INNATE IMMUNE CELLS IN VACCINATION

EDITED BY: Michael Schotsaert, Jordi Ochando and Matthias Tenbusch
PUBLISHED IN: Frontiers in Immunology

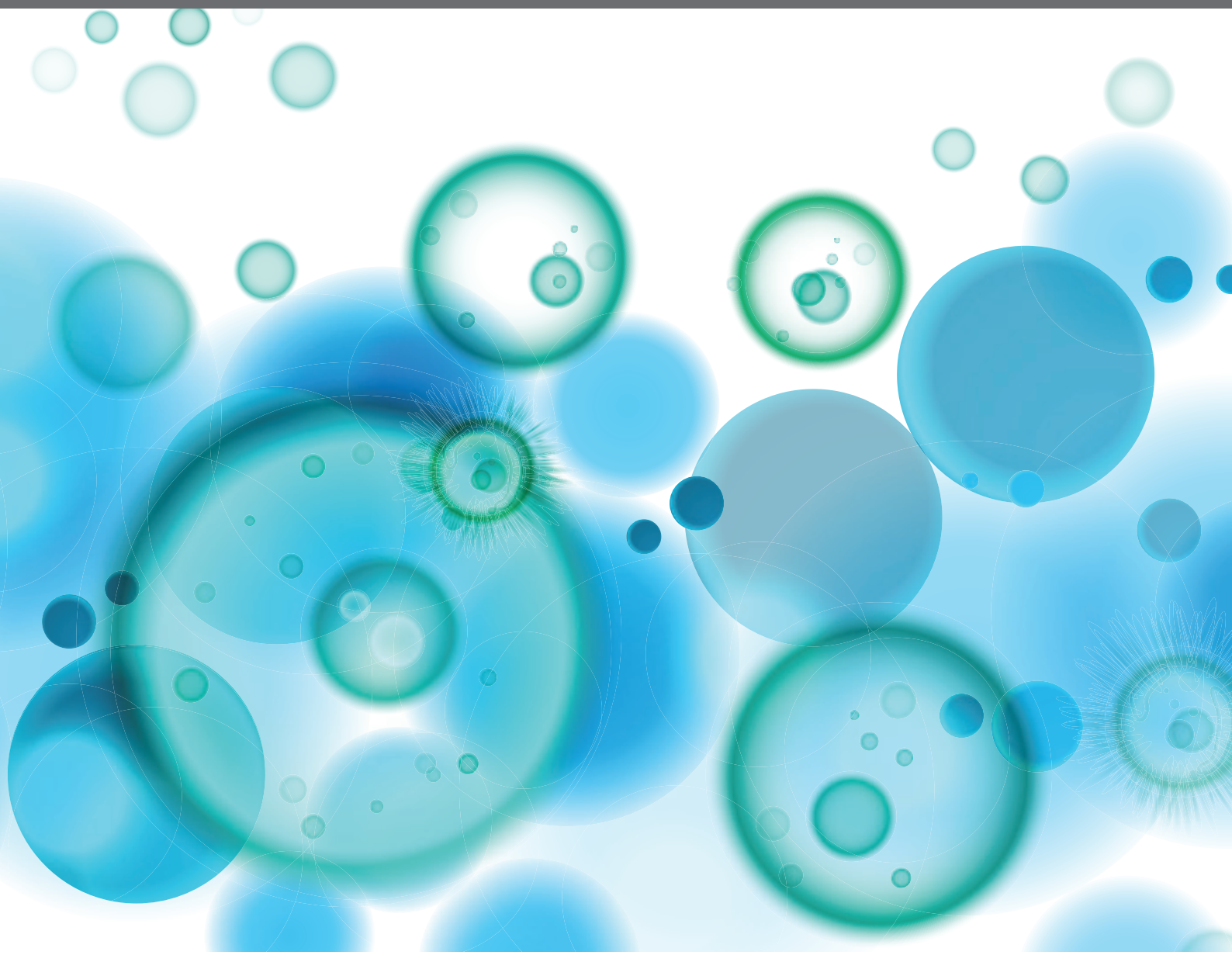

frontiers Research Topics

ISSN 1664-8714
ISBN 978-2-88966-660-7
DOI 10.3389/978-2-88966-660-7

About Frontiers

Frontiers is more than just an open-access publisher of scholarly articles: it is a pioneering approach to the world of academia, radically improving the way scholarly research is managed. The grand vision of Frontiers is a world where all people have an equal opportunity to seek, share and generate knowledge. Frontiers provides immediate and permanent online open access to all its publications, but this alone is not enough to realize our grand goals.

Frontiers Journal Series

The Frontiers Journal Series is a multi-tier and interdisciplinary set of open-access, online journals, promising a paradigm shift from the current review, selection and dissemination processes in academic publishing. All Frontiers journals are driven by researchers for researchers; therefore, they constitute a service to the scholarly community. At the same time, the Frontiers Journal Series operates on a revolutionary invention, the tiered publishing system, initially addressing specific communities of scholars, and gradually climbing up to broader public understanding, thus serving the interests of the lay society, too.

Dedication to Quality

Each Frontiers article is a landmark of the highest quality, thanks to genuinely collaborative interactions between authors and review editors, who include some of the world's best academicians. Research must be certified by peers before entering a stream of knowledge that may eventually reach the public - and shape society; therefore, Frontiers only applies the most rigorous and unbiased reviews.
Frontiers revolutionizes research publishing by freely delivering the most outstanding research, evaluated with no bias from both the academic and social point of view. By applying the most advanced information technologies, Frontiers is catapulting scholarly publishing into a new generation.

What are Frontiers Research Topics?

Frontiers Research Topics are very popular trademarks of the Frontiers Journals Series: they are collections of at least ten articles, all centered on a particular subject. With their unique mix of varied contributions from Original Research to Review Articles, Frontiers Research Topics unify the most influential researchers, the latest key findings and historical advances in a hot research area! Find out more on how to host your own Frontiers Research Topic or contribute to one as an author by contacting the Frontiers Editorial Office: frontiersin.org/about/contact

INNATE IMMUNE CELLS IN VACCINATION

Topic Editors:
Michael Schotsaert, Icahn School of Medicine at Mount Sinai, United States
Jordi Ochando, Icahn School of Medicine at Mount Sinai, United States
Matthias Tenbusch, University Hospital Erlangen, Germany

Citation: Schotsaert, M., Ochando, J., Tenbusch, M., eds. (2021). Innate Immune Cells in Vaccination. Lausanne: Frontiers Media SA. doi: 10.3389/978-2-88966-660-7

Table of Contents

frontiers in Immunology

REVIEW
published: 14 February 2020
doi: 10.3389/fimmu.2020.00226

Thinking Outside the Box: Innate- and B Cell-Memory Responses as Novel Protective Mechanisms Against Tuberculosis

José Alberto Choreño-Parra[1,2†], *León Islas Weinstein*[3†], *Edmond J. Yunis*[4,5], *Joaquín Zúñiga*[2,6*] *and Rogelio Hernández-Pando*[3*]

[1] Escuela Nacional de Ciencias Biológicas, Instituto Politécnico Nacional, Mexico City, Mexico, [2] Laboratory of Immunobiology and Genetics, Instituto Nacional de Enfermedades Respiratorias Ismael Cosío Villegas, Mexico City, Mexico, [3] Section of Experimental Pathology, Department of Pathology, Instituto Nacional de Ciencias Médicas y Nutrición Salvador Zubirán, Mexico City, Mexico, [4] Department of Cancer Immunology and AIDS, Dana-Farber Cancer Institute, Boston, MA, United States, [5] Department of Pathology, Harvard Medical School, Boston, MA, United States, [6] Tecnologico de Monterrey, Escuela de Medicina y Ciencias de la Salud, Mexico City, Mexico

OPEN ACCESS

Edited by:
Matthias Tenbusch,
University Hospital Erlangen, Germany

Reviewed by:
Suraj Sable,
Centers for Disease Control and Prevention, United States
Roland Lang,
University Hospital Erlangen, Germany

***Correspondence:**
Joaquín Zúñiga
joazu@yahoo.com;
joazu@tec.mx
Rogelio Hernández-Pando
rhdezpando@hotmail.com;
rhpando@quetzal.innsz.mx

†These authors have contributed equally to this work

Specialty section:
This article was submitted to Molecular Innate Immunity, a section of the journal Frontiers in Immunology

Received: 02 October 2019
Accepted: 28 January 2020
Published: 14 February 2020

Citation:
Choreño-Parra JA, Weinstein LI, Yunis EJ, Zúñiga J and Hernández-Pando R (2020) Thinking Outside the Box: Innate- and B Cell-Memory Responses as Novel Protective Mechanisms Against Tuberculosis. Front. Immunol. 11:226. doi: 10.3389/fimmu.2020.00226

Tuberculosis (TB) is currently the deadliest infectious disease worldwide. Failure to create a highly effective vaccine has limited the control of the TB epidemic. Historically, the vaccine field has relied on the paradigm that IFN-γ-mediated CD4+ T cell memory responses are the principal correlate of protection in TB. Nonetheless, the demonstration that other cellular subsets offer protective memory responses against *Mycobacterium tuberculosis* (Mtb) is emerging. Among these are memory-like features of macrophages, myeloid cell precursors, natural killer (NK) cells, and innate lymphoid cells (ILCs). Additionally, the dynamics of B cell memory responses have been recently characterized at different stages of the clinical spectrum of Mtb infection, suggesting a role for B cells in human TB. A better understanding of the immune mechanisms underlying such responses is crucial to better comprehend protective immunity in TB. Furthermore, targeting immune compartments other than CD4+ T cells in TB vaccine strategies may benefit a significant proportion of patients co-infected with Mtb and the human immunodeficiency virus (HIV). Here, we summarize the memory responses of innate immune cells and B cells against Mtb and propose them as novel correlates of protection that could be harnessed in future vaccine development programs.

Keywords: *Mycobacterium tuberculosis*, trained immunity, B-cells, memory-like NK cells, ILCs

INTRODUCTION

Mycobacterium tuberculosis (Mtb), the causative agent of pulmonary tuberculosis (TB), remains the most important pathogen worldwide in terms of accumulated mortality. The World Health Organization has estimated that 10 million new cases of TB and 1.421 million deaths caused by Mtb occurred in 2018 (1). The convergence of the Mtb and human immunodeficiency virus (HIV) epidemics, as well as the lack of new vaccines capable of conferring significant protection against TB have limited the control of this global health treat. Failure to create an effective vaccine for TB has been largely due to an incomplete understanding of the immune mechanisms associated with protective immunity against Mtb. In fact, for many years, the TB vaccine field has established

the paradigm that CD4+ T memory cell responses mediated by IFN-γ are the chief immune mechanism which controls the spread of Mtb within the infected lung (2, 3). Despite its relevance, this mechanism has erroneously been considered the sole correlate of protection in TB (4). Moreover, recent findings have raised uncertainty about the protective capacity of IFN-γ-mediated CD4+ T cell memory against Mtb. For instance, T cell epitopes have been demonstrated to be well-conserved in Mtb, suggesting that the pathogen may take advantage of its recognition by T cells (5). Furthermore, recent TB vaccine candidates targeting IFN-γ-mediated T cell functions have failed to provide improved effectiveness compared to the *Mycobacterium bovis* Bacillus Calmette-Guerin (BCG) vaccine (6). Finally, IFN-γ has shown a poor predictive value in discriminating between subjects receiving BCG vaccination that will receive protection from those that will develop active TB (7). The discussion of the protective capacity of T cell memory responses against Mtb is beyond the scope of the present review, but further evidence has been extensively revised and analyzed by other researchers (8).

Hence, the TB vaccination field would benefit from the exploration of novel correlates of protection and the development of new strategies to disrupt the natural immune responses induced by Mtb to ensure its survival. Recently, some authors have proposed that this goal could be achieved through two complementary approaches: 1) inducing immune memory responses lacking or being strong enough to overcome the characteristics of the natural anti-Mtb immune responses that are beneficial for the pathogen, but with minimal risk of immunopathology, or 2) triggering very early protective responses that prevent the establishment of evasive mechanisms used by Mtb to manipulate the innate immune response (9). A growing body of evidence suggests that these approaches could be achieved by targeting immune cell populations other than T cells (10–13). In particular, it has been increasingly accepted that B cells actively participate in anti-Mtb immunity, either as secondary actors providing support and shaping the quality of T cell-memory responses, or as protagonists mediating direct effector functions against Mtb (14). Similarly, different subpopulations of innate immune cells that possess a previously unrecognized capacity to mount secondary "memory-like" responses are equally capable of limiting Mtb growth (11, 15). Therefore, in this review we summarize the memory responses of innate immune cells and B cells against Mtb and analyze how their functions may constitute novel correlates of protection that can be potentially harnessed for TB vaccine development.

MEMORY RESPONSES AGAINST Mtb WITHIN THE INNATE IMMUNE SYSTEM

As mentioned before, the study of the mechanisms underlying immunity to Mtb infection has focused on immunological memory mediated by adaptive immune cells, mainly CD4+ T helper lymphocytes. However, human studies have shown that up to a quarter of the individuals that are in close contact with active TB patients remain clear of the infection (16). These individuals test negatively in the purified protein derivative (PPD) skin test and IFN-γ release assays (IGRAs) (16, 17), which are two indirect readouts of adaptive responses against immune-dominant Mtb antigens. A positive BCG vaccination history has been associated with this state of immune protection (16). This suggests that in such "resistant" close-contacts, innate immune responses potentiated by BCG vaccination are sufficient to restraint Mtb infection.

Notably, recent investigations have uncovered the role of "trained immunity" in the pathogenesis of different infectious diseases. This concept describes an enhanced capacity of innate leukocytes to respond to secondary challenges by the same or by unrelated microorganisms after an initial antigenic exposure (18). The first hints of trained immunity induced by mycobacterial components were observed in mice treated with muramyl dipeptide (19), Freund's complete adjuvant (20), and BCG/PPD (21). Mycobacterial component preparations conferred protection against *Klebsiella pneumoniae*, foot and mouth disease virus (FMDV), and *Candida albicans* infection, respectively. Interestingly, protection from FMDV was independent of neutralizing antibodies (20), whereas control of systemic candidiasis occurred before the development of delayed-type hypersensitivity (21). Similarly, BCG exposure was shown to limit *Schistosoma mansoni* infestation in nude mice, suggesting a role for trained immunity in BCG-induced cross-protection (22). In humans, BCG vaccination conferred heterologous immunity against lower respiratory tract pathogens (23, 24), yellow fever virus (25), and neonatal sepsis (24). Furthermore, BCG vaccination was demonstrated to induce protection against intestinal parasites (26), even in individuals infected with HIV, suggesting that innate immune cells mediate such cross-protection.

Epigenetic changes that facilitate the expression of inflammatory genes and generate metabolic reprogramming are responsible for inducing trained immunity against mycobacterial and other microbial components. In these epigenetic changes, long non-coding RNAs participate in the formation of chromatin loops that bring several genes into a close spatial relationship, making these genetic regions more accessible to the enzymatic complexes responsible for epigenetic priming. Three cellular subsets appear to be involved in the trained immune response against Mtb: monocyte-macrophages, myeloid cell precursors, and innate lymphoid cells (ILCs), these latter including natural killer (NK) cells (18).

Myeloid Cells in Memory Responses Against Mtb

Infected cell recognition is needed for the clearance of any infection. The adequate induction of protective immune responses against Mtb is initiated through efficient bacterial antigen recognition via pattern recognition receptors (PRRs) present in antigen presenting cells (APCs). Monocytes and macrophages are myeloid cells that participate in pathogen clearance at different organs. Irrespective of their origin, macrophages acquire a distinctive tissue-residency phenotype under the influence of local signals (27). In the lung, two

subpopulations of macrophages maintain tissue homeostasis. Precursors of alveolar macrophages (AMs) from the yolk sac infiltrate the alveolar epithelium during fetal development, maintaining themselves through a self-renewal process independent of circulating monocytes (28). These phagocytes eliminate infectious agents that reach the lumen of distal airways, including Mtb (29). On the other hand, monocyte-derived macrophages migrate to the lung interstitium to participate in the elimination of pathogens, as well as in antigen presentation, and the recruitment of other leukocytes during inflammation (30).

AMs are among the first cells of the host immune system to encounter Mtb. After engulfing the bacillus, they leave the airways and initiate a cascade of inflammatory signals that will lead to the recruitment of more leukocytes around the sites of Mtb exposure (29). Over time, infiltrating leukocytes form structures called "granulomas" where different subtypes of phagocytes interact with the bacillus (31). Phagocytosis, antigenic processing, and cytokine production by myeloid cells shape the subsequent adaptive immune response (32). Nevertheless, Mtb employs mechanisms to evade the bactericidal activity of macrophages within immature phagosomes (i.e., Rab5 blockage, respiratory oxidative burst avoidance, etc.) establishing a proliferative niche (33). Hence, it was believed that pulmonary Mtb infection was contained only when primed antigen specific CD4+ T cells migrated to the lung parenchyma to stimulate antimicrobial mechanisms of local macrophages (34, 35). As a result, researchers have attributed excessive importance to the adaptive immune response in TB and far fewer significance to the trained immune response. The current view has probably limited the potential of basic and clinical research in TB vaccination strategies. Notwithstanding, this dogma is changing as emerging evidence demonstrates that the outcome of TB might be significantly influenced by special features present in innate immune cells, including their capacity to develop trained immunity. Moreover, the qualities that resemble memory in monocytes and macrophages are fueling the investigation of novel methods to potentiate innate defenses against Mtb (11).

Early studies in mice showed that BCG-induced trained immunity was mediated by macrophages (20, 21). Indeed, macrophages from animals treated with BCG produce more reactive oxygen species (ROS) and have increased *Candida albicans* growth restriction (21). In humans, BCG vaccination greatly enhances the ability of monocytes to produce inflammatory cytokines, such as IL-1β, TNF-α, and IFN-γ, after secondary encounters with Mtb and other microorganisms (36). Moreover, these monocytes expressed larger quantities of CD11b and toll-like receptor 4 (TLR4), two important pattern recognition receptors that initiate phagocytosis (37–39), suggesting that trained-monocytes may be more efficient at detecting and engulfing Mtb. The innate memory responses of monocytes depend on the intracellular recognition of BCG via NOD2 receptor and downstream Rip2 kinase signaling (36). NOD2 is one of the main receptors triggering immune activation after Mtb uptake (40) and is also involved in the initiation of autophagy (41). Thus, autophagy mediated by the NODS-Rip2 pathway is one of the mechanisms necessary for the development of trained immunity. Moreover, pharmacological inhibition of autophagy abolishes trained immunity in BCG-treated human monocytes (42). Interestingly, in some trials, the effect of BCG-induced training of human monocytes was still present 3 months after vaccination (36). This raised questions about the processes implicated in the maintenance of innate memory in monocytes because of the short half-life of these circulating cells (43).

Besides monocytes and macrophages, bone-marrow myeloid precursors were also reported to receive epigenetic reprogramming after microbiota exposure (44). Based on this finding, Kaufmann et al. exposed mice to intravenous BCG and observed an IFN-γ-dependent expansion of hematopoietic stem cells (HSCs) within the bone marrow (11). These HSCs displayed an increased expression of genes implicated in myeloid cell differentiation, inflammation, and IFN-γ signaling responses. Furthermore, bone marrow-derived macrophages (BMDMs) from mice exposed to intravenous BCG possessed an increased capacity to restrict Mtb growth *in vitro*, and conferred protection from aerosol Mtb infection when adoptively transferred into Rag1 immunodeficient mice (11). Such protection was independent of antigenic persistence in donor mice exposed to intravenous BCG, as antibiotic administration to donor mice before adoptive transfer did not influence the capacity of BMDMs to confer protection against Mtb *in vivo*. Interestingly, the epigenetic changes associated with immune training of BMDMs were similar to those observed in human innate immune cells trained by BCG vaccination (36), as well as by exposure to other microbial components (45). These epigenetic modifications consisted of increased H3K4me3 histone marks at promoters of genes involved in inflammation and anti-Mtb responses (11, 36). Accordingly, pharmacologic inhibition of histone methylation reversed BCG-induced training of human monocytes (36). Thus, trained monocytes/macrophages mount enhanced secondary responses to Mtb because they carry epigenetic modifications that make inflammatory genes more accessible to the transcriptional machinery. In addition, BCG-induced histone modifications in trained-myeloid cells cause a metabolic shift in these cells which potentiates glycolysis and glutamine consumption pathways (46). Hence, the improved effector capacity of BCG-trained macrophages is related to their increased catabolic activity and energetic production required to sustain their pro-inflammatory and bactericidal actions.

These findings open the possibility for evaluating novel vaccination strategies targeting the bone marrow (**Figure 1A**). However, it is crucial to confirm the occurrence of epigenetic priming of myeloid precursors after BCG administration or during natural pulmonary TB infection in humans. Equally important is determining whether innate immune memory responses of HSCs and their progeny can generate significant adverse effects in the host. In fact, there is evidence showing that systemic inflammatory stimuli induce training of monocytes/macrophages which then mediate local tissue damage at different anatomical sites (47–49). Conversely, a recent study in macaques receiving intravenous BCG demonstrated that this route of vaccination, which perhaps reaches the bone marrow, is effective at conferring protection against Mtb infection

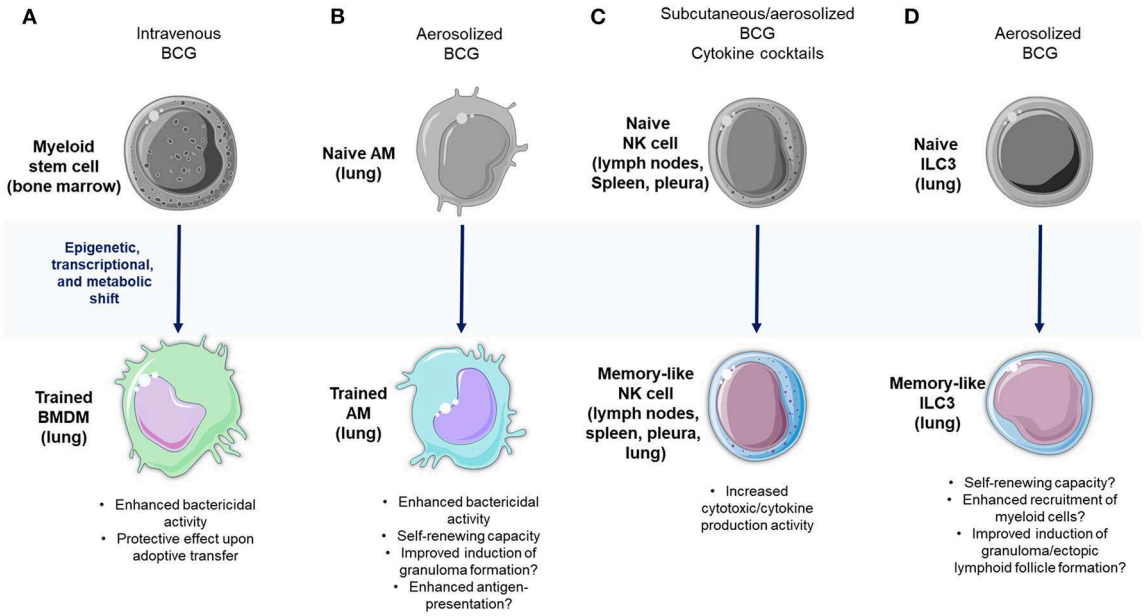

FIGURE 1 | Memory-like responses against Mtb within the innate immune system**. (A)** Intravenous Bacillus Calmette-Guerin (BCG) vaccination induces the expansion of human stem cells (HSCs) and a bias toward the production of myeloid precursors carrying epigenetic imprints that reprogram their transcriptional and metabolic profiles. These cells subsequently generate a progeny of myeloid cells with enhanced effector functions that confer protection against aerosol infection in Mtb-infected mice. **(B)** Alveolar macrophages (AMs) display characteristics of trained immunity, which may provide protection against Mtb infection. **(C)** BCG as well as natural Mtb infection potentiate the effector functions of natural killer (NK) cells, and induce the expansion of memory-like NK cell subpopulations. **(D)** Similarly, innate lymphoid cells (ILCs) possess characteristics of adaptive immunity that may confer protection in TB, thus placing these cells as potential targets for vaccine development programs. The art pieces used in this figure were modified from Servier Medical Art by Servier, licensed under a Creative Commons Attribution 3.0 Unported License (https://smart.servier.com/).

without generating pathological effects (50). However, in this study, the participation of trained myeloid cell precursors in protective immunity against TB was not addressed. Training of tissue-resident macrophages located solely within the lung may constitute a more prudent strategy to improve innate immunity at the sites of natural Mtb exposure. In this context, recent findings provide evidence that AMs can also display memory characteristics in mice (51). The local priming of memory AMs has been triggered by mucosal infection of mice with an adenoviral vaccine vector, which caused an increased expression of MHC-II molecules and a metabolic shift toward glycolysis in these cells. Trained AMs protected animals against secondary infection with *Streptococcus pneumoniae*, maintaining their memory responses through a process of self-renewing which was independent of circulating monocytes. Hence, these data demonstrate that induction of trained immunity in lung AMs can be achieved by local antigen delivery and may explain why mucosal BCG vaccination is a better approach to confer protection against Mtb infection as compared to subcutaneous BCG administration (52–54). However, direct evidence of trained immunity induced by BCG in AMs is currently inexistent. Furthermore, although trained AMs contribute to the clearance of other respiratory pathogens (51), recent findings suggest that AMs are indeed more permissive than blood-derived monocytes to sustain the intracellular growth of Mtb (55). This contrasts with other data showing that CCR2+ AMs induce protective responses against Mtb (29). Therefore, it is likely that different subpopulations of AMs with variable bactericidal capacity against Mtb exist, mirroring M1 and M2 macrophages. Future studies are warranted to define whether memory AMs generate enhanced protection after mucosal BCG vaccination, as well as to determine the duration of their trained responses (**Figure 1B**). In addition, the pathogenic potential of trained AMs during TB must be addressed. If trained immunity is documented as a protective long-lasting response with limited adverse effects in TB, then it could emerge as a novel correlate of protection suitable to be targeted in vaccine development programs.

NK Cell Memory in TB

NK cells participate in the defense against pathogens by mediating cytotoxicity against infected cells and through the production of a wide range of cytokines that influence the effector functions of other leukocytes (56). Activation of NK cells can be triggered by ligand recognition of infected cells via their activating receptors and through PRR microbial component recognition (57, 58). Furthermore, NK cells possess various inhibitory receptors that bind to MHC-I molecules and other related surface proteins (59). Cells disturbed by an intracellular infection lose the expression of their inhibitory ligands, allowing NK cells to react to the "missing self" signals by activating their effector functions (60).

NK cells are an important source of cytokines, chemokines and growth factors crucial for anti-Mtb immunity. In fact, they produce high amounts of IFN-γ (61), TNF-α (62), IL-17 (63), IL-22 (64, 65), and GM-CSF (66), all of which participate in TB pathogenesis (67). Thus, these cells have attracted the attention of researchers as they may play a relevant role in pulmonary TB. In this regard, it is known that NK cells can recognize several components of the Mtb cell wall through their activating receptors and PRRs (58, 68, 69). These interactions result in the production of proinflammatory cytokines that can increase the bactericidal activity of macrophages (70–72), as well as cytotoxic proteins that can kill bacilli-loaded phagocytes (73). *In vitro* assays have demonstrated that NK cells can even eliminate extracellular Mtb through cytotoxic mechanisms (74), although the relevance of this function has not been confirmed *in vivo*. In animal models, NK cells play a relevant role for protective immunity against Mtb only when T and B-cell responses are compromised (75). NK cells-derived IFN-γ and other proinflammatory cytokines (75, 76), potentiate the control of Mtb infection by macrophages. These functions are dependent on IL-12 and IL-21 production by T cells (75, 76). However, in immunocompetent animals NK cells play a minimal role in protective immunity against Mtb (77). In humans, NK cells can be found in lung tissue specimens from patients with chronic Mtb infection (78), suggesting their involvement in TB pathogenesis. Current evidence suggests a beneficial role of NK cells during human TB as changes in their immunophenotype and function are associated with the development of active TB (79–88). NK cells support the activity of CD8+ T cells during Mtb infection (89), shape the maturation process and Mtb-antigen processing in dendritic cells (DCs) (90), limit the expansion of regulatory CD25+ T cells (91), and even participate in the mechanisms underlying protection induced by BCG vaccination (92).

In a similar fashion to monocytes and macrophages, NK cells display characteristics of adaptive immune cells that allow them to mount recall responses against haptens, viruses, and bacteria (93–95). However, NK cell memory differs from trained immunity in myeloid cells in terms of the response specificity. In some cases, NK cell memory responses against specific antigens are mediated by a single subset of NK cells expressing a particular receptor (93, 94, 96). For instance, memory-like NK cells expressing CD94/NKG2C expand rapidly after cytomegalovirus (CMV) infection in humans (96). On the other hand, cytokine priming of NK cells can induce the expansion and development of memory responses against antigenic and non-antigenic stimuli (97, 98). Importantly, NK cell memory can be induced after BCG vaccination and after natural Mtb exposure in both mice and humans (99). For instance, NK cells isolated from BCG-vaccinated humans show an increased capacity of proinflammatory cytokine production after *ex vivo* re-challenge with Mtb, BCG, and other bacteria and fungi (99). Such enhanced responses are long-lasting and can be observed 1 year after BCG revaccination in LTBI patients (100). Human NK cells can also be primed during natural pulmonary Mtb infection in humans, as suggested by the expression of CD45RO, a molecular marker classically used to identify memory T cells subsets (101, 102). These human CD45RO+ NK cells demonstrate increased cytotoxicity and IFN-γ production capacity after *ex vivo* stimulation with IL-12, as compared to CD45RO- NK cells (102). Additionally, CD45RO+ NK cells produce more IL-22 in response to IL-15 and BCG (101). However, the relevance of such trained-NK cell responses in protective immunity against Mtb infection in humans remains unclear.

In a recent study, a protective effect of memory-like NK cells against murine pulmonary TB was observed (15). BCG-vaccinated mice showed an IL-21 dependent expansion of NKp46+CD27+KLRG1+ NK cells in the lymph nodes and spleen. Such cells produced more IFN-γ than their NKp46+CD27− counterparts and were able to improve Mtb infection control both in isolated macrophages as well as in mouse TB-infected lungs after their adoptive transfer. The specificity of BCG-induced memory-like responses mediated by NK cells seemed to be limited to Mtb, as these cells did not respond to *Candida albicans*. In addition, higher amounts of CD56+CD27+ NK cells were observed in humans with LTBI compared to healthy donors, providing evidence of memory-like NK cell expansion in humans with controlled TB. Interestingly, human CD56+CD27+ NK cells have a higher capacity of limiting intracellular Mtb growth in macrophages compared to CD56+CD27-NK cells. Nevertheless, the protective role of memory-like NK cells in human TB remains unknown as this NK cell subpopulation was only evaluated in individuals with LTBI, but not in patients with active TB (15). In summary, memory-like NK cells promise to be new targets for TB vaccine development due to their possible protective functions (**Figure 1C**). Nonetheless, uncovering their precise role in human anti-Mtb immunity remains a challenge. Collectively, the evidence suggests that despite the apparent redundancy of NK cell functions during Mtb infection in immunocompetent hosts (77), the potentiation of their memory properties may be beneficial in subjects with impaired adaptive responses (75), such as those infected with HIV.

Memory of ILCs in TB

ILCs are lymphocytes that functionally mirror adaptive T helper cells except for their lack of rearranged antigen-specific receptor expression. Hence, these cells are considered as part of the innate branch of the immune system. Type 1 ILCs are the innate counterpart of Th1 lymphocytes and, as such, produce high amounts of IFN-γ upon stimulation. ILC2s resemble Th2 cells, produce IL-4, IL-5, and IL-13, and play a role in allergic disorders and defense against parasites. ILC3s functionally mirror Th17 cells and produce IL-17 and IL-22 (103). Recently, ILCs have been implicated in the immune response to Mtb. Compared to healthy controls, all ILC subsets are diminished in the peripheral blood of humans with active TB. The proportion of circulating ILC1s and ILC3s is restored after infection clearance following antibiotic treatment (12). The depletion of circulating ILCs has been linked to their migration toward sites of Mtb exposure within the lung. In fact, during advanced pulmonary TB, ILCs are enriched in both mice and human lung tissue. Their recruitment is apparently regulated via the CXCL13/CXCR5 axis. Additionally, in humans, ILC2s and ILC3s localize within the infected lung and overexpress genes involved in inflammation

and myeloid cell chemotaxis, such as CXCL17 (104). In mice, the maximum migration of ILCs to the lungs coincides with the peak recruitment of AMs. Absence of ILCs, particularly of ILC3s, results in a reduction of lung AMs recruitment, higher bacterial burden, and altered tertiary lymphoid nodule (TLN) and granuloma formation during TB infection (12). Similar findings were reported in type 2 diabetes mellitus (T2DM) mice infected with Mtb, in which the adoptive transfer of ILC3s prolonged their survival, limiting neutrophil accumulation within the lung, and preventing damage to the alveolar epithelium via the production of IL-22 (105). These findings suggest that ILCs, specifically ILC3s, participate in the immune response to Mtb. Nonetheless, additional TB models in animals with specific deletion of ILC3s are required to confirm these data.

Interestingly, recent investigations have uncovered the ability of ILCs to display features that resemble the trained immune responses of macrophages and the memory-like responses of NK cells (106). These innate memory-like responses of ILCs could be targeted via vaccination (**Figure 1D**). For instance, BCG vaccination in mice has already shown to induce rapid accumulation of ILCs within the lungs (107). In such animals, the intranasal route of BCG administration generated a stronger recruitment of lung ILCs which possess an enhanced ability to produce IFN-γ compared to the intradermal route of BCG administration. These data suggest that mucosal BCG vaccination may trigger the development of lung memory-like ILCs. Nevertheless, further experimental demonstration of the adaptive characteristics of such cells and their protective or pathogenic nature in the context of TB is required.

B CELLS IN MEMORY RESPONSES AGAINST Mtb

The role of B cells in the defense against pathogens greatly relies on their capacity to generate immune memory, providing the host with a durable reservoir of antigen-specific antibodies, as well as a pool of long-lasting antibody-producing cells that can re-expand in case of a secondary challenge. During a primary response to an antigen, naïve B cells may transform into effector B cells and subsequently experience class switching, recombination, and affinity maturation within germinal centers (GC), with the support of follicular T helper (Tfh) cells. This GC reaction is a common pathway that gives rise to memory B cells (MBCs) and plasmablasts. MBCs secrete null amounts of antibodies but in case of a re-encounter with the same pathogen, they can generate plasmablasts within hours. Plasmablasts are B cells capable of secreting reduced amounts of antibodies and more importantly, are precursors of plasma cells (PCs), short-lived cellular units that use their protein machinery for the production and secretion of massive amounts of antigen-specific antibodies. PCs are unable to proliferate without antigenic stimulation; however, a selected minority of PCs can generate anti-apoptotic processes and migrate to the bone marrow, thus becoming long-lived PCs (LLPCs, also termed memory PCs). These LLPCs survive without antigenic stimulation and continuously liberate antigen-specific antibodies to the circulation (108, 109).

For many years, the role of antibody-mediated B cell memory responses in TB has remained controversial (110). However, several studies have demonstrated the importance of this response in combatting this disease. In fact, elevated serum titers of PPD-specific antibodies correlate with protection against TB in high-risk individuals and are a better indicator of LTBI than the skin test reaction (111). Such antibodies induce the stimulation of PBMCs *in vitro*, suggesting that after biding to its specific antigen, these immunoglobulins can trigger effector responses of different immune cells. In line with these findings, it has been recently described that the antibodies from LTBI subjects have an increased capacity to bind to the FcγRIII and trigger the effector activities of NK cells and macrophages (10). This functional difference is associated with distinctive patterns of glycosylation of the Fab domain of antibodies from LTBI patients compared to individuals with active TB (10). Functional humoral responses have also been linked to the development of sterilizing immunity in individuals resistant to TB. In such resistant subjects an IFNγ-independent response mediated by CD4+CD40L/CD154+ T cells induces T-follicular B cell help and the production of several non-Th subset-specific cytokines critical for B cell activation (112). Furthermore, in a recent study, the humoral response of this human population was characterized by an IgG1-dominant state specific to ESAT6/ CFP10, LAM and PPD. Conversely LTBI individuals displayed a diversified IgG subclass response (112). Additionally, antibodies from individuals with LTBI can restrict Mtb intracellular growth in a more successful fashion compared with antibodies from patients with active TB (113). Whether antibodies contribute to the "resistant" phenotype observed in some individuals remains an undetermined matter at this moment, however it is currently known that post-vaccination serum favors Mtb phagocytosis by macrophages, enhances phagolysosome fusion and inhibits intracellular Mtb growth (113). Furthermore, pooled IgG from LTBI individuals may eradicate intracellular bacilli through a process that likely involves the inflammasome (114). These findings suggest that antibody-mediated B-cell memory responses play a role in the defense against Mtb infection and may be targeted to induce protective immunity through vaccination. Unfortunately, the dynamics of the antibody mediated immune responses (AMIR) during TB progression remain insufficiently characterized. Nonetheless, as MBCs are not only located in lymphoid organs but can also be found in peripheral blood, some studies have examined the kinetics of circulating MBC populations in patients with distinct forms of TB.

Some preliminary findings suggest that the proportion of distinct MBC subsets may predict the clinical status of Mtb-infected patients (**Figure 2**), arguing in favor of a role of B cell memory in TB (108, 115–119). For instance, MBC, plasmablasts, and PCs subsets are significantly enriched in the circulation of patients with active TB, and their proportions diminish after the conclusion of anti-TB treatment, suggesting that these B cells subsets undergo a contraction phase after antigen clearance (119). Indeed, the maintenance of MBCs in circulation is dependent on the presence of Mtb antigens and can be eliminated after 12 weeks of antibiotic treatment (116), but serum IgG levels remain augmented even after a 6 month course

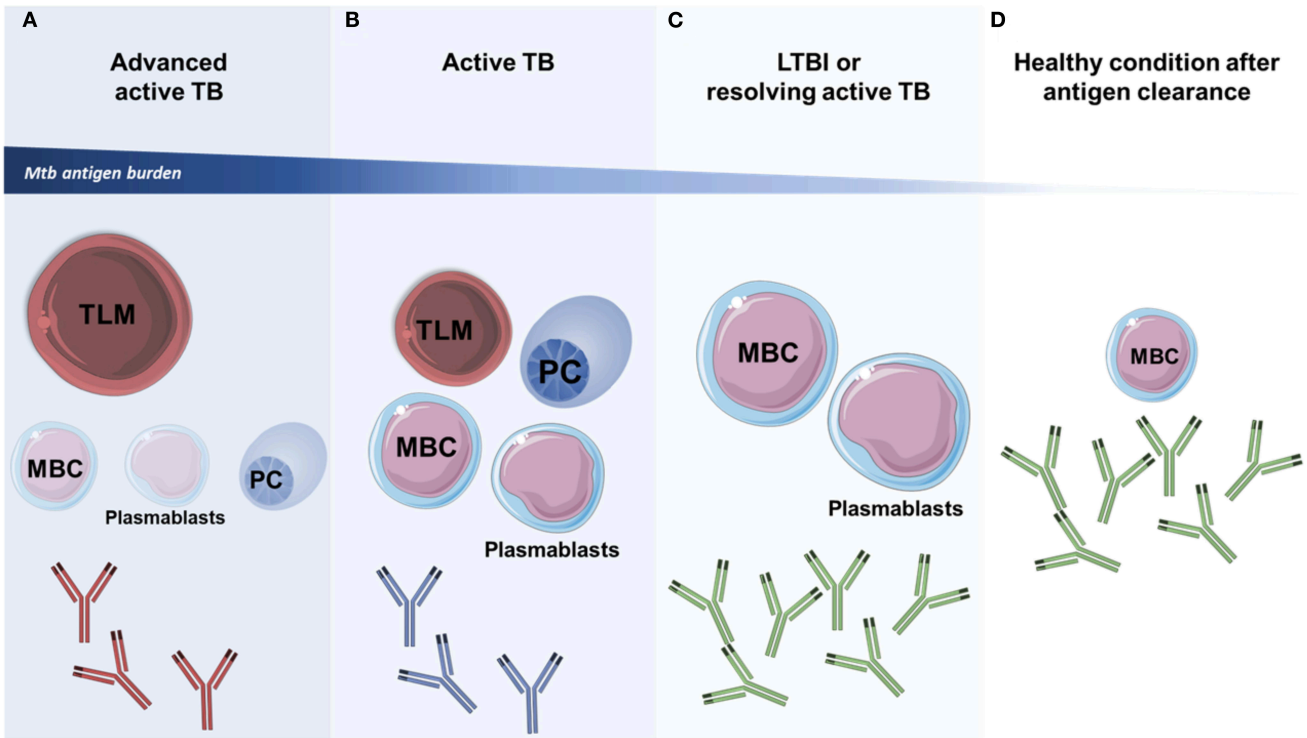

FIGURE 2 | Profiles of circulating memory B cell subpopulations during TB. The characterization of the profile of circulating B cell subsets may help to discriminate different forms of the clinical spectrum of TB. **(A,B)** Most memory B-cells (MBCs), plasma cells (PCs), and plasmablasts subsets expand during active TB and depend on antigenic persistence. These subsets are depleted from the circulation of individuals with advanced TB, which show increased numbers of tissue-like memory B cells (TLMs) that have an exhaustion phenotype and are associated with disease progression. The humoral response in patients with active TB is characterized by the presence of antibodies that induce poor activation of effector activities in innate immune cells (antibodies in red and blue color). **(C)** Individuals with LTBI and those with resolving active TB are characterized by a strong functional antibody response (antibodies in green color), as well as by elevated numbers of circulating MBCs and plasmablasts. **(D)** In healthy individuals that are able to clear the infection, and in those that received antibiotic treatment, an increased proportion of circulating MBCs is observed. This cellular population may decrease over time in a parallel fashion to the antigenic burden. In these patients, a persistent functional antibody-mediated immune response is also observed (antibodies in green color). The size of B cell subsets at each specific stage of TB disease indicate their predominance (larger drawings) or downregulation (smaller drawings). The art pieces used in this figure were modified from Servier Medical Art by Servier, licensed under a Creative Commons Attribution 3.0 Unported License (https://smart.servier.com/).

of antibiotic therapy in TB patients (119). Thus, during active TB, the presence of the pathogen may trigger the generation of high-affinity antibody-mediated memory responses to Mtb antigens. Plasmablasts can readily induce class-switched and cytokine-producing PCs upon antigen exposure or re-exposure if they are derived from naïve B cells or antigen-experienced MBCs, respectively (14, 119). These responses may reduce Mtb burden in active TB patients and curb their disease outcome, as well as maintain a LTBI status. In fact, it was demonstrated that PCs derived from peripheral blood cells of LTBI subjects produce significant amounts of antibodies and IL-17 when exposed to Mtb antigens (115). Thus, the dual presence of MBCs and plasmablasts in the peripheral blood has been proposed as a marker of resolving active disease and LTBI. On the other hand, the presence of activated antigen-specific plasmablasts but not MBCs in the peripheral circulation may reflect the initial stages of active TB and the lack of both MBCs and plasmablasts in circulation may indicate uncontrolled infection (118). Particularly, non-switched IgD+ MBCs have been found reduced in distinct tissue compartments during advanced active TB (120, 121). Other studies have found that higher proportions of circulating MBCs but not plasmablasts in peripheral blood along with a prominent serum antibody-mediated memory response is indicative of a healthy condition after sterilizing immunity following Mtb infection (118). This coincides with the observation that healthy subjects who have resided in TB-endemic areas have greater frequencies of peripheral blood MBCs and antibody-mediated responses compared to subjects from other world areas (122). Therefore, although MBCs might contract after Mtb control, they remain preconditioned to mount secondary responses in case of reinfection.

The role and dynamics of LLPCs and marginal zone (MZ) B cells during TB is still under investigation. Recently, it was observed that BCG vaccination can elicit the generation of PPD-specific LLPCs in humans (122). Additionally, another study found that LLPCs are important contributors of cytokine production during LTBI (115). MBCs and LLPCs generate the AMIR through the production of IL-21 and the subsequent

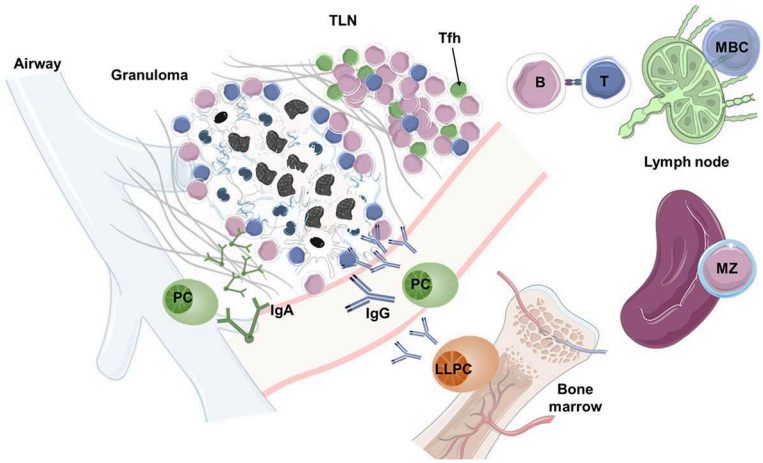

FIGURE 3 | B cell functions in TB. During pulmonary Mtb infection, granulomas and peripheral tertiary lymphoid nodes (TLNs), which resemble germinal centers (GCs), develop in the lungs and shape the protective immune response. Within TLNs and local lymph nodes, B cells interact with Tfh cells, mediate antigen presentation, and produce soluble mediators that support the development of T cell memory responses. However, the identity of B cells that are present in TLNs needs detail characterization. In the bone marrow, strong antibody responses are generated by long-lived plasma cells (LLPCs) and circulating plasma cells (PCs), which are derived from memory B cells (MBCs). The antibody response generated by PCs may help to neutralize Mtb in both the mucosa (via IgA) and the peripheral circulation (via IgG). In case of reinfection, MBCs convert into plasmablasts and PCs, mounting a secondary antibody response within days. The art pieces used in this figure were modified from Servier Medical Art by Servier, licensed under a Creative Commons Attribution 3.0 Unported License (https://smart.servier.com/).

induction of a B cell maturation loop involving the formation of PCs (108, 116). Preliminary evidence suggests that this response is crucial for controlling Mtb infection (108, 116). The role of MZ B cells during TB has not been adequately characterized and inconsistencies have arisen between mouse and human studies (121). These cells are normally activated by T cell independent antigens and have innate-like B cell memory characteristics. MZ B cells contribute to the AMIR through the production of IgM and IgG3 antibodies (117). Interestingly, a pilot study indicated that MZ B cells are present in the peripheral circulation during active TB at significantly lower levels compared to healthy controls (116).

Beyond antibody production, B cells play a crucial role in regulating innate and adaptive immune responses to infectious agents even in disease states dominated by T lymphocytes, as is the case of TB. B cells impact cellular adaptive immunity and are necessary for the adequate activation and maturation of memory T cells (123–125). This regulation is achieved through direct interactions between B and T cells that occur during both primary and secondary antigen responses. Such interactions are varied and include antigen presentation, co-stimulatory signaling, cytokine priming and antibody-mediated effector functions, as shown in **Figure 3**. In fact, B cell-deficient mice and human patients receiving B cell depletion therapy generally present alterations in their CD4+ T cell and CD8+ T cell repertoires (126). However, B cells exert contrasting effects on T cell responses. For instance, B1 and B2 cell subsets are capable of producing IFN-γ, TNF-α, IL-12 or IL-2, IL-13, and IL-4, thus inducing Th1 or Th2 immune responses, respectively. Furthermore, B-cells also display different regulatory phenotypes capable of generating Th10 responses via IL-10, TGF-β, IL-35, FasL, or PD-L1. Besides T cell activation, B cells also regulate T cell proliferation and contraction during acute immune responses and participate in the maintenance and reactivation of T cell memory responses via antibody-independent mechanisms (127). Most of these B cell functions have not been adequately characterized during TB, although it is currently known that B cells can get infected by Mtb via micropinocytosis (128), and B cells can produce cytokines in response to infection with Mtb *in vivo* (129).

In addition, B cells are also crucial for the induction and maturation of antigen-presenting environments (APEs) and APCs (127). In TB, B cells participate in the formation of granulomas and play a pivotal role in the development of TLNs (**Figure 3**), two APEs that are critical for Mtb control (123, 124). As such, B cell-deficient mice infected with Mtb display disrupted lung granuloma and TLN formation (34). Moreover, the production of cytokines and antibodies by B cells contributes to set up activation thresholds for macrophages, DCs and other non-professional APCs within and outside APEs during TB (123), which subsequently will determine the quality and dynamics of effector and memory T cell responses. In this regard, during active pulmonary TB, humans, mice, and non-human primates develop TLNs in the surroundings of granulomas. These TLNs assume the structure and function of GCs containing B cells with different maturation profiles, Tfh-like CXCR5+ cells, and follicular DCs (34, 130). Additionally, pulmonary TLNs facilitate the interaction between these and other immune cells and become the anatomical foci that possess the highest levels of cellular proliferation during active TB. The presence and organization of these TLNs is associated with immune protection and LTBI, and their absence or

disorganization may lead to uncontrolled progression of active TB (34).

Importantly, the possibility that Mtb might manipulate B cell and B cell memory responses exists, as B cells are susceptible to multiple effects of the bacteria including their direct infection via micropinocytosis (128). For instance, tissue-like memory B-cells (TLMs) are increased in the blood of patients with active TB and reduced in healthy controls (**Figure 2**). TLMs constitute a population of MBCs, also known as exhausted B-cells, that express low levels of CD21 and CD27 and increased levels of inhibitory receptors, having a diminished capacity to respond to antigenic stimuli. The presence of these cells in the circulation is associated with adverse clinical outcomes in chronic viral infections and is likely associated with active TB as well (128). Additionally, a population of B CD27-/IgD-memory cells has been shown to be increased in the pleural fluid of patients with tuberculous pleurisy as compared to healthy subjects. In these patients, pleural B cells interfered with the protective production of IFN-γ by NK cells and T lymphocytes (121). Collectively, these data indicate that targeting B cell functions for vaccination purposes in TB must be conducted carefully to avoid possible detrimental effects to the host.

CONCLUSIONS AND FUTURE DIRECTIONS

Humoral responses characterized by the production of high-affinity neutralizing antibodies have been the main target for the development of vaccines that confer protective immunity against several bacterial pathogens (108). Currently, the exception to the rule seems to be TB, as most of the TB vaccine candidates that are being evaluated in clinical trials are designed to exploit cell-mediated immunity rather than humoral immunity (131). Despite this, the evidence reviewed here suggests that both arms of the adaptive immune response should be evaluated in vaccine-development programs. Induction strategies should attempt to provide the host with a pool of antigen-specific MBCs capable of producing high-affinity neutralizing and polyfunctional antibodies which can potentiate macrophage and NK cell effector functions. Antibody-mediated activation of innate immunity may contribute to prevent the establishment of an immune microenvironment manipulated by Mtb. Vaccines targeting B cell responses can also promote the cooperation between B and T cells necessary for efficient T cell memory responses. For example, in a preclinical mouse model, the adoptive transfer of B cells that had internalized the naked plasmid pcDNA3 encoding the *Mycobacterium leprae* 65-kDa heat shock protein into B cell deficient mice resulted in the establishment of strong CD8+ T cell memory responses that conferred protection against Mtb challenge (132). Furthermore, novel ways to promote the formation of protective TLNs within the lungs deserves further investigation. Finally, the fact that a robust MBC response can be induced in the adjacent mesothelium upon primary mucosal Mtb exposure advocates in favor of using novel routes of vaccine administration (119, 121).

On the other hand, the memory-like properties of innate immune cells must also prompt us to discover novel ways to potentiate protective long-lasting anti-TB innate immune mechanisms. These strategies must aim to provide the host with a pool of primed long-lived innate cells with enhanced capacity to directly respond to the invading pathogen and with an increased adjuvant activity to support the correct development of effective T-cell memory responses. For instance, targeting trained immunity in myeloid cells may provide the host with metabolically and epigenetically reprogramed phagocytes ready to act before the contact with Mtb. Furthermore, memory-like AMs could initiate the early formation of protective granulomas around the sites of Mtb exposure, while the enhancement of ILCs activity could promote the establishment of an early immunological microenvironment advantageous for the host. Finally, Mtb-induced memory-like NK cells may serve as innate effector cells with increased cytokine production and cytotoxic activity. Targeting innate immunity in TB vaccination strategies may benefit a significant proportion of patients co-infected with Mtb and HIV by conferring them with T-cell independent protective immunity. HIV/AIDS remains the leading comorbidity in TB, and according to the 2019 WHO TB report, a third of HIV-related deaths were due to TB (1).

In conclusion, we must think outside the box and look for novel protective immune responses against Mtb beyond T cell memory responses. Future investigations in the TB field warrant the study of mechanisms implicated in trained immunity and B cell memory, as well as the discovery of routes and adjuvants for TB vaccine administration that may potentiate these and other overlooked protective immune responses against Mtb infection (131, 133).

AUTHOR CONTRIBUTIONS

JC-P and LW designed the study and drafted the manuscript. EY, JZ, and RH-P contributed in the writing process of the manuscript and revised it for intellectual content. All the authors revised and approved the final version of the manuscript.

FUNDING

This work was supported by the NIAID of the National Institutes of Health (NIH) and by the Research Founds of the National Institute of Respiratory Diseases in Mexico. JC-P was supported by the National Council of Science and Technology of Mexico (CONACyT, CVU 737347) to achieve his Ph.D. degree. LW is a doctoral student from the Programa de doctorado en Ciencias Biomédicas of the Universidad Nacional Autónoma de México (UNAM).

ACKNOWLEDGMENTS

To all the members of the JZ's lab and RH-P's lab, for their critical comments about the manuscript.

REFERENCES

1. World Health Organization. WHO global tuberculosis report 2019. World Health Organization (2019). Available online at: https://apps.who.int/iris/bitstream/handle/10665/329368/9789241565714-eng.pdf?ua=1 (accessed on December 31, 2019).
2. Orme IM, Roberts AD, Griffin JP, Abrams JS. Cytokine secretion by CD4 T lymphocytes acquired in response to *Mycobacterium tuberculosis* infection. *J Immunol*. (1993) 151:518–25.
3. Shimokata K, Kishimoto H, Takagi E, Tsunekawa H. Determination of the T-cell subset producing gamma-interferon in tuberculous pleural effusion. *Microbiol Immunol*. (1986) 30:353–61. doi: 10.1111/j.1348-0421.1986.tb00952.x
4. Nunes-Alves C, Booty MG, Carpenter SM, Jayaraman P, Rothchild AC, Behar SM. In search of a new paradigm for protective immunity to TB. *Nat Rev Microbiol*. (2014) 12:289–99. doi: 10.1038/nrmicro3230
5. Comas I, Chakravartti J, Small PM, Galagan J, Niemann S, Kremer K, et al. Human T cell epitopes of *Mycobacterium tuberculosis* are evolutionarily hyperconserved. *Nat Genet*. (2010) 42:498–503. doi: 10.1038/ng.590
6. Tameris MD, Hatherill M, Landry BS, Scriba TJ, Snowden MA, Lockhart S, et al. Safety and efficacy of MVA85A, a new tuberculosis vaccine, in infants previously vaccinated with BCG: a randomised, placebo-controlled phase 2b trial. *Lancet*. (2013) 381:1021–8. doi: 10.1016/S0140-6736(13)60177-4
7. Kagina BM, Abel B, Scriba TJ, Hughes EJ, Keyser A, Soares A, et al. Specific T cell frequency and cytokine expression profile do not correlate with protection against tuberculosis after bacillus Calmette-Guerin vaccination of newborns. *Am J Respir Crit Care Med*. (2010) 182:1073–9. doi: 10.1164/rccm.201003-0334OC
8. Steigler P, Verrall AJ, Kirman JR. Beyond memory T cells: mechanisms of protective immunity to tuberculosis infection. *Immunol Cell Biol*. (2019) 97:647–55. doi: 10.1111/imcb.12278
9. Hansen SG, Zak DE, Xu G, Ford JC, Marshall EE, Malouli D, et al. Prevention of tuberculosis in rhesus macaques by a cytomegalovirus-based vaccine. *Nat Med*. (2018) 24:130–43. doi: 10.1038/nm.4473
10. Lu LL, Chung AW, Rosebrock TR, Ghebremichael M, Yu WH, Grace PS, et al. A functional role for antibodies in tuberculosis. *Cell*. (2016) 167:433–43.e14. doi: 10.1016/j.cell.2016.08.072
11. Kaufmann E, Sanz J, Dunn JL, Khan N, Mendonca LE, Pacis A, et al. BCG educates hematopoietic stem cells to generate protective innate immunity against tuberculosis. *Cell*. (2018) 172:176–90.e19. doi: 10.1016/j.cell.2017.12.031
12. Ardain A, Domingo-Gonzalez R, Das S, Kazer SW, Howard NC, Singh A, et al. Group 3 innate lymphoid cells mediate early protective immunity against tuberculosis. *Nature*. (2019) 570:528–32. doi: 10.1038/s41586-019-1276-2
13. Choreño Parra JA, Martinez Zuniga N, Jimenez Zamudio LA, Jimenez Alvarez LA, Salinas Lara C, Zuniga J. Memory of natural killer cells: a new chance against *Mycobacterium tuberculosis*? *Front Immunol*. (2017) 8:967. doi: 10.3389/fimmu.2017.00967
14. Rao M, Valentini D, Poiret T, Dodoo E, Parida S, Zumla A, et al. B in TB: B cells as mediators of clinically relevant immune responses in tuberculosis. *Clin Infect Dis*. (2015) 61(Suppl 3):S225–34. doi: 10.1093/cid/civ614
15. Venkatasubramanian S, Cheekatla S, Paidipally P, Tripathi D, Welch E, Tvinnereim AR, et al. IL-21-dependent expansion of memory-like NK cells enhances protective immune responses against *Mycobacterium tuberculosis*. *Mucosal Immunol*. (2017) 10:1031–42. doi: 10.1038/mi.2016.105
16. Verrall AJ, Alisjahbana B, Apriani L, Novianty N, Nurani AC, van Laarhoven A, et al. Early clearance of *Mycobacterium tuberculosis*: the INFECT case contact cohort study in Indonesia. *J Infect Dis*. (2019). doi: 10.1093/infdis/jiz168. [Epub ahead of print].
17. Ewer K, Millington KA, Deeks JJ, Alvarez L, Bryant G, Lalvani A. Dynamic antigen-specific T-cell responses after point-source exposure to *Mycobacterium tuberculosis*. *Am J Respir Crit Care Med*. (2006) 174:831–9. doi: 10.1164/rccm.200511-1783OC
18. Netea MG, Joosten LA, Latz E, Mills KH, Natoli G, Stunnenberg HG, et al. Trained immunity: a program of innate immune memory in health and disease. *Science*. (2016) 352:aaf1098. doi: 10.1126/science.aaf1098
19. Chedid L, Parant M, Parant F, Lefrancher P, Choay J, Lederer E. Enhancement of nonspecific immunity to *Klebsiella pneumoniae* infection by a synthetic immunoadjuvant (N-acetylmuramyl-L-alanyl-D-isoglutamine) and several analogs. *Proc Natl Acad Sci USA*. (1977) 74:2089–93. doi: 10.1073/pnas.74.5.2089
20. Gorhe DS. Inhibition of multiplication of foot and mouth disease virus in adult mice pretreated with Freund's complete adjuvant. *Nature*. (1967) 216:1242–4. doi: 10.1038/2161242a0
21. van 't Wout JW, Poell R, van Furth R. The role of BCG/PPD-activated macrophages in resistance against systemic candidiasis in mice. *Scand J Immunol*. (1992) 36:713–9. doi: 10.1111/j.1365-3083.1992.tb03132.x
22. Tribouley J, Tribouley-Duret J, Appriou M. Effect of Bacillus Callmette Guerin (BCG) on the receptivity of nude mice to *Schistosoma mansoni*. *C R Seances Soc Biol Fil*. (1978) 172:902–4.
23. Hollm-Delgado MG, Stuart EA, Black RE. Acute lower respiratory infection among Bacille Calmette-Guerin (BCG)-vaccinated children. *Pediatrics*. (2014) 133:e73–81. doi: 10.1542/peds.2013-2218
24. de Castro MJ, Pardo-Seco J, Martinon-Torres F. Nonspecific (Heterologous) protection of neonatal bcg vaccination against hospitalization due to respiratory infection and sepsis. *Clin Infect Dis*. (2015) 60:1611–9. doi: 10.1093/cid/civ144
25. Arts RJW, Moorlag S, Novakovic B, Li Y, Wang SY, Oosting M, et al. BCG vaccination protects against experimental viral infection in humans through the induction of cytokines associated with trained immunity. *Cell Host Microbe*. (2018) 23:89–100.e5. doi: 10.1016/j.chom.2017.12.010
26. Elliott AM, Nakiyingi J, Quigley MA, French N, Gilks CF, Whitworth JA. Inverse association between BCG immunisation and intestinal nematode infestation among HIV-1-positive individuals in Uganda. *Lancet*. (1999) 354:1000–1. doi: 10.1016/S0140-6736(99)03290-0
27. Davies LC, Jenkins SJ, Allen JE, Taylor PR. Tissue-resident macrophages. *Nat. Immunol.* (2013) 14:986–95. doi: 10.1038/ni.2705
28. Yona S, Kim KW, Wolf Y, Mildner A, Varol D, Breker M, et al. Fate mapping reveals origins and dynamics of monocytes and tissue macrophages under homeostasis. *Immunity*. (2013) 38:79–91. doi: 10.1016/j.immuni.2012.12.001
29. Dunlap MD, Howard N, Das S, Scott N, Ahmed M, Prince O, et al. A novel role for C-C motif chemokine receptor 2 during infection with hypervirulent *Mycobacterium tuberculosis*. *Mucosal Immunol*. (2018) 11:1727–42. doi: 10.1038/s41385-018-0071-y
30. Cai Y, Sugimoto C, Arainga M, Alvarez X, Didier ES, Kuroda MJ. *In vivo* characterization of alveolar and interstitial lung macrophages in rhesus macaques: implications for understanding lung disease in humans. *J Immunol*. (2014) 192:2821–9. doi: 10.4049/jimmunol.1302269
31. Tsai MC, Chakravarty S, Zhu G, Xu J, Tanaka K, Koch C, et al. Characterization of the tuberculous granuloma in murine and human lungs: cellular composition and relative tissue oxygen tension. *Cell Microbiol*. (2006) 8:218–32. doi: 10.1111/j.1462-5822.2005.00612.x
32. Zuñiga J, Torres-García D, Santos-Mendoza T, Rodriguez-Reyna TS, Granados J, Yunis EJ. Cellular and humoral mechanisms involved in the control of tuberculosis. *Clin Dev Immunol*. (2012) 2012:193923. doi: 10.1155/2012/193923
33. Ernst JD. Mechanisms of *M. tuberculosis* immune evasion as challenges to TB vaccine design. *Cell Host Microbe*. (2018) 24:34–42. doi: 10.1016/j.chom.2018.06.004
34. Slight SR, Rangel-Moreno J, Gopal R, Lin Y, Fallert Junecko BA, Mehra S, et al. CXCR5(+) T helper cells mediate protective immunity against tuberculosis. *J Clin Invest*. (2013) 123:712–26. doi: 10.1172/JCI65728
35. Sakai S, Kauffman KD, Schenkel JM, McBerry CC, Mayer-Barber KD, Masopust D, et al. Cutting edge: control of *Mycobacterium tuberculosis* infection by a subset of lung parenchyma-homing CD4 T cells. *J Immunol*. (2014) 192:2965–9. doi: 10.4049/jimmunol.1400019
36. Kleinnijenhuis J, Quintin J, Preijers F, Joosten LA, Ifrim DC, Saeed S, et al. Bacille Calmette-Guerin induces NOD2-dependent nonspecific protection from reinfection via epigenetic reprogramming of monocytes. *Proc Natl Acad Sci USA*. (2012) 109:17537–42. doi: 10.1073/pnas.1202870109
37. Cywes C, Hoppe HC, Daffe M, Ehlers MR. Nonopsonic binding of *Mycobacterium tuberculosis* to complement receptor type 3 is mediated by capsular polysaccharides and is strain dependent. *Infect Immun*. (1997) 65:4258–66. doi: 10.1128/IAI.65.10.4258-4266.1997

38. Melo MD, Catchpole IR, Haggar G, Stokes RW. Utilization of CD11b knockout mice to characterize the role of complement receptor 3 (CR3, CD11b/CD18) in the growth of *Mycobacterium tuberculosis* in macrophages. *Cell Immunol*. (2000) 205:13–23. doi: 10.1006/cimm.2000.1710
39. Lv J, He X, Wang H, Wang Z, Kelly GT, Wang X, et al. TLR4-NOX2 axis regulates the phagocytosis and killing of *Mycobacterium tuberculosis* by macrophages. *BMC Pulm Med*. (2017) 17:194. doi: 10.1186/s12890-017-0517-0
40. Brooks MN, Rajaram MV, Azad AK, Amer AO, Valdivia-Arenas MA, Park JH, et al. NOD2 controls the nature of the inflammatory response and subsequent fate of *Mycobacterium tuberculosis* and *M. bovis* BCG in human macrophages. *Cell Microbiol*. (2011) 13:402–18. doi: 10.1111/j.1462-5822.2010.01544.x
41. Homer CR, Kabi A, Marina-Garcia N, Sreekumar A, Nesvizhskii AI, Nickerson KP, et al. A dual role for receptor-interacting protein kinase 2 (RIP2) kinase activity in nucleotide-binding oligomerization domain 2 (NOD2)-dependent autophagy. *J Biol Chem*. (2012) 287:25565–76. doi: 10.1074/jbc.M111.326835
42. Buffen K, Oosting M, Quintin J, Ng A, Kleinnijenhuis J, Kumar V, et al. Autophagy controls BCG-induced trained immunity and the response to intravesical BCG therapy for bladder cancer. *PLoS Pathog*. (2014) 10:e1004485. doi: 10.1371/journal.ppat.1004485
43. Patel AA, Zhang Y, Fullerton JN, Boelen L, Rongvaux A, Maini AA, et al. The fate and lifespan of human monocyte subsets in steady state and systemic inflammation. *J Exp Med*. (2017) 214:1913–23. doi: 10.1084/jem.20170355
44. Burgess SL, Buonomo E, Carey M, Cowardin C, Naylor C, Noor Z, et al. Bone marrow dendritic cells from mice with an altered microbiota provide interleukin 17A-dependent protection against Entamoeba histolytica colitis. *MBio*. (2014) 5:e01817. doi: 10.1128/mBio.01817-14
45. Saeed S, Quintin J, Kerstens HH, Rao NA, Aghajanirefah A, Matarese F, et al. Epigenetic programming of monocyte-to-macrophage differentiation and trained innate immunity. *Science*. (2014) 345:1251086. doi: 10.1126/science.1251086
46. Arts RJW, Carvalho A, La Rocca C, Palma C, Rodrigues F, Silvestre R, et al. Immunometabolic pathways in BCG-induced trained immunity. *Cell Rep*. (2016) 17:2562–2571. doi: 10.1016/j.celrep.2016.11.011
47. Wendeln AC, Degenhardt K, Kaurani L, Gertig M, Ulas T, Jain G, et al. Innate immune memory in the brain shapes neurological disease hallmarks. *Nature*. (2018) 556:332–8. doi: 10.1038/s41586-018-0023-4
48. Christ A, Bekkering S, Latz E, Riksen NP. Long-term activation of the innate immune system in atherosclerosis. *Semin Immunol*. (2016) 28:384–93. doi: 10.1016/j.smim.2016.04.004
49. Groh L, Keating ST, Joosten LAB, Netea MG, Riksen NP. Monocyte and macrophage immunometabolism in atherosclerosis. *Semin Immunopathol*. (2018) 40:203–14. doi: 10.1007/s00281-017-0656-7
50. Darrah PA, Zeppa JJ, Maiello P, Hackney JA, Wadsworth MH 2nd, Hughes TK, et al. Prevention of tuberculosis in macaques after intravenous BCG immunization. *Nature*. (2020) 577:95–102. doi: 10.1038/s41586-019-1817-8
51. Yao Y, Jeyanathan M, Haddadi S, Barra NG, Vaseghi-Shanjani M, Damjanovic D, et al. Induction of autonomous memory alveolar macrophages requires T cell help and is critical to trained immunity. *Cell*. (2018) 175:1634–50.e17. doi: 10.1016/j.cell.2018.09.042
52. Chen L, Wang J, Zganiacz A, Xing Z. Single intranasal mucosal Mycobacterium bovis BCG vaccination confers improved protection compared to subcutaneous vaccination against pulmonary tuberculosis. *Infect Immun*. (2004) 72:238–46. doi: 10.1128/IAI.72.1.238-246.2004
53. Perdomo C, Zedler U, Kuhl AA, Lozza L, Saikali P, Sander LE, et al. Mucosal BCG vaccination induces protective lung-resident memory T Cell populations against tuberculosis. *MBio*. (2016) 7:e01686–16. doi: 10.1128/mBio.01686-16
54. Dijkman K, Sombroek CC, Vervenne RAW, Hofman SO, Boot C, Remarque EJ, et al. Prevention of tuberculosis infection and disease by local BCG in repeatedly exposed rhesus macaques. *Nat Med*. (2019) 25:255–62. doi: 10.1038/s41591-018-0319-9
55. Huang L, Nazarova EV, Tan S, Liu Y, Russell DG. Growth of *Mycobacterium tuberculosis in vivo* segregates with host macrophage metabolism and ontogeny. *J Exp Med*. (2018) 215:1135–52. doi: 10.1084/jem.20172020
56. Lodoen MB, Lanier LL. Natural killer cells as an initial defense against pathogens. *Curr Opin Immunol*. (2006) 18:391–8. doi: 10.1016/j.coi.2006.05.002
57. Sivori S, Falco M, Della Chiesa M, Carlomagno S, Vitale M, Moretta L, et al. CpG and double-stranded RNA trigger human NK cells by Toll-like receptors: induction of cytokine release and cytotoxicity against tumors and dendritic cells. *Proc Natl Acad Sci USA*. (2004) 101:10116–21. doi: 10.1073/pnas.0403744101
58. Marcenaro E, Ferranti B, Falco M, Moretta L, Moretta A. Human NK cells directly recognize Mycobacterium bovis via TLR2 and acquire the ability to kill monocyte-derived DC. *Int Immunol*. (2008) 20:1155–67. doi: 10.1093/intimm/dxn073
59. Long EO, Kim HS, Liu D, Peterson ME, Rajagopalan S. Controlling natural killer cell responses: integration of signals for activation and inhibition. *Annu Rev Immunol*. (2013) 31:227–58. doi: 10.1146/annurev-immunol-020711-075005
60. Lanier LL. Up on the tightrope: natural killer cell activation and inhibition. Nat Immunol. (2008) 9:495–502. doi: 10.1038/ni1581
61. Orange JS, Wang B, Terhorst C, Biron CA. Requirement for natural killer cell-produced interferon gamma in defense against murine cytomegalovirus infection and enhancement of this defense pathway by interleukin 12 administration. *J Exp Med*. (1995) 182:1045–56. doi: 10.1084/jem.182.4.1045
62. Wang R, Jaw JJ, Stutzman NC, Zou Z, Sun PD. Natural killer cell-produced IFN-gamma and TNF-alpha induce target cell cytolysis through up-regulation of ICAM-1. *J Leukoc Biol*. (2012) 91:299–309. doi: 10.1189/jlb.0611308
63. Passos ST, Silver JS, O'Hara AC, Sehy D, Stumhofer JS, Hunter CA. IL-6 promotes NK cell production of IL-17 during toxoplasmosis. *J Immunol*. (2010) 184:1776–83. doi: 10.4049/jimmunol.0901843
64. Kumar P, Thakar MS, Ouyang W, Malarkannan S. IL-22 from conventional NK cells is epithelial regenerative and inflammation protective during influenza infection. *Mucosal Immunol*. (2013) 6:69–82. doi: 10.1038/mi.2012.49
65. Xu X, Weiss ID, Zhang HH, Singh SP, Wynn TA, Wilson MS, et al. Conventional NK cells can produce IL-22 and promote host defense in *Klebsiella pneumoniae* pneumonia. *J Immunol*. (2014) 192:1778–86. doi: 10.4049/jimmunol.1300039
66. Cuturi MC, Anegon I, Sherman F, Loudon R, Clark SC, Perussia B, et al. Production of hematopoietic colony-stimulating factors by human natural killer cells. *J Exp Med*. (1989) 169:569–83. doi: 10.1084/jem.169.2.569
67. Domingo-Gonzalez R, Prince O, Cooper A, Khader SA. Cytokines and chemokines in *Mycobacterium tuberculosis* infection. *Microbiol Spectr*. (2016) 4:TBTB2-0018-2016. doi: 10.1128/microbiolspec.TBTB2-0018-2016
68. Esin S, Batoni G, Counoupas C, Stringaro A, Brancatisano FL, Colone M, et al. Direct binding of human NK cell natural cytotoxicity receptor NKp44 to the surfaces of mycobacteria and other bacteria. *Infect Immun*. (2008) 76:1719–27. doi: 10.1128/IAI.00870-07
69. Esin S, Counoupas C, Aulicino A, Brancatisano FL, Maisetta G, Bottai D, et al. Interaction of *Mycobacterium tuberculosis* cell wall components with the human natural killer cell receptors NKp44 and Toll-like receptor 2. *Scand J Immunol*. (2013) 77:460–9. doi: 10.1111/sji.12052
70. Dhiman R, Indramohan M, Barnes PF, Nayak RC, Paidipally P, Rao LV, et al. IL-22 produced by human NK cells inhibits growth of *Mycobacterium tuberculosis* by enhancing phagolysosomal fusion. *J Immunol*. (2009) 183:6639–45. doi: 10.4049/jimmunol.0902587
71. Guerra C, Johal K, Morris D, Moreno S, Alvarado O, Gray D, et al. Control of *Mycobacterium tuberculosis* growth by activated natural killer cells. *Clin Exp Immunol*. (2012) 168:142–52. doi: 10.1111/j.1365-2249.2011.04552.x
72. Dhiman R, Venkatasubramanian S, Paidipally P, Barnes PF, Tvinnereim A, Vankayalapati R. Interleukin 22 inhibits intracellular growth of *Mycobacterium tuberculosis* by enhancing calgranulin A expression. *J Infect Dis*. (2014) 209:578–87. doi: 10.1093/infdis/jit495
73. Vankayalapati R, Garg A, Porgador A, Griffith DE, Klucar P, Safi H, et al. Role of NK cell-activating receptors and their ligands in the lysis of mononuclear phagocytes infected with an intracellular bacterium. *J Immunol*. (2005) 175:4611–7. doi: 10.4049/jimmunol.175.7.4611

74. Lu CC, Wu TS, Hsu YJ, Chang CJ, Lin CS, Chia JH, et al. NK cells kill mycobacteria directly by releasing perforin and granulysin. *J Leukoc Biol*. (2014) 96:1119–29. doi: 10.1189/jlb.4A0713-363RR
75. Feng CG, Kaviratne M, Rothfuchs AG, Cheever A, Hieny S, Young HA, et al. NK cell-derived IFN-gamma differentially regulates innate resistance and neutrophil response in T cell-deficient hosts infected with *Mycobacterium tuberculosis*. *J Immunol*. (2006) 177:7086–93. doi: 10.4049/jimmunol.177.10.7086
76. Paidipally P, Tripathi D, Van A, Radhakrishnan RK, Dhiman R, Venkatasubramanian S, et al. Interleukin-21 regulates natural killer cell responses during *Mycobacterium tuberculosis* infection. *J Infect Dis*. (2018) 217:1323–33. doi: 10.1093/infdis/jiy034
77. Junqueira-Kipnis AP, Kipnis A, Jamieson A, Juarrero MG, Diefenbach A, Raulet DH, et al. NK cells respond to pulmonary infection with *Mycobacterium tuberculosis*, but play a minimal role in protection. *J Immunol*. (2003) 171:6039–45. doi: 10.4049/jimmunol.171.11.6039
78. Portevin D, Via LE, Eum S, Young D. Natural killer cells are recruited during pulmonary tuberculosis and their ex vivo responses to mycobacteria vary between healthy human donors in association with KIR haplotype. *Cell Microbiol*. (2012) 14:1734–44. doi: 10.1111/j.1462-5822.2012.01834.x
79. Mendez A, Granda H, Meenagh A, Contreras S, Zavaleta R, Mendoza MF, et al. Study of KIR genes in tuberculosis patients. *Tissue Antigens*. (2006) 68:386–9. doi: 10.1111/j.1399-0039.2006.00685.x
80. Mahfouz R, Halas H, Hoteit R, Saadeh M, Shamseddeen W, Charafeddine K, et al. Study of KIR genes in Lebanese patients with tuberculosis. *Int J Tuberc Lung Dis*. (2011) 15:1688–91. doi: 10.5588/ijtld.11.0138
81. Pydi SS, Sunder SR, Venkatasubramanian S, Kovvali S, Jonnalagada S, Valluri VL. Killer cell immunoglobulin like receptor gene association with tuberculosis. *Hum Immunol*. (2013) 74:85–92. doi: 10.1016/j.humimm.2012.10.006
82. Salie M, Daya M, Moller M, Hoal EG. Activating KIRs alter susceptibility to pulmonary tuberculosis in a South African population. *Tuberculosis*. (2015) 95:817–21. doi: 10.1016/j.tube.2015.09.003
83. Batoni G, Esin S, Favilli F, Pardini M, Bottai D, Maisetta G, et al. Human CD56bright and CD56dim natural killer cell subsets respond differentially to direct stimulation with *Mycobacterium bovis* bacillus Calmette-Guerin. *Scand J Immunol*. (2005) 62:498–506. doi: 10.1111/j.1365-3083.2005.01692.x
84. Bozzano F, Costa P, Passalacqua G, Dodi F, Ravera S, Pagano G, et al. Functionally relevant decreases in activatory receptor expression on NK cells are associated with pulmonary tuberculosis *in vivo* and persist after successful treatment. *Int Immunol*. (2009) 21:779–91. doi: 10.1093/intimm/dxp046
85. Barcelos W, Sathler-Avelar R, Martins-Filho OA, Carvalho BN, Guimaraes TM, Miranda SS, et al. Natural killer cell subpopulations in putative resistant individuals and patients with active *Mycobacterium tuberculosis* infection. *Scand J Immunol*. (2008) 68:92–102. doi: 10.1111/j.1365-3083.2008.02116.x
86. Fan R, Xiang Y, Yang L, Liu Y, Chen P, Wang L, et al. Impaired NK cells' activity and increased numbers of CD4 + CD25+ regulatory T cells in multidrug-resistant *Mycobacterium tuberculosis* patients. *Tuberculosis*. (2016) 98:13–20. doi: 10.1016/j.tube.2016.02.001
87. Garand M, Goodier M, Owolabi O, Donkor S, Kampmann B, Sutherland JS. Functional and phenotypic changes of natural killer cells in whole blood during *Mycobacterium tuberculosis* infection and disease. *Front Immunol*. (2018) 9:257. doi: 10.3389/fimmu.2018.00257
88. Roy Chowdhury R, Vallania F, Yang Q, Lopez Angel CJ, Darboe F, Penn-Nicholson A, et al. A multi-cohort study of the immune factors associated with *M. tuberculosis* infection outcomes. *Nature*. (2018) 560:644–8. doi: 10.1038/s41586-018-0439-x
89. Vankayalapati R, Klucar P, Wizel B, Weis SE, Samten B, Safi H, et al. NK cells regulate CD8+ T cell effector function in response to an intracellular pathogen. *J Immunol*. (2004) 172:130–7. doi: 10.4049/jimmunol.172.1.130
90. Ferlazzo G, Tsang ML, Moretta L, Melioli G, Steinman RM, Munz C. Human dendritic cells activate resting natural killer (NK) cells and are recognized via the NKp30 receptor by activated NK cells. *J Exp Med*. (2002) 195:343–51. doi: 10.1084/jem.20011149
91. Roy S, Barnes PF, Garg A, Wu S, Cosman D, Vankayalapati R. NK cells lyse T regulatory cells that expand in response to an intracellular pathogen. *J Immunol*. (2008) 180:1729–36. doi: 10.4049/jimmunol.180.3.1729
92. Dhiman R, Periasamy S, Barnes PF, Jaiswal AG, Paidipally P, Barnes AB, et al. NK1.1+ cells and IL-22 regulate vaccine-induced protective immunity against challenge with *Mycobacterium tuberculosis*. *J Immunol*. (2012) 189:897–905. doi: 10.4049/jimmunol.1102833
93. O'Leary JG, Goodarzi M, Drayton DL, von Andrian UH. T cell- and B cell-independent adaptive immunity mediated by natural killer cells. *Nat Immunol*. (2006) 7:507–16. doi: 10.1038/ni1332
94. Sun JC, Beilke JN, Lanier LL. Adaptive immune features of natural killer cells. *Nature*. (2009) 457:557–61. doi: 10.1038/nature07665
95. Habib S, El Andaloussi A, Hisham A, Ismail N. NK cell-mediated regulation of protective memory responses against intracellular ehrlichial pathogens. *PLoS ONE*. (2016) 11:e0153223. doi: 10.1371/journal.pone.0153223
96. Foley B, Cooley S, Verneris MR, Curtsinger J, Luo X, Waller EK, et al. Human cytomegalovirus (CMV)-induced memory-like NKG2C(+) NK cells are transplantable and expand *in vivo* in response to recipient CMV antigen. *J Immunol*. (2012) 189:5082–8. doi: 10.4049/jimmunol.1201964
97. Cooper MA, Elliott JM, Keyel PA, Yang L, Carrero JA, Yokoyama WM. Cytokine-induced memory-like natural killer cells. *Proc Natl Acad Sci USA*. (2009) 106:1915–9. doi: 10.1073/pnas.0813192106
98. Romee R, Schneider SE, Leong JW, Chase JM, Keppel CR, Sullivan RP, et al. Cytokine activation induces human memory-like NK cells. *Blood*. (2012) 120:4751–60. doi: 10.1182/blood-2012-04-419283
99. Kleinnijenhuis J, Quintin J, Preijers F, Joosten LA, Jacobs C, Xavier RJ, et al. BCG-induced trained immunity in NK cells: role for non-specific protection to infection. *Clin Immunol*. (2014) 155:213–9. doi: 10.1016/j.clim.2014.10.005
100. Suliman S, Geldenhuys H, Johnson JL, Hughes JE, Smit E, Murphy M, et al. Bacillus Calmette-Guerin (BCG) revaccination of adults with latent *Mycobacterium tuberculosis* infection induces long-lived BCG-reactive NK cell responses. *J Immunol*. (2016) 197:1100–10. doi: 10.4049/jimmunol.1501996
101. Fu X, Yu S, Yang B, Lao S, Li B, Wu C. Memory-like antigen-specific human NK cells from TB pleural fluids produced IL-22 in response to IL-15 or *Mycobacterium tuberculosis* antigens. *PLoS ONE*. (2016) 11:e0151721. doi: 10.1371/journal.pone.0151721
102. Fu X, Liu Y, Li L, Li Q, Qiao D, Wang H, et al. Human natural killer cells expressing the memory-associated marker CD45RO from tuberculous pleurisy respond more strongly and rapidly than CD45RO- natural killer cells following stimulation with interleukin-12. *Immunology*. (2011) 134:41–9. doi: 10.1111/j.1365-2567.2011.03464.x
103. Diefenbach A, Colonna M, Koyasu S. Development, differentiation, and diversity of innate lymphoid cells. *Immunity*. (2014) 41:354–65. doi: 10.1016/j.immuni.2014.09.005
104. Burkhardt AM, Maravillas-Montero JL, Carnevale CD, Vilches-Cisneros N, Flores JP, Hevezi PA, et al. CXCL17 is a major chemotactic factor for lung macrophages. *J Immunol*. (2014) 193:1468–74. doi: 10.4049/jimmunol.1400551
105. Tripathi D, Radhakrishnan RK, Sivangala Thandi R, Paidipally P, Devalraju KP, Neela VSK, et al. IL-22 produced by type 3 innate lymphoid cells (ILC3s) reduces the mortality of type 2 diabetes mellitus (T2DM) mice infected with *Mycobacterium tuberculosis*. *PLoS Pathog*. (2019) 15:e1008140. doi: 10.1371/journal.ppat.1008140
106. Wang X, Peng H, Tian Z. Innate lymphoid cell memory. *Cell Mol Immunol*. (2019) 16:423–9. doi: 10.1038/s41423-019-0212-6
107. Steigler P, Daniels NJ, McCulloch TR, Ryder BM, Sandford SK, Kirman JR. BCG vaccination drives accumulation and effector function of innate lymphoid cells in murine lungs. *Immunol Cell Biol*. (2018) 96:379–89. doi: 10.1111/imcb.12007
108. Neuberger MS, Ehrenstein MR, Rada C, Sale J, Batista FD, Williams G, et al. Memory in the B-cell compartment: antibody affinity maturation. *Philos Trans R Soc Lond B Biol Sci*. (2000) 355:357–60. doi: 10.1098/rstb.2000.0573
109. De Silva NS, Klein U. Dynamics of B cells in germinal centres. *Nat Rev Immunol*. (2015) 15:137–48. doi: 10.1038/nri3804
110. Glatman-Freedman A, Casadevall A. Serum therapy for tuberculosis revisited: reappraisal of the role of antibody-mediated immunity against *Mycobacterium tuberculosis*. *Clin Microbiol Rev*. (1998) 11:514–32. doi: 10.1128/CMR.11.3.514

111. Encinales L, Zuniga J, Granados-Montiel J, Yunis M, Granados J, Almeciga I, et al. Humoral immunity in tuberculin skin test anergy and its role in high-risk persons exposed to active tuberculosis. *Mol Immunol*. (2010) 47:1066–73. doi: 10.1016/j.molimm.2009.11.005
112. Lu LL, Smith MT, Yu KKQ, Luedemann C, Suscovich TJ, Grace PS, et al. IFN-γ-independent immune markers of *Mycobacterium tuberculosis* exposure. *Nat Med*. (2019) 25:977–987. doi: 10.1038/s41591-019-0441-3
113. Li H, Javid B. Antibodies and tuberculosis: finally coming of age? *Nat Rev Immunol*. (2018) 18:591–596. doi: 10.1038/s41577-018-0028-0
114. Simmons JD, Stein CM, Seshadri C, Campo M, Alter G, Fortune S, et al. Immunological mechanisms of human resistance to persistent *Mycobacterium tuberculosis* infection. *Nat Rev Immunol*. (2018) 18:575–589. doi: 10.1038/s41577-018-0025-3
115. du Plessis WJ, Kleynhans L, du Plessis N, Stanley K, Malherbe ST, Maasdorp E, et al. The functional response of B cells to antigenic stimulation: a preliminary report of latent tuberculosis. *PLoS ONE*. (2016) 11:e0152710. doi: 10.1371/journal.pone.0152710
116. du Plessis WJ, Keyser A, Walzl G, Loxton AG. Phenotypic analysis of peripheral B cell populations during *Mycobacterium tuberculosis* infection and disease. *J Inflamm*. (2016) 13:23. doi: 10.1186/s12950-016-0133-4
117. du Plessis WJ, Walzl G, Loxton AG. B cells as multi-functional players during *Mycobacterium tuberculosis* infection and disease. *Tuberculosis*. (2016) 97:118–25. doi: 10.1016/j.tube.2015.10.007
118. Sebina I, Biraro IA, Dockrell HM, Elliott AM, Cose S. Circulating B-lymphocytes as potential biomarkers of tuberculosis infection activity. *PLoS ONE*. (2014) 9:e106796. doi: 10.1371/journal.pone.0106796
119. Zimmermann N, Thormann V, Hu B, Köhler AB, Imai-Matsushima A, Locht C, et al. Human isotype-dependent inhibitory antibody responses against *Mycobacterium tuberculosis*. *EMBO Mol Med*. (2016) 8:1325–39. doi: 10.15252/emmm.201606330
120. Abreu MT, Carvalheiro H, Rodrigues-Sousa T, Domingos A, Segorbe-Luis A, Rodrigues-Santos P, et al. Alterations in the peripheral blood B cell subpopulations of multidrug-resistant tuberculosis patients. *Clin Exp Med*. (2014) 14:423–9. doi: 10.1007/s10238-013-0258-1
121. Schierloh P, Landoni V, Balboa L, Musella RM, Castagnino J, Morana E, et al. Human pleural B-cells regulate IFN-gamma production by local T-cells and NK cells in a *Mycobacterium tuberculosis*-induced delayed hypersensitivity reaction. *Clin Sci*. (2014) 127:391–403. doi: 10.1042/CS20130769
122. Sebina I, Cliff JM, Smith SG, Nogaro S, Webb EL, Riley EM, et al. Long-lived memory B-cell responses following BCG vaccination. *PLoS ONE*. (2012) 7:e51381. doi: 10.1371/journal.pone.0051381
123. Maglione PJ, Xu J, Chan J. B cells moderate inflammatory progression and enhance bacterial containment upon pulmonary challenge with *Mycobacterium tuberculosis*. *J Immunol*. (2007) 178:7222–34. doi: 10.4049/jimmunol.178.11.7222
124. Chan J, Mehta S, Bharrhan S, Chen Y, Achkar JM, Casadevall A, et al. The role of B cells and humoral immunity in *Mycobacterium tuberculosis* infection. *Semin Immunol*. (2014) 26:588–600. doi: 10.1016/j.smim.2014.10.005
125. Loxton AG. B cells and their regulatory functions during tuberculosis: latency and active disease. *Mol Immunol*. (2019) 111:145–51. doi: 10.1016/j.molimm.2019.04.012
126. HayGlass KT, Naides SJ, Benacerraf B, Sy MS. T cell development in B cell deficient mice. III. Restriction specificity of suppressor T cell factor(s) produced in mice treated chronically with rabbit anti-mouse mu chain antibody. *J Mol Cell Immunol*. (1985) 2:107–17.
127. van Rensburg IC, Wagman C, Stanley K, Beltran C, Ronacher K, Walzl G, et al. Successful TB treatment induces B-cells expressing FASL and IL5RA mRNA. *Oncotarget*. (2017) 8:2037–43. doi: 10.18632/oncotarget.12184
128. Joosten SA, van Meijgaarden KE, Del Nonno F, Baiocchini A, Petrone L, Vanini V, et al. Patients with tuberculosis have a dysfunctional circulating B-cell compartment, which normalizes following successful treatment. *PLoS Pathog*. (2016) 12:e1005687. doi: 10.1371/journal.ppat.1005687
129. Phuah J, Wong EA, Gideon HP, Maiello P, Coleman MT, Hendricks MR, et al. Effects of B cell depletion on Early *Mycobacterium tuberculosis* infection in cynomolgus macaques. *Infect Immun*. (2016) 84:1301–11. doi: 10.1128/IAI.00083-16
130. Ulrichs T, Kosmiadi GA, Trusov V, Jorg S, Pradl L, Titukhina M, et al. Human tuberculous granulomas induce peripheral lymphoid follicle-like structures to orchestrate local host defence in the lung. *J Pathol*. (2004) 204:217–28. doi: 10.1002/path.1628
131. Sable SB, Posey JE, Scriba TJ. Tuberculosis vaccine development: progress in clinical evaluation. *Clin Microbiol Rev*. (2019) 33:e00100–19. doi: 10.1128/CMR.00100-19
132. Almeida LP, Trombone AP, Lorenzi JC, Rocha CD, Malardo T, Fontoura IC, et al. B cells can modulate the CD8 memory T cell after DNA vaccination against experimental tuberculosis. *Genet Vaccines Ther*. (2011) 9:5. doi: 10.1186/1479-0556-9-5
133. Khader SA, Divangahi M, Hanekom W, Hill PC, Maeurer M, Makar KW, et al. Targeting innate immunity for tuberculosis vaccination. *J Clin Invest*. (2019) 129:3482–91. doi: 10.1172/JCI128877

Conflict of Interest: The authors declare that the research was conducted in the absence of any commercial or financial relationships that could be construed as a potential conflict of interest.

frontiers in Immunology

ORIGINAL RESEARCH
published: 25 February 2020
doi: 10.3389/fimmu.2020.00327

Adjuvant Screen Identifies Synthetic DNA-Encoding Flt3L and CD80 Immunotherapeutics as Candidates for Enhancing Anti-tumor T Cell Responses

*Amy Haseley Thorne[1†], Kirsten N. Malo[1†], Ashley J. Wong[1], Tricia T. Nguyen[1], Neil Cooch[2], Charles Reed[2], Jian Yan[2], Kate E. Broderick[1], Trevor R. F. Smith[1], Emma L. Masteller[1] and Laurent Humeau[1]**

[1] Inovio Pharmaceuticals Inc., San Diego, CA, United States, [2] Inovio Pharmaceuticals Inc., Plymouth, PA, United States

OPEN ACCESS

Edited by:
Matthias Tenbusch,
University Hospital Erlangen, Germany

Reviewed by:
Gaelle Vandermeulen,
Catholic University of Louvain, Belgium
David Pejoski,
Université de Genève, Switzerland

***Correspondence:**
Laurent Humeau
lhumeau@inovio.com

[†]These authors have contributed equally to this work

Specialty section:
This article was submitted to Vaccines and Molecular Therapeutics, a section of the journal Frontiers in Immunology

Received: 08 November 2019
Accepted: 10 February 2020
Published: 25 February 2020

Citation:
Thorne AH, Malo KN, Wong AJ, Nguyen TT, Cooch N, Reed C, Yan J, Broderick KE, Smith TRF, Masteller EL and Humeau L (2020) Adjuvant Screen Identifies Synthetic DNA-Encoding Flt3L and CD80 Immunotherapeutics as Candidates for Enhancing Anti-tumor T Cell Responses. Front. Immunol. 11:327. doi: 10.3389/fimmu.2020.00327

Overcoming tolerance to tumor-associated antigens remains a hurdle for cancer vaccine-based immunotherapy. A strategy to enhance the anti-tumor immune response is the inclusion of adjuvants to cancer vaccine protocols. In this report, we generated and systematically screened over twenty gene-based molecular adjuvants composed of cytokines, chemokines, and T cell co-stimulators for the ability to increase anti-tumor antigen T cell immunity. We identified several robust adjuvants whose addition to vaccine formulations resulted in enhanced T cell responses targeting the cancer antigens STEAP1 and TERT. We further characterized direct T cell stimulation through CD80-Fc and indirect T cell targeting via the dendritic cell activator Flt3L-Fc. Mechanistically, intramuscular delivery of Flt3L-Fc into mice was associated with a significant increase in infiltration of dendritic cells at the site of administration and trafficking of activated dendritic cells to the draining lymph node. Gene expression analysis of the muscle tissue confirmed a significant up-regulation in genes associated with dendritic cell signaling. Addition of CD80-Fc to STEAP1 vaccine formulation mimicked the engagement provided by DCs and increased T cell responses to STEAP1 by 8-fold, significantly increasing the frequency of antigen-specific cells expressing IFNγ, TNFα, and CD107a for both $CD8^+$ and $CD4^+$ T cells. CD80-Fc enhanced T cell responses to multiple tumor-associated antigens including Survivin and HPV, indicating its potential as a universal adjuvant for cancer vaccines. Together, the results of our study highlight the adjuvanting effect of T cell engagement either directly, CD80-Fc, or indirectly, Flt3L-Fc, for cancer vaccines.

Keywords: Flt3L, CD80, vaccine, immune, cancer

INTRODUCTION

Much progress has been made in the field of immuno-oncology in recent years, revealing the promise of harnessing an individual's immune system to effectively target cancer cells. An effective immune response requires a coordination of several working parts: tumor-associated antigens must be processed and presented to antigen-specific T cells, the T cells must be activated and

expanded, and then traffic to and accumulate at the tumor site, maintaining activity long enough to effectively destroy a tumor in an immuno-suppressive microenvironment (1). Although immune checkpoint therapy has made some of the greatest strides in this field to date (2), therapy-associated toxicities can be prohibitive and not all tumors respond (3, 4). Importantly, studies with the dendritic cell vaccine Sipuleucel-T (Provenge®) have shown that using a vaccination strategy to target cancer is a viable therapeutic option. However, this therapy has shown only modest efficacy, is cost-prohibitive, and requires extensive *ex vivo* manipulation: immune cells are isolated from the patient's blood, activated in a laboratory, and then infused back into the patient (5, 6). Plasmid DNA vaccination provides a simple and accessible approach to immune therapy, generating an activated immune response to tumor-associated antigens *in vivo*. Vaccination with highly optimized DNA cancer vaccines and delivered by the CELLECTRA® electroporation (EP) device for cancer has been highly effective in the preclinical space (7–11) and results from a phase 2b clinical trial testing VGX-3100 for patients with cervical intraepithelial neoplasia showed this therapy to be safe, efficacious, and immunogenic (12). It has been well-documented that the specific targeting of immune cells by molecular adjuvants increases the immune response to viral associated antigens (13–16), thus the potential exists to further increase the magnitude of the vaccine-elicited responses against tumor-associated antigens (TAAs) enabling tumor control.

Dendritic cells (DCs) are professional antigen-presenting cells that play a central role in priming T lymphocytes. At the initiation of the immune response, DCs both present antigen and up-regulate co-stimulatory molecules. In response to intramuscular injection and electroporation (IM/EP) of plasmid DNA, DCs migrate to the site of inoculation and present antigen either via cross-presentation or direct transfection (17–19). However, DCs are usually found in small numbers in the muscle and they typically present as functionally immature (20). Thus, enhancing DC activity to prime T cells with optimal efficiency in this setting could improve anti-tumor immune responses. FMS-like tyrosine kinase 3 ligand (Flt3L) is a potent DC specific growth factor that has been shown to expand and mature DCs in both mice and humans (21). Studies have shown that administration of recombinant Flt3L increases the total number of lymphocytes, granulocytes, and monocytes, and massively mobilizes lymphoid/myeloid $CD34^+$ progenitor cells into peripheral blood (22, 23). Synergy between Flt3L and DC recruitment for the advantage of immune therapy has been well-documented (24–26). CD80 is an activation molecule on APCs including DCs that interacts with CD28 on T cells enabling T cell proliferation and activation (27). CD80-T cell interaction mechanisms have been shown to maintain a strong T cell activation through both co-stimulation and by blocking inhibition induced by PD-1 and PD-L1 (28). Thus, Flt3L and CD80 represent targets for adjuvant interventions to enhance T cell-mediated anti-tumor immune responses.

In this study, we explored the ability of plasmid-encoded adjuvants to mediate T cell responses to tumor antigens in mice. We screened over twenty synthetic DNA-encoded adjuvants targeting immune processes thought to be associated with anti-tumor responses. We show that formulating the DNA vaccine STEAP1 with Flt3L-Fc mobilized DCs to the site of injection and resulted in a significant increase in the antigen-specific immune response to the target tumor antigen. Several of the candidate adjuvants which enhanced the immune response to the target tumor antigen were involved in direct T cell activation. CD80-Fc provided the most robust antigen-specific immune response to STEAP1 and may be considered a potential universal adjuvant as it significantly boosted several additional cancer vaccines of interest. Together, our data suggests that cancer vaccines may be boosted by both indirectly engaging T cells via influx of DCs and also by directly engaging T cells through co-stimulation and warrants the further investigation of CD80-Fc and Flt3L-Fc as potential "off the shelf" adjuvants to enhance tumor targeting immune responses.

RESULTS

Adjuvant Screen Identifies T Cell Co-stimulators and the Dendritic Cell Activator Flt3L as Potential Candidates to Enhance Anti-cancer Vaccines

We designed and tested over twenty plasmid DNA-encoded genetic adjuvant candidates, chosen based on defined biological mechanisms of action (chemokines, cytokines, and ligands for T cell co-stimulation) associated with anti-tumor immune responses. Plasmids were individually formulated with a DNA vaccine targeting a synthetic consensus (SynCon®) antigen of either human Six-Transmembrane Epithelial Antigen of Prostate 1 (STEAP1) or murine Telomerase Reverse Transcriptase (TERT) and administered intramuscularly to mice using the CELLECTRA® 3P device (IM/EP). Antigen-specific immune responses from splenocytes were measured following peptide stimulation by IFNγ ELISpot (**Figure 1**). Of the 21 adjuvants tested, 10 significantly boosted the immune response to hSTEAP1 tumor antigen by at least 2-fold (**Figure 1B**), and six boosted the immune response to TERT tumor antigen by at least 2-fold (**Figure 1C**). Overall, the candidate adjuvants which play a role in direct T cell activation (CD80, OX-40L, and 4-1BB-L) showed the greatest enhancement in antigen-specific T cell responses to vaccination with either STEAP1 or TERT. The T cell co-stimulator CD80 was the strongest immuno-enhancer: increasing STEAP1-specific T cell responses by 11.6 fold and increasing TERT-specific T cell responses by 6.44 fold. Independent to direct T cell engagement, vaccine formulation with Flt3L was associated with enhanced T cell responses to both tumor antigens by >2-fold (STEAP1: 2.67 fold; TERT: 2.7 fold). Therefore, we focused the following studies on CD80 and Flt3L.

Synthetic DNA-Encoded Murine CD80-Fc and Flt3L-Fc Design and Expression *in vitro* and *in vivo*

Murine CD80-Fc and murine Flt3L-Fc were designed based on type I single pass transmembrane proteins with well-defined extracellular, transmembrane, and intracellular domains.

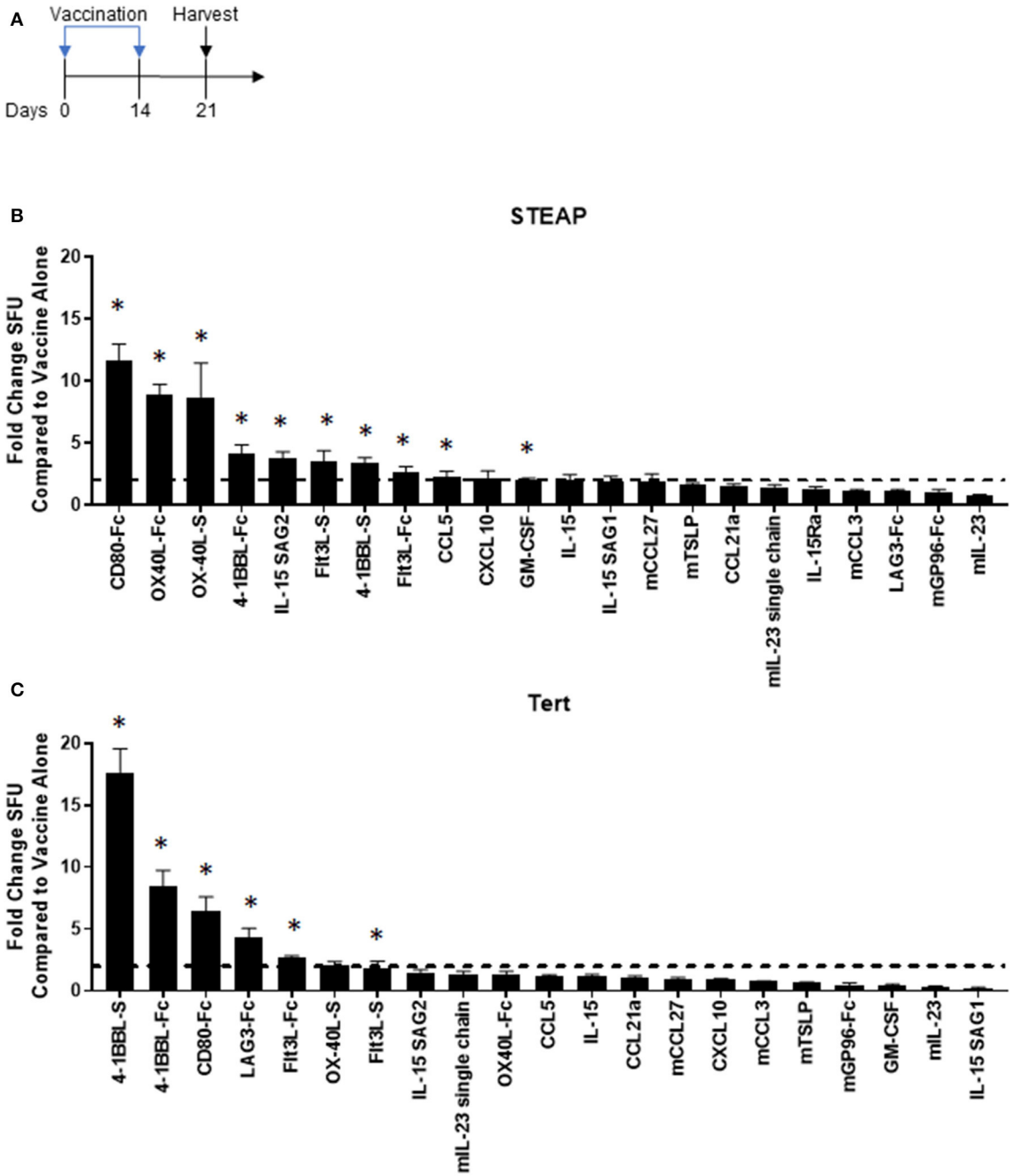

FIGURE 1 | Adjuvant screen identifies T cell co-stimulators and the dendritic cell activator Flt3L as candidates for cancer vaccines. **(A)** Diagram of the experiment. Mice were vaccinated on days 0 and 14 and spleens were harvested on day 21 for analysis. **(B,C)** Immunogenicity fold change of STEAP1 or TERT plus adjuvant compared to STEAP1 or TERT alone by IFNγ ELISpot responses. The fold change boost is defined as an increase in IFNγ ELISpot response in stimulated splenocytes from mice treated with adjuvant plus antigen as compared to mice treated with antigen alone. $N = 8–10$ mice. $^*p < 0.05$.

Both of these proteins possess native signal peptides which were incorporated into the design. For the Fc fusions, the extracellular regions were harvested and fused with a fully murine IgG2A Fc. We performed comparative modeling of these constructs using the MacroModel and Crosslink Proteins features as implemented in Bioluminate (Schrödinger, LLC, New York, NY, 2019), to better understand the potential implications of putatively unstructured regions between the more well-ordered domains, and also to enable identification of sites for optimization if necessary (**Figures 2A,B**). To ensure expression of these novel constructs, we first transfected 293T cells with either the construct of interest or the

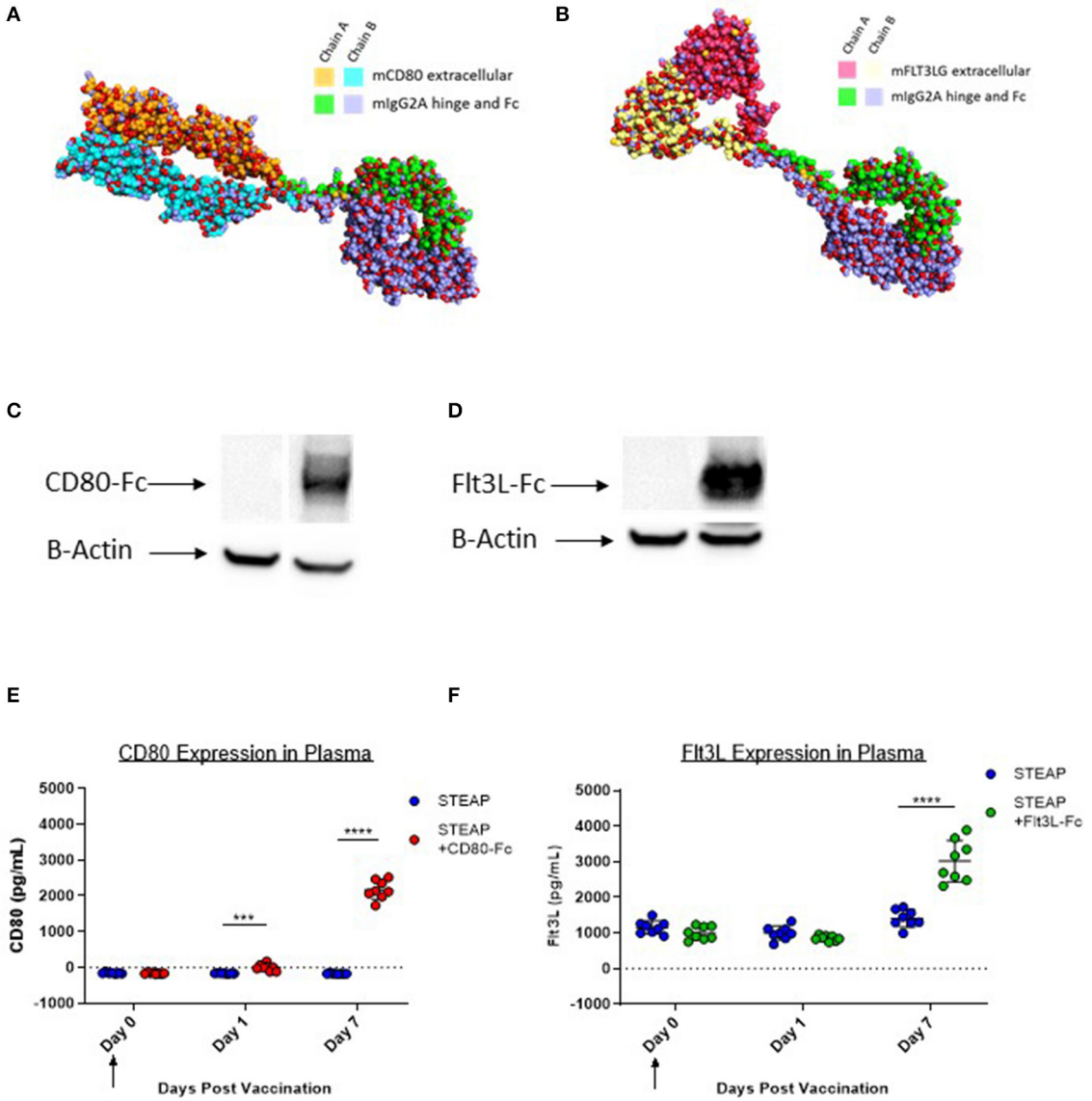

FIGURE 2 | CD80-Fc and Flt3L-Fc express *in vitro* and *in vivo*. **(A)** Comparative model of murine Flt3L extracellular domain-murine IgG2A fusion. **(B)** Comparative model of murine CD80 extracellular domain-murine IgG2A fusion **(C,D)** 293T cells were transfected and Flt3L-Fc **(C)** and CD80-Fc **(D)** expression was analyzed by Western blot and compared to pVAX control. **(E,F)** Mice were immunized and Flt3L-Fc **(E)** and CD80-Fc **(F)** expression was measured in the plasma over time. $N = 8$ mice, $^{***}p < 0.001$, $^{****}p < 0.0001$.

control empty vector plasmid (modified pVAX). Cell lysates were analyzed by western blot. Our results indicate that both CD80-Fc and Flt3L-Fc proteins properly express *in vitro* (**Figures 2C,D**). To address *in vivo* expression following plasmid DNA administration via IM/EP, we administered formulations of STEAP1 or STEAP1 with adjuvant, and then assayed systemic levels of each protein at days 0, 1, and 7 by ELISA. We show in **Figures 2E,F** that IM/EP injection of plasmid-DNA encoding CD80-Fc or Flt3L-Fc results in expression of the respective proteins with values of 2,341 and 1,610 pg/ml, respectively, in the plasma of mice 7 days post treatment.

Flt3L-Fc Significantly Increases Antigen-Specific T Cell Responses to STEAP1 Tumor Antigen

Our initial adjuvant screen examined one dose level for antigen and adjuvant, next we proceeded to examine the effect of STEAP1 dose range on T cell responses. We compared two different dose levels of STEAP1, 5, and 20 ug, where 5 ug was chosen as a sub-optimal dose for the initial screen to assess adjuvanting, and 20 ug is the dose level which affords maximal T cell response prior to plateau (data not shown). There was a significant increase in STEAP1-specific T cell responses at a 20 ug dose of STEAP1 compared to a 5 ug dose (**Figure 3A**). The addition

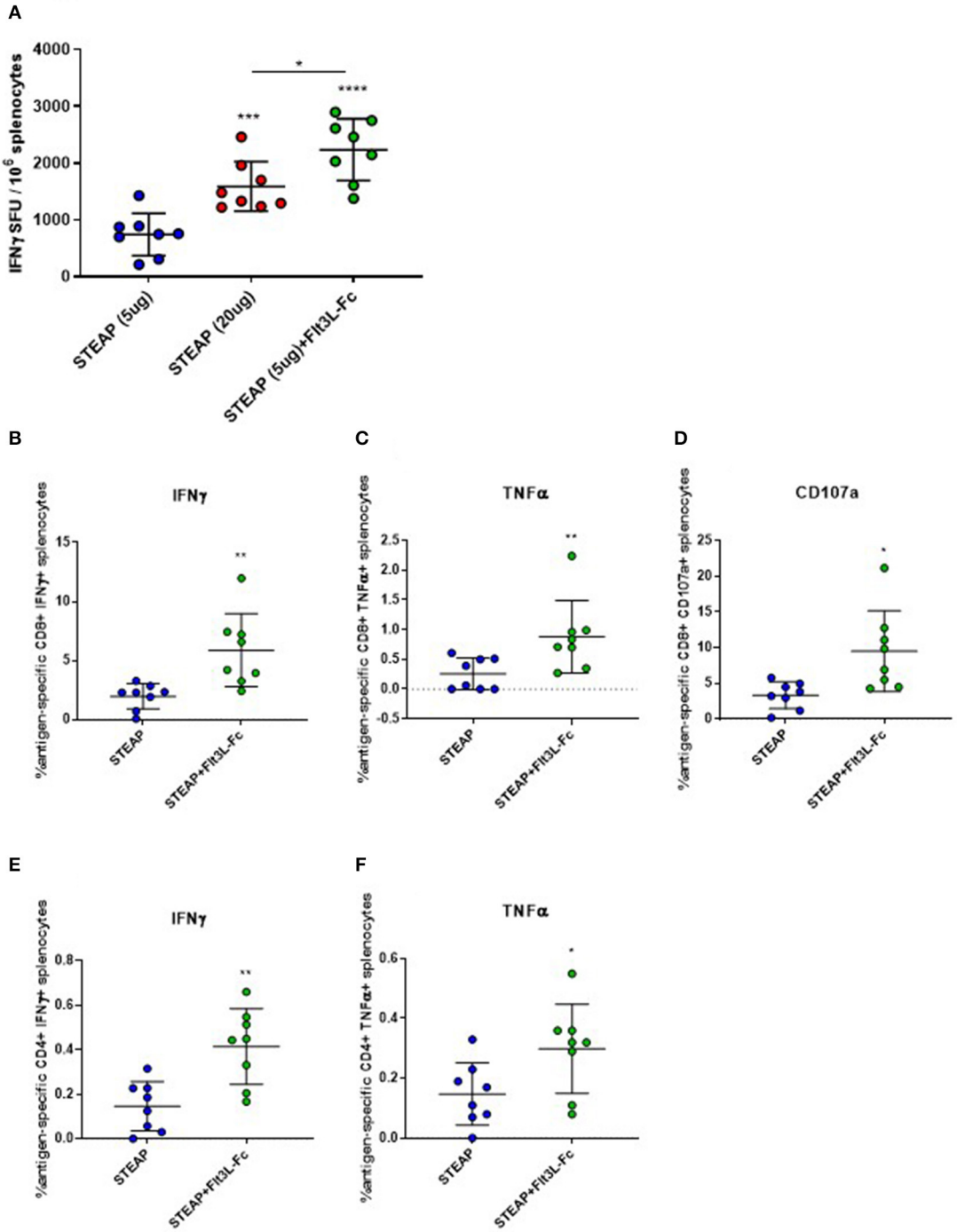

FIGURE 3 | Flt3L-Fc increases antigen specific T cell responses to STEAP1. **(A)** Mice were immunized biweekly according to **Figure 1A** and an IFNγ ELISpot was run on splenocytes to assess antigen-specific T cell responses to STEAP1. **(B–F)** Intracellular cytokine staining was done on splenocytes to characterize $CD8^+$ **(B–D)** and $CD4^+$ **(E,F)** functional T cell responses from mice immunized with STEAP1 alone or in combination with Flt3L-Fc. $N = 8$, $^*p < 0.05$, $^{**}p < 0.01$, $^{***}p < 0.001$, $^{****}p < 0.0001$.

of 19 ug Flt3L-Fc to 5 ug of STEAP1 significantly enhanced the antigen-specific T cell response to levels greater than the plateau level afforded by STEAP1 alone at 20 ug, indicating that the addition of Flt3L-Fc to STEAP1 vaccination is not merely dose-sparing.

We proceeded to characterize the effect of Flt3L-Fc by specifically analyzing the T lymphocyte phenotype by flow cytometry. We performed intracellular cytokine staining on peptide-stimulated spleen cells from mice treated with STEAP1 formulated with Flt3L-Fc compared to STEAP1 alone. Results

show that both $CD8^+$ and $CD4^+$ T cell populations from mice treated with STEAP1 formulated with Flt3L-Fc possess a significantly greater frequency of STEAP1-specific cells expressing IFNγ and TNFα compared to mice treated with STEAP1 alone (**Figures 3B,C,E,F**). The $CD8^+$ T cell population also displayed a significantly enhanced frequency of cells expressing the degranulation marker, CD107a, when Flt3L-Fc is formulated with STEAP1 (**Figure 3D**). In summary, these results indicate that Flt3L-Fc formulated with STEAP1 drives an increase in the quantitative and qualitative functional T cell response.

Flt3L-Fc Mobilizes and Activates Dendritic Cell Populations

To investigate the mechanism of action associated with enhanced T cell responses with the addition of Flt3L-Fc, mice were vaccinated weekly with STEAP1 alone or STEAP1 formulated with Flt3L-Fc. Draining lymph nodes and TA muscle were harvested 24 h following each vaccination and dendritic cell populations were analyzed by flow cytometry. Twenty four hours following the first vaccination, we observed no significant effect of Flt3L-Fc on DC populations at either tissue site (**Figures 4A,B**). Seven days later, mice administered STEAP1 formulated with Flt3L-Fc showed a significantly increased percentage of $CD11c^+MHCII^{hi}$ and $CD11c^+MHCII^{lo}$ dendritic cell populations at the site of administration, as well as a significant increase in the percent of $CD11c^+MHCII^{hi}$ DCs in the draining lymph node which displayed the activation markers CD80/CD86 (**Figures 4C,D**). The effect at the site of administration was lost 7 days later, however the percentage of both $CD11c^+MHCII^{hi}$ and $CD11c^+MHCII^{lo}$ populations was significantly increased at the lymph node at this time (**Figures 4E,F**).

To further investigate the effect of Flt3L-Fc formulation at the site of administration, we extracted RNA from the TA muscle 7 days following vaccination and analyzed gene expression via the nCounter PanCancer Immune Profiling panel on the Nanostring Max Analysis System. Global differences in gene expression between mice administered STEAP1 and mice administered STEAP1 formulated with Flt3L-Fc were assessed by heat-map and volcano plot analyses (**Figures 5A,B**). Volcano plot analysis shows there is over 100 differentially expressed genes in TA muscles isolated from mice treated with STEAP1 plus Flt3L-Fc as compared to mice treated with STEAP1 alone ($p < 0.01$, false-discovery rate < 5%). Specifically, genes involved in DC function and/or migration such as CD86 and ITGAE were significantly upregulated (**Figure 5A**). Specific analysis of genes involved in DC activation and function showed that when Flt3L-Fc is formulated with STEAP1 there is a significant increase in CCL5, CD40L, CD83, and CD86 (**Figure 5C**). We further analyzed this dataset using DAVID (the database for annotation, visualization, and integrated discovery), a functional annotation bioinformatics resource. Biological processes which were up-regulated when Flt3L-Fc was formulated with STEAP1 included leukocyte activation, hemopoiesis, antigen processing and presentation, IFNγ production, and dendritic cell differentiation (**Figure 5D**, complete list of genes included in **Supplementary Table 1**). Combined, FACS and gene expression data show that Flt3L-Fc formulated with STEAP1 significantly enhances the DC response STEAP1 vaccine.

Vaccine Formulation With CD80-Fc Enhances T Cell Immune Responses to Multiple Cancer Antigens

Thus far, we have shown that indirect activation of T cells via the Flt3L adjuvant significantly boosts the antigen-specific T cell response to STEAP1. To determine the role of direct T cell engagement in our vaccination paradigm, we further investigated the effect of CD80-Fc formulation with STEAP1 on antigen-specific T cell responses. We compared two dose levels of STEAP1 (5 and 20 ug) formulated with CD80-Fc at 20 ug. As in our previous results, the addition of CD80-Fc to STEAP1 formulation at 5 ug significantly boosted the antigen-specific T cell response (**Figure 6A**). When STEAP1 was dosed at the maximal level, there was no further increase in antigen-specific T cell responses and both doses of STEAP1 with CD80-Fc generated antigen-specific T cell responses which were >5-fold as compared to STEAP1 alone at 5 ug. As STEAP1 alone at 20 ug compared to 5 ug resulted in a 2-fold increase only, these results indicate that this combination was not merely dose-sparing.

We proceeded to characterize the effect of CD80-Fc by specifically analyzing the T lymphocyte phenotype by flow cytometry. We performed intracellular cytokine staining on peptide-stimulated spleen cells from mice treated with STEAP1 formulated with CD80-Fc compared to STEAP1 alone. Results show that both $CD8^+$ and $CD4^+$ T cell populations from mice treated with STEAP1 formulated with CD80-Fc possess a significantly greater frequency of antigen-specific cell expressing IFNγ, TNFα, and CD107a compared to mice treated with STEAP1 alone (**Figures 6B–G**). In summary, these results indicate that CD80-Fc formulated with STEAP1 drives an increase in the quantitative and qualitative functional T cell response to the STEAP1 antigen.

Given the highly robust effect of CD80-Fc formulation with STEAP1, we examined the effect of CD80-Fc in combination with the tumor associated antigen Survivin. We compared two different dose levels of Survivin, 20 and 40 ug, chosen as the sub-optimal and maximal dose, respectively. There was a significant increase in Survivin-specific T cell responses at the 40 ug dose of Survivin compared to the 20 ug dose (**Figure 6H**). The addition of CD80-Fc to 20 ug of Survivin significantly enhanced the antigen-specific T cell response to levels greater than the maximal dose, indicating that the addition of CD80-Fc to Survivin vaccination was not merely dose-sparing.

We proceeded to characterize the effect of CD80-Fc by specifically analyzing the T lymphocyte phenotype by flow cytometry. We performed intracellular cytokine staining on peptide-stimulated spleen cells from mice treated with Surivivin formulated with CD80-Fc compared to Survivin alone. Results show that the $CD8^+$ T cell population from mice treated with Survivin formulated with CD80-Fc possesses a significantly greater frequency of antigen-specific cells expressing CD107a compared to mice treated with Survivin alone

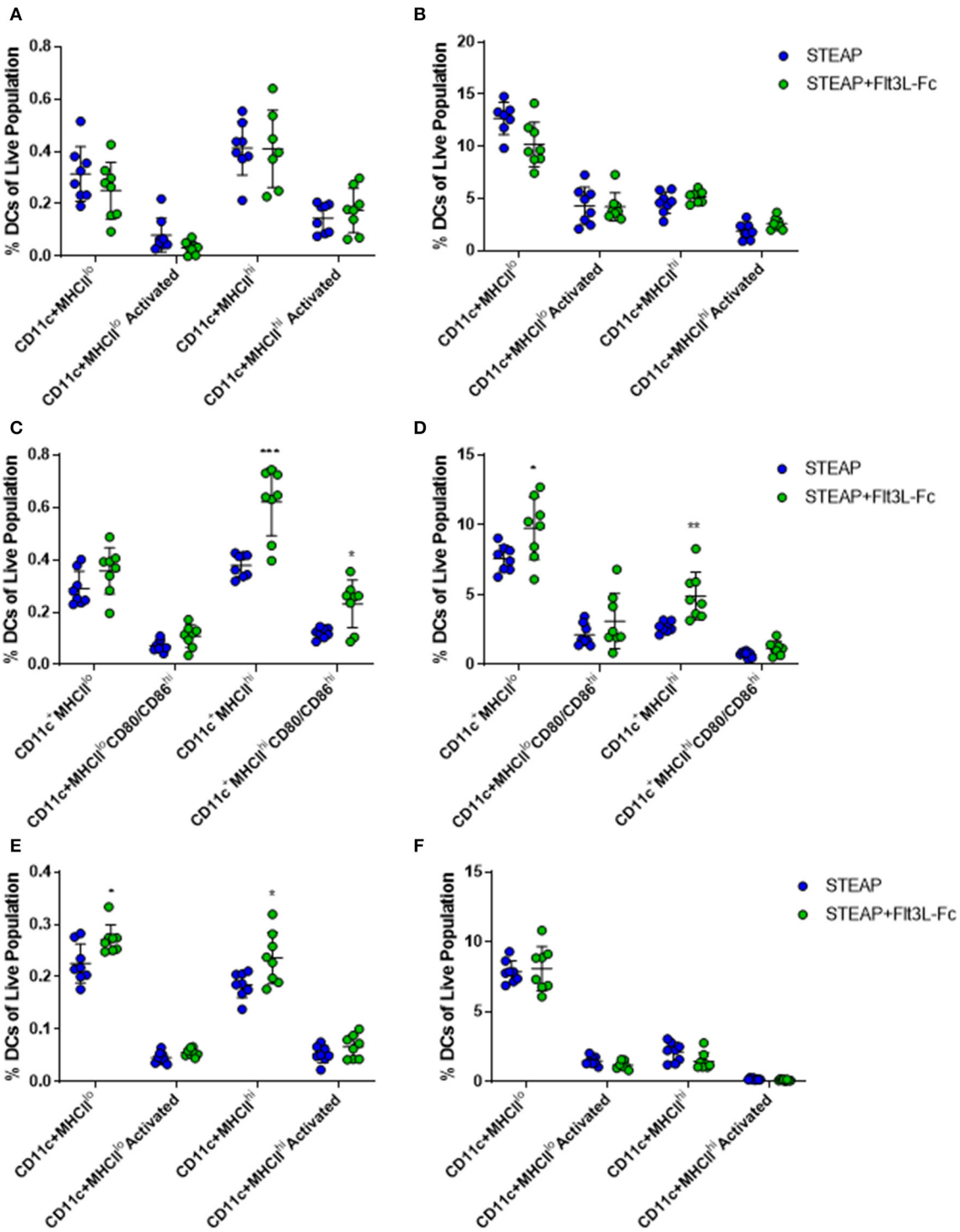

FIGURE 4 | Flt3L-Fc significantly increases dendritic cell migration and trafficking. Mice were immunized weekly and the draining lymph node and TA muscle were harvested 24 h following each treatment. **(A–F)** Flow cytometry was performed on cells harvested from the dLN **(A,C,E)** and TA muscle **(B,D,F)** to assess DC populations 24 h after the first **(A,B)**, second **(C,D)**, and third **(E,F)** doses. $N = 8$, $^{*}p < 0.05$, $^{**}p < 0.01$, $^{***}p < 0.001$.

(**Figure 6I**). Additionally, the $CD4^{+}$ T cell population possessed a significantly greater frequency of antigen-specific cells expressing IFNγ compared to mice treated with Survivin alone (**Figure 6J**). In summary, these results indicate that CD80-Fc formulated with Survivin drives an increase in the quantitative and qualitative functional T cell response to Survivin vaccination.

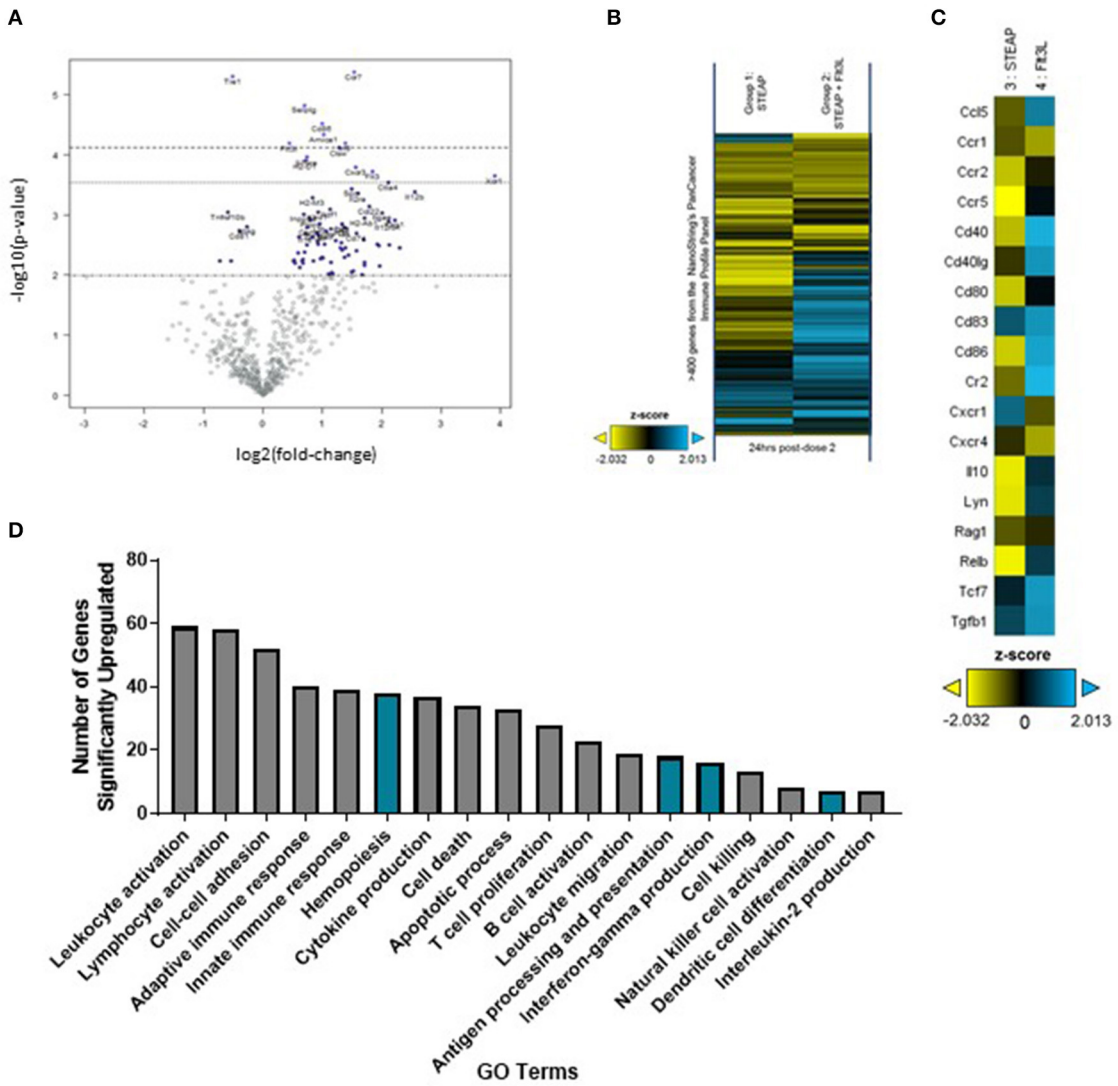

FIGURE 5 | Flt3L-Fc promotes dendritic cell signaling at the site of administration. Mice were immunized weekly and the TA muscle was harvest 24 h post-dose 2. **(A)** Volcano plot analysis of differentially expressed genes at post-dose 2. **(B)** Heatmap depicting global differences in gene expression between treatment groups, following the second immunization. **(C)** Heatmap of DC function and activation genes. **(D)** Biological processes significantly upregulated by Flt3L-Fc as indicated by DAVID Gene Ontology (GO) terms. Pathways specifically associated with dendritic cells are highlighted in blue.

Next, we examined the effect of CD80-Fc as an adjuvant to vaccination with the HPV 16 associated oncoproteins E6/E7. We measured the generation of antigen-specific T cells in the peripheral blood using a tetramer specific to the dominant epitope E7 (H-2D^{b} RAHYNIVTF). Mice were administered either HPV 16 E6/E7 pDNA alone or formulated with CD80-Fc, and RAHYNIVTF-specific T cells from the peripheral blood were quantified 2 weeks following immunization by flow cytometry. **Figure 6K** shows that the addition of CD80-Fc significantly increased RAHYNIVTF-specific T cells in the peripheral blood, indicating an adjuvant effect of this molecule for viral-associated cancer driving antigens. Together, these results indicate that the T cell engager and activator CD80-Fc, significantly boosts the antigen-specific T cell immune response to a diverse range of cancer-antigen targets.

CD80-Fc in Combination With STEAP1 Reduces Tumor Burden in Mice

Lastly, we sought to determine the relevance of the addition of CD80-Fc with the STEAP1 vaccine in a tumor challenge model. We subcutaneously implanted CT-26 tumor cells into Balb/c mice and began vaccination when the tumors reached an average size of 100 mm^3. Mice were vaccinated bi-weekly and tumors measured over time. **Figure 7** shows that when mice were treated with STEAP1 plus CD80-Fc, there is a significant reduction in tumor growth and a significant increase in animal survival compared to mice treated with STEAP1 alone.

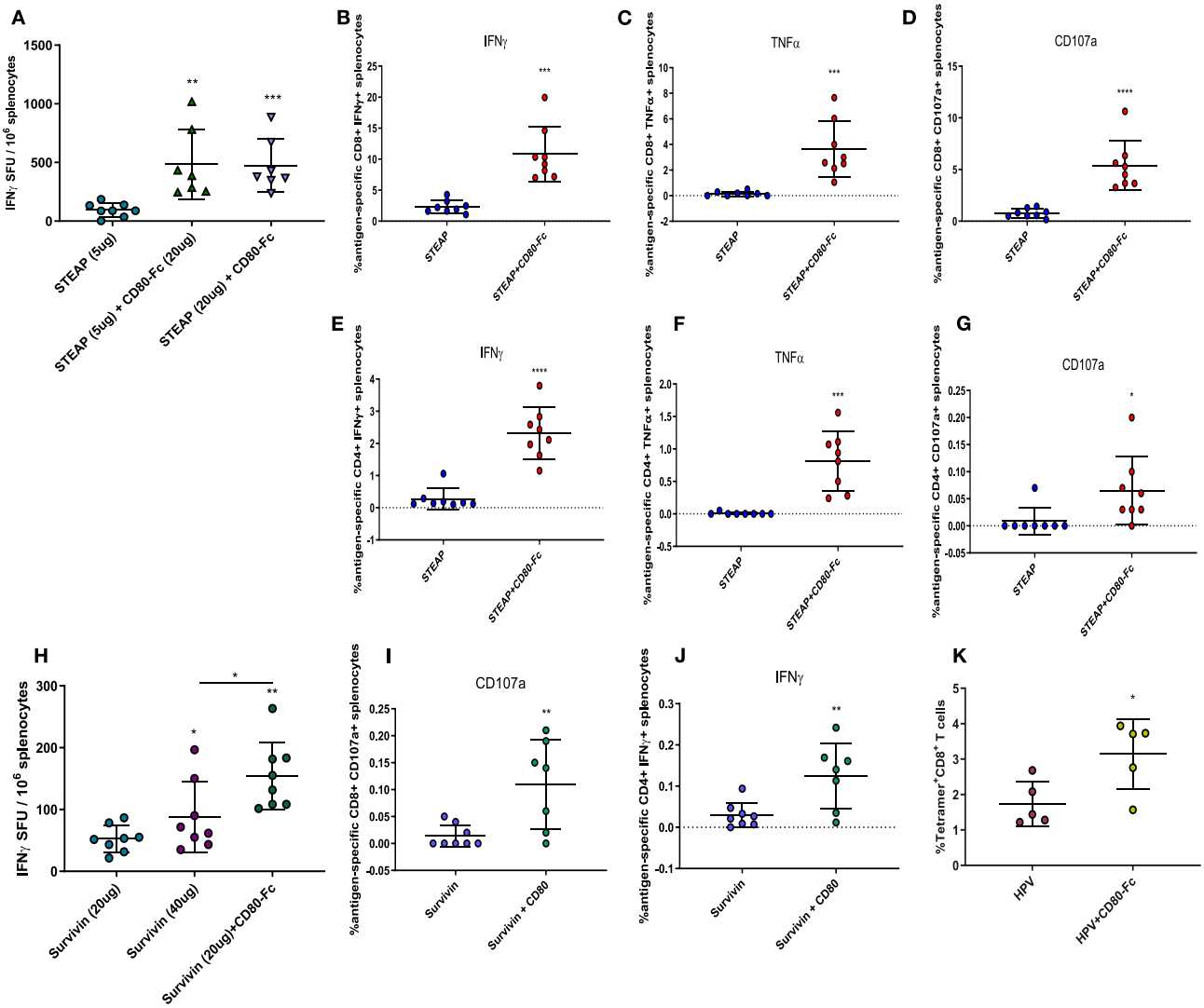

FIGURE 6 | Direct targeting of T cells via CD80 ligand enhances anti-tumor antigen responses. **(A–J)** Mice were immunized biweekly according to **Figure 1B** and splenocytes harvested. **(B)** IFNγ ELISpot was performed to assess antigen-specific T cell responses to STEAP1. **(B–G)** Intracellular cytokine staining was done on splenocytes to characterize $CD8^+$ and $CD4^+$ T cell functional responses from mice immunized with STEAP1 alone or in combination with CD80-Fc. **(H)** IFNγ ELISpot was performed to assess antigen-specific T cell responses to Survivin. **(I,J)** Intracellular cytokine staining was done on splenocytes to characterize $CD8^+$ and $CD4^+$ T cell functional responses from mice immunized with Survivin alone or in combination with CD80-Fc. **(K)** Mice were immunized at day 0 and 21 and serially bled. PBMCs were stained with HPV E7 (H-$2D^b$ RAHYNIVTF) tetramer on day 17. $N = 8$, $^*p < 0.05$, $^{**}p < 0.01$, $^{***}p < 0.001$, $^{****}p < 0.0001$.

Collectively, the results of these data indicate that the addition of this adjuvant has a robust effect on the antigen-specific T cell response and CD80-Fc reduces tumor burden in a syngeneic mouse tumor model.

DISCUSSION

Robust antigen-specific T cell generation following CELLECTRA® EP enhanced delivery of pDNA vaccines has been demonstrated in several clinical trials examining a variety of antigens (12, 29). This platform has recently been expanded upon by the delivery of DNA-encoded monoclonal antibodies (dMAbs) with excellent expression kinetics *in vivo* (30–32), and a first in-human clinical trial that commenced this year (NCT03831503). The versatility of this platform is further exemplified by the recent publication describing the utility of a DNA-encoded bispecific antibody targeting Her2, which abolishes tumor growth and maintains expression in mice for several months (33). Here we further expand on the potential of our platform by showing that synthetic DNA constructs-encoding immune adjuvants can significantly enhance antigen-specific T cell responses to cancer vaccines.

In this study we designed over twenty DNA-encoded genetic adjuvants and tested their ability to enhance antigen-specific T cell responses to vaccination against two different

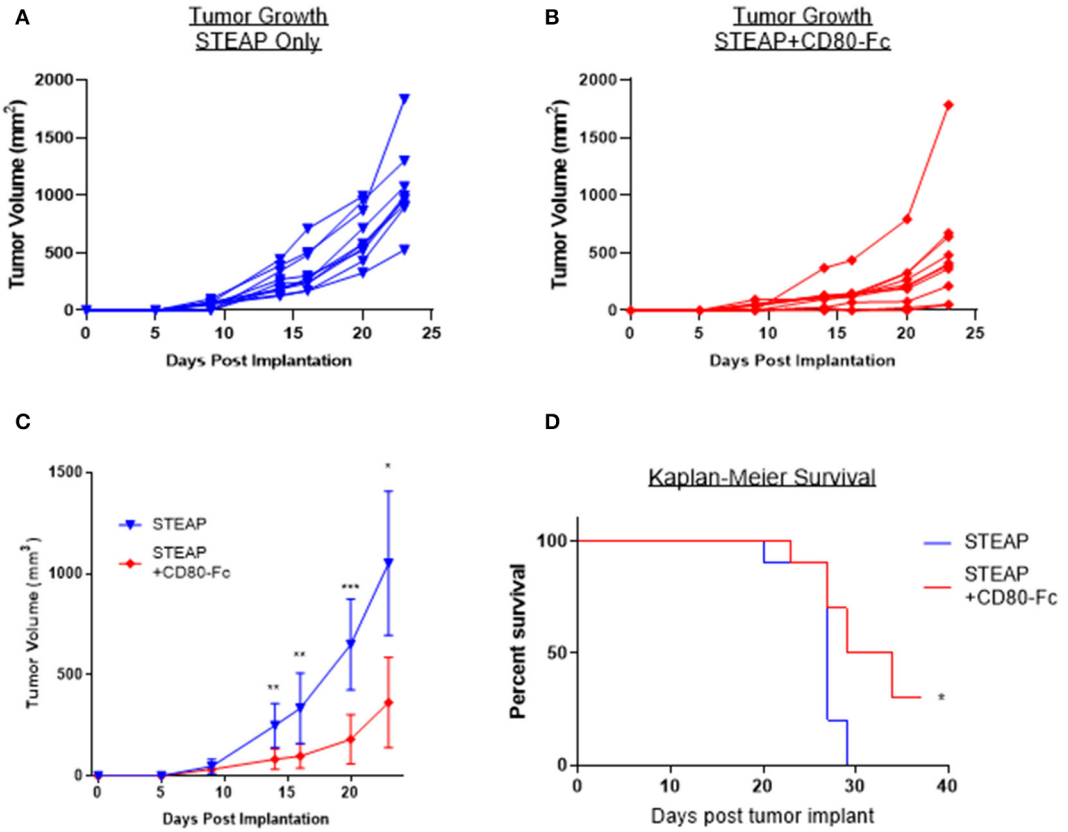

FIGURE 7 | CD80-Fc in combination with STEAP1 significantly reduces tumor burden compared to STEAP1 alone. Balb/c mice were implanted subcutaneously with CT-26 tumor cells and allowed to grow to 100 mm^3. At this time, they were separated into two groups and vaccinated with either STEAP1 alone of STEAP1 formulated with CD80-Fc. **(A,B)** Individual tumor growth curves. **(C)** Averages of A and B plotted together. **(D)** Kaplan-Meier survival curves taken at time of mouse sacrifice. $N = 10$, $^*p < 0.05$, $^{**}p < 0.01$, $^{***}p < 0.001$.

tumor-associated antigens, STEAP1, and TERT. Although this manuscript specifically analyzed the effect of these adjuvants against these two self antigens, we hypothesize that they would also be beneficial against a personalized or neoantigen approach and future studies are underway to test this hypothesis. A more commonly used adjuvant to date is the pro-inflammatory cytokine IL-12, which has been added to vaccination trials for both infectious diseases (NCT02431767) as well as cancer vaccines (NCT03491683, NCT01440816). The utility of IL-12 stands from its ability to induce the production of IFNγ from NK and cytotoxic T cells (34) responses. In this report, we show enhanced antigen specific T cell responses to SynCon® vaccination, via directly co-stimulating T cells through the addition of a plasmid encoding CD80-Fc as well as indirectly affecting T cell activation through enhanced dendritic cell recruitment and trafficking mediated by Flt3L-Fc. It will be interesting to compare these adjuvants head-to-head with IL-12, to gain further insight to the efficacy afforded by each adjuvant tested. Additionally, while the initial screen was performed with a single dose level of antigen plus adjuvant, and therefore it is possible that other adjuvants would show benefit to vaccination following a dose level optimization analysis, dose-range follow-up studies with CD80-Fc and Flt3L-Fc indicate that the initial dose chosen was indeed optimal for these two adjuvants in combination with the STEAP1 antigen.

For optimal stimulation of naïve T cells and the induction of protective immunity three signals are required: binding of the TCR to the peptide-MHC complex, the interaction of costimulatory molecules at the interface between APCs and T cells, and cytokine production (35). Here we have focused on signal 2: stimulation of the T cell. Previous studies have revealed enhancement of signal one through advancements in pDNA delivery technology resulting in increased antigen expression. Additionally, cytokines such as IL-12 have been employed to enhance the immune response via signal 3. The data from these studies reveals that the T cell stimulation requirement could be addressed both indirectly, by enhancing their engagement with DCs via Flt3L, and directly, by the specific expression of co-stimulatory molecules such as CD80.

The use of Flt3L as an adjuvant to cancer vaccines has been previously reported (25, 36), however, this is the first study to examine the effect of Flt3L formulation with the STEAP1 antigen. We show that the addition of Flt3L-Fc to STEAP1 vaccination resulted in significantly increased antigen-specific T cell responses. The addition of Flt3L-Fc also resulted in increased migration of DCs to the site of administration

and increased trafficking to the draining lymph nodes. Gene expression analysis of the treated muscle showed a significant up-regulation of genes related to DC migration and activation at day 7, however there was also increased expression of several immune checkpoint proteins including CTLA4 and PSGL1. A series of previously published studies describe a significant benefit of combining checkpoint inhibition with Flt3L therapy for the benefit of anti-tumor vaccination (37–39). Thus, it is plausible that combining the Flt3L-Fc plasmid with CTLA-4 inhibition would be synergistic and future studies will examine this combination strategy. Indeed, several papers describing the adjuvant effect of Flt3L for cancer vaccines do so in the context of a combination therapy. For example, Song et al. showed in an aggressive HBc-expressing B16 melanoma model that the addition of Flt3L combined with RANTEs to an HBc prime-boost DNA vaccination regime resulted a strong antitumor response (40). In another study, when mice were treated with a DNA vaccine encoding pN-neu in combination with either two separate monocistronic plasmids encoding Flt3L and GM-CSF, or a bicistronic plasmid encoding both cytokines, authors showed moderate, and exceptional tumor control, respectively (41). Although neither of these studies examined the effect of Flt3L alone, they do warrant the further examination of Flt3L in combination with RANTES and/or GM-CSF in CELLECTRA®-enhanced pDNA delivery protocols.

The DC-based vaccine Provenge® is the first FDA-approved vaccine for cancer therapy. DC-based vaccines, in general, are a result of the realization that DCs are a critical component to the immune response necessary to effectively target cancer, and yet are possibly defective or present in inadequate numbers (42). Of the over two dozen candidate adjuvants we screened, including chemokines and cytokines with known roles in generating an active immune response, our study showed that the T cell co-stimulators 4-1BBL, OX-40L, and CD80-Fc all significantly and robustly increased the antigen-specific T cell response to both STEAP1 and Tert, and Flt3L-Fc followed closely behind. While the Phase III clinical trial showed that Provenge® extended median survival by 4.1 months for patients with metastatic hormone-refractory prostate cancer (5), DC-based vaccines require complex *ex vivo* manipulation of cells which are then administered back to the patient for treatment. In this study we show the potential to override the defective nature of DCs harnessing their co-stimulation through the addition of CD80-Fc which directly acts on the T cells themselves. In addition to CD28, CD80 also binds PD-L1 and CTLA-4 expressed on T cells. While CTLA-4 is involved in the negative regulation of T cell activation, it is possible that CD80-FC could decrease T cell function by interacting with CTLA-4. However, numerous studies performed *in vitro* suggest that soluble CD80-Fc does not suppress T cell activation through CTLA-4 or the effect is minimal (28, 43, 44). This data is consistent with the hypothesis that CTLA-4 functions primarily as a decoy receptor for preventing CD80 activation through CD28 (45). Interestingly, our gene expression data shows that the addition of Flt3L-Fc to vaccination with STEAP1 results in an increase in CTLA-4 expression. It would be interesting to explore the combined effect of Flt3L-Fc with CD80-Fc. We would expect that the addition of CD80-Fc to a Flt3L-Fc adjuvanted vaccination could help overcome any negative regulation of T effector cells by directly engaging them via CD28, resulting in an additive or synergistic boosting. We further analyzed CD80-Fc with a variety of cancer vaccines and show that it universally led to an increased antigen-specific T cell response. Therefore, CD80-Fc presents as a potentially "off-the-shelf" approach for enhancing anti-tumor DNA vaccination.

In this article, we reveal two different methods for enhancing anti-tumor T cell responses to synthetic DNA vaccines: indirectly via Flt3L and directly via CD80. Future studies will be performed to analyze the functionality of these combinations in tumor models, however, they stand as exciting combinations for cancer vaccination and warrant further attention.

MATERIALS AND METHODS

DNA Constructs

The SynCon® TERT and HPV type-16, E6 and E7 were generated as previously described (46–48). The SynCon® STEAP1 sequence that shares 95.6% sequence identity with human native STEAP1 was generated after performing ClustalW multiple sequence alignment using 36 STEAP1 sequences collected from human and other species. To design mouse SynCon® Survivin, four mouse survivin sequences were collected from GenBank to generate a consensus sequence. In order to abolish the potential biological function of the resulting consensus mouse survivin protein, three mutations (T34A, T48A, C84A) were introduced to abolish the anti-apoptotic activity of survivin. The resulting mouse SynCon® Survivin protein shares 95.0% identity with mouse native survivin. Once the SynCon® STEAP1 and mouse SynCon® Survivin sequences were obtained, an upstream Kozak sequence and IgE leader sequence were added to the N-terminus to have a higher level of expression. Codon/RNA optimization was also performed. The synthesized SynCon® STEAP1 and mouse SynCon® Survivin genes were cloned into Inovio's expression vector pGX0001 under the control of the human cytomegalovirus immediate-early promoter, and sequence verified for further immunogenicity study. Plasmids were purified using the Charles River Laboratories Endochrome-K Kit (Fisher Scientific), all endotoxin levels were below the detectable limit.

For the adjuvants, a series of DNA encoded murine signaling molecules with known biological effects were selected for screening in the platform. In all cases, soluble versions of molecules were designed based on known protein topologies. In some cases, murine Fc-linked versions were also constructed. Comparative protein modeling using Discovery Studio 2017 (Dassault Systèmes BIOVIA, San Diego) or Bioluminate (Schrödinger, LLC, New York, NY, 2019) was used when necessary to improve decisions based on molecule truncations and fusions, and to help in understanding potential higher-order assemblies such as dimerization upon Fc linkage.

The nucleic sequences of adjuvants used in this manuscript can be found using the following Genbank Accession Numbers: CD80–Q00609, OX40-L–P43488, 4-1BBL–P41274,

IL-15–P48346, Flt3L–P49772, CCL5–CAJ18523.1, CXCL10–NP_067249.1, GM-CSF–CAA26820.1, mmCCL27–Q9Z1X0, mTSLP–Q9JIE6, CCL21a–NP_035254.1, mIL-23–Q9EQ14, IL-15RA–Q60819, mCCL3, LAG3–Q61790, mGP96–P08113. Where designs are not indicated denotes proprietary modifications to existing sequences.

Animal Immunizations

Female BALB/c mice (6–8 weeks old) were purchased from Jackson Laboratory. All mice were housed in compliance with the Institutional Animal Care and Use Committee (IACUC) at the USDA-approved, AAALAC accredited facility ACCULAB (Sorrento Valley, San Diego, CA). Mice were immunized with 5 ug of STEAP1 plasmid with or without 20 ug of the indicated adjuvant plasmid unless otherwise described in the figure legend. DNA was formulated in Saline Sodium Citrate Buffer (SSC). Mice were injected intramuscularly (IM) into the tibialis anterior (TA) muscle followed by electroporation (EP) with the CELLECTRA® 3P device (Inovio Pharmaceuticals) as previously described (47). Briefly, two 0.1-amp constant current square-wave pulses were delivered and each pule was 52 ms in length with a 1-s delay between pulses. Vaccination schedules are indicated in the respective figures.

ELISpot

Mouse spleens were dissociated using gentleMACS C Tubes (Miltenyi Biotec) in R10 (RPMI 1640 media supplemented with 10% FBS (Seradigm), 1% Penicillin-Streptomycin, and 0.1% 2-mercaptoethanol), followed by filtration through 40 um cell strainers (Falcon) and ACK lysis (Lonza). Splenocytes were counted and 2×10^5 were added to pre-coated Mouse IFN-γ ELISpot^{PLUS} (ALP) plates (Mabtech) and stimulated with overlapping 15 mer peptide pools corresponding to SynCon® or native mouse STEAP1. After 18 h at 37°C, cytokine secretion was detected according to the manufacturer's instructions. Spots were counted using an ImmunoSpot CTL reader and spot-forming units (SFU) were calculated by subtracting media alone wells from stimulated wells. Concanavalin A was used as a positive control.

ELISA

Mouse plasma was obtained by bleeding mice through heparinized capillary tubes. Tubes were spun and the top clear layer was collected. Plasma was plated on a pre-coated Mouse Flt 3 Ligand ELISA Kit (abcam) or Mouse B7-1 ELISA Kit (abcam) and run according to the instructions of the manufacturer. Plates were analyzed at 450 nm and cytokine expression was calculated from the standard curve of each assay.

Isolation of Peripheral Blood Mononuclear Cells (PBMCs), Lymph Node, and TA Muscle Dissociation

To isolate PBMCs, blood was collected in tubes containing 4% sodium citrate (Sigma-Aldrich) and then layered over Histopaque-1083 (Sigma-Aldrich). Tubes were spun to create a gradient and cells from the buffy coat were collected and stained for flow cytometry. Lymph nodes were mechanically disrupted using a scalpel and dissociated using an enzymatic cocktail containing R10, 100 U/ml DNase (Qiagen), and 1 mg/ml Collagenase D (Sigma-Aldrich) at 37°C for 1 h. TA muscles were dissociated using the Skeletal Muscle Dissociation kit, mouse and rat (Miltenyl Biotec, USA). Single cell suspensions were filtered and stained for flow cytometry.

Flow Cytometry

To assess DC phenotypes, cells isolated from spleens, TA muscles, or lymph nodes were surface stained with LIVE/DEAD Aqua (Invitrogen), CD3 (145-2C11; BD Biosciences), CD19 (6D5, Biolegend), CD11c (HL3, BD Biosciences), MHC class II (M5/114.15.2, BD Biosciences), CD80 (16-10A1, BD Biosciences), and CD86 (GL1, BD Biosciences). Cell suspensions were then washed and fixed in PBS containing 1% paraformaldehyde. Samples were acquired on a FACSCanto (BD Biosciences) and analyzed using FlowJo (BD Biosciences) software. Gated $CD3^-CD19^-CD11c^+$MHC $II^{+/-}$ DCs were quantitated and expression of either CD80 or CD86 was considered activated.

For intracellular cytokine staining, splenocytes were stimulated with STEAP peptide pools in the presence of GolgiStop^{TM} GolgiPlug^{TM} (BD Bioscience) and CD107a (1D4B; BD Biosciences). Media alone and Cell Stimulation Cocktail (eBioscience) were used as negative and positive controls, respectively. Following stimulation, cells were washed and surface stained using LIVE/DEAD Aqua (Invitrogen), CD4 (RM4-5; BD Biosciences), CD8 (53-6.7; BD Biosciences), and CD45 (30-F11; BD Biosciences). Cells were permeabilized using the Foxp3/Transcription Factor Fixation/Permeabilization kit (eBioscience), followed by intracellular staining with CD3 (145-2C11; BD Biosciences), IFN-γ (XMG1.2; Biolegend), IL-2 (JES6-5H4, Biolegend), and TNF-α (MP6-XT22; BD Biosciences). Cells were fixed in PBS containing 1% paraformaldehyde. Samples were acquired on a FACSCanto (BD Biosciences) and analyzed using FlowJo (BD Biosciences) software. For more information on flow panels see **Supplementary Tables 2**, **3**.

For tetramer analysis, PBMCs were washed and stained with anti-CD3 (145-2C11; eBioscience), anti-CD45 (30-F11; Biolegend), anti-CD8 (53-6.7; Biolegend), anti-CD4 (RM4-5; BD Biosciences), and the iTAg tetramer H-2Db HPV16E7 tetramer (RAHYNIVTF) (MBL). Cells were then fixed and permabilized using the FoxP3/Transcription factor fixation/permeabilization kit (eBioscience). Example FACs gating strategy for all immune cell populations can found in **Supplementary Figure 1**.

Nanostring

Mouse TA muscles were extracted and flash frozen in a dry ice-methanol bath. Tissue was homogenized using a Bessman Tissue Pulverizer (VWR) in liquid nitrogen. RNA was isolated from the pulverized muscle using the RNeasy Fibrous Tissue Mini Kit (Qiagen) following the manufacturer's instructions. RNA purity was measured using a NanoDrop. The nCounter PanCancer Immune Profiling Panel (NanoString Technologies)

was run according to the manufacturer's instructions and data was analyzed using nSolver Software (NanoString Technologies).

Statistical Analysis

Statistical analysis was performed using a two-tailed unpaired Student's *t* test. Error bars represent the standard deviation. All statistical analyses were done using GraphPad Prism. $p < 0.05$ was considered statistically significant.

DATA AVAILABILITY STATEMENT

All datasets generated for this study are included in the article/**Supplementary Material**.

ETHICS STATEMENT

The animal study was reviewed and approved by Institutional Animal Care and Use Committee at Acculab Life Sciences, San Diego CA.

AUTHOR CONTRIBUTIONS

AT, KM, and EM: conceptualization. AT and EM: methodology and supervision. AT, KM, and AW: formal analysis and writing—original. AT, KM, AW, and TN: investigation. CR, JY, NC, KB, and LH: resources. AT, TS, and EM: writing—review and editing. AT and KM: visualization.

SUPPLEMENTARY MATERIAL

The Supplementary Material for this article can be found online at: https://www.frontiersin.org/articles/10.3389/fimmu.2020.00327/full#supplementary-material

Supplementary Figure 1 | FACs gating strategies. Example gating strategies for **(A)** functional antigen-specific T cells, **(B)** tetramer-positive T cells, and **(C)** dendritic cells.

Supplementary Table 1 | Specific genes Up-regulated.

Supplementary Table 2 | T cell flow cytometry panel.

Supplementary Table 3 | Dendritic cell flow cytometry panel.

REFERENCES

1. Makkouk A, Weiner GJ. Cancer immunotherapy and breaking immune tolerance: new approaches to an old challenge. *Cancer Res*. (2015) 75:5–10. doi: 10.1158/0008-5472.CAN-14-2538
2. Hoos A. Development of immuno-oncology drugs - from CTLA4 to PD1 to the next generations. *Nat Rev Drug Discov*. (2016) 15:235–47. doi: 10.1038/nrd.2015.35
3. Walters JN, Ferraro B, Duperret EK, Kraynyak KA, Chu J, Saint-Fleur A, et al. A novel DNA vaccine platform enhances neo-antigen-like T cell responses against WT1 to break tolerance and induce anti-tumor immunity. *Mol Ther*. (2017) 25:976–88. doi: 10.1016/j.ymthe.2017.01.022
4. Marin-Acevedo JA, Chirila RM, Dronca RS. Immune checkpoint inhibitor toxicities. *Mayo Clin Proc*. (2019) 94:1321–9. doi: 10.1016/j.mayocp.2019.03.012
5. Kantoff PW, Higano CS, Shore ND, Berger ER, Small EJ, Penson DF, et al. Sipuleucel-T immunotherapy for castration-resistant prostate cancer. *N Engl J Med*. (2010) 363:411–22. doi: 10.1056/NEJMoa1001294
6. Cheever MA, Higano CS. PROVENGE (Sipuleucel-T) in prostate cancer: the first FDA-approved therapeutic cancer vaccine. *Clin Cancer Res*. (2011) 17:3520–6. doi: 10.1158/1078-0432.CCR-10-3126
7. Duperret EK, Liu S, Paik M, Trautz A, Stoltz R, Liu X, et al. A designer cross-reactive DNA immunotherapeutic vaccine that targets multiple MAGE-A family members simultaneously for cancer therapy. *Clin Cancer Res*. (2018) 24:6015–27. doi: 10.1158/1078-0432.CCR-18-1013
8. Duperret EK, Trautz A, Ammons D, Perales-Puchalt A, Wise MC, Yan J, et al. Alteration of the tumor stroma using a consensus DNA vaccine targeting fibroblast activation protein (FAP) synergizes with antitumor vaccine therapy in mice. *Clin Cancer Res*. (2018) 24:1190–201. doi: 10.1158/1078-0432.CCR-17-2033
9. Perales-Puchalt A, Svoronos N, Rutkowski MR, Allegrezza MJ, Tesone AJ, Payne KK, et al. Follicle-stimulating hormone receptor is expressed by most ovarian cancer subtypes and is a safe and effective immunotherapeutic target. *Clin Cancer Res*. (2017) 23:441–53. doi: 10.1158/1078-0432.CCR-16-0492
10. Perales-Puchalt A, Wojtak K, Duperret EK, Yang X, Slager AM, Yan J, et al. Engineered DNA vaccination against follicle-stimulating hormone receptor delays ovarian cancer progression in animal models. *Mol Ther*. (2019) 27:314–25. doi: 10.1016/j.ymthe.2018.11.014
11. Shore N. *Evaluation of an Immunotherapeutic DNA-Vaccine in Biochemically Relapsed PCa*. In: *ASCO Annual Meeting*. Chicago: IL (2018).
12. Trimble CL, Morrow MP, Kraynyak KA, Shen X, Dallas M, Yan J, et al. Safety, efficacy, and immunogenicity of VGX-3100, a therapeutic synthetic DNA vaccine targeting human papillomavirus 16 and 18 E6 and E7 proteins for cervical intraepithelial neoplasia 2/3: a randomised, double-blind, placebo-controlled phase 2b trial. *Lancet*. (2015) 386:2078–88.
13. Louis L, Wise MC, Choi H, Villarreal DO, Muthumani K, Weiner DB. Designed DNA-encoded IL-36 gamma acts as a potent molecular adjuvant enhancing zika synthetic DNA vaccine-induced immunity and protection in a lethal challenge model. *Vaccines*. (2019) 7:E42. doi: 10.3390/vaccines7020042
14. Kutzler MA, Wise MC, Hutnick NA, Moldoveanu Z, Hunter M, Reuter M, et al. Chemokine-adjuvanted electroporated DNA vaccine induces substantial protection from simian immunodeficiency virus vaginal challenge. *Mucosal Immunol*. (2016) 9:13–23. doi: 10.1038/mi.2015.31
15. Villarreal DO, Svoronos N, Wise MC, Shedlock DJ, Morrow MP, Conejo-Garcia JR, et al. Molecular adjuvant IL-33 enhances the potency of a DNA vaccine in a lethal challenge model. *Vaccine*. (2015) 33:4313–20. doi: 10.1016/j.vaccine.2015.03.086
16. Fagone P, Shedlock DJ, Bao H, Kawalekar OU, Yan J, Gupta D, et al. Molecular adjuvant HMGB1 enhances anti-influenza immunity during DNA vaccination. *Gene Ther*. (2011) 18:1070–7. doi: 10.1038/gt.2011.59
17. Casares S, Inaba K, Brumeanu TD, Steinman RM, Bona CA. Antigen presentation by dendritic cells after immunization with DNA encoding a major histocompatibility complex class II-restricted viral epitope. *J Exp Med*. (1997) 186:1481–6. doi: 10.1084/jem.186.9.1481
18. Haddad D, Ramprakash J, Sedegah M, Charoenvit Y, Baumgartner R, Kumar S, et al. Plasmid vaccine expressing granulocyte-macrophage colony-stimulating factor attracts infiltrates including immature dendritic cells into injected muscles. *J Immunol*. (2000) 165:3772–81. doi: 10.4049/jimmunol.165.7.3772
19. Akbari O, Panjwani N, Garcia S, Tascon R, Lowrie D, Stockinger B. DNA vaccination: transfection and activation of dendritic cells as key events for immunity. *J Exp Med*. (1999) 189:169–78. doi: 10.1084/jem.189.1.169
20. Chattergoon MA, Robinson TM, Boyer JD, Weiner DB. Specific immune induction following DNA-based immunization through *in vivo* transfection and activation of macrophages/antigen-presenting cells. *J Immunol*. (1998) 160:5707–18.
21. Maraskovsky E, Brasel K, Teepe M, Roux ER, Lyman SD, Shortman K, et al. Dramatic increase in the numbers of functionally mature dendritic cells in Flt3 ligand-treated mice: multiple dendritic cell subpopulations identified. *J Exp Med*. (1996) 184:1953–62. doi: 10.1084/jem.184.5.1953
22. Karsunky H, Merad M, Cozzio A, Weissman IL, Manz MG. Flt3 ligand regulates dendritic cell development from Flt3+ lymphoid and myeloid-committed progenitors to Flt3+ dendritic cells *in vivo*. *J Exp Med*. (2003) 198:305–13. doi: 10.1084/jem.20030323

23. Reeves RK, Wei Q, Fultz PN. Mobilization of CD34+ progenitor cells in association with decreased proliferation in the bone marrow of macaques after administration of the Fms-like tyrosine kinase 3 ligand. *Clin Vaccine Immunol*. (2010) 17:1269–73. doi: 10.1128/CVI.00166-10
24. Sumida SM, McKay PF, Truitt DM, Kishko MG, Arthur JC, Seaman MS, et al. Recruitment and expansion of dendritic cells in vivo potentiate the immunogenicity of plasmid DNA vaccines. *J Clin Invest*. (2004) 114:1334–42. doi: 10.1172/JCI200422608
25. Kreiter S, Diken M, Selmi A, Diekmann J, Attig S, Hüsemann Y, et al. FLT3 ligand enhances the cancer therapeutic potency of naked RNA vaccines. *Cancer Res*. (2011) 71:6132–42. doi: 10.1158/0008-5472.CAN-11-0291
26. Anandasabapathy N, Feder R, Mollah S, Tse SW, Longhi MP, Mehandru S, et al. Classical Flt3L-dependent dendritic cells control immunity to protein vaccine. *J Exp Med*. (2014) 211:1875–91. doi: 10.1084/jem.20131397
27. Subauste CS, de Waal Malefyt R, Fuh F. Role of CD80 (B7.1) and CD86 (B7.2) in the immune response to an intracellular pathogen. *J Immunol*. (1998) 160:1831–40.
28. Haile ST, Horn LA, Ostrand-Rosenberg S. A soluble form of CD80 enhances antitumor immunity by neutralizing programmed death ligand-1 and simultaneously providing costimulation. *Cancer Immunol Res*. (2014) 2:610–5. doi: 10.1158/2326-6066.CIR-13-0204
29. Tebas P, Roberts CC, Muthumani K, Reuschel EL, Kudchodkar SB, Zaidi FI, et al. Safety and immunogenicity of an anti-zika virus DNA vaccine - preliminary report. *N Engl J Med*. (2017). doi: 10.1056/NEJMoa1708120. [Epub ahead of print].
30. Duperret EK, Trautz A, Stoltz R, Patel A, Wise MC, Perales-Puchalt A, et al. Synthetic DNA-encoded monoclonal antibody delivery of anti-CTLA-4 antibodies induces tumor shrinkage *in vivo*. *Cancer Res*. (2018) 78:6363–70. doi: 10.1158/0008-5472.CAN-18-1429
31. Perales-Puchalt A, Duperret EK, Muthumani K, Weiner DB. Simplifying checkpoint inhibitor delivery through in vivo generation of synthetic DNA-encoded monoclonal antibodies (DMAbs). *Oncotarget*. (2019) 10:13–6. doi: 10.18632/oncotarget.26535
32. Esquivel RN, Patel A, Kudchodkar SB, Park DH, Stettler K, Beltramello M, et al. *In vivo* delivery of a DNA-encoded monoclonal antibody protects non-human primates against zika virus. *Mol Ther*. (2019) 27:974–85. doi: 10.1016/j.ymthe.2019.03.005
33. Perales-Puchalt A, Duperret EK, Yang X, Hernandez P, Wojtak K, Zhu X, et al. DNA-encoded bispecific T cell engagers and antibodies present long-term antitumor activity. *JCI Insight*. (2019) 4:126086. doi: 10.1172/jci.insight.126086
34. Liu J, Cao S, Kim S, Chung EY, Homma Y, Guan X, et al. Interleukin-12: an update on its immunological activities, signaling and regulation of gene expression. *Curr Immunol Rev*. (2005) 1:119–37. doi: 10.2174/1573395054065115
35. Tai Y, Wang Q, Korner H, Zhang L, Wei W. Molecular mechanisms of T cells activation by dendritic cells in autoimmune diseases. *Front Pharmacol*. (2018) 9:642. doi: 10.3389/fphar.2018.00642
36. Gao FS, Zhan YT, Wang XD, Zhang C. Enhancement of anti-tumor effect of plasmid DNA-carrying MUC1 by the adjuvanticity of FLT3L in mouse model. *Immunopharmacol Immunotoxicol*. (2018) 40:353–7. doi: 10.1080/08923973.2018.1498099
37. Curran MA, Montalvo W, Yagita H, Allison JP. PD-1 and CTLA-4 combination blockade expands infiltrating T cells and reduces regulatory T and myeloid cells within B16 melanoma tumors. *Proc Natl Acad Sci USA*. (2010) 107:4275–80. doi: 10.1073/pnas.0915174107
38. Curran MA, Allison JP. Tumor vaccines expressing flt3 ligand synergize with ctla-4 blockade to reject preimplanted tumors. *Cancer Res*. (2009) 69:7747–55. doi: 10.1158/0008-5472.CAN-08-3289
39. Curran MA, Kim M, Montalvo W, Al-Shamkhani A, Allison JP. Combination CTLA-4 blockade and 4-1BB activation enhances tumor rejection by increasing T-cell infiltration, proliferation, and cytokine production. *PLoS ONE*. (2011) 6:e19499. doi: 10.1371/journal.pone.0019499
40. Song S, Liu C, Wang J, Zhang Y, You H, Wang Y, et al. Vaccination with combination of Fit3L and RANTES in a DNA prime-protein boost regimen elicits strong cell-mediated immunity and antitumor effect. *Vaccine*. (2009) 27:1111–8. doi: 10.1016/j.vaccine.2008.11.095
41. Yo YT, Hsu KF, Shieh GS, Lo CW, Chang CC, Wu CL, et al. Coexpression of Flt3 ligand and GM-CSF genes modulates immune responses induced by HER2/neu DNA vaccine. *Cancer Gene Ther*. (2007) 14:904–17. doi: 10.1038/sj.cgt.7701081
42. Palucka K, Banchereau J. Cancer immunotherapy via dendritic cells. *Nat Rev Cancer*. (2012) 12:265–77. doi: 10.1038/nrc3258
43. Haile ST, Dalal SP, Clements V, Tamada K, Ostrand-Rosenberg S. Soluble CD80 restores T cell activation and overcomes tumor cell programmed death ligand 1-mediated immune suppression. *J Immunol*. (2013) 191:2829–36. doi: 10.4049/jimmunol.1202777
44. Horn LA, Long TM, Atkinson R, Clements V, Ostrand-Rosenberg S. Soluble CD80 protein delays tumor growth and promotes tumor-infiltrating lymphocytes. *Cancer Immunol Res*. (2018) 6:59–68. doi: 10.1158/2326-6066.CIR-17-0026
45. Walker LS, Sansom DM. Confusing signals: recent progress in CTLA-4 biology. *Trends Immunol*. (2015) 36:63–70. doi: 10.1016/j.it.2014.12.001
46. Duperret EK, Wise MC, Trautz A, Villarreal DO, Ferraro B, Walters J, et al. Synergy of immune checkpoint blockade with a novel synthetic consensus DNA vaccine targeting TERT. *Mol Ther*. (2018) 26:435–45. doi: 10.1016/j.ymthe.2017.11.010
47. Yan J, Harris K, Khan AS, Draghia-Akli R, Sewell D, Weiner DB. Cellular immunity induced by a novel HPV18 DNA vaccine encoding an E6/E7 fusion consensus protein in mice and rhesus macaques. *Vaccine*. (2008) 26:5210–5. doi: 10.1016/j.vaccine.2008.03.069
48. Yan J, Reichenbach DK, Corbitt N, Hokey DA, Ramanathan MP, McKinney KA, et al. Induction of antitumor immunity in vivo following delivery of a novel HPV-16 DNA vaccine encoding an E6/E7 fusion antigen. *Vaccine*. (2009) 27:431–40. doi: 10.1016/j.vaccine.2008.10.078

Conflict of Interest: JY, TS, KB, and LH are employees of Inovio Pharmaceuticals and as such receive salary and benefits, including ownership of stock and stock options. AT, KM, AW, TN, NC, EM, and CR are former employees of Inovio Pharmaceuticals.

frontiers in Immunology

REVIEW
published: 19 March 2020
doi: 10.3389/fimmu.2020.00460

Targeting Autophagy in Innate Immune Cells: Angel or Demon During Infection and Vaccination?

Sha Tao and Ingo Drexler*

Institute for Virology, Düsseldorf University Hospital, Heinrich-Heine-University, Düsseldorf, Germany

Innate immune cells are the "doorkeepers" in the immune system and are important for the initiation of protective vaccine responses against infection. Being an essential regulatory component of the immune system in these cells, autophagy not only mediates pathogen clearance and cytokine production, but also balances the immune response by preventing harmful overreaction. Interestingly, recent literature indicates that autophagy is positively or negatively regulating the innate immune response in a cell type-specific manner. Moreover, autophagy serves as a bridge between innate and adaptive immunity. It is involved in antigen presentation by delivering pathogen compounds to B and T cells, which is important for effective immune protection. Upon infection, autophagy can also be hijacked by some pathogens for replication or evade host immune responses. As a result, autophagy seems like a double-edged sword to the immune response, strongly depending on the cell types involved and infection models used. In this review, the dual role of autophagy in regulating the immune system will be highlighted in various infection models with particular focus on dendritic cells, monocytes/macrophages and neutrophils. Targeting autophagy in these cells as for therapeutic application or prophylactic vaccination will be discussed considering both roles of autophagy, the "angel" enhancing innate immune responses, antigen presentation, pathogen clearance and dampening inflammation or the "demon" enabling viral replication and degrading innate immune components. A better understanding of this dual potential will help to utilize autophagy in innate immune cells in order to optimize vaccines or treatments against infectious diseases.

Keywords: autophagy, dendritic cells, macrophages, innate immunity, adaptive immunity, vaccines and therapies against infectious diseases

OPEN ACCESS

Edited by:
Matthias Tenbusch,
University Hospital Erlangen, Germany

Reviewed by:
Eun-Kyeong Jo,
Chungnam National University, South Korea
Heinz Laubli,
University of Basel, Switzerland

****Correspondence:***
Sha Tao
sha.tao@med.uni-duesseldorf.de

Specialty section:
This article was submitted to Vaccines and Molecular Therapeutics, a section of the journal Frontiers in Immunology

Received: *13 December 2019*
Accepted: *28 February 2020*
Published: *19 March 2020*

Citation:
Tao S and Drexler I (2020) Targeting Autophagy in Innate Immune Cells: Angel or Demon During Infection and Vaccination? Front. Immunol. 11:460. doi: 10.3389/fimmu.2020.00460

INTRODUCTION

The awarding of the Nobel Prize in 2016 to Yoshinori Ohsumi reflects the importance of autophagy in human health and disease. Autophagy is a homeostatic degradation process that enables cells to survive in case of stress, like accumulation of misfolded proteins and damaged organelles or starvation and energy deprivation. Mammalian cells deliver those "unwanted" materials to lysosomes for degradation. Three major ways can be distinguished: microautophagy, chaperone-mediated autophagy, and macroautophagy. The latter has been intensively characterized in recent years because of its high impact on human health and disease (1). In this review, we will focus on macroautophagy, simply referred to as autophagy in the following.

The autophagic pathway has been widely discussed and reviewed (1–3). Here, only a brief summary will be provided, including the four major steps in the pathway: initiation, membrane elongation, maturation/fusion and degradation. In mammalian cells, after a strong stimulus such as starvation, autophagosomes initiate as omegasomes at the endoplasmic reticulum (ER). Autophagy can be induced by two different arms of upstream signaling based on either mammalian target of rapamycin (mTOR) inactivation or adenosine monophosphate (AMP) activated protein kinase (AMPK) activation which leads to distinct Unc-51-like autophagy activating kinase 1 (ULK1) activation. mTOR typically responds to nutrient signals while AMPK responds to the energy status of the cell. Two protein complexes are important for phagophore formation: ULK and PI3K (phosphoinositide 3-kinase catalytic subunit type III) complex. The ULK complex consists of autophagy-related (ATG)13, FIP200, ATG101, and ULK1. The PI3K complex comprises Beclin1, VPS34 (vacuolar protein sorting 34), VPS15 and ATG14L. Furthermore, two ubiquitin-like (UBL) conjugation complexes are important for the membrane extension. One is ATG16L1 complex, in which ATG12 is conjugated to ATG5 and then bind to ATG16L1. This facilitates another ubiquitin cascade involving ATG7 and ATG3, namely microtubule-associated protein 1A/1B-light chain 3 (LC3/ATG8) lipidation (conjugation to phosphatidylethanolamine-PE). LC3-PE mediates membrane tethering and fusion to extend the isolation membrane by recruiting membranes from multiple sources, leading to the formation of autophagosomes. During the final maturation, autophagosomes are decorated with Rab7 and tail-anchored SNAP receptor (SNARE) syntaxin 17 (STX17), which leads to the fusion with lysosomes and degradation of sequestered substrates (**Figure 1**). Recent findings suggest that autophagy can also occur in the absence of some key autophagy-related proteins (ATGs) through unconventional autophagy pathways, also called "non-canonical autophagy" (4–6). Furthermore, the double membrane does not necessarily elongate from a single source. Such variation gives alternatives to recognize or eliminate pathogens, for instance, receptor mediate internalization and LC3-associated phagocytosis (LAP).

The immune system is a big network with crosstalk of cells from innate and adaptive immunity. Autophagy is a key mechanism against invading bacteria, parasites, and viruses in innate immune cells including monocytes/macrophages, dendritic cells (conventional dendritic cells-cDCs and plasmacytoid dendritic cells-pDCs) and neutrophils. In the past few years, a number of studies have highlighted the potential

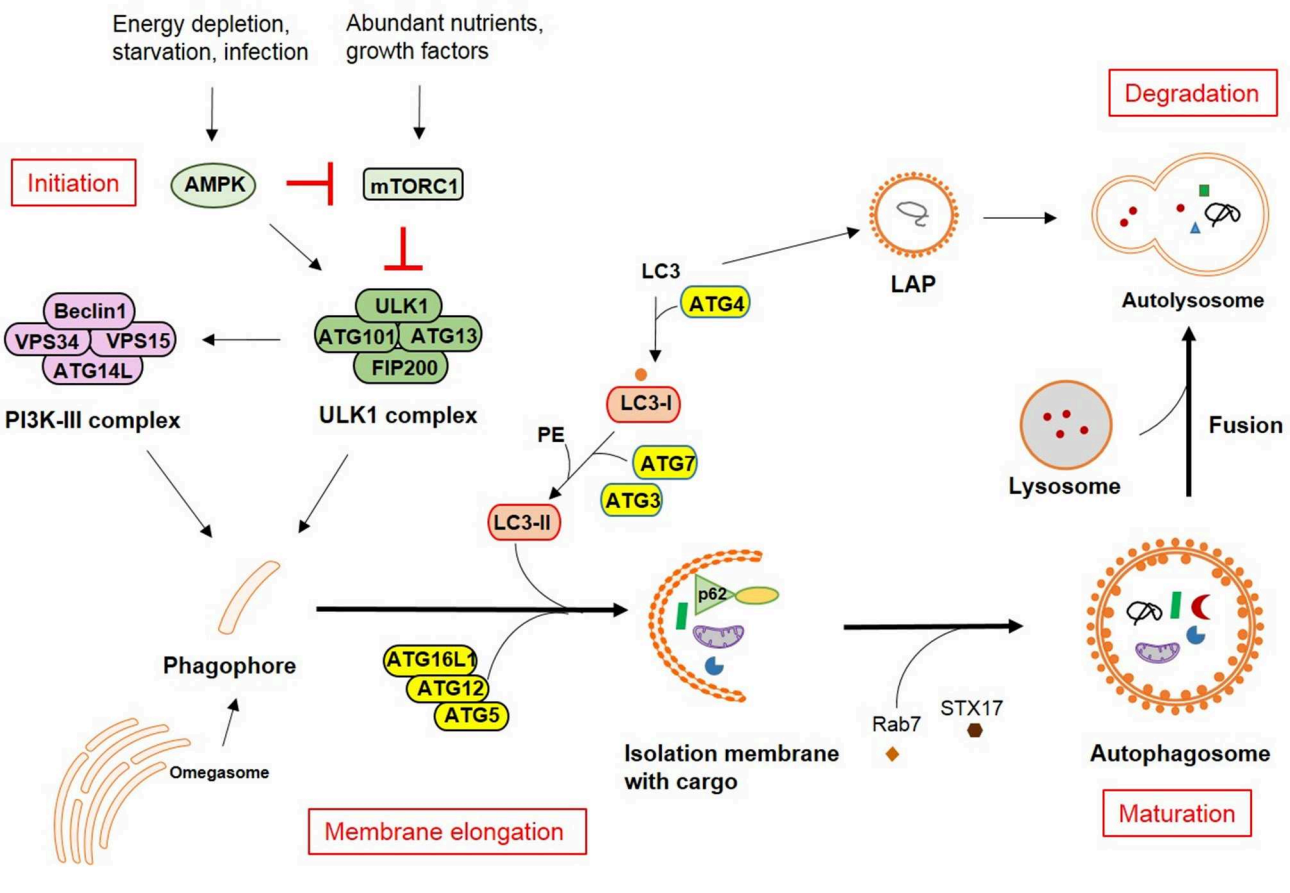

FIGURE 1 | Autophagy pathways in mammalian cells. The molecular pathway comprised of the core autophagy-related proteins (ATGs) is illustrated together with the respective associated autophagy membrane compartments. The four major steps in the autophagolysosomal pathway are indicated in red.

of targeting autophagy for the control of infections. These data combined with the emerging role of autophagy for immune impairment in some infectious diseases have attracted significant interest in developing autophagy modulators or targets as a new approach for vaccination.

VACCINES TARGETING AUTOPHAGY FOR EFFECTIVE ANTIGEN PROCESSING AND PRESENTATION

DCs as one of most potent professional antigen-presenting cells (APCs) bridge between the innate and adaptive immune system. They are particularly critical for naïve T cell activation and drive protective immunity against infection. An increasing number of recent studies have characterized the involvement of autophagy in various DC functions in physiological as well as pathological context (7), especially with regard to T cell activation (8, 9) (**Figure 2**).

Autophagy has been shown to be involved in antigen processing and presentation in DCs, especially for MHC class II restricted peptides. Those peptides are often derived from lysosomal degradation, either from LAP (non-canonical pathway) (10) or from macroautophagy (canonical pathway). In the latter, cytosolic antigens are recognized by a group of SQSTM1-like receptors (SLRs) such as p62, NDP52, OPTN or NBR1. This selective form of autophagy is also called "xenophagy" (3, 11). SLRs serve as links to ubiquitin (tagged with substrates) and LC3 homologs on the autophagosomal membrane. Peptides are further loaded on MHC class II in late endosomal MHC class II containing compartments (MIIC) (12). LAP involves single-membraned phagosomes, but also leads to MHC class II presentation (5). As a result, it is not surprising that autophagy promoted MHC class II antigen presentation to CD4+ T cells in various infection models, such as modified vaccinia virus Ankara (13) or herpes simplex virus 1 (HSV-1) (14–17) or was able to enhance cytokine production by CD4+ T cells in *Toxoplasma gondii* (*T. gondii*) (18) or respiratory syncytial virus (RSV) infection (19). Indeed, enabling access of antigens to autophagolysosomes by genetic engineering to link them to key components like LC3-II, greatly enhanced vaccine efficacy. For instance, human immunodeficiency virus-1 (HIV-1) Gag and Env fail to colocalize with LC3 containing vesicles during infection. However, once antigens were targeted to LC3b, the autophagic degradation process was enhanced and could efficiently stimulate CD4+ T cell responses (20, 21). Besides, autophagy also indirectly promoted antigen presentation by benefitting lysosomal enzyme activity during HIV-1 infection (22). Further examples include the conjugation of influenza A virus (IAV) matrix protein 1 (M1) to LC3 in DCs which led to enhanced antigen-specific CD4+ T cell responses (23). Japanese encephalitis (JEV) prM and E proteins fused to LC3 (pJME-LC3 DNA vaccine) allowed for increased T cell responses and long lasting antibody-mediated protection after immunization (24).

In addition to MHC class II presentation to CD4+ T cells, autophagy in several APCs has been considered to contribute to MHC class I presentation to CD8+ T cells. Indeed, pDCs (25) as well as some subtypes of macrophages (26) showed potential for antigen capture and processing, and promoted T cell priming in infection models. Viral peptides derived from autophagosomes were further processed by proteasomes in HIV-1 infected macrophages (27). The MHC class I presentation of human cytomegalovirus (HCMV) protein pUL138-derived peptide epitopes was autophagy-mediated and TAP-independent (28). H1N1 infected bone marrow-derived DCs (BMDCs) were activating strong CD4+ T cell proliferation and additionally, were more efficiently cross-presenting antigen to CD8+ T cells (29). All these reports suggest an interaction between vacuolar and MHC class I presentation pathways. Dribbles are autophagosomal structures derived from tumor cells after proteasomal inhibition and are currently tested as tools to enhance cross-presentation. Human DCs loaded with DRibbles isolated from tumor cells expressing CMV peptide epitopes were significantly more efficient in stimulating CD8+ memory T cells (30). Similarly, DCs loaded with DRibbles containing CMV proteins revealed a superior ability to induce CMV-specific T cells (31).

Among SLRs, p62 and NDP52 are considered most important for pathogen recognition through autophagy. p62 delivers ubiquitinated *Mycobacterium tuberculosis* (Mtb) proteins into

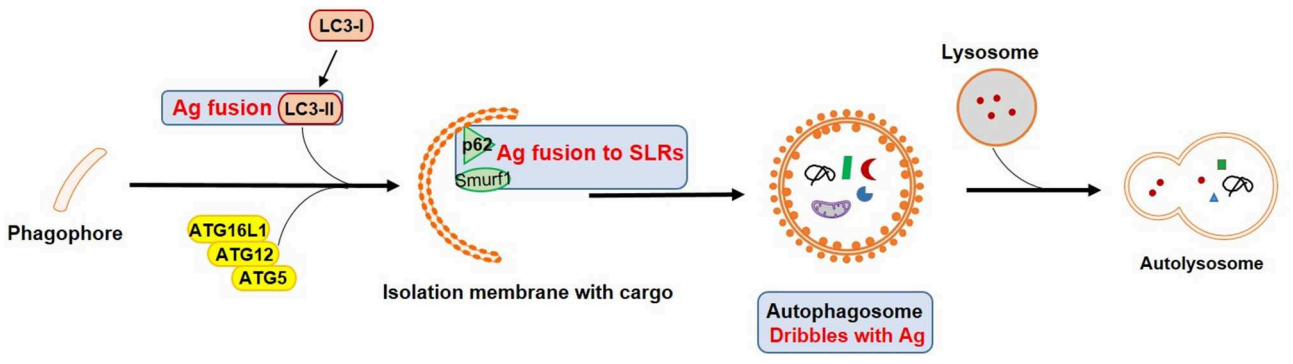

FIGURE 2 | Vaccines targeting autophagy for enhanced antigen processing and presentation. Blue squares mark important autophagy components that could be targets in APCs for vaccine design by enhancing antigen presentation and T cell activation. Ag refers to antigen.

autolysosomes for clearance (32, 33), while clearance of Bacillus anthracis is based on rapid induction of LC3 conversion, Beclin1 expression and p62-mediated degradation in neutrophils (34). Redirection of vaccine antigens from proteasomal degradation into autophagosomal pathways could increase the generation and variability of antigen-specific T cells. Fusion of HIV-1 Gagp24 to the selective autophagy receptor sequestosome 1 (SQSTM1)/p62 complex enhanced antigen delivery and increased antigen-specific T cell responses in comparison to Gagp24 alone (35). The connection of p62 and autophagy is highly conserved between species and could be an interesting candidate for T-cell-based vaccine strategies in humans. More recently, another recognition molecule in selective autophagy captured attention regarding autophagy-mediated host defense against infection. Smurf1 is an E3 ubiquitin ligase and a key component in autophagic targeting of Mtb in macrophages supporting host defense *in vivo* (36) which may suggest a new potential target for enhancing xenophagic degradation.

Recently, a self-assembling peptide vaccine in which the amphipathic peptide KFE8 (FKFEFKFE) was either combined with MHC class II restricted epitopes from Mtb Ag85B or MHC class I restricted peptides from ovalbumin. These conjugate vaccines were tested *in vitro* in APCs with known ability to induce strong antibody and cellular responses to conjugated antigens. Interestingly, both variations were processed through autophagy and displayed a highly efficient antigen presentation capacity to T cells (37). However, the vaccine efficacy still needs to be established *in vivo* and for other target antigens.

ADJUVANTS THAT ENHANCE VACCINE EFFICIENCY THROUGH AUTOPHAGY

Some vaccines are derived from attenuated strains of pathogens. Deleting virulence genes increases the vaccine safety but sometimes also reduces immunogenicity, especially when the lost genes are associated with autophagy functions. In order to enhance vaccine efficacy, the boosting of host immune responses with adjuvants which induce autophagy may increase phagocytosis and clearance of pathogens as well as antigen presentation by innate immune cells (**Figure 3**).

For instance, Bacillus Calmette-Guerin (BCG) representing a live attenuated strain from *Mycobacterium tuberculosis* (Mtb) is still used as a vaccine for tuberculosis (TB). However, it's efficiency varies and is especially low in adults. Therefore, vaccine adjuvants have gained great interest to improve BCG vaccines. Compared to Mtb, the attenuated BCG lacks a functional ESX-1 system (secreting ESAT-6 and CFP-10). This system allows cytosolic components of ubiquitin-mediated autophagy to access phagosomes and to free contained mycobacteria which supports bacterial evasion from xenophagic elimination (38) and reduces antigen presentation (39). Combination of BCG vaccines with autophagy inducers or with peptides from the above mentioned

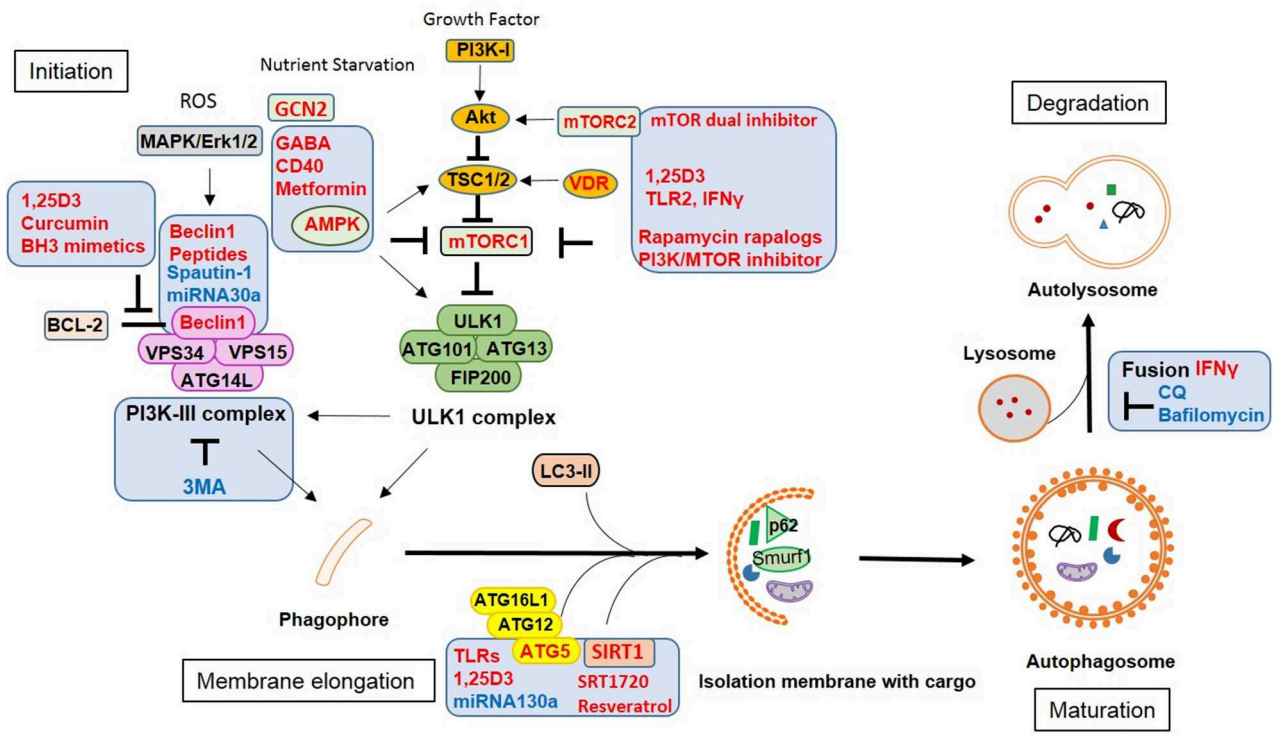

FIGURE 3 | Vaccine adjuvants and therapeutic strategies against infection by modulating autophagy. Approaches or targets aiming to enhance autophagy are labeled in red, those inhibiting autophagic functions are labeled in blue.

virulence proteins showed better protection *in vivo* than BCG alone. A BCG vaccine that overexpressed immunogenic Ag85B has been proven superior compared to the wild-type BCG vaccine. Particularly, additional application of rapamycin enhanced Ag85B-specific MHC class II presentation by DCs via autophagy and thus increased vaccine efficacy (40). An autophagy inducing and TLR2 activating C5 peptide from Mtb-derived CFP-10 protein was overexpressed in BCG in combination with Ag85B (BCG^{85C5}). This recombinant BCG^{85C5} induced robust LC3-dependent autophagy in macrophages which increased antigen presentation to CD4+ T cells *in vitro* and enhanced effector and central memory T cell responses *in vivo* (39). Accordingly, a recombinant BCG ΔureC::hly(+) (rBCG) vaccine with enhanced AIM2 inflammasome activation and autophagy was more efficient against TB in preclinical animal models than parental BCG (41). Consequently, triggering other synergistic innate pathways in conjunction with autophagy should boost the immune response and vaccine efficacy.

DCs play a key role for antigen presentation and T cell induction during viral infections. Autophagy has been shown to be involved in DC maturation during RSV infection (42) which enabled DCs to migrate to secondary lymphoid tissues, interact with naïve T cells and trigger effector T cell responses (43). HIV-1 protein Env has been proposed to downregulate autophagy by activating mTOR and reducing lysosomal enzyme activity in DCs, thereby inhibiting antigen presentation and enhancing the transfer of infection into CD4+ T cells (22, 44). However, viral inhibition was bypassed by rapamycin-mediated stimulation of autophagy in DCs and restored CD4+ T cell responses (44). Starvation is an efficient way to induce autophagy. By activating the cellular starvation sensor general control non-derepressible 2 (GCN2) kinase, yellow fever vaccine YF-17D induced autophagy in human DCs which operated via the induction of cell death in infected "donor" cells and the enhanced uptake by bystander DCs through LAP, which subsequently resulted in enhanced antigen presentation and robust T cell responses (45). Beclin1, one important component of canonical autophagy also proved to act as a potent vaccine adjuvant. By enhancing autophagy-mediated antigen presentation, a combinatory HPV-16 E7/Beclin1 DNA vaccine led to superior lymphocyte proliferation and cytotoxicity as compared to the HPV-16 E7 DNA vaccine alone (46).

Additional to traditional adjuvants inducing autophagy such as rapamycin, several drugs may be repurposed from their original usage (e.g., against cancer or diabetes), since they activate autophagy and increase vaccine-specific immune responses. For instance, curcumin is known for inducing autophagy in tumor cells and is currently tested for tumor therapy. Due to its poor intestinal absorption and rapid metabolism, this drug has clinical limitations. However, a recent paper demonstrated that a nanoparticle-formulated version of curcumin could overcome these limitations and optimized various APC functions including autophagy and finally enhanced BCG vaccine efficacy by inducing central memory T cell as well as Th1 and Th17 responses (47). Another biological, the antioxidant glutathione (GSH), improved BCG vaccination by increasing autophagy and the production of IFNγ and TNFα which prevented loss of T cells by decreasing the expression of PD-1 (48). However, those adjuvants have not been widely used in other infection models and the effect could be pathogen-specific.

THERAPEUTIC APPROACHES AGAINST INFECTIONS BY MODULATING AUTOPHAGY

Since autophagy has important functions in innate and adaptive immunity, it is not surprising that pathogens employ autophagy to escape the host immune response. In macrophages, the Gram-positive bacteria *Listeria monocytogenes* (Lm), mycobacteria (Mtb) including BCG, and parasites such as *Toxoplasma gondii* (*T. gondii*) are well-studied intracellular pathogens that have different strategies to utilize autophagy for long-term survival or replication (49), while LAP (5) as well as xenophagy (11) usually result in bacterial degradation by lysosome fusion. However, Lm masks its surface with ActA and InlK to avoid recognition (50, 51), while Mtb evades killing by CpsA which prevents a robust oxidative response (ROS) and further leads to LAP (52). To bypass these defects, treatment of innate immune cells with autophagy inducers could enhance pathogen killing (**Figure 3**). Common therapies include adenosine monophosphate–activated protein kinase (AMPK) modulators. CD40 may stimulate autophagic killing of *T. gondii* in macrophages via calcium/calmodulin-dependent kinase kinase ß (CaMKKß), AMPK and ULK1 (53) and subsequent fusion of vacuoles and late lysosomes (54). Gamma-aminobutyric acid (GABA) or GABAergic drugs promote autophagy via intracellular calcium release and AMPK signaling resulting in enhanced phagosomal maturation and subsequently antimicrobial responses against mycobacterial infection (55). The U.S. Food and Drug Administration (FDA)-approved antidiabetic drug metformin increases the production of mitochondrial reactive oxygen species (ROS) and facilitates phagosome-lysosome fusion which has been shown to limit Mtb growth and to reduce chronic inflammation in infected mice (56).

Another option to enhance autophagy is through vitamin D receptor (VDR) activation and cathelicidin induction. The active form of vitamin D, 1,25-dihydroxyvitamin D3 (1,25D3), induces autophagy in human monocytes and activates transcription of the autophagy-related genes Beclin1 and ATG5 (57). A combination of retinoic acid (RA) and vitamin D3 (VD) (RAVD) enhanced the levels of DC-SIGN and mannose receptors on THP-1 macrophages which increased mycobacterial uptake and inhibited the subsequent intracellular growth of Mtb by inducing ROS and autophagy (58). TLR2/1/CD14 stimulation activates antibacterial autophagy through VDR and cathelicidin in human primary monocytes (59). Additionally, some effector cytokines such as IFNγ activate autophagy in macrophages. IFNγ treated macrophages could overcome the inhibition of phagosome-lysosome fusion by Mtb and controlled intracellular Mtb growth (60). In severely ill TB patients, IFNγ as well as Th1 and Th17 immune responses are required to eliminate Mtb. Interestingly, IL17a alone was unable to augment autophagy because of a disease-associated defect in MAPK1/3 signaling. Adding IFNγ to IL17a increased autophagy levels in the patients'

monocytes resulting in strong immunity to Mtb and promoting mycobacterial killing (61).

Though autophagy plays a key role in macrophages and neutrophils for pathogen clearance through xenophagy or LAP, it is still unclear how phagosomes trigger autophagy. One paper suggests a connection to TLR signaling, but this has not been investigated in infectious context (62). Autophagy may not always work best to eliminate pathogens. Previous reports have shown that phagocytosis of Escherichia coli triggers the autophagic machinery in neutrophils (63). On the other hand, autophagy may reduce the phagocytosis rate of mycobacteria in murine macrophages (64) and neutrophils (65). The reduced internalization is due to decreased expression of two class A scavenger receptors, namely macrophage receptor with collagenous structure (MARCO) and macrophage scavenger receptor 1 (MSR1) (66). Therefore, pharmacological modulation of autophagy should aim to target both, autophagy and phagocytosis, and should be carefully designed for each pathogen.

Clearing blood-borne pathogens is a hallmark feature of the spleen. In this secondary lymphoid organ, pDCs and red pulp macrophages efficiently cleared malaria parasites after boosting autophagy with rapamycin (67, 68). The treatment enhanced antigen presentation in these cells and shifted the cytokine and chemokines profile *in vivo* which recruited effector cells into the spleen and enhanced T cell responses. Thus, targeting autophagy in pDCs and red pulp macrophages may open new prospects for the development of novel antimalarial drugs.

When it comes to viral infection, some viral proteins directly inhibit autophagy. For instance, HIV-1 Nef is interacting with Beclin1 which blocks the late stage of autophagy in macrophages, thereby protecting virus particles from degradation (69). That is able to suppress IFNγ-induced autophagy in infected macrophages (70) as well as in bystander macrophages through Src-Akt and STAT3 signaling (71). Rescue of autophagy function could be a novel approach to prevent and treat HIV-1 infection and related opportunistic infections. The PI3K/MTOR inhibitor (dactolisib) and PI3K/MTOR/BRD4 inhibitor (SF2523, JQ1) restrain HIV replication through degradative autophagy without altering the initial susceptibility of macrophages to infection (72). Low vitamin D levels in HIV-1 infected patients are associated with more rapid disease progression and increased risk for other infections such as Mtb. 1,25D3 targets multiple steps in autophagy and inhibits HIV replication and mycobacterial growth in co-infected human macrophages through the induction of autophagy (73). In RSV infection, Sirtuin 1 (SIRT1) an NAD+ dependent deacetylase regulates autophagy depending on the nutrient status. SIRT1 may induce autophagy directly by deacetylating TAG5 and 7 and LC3. Activated DCs produce crucial cytokines promoting antiviral Th1 responses, while pathologic Th2 and Th17 responses are suppressed during infection (74). SIRT1 inducers like SRT1720 could be a therapeutic alternative for RSV patients.

Autophagy may have distinct functions depending on the stage of infection or the host cell type infected (75, 76). In the early phase of HSV-1 infection, autophagy was found to be transiently induced in human THP-1 cells favoring viral replication (77). In the later phase, however, viral protein ICP34.5 blocked the maturation of autophagosomes which reduced viral antigen presentation by DCs (17). Alternatively, human gamma herpesviruses EBV and KSHV regulate autophagy in immune cells during *de novo* infection, while autophagy plays a distinct role in chronic murine gamma herpesvirus 68 (MHV-68) infection by triggering virus reactivation from latency (78). Thus, opposing effects of the same drug may occur depending on the infection settings. While rapamycin induces killing of Mtb in macrophages, it supports Mtb growth during low-dose and controlled infection when co-infected with HIV-1 by interfering with phagosomal maturation (35). Therefore, a detailed knowledge of how pathogens modulate autophagy during the infection cycle will help to develop more specific targets for autophagy-based strategies against infectious diseases.

Various viral virulence factors such as ICP34.5 (HSV-1), Nef (HIV-1), or M11 (MHV-68) have been shown to specifically interact with autophagy-related proteins such as Beclin1 to exploit autophagy for viral replication. New therapy approaches that target specific components of autophagy pathways, which are manipulated by pathogens, should maximize clinical benefits while minimizing toxicity. For instance, an autophagy inducing cell-permeable peptide (Tat–Beclin1) has been generated by mapping the functional region of Beclin1 with the HIV-1 Tat transduction domain (PTD). Therapeutic application of Tat-Beclin1 was associated with reduced HIV-1 replication, decreased intracellular survival of the bacterium Lm in human macrophages and reduced mortality of mice infected with chikungunya or West Nile virus (79). Inhibitors of interactions between viral and autophagic proteins may also have potential benefits for the prevention and treatment of a broad range of human diseases. Bcl-2 binds to Beclin1 preventing assembly of pre-autophagosomal structures which inhibits autophagy. This interaction involves a Bcl-2 homology 3 (BH3) domain in Beclin1. Proteins containing BH3 domains such as BH3 mimetics (80, 81) can competitively disrupt the interaction between Beclin1 and Bcl-2 and thereby induce autophagy (82). Another example is MHV-68 M11 which binds to one BH3 domain of Beclin1 and inhibits autophagy. Alternatively, a Beclin1 BH3 domain-derived peptide which selectively binds to M11, but not to Bcl-2, abrogated M11-mediated down-regulation of autophagy (83) (**Figure 3**).

Autophagy is additionally regulated by mitochondrial integrity and contributes to the elimination of damaged organelles. Autophagy may selectively degrade inflammasome components such as NLRP3 and products such as Pro-IL1ß (84) thereby limiting the secretion of pro-inflammatory cytokines. As a result, the dampening of inflammation is another important role of autophagy in innate immune cells which so far has been exclusively shown in myeloid cells. For instance, loss of autophagy-related proteins in macrophages causes massive inflammation after infection which may lead to host tissue damage such as lung injury in IAV (85, 86) and Mtb infection (87) as well as in pseudomonas aeruginosa-driven abdominal infection (88). Autophagy also helps to curtail virus-induced systemic inflammation by creating an environment that prevents host injury mediated by pro-inflammatory cytokines.

Trichostatin A (TSA), an autophagy inducer used to reduce systemic inflammation and to attenuate sepsis-induced organ injury, promotes M2 polarization in peritoneal macrophages and ultimately improved the survival of mice with polymicrobial sepsis (89). In some autoimmune diseases such as inflammatory bowel disease (IBD), the containment of inflammation may prevent the development of disease and reduce the risk of infections. Enhancing autophagy may be therapeutically beneficial by regulating inflammation and clearing intestinal pathogens. Recently, IL-10 was reported to induce mitophagy (autophagy-mediated mitochondria degradation) to prevent accumulation of dysfunctional mitochondria and production of mitochondrial ROS in macrophages from IBD patients (90) (**Figure 3**).

THERAPEUTIC STRATEGIES AIMING TO INHIBIT AUTOPHAGY TO BLOCK VIRUS REPLICATION AND IMMUNE EVASION

Autophagy seems to be an angel for most infection scenarios, except for two: first, autophagy may benefit virus replication rather than support host immune protection as seen for flaviviruses. Second, autophagy may degrade components of innate immune pathways which negatively affects innate sensing of pathogens and antiviral cytokine production. The former represents a potential therapeutic target for several (re-)emerging diseases for which we currently have no vaccine available due to rapid spread and high virulence. The latter is exemplified by multiple targets in the cGAS/STING DNA sensing pathway aiming to halt IFN production. A direct interaction between cGAS and Beclin1 has been described in macrophages during HSV-1 infection (91). Similarly, p62-mediated degradation of cGAS in HSV-1 and VSV infection (92) as well as poxin-mediated cGAMP degradation by various poxviruses has been reported (93). The latter has not been associated with autophagy so far, but the therapeutic potential of any autophagy modulator that may arise from these studies has not been assed and molecular mechanisms still need to be elucidated.

Some viruses induce autophagy for their own replication by taking advantage of membrane structures produced in this process as reported for flaviviruses [hepatitis C virus (HCV), dengue virus (DENV), zika virus (ZIKV)] or hepatitis B virus (HBV) (94). For viruses that infect specific organs or tissues like HBV or HCV, tissue-specific targeting of autophagy e.g., hepatocytes, would be favorable. HCV genomic RNA is recognized by RIG-I, MDA5 and TLRs to activate IFN signaling and pro-inflammatory cytokine secretion. HCV induces autophagy in hepatocytes which enables its replication and trafficking, additionally, attenuates the innate immune response by viral proteins NS3 and NS5A (95). Consequently, knockdown of autophagy-related proteins (Beclin1 or ATG7) in immortalized human hepatocytes (IHH) could inhibit HCV growth (96) and block exosome-mediated virus transmission (97).

For DENV and ZIKV, some autophagy pathway components are crucial for replication including maturation and packaging. The induction of autophagy by ZIKV appears to be linked to the activation of AMPK, while DENV induces autophagy by activation of VPS34 (98). USP10 and USP13 are needed to reverse ubiquitination and subsequently degradation of the Beclin1-VPS34-ATG14 complex. Targeting this complex by Spautin1 which inhibits the deubiquitination activity of the two molecules inhibited DENV infection (99). In innate immune cells, the pro-inflammatory cytokine macrophage migration inhibitory factor (MIF) induces autophagy and facilitates DENV replication. Inhibition of MIF-induced autophagy by minocycline might represent an alternative therapeutic approach against DENV infection (100). Pharmacological inhibitors of autophagolysosomal activity such as chloroquine (CQ) prevents endosomal viral RNA release and autophagy-dependent viral replication and is currently used to prevent maternal to fetal transmission of ZIKV (101–103) (**Figure 3**).

MicroRNAs (miRNAs) represent a new tool to regulate autophagy by specifically targeting the expression of autophagy-related genes. They bind to the target mRNA through specific base-pairing interactions between the "seed" region of miRNA and sites within coding and untranslated regions (UTRs) of mRNAs, especially 3′UTRs, to suppress gene expression. Several miRNAs have been shown to augment or repress virus replication through interfering with autophagy. Therefore, manipulation of cellular miRNAs which target autophagy components represent a novel approach for purging pathogens. Administration of miRNA130a diminished HCV replication by interfering with ATG5-dependent autophagy (104), while miRNA146a targets TRAF6 which blocked DENV-induced autophagy in THP-1 cells (105). Enterovirus 71 (EV71)-induced autophagy is mediated by Beclin1 which contains a potential binding site for miRNA30a. By using a miRNA30a mimic, EV71 replication was suppressed by blocking virus-induced autophagy (106). This therapeutic approach is widely used in the tumor field, but the options for different pathogens may vary, since miRNA expression is altered during conditions of stress and disease (**Figure 3**).

FUTURE PROSPECTS

Innate immune cells are the first line of defense against infection. Targeting autophagy in those cells is an attractive approach to augment vaccination efficacy or to improve immunotherapeutic strategies against infectious diseases. Vaccines which are based on genetic fusion of antigens to important components of autophagy pathways improved adaptive immune responses by enhancing antigen processing and presentation in APCs. Combination with autophagy modulators as adjuvants has been proven to further boost host immune responses by triggering innate immunity as well as increasing immune cell functions such as cytokine/chemokine production, maturation, and migration. Pharmacological induction of autophagy could increase pathogen clearance in phagocytes through xenophagy or LAP. Furthermore, given the potent anti-inflammatory effect associated with autophagy, employing autophagic functions in myeloid cells might also help to control infections in some

autoimmune diseases. The functions or effector mechanisms exerted by or related to autophagy during infection may vary among cell types, the type of pathogen or the stage of infection. The impact of autophagy goes beyond single cell types and involves intensive cross-talk within the whole immune system and therapeutic strategies may have to be determined individually for a given pathogen. Future studies will have to focus on investigating the role of autophagy for pathogen–host-specific interplay *in vivo* and identify relevant steps in the course of infection in which the targeting of autophagy—possibly in selected cell types—proves to be most efficient for pathogen clearance and protection. This will allow to develop new strategies for vaccines or therapeutic approaches with optimized efficacy against infectious diseases and help to minimize unwanted off-target effects or toxicity.

AUTHOR CONTRIBUTIONS

ST and ID wrote the manuscript. ST generated images.

FUNDING

This work was supported by research funding from the Deutsche Forschungsgemeinschaft (DFG) grant 1949/1 to ID, the European Union grant 812915 VacPath to ID, and the MOI III Graduate School.

REFERENCES

1. Kuballa P, Nolte WM, Castoreno AB, Xavier RJ. Autophagy and the immune system. *Annu Rev Immunol*. (2012) 30:611–46. doi: 10.1146/annurev-immunol-020711-074948
2. Ma Y, Galluzzi L, Zitvogel L, Kroemer G. Autophagy and cellular immune responses. *Immunity*. (2013) 39:211–27. doi: 10.1016/j.immuni.2013.07.017
3. Choi Y, Bowman JW, Jung JU. Autophagy during viral infection - a double-edged sword. *Nat Rev Microbiol*. (2018) 16:341–54. doi: 10.1038/s41579-018-0003-6
4. Codogno P, Mehrpour M, Proikas-Cezanne T. Canonical and non-canonical autophagy: variations on a common theme of self-eating? *Nat Rev Mol Cell Biol*. (2011) 13:7–12. doi: 10.1038/nrm3249
5. Munz C. Non-canonical functions of macroautophagy proteins during endocytosis by myeloid antigen presenting cells. *Front Immunol*. (2018) 9:2765. doi: 10.3389/fimmu.2018.02765
6. Gui X, Yang H, Li T, Tan X, Shi P, Li M, et al. Autophagy induction via STING trafficking is a primordial function of the cGAS pathway. *Nature*. (2019) 567:262–6. doi: 10.1038/s41586-019-1006-9
7. Ghislat G, Lawrence T. Autophagy in dendritic cells. *Cell Mol Immunol*. (2018) 15:944–52. doi: 10.1038/cmi.2018.2
8. Munz C. Autophagy beyond intracellular MHC class II antigen presentation. *Trends Immunol*. (2016) 37:755–63. doi: 10.1016/j.it.2016.08.017
9. Merkley SD, Chock CJ, Yang XO, Harris J, Castillo EF. Modulating T cell responses via autophagy: the intrinsic influence controlling the function of both antigen-presenting cells and T Cells. *Front Immunol*. (2018) 9:2914. doi: 10.3389/fimmu.2018.02914
10. Romao S, Munz C. LC3-associated phagocytosis. *Autophagy*. (2014) 10:526–8. doi: 10.4161/auto.27606
11. Sharma V, Verma S, Seranova E, Sarkar S, Kumar D. Selective autophagy and xenophagy in infection and disease. *Front Cell Dev Biol*. (2018) 6:147. doi: 10.3389/fcell.2018.00147
12. Blum JS, Wearsch PA, Cresswell P. Pathways of antigen processing. *Annu Rev Immunol*. (2013) 31:443–73. doi: 10.1146/annurev-immunol-032712-095910
13. Thiele F, Tao S, Zhang Y, Muschaweckh A, Zollmann T, Protzer U, et al. Modified vaccinia virus Ankara-infected dendritic cells present $CD4^+$ T-cell epitopes by endogenous major histocompatibility complex class II presentation pathways. *J Virol*. (2015) 89:2698–709. doi: 10.1128/JVI.03244-14
14. Lee HK, Mattei LM, Steinberg BE, Alberts P, Lee YH, Chervonsky A, et al. In vivo requirement for Atg5 in antigen presentation by dendritic cells. *Immunity*. (2010) 32:227–39. doi: 10.1016/j.immuni.2009.12.006
15. Gobeil PA, Leib DA. Herpes simplex virus gamma34.5 interferes with autophagosome maturation and antigen presentation in dendritic cells. *MBio*. (2012) 3:e00267–12. doi: 10.1128/mBio.00267-12
16. Jiang Y, Yin X, Stuart PM, Leib DA. Dendritic cell autophagy contributes to herpes simplex virus-driven stromal keratitis and immunopathology. *MBio*. (2015) 6:e01426–15. doi: 10.1128/mBio.01426-15
17. Budida R, Stankov MV, Dohner K, Buch A, Panayotova-Dimitrova D, Tappe KA, et al. Herpes simplex virus 1 interferes with autophagy of murine dendritic cells and impairs their ability to stimulate CD8(+) T lymphocytes. *Eur J Immunol*. (2017) 47:1819–34. doi: 10.1002/eji.201646908
18. Liu E, Van Grol J, Subauste CS. Atg5 but not Atg7 in dendritic cells enhances IL-2 and IFN-gamma production by *Toxoplasma gondii*-reactive CD4+ T cells. *Microbes Infect*. (2015) 17:275–84. doi: 10.1016/j.micinf.2014.12.008
19. Reed M, Morris SH, Jang S, Mukherjee S, Yue Z, Lukacs NW. Autophagy-inducing protein beclin-1 in dendritic cells regulates CD4 T cell responses and disease severity during respiratory syncytial virus infection. *J Immunol*. (2013) 191:2526–37. doi: 10.4049/jimmunol.1300477
20. Jin Y, Sun C, Feng L, Li P, Xiao L, Ren Y, et al. Regulation of SIV antigen-specific CD4+ T cellular immunity via autophagosome-mediated MHC II molecule-targeting antigen presentation in mice. *PLoS ONE*. (2014) 9:e93143. doi: 10.1371/journal.pone.0093143
21. Coulon PG, Richetta C, Rouers A, Blanchet FP, Urrutia A, Guerbois M, et al. HIV-infected dendritic cells present endogenous MHC class II-restricted antigens to HIV-specific CD4+ T cells. *J Immunol*. (2016) 197:517–32. doi: 10.4049/jimmunol.1600286
22. Harman AN, Kraus M, Bye CR, Byth K, Turville SG, Tang O, et al. HIV-1-infected dendritic cells show 2 phases of gene expression changes, with lysosomal enzyme activity decreased during the second phase. *Blood*. (2009) 114:85–94. doi: 10.1182/blood-2008-12-194845
23. Schmid D, Pypaert M, Munz C. Antigen-loading compartments for major histocompatibility complex class II molecules continuously receive input from autophagosomes. *Immunity*. (2007) 26:79–92. doi: 10.1016/j.immuni.2006.10.018
24. Zhao F, Zhai Y, Zhu J, Xiao P, Feng G. Enhancement of autophagy as a strategy for development of new DNA vaccine candidates against Japanese encephalitis. *Vaccine*. (2019) 37:5588–95. doi: 10.1016/j.vaccine.2019.07.093
25. Villadangos JA, Young L. Antigen-presentation properties of plasmacytoid dendritic cells. *Immunity*. (2008) 29:352–61. doi: 10.1016/j.immuni.2008.09.002
26. Sheng J, Chen Q, Soncin I, Ng SL, Karjalainen K, Ruedl C. A Discrete subset of monocyte-derived cells among typical conventional type 2 dendritic cells can efficiently cross-present. *Cell Rep*. (2017) 21:1203–14. doi: 10.1016/j.celrep.2017.10.024
27. English L, Chemali M, Duron J, Rondeau C, Laplante A, Gingras D, et al. Autophagy enhances the presentation of endogenous viral antigens on MHC class I molecules during HSV-1 infection. *Nat Immunol*. (2009) 10:480–7. doi: 10.1038/ni.1720
28. Tey SK, Khanna R. Autophagy mediates transporter associated with antigen processing-independent presentation of viral epitopes through MHC class I pathway. *Blood*. (2012) 120:994–1004. doi: 10.1182/blood-2012-01-402404
29. Zang F, Chen Y, Lin Z, Cai Z, Yu L, Xu F, et al. Autophagy is involved in regulating the immune response of dendritic cells to influenza A (H1N1) pdm09 infection. *Immunology*. (2016) 148:56–69. doi: 10.1111/imm.12587
30. Ye W, Xing Y, Paustian C, Van De Ven R, Moudgil T, Hilton TL, et al. Cross-presentation of viral antigens in dribbles leads to efficient activation

of virus-specific human memory T cells. *J Transl Med*. (2014) 12:100. doi: 10.1186/1479-5876-12-100
31. Fan J, Wu Y, Jiang M, Wang L, Yin D, Zhang Y, et al. IFN-DC loaded with autophagosomes containing virus antigen is highly efficient in inducing virus-specific human T cells. *Int J Med Sci*. (2019) 16:741–50. doi: 10.7150/ijms.31830
32. Ponpuak M, Davis AS, Roberts EA, Delgado MA, Dinkins C, Zhao Z, et al. Delivery of cytosolic components by autophagic adaptor protein p62 endows autophagosomes with unique antimicrobial properties. *Immunity*. (2010) 32:329–41. doi: 10.1016/j.immuni.2010.02.009
33. Kimmey JM, Huynh JP, Weiss LA, Park S, Kambal A, Debnath J, et al. Unique role for ATG5 in neutrophil-mediated immunopathology during *M. tuberculosis* infection. *Nature*. (2015) 528:565–9. doi: 10.1038/nature16451
34. Ramachandran G, Gade P, Tsai P, Lu W, Kalvakolanu DV, Rosen GM, et al. Potential role of autophagy in the bactericidal activity of human PMNs for Bacillus anthracis. *Pathog Dis*. (2015) 73:ftv080. doi: 10.1093/femspd/ftv080
35. Andersson AM, Andersson B, Lorell C, Raffetseder J, Larsson M, Blomgran R. Autophagy induction targeting mTORC1 enhances *Mycobacterium tuberculosis* replication in HIV co-infected human macrophages. *Sci Rep*. (2016) 6:28171. doi: 10.1038/srep28171
36. Franco LH, Nair VR, Scharn CR, Xavier RJ, Torrealba JR, Shiloh MU, et al. The ubiquitin ligase smurf1 functions in selective autophagy of *Mycobacterium tuberculosis* and anti-tuberculous host defense. *Cell Host Microbe*. (2017) 21:59–72. doi: 10.1016/j.chom.2016.11.002
37. Rudra JS, Khan A, Clover TM, Endsley JJ, Zloza A, Wang J, et al. Supramolecular peptide nanofibers engage mechanisms of autophagy in antigen-presenting cells. *ACS Omega*. (2017) 2:9136–43. doi: 10.1021/acsomega.7b00525
38. Watson RO, Manzanillo PS, Cox JS. Extracellular *M. tuberculosis* DNA targets bacteria for autophagy by activating the host DNA-sensing pathway. *Cell*. (2012) 150:803–15. doi: 10.1016/j.cell.2012.06.040
39. Khan A, Bakhru P, Saikolappan S, Das K, Soudani E, Singh CR, et al. An autophagy-inducing and TLR-2 activating BCG vaccine induces a robust protection against tuberculosis in mice. *NPJ Vaccines*. (2019) 4:34. doi: 10.1038/s41541-019-0122-8
40. Jagannath C, Lindsey DR, Dhandayuthapani S, Xu Y, Hunter RL Jr, Eissa NT. Autophagy enhances the efficacy of BCG vaccine by increasing peptide presentation in mouse dendritic cells. *Nat Med*. (2009) 15:267–76. doi: 10.1038/nm.1928
41. Saiga H, Nieuwenhuizen N, Gengenbacher M, Koehler AB, Schuerer S, Moura-Alves P, et al. The Recombinant BCG DeltaureC::hly vaccine targets the AIM2 inflammasome to induce autophagy and inflammation. *J Infect Dis*. (2015) 211:1831–41. doi: 10.1093/infdis/jiu675
42. Morris S, Swanson MS, Lieberman A, Reed M, Yue Z, Lindell DM, et al. Autophagy-mediated dendritic cell activation is essential for innate cytokine production and APC function with respiratory syncytial virus responses. *J Immunol*. (2011) 187:3953–61. doi: 10.4049/jimmunol.1100524
43. Dalod M, Chelbi R, Malissen B, Lawrence T. Dendritic cell maturation: functional specialization through signaling specificity and transcriptional programming. *EMBO J*. (2014) 33:1104–16. doi: 10.1002/embj.201488027
44. Blanchet FP, Moris A, Nikolic DS, Lehmann M, Cardinaud S, Stalder R, et al. Human immunodeficiency virus-1 inhibition of immunoamphisomes in dendritic cells impairs early innate and adaptive immune responses. *Immunity*. (2010) 32:654–69. doi: 10.1016/j.immuni.2010.04.011
45. Ravindran R, Khan N, Nakaya HI, Li S, Loebbermann J, Maddur MS, et al. Vaccine activation of the nutrient sensor GCN2 in dendritic cells enhances antigen presentation. *Science*. (2014) 343:313–7. doi: 10.1126/science.1246829
46. Naziri H, Tahamtan A, Dadmanesh M, Barati M, Ghorban K. Antitumor effects of HPV DNA vaccine adjuvanted with beclin-1 as an autophagy inducer in a mice model. *Iran Biomed J*. (2019) 23:388–94. doi: 10.29252/ibj.23.6.388
47. Ahmad S, Bhattacharya D, Kar S, Ranganathan A, Van Kaer L, Das G. Curcumin nanoparticles enhance *Mycobacterium bovis* BCG vaccine efficacy by modulating host immune responses. *Infect Immun*. (2019) 87:e00291-19. doi: 10.1128/IAI.00291-19
48. Abrahem R, Cao R, Robinson B, Munjal S, Cho T, To K, et al. Elucidating the efficacy of the bacille calmette-guerin vaccination in conjunction with first line antibiotics and liposomal glutathione. *J Clin Med*. (2019) 8:1556. doi: 10.3390/jcm8101556
49. Mitchell G, Chen C, Portnoy DA. Strategies Used by Bacteria to Grow in Macrophages. *Microbiol Spectr*. (2016) 4:MCHD-0012-2015. doi: 10.1128/microbiolspec.MCHD-0012-2015
50. Mitchell G, Ge L, Huang Q, Chen C, Kianian S, Roberts MF, et al. Avoidance of autophagy mediated by PlcA or ActA is required for *Listeria monocytogenes* growth in macrophages. *Infect Immun*. (2015) 83:2175–84. doi: 10.1128/IAI.00110-15
51. Mitchell G, Cheng MI, Chen C, Nguyen BN, Whiteley AT, Kianian S, et al. *Listeria monocytogenes* triggers noncanonical autophagy upon phagocytosis, but avoids subsequent growth-restricting xenophagy. *Proc Natl Acad Sci USA*. (2018) 115:E210–7. doi: 10.1073/pnas.1716055115
52. Koster S, Upadhyay S, Chandra P, Papavinasasundaram K, Yang G, Hassan A, et al. *Mycobacterium tuberculosis* is protected from NADPH oxidase and LC3-associated phagocytosis by the LCP protein CpsA. *Proc Natl Acad Sci USA*. (2017) 114:E8711–20. doi: 10.1073/pnas.1707792114
53. Liu E, Lopez Corcino Y, Portillo JA, Miao Y, Subauste CS. Identification of signaling pathways by which CD40 stimulates autophagy and antimicrobial activity against *Toxoplasma gondii* in macrophages. *Infect Immun*. (2016) 84:2616–26. doi: 10.1128/IAI.00101-16
54. Andrade RM, Wessendarp M, Gubbels MJ, Striepen B, Subauste CS. CD40 induces macrophage anti-*Toxoplasma gondii* activity by triggering autophagy-dependent fusion of pathogen-containing vacuoles and lysosomes. *J Clin Invest*. (2006) 116:2366–77. doi: 10.1172/JCI28796
55. Kim JK, Kim YS, Lee HM, Jin HS, Neupane C, Kim S, et al. GABAergic signaling linked to autophagy enhances host protection against intracellular bacterial infections. *Nat Commun*. (2018) 9:4184. doi: 10.1038/s41467-018-06487-5
56. Singhal A, Jie L, Kumar P, Hong GS, Leow MK, Paleja B. et al. Metformin as adjunct antituberculosis therapy. *Sci Transl Med*. (2014) 6:263ra159. doi: 10.1126/scitranslmed.3009885
57. Yuk JM, Shin DM, Lee HM, Yang CS, Jin HS, Kim KK, et al. Vitamin D3 induces autophagy in human monocytes/macrophages via cathelicidin. *Cell Host Microbe*. (2009) 6:231–43. doi: 10.1016/j.chom.2009.08.004
58. Estrella JL, Kan-Sutton C, Gong X, Rajagopalan M, Lewis DE, Hunter RL, et al. A Novel in vitro Human Macrophage Model to Study the Persistence of *Mycobacterium tuberculosis* using Vitamin D(3) and retinoic acid activated THP-1 macrophages. *Front Microbiol*. (2011) 2:67. doi: 10.3389/fmicb.2011.00067
59. Shin DM, Yuk JM, Lee HM, Lee SH, Son JW, Harding CV, et al. Mycobacterial lipoprotein activates autophagy via TLR2/1/CD14 and a functional vitamin D receptor signalling. *Cell Microbiol*. (2010) 12:1648–65. doi: 10.1111/j.1462-5822.2010.01497.x
60. Gutierrez MG, Master SS, Singh SB, Taylor GA, Colombo MI, Deretic V. Autophagy is a defense mechanism inhibiting BCG and *Mycobacterium tuberculosis* survival in infected macrophages. *Cell*. (2004) 119:753–66. doi: 10.1016/j.cell.2004.11.038
61. Tateosian NL, Pellegrini JM, Amiano NO, Rolandelli A, Casco N, Palmero DJ, et al. IL17A augments autophagy in *Mycobacterium tuberculosis*-infected monocytes from patients with active tuberculosis in association with the severity of the disease. *Autophagy*. (2017) 13:1191–204. doi: 10.1080/15548627.2017.1320636
62. Sanjuan MA, Dillon CP, Tait SW, Moshiach S, Dorsey F, Connell S, et al. Toll-like receptor signalling in macrophages links the autophagy pathway to phagocytosis. *Nature*. (2007) 450:1253–7. doi: 10.1038/nature06421
63. Mitroulis I, Kourtzelis I, Kambas K, Rafail S, Chrysanthopoulou A, Speletas M, et al. Regulation of the autophagic machinery in human neutrophils. *Eur J Immunol*. (2010) 40:1461–72. doi: 10.1002/eji.200940025
64. Lima JG, De Freitas Vinhas C, Gomes IN, Azevedo CM, Dos Santos RR, Vannier-Santos MA, et al. Phagocytosis is inhibited by autophagic induction in murine macrophages. *Biochem Biophys Res Commun*. (2011) 405:604–9. doi: 10.1016/j.bbrc.2011.01.076
65. Jin L, Batra S, Jeyaseelan S. Deletion of Nlrp3 augments survival during polymicrobial sepsis by decreasing autophagy and enhancing phagocytosis. *J Immunol*. (2017) 198:1253–62. doi: 10.4049/jimmunol.1601745

66. Bonilla DL, Bhattacharya A, Sha Y, Xu Y, Xiang Q, Kan A, et al. Autophagy regulates phagocytosis by modulating the expression of scavenger receptors. *Immunity*. (2013) 39:537–47. doi: 10.1016/j.immuni.2013.08.026
67. Sengupta A, Keswani T, Sarkar S, Ghosh S, Mukherjee S, Bhattacharyya A. Autophagic induction modulates splenic plasmacytoid dendritic cell mediated immune response in cerebral malarial infection model. *Microbes Infect*. (2019) 21:475–84. doi: 10.1016/j.micinf.2019.05.004
68. Sengupta A, Sarkar S, Keswani T, Mukherjee S, Ghosh S, Bhattacharyya A. Impact of autophagic regulation on splenic red pulp macrophages during cerebral malarial infection. *Parasitol Int*. (2019) 71:18–26. doi: 10.1016/j.parint.2019.03.008
69. Kyei GB, Dinkins C, Davis AS, Roberts E, Singh SB, Dong C, et al. Autophagy pathway intersects with HIV-1 biosynthesis and regulates viral yields in macrophages. *J Cell Biol*. (2009) 186:255–68. doi: 10.1083/jcb.200903070
70. Li JC, Au KY, Fang JW, Yim HC, Chow KH, Ho PL, et al. HIV-1 trans-activator protein dysregulates IFN-gamma signaling and contributes to the suppression of autophagy induction. *AIDS*. (2011) 25:15–25. doi: 10.1097/QAD.0b013e328340fd61
71. Van Grol J, Subauste C, Andrade RM, Fujinaga K, Nelson J, Subauste CS. HIV-1 inhibits autophagy in bystander macrophage/monocytic cells through Src-Akt and STAT3. *PLoS ONE*. (2010) 5:e11733. doi: 10.1371/journal.pone.0011733
72. Campbell GR, Bruckman RS, Herns SD, Joshi S, Durden DL, Spector SA. Induction of autophagy by PI3K/MTOR and PI3K/MTOR/BRD4 inhibitors suppresses HIV-1 replication. *J Biol Chem*. (2018) 293:5808–20. doi: 10.1074/jbc.RA118.002353
73. Campbell GR, Spector SA. Vitamin D inhibits human immunodeficiency virus type 1 and *Mycobacterium tuberculosis* infection in macrophages through the induction of autophagy. *PLoS Pathog*. (2012) 8:e1002689. doi: 10.1371/journal.ppat.1002689
74. Owczarczyk AB, Schaller MA, Reed M, Rasky AJ, Lombard DB, Lukacs NW. Sirtuin 1 regulates dendritic cell activation and autophagy during respiratory syncytial virus-induced immune responses. *J Immunol*. (2015) 195:1637–46. doi: 10.4049/jimmunol.1500326
75. Munz C. Autophagy proteins in viral exocytosis and anti-viral immune responses. *Viruses*. (2017) 9:288. doi: 10.3390/v9100288
76. Ahmad L, Mostowy S, Sancho-Shimizu V. Autophagy-virus interplay: from cell biology to human disease. *Front Cell Dev Biol*. (2018) 6:155. doi: 10.3389/fcell.2018.00155
77. Siracusano G, Venuti A, Lombardo D, Mastino A, Esclatine A, Sciortino MT. Early activation of MyD88-mediated autophagy sustains HSV-1 replication in human monocytic THP-1 cells. *Sci Rep*. (2016) 6:31302. doi: 10.1038/srep31302
78. Park S, Buck MD, Desai C, Zhang X, Loginicheva E, Martinez J, et al. Autophagy genes enhance murine gammaherpesvirus 68 reactivation from latency by preventing virus-induced systemic inflammation. *Cell Host Microbe*. (2016) 19:91–101. doi: 10.1016/j.chom.2015.12.010
79. Shoji-Kawata S, Sumpter R, Leveno M, Campbell GR, Zou Z, Kinch L, et al. Identification of a candidate therapeutic autophagy-inducing peptide. *Nature*. (2013) 494:201–6. doi: 10.1038/nature11866
80. Maiuri MC, Criollo A, Tasdemir E, Vicencio JM, Tajeddine N, Hickman JA, et al. BH3-only proteins and BH3 mimetics induce autophagy by competitively disrupting the interaction between Beclin 1 and Bcl-2/Bcl-X(L). *Autophagy*. (2007) 3:374–6. doi: 10.4161/auto.4237
81. Rubinsztein DC, Codogno P, Levine B. Autophagy modulation as a potential therapeutic target for diverse diseases. *Nat Rev Drug Discov*. (2012) 11:709–30. doi: 10.1038/nrd3802
82. Levine B, Sinha S, Kroemer G. Bcl-2 family members: dual regulators of apoptosis and autophagy. *Autophagy*. (2008) 4:600–6. doi: 10.4161/auto.6260
83. Su M, Mei Y, Sanishvili R, Levine B, Colbert CL, Sinha S. Targeting gammaherpesvirus 68 Bcl-2-mediated down-regulation of autophagy. *J Biol Chem*. (2014) 289:8029–40. doi: 10.1074/jbc.M113.515361
84. Harris J, Hartman M, Roche C, Zeng SG, O'shea A, Sharp FA, et al. Autophagy controls IL-1beta secretion by targeting pro-IL-1beta for degradation. *J Biol Chem*. (2011) 286:9587–97. doi: 10.1074/jbc.M110.202911
85. Lupfer C, Thomas PG, Anand PK, Vogel P, Milasta S, Martinez J, et al. Receptor interacting protein kinase 2-mediated mitophagy regulates inflammasome activation during virus infection. *Nat Immunol*. (2013) 14:480–8. doi: 10.1038/ni.2563
86. Lu Q, Yokoyama CC, Williams JW, Baldridge MT, Jin X, Desrochers B, et al. Homeostatic control of innate lung inflammation by vici syndrome gene Epg5 and additional autophagy genes promotes influenza pathogenesis. *Cell Host Microbe*. (2016) 19:102–13. doi: 10.1016/j.chom.2015.12.011
87. Castillo EF, Dekonenko A, Arko-Mensah J, Mandell MA, Dupont N, Jiang S, et al. Autophagy protects against active tuberculosis by suppressing bacterial burden and inflammation. *Proc Natl Acad Sci USA*. (2012) 109:E3168–76. doi: 10.1073/pnas.1210500109
88. Pu Q, Gan C, Li R, Li Y, Tan S, Li X, et al. Atg7 deficiency intensifies inflammasome activation and pyroptosis in pseudomonas sepsis. *J Immunol*. (2017) 198:3205–13. doi: 10.4049/jimmunol.1601196
89. Cui SN, Chen ZY, Yang XB, Chen L, Yang YY, Pan SW, et al. Trichostatin A modulates the macrophage phenotype by enhancing autophagy to reduce inflammation during polymicrobial sepsis. *Int Immunopharmacol*. (2019) 105973. doi: 10.1016/j.intimp.2019.105973
90. Ip WKE, Hoshi N, Shouval DS, Snapper S, Medzhitov R. Anti-inflammatory effect of IL-10 mediated by metabolic reprogramming of macrophages. *Science*. (2017) 356:513–9. doi: 10.1126/science.aal3535
91. Liang Q, Seo GJ, Choi YJ, Kwak MJ, Ge J, Rodgers MA, et al. Crosstalk between the cGAS DNA sensor and Beclin-1 autophagy protein shapes innate antimicrobial immune responses. *Cell Host Microbe*. (2014) 15:228–38. doi: 10.1016/j.chom.2014.01.009
92. Chen M, Meng Q, Qin Y, Liang P, Tan P, He L, et al. TRIM14 inhibits cGAS degradation mediated by selective autophagy receptor p62 to promote innate immune responses. *Mol Cell*. (2016) 64:105–19. doi: 10.1016/j.molcel.2016.08.025
93. Eaglesham JB, Pan Y, Kupper TS, Kranzusch PJ. Viral and metazoan poxins are cGAMP-specific nucleases that restrict cGAS-STING signalling. *Nature*. (2019) 566:259–63. doi: 10.1038/s41586-019-0928-6
94. Sir D, Tian Y, Chen WL, Ann DK, Yen TS, Ou JH. The early autophagic pathway is activated by hepatitis B virus and required for viral DNA replication. *Proc Natl Acad Sci USA*. (2010) 107:4383–8. doi: 10.1073/pnas.0911373107
95. Chan ST, Ou JJ. Hepatitis C virus-induced autophagy and host innate immune response. *Viruses*. (2017) 9:224. doi: 10.3390/v9080224
96. Shrivastava S, Raychoudhuri A, Steele R, Ray R, Ray RB. Knockdown of autophagy enhances the innate immune response in hepatitis C virus-infected hepatocytes. *Hepatology*. (2011) 53:406–14. doi: 10.1002/hep.24073
97. Shrivastava S, Devhare P, Sujijantarat N, Steele R, Kwon YC, Ray R, et al. Knockdown of autophagy inhibits infectious hepatitis C virus release by the exosomal pathway. *J Virol*. (2016) 90:1387–96. doi: 10.1128/JVI.02383-15
98. Gratton R, Agrelli A, Tricarico PM, Brandao L, Crovella S. Autophagy in Zika virus infection: a possible therapeutic target to counteract viral replication. *Int J Mol Sci*. (2019) 20. doi: 10.3390/ijms20051048
99. Mateo R, Nagamine CM, Spagnolo J, Mendez E, Rahe M, Gale MJr, et al. Inhibition of cellular autophagy deranges dengue virion maturation. *J Virol*. (2013) 87:1312–21. doi: 10.1128/JVI.02177-12
100. Lai YC, Chuang YC, Chang CP, Lin YS, Perng GC, Wu HC, et al. Minocycline suppresses dengue virus replication by down-regulation of macrophage migration inhibitory factor-induced autophagy. *Antiviral Res*. (2018) 155:28–38. doi: 10.1016/j.antiviral.2018.05.002
101. Cao B, Parnell LA, Diamond MS, Mysorekar IU. Inhibition of autophagy limits vertical transmission of Zika virus in pregnant mice. *J Exp Med*. (2017) 214:2303–13. doi: 10.1084/jem.20170957
102. Shiryaev SA, Mesci P, Pinto A, Fernandes I, Sheets N, Shresta S, et al. Repurposing of the anti-malaria drug chloroquine for Zika Virus treatment and prophylaxis. *Sci Rep*. (2017) 7:15771. doi: 10.1038/s41598-017-15467-6
103. Zhang S, Yi C, Li C, Zhang F, Peng J, Wang Q, et al. Chloroquine inhibits endosomal viral RNA release and autophagy-dependent viral replication and effectively prevents maternal to fetal transmission of Zika virus. *Antiviral Res*. (2019) 169:104547. doi: 10.1016/j.antiviral.2019.104547

104. Duan X, Liu X, Li W, Holmes JA, Kruger AJ, Yang C, et al. Microrna-130a downregulates HCV replication through an atg5-dependent autophagy pathway. *Cells*. (2019) 8:338. doi: 10.3390/cells 8040338
105. Pu J, Wu S, Xie H, Li Y, Yang Z, Wu X, et al. miR-146a Inhibits dengue-virus-induced autophagy by targeting TRAF6. *Arch Virol*. (2017) 162:3645–59. doi: 10.1007/s00705-017-3516-9
106. Fu Y, Xu W, Chen D, Feng C, Zhang L, Wang X, et al. Enterovirus 71 induces autophagy by regulating has-miR-30a expression to promote viral replication. *Antiviral Res*. (2015) 124:43–53. doi: 10.1016/j.antiviral.2015.09.016

Conflict of Interest: The authors declare that the research was conducted in the absence of any commercial or financial relationships that could be construed as a potential conflict of interest.

frontiers in Immunology

ORIGINAL RESEARCH
published: 27 March 2020
doi: 10.3389/fimmu.2020.00438

Dual Pro- and Anti-Inflammatory Features of Monocyte-Derived Dendritic Cells

Waqas Azeem[1,2]*, *Ragnhild Maukon Bakke*[1], *Silke Appel*[2,3], *Anne Margrete Øyan*[2,4] and *Karl-Henning Kalland*[1,2,5]*

[1] Department of Microbiology, Haukeland University Hospital, Helse Bergen, Bergen, Norway, [2] Department of Clinical Science, University of Bergen, Bergen, Norway, [3] Broegelmann Research Laboratory, University of Bergen, Bergen, Norway, [4] Department of Immunology and Transfusion Medicine, Haukeland University Hospital, Helse Bergen, Bergen, Norway, [5] Norway Centre for Cancer Biomarkers, University of Bergen, Bergen, Norway

The transcription factor β-catenin is able to induce tolerogenic/anti-inflammatory features in different types of dendritic cells (DCs). Monocyte-derived dendritic cells (moDCs) have been widely used in dendritic cell-based cancer therapy, but so far with limited clinical efficacy. We wanted to investigate the hypothesis that aberrant differentiation or induction of dual pro- and anti-inflammatory features may be β-catenin dependent in moDCs. β-catenin was detectable in both immature and lipopolysaccharide (LPS)-stimulated DCs. The β-catenin inhibitor ICG-001 dose-dependently increased the pro-inflammatory signature cytokine IL-12p70 and decreased the anti-inflammatory signature molecule IL-10. The β-catenin activator 6-bromoindirubin-3′-oxime (6-BIO) dose-dependently increased total and nuclear β-catenin, and this was associated with decreased IL-12p70, increased IL-10, and reduced surface expression of activation markers, such as CD80 and CD86, and increased expression of inhibitory markers, such as PD-L1. 6-BIO and ICG-001 competed dose-dependently regarding these features. Genome-wide mRNA expression analyses further underscored the dual development of pro- and anti-inflammatory features of LPS-matured moDCs and suggest a role for β-catenin inhibition in production of more potent therapeutic moDCs.

Keywords: monocyte-derived dendritic cell, pro-inflammatory, tolerogenic, immunotherapy, beta-catenin

OPEN ACCESS

Edited by:
Jordi Ochando, Icahn School of Medicine at Mount Sinai, United States

Reviewed by:
Robert Adam Harris, Karolinska Institutet (KI), Sweden
Estanislao Nistal-Villan, San Pablo CEU University, Spain

***Correspondence:**
Waqas Azeem
waqas.azeem@uib.no
Karl-Henning Kalland
karl.kalland@uib.no

Specialty section:
This article was submitted to Molecular Innate Immunity, a section of the journal Frontiers in Immunology

Received: *28 October 2019*
Accepted: *25 February 2020*
Published: *27 March 2020*

Citation:
Azeem W, Bakke RM, Appel S, Øyan AM and Kalland K-H (2020) Dual Pro- and Anti-Inflammatory Features of Monocyte-Derived Dendritic Cells. Front. Immunol. 11:438. doi: 10.3389/fimmu.2020.00438

INTRODUCTION

Dendritic cells (DCs) are the most efficient antigen-presenting cells of the immune system and play a vital role in initiating the adaptive immune response and maintaining tolerance to self-antigens (1). Immature DCs continually search their environment for antigens, while mature DCs migrate to the lymph nodes and present processed antigens on their major histocompatibility (MHC) molecules to T cells. Traditionally, three different types of DCs have been considered in peripheral blood, plasmacytoid DCs (pDC) and classical or conventional DC type 1 (cDC1) and type 2 (cDC2) (2–4). Recent high-resolution technologies have revealed additional types of human blood DCs and progenitors (5, 6). Altogether, DCs comprise less than 1% of circulating blood leukocytes, and for this reason, most DC-based therapies have relied on DCs generated *in vitro* from the more plentiful

blood monocytes [reviewed in (2–4, 7, 8)]. Monocyte-derived DCs (moDCs) are able to activate the immune system, but it may be anticipated that there is a considerable potential for the generation of more potent and robust DCs for cancer therapy.

Depending on their phenotype and type of secreted cytokines, DCs may exert either pro-inflammatory or tolerogenic function as their response to newly encountered antigens. The transcription factor β-catenin can be activated to stimulate tolerogenic features of DCs, such as cytokine, surface marker, and metabolic profiles (9–12). Surface markers associated with pro-inflammatory activation include CD80 and CD86, whereas PD-L1 and PD-L2 are considered inhibitory or tolerogenic markers (7). Interleukin 12 (IL-12p70) represents a pro-inflammatory cytokine (13) and interleukin 10 (IL-10) an anti-inflammatory or tolerogenic cytokine (14) that can be secreted from mature DCs.

Inhibiting β-catenin signaling could have a dual effect in cancer therapy, as this pathway promotes tolerogenic features of the local dendritic cells and is often activated in cancer and cancer stem cells. In the present study, β-catenin activation was achieved using a specific inhibitor of the β-catenin destruction complex, 6-bromoindirubin-3′-oxime (6-BIO) that has been found to increase β-catenin in the cell nucleus of different cell types (15). In this way the central, final part of β-catenin signaling downstream of the destruction complex can be investigated. This approach has experimental advantages because β-catenin activation is impacted by different up-stream pathways with complicated cross-talks (16). Likewise, central β-catenin inhibition was attempted using the small molecule ICG-001 that binds CREB-binding protein (CBP) to disrupt its interaction with β-catenin and inhibits CBP function as a co-activator of β-catenin-mediated transcription at regulatory genomic elements (17).

In the present study, moDCs derived from buffy coats of healthy donors were investigated and revealed the potential of mature moDCs to co-develop both pro-inflammatory and tolerogenic features assayed by IL-12p70 and IL-10 secretion, DC surface markers, and whole-genome mRNA quantification.

MATERIALS AND METHODS

Generation of Monocyte-Derived Dendritic Cells

Buffy coats of healthy blood donors at the Blood bank of Haukeland University Hospital, Bergen, were used to generate human monocyte-derived dendritic cells (moDCs). Informed consents were obtained from all donors, and samples were anonymized according to the approval by the Regional Ethical Committee (#64205). Healthy donors were above 23 years of age. Peripheral blood mononuclear cells (PBMCs) were isolated by gradient centrifugation using Lymphoprep™ (Cat. No. 1114545; Axis-Shield). Pan Monocyte Isolation Kit (Cat. No. 130-096-537; MiltenyiBiotec) with the addition of CD61 MicroBeads (Cat. No. 130-051-101; MiltenyiBiotec) and LS columns (Cat. No. 130-042-401; MiltenyiBiotec) were used to separate untouched monocytes from PBMCs by indirect magnetic labeling. Monocytes were then cultured in CellGenix GMP DC medium (Cat. No. 20801-0500; CellGenix) supplemented with 20 ng/ml of IL-4 (Cat. No. 11340047; Immunotools) and 100 ng/ml of GM-CSF (Cat. No. 11343128; Immunotools) at cell densities of 1.5×10^6 per 3 ml/well in six-well plates or 0.75×10^6 per 1.5 ml/well in 12-well plates for 4 days. IL-4 and GM-CSF were replenished on day 3. The fourth-day cultures were treated with compounds at different concentrations, i.e., 6-bromoindirubin-3-oxime (6-BIO; Cat. No. S7198; Selleckchem) 1 nM to 2 μM and/or ICG-001 (Cat. No. S2662; Selleckchem) 0.5 to 8 μM (for 24 h), and 1 h later with 30 ng/ml of LPS (for 23 h). As controls, the vehicle DMSO was added in LPS-treated and un-treated (iDC) populations. The moDCs were harvested on day 5.

Western Blots

Western blots were performed as previously described (18). moDCs were lysed in RIPA-buffer (Cat. No. ab156034; Abcam) supplemented with 1:100 Protease Inhibitor Cocktail Set I (Cat. No. 535142; Calbiochem). The protein concentration was quantified using Direct Detect® Infrared Spectrometer (EMD Millipore) using Direct Detect® Assay-free Cards (Cat. No. DDAC00010-GR; Millipore). Twenty micrograms was used for each sample loaded onto BoltTM Bis-Tris Plus Gels (Cat. No. NW04120BOX; Novex; Life Technologies). The proteins were separated by SDS electrophoresis and blotted on Amersham Hybond P 0.45 PVDF blotting membrane (Cat. No. 10600069; GE Healthcare). The primary antibodies used were anti-β-catenin (Cat. No. 16051; Abcam) and anti-GAPDH (Cat. No. MAI-16757 Invitrogen). The horseradish peroxidase (HRP)-conjugated secondary antibodies used were anti-rabbit (dilution 1:2,000; Cat. No. NA934; Amersham) and anti-mouse (dilution 1:2,000; Cat. No. 170-501; Bio-RAD). SuperSignal™ West Pico PLUS Chemiluminescent Substrate (Cat. No. 34580; Thermo Scientific) was used for visualization with Chemidoc XRS, and images were captured using Quantity One 4.6.5 software (Bio-Rad). MagicMark™ XP Western Protein Standard (Cat. No. LC5602; Invitrogen) was used as molecular weight marker. ImageJ 1.50i software (National Institutes of Health, Bethesda, MD, USA) was used to quantify the band intensity of each protein followed by normalization to its corresponding GAPDH control.

Indirect Immunofluorescence Assay

Indirect immunofluorescence assays were performed as previously described (19). The primary antibody used was anti-β-catenin (Cat. No. 16051; Abcam) at 1 μg/ml dilution, and FITC-conjugated Pierce™ goat anti-rabbit IgG (H + L) secondary antibody (Cat. No. 31635; Thermo Scientific) was used at 1:50 dilution. Cells grown on coverslips were mounted on glass slides in SlowFade™ Gold Antifade Mountant w/DAPI (Cat. No. S36939; Invitrogen). The images were captured on Leica TCS SP8 STED 3× confocal microscope using Leica Application Suite X 2.0.2.15022 software (Leica Microsystems).

Enzyme-Linked Immunosorbent Assay (ELISA)

Secretion of IL-12p70 and IL-10 in the supernatant of moDC cultures were measured using IL-12p70 Human Uncoated

ELISA Kit (Cat. No. 88-7126-88; Invitrogen) and IL-10 Human Uncoated ELISA Kit (Cat. No. 88-7106-88; Invitrogen), respectively. The absorbance was measured with Synergy H1 Hybrid Multi-Mode Reader and analyzed using Gen5 2.00.18 software (BioTek). Data are presented as fold change to DMSO-treated control sample, as absolute levels of IL-10 and IL-12 secretion varied considerably between the donors.

Flow Cytometry

The phenotype of the generated moDC populations was determined by flow cytometry as described previously (20). In short, 1×10^5 moDCs were incubated with FcR-blocking reagent (Cat. No. 130-059-901; MiltenyiBiotec) before titrated amounts of a panel of nine antibodies were added for 10 min at room temperature in the dark. The antibodies used were as follows: CD83 PE-CF594 (Cat. No. 562631; BD Biosciences), HLA-DR Horizon V500 (Cat. No. 561224; BD Biosciences), CD80 Brilliant Violet 605 (Cat. No. 305225; Biolegend), CCR7 Brilliant Violet 421 (Cat. No. 353208; Biolegend), CD86 Alexa Fluor 647 (Cat. No. 305416; Biolegend), CD274 PE-Cyanine7 (Cat. No. 46-5983-42; eBioscience), CD273 PerCP-Fluor 710 (Cat. No. 46-5888-42), CD14 FITC (Cat. No. 21620143; Immunotools), and CD1a PE (Cat. No. 21270014; Immunotools). The cells were analyzed on LSR Fortessa (BD Biosciences), and further analysis was performed using FlowJo V10 software (FlowJo, LLC). Unstained samples were used to set the gates, and 1% false-positive events were accepted throughout the analysis. For each experiment, a minimum of 5,000 single events were recorded.

Luminex Microbead Cytokine Assay

The cell-free supernatants collected from the MLR cultures were thawed and measured for cytokines using Human Magnetic 25-Plex Panel (Cat. No. LHC009M; Invitrogen) according to the manufacturer's instructions. We measured and analyzed seven cytokines including interferon-α (IFN-α), interferon-γ (IFN-γ), tumor necrosis factor-α (TNF-α), interleukin (IL)-6, IL-2R, IL-10, and IL-12. Luminex plates were read using the Luminex 100 System (Luminex Corporation, Austin, TX, USA) following the manufacturer's instructions. STarStation V3.0 (Build: 3810.0; Applied Cytometry Systems, Sheffield, UK) was used to analyze the data.

Mixed Leukocyte Reaction (MLR)

Allogeneic MLR was performed as previously described (20). In short, 2×10^5 monocyte-depleted allogeneic PBMCs were labeled with CFSE using Vybrant™ CFDA SE Cell Tracer Kit (Cat. No. V12883; Invitrogen) and co-cultured with 5×10^4 moDCs of different donors for 5 days in X-Vivo 20 medium (Cat. No. 04-448Q; Lonza) supplemented with 50 U/ml of IL-2 (Cat. No. 11340023; Immunotools) and 10 ng/ml of IL-7 (Cat. No. 11340073; Immunotools). The cells were harvested and analyzed on Accuri C6 flow cytometer (BD Biosciences). For each experiment, a minimum of 20,000 single events were recorded.

DNA Microarray Analyses

Genome-wide transcription profiling using Agilent microarrays has been described previously (21). Total RNA was isolated and tested for RNA integrity by 1% agarose gel electrophoresis, then converted to Cy3-labeled cRNA targets and hybridized to Agilent Whole Human Genome 44k Microarrays (Cat. No. G4845A; Agilent Technologies). Raw data were imported and analyzed in J-Express software (http://www.molmine.com) (22). We used mean spot signals as intensity measure, normalized the expression data over the entire arrays, and log2-transformed and considered genes changed more than 1.5-fold with FDR value <5% as differentially expressed genes. DNA microarray data have been deposited into the ArrayExpress database under accession number E-MTAB-8330.

RNA Sequencing and Analyses

All experiments were conducted at QIAGEN Genomic Services. The library preparation was done using TruSeq® Stranded mRNA Sample preparation kit (Illumina Inc.). The starting material (500 ng) of total RNA was mRNA enriched using the oligodT bead system. The isolated mRNA was subsequently enzymatically fragmented. Then first-strand synthesis and second-strand synthesis were performed, and the double-stranded cDNA was purified (AMPure XP, Beckman Coulter). The cDNA was end repaired, 3′ adenylated and Illumina sequencing adaptors ligated onto the fragments ends, and the library was purified (AMPure XP). The mRNA stranded libraries were pre-amplified with PCR and purified (AMPure XP). The libraries' size distribution was validated and quality inspected on a Bioanalyzer 2100 or BioAnalyzer 4200tape Station (Agilent Technologies). High-quality libraries were pooled based in equimolar concentrations based on the Bioanalyzer Smear Analysis tool (Agilent Technologies). The library pool(s) were quantified using qPCR, and the optimal concentration of the library pool was used to generate the clusters on the surface of a flow cell before sequencing on a NextSeq 500 instrument (75 cycles) according to the manufacturer instructions (Illumina Inc.).

Software Tools Used for RNA-Seq Analysis

NGS data analysis pipeline was based on the Tuxedo software package, which is a combination of open-source software, and implements peer-reviewed statistical methods. In addition, specialized software developed internally at QIAGEN Genomic Services was employed to interpret and improve the readability of the final results. The components of NGS data analysis pipeline for RNA-seq include Bowtie2 (v. 2.2.2), see (23), Tophat (v2.0.11), see (24, 25), and Cufflinks (v2.2.1), see (26, 27).

To guide the assembly process, an existing transcript annotation was used (RABT assembly). In addition, fragment bias correction was used to correct for sequence bias during library preparation (28). When comparing groups, Cuffdiff was used to calculate the FPKM (number of fragments per kilobase of transcript per million mapped fragments) and test for differential expression.

Statistical Analysis

All data were analyzed using GraphPad Prism 8 (GraphPad software). Statistical significance of the difference was calculated using one-way analysis of variance (ANOVA) with Dunnett's

multiple comparisons test or two-way ANOVA with Tukey's multiple comparisons test, and 95% confidence interval. A value of $p \leq 0.05$ was considered statistically significant.

RESULTS

β-Catenin Accumulation in Monocyte-Derived Dendritic Cells

β-catenin was detectable in immature moDCs (iDCs) by Western blotting, and this concentration increased slightly in moDCs matured for 23 h using LPS (**Figure 1A**). 6-BIO dose-dependently increased the accumulation of β-catenin when moDCs were treated with 6-BIO for 24 h and with concomitant LPS for the last 23 h prior to cell harvesting according to Western blot analyses (**Figure 1A**). Indirect fluorescent confocal microscopy revealed β-catenin accumulation in the cell nuclei of moDCs treated with 0.25 to 1 μM 6-BIO (**Figure 1B** and **Supplementary Figure 1**).

6-BIO Dose-Dependently Promoted Anti-Inflammatory Features of moDCs

In order to further investigate possible immune-relevant consequences of 6-BIO-induced β-catenin in mature moDCs, we quantified IL-12p70 and IL-10 of cell culture supernatants using ELISA. As exemplified in **Figure 2A**, the IL-12 concentration decreased significantly with increasing 6-BIO concentrations following LPS maturation for 23 h. 6-BIO concentrations down to 1 nM decreased IL-12 levels compared to cultures with only vehicle and with pronounced dose-dependent IL-12 decrease at 10, 100, and 250 nM. On the contrary, IL-10 secretion increased dose dependently and significantly with increasing 6-BIO in LPS-matured moDCs (**Figure 2B**). Absolute levels of IL-10 and IL-12 secretion varied considerably in moDCs of buffy coats donated by different healthy persons, although the above trends were in common, for which reason fold change was used for the Y-axis of **Figure 2**. Quantitative levels in picogram/milliliter are shown in **Supplementary Figure 2**.

ICG-001 Increased IL-12 and Decreased IL-10 Secretion of Mature moDCs

In order to examine the possibility that β-catenin signaling was activated in LPS-matured moDCs even without the use of 6-BIO, cells were treated with the commercially available β-catenin inhibitor ICG-001 for 24 h and with LPS added for the last 23 h before harvest of supernatants. ICG-001 between 1 and 8 μM dose-dependently increased the secretion of IL-12p70 (**Figure 2C**). In the same supernatants, a dose-dependent decrease in IL-10 was found with significantly increasing effect from 1 to 8 μM ICG-001 (**Figure 2D**).

6-BIO and ICG-001 Competed Against Each Other Regarding Pro- and Anti-Inflammatory Features

To examine any direct competition between 6-BIO and ICG-001, ELISA was used to quantify IL-12 and IL-10 secretion of LPS-matured DCs (**Figure 3**). IL-12 induced by either LPS alone or by LPS plus 8 μM ICG-001 was dose-dependently competed by 6-BIO (**Figure 3A**). Correspondingly, IL-10 induced by either LPS alone or by LPS plus 6-BIO was efficiently competed by 8 μM ICG-001 (**Figure 3B**). Western blots showed that ICG-001 did not significantly affect the 6-BIO-induced accumulation of β-catenin (**Figure 3C**). Quantification of mRNA levels using Agilent microarray and RNA-seq profiling showed that β-catenin mRNA levels remained relatively unaffected by ICG-001 treatment and was reduced by possible negative feedback following 6-BIO treatment (**Supplementary Figure 3**).

Effect of 6-BIO and ICG-001 on Maturation and Activation Markers of DCs

Flow cytometry was used to examine how relevant DC surface markers were affected by β-catenin stimulation or inhibition. A representative gating strategy is shown in **Supplementary Figure 4**. Retained monocyte marker CD14, along with decreased CD1a, suggests deviated maturation of DCs (29). ICG-001 treatment decreased the percentage of LPS-matured DCs that expressed CD14. 6-BIO (100 and 250 nM) increased the CD14 expression, and this was counteracted by the addition of 8 μM ICG-001 (**Figure 4**). CD1a expression was not affected by either treatment. The maturation markers HLA-DR and CD83 showed, as expected, a clear upregulation following LPS treatment for 23 h. HLA-DR was not strongly affected by either ICG-001 or 6-BIO. 6-BIO was moderately inhibitory and ICG-001 moderately stimulatory to CD83 expression at the concentrations tested (**Figure 4**).

The activation markers CD80 and CD86 increased strongly as expected when iDCs were stimulated for 23 h with LPS. 6-BIO clearly reduced expression of LPS-induced CD80 and CD86, while the effect of ICG-001 was less clear (**Figure 4**). The inhibitory marker PD-L1 increased strongly following LPS maturation of iDC for 23 h with or without 6-BIO. ICG-001 (8 μM) tended to decrease the LPS-induced PD-L1 with or without 100 or 250 nM 6-BIO. The PD-L2 marker was not increased by LPS, but was moderately decreased by 8 μM ICG-001 (**Figure 4**). The DC migration marker CCR7 was upregulated during LPS maturation, as expected, and was clearly reduced by 6-BIO treatment. ICG-001 increased CCR7 expression and competed the 6-BIO-associated downregulation of CCR7.

Effect of 6-BIO and ICG-001 on Gene Expression Patterns

In order to obtain a broader overview of potential pro- and anti-inflammatory features of LPS-matured moDCs, mRNA transcription was profiled using both Agilent 44k microarrays and Illumina RNA-seq. **Figure 5** shows a selection of 26 genes known to be relevant in pro- and anti-inflammatory regulation. The performance of the model with gene expression analyses was exemplified by the known β-catenin target gene *LRP5* (30). Both Agilent 44k microarrays and Illumina RNA-seq showed a significant, but low level, iDC expression of *LRP5* mRNA, with almost 48-fold induction of *LRP5* in LPS-matured moDCs treated with 6-BIO. In contrast, *LRP5*

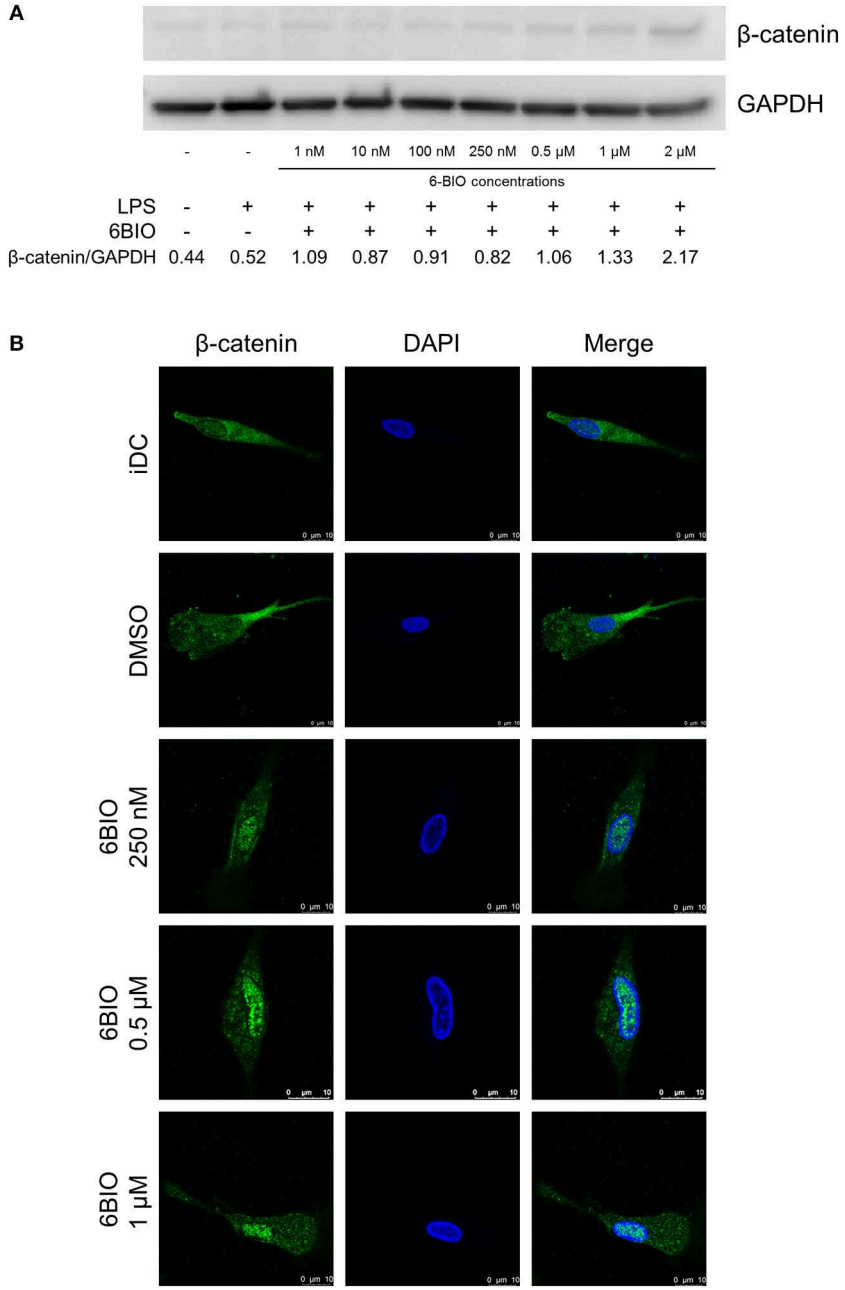

FIGURE 1 | Monocyte-derived dendritic cells (moDCs) obtained from healthy donors were treated with indicated concentrations of 6-bromoindirubin-3′-oxime (6-BIO) or DMSO (vehicle) for 24 h together with 30 ng/ml of lipopolysaccharide (LPS) for the last 23 h or left untreated as iDC. **(A)** β-catenin protein levels were measured by Western blot in whole-cell lysates. Representative Western blot of three independent experiments is shown. **(B)** Fluorescein (FITC) indirect immunofluorescent detection of β-catenin proteins according to confocal microscopy analyses.

was reduced in ICG-001-treated LPS-matured moDCs. The classical β-catenin target gene *AXIN2* was relatively weakly expressed as mRNA, but with significant induction with concomitant 6-BIO in LPS-matured moDCs (**Figures 5A,B**). *CTNNB1* (β-catenin) mRNA was relatively abundant and was reduced by 6-BIO and little affected by ICG-001 in LPS-matured moDCs.

Transcription Levels of Pro- and Anti-Inflammatory Interleukins

According to Agilent 44k microarray data (**Figure 5A**) pro-inflammatory interleukins, *IL-6*, *IL-12B*, and *IL-18* were strongly induced in LPS-matured moDCs compared to their immature origins. RNA-seq data validated the increase in *IL-6* and *IL-12B* (**Figure 5B**). Parallel treatment with 1 μM 6-BIO clearly reduced

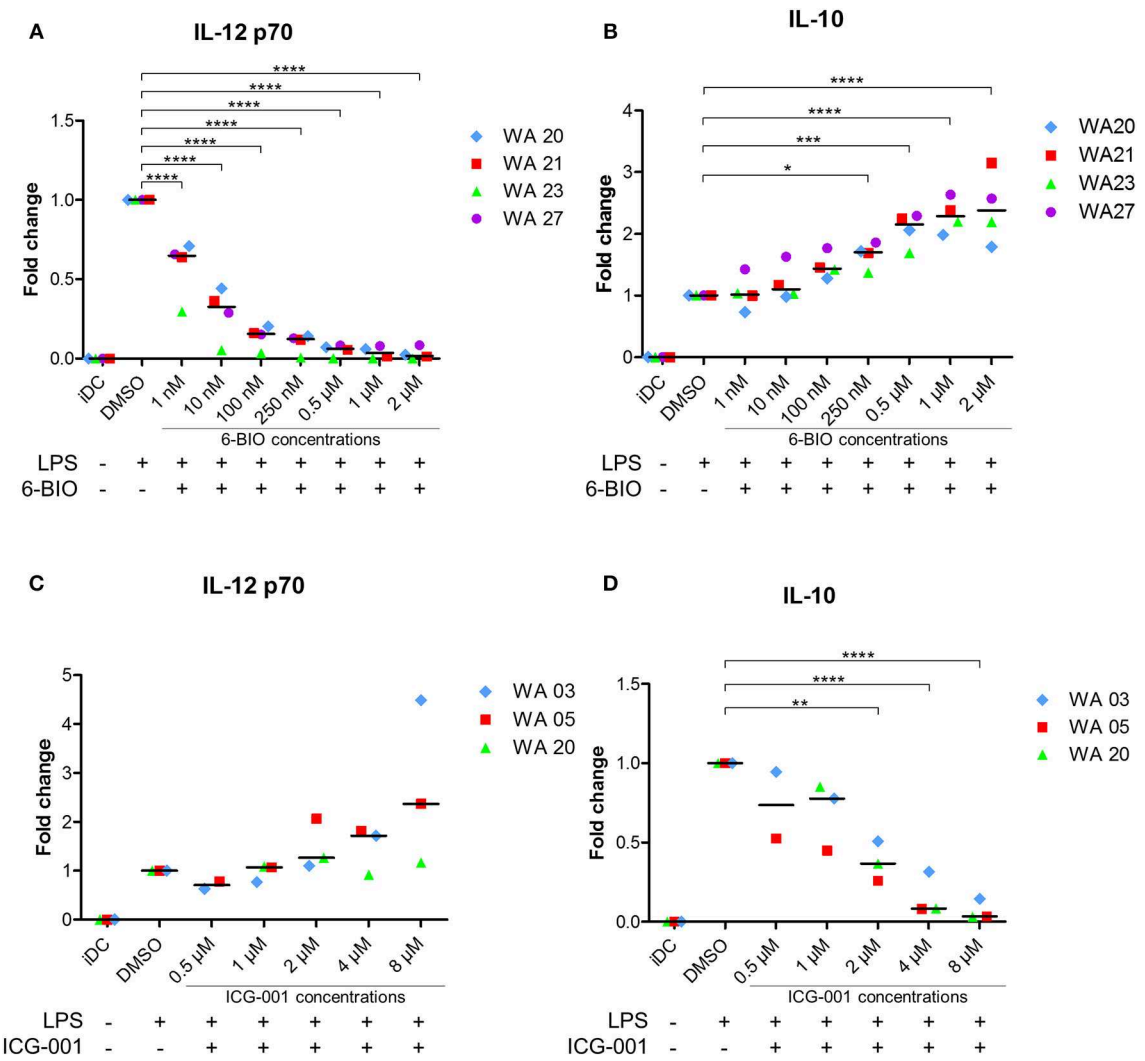

FIGURE 2 | moDCs obtained from healthy donors were treated with indicated concentrations of 6-BIO or ICG-001 or DMSO for 24 h with 30 ng/ml of LPS for the last 23 h or left untreated with those compounds as iDC. **(A–D)** The fold changes compared to DMSO controls of IL-12p70 and IL-10 in supernatants were measured by enzyme-linked immunosorbent assay (ELISA). Each symbol represents a different donor, and lines represent the median. *$p \leq 0.05$, **$p \leq 0.01$, ***$p \leq 0.001$, ****$p \leq 0.0001$ using one-way ANOVA with Dunnett's multiple comparisons test and 95% confidence interval.

mRNA levels of all of *IL-6*, *IL-12B*, *IL18*, and *IL-12A* according to both microarray and RNA-seq analyses. ICG-001 (4 μM) induced the opposite effect and a clear increase in these pro-inflammatory mRNA markers in LPS-matured moDCs according to both data sets. The anti-inflammatory *IL-10* mRNA was increased in LPS-matured moDCs compared to iDCs according to microarray data, but this was not validated by RNA-seq data. Concomitant 6-BIO-treatment, however, was associated with increased *IL-10* mRNA according to both data sets with less clear effect of concomitant ICG-001 treatment.

Transcription Levels of Activating and Inhibitory Membrane Markers

The DC activation markers *CD40*, *CD80*, and *CD86* were clearly increased in LPS-matured moDCs according to microarrays (**Figure 5A**). These results were validated by RNA-seq data for *CD86*, but not for *CD40* and *CD80*. Concomitant 6-BIO and LPS treatment showed consistently lower levels of all these cell surface activation markers according to microarrays in comparison with only LPS and, in particular, with concomitant LPS and ICG-001 treatment. RNA-seq data validated the 6-BIO results for *CD40*, *CD80*, and *CD86* and showed clearly higher expression levels when ICG-001 was used instead of 6-BIO in LPS-matured moDCs (**Figure 5B**). DC membrane inhibitory markers *PDCD1LG2* (PD-L1) and *CD274* (PD-L2) mRNAs were induced in LPS-matured moDCs according to both data sets, while concomitant 6-BIO treatment reduced transcription and ICG-001 increased transcription according to RNA-seq data. *TNFS4* (OX40 ligand) is typically expressed on DCs and its receptor *TNFRSF4* (OX40) typically on T

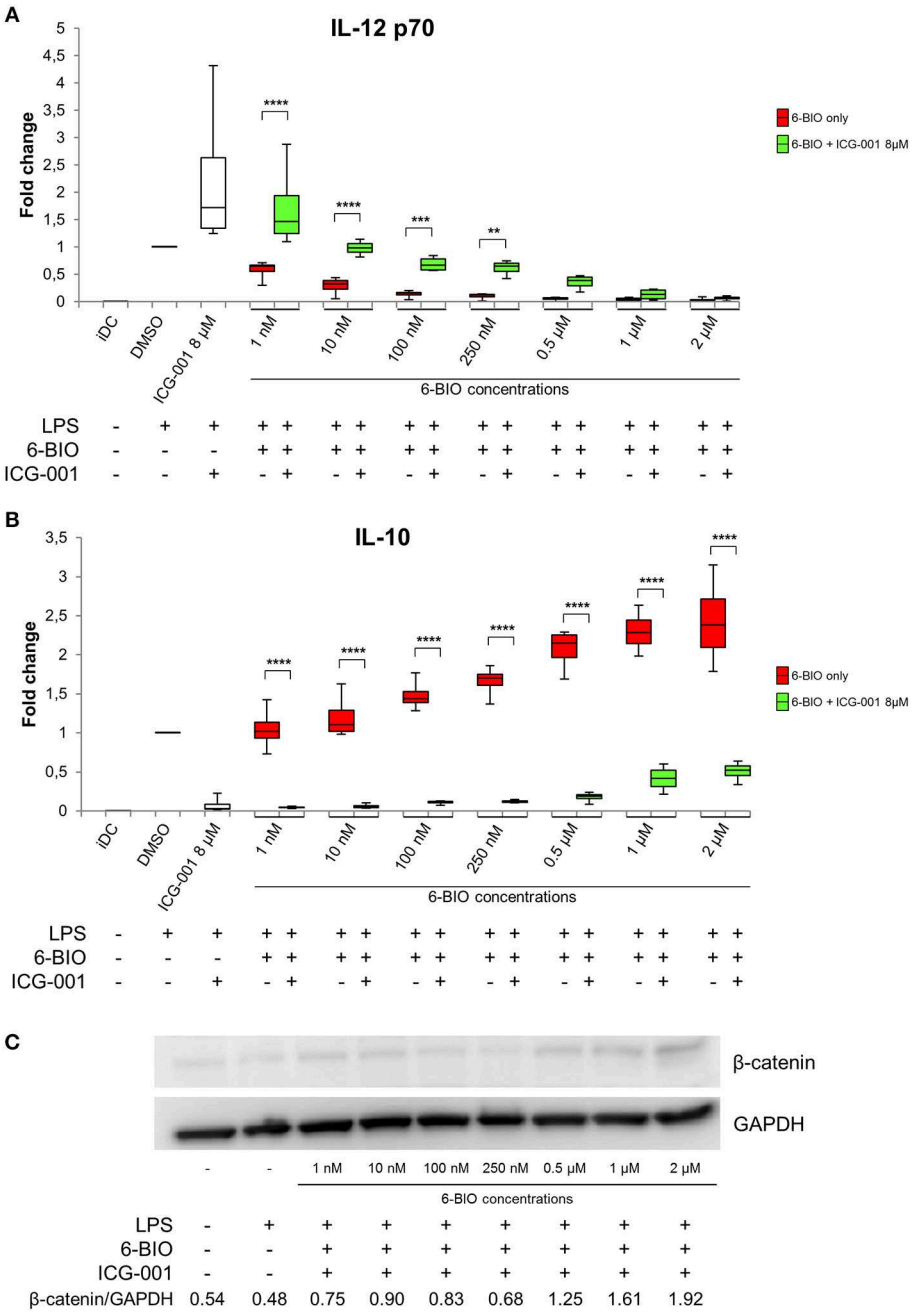

FIGURE 3 | moDCs obtained from healthy donors were treated with 8 μM ICG-001 and/or indicated concentrations of 6-BIO or DMSO (vehicle) for 24 h with 30 ng/ml of LPS for the last 23 h or left untreated as iDC. **(A,B)** Each vertical box and whisker plot shows the fold change compared to untreated DMSO controls of IL-12p70 and IL-10, respectively, measured by ELISA. The lines represent the median, edges of the box represent 25th and 75th percentiles, and whiskers display the smallest and highest value, $n = 5$. **(C)** β-catenin protein levels were measured by Western blot in whole-cell lysates. $^{*}p \leq 0.05$, $^{**}p \leq 0.01$, $^{***}p \leq 0.001$, $^{****}p \leq 0.0001$ using two-way ANOVA with Tukey's multiple comparisons test and 95% confidence interval.

lymphocytes (31). According to microarray data, *TNFRSF4* increased substantially in LPS-matured DCs and was reduced by concomitant 6-BIO and increased by ICG-001 according to both microarrays and RNA-seq (**Figures 5A,B**). *TNFSF9* (4-1BBL; CD137L) expressed on DCs activate lymphocytes via binding to *TNFRSF9* (CD137) (32). Microarray data showed strongly induced expression of both *TNFSF9* and *TNFRSF9* mRNAs in LPS-matured moDCs. Concomitant 6-BIO treatment was associated with lower, and ICG-001 treatment with higher, *TNFSF9* expression (**Figures 5A,B**). CD70 is a cell-membrane-bound TNF superfamily (TNFSR) member that activates T lymphocytes via TNFRSF member CD27 (31).

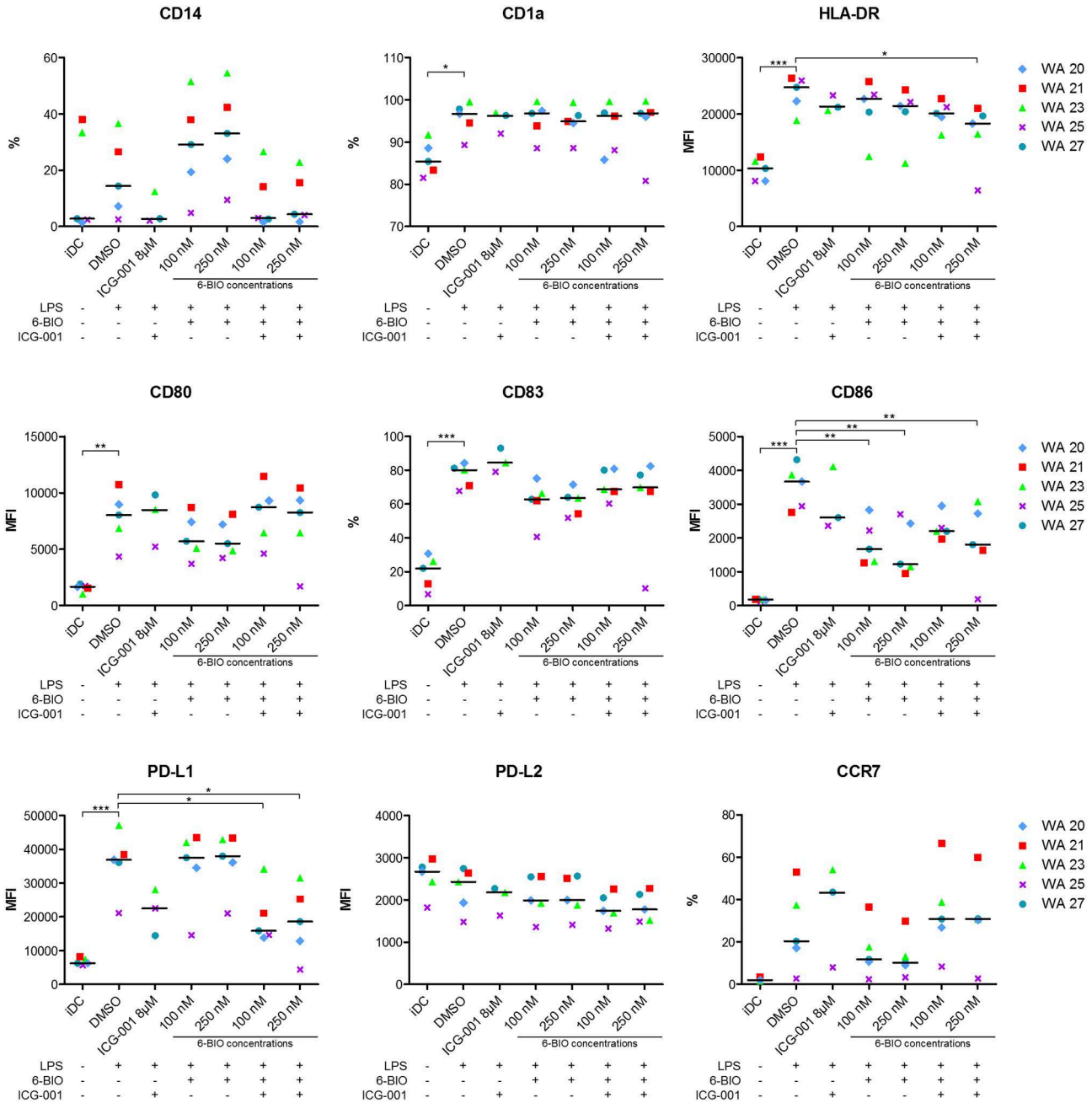

FIGURE 4 | moDCs obtained from healthy donors were treated with 8 µM ICG-001 and/or indicated concentrations of 6-BIO or DMSO for 24 h with 30 ng/ml of LPS for the last 23 h or left untreated as iDC. Flow cytometry analyses of cell surface markers were performed. Each symbol represents a different donor and lines represent the median. $^{*}P \leq 0.05$, $^{**}P \leq 0.01$, $^{***}P \leq 0.001$, using one-way ANOVA with Dunnett's multiple comparisons test and 95% confidence interval. %, percentage of positive cells; MFI, median fluorescence intensity.

According to microarray data, *CD70* mRNA was strongly induced by LPS maturation of moDCs, and this was reduced by 6-BIO and increased by ICG-001 (**Figures 5A,B**). CD200 is a surface glycoprotein that can induce IDO expression following engagement of pDC-expressed CD200R1. According to microarray data, *CD200* mRNA was strongly induced in LPS-matured moDCs. According to both microarray and RNA-seq data, *CD200* expression is further increased by concomitant ICG-001, but reduced by concomitant 6-BIO (**Figures 5A,B**). *CD200R1* was clearly reduced in LPS-matured moDCs, but was increased by concomitant 6-BIO treatment (**Figures 5A,B**).

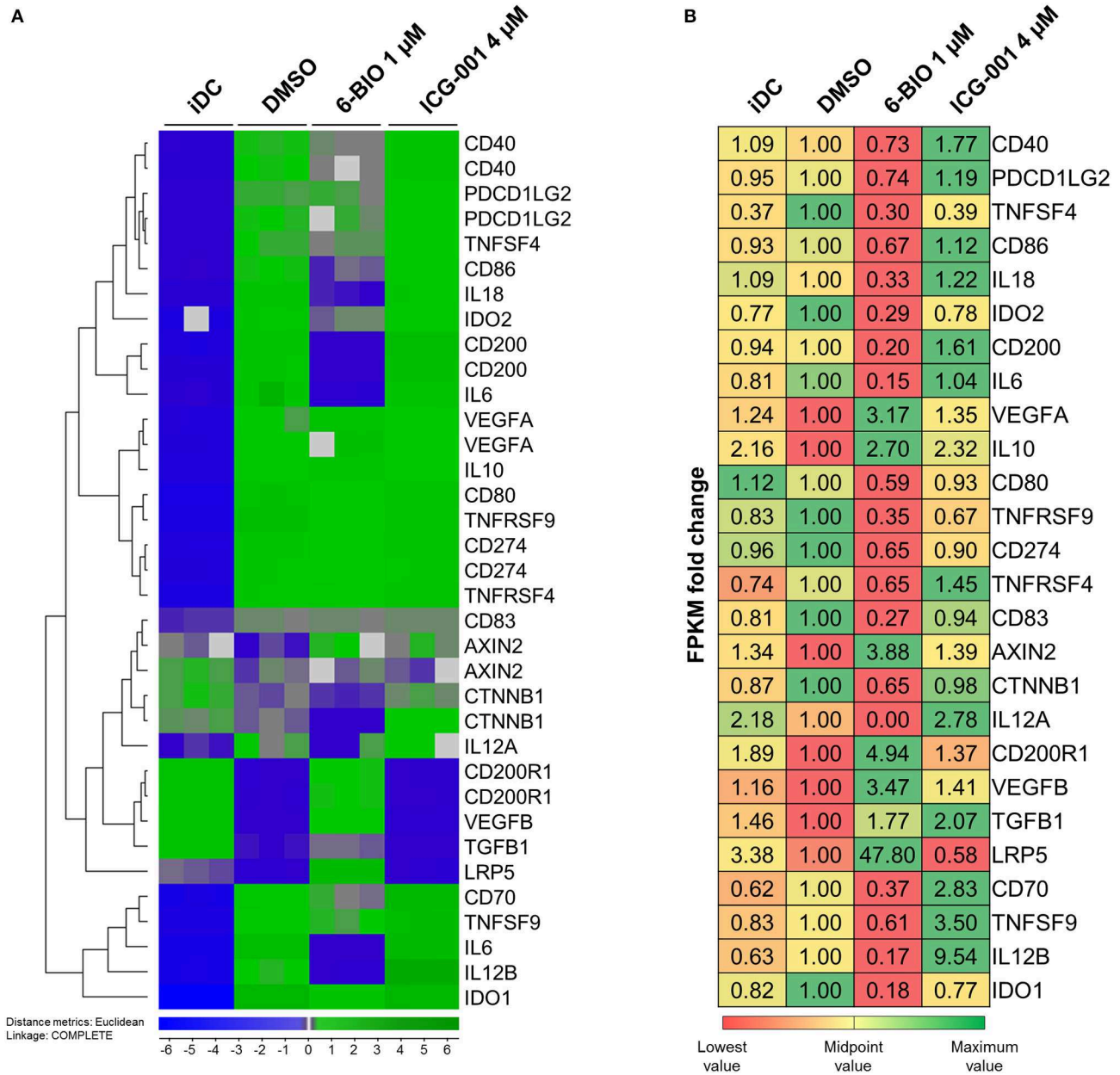

FIGURE 5 | moDCs obtained from healthy donor and treated with DMSO, 1 µM 6-BIO or 8 µM ICG-001 for 24 h with 30 ng/ml of LPS for the last 23 h, or left untreated as iDC. **(A)** Total RNA was subjected to whole-genome microarray analysis. Heat map of selected gene expression data based on the supervised hierarchical cluster analysis (J-Express™ software) of different treatments. **(B)** Total RNA (500 ng) was used to generate RNA-seq libraries. Values of the expression of selected genes were based on fold change of normalized fragments per kilobase of transcript per million mapped fragments (FPKM) for each gene of each sample. Fold change was compared to untreated DMSO (vehicle) controls.

Transcription Levels of Inhibitory Enzymes and Secreted Proteins

Indoleamine 2,3-dioxygenase (IDO-1) activity, via enzymatic catalysis of tryptophan metabolites, converts mature DCs into tolerogenic antigen-presenting cells that suppress T effector cells and promote T regulatory cells, thereby promoting tolerance (33). *IDO1* was found strongly upregulated in LPS-stimulated moDCs. Concomitant 6-BIO reduced *IDO1* (**Figures 5A,B**). TGFB is a secreted immunomodulatory molecule of DCs (10, 31). According to both microarray and RNA-seq data, *TGFB1* is reduced in LPS-stimulated moDCs compared to iDCs. Concomitant 6-BIO treatment stimulated *TGFB1* expression (**Figures 5A,B**). VEGF expression and secretion are associated both with aberrant DC maturation and anti-inflammatory DCs (34), and both *VEGFA* and *VEGFB* increased strongly in LPS-plus 6-BIO-treated moDCs (**Figures 5A,B**).

Functional Effects of 6-BIO and ICG-001 in the Allogeneic Mixed Leukocyte Reaction (MLR)

Allogeneic MLRs were performed to analyze T-cell stimulatory capacity of the generated DC populations. The cells were co-cultured with monocyte-depleted allogeneic CFDA-SE-stained PBMCs, and proliferation was determined by the reduction in CFSE intensity. All DC populations showed T-cell stimulatory capacity with LPS-matured moDCs inducing more proliferation than iDC (**Figure 6A**). The addition of 6-BIO did not, however, show any significant variation in T-cell proliferation compared to DMSO control, although a slight decrease was observed at 0.5 and 2 μM 6-BIO. Neither did up to 8 μM ICG-001 significantly affect the recorded T-cell proliferation (result not shown). In order to examine further the apparent minimal effect of β-catenin modulation of the MLR assay, co-culture supernatants were investigated for cytokines using the Luminex microbead assay (**Figure 6B**). There was a trend toward 6-BIO dose-dependent reduction in pro-inflammatory cytokines IFN-γ, TNF-α, and IL-6. Among those cytokines, only IL-6 level reached statistical significance. Soluble IL-2R showed a statistically significant and dose-dependent decrease with increasing 6-BIO. It was additionally noted that the 6-BIO dose-dependent effects on IL-10 and IL-12 that we found in pure DC cultures seemed to be abrogated in co-cultures with allogeneic lymphocytes.

DISCUSSION

Improved DCs are much needed for next-generation cancer immunotherapy (2, 7, 8, 35). One attractive possibility is that β-catenin signaling can be exploited to generate more robust and potent therapeutic DCs. The transcription factor β-catenin is an important immune regulator that can affect pro-inflammatory and anti-inflammatory/tolerogenic features of mouse and human DCs of different subtypes (11, 12, 36–40), but the therapeutic potential of β-catenin inhibition in moDCs needs further clarification (41–47).

In the present work, we established a model system of moDCs derived from buffy coats of healthy blood donors. Monocytes were induced to become immature DCs (iDCs) using GM-CSF and IL-4 for 4 days. Thereafter, small molecular compounds were added to iDCs for 24 h with concomitant LPS for the last 23 hours, followed by assays of secreted IL-10 and IL-12p70 and surface markers of maturation, activation, and inhibition.

In order to investigate the possibility that a basal β-catenin activation was present in LPS-matured moDCs (48), even in the absence of 6-BIO, we tested our model with the β-catenin inhibitor ICG-001, previously found to inhibit β-catenin-stimulated transcription in both cancer cells (49) and dendritic cells (42). A pronounced ICG-001 dose-dependent increase in IL-12p70 and a corresponding dose-dependent decrease in IL-10 secretion was observed when iDCs were treated for 24 h with ICG-001. This suggested that β-catenin is activated in mature moDCs to promote anti-inflammatory features and, furthermore, is accessible to β-catenin inhibition, even in the absence of Wnt ligands or other specific activators of Wnt or β-catenin signaling added to the culture medium.

Addition of the small molecular compound 6-BIO indicated, however, that the basal β-catenin activity of LPS-matured moDCs can be augmented by external stimulation. Western blot analyses of moDC whole-cell lysates detected β-catenin both in iDCs and LPS-matured moDCs with dose-dependent increase in β-catenin accumulation detectable from low 6-BIO concentrations. Confocal microscopy revealed obvious nuclear accumulation of β-catenin at 250 nM and higher concentrations of 6-BIO. This *in situ* localization method was preferred over nuclear and cytoplasmic fractionation, consistent with our previous results that fractionation is associated with loss of labile nuclear proteins due to the drop of colloid osmotic pressure during fractionation (50).

The small molecule ICG-001 binds CREB-binding protein (CBP) to disrupt its interaction with β-catenin and inhibits CBP function as a co-activator of Wnt/β-catenin-mediated transcription (17). This mechanism of β-catenin inhibition is consistent with our present findings. According to our Western blot assays, ICG-001 did not affect β-catenin at the protein synthesis/stability level. According to microarray and RNA-seq data, β-catenin (*CTNNB1*) mRNA levels were similar in ICG-treated and non-treated moDCs. ICG-001 was consequently used to examine further the association between β-catenin inhibition and anti-inflammatory features of mature moDCs. Competition assays between 6-BIO and ICG-001 showed that these compounds had inverse effects on IL-10 and IL-12p70 secretion and on dendritic cell markers of activation, inhibition, and migration. 6-BIO dose-dependently promoted anti-inflammatory patterns of the examined cytokines and several surface markers. ICG-001 exhibited the opposite and the competing effect on cytokine and several surface markers. The pronounced upregulation of the β-catenin target gene *LRP5* in 6-BIO-treated and downregulation in ICG-001-treated LPS-matured moDCs additionally support the existence of a basal and dynamic β-catenin activation status.

IL-10 is considered an anti-inflammatory cytokine that is induced by β-catenin signaling (11) and by non-canonical Wnt5a signaling in mouse DCs (39). Stimulation of toll-like-receptors (TLR2, TLR4, TLR5, TLR7, and TLR9) has been shown to induce IL-10 production of DCs [reviewed in (14)]. The TLR4 stimulator LPS induced dual production of IL-10 and IL-12 in human moDCs, but with significant donor-to-donor variation (13, 51), consistent with our present findings. In the LPS-matured moDCs, the level of β-catenin was dose-dependently increased by 6-BIO. It may offer experimental advantages to activate β-catenin downstream of the cytoplasmic destruction complex because several upstream and parallel pathways, such as WNTs, tankyrases (52, 53), and TLR2 stimulation via PI3 kinase and ERK in moDCs (54, 55) may activate nuclear β-catenin signaling. In parallel with increasing β-catenin levels, 6-BIO dose-dependently increased IL-10 and dose-dependently decreased IL-12p70. These experiments, therefore, reveal the potential of β-catenin signaling to modulate important pro-

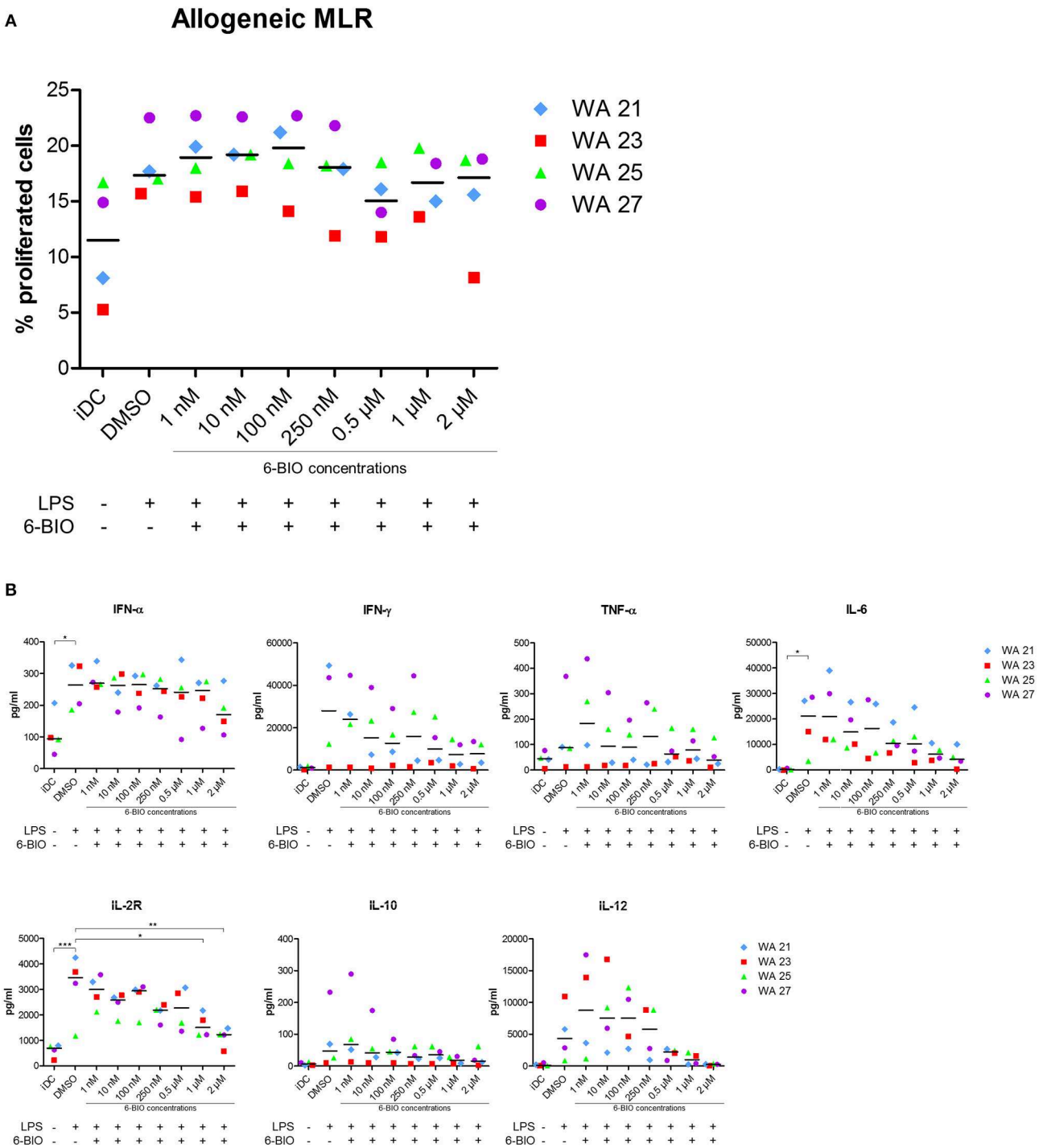

FIGURE 6 | Mixed leukocyte reaction (MLR) between moDCs and allogeneic peripheral blood mononuclear cells (PBMCs) obtained from healthy donors. moDCs were treated with indicated concentrations of 6-BIO or DMSO for 24 h with 30 ng/ml of LPS treatment for 23 h, or left untreated as iDC. Allogeneic PBMCs were pre-labeled with CFSE and co-cultured with treated moDCs for 5 days. **(A)** Percentage proliferated cells was measured by reduction in CFSE intensity. **(B)** The amount of secreted cytokines was analyzed using 25-Plex Panel, and the concentrations are given in pg/ml. Each symbol represents a different donor, and lines represent the median. $^{*}p \leq 0.05$, $^{**}p \leq 0.01$, $^{***}p \leq 0.001$, using one-way ANOVA with Dunnett's multiple comparisons test and 95% confidence interval.

and anti-inflammatory cytokine production of moDCs. The IL-10 promoter has been shown to contain several response elements that can bind β-catenin to activate IL-10 transcription (56). Both microarray and RNA-seq data showed increased IL-10 mRNA in 6-BIO-treated moDCs. The relationship between β-catenin signaling and IL-12 stimulation is additionally complex

due to the ability of IL-10 to decrease IL-12 production in DCs (13).

In mice, DC-specific deletion of the Wnt co-receptors LRP5/6 or β-catenin led to an increased expression of IL-6, TNF-α, IL-1β, IL-12p40, and IL-12p70 with diminished production of IL-10 and TGF-β (57). In another study on mouse splenic DC precursors, CD11c-specific constitutive β-catenin activation upregulated Irf8 through targeting of the Irf8 promoter, β-catenin-stabilized CD8a + DCs secreted elevated IL-12 upon *in vitro* microbial stimulation, and pharmacological β-catenin inhibition using ICG-001 blocked this response in wild-type cells (42). Also, knock-down of the non-canonical Wnt5a in human moDCs, presumed not to signal via β-catenin, compromised IL-12 secretion (58).

In order to obtain an additional impression of potential pro- and anti-inflammatory features of LPS-matured moDCs, whole-genome mRNA analyses of moDCs was done, using both Agilent microarray and Illumina RNA sequence quantifications. Recently, it was published that β-catenin directly stimulates the *IDO1* transcription and additionally the peroxisome proliferator-activated receptor-γ (PPAR-γ), thus, causing the metabolic shift required for protoporphyrin X synthesis, the heme prosthetic group required for full IDO1 enzymatic activity in DCs (12). According to our mRNA expression data, *IDO1* was strongly induced and abundantly expressed in LPS-matured moDCs, while *PPARG* was relatively abundantly expressed in both immature and LPS-matured DCs (ArrayExpress E-MTAB-8330). Surprisingly, 6-BIO dose-dependently reduced *IDO1* mRNA levels in our LPS-matured moDCs, although significant *IDO1* mRNA was still expressed even at high 6-BIO concentrations. Interestingly, CD200 binding to CD200R1 on murine pDCs has been reported among stimulators of IDO1 expression (59). Expressions of *CD200* and *CD200R1* were strongly affected during LPS maturation and by concomitant 6-BIO and ICG-001 treatment. These findings have to be followed up separately.

It has been shown in both murine and human models that Wnt5a from melanomas affects the local DCs to express indoleamine 2,3-dioxygenase-1 (IDO1) that stimulates development of T regulatory cells (TRegs) through kynurenine (60). Wnt5a has been considered to be a ligand of the non-canonical Wnt pathway (β-catenin independent), but appears to be able to context-dependent stimulation of β-catenin signaling, in some cases stronger than the "canonical" Wnt3a stimulation (12, 60).

TGF-β induces T regulatory cells and thereby promotes tolerance when secreted from antigen-presenting cells [(10, 31, 48) and references therein]. It has been reported that TGF-β antagonizes β-catenin in DCs, thereby selectively suppressing signaling associated with tolerogenic DC activation while having no impact on LPS-induced, β-catenin-independent immunogenic activation (61). According to our microarray and RNA-seq data, *TGFB1* was clearly reduced during LPS-mediated maturation of moDCs, but this decrease was counteracted by both concomitant 6-BIO and ICG-001 treatment. This could represent indirect effects of β-catenin, also because *TGFB1* is not a known β-catenin target gene.

VEGF has been shown to be a direct β-catenin target gene in different cell types (62). The strong 6-BIO-enhanced expression of both *VEGFA* and *VEGFB* would suggest this to be the case in LPS-matured moDCs. VEGF has been shown to be immunosuppressive in different ways: it can inhibit the function of T cells, increase the recruitment of T regulatory cells and myeloid-derived suppressor cells (MDSCs), and hinder the differentiation and activation of DCs (34).

Additional transcriptional determinants of tolerogenic and immunogenic states during dendritic cell maturation have been published (63). All our genome-wide Agilent microarray and Illumina RNA-seq data have been made publicly available and can be further explored regarding β-catenin targets and pro- and anti-inflammatory transcription of LPS-matured moDCs.

Mixed leukocyte reaction (MLR) was employed for the assessment of T-cell stimulatory capacity of the generated cell populations and showed the ability of the LPS-stimulated moDCs to induce allogeneic T-cell proliferation. The minor effects of either 6-BIO or ICG-001 in the MLR assay could reflect that the outcome of conflicting pro- and anti-inflammatory cues could be complex. It is possible that negative feedback effects due to moDC and allogeneic cross-talk could result in the abrogation of the pronounced dose-dependent effects on both IL-10 and IL-12 secretion by either 6-BIO or ICG-001 in pure moDC. Expanded cytokine profiling of MLR culture supernatants showed 6-BIO dose-dependent decreases of several relevant cytokines. Presently, this is a reminder of increased complexity once different immune cells are brought into interaction. Future work will address such interactions in MLR assays and in DC and patient-derived cell co-cultures with expanded assays including parallel multi-variable mass cytometric analyses of supernatants and cells.

Much understanding is lacking regarding β-catenin signaling in moDCs, although a critical role of β-catenin signaling in DC function and differentiation of pro- and anti-inflammatory features *in vivo* is already established [reviewed in (37, 46)]. In both freshly isolated and Flt3-stimulated CD11c+ DCs from mouse lymph nodes, the main conclusion was that Wnts upregulate immune suppressive cytokines (IL-10, VEGF, TGF-β) without inhibiting LPS-induced maturation and activation, thus allowing development of a mature tolerogenic phenotype (39). Minimal effects were detected on the MHCII maturation marker or CD80 or CD86 activation markers or the migration marker CCR7 (39). IL-12p70 secretion was additionally found to be little affected by either canonical (Wnt3a) or non-canonical (Wnt5a) signaling in that study (39). In another study, however, deletion of β-catenin in a mouse model was found to increase expression of DC co-stimulatory markers (CD40, CD80, CD86) and to decrease the inhibitory markers PD-L1 and PD-L2 (64). Different murine tumor models have documented the ability of Wnt ligands to stimulate DCs to produce tolerogenic factors, such as IL-10, Raldh, and Ido-1 [reviewed in (11)]. In one study of human cancer, melanoma-intrinsic β-catenin signaling was found to inhibit DC migration and lead to immune evasion (65). The important mechanisms involved have been reviewed (38, 40, 66, 67).

CONCLUSION

LPS-matured moDCs co-developed pro- and anti-inflammatory surface and secretory markers with considerable quantitative person-to-person variation. A basal β-catenin activation was present in LPS-matured moDCs and could be boosted dose dependently by the β-catenin activator 6-BIO and counteracted dose-dependently by the β-catenin transcription complex inhibitor ICG-001 with inverse effects on IL-10 and IL-12 secretion. These observations should be taken into consideration for the production of more potent and robust therapeutic DCs.

DATA AVAILABILITY STATEMENT

DNA microarray data have been deposited into the ArrayExpress database under accession number E-MTAB-8330.

AUTHOR CONTRIBUTIONS

WA, RB, and AØ did the experiments. WA prepared the figures. All authors contributed to experimental design, evaluation of results, manuscript revisions, and approved the submitted version.

FUNDING

The Research Council of Norway (Norges Forskningsråd) has funded positions and running costs. The Norwegian Cancer Society (Kreftforeningen) has funded positions and running costs. This work received funding from Helse Vest (grant numbers 912062, 911626, 911747, 911582, 911778, 912226, and 980058), the Helse Vest Strategic grants of Personalized Therapy (grant number 303484) and Bergen Stem Cell Consortium (grant number 502027), Centre for Cancer Biomarkers, CCBIO, a Centre of Excellence in Cancer Biomarkers authorized and funded by the Research Council of Norway, the Research Council of Norway NFR BEHANDLING program (project number 287829); the Norwegian Cancer Society (project number 204947) and Bergen Research Foundation/Trond Mohn Stiftelse. All flow cytometry experiments were performed at the Core Facility for Flow Cytometry, Department of Clinical Science, University of Bergen.

ACKNOWLEDGMENTS

Hua My Hoang is acknowledged for expert technical assistance and Kjell Petersen and the Computational Biology Unit, Department of Informatics, University of Bergen, for J-Express and microarray data handling. Illumina RNA-sequencing was done by Qiagen GmbH, Hilden, Germany. We thank Michael Gombert and Charlotte B. Ahler for help in data analyses. We thank blood donors and staff at the Blood bank, Haukeland University Hospital. We greatly acknowledge the contributions to this study by Einar Galtung Døsvig, Espen Galtung Døsvig, Bjarne Rieber, Trond Mohn, Herman Friele, Jan Einar Greve, Kåre Rommetveit, and Thorstein Selvik.

SUPPLEMENTARY MATERIAL

The Supplementary Material for this article can be found online at: https://www.frontiersin.org/articles/10.3389/fimmu.2020.00438/full#supplementary-material

REFERENCES

1. Banchereau J, Steinman, RM. Dendritic cells and the control of immunity. *Nature*. (1998) 392:245–52. doi: 10.1038/32588
2. Bol KF, Schreibelt G, Rabold K, Wculek SK, Schwarze JK, Dzionek A, et al. The clinical application of cancer immunotherapy based on naturally circulating dendritic cells. *J Immunother Cancer*. (2019) 7:109. doi: 10.1186/s40425-019-0580-6
3. Chrisikos TT, Zhou Y, Slone N, Babcock R, Watowich SS, Li HS. Molecular regulation of dendritic cell development and function in homeostasis, inflammation, and cancer. *Mol Immunol*. (2019) 110:24–39. doi: 10.1016/j.molimm.2018.01.014
4. Collin M, Bigley V. Human dendritic cell subsets: an update. *Immunology*. (2018) 154:3–20. doi: 10.1111/imm.12888
5. Alcantara-Hernandez M, Leylek R, Wagar LE, Engleman EG, Keler T, Marinkovich MP, et al. High-dimensional phenotypic mapping of human dendritic cells reveals interindividual variation and tissue specialization. *Immunity*. (2017) 47:1037–50.e6. doi: 10.1016/j.immuni.2017.11.001
6. Villani AC, Satija R, Reynolds G, Sarkizova S, Shekhar K, Fletcher J, et al. Single-cell RNA-seq reveals new types of human blood dendritic cells, monocytes, and progenitors. *Science*. (2017) 356:eaah4573. doi: 10.1126/science.aah4573
7. Sabado RL, Balan S, Bhardwaj N. Dendritic cell-based immunotherapy. *Cell Res*. (2017) 27:74–95. doi: 10.1038/cr.2016.157
8. Saxena M, Bhardwaj N. Re-emergence of dendritic cell vaccines for cancer treatment. *Trends Cancer*. (2018) 4:119–37. doi: 10.1016/j.trecan.2017.12.007
9. Jiang A, Bloom O, Ono S, Cui W, Unternaehrer J, Jiang S, et al. Disruption of E-cadherin-mediated adhesion induces a functionally distinct pathway of dendritic cell maturation. *Immunity*. (2007) 27:610–24. doi: 10.1016/j.immuni.2007.08.015
10. Manicassamy S, Pulendran B. Dendritic cell control of tolerogenic responses. *Immunol Rev*. (2011) 241:206–27. doi: 10.1111/j.1600-065X.2011.01015.x
11. Suryawanshi A, Tadagavadi RK, Swafford D, Manicassamy S. Modulation of inflammatory responses by Wnt/beta-catenin signaling in dendritic cells: a novel immunotherapy target for autoimmunity and cancer. *Front Immunol*. (2016) 7:460. doi: 10.3389/fimmu.2016.00460
12. Zhao F, Xiao C, Evans KS, Theivanthiran T, DeVito N, Holtzhausen A, et al. Paracrine Wnt5a-beta-catenin signaling triggers a metabolic program that drives dendritic cell tolerization. *Immunity*. (2018) 48:147–60.e7. doi: 10.1016/j.immuni.2017.12.004
13. Zheng H, Ban Y, Wei F, Ma X. Regulation of interleukin-12 production in antigen-presenting cells. *Adv Exp Med Biol*. (2016) 941:117–38. doi: 10.1007/978-94-024-0921-5_6
14. Rutz S, Ouyang W. Regulation of interleukin-10 expression. *Adv Exp Med Biol*. (2016) 941:89–116. doi: 10.1007/978-94-024-0921-5_5
15. Sato N, Meijer L, Skaltsounis L, Greengard P, Brivanlou AH. Maintenance of pluripotency in human and mouse embryonic stem cells through activation of Wnt signaling by a pharmacological GSK-3-specific inhibitor. *Nat Med*. (2004) 10:55–63. doi: 10.1038/nm979
16. Qu Y, Gharbi N, Yuan X, Olsen JR, Blicher P, Dalhus B, et al. Axitinib blocks Wnt/beta-catenin signaling and directs asymmetric cell division in cancer. *Proc Natl Acad Sci USA*. (2016) 113:9339–44. doi: 10.1073/pnas.1604520113

17. Emami KH, Nguyen C, Ma H, Kim DH, Jeong KW, Eguchi M, et al. A small molecule inhibitor of beta-catenin/CREB-binding protein transcription [corrected]. *Proc Natl Acad Sci USA*. (2004) 101:12682–7. doi: 10.1073/pnas.0404875101
18. Olsen JR, Azeem W, Hellem MR, Marvyin K, Hua Y, Qu Y, et al. Context dependent regulatory patterns of the androgen receptor and androgen receptor target genes. *BMC Cancer*. (2016) 16:377. doi: 10.1186/s12885-016-2453-4
19. Azeem W, Hellem MR, Olsen JR, Hua Y, Marvyin K, Qu Y, et al. An androgen response element driven reporter assay for the detection of androgen receptor activity in prostate cells. *PLoS ONE*. (2017) 12:e0177861. doi: 10.1371/journal.pone.0177861
20. Sprater F, Azeem W, Appel S. Activation of peroxisome proliferator-activated receptor gamma leads to upregulation of ESE-3 expression in human monocyte-derived dendritic cells. *Scand J Immunol*. (2014) 79:20–6. doi: 10.1111/sji.12126
21. Qu Y, Oyan AM, Liu R, Hua Y, Zhang J, Hovland R, et al. Generation of prostate tumor-initiating cells is associated with elevation of reactive oxygen species and IL-6/STAT3 signaling. *Cancer Res*. (2013) 73:7090–100. doi: 10.1158/0008-5472.CAN-13-1560
22. Dysvik B, Jonassen I. J-Express: exploring gene expression data using Java. *Bioinformatics*. (2001) 17:369–70. doi: 10.1093/bioinformatics/17.4.369
23. Langmead B, Salzberg SL. Fast gapped-read alignment with Bowtie 2. *Nat Methods*. (2012) 9:357–9. doi: 10.1038/nmeth.1923
24. Trapnell C, Pachter L, Salzberg SL. TopHat: discovering splice junctions with RNA-Seq. *Bioinformatics*. (2009) 25:1105–11. doi: 10.1093/bioinformatics/btp120
25. Trapnell C, Salzberg SL. How to map billions of short reads onto genomes. *Nat Biotechnol*. (2009) 27:455–7. doi: 10.1038/nbt0509-455
26. Trapnell C, Roberts A, Goff L, Pertea G, Kim D, Kelley DR, et al. Differential gene and transcript expression analysis of RNA-seq experiments with TopHat and Cufflinks. *Nat Protoc*. (2012) 7:562–78. doi: 10.1038/nprot.2012.016
27. Trapnell C, Williams BA, Pertea G, Mortazavi A, Kwan G, van Baren MJ, et al. Transcript assembly and quantification by RNA-Seq reveals unannotated transcripts and isoform switching during cell differentiation. *Nat Biotechnol*. (2010) 28:511–5. doi: 10.1038/nbt.1621
28. Roberts A, Trapnell C, Donaghey J, Rinn JL, Pachter L. Improving RNA-Seq expression estimates by correcting for fragment bias. *Genome Biol*. (2011) 12:R22. doi: 10.1186/gb-2011-12-3-r22
29. Wolfle SJ, Strebovsky J, Bartz H, Sahr A, Arnold C, Kaiser C, et al. PD-L1 expression on tolerogenic APCs is controlled by STAT-3. *Eur J Immunol*. (2011) 41:413–24. doi: 10.1002/eji.201040979
30. Hong Y, Manoharan I, Suryawanshi A, Shanmugam A, Swafford D, Ahmad S, et al. Deletion of LRP5 and LRP6 in dendritic cells enhances antitumor immunity. *Oncoimmunology*. (2016) 5:e1115941. doi: 10.1080/2162402X.2015.1115941
31. Bourque J, Hawiger D. Immunomodulatory bonds of the partnership between dendritic cells and T cells. *Crit Rev Immunol*. (2018) 38:379–401. doi: 10.1615/CritRevImmunol.2018026790
32. Chu DT, Bac ND, Nguyen KH, Tien NLB, Thanh VV, Nga VT, et al. An update on anti-CD137 antibodies in immunotherapies for cancer. *Int J Mol Sci*. (2019) 20:1822. doi: 10.3390/ijms20081822
33. Mellor AL, Lemos H, Huang L. Indoleamine 2,3-dioxygenase and tolerance: where are we now? *Front Immunol*. (2017) 8:1360. doi: 10.3389/fimmu.2017.01360
34. Yang J, Yan J, Liu B. Targeting VEGF/VEGFR to modulate antitumor immunity. *Front Immunol*. (2018) 9:978. doi: 10.3389/fimmu.2018.00978
35. Saxena M, Balan S, Roudko V, Bhardwaj N. Towards superior dendritic-cell vaccines for cancer therapy. *Nat Biomed Eng*. (2018) 2:341–6. doi: 10.1038/s41551-018-0250-x
36. Fu C, Jiang A. Dendritic cells and CD8 T cell immunity in tumor microenvironment. *Front Immunol*. (2018) 9:3059. doi: 10.3389/fimmu.2018.03059
37. Galluzzi L, Spranger S, Fuchs E, Lopez-Soto A. WNT signaling in cancer immunosurveillance. *Trends Cell Biol*. (2019) 29:44–65. doi: 10.1016/j.tcb.2018.08.005
38. Luke JJ, Bao R, Sweis RF, Spranger S, Gajewski TF. WNT/β-catenin pathway activation correlates with immune exclusion across human cancers. *Clin Cancer Res*. (2019). 25:3074–83. doi: 10.1158/1078-0432.CCR-18-1942
39. Oderup C, LaJevic M, Butcher EC. Canonical and noncanonical Wnt proteins program dendritic cell responses for tolerance. *J Immunol*. (2013) 190:6126–34. doi: 10.4049/jimmunol.1203002
40. Spranger S, Gajewski TF. Impact of oncogenic pathways on evasion of antitumour immune responses. *Nat Rev Cancer*. (2018) 18:139–47. doi: 10.1038/nrc.2017.117
41. Alessandrini A, De Haseth S, Fray M, Miyajima M, Colvin RB, Williams WW, et al. Dendritic cell maturation occurs through the inhibition of GSK-3beta. *Cell Immunol*. (2011) 270:114–25. doi: 10.1016/j.cellimm.2011.04.007
42. Cohen SB, Smith NL, McDougal C, Pepper M, Shah S, Yap GS, et al. Beta-catenin signaling drives differentiation and proinflammatory function of IRF8-dependent dendritic cells. *J Immunol*. (2015) 194:210–22. doi: 10.4049/jimmunol.1402453
43. Feng M, Jin JQ, Xia L, Xiao T, Mei S, Wang X, et al. Pharmacological inhibition of beta-catenin/BCL9 interaction overcomes resistance to immune checkpoint blockades by modulating Treg cells. *Sci Adv*. (2019) 5:eaau5240. doi: 10.1126/sciadv.aau5240
44. Fu C, Liang X, Cui W, Ober-Blobaum JL, Vazzana J, Shrikant PA, et al. β-Catenin in dendritic cells exerts opposite functions in cross-priming and maintenance of CD8+ T cells through regulation of IL-10. *Proc Natl Acad Sci USA*. (2015) 112:2823–8. doi: 10.1073/pnas.1414167112
45. Kafer R, Usanova S, Montermann E, Loquai C, Reske-Kunz AB, Bros M. Inhibitors of beta-catenin affect the immuno-phenotype and functions of dendritic cells in an inhibitor-specific manner. *Int Immunopharmacol*. (2016) 32:118–24. doi: 10.1016/j.intimp.2016.01.018
46. Wang B, Tian T, Kalland KH, Ke X, Qu Y. Targeting Wnt/β-catenin signaling for cancer immunotherapy. *Trends Pharmacol Sci*. (2018) 39:648–58. doi: 10.1016/j.tips.2018.03.008
47. Zizzari IG, Napoletano C, Botticelli A, Caponnetto S, Calabro F, Gelibter A, et al. TK inhibitor pazopanib primes DCs by downregulation of the beta-catenin pathway. *Cancer Immunol Res*. (2018) 6:711–22. doi: 10.1158/2326-6066.CIR-17-0594
48. Manicassamy S, Reizis B, Ravindran R, Nakaya H, Salazar-Gonzalez RM, Wang YC. Activation of beta-catenin in dendritic cells regulates immunity versus tolerance in the intestine. *Science*. (2010) 329:849–53. doi: 10.1126/science.1188510
49. Ma H, Nguyen C, Lee KS, Kahn M. Differential roles for the coactivators CBP and p300 on TCF/beta-catenin-mediated survivin gene expression. *Oncogene*. (2005) 24:3619–31. doi: 10.1038/sj.onc.1208433
50. Kalland KH, Szilvay AM, Brokstad KA, Saetrevik W, Haukenes G. The human immunodeficiency virus type 1 Rev protein shuttles between the cytoplasm and nuclear compartments. *Mol Cell Biol*. (1994) 14:7436–44. doi: 10.1128/MCB.14.11.7436
51. Lovgren T, Sarhan D, Truxova I, Choudhary B, Maas R, Melief J, et al. Enhanced stimulation of human tumor-specific T cells by dendritic cells matured in the presence of interferon-gamma and multiple toll-like receptor agonists. *Cancer Immunol Immunother*. (2017) 66:1333–44. doi: 10.1007/s00262-017-2029-4
52. Nusse R, Clevers H. Wnt/β-catenin signaling, disease, and emerging therapeutic modalities. *Cell*. (2017) 169:985–99. doi: 10.1016/j.cell.2017.05.016
53. Wiese KE, Nusse R, van Amerongen R. Wnt signalling: conquering complexity. *Development*. (2018) 145:dev165902. doi: 10.1242/dev.165902
54. Agrawal S, Agrawal A, Doughty B, Gerwitz A, Blenis J, Van Dyke T, et al. Cutting edge: different Toll-like receptor agonists instruct dendritic cells to induce distinct Th responses via differential modulation of extracellular signal-regulated kinase-mitogen-activated protein kinase and c-Fos. *J Immunol*. (2003) 171:4984–9. doi: 10.4049/jimmunol.171.10.4984
55. Manoharan I, Hong Y, Suryawanshi A, Angus-Hill ML, Sun Z, Mellor AL, et al. TLR2-dependent activation of beta-catenin pathway in dendritic cells induces regulatory responses and attenuates autoimmune inflammation. *J Immunol*. (2014) 193:4203–13. doi: 10.4049/jimmunol.1400614

56. Yaguchi T, Goto Y, Kido K, Mochimaru H, Sakurai T, Tsukamoto N, et al. Immune suppression and resistance mediated by constitutive activation of Wnt/beta-catenin signaling in human melanoma cells. *J Immunol.* (2012) 189:2110–7. doi: 10.4049/jimmunol.1102282
57. Suryawanshi A, Manoharan I, Hong Y, Swafford D, Majumdar T, Taketo MM, et al. Canonical wnt signaling in dendritic cells regulates Th1/Th17 responses and suppresses autoimmune neuroinflammation. *J Immunol.* (2015) 194:3295–304. doi: 10.4049/jimmunol.1402691
58. Valencia J, Martinez VG, Hidalgo L, Hernandez-Lopez C, Canseco NM, Vicente A, et al. Wnt5a signaling increases IL-12 secretion by human dendritic cells and enhances IFN-gamma production by CD4+ T cells. *Immunol Lett.* (2014) 162(1 Pt A):188–99. doi: 10.1016/j.imlet.2014.08.015
59. Fallarino F, Asselin-Paturel C, Vacca C, Bianchi R, Gizzi S, Fioretti MC, et al. Murine plasmacytoid dendritic cells initiate the immunosuppressive pathway of tryptophan catabolism in response to CD200 receptor engagement. *J Immunol.* (2004) 173:3748–54. doi: 10.4049/jimmunol.173.6.3748
60. Holtzhausen A, Zhao F, Evans KS, Tsutsui M, Orabona C, Tyler DS, et al. Melanoma-derived Wnt5a promotes local dendritic-cell expression of IDO and immunotolerance: opportunities for pharmacologic enhancement of immunotherapy. *Cancer Immunol Res.* (2015) 3:1082–95. doi: 10.1158/2326-6066.CIR-14-0167
61. Vander Lugt B, Beck ZT, Fuhlbrigge RC, Hacohen N, Campbell JJ, Boes M. TGF-beta suppresses beta-catenin-dependent tolerogenic activation program in dendritic cells. *PLoS ONE.* (2011) 6:e20099. doi: 10.1371/journal.pone.0020099
62. Wang Y, Sang A, Zhu M, Zhang G, Guan H, Ji M, et al. Tissue factor induces VEGF expression via activation of the Wnt/beta-catenin signaling pathway in ARPE-19 cells. *Mol Vis.* (2016) 22:886–97.
63. Vander Lugt B, Riddell J, Khan AA, Hackney JA, Lesch J, DeVoss J, et al. Transcriptional determinants of tolerogenic and immunogenic states during dendritic cell maturation. *J Cell Biol.* (2017) 216:779–92. doi: 10.1083/jcb.201512012
64. Hong Y, Manoharan I, Suryawanshi A, Majumdar T, Angus-Hill ML, Koni PA, et al. β-catenin promotes regulatory T-cell responses in tumors by inducing vitamin A metabolism in dendritic cells. *Cancer Res.* (2015) 75:656–65. doi: 10.1158/0008-5472.CAN-14-2377
65. Spranger S, Bao R, Gajewski TF. Melanoma-intrinsic β-catenin signalling prevents anti-tumour immunity. *Nature.* (2015) 523:231–5. doi: 10.1038/nature14404
66. Binnewies M, Roberts EW, Kersten K, Chan V, Fearon DF, Merad M, et al. Understanding the tumor immune microenvironment (TIME) for effective therapy. *Nat Med.* (2018) 24:541–50. doi: 10.1038/s41591-018-0014-x
67. Spranger S, Dai D, Horton B, Gajewski TF. Tumor-residing batf3 dendritic cells are required for effector T cell trafficking and adoptive T cell therapy. *Cancer Cell.* (2017) 31:711–23.e4. doi: 10.1016/j.ccell.2017.04.003

Conflict of Interest: AØ and K-HK own stocks in the Company Alden Cancer Therapy II AS that has sponsored and will sponsor dendritic cell-based cancer immunotherapy, including the trial registered at ClinicalTrials.gov Identifier: NCT02423928. AØ and K-HK additionally are co-inventors of the United States Patent Application No. 15/771496 (US-2018-0344715) regarding novel beta-catenin inhibitor compounds for cancer therapy. None of these compounds have been used or addressed in the present manuscript.

The remaining authors declare that the research was conducted in the absence of any commercial or financial relationships that could be construed as a potential conflict of interest.

frontiers in Immunology

REVIEW
published: 19 May 2020
doi: 10.3389/fimmu.2020.00909

Factors Which Contribute to the Immunogenicity of Non-replicating Adenoviral Vectored Vaccines

Lynda Coughlan[*†]

Department of Microbiology, Icahn School of Medicine at Mount Sinai, New York, NY, United States

Adenoviral vectors are a safe and potently immunogenic vaccine delivery platform. Non-replicating Ad vectors possess several attributes which make them attractive vaccines for infectious disease, including their capacity for high titer growth, ease of manipulation, safety, and immunogenicity in clinical studies, as well as their compatibility with clinical manufacturing and thermo-stabilization procedures. In general, Ad vectors are immunogenic vaccines, which elicit robust transgene antigen-specific cellular (namely $CD8^+$ T cells) and/or humoral immune responses. A large number of adenoviruses isolated from humans and non-human primates, which have low seroprevalence in humans, have been vectorized and tested as vaccines in animal models and humans. However, a distinct hierarchy of immunological potency has been identified between diverse Ad vectors, which unfortunately limits the potential use of many vectors which have otherwise desirable manufacturing characteristics. The precise mechanistic factors which underlie the profound disparities in immunogenicity are not clearly defined and are the subject of ongoing, detailed investigation. It has been suggested that a combination of factors contribute to the potent immunogenicity of particular Ad vectors, including the magnitude and duration of vaccine antigen expression following immunization. Furthermore, the excessive induction of Type I interferons by some Ad vectors has been suggested to impair transgene expression levels, dampening subsequent immune responses. Therefore, the induction of balanced, but not excessive stimulation of innate signaling is optimal. Entry factor binding or receptor usage of distinct Ad vectors can also affect their *in vivo* tropism following administration by different routes. The abundance and accessibility of innate immune cells and/or antigen-presenting cells at the site of injection contributes to early innate immune responses to Ad vaccination, affecting the outcome of the adaptive immune response. Although a significant amount of information exists regarding the tropism determinants of the common human adenovirus type-5 vector, very little is known about the receptor usage and tropism of rare species or non-human Ad vectors. Increased understanding of how different facets of the host response to Ad vectors contribute to their immunological potency will be essential for the development of optimized and customized Ad vaccine platforms for specific diseases.

Keywords: adenovirus, adenoviral, vector, vaccine, immunogenicity

OPEN ACCESS

Edited by:
Matthias Tenbusch,
University Hospital Erlangen, Germany

Reviewed by:
Wibke Bayer,
Essen University Hospital, Germany
Marc Paul Girard,
Université Paris Diderot, France

***Correspondence:**
Lynda Coughlan
lynda.coughlan@mssm.edu

†ORCID:
Lynda Coughlan
orcid.org/0000-0001-9880-6560

Specialty section:
This article was submitted to Vaccines and Molecular Therapeutics, a section of the journal Frontiers in Immunology

Received: *30 January 2020*
Accepted: *20 April 2020*
Published: *19 May 2020*

Citation:
Coughlan L (2020) Factors Which Contribute to the Immunogenicity of Non-replicating Adenoviral Vectored Vaccines. Front. Immunol. 11:909. doi: 10.3389/fimmu.2020.00909

INTRODUCTION

Use of Adenoviral Vectors as Vaccines for Infectious Disease

Adenoviruses (Ad) represent a promising vector platform for the development of vaccines for infectious disease, largely due to their safety and ability to stimulate robust cellular and/or humoral immune responses in multiple species (1–8), as compared with other genetic vaccine platforms (5, 9–12). Adenoviruses derived from humans and non-human primates (NHP) belong to the family *Adenoviridae* and the genus *Mastadenoviridae,* and are further subdivided into species A-G (i.e., for species A viruses, these are denoted HAdV-A followed by the type number). Accounting for the inclusion of many Ad recombinants (13, 14), ∼103 human Ads (http://hadvwg.gmu.edu/) and >200 non-human Ad serotypes have been identified to date. Adenoviruses are non-enveloped viruses which contain a double-stranded DNA genome. The virion exterior is composed of three major structural proteins, the fiber, the penton base and the hexon [(15–18); **Figure 1**]. Recombinant Ad (rAd) vectors can easily be rendered replication-incompetent (non-replicating) through deletion of the essential viral gene E1 from their genome and can be vectorized for easy manipulation (16, 19–21). Further improvements to these first-generation Ad vectors have been developed in which the E3 region is also deleted, to accommodate a larger heterologous transgene capacity of ∼7.5 kbp. Ad vectors display a number of desirable characteristics which make them particularly well-suited to prophylactic vaccine applications. Their genome is stable and easy to manipulate, they can be amplified and produced to high titers using various complementing cell lines which adhere with good clinical practice (GCP) procedures (22), and they have an outstanding track-record as safe and immunogenic vaccines in numerous human clinical trials (1–7, 23–25). Historically, the most commonly used rAd has been *Human mastadenovirus C*, Human Adenovirus Type-5 (HAdV-C5, *referred to Ad5 throughout this manuscript*). However, despite its well-characterized biology and robust immunogenicity, high seroprevalence has limited its widespread use in humans and has prompted the development and investigation of novel Ad species, either rare species human Ads (6, 20, 26) or those derived from NHPs (5, 8, 27), many of which have very low seroprevalence (27–31). For the purpose of this review, the nomenclature of Ad types will use reference to the vertebrate species from which the vector was derived (i.e., H for human or Ch for chimpanzee) followed by the virus type number, as outlined in **Table 1**. Human Ad vectors will include their assigned adenovirus species group (i.e., A-G). This nomenclature has been proposed to ICTV by Dr. Don Seto, George Mason University and Dr. James Chodosh, Harvard University (*personal communication*).

The use of non-replicating viral vectors as a vaccine platform has several advantages over other vaccine formulations (i.e., recombinant protein, inactivated particles). Viral vectored vaccines retain some characteristics of a live attenuated vaccine in terms of their ability to enter target cells, engage intracellular trafficking pathways to deliver their genome and facilitate antigen (Ag) expression and subsequent Ag-presentation *in vivo,* but possess additional safety features. Furthermore, in order to drive the expression of substantial quantities of transcripts which correspond to the encoded vaccine Ag, non-replicating Ad vectors make use of powerful exogenous promoters, such as the cytomegalovirus (CMV) promoter (32). Unlike recombinant protein or inactivated vaccines in which antigen quantity is limited to the input vaccine dose, the use of exogenous promoters facilitates more sustained transgene antigen expression *in vivo*.

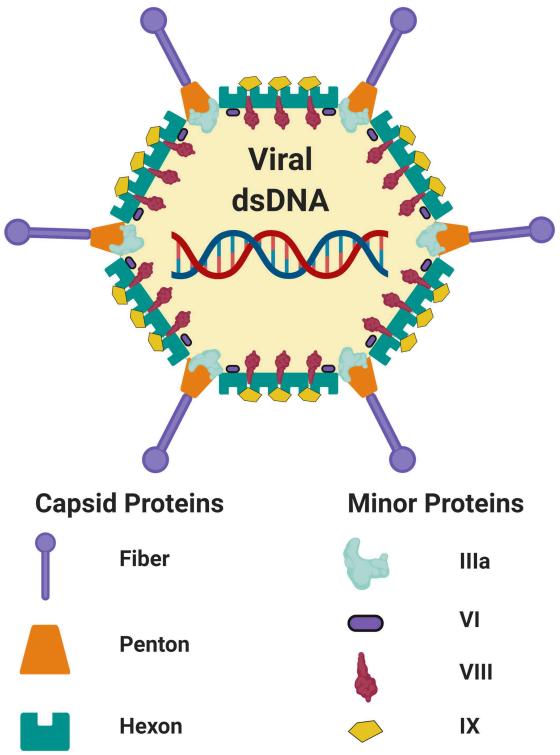

FIGURE 1 | Schematic adenovirus structure. Schematic representation of the capsid and minor structural proteins of an adenovirus. Internal core proteins are not shown. The adenoviral virion contains linear double-stranded DNA genome (dsDNA). Figure is adapted from Russell (17) and was created with ©BioRender - biorender.com. Proteins are not to scale.

In general, Ad vectors are well-established to stimulate $CD8^+$ T cell responses directed toward transgene Ag, with selected Ad types confirmed to elicit robust cellular immunity in both animal models (8, 32–36) and humans [(1, 3, 6, 23, 33, 37); see **Table 2**]. Memory $CD8^+$ T cell responses elicited following vaccination with Ad vectors exhibit an extended contraction phase (38). Importantly, the persistent Ag expression following immunization with Ad vaccines enables the induction of sustained immune responses (5, 36, 39–41), making them very attractive vaccine vectors for conferring long-lasting immunity. It is believed that the prolonged expression of vaccine Ag facilitates the maintenance of effector $CD8^+$ T cells while simultaneously permitting their differentiation into central memory populations (36). Improved understanding into how Ad vectors prime and maintain such long-lived responses will be crucial not only in designing improved Ad vaccines, but also other vaccine

TABLE 1 | Nomenclature of adenoviruses discussed in this review.

Ad name (*this review*)	Description (vertebrate species, type)	Species/Group classification	Alternative names reported in the literature
HAdV-B3	Human adenovirus type 3	B	Ad3, rAd3
*HAdV-B35	Human adenovirus type 35	B	Ad35, rAd35
HAdV-C2	Human adenovirus type 2	C	Ad2, rAd2
*HAdV-C5	Human adenovirus type 5	C	Ad5, rAd5, AdHu5
*HAdV-C6	Human adenovirus type 6	C	Ad6, rAd6, AdHu6
HAdV-D11	Human adenovirus type 11	D	Ad11, rAd11
*HAdV-D26	Human adenovirus type 26	D	Ad26, rAd26
HAdV-D28	Human adenovirus type 28	D	Ad28, rAd28
*HAdV-E4	Human adenovirus type 4	E	Ad4, rAd4
ChAdV-1	Chimpanzee adenovirus type 1	B2	ChAd1, AdC1, SAd21
*ChAdV-3	Chimpanzee adenovirus type 3	C	ChAd3
ChAdV-7	Chimpanzee adenovirus type 7	E	AdC7, ChAd7, SAd24, Pan7
*ChAdV-63	Chimpanzee adenovirus type 63	E	ChAd63
ChAdV-68	Chimpanzee adenovirus type 68	E	AdC68, ChAd68, SAd25, Pan9, ChAdOx2
*ChAdOx1	Chimpanzee adenovirus type Y25	E	Y25
SAdV-11	Simian adenovirus type 11	Yet undefined	SAd11, sAd11
SAdV-16	Simian adenovirus type 16	Yet undefined	SAd16, sAd16
SAdV-23	Simian adenovirus type 23	E	ChAdV-6, AdC6, ChAd6, Pan6
*PanAdV-3	Pan (*paniscus*) adenovirus type 3	C	PanAd3

Adenovirus classification for human and non-human Ad vectors referred to in this review. The nomenclature of Ad vectors derived from non-human primates, including chimpanzees, is not standardized, resulting in the confusing use of multiple names assigned by individuals who vectorized these constructs. In this review text, we propose to follow current standards for human Ad vectors, such as HAdV-C5, as outlined by ICTV, for descriptions of Ad vectors derived from chimpanzees or non-human primates. Abbreviated "alternative" names are used in ***Table 2*** *due to space constraints. H, human; Ch, chimpanzee; S, simian. *Vectors used in human clinical trial.*

platforms which are optimized for diverse disease targets. However, the precise factors which contribute to the robust immunogenicity associated with particular Ad-vectored vaccines are currently unclear.

It is widely appreciated in the Ad vaccine field that Ad vectors can act as a "self-adjuvant," allowing the stimulation of multiple innate immune signaling pathways upon viral entry, which can augment the immunogenicity of the encoded Ag (although conversely, stimulation of certain signaling pathways can also be detrimental to their immunogenicity, as discussed below). Although we have some understanding of how individual pathways work *in vitro* in defined cell types (i.e., dendritic cells, macrophages), understanding how these pathways intersect, or cooperate in the development of protective immunity *in vivo,* is complex and our understanding is incomplete. Additionally, it is apparent that there is a clear hierarchy of immunological potency when evaluating distinct Ad species and serotypes as vaccine vectors in animal models. Although a few selected vectors display robust immunogenicity *in vivo* which is comparable to that of Ad5, most are less immunogenic (5, 8, 15, 29, 31), and there are considerable differences in the phenotype and functionality of immune response elicited (8, 42, 43). In recent years, investigators have begun to identify several crucial factors which could contribute to these profound disparities in immunological potency. It is now believed that differences in (i) cellular receptor and/or co-receptor usage, viral entry, trafficking, endosomal escape, and *in vivo* tropism can contribute to the (ii) differential activation of innate immune signaling which influences subsequent immune responses (44). In addition, it is apparent that the (iii) magnitude and persistence of transgene expression can also shape the ensuing immune response (33) and all of these factors are in turn affected by the (iv) vaccine dose (8) and route of administration (45). Increased understanding of, and implementation of efforts to overcome these striking differences in immunological potency or quality, will absolutely be required for the development of optimal Ad vectors for clinical use.

Viral Entry and Cellular Tropism

Entry in non-immune cells

As a result of extensive study over the past few decades, we have a clear understanding of the *in vitro* tropism determinants of vectors derived from species C HAdVs (i.e., HAdV-C5/Ad5) (18). The classical entry pathway of rAd5-based vectors in non-immune cells is mediated by binding of the fiber knob domain (**Figure 2**) to the Coxsackie and Adenovirus receptor (CAR). Following this "docking" interaction, viral internalization is facilitated through interactions between the arginine-glycine-aspartate (RGD) motif within the viral penton base and cellular integrins (namely αvβ3 and αvβ5) on the surface of cells (46, 47). Adenovirus capsid disassembly then proceeds in a systematic and stepwise process. Initial binding to CAR is a motile interaction, whereas the subsequent interaction with immobile αv integrins results in the ripping or shedding of fibers from the virion, initiating partial disassembly of the virion at the plasma membrane (48, 49). It was previously believed

TABLE 2 | Summary of the comparative immunogenicity of diverse AdV vaccines.

A. Ad vectors compared	B. Vaccine antigen	C. Parameters used to define hierarchy of immunogenicity	Optimal vector	PMID
SPECIES: MICE				
Human Ads **B:** Ad34, Ad35 **C:** Ad5, Ad6 **D:** Ad24	HIV-1 *gag*	**Maintenance of Gag$^+$CD8$^+$IFNγ$^+$ responses with dose de-escalation (10^{10}-10^6 vp):** Ad5, Ad6 > Ad24 > Ad35 > Ad34 (*Balb/c mice,* intramuscular immunization) • Ad5 and Ad6 were capable of eliciting T cell responses at a vaccine dose of 10^6 viral particles (vp). Ad24 = 10^8 vp, Ad35 = 10^9 vp, and Ad34 = 10^{10} vp.	**Ad5, Ad6**	22218691
Non-human Ads **B:** ChAd30 **C:** ChAd3, PanAd3, PanAd1, PanAd2, ChAd11, ChAd19, ChAd20, ChAd24, ChAd31 (listed in order of immunogenicity) **E:** ChAd63, ChAd83, ChAd6, ChAd9, ChAd10, ChAd43, ChAd55, ChAd147, ChAd4, ChAd5, ChAd7, ChAd16, ChAd38, ChAd146, ChAd149, ChAd150 (listed in order of immunogenicity)		**Maintenance of Gag$^+$CD8$^+$IFNγ$^+$ responses with dose de-escalation (10^{10}-10^6 vp):** ChAd3, PanAd3 > ChAd63 > PanAd1 > as listed in column A (*Balb/c mice,* intramuscular immunization) • 26 chimpanzee adenoviral isolates were screened for immunological potency. • Group C Ad vectors were most potently immunogenic, followed by Group E. Group B ChAd30 was weakly immunogenic. • ChAd3 and PanAd3 were capable of eliciting T cell responses at a dose of 10^6 viral particles (vp), ranking them as comparable with the immunogenicity of Ad5. • ChAd63 also elicited T cell responses at 3×10^6 vp making it only slightly less immunogenic than ChAd3 and PanAd3.	**ChAd3, PanAd3, ChAd63**	
Human Ads **B:** Ad35 **C:** Ad5 **D:** Ad28 **Non-human Ads** **C:** ChAd3 **E:** ChAd63 **ND:** SAd11, SAd16	SIV *gag*	**Magnitude and protective efficacy of CD8$^+$ with dose de-escalation (10^9-10^7 particle units PU):** Efficacy ranking: Ad5+ChAd3 > Ad28+SAd11 > ChAd63 > SAd16 > Ad35 (*C57BL/6 mice*, sub-cutaneous immunization) • Study performed a dose titration of vaccines with detailed phenotyping of T cell response at peak and memory timepoints. • Ad5, Ad28, SAd11, and ChAd3 were comparable in conferring CD8$^+$ mediated protection in challenge model using gag-expressing *Listeria monocytogenes.*	**Ad5, Ad28** **ChAd3** **SAd11**	23390298
Human Ads **B:** Ad35 **C:** Ad5 **D:** Ad28 **Non-human Ads** **C:** ChAd3 **E:** ChAd63 **ND:** SAd11, SAd16	SIV *gag* *eGFP*	**Memory (D70) Gag Tetramer$^+$CD8$^+$ at 10^8 PU and protection from challenge:** Ad5, ChAd3 > ChAd63 (*C57BL/6 mice*, sub-cutaneous immunization) • The protective efficacy of Ad vectors in a murine challenge model of *gag*-expressing *Listeria monocytogenes* was tested. • Ad5 and ChAd3 were most potently protective, followed by ChAd63. • Vaccination with Ads expressing reporter eGFP resulted in higher frequencies of eGFP$^+$ CD11c$^+$ dendritic cells in draining lymph nodes (dLNs) for Ad5, ChAd3 > ChAd63. • Transcriptional profiling of dLNs revealed that the most potently protective vectors, Ad5 and ChAd3, exhibited weak induction of IFN-stimulated genes, unlike other Ad vectors (8–24 h). • More pronounced upregulation of IFN-responsive gene modules in dLNs at 24 h were associated with reducing Ad transgene expression levels and thereby limiting their immunological potency.	**Ad5** **ChAd3, ChAd63**	25642773
Human Ads **B:** Ad11, Ad35, Ad50 **C:** Ad5 **D:** Ad26, Ad48, Ad49	SIV *gag*	**Maintenance of Gag$^+$CD8$^+$IFNγ$^+$ responses with dose de-escalation (10^{10}-10^7 vp):** Ad5 > Ad26 (*C57BL/6 mice*, intramuscular immunization) • A head-to-head comparison of species B and D Ad-based vaccine vectors was performed compared with species C Ad5. • At a dose of 10^7 vp, Ad5 and Ad26 were more potent than all other Ad vectors, but only Ad5 was immunogenic at a dose of 10^6 vp.	**Ad5, Ad26**	17329340

(Continued)

TABLE 2 | Continued

A. Ad vectors compared	B. Vaccine antigen	C. Parameters used to define hierarchy of immunogenicity	Optimal vector	PMID
Human Ads **C:** Ad5 **D:** Ad26	HIV-1 *gag*	**Magnitude of Gag$^+$CD8$^+$IFNγ$^+$ responses at 10^9 or 10^8 vp:** Ad5 > Ad26, AdC6, AdC7 (*Balb/c mice*, intramuscular immunization) • At 10^{10} vp gag-specific CD8+ responses were comparable for Ad5, Ad26, AdC6, and AdC7. • At 10^8 vp, Ad5 was superior to all.	**Ad5, Ad26**	20686035
Non-human Ads **E:** AdC6 (SAdV-23), AdC7 (SAdV-24)	Rabies *glycoprotein*	**Induction of NAbs to Rabies GP and Protective Efficacy at 10^{11}-10^9 vp:** Ad5 > Ad26, AdC6, AdC7 (*ICR outbred mice*, intramuscular immunization) • At all doses neutralizing antibodies considered protective according to comparison with WHO standard serum samples (>0.5 IU) were induced, but Ad5 was the best. • Ad5 had superior protective efficacy from challenge with rabies virus strain CVS-24 at all doses, survival with other Ads was reduced, even at 10^{11} vp. • Ad26 displayed 60% survival, AdC6 was ∼50% survival at 10^{11} vp.	**Ad26, AdC6**	

We are only including murine studies that performed a head-to-head comparison of vector immunogenicity for Ad vaccines derived from more than three Ad species groups. Please note, vector type names are listed as shortened versions due to space constraints within the Table. IFNγ, interferon gamma; vp, viral particle; PU, particle unit; HIV, human immunodeficiency virus; SIV, simian immunodeficiency virus; eGFP, enhanced green fluorescent protein; dLN, draining lymph node; GP, glycoprotein. Abbreviated "alternative" names for Ad vectors are used in this table due to space constraints. See ***Table 1*** *for their standardized nomenclature.*

that endosomal escape was pH-dependent (50). However, it has subsequently been demonstrated that exposure of protein VI from the capsid interior (51) at the cell surface, as a result of mechanical strain induced by the antagonistic CAR:integrin interaction (48), facilitates access to the cytoplasm through the action of its pH-independent membrane lytic activity (52–54). Following endosomal escape, the virion is transported to the nuclear pore complex via the microtubule network (50, 52). Once the virion has docked at the nuclear pore complex, interactions with cellular proteins trigger further capsid disassembly and allow the viral DNA to extrude into the nucleus for subsequent gene expression (18).

However, unlike Ad5, adenoviral types derived from species B or D viruses such as HAdV-B35, HAdV-B3, HAdV-D11, or HAdV-D26 can use alternative binding/entry factors or receptors to CAR, such as CD46 (55–57), desmoglein-2 (DSG-2) (58), or sialic acid (59). The post-entry steps of these rare species Ad viruses in diverse cell types are not as well-characterized as the CAR-mediated entry of Ad5. However, it is considered that the use of alternative entry pathways or different receptors can not only result in differences in endosomal escape, trafficking to the nucleus and subsequent transgene expression (60), but can also impact on the *in vivo* tropism of the vector following different routes of vaccine administration (i.e., intramuscular vs. intranasal). As a result, triggering of innate immune signaling pathways may also differ at each step of the entry process (33, 61). Less efficient trafficking pathways could result in weak or limited induction of cytokines/chemokines (62), or increased uptake in cell types which result in vector degradation with minimal transgene expression (63–66). Consequently, such differences between diverse Ad vectors can impact on the magnitude and phenotype of the ensuing adaptive immune response when they are used as a vaccine platform (8, 33, 44).

Entry in immune cells

Macrophages. In addition to the classical *in vitro* entry pathways described above, Ad vectors can infect mononuclear phagocytes efficiently both *in vitro* and *in vivo*, independently of their described surface receptors (i.e., CAR, DSG-2) (67), which are absent on murine macrophages. *In vivo* interactions with tissue resident macrophages, such as Kupffer cells in the liver or alveolar macrophages in the lung, can result in scavenging and degradation of significant amounts of input Ad vector (64–66). Not only can these interactions result in limited transgene expression which could affect the therapeutic efficacy, but the phagocytosis of Ad particles can trigger inflammatory responses (68, 69), leading to undesirable off-target toxicity (70). This is a particularly important consideration for therapeutic applications which require systemic administration or are designed for use in immunocompromised individuals (i.e., oncolytic viral therapy for disseminated metastases) (18). As a result, efforts have been made to characterize the mechanisms of Ad viral entry in macrophages and to better understand how these interactions contribute to the induction of inflammatory responses within defined anatomical compartments following different routes of administration (i.e., intramuscular, intranasal vs. intravenous).

Opsonization of Ad viral particles by complement or antibodies (natural or anti-viral) can bridge entry into macrophages by engaging Fc-receptors (FcRs) or complement receptors (71–73). Additionally, a role for scavenging receptors in facilitating viral entry into murine macrophages, both *in vitro* and *in vivo*, has been outlined (62, 67, 74). Scavenging receptors are a heterogenous and structurally diverse family of receptors capable of interacting with endogenous proteins and lipids, microbial ligands, and non-opsonized particles, including viruses (75). In addition to contributing to the clearance of particulate Ag, scavenging receptors have been

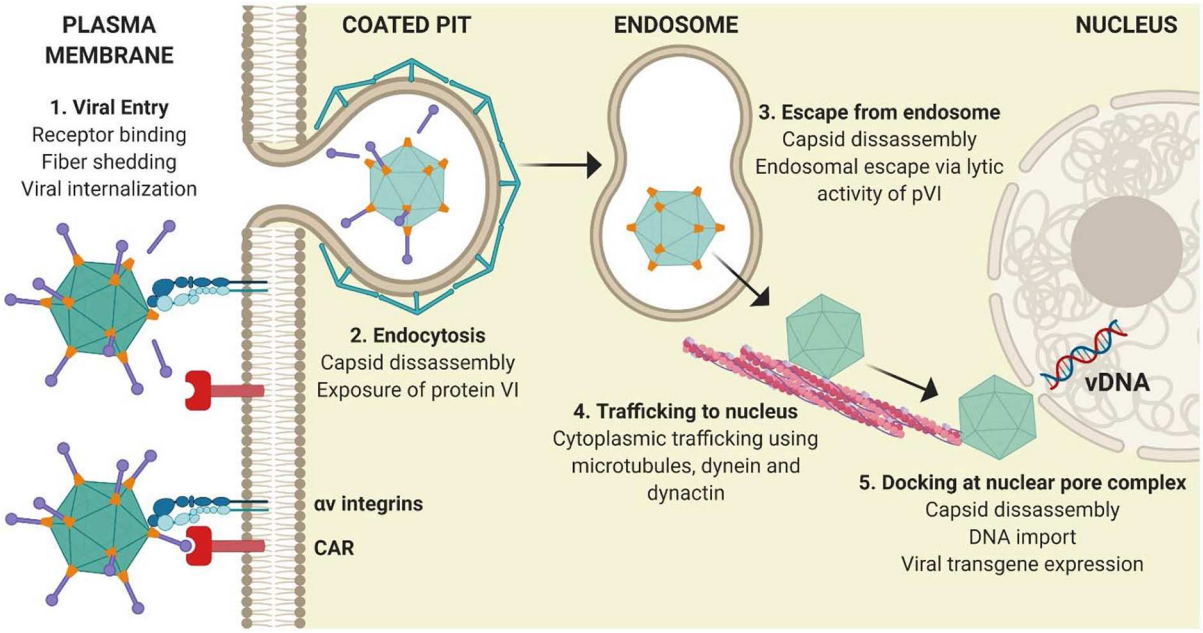

FIGURE 2 | Classical adenoviral entry pathway. **(1)** Attachment of the Ad5 adenoviral fiber knob mediates primary receptor interactions with CAR, followed by an interaction between the RGD motif within the penton base and cellular integrins on the surface of cells, which initiate partial capsid disassembly by fiber shedding. **(2)** Internalization of virions is mediated by integrins. **(3)** Exposure of pVI from the virion interior facilitates its lytic activity and allows endosomal escape. **(4)** Partially disassembled nucleocapsid cores traffic to the nucleus using the microtubule network before docking at the nuclear pore complex. **(5)** Viral DNA enters the nucleus and viral transgene expression is initiated. Figure is updated from Coughlan et al. (18) and was created with ©BioRender - biorender.com.

implicated in innate immune sensing, due to their ability to recognize pathogen-associated molecular patterns (PAMPs). Murine SR-A1 (74), SR-AII (76), and MARCO (SR-A6) (67) have been described as receptors for rAd vectors, and MARCO$^+$ marginal zone macrophages in the spleen have been shown to accumulate Ad5-based vectors following intravenous (*i.v.*) delivery in mice (28, 77). The fiber knob (i.e., SR-A1), or hexon protein has been implicated in mediating these interactions (i.e., SR-AII and SR-A6). Interestingly, SR-A6 (MARCO) was shown to not only facilitate entry and efficient gene transduction with Ad5, but also with HAdV-C2, HAdV-B35, and HAdV-D26 (67). The mechanism of interaction between Ad and SR-AII/SR-A6 was proposed to involve the negative charge conferred by specific hypervariable regions (HVRs) of the viral hexon, namely HVR1. In support of this, preferential scavenging of negatively charged particles has previously been shown to contribute to the differential recognition of Ad vectors by macrophages *in vivo* (76, 78, 79).

Dendritic cells. Dendritic cells (DCs) are a specialized subset of professional Ag presenting cells which are central to the development of protective immunity. DCs can process Ag using several methods; (i) direct presentation, in which an infected DC presents peptide:major histocompatibility complex class (MHC) complexes directly to T cells, (ii) cross-presentation in which Ag derived from other infected cells is phagocytosed by DCs, processed and then presented to T cells, and (iii) cross-dressing (80), in which peptide:MHC complexes are acquired from other professional or non-professional antigen presenting cells (APCs) and are transferred to the DC through a process of trogocytosis, in which fragments of the plasma membrane containing the MHC complex merges with the recipient cell. Cross-dressing is also hypothesized to occur through the intercellular transfer of pre-formed peptide:MHC complexes by extracellular vesicles, such as exosomes [(81–84); **Figure 3**].

A critical role for DCs in the robust induction of CD8$^+$ T cell responses following immunization with rAd vectors has been demonstrated (86, 87). It has been shown that CD8$^+$, but not CD4$^+$ T cell responses elicited by Ad vaccines, are dependent on cross-presentation by specific sub-populations of DCs, including CD8α$^+$ DCs (33). In support of this, Ag-specific CD8$^+$ T cell responses in BATF3-deficient mice (*Batf3*$^{-/-}$), which preclude the development of the latter DC population (CD8α$^+$ DCs), were shown to be ∼80% lower following immunization with several Ad vectors (33). DCs infected with Ads upregulate MHC, as well as co-stimulatory molecules including CD40, CD80, or CD86, leading to the activation or maturation of DCs (88), in a manner which is believed to be dependent on nuclear factor kappa-light-chain-enhancer of activated B cells (NF-κB) signaling (89). The maturation of murine DCs has been proposed to be mediated by the fiber knob domain of Ad5 (90). *In vivo* experiments in mice have shown that uptake of rAd5-based vaccines in draining lymph nodes (dLNs) following intramuscular (*i.m.*) or subcutaneous (*s.c.*) vaccination is highest in CD11c$^+$ CD8$^-$ B220$^-$ DCs, although CD11c$^+$ CD8$^+$ B220$^-$ DCs were the most potent for eliciting naïve Ag-specific T cell proliferation (86). As

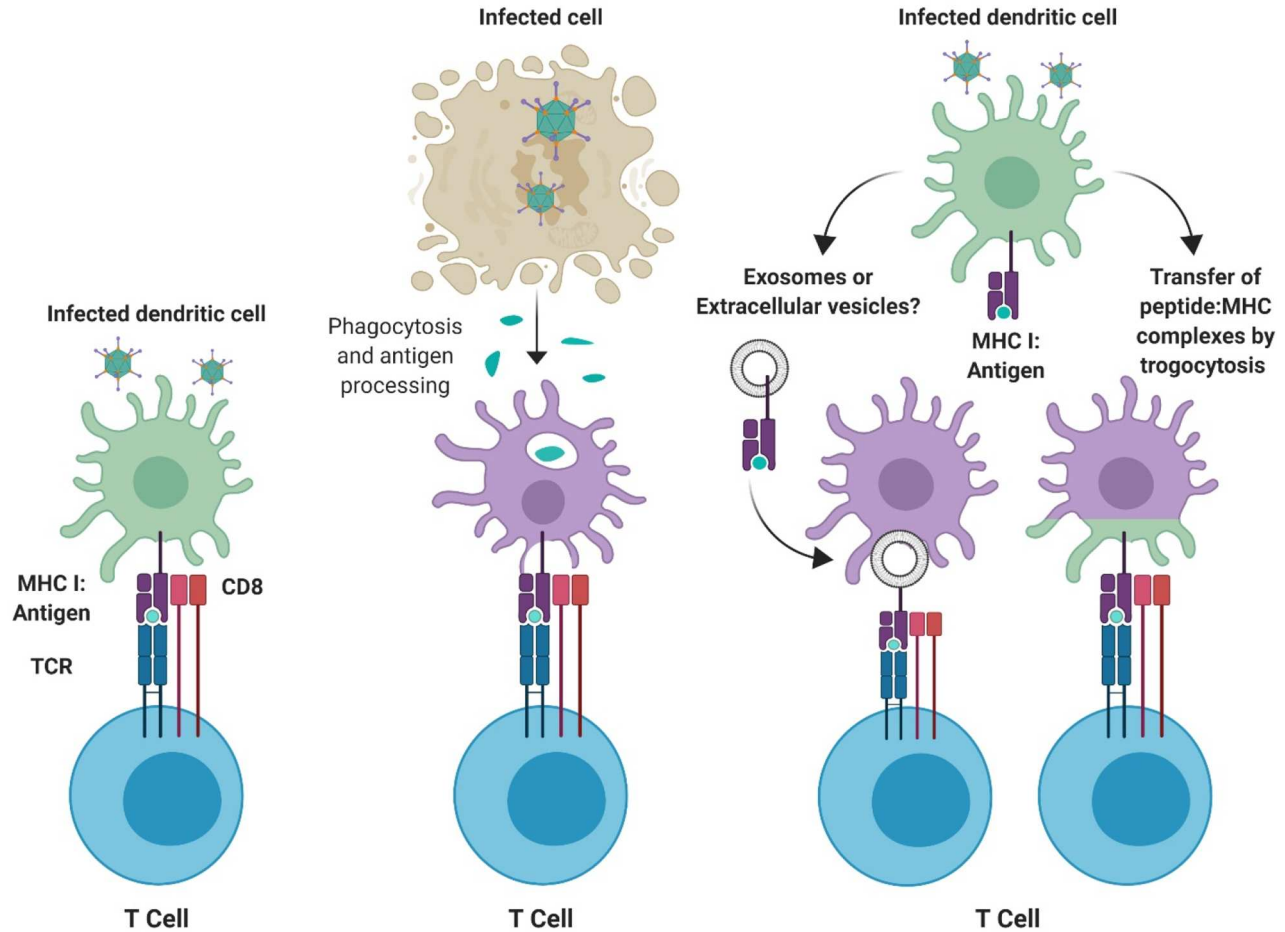

FIGURE 3 | Pathways for antigen presentation. **(1)** *Direct-presentation:* Antigen from virally infected cells is degraded by the proteasome and processed for peptide presentation to $CD8^+$ T cells on MHC I. **(2)** *Cross-presentation:* Antigen fragments derived from virally infected cells are phagocytosed by professional APCs and peptide processed and presented to T cells via appropriate MHC molecules. **(3)** *Cross-dressing:* Peptide:MHC complexes can be acquired through transfer via extracellular vesicles or exosomes, or by a process of membrane gnawing called trogocytosis. Figure is adapted from Yewdell and Dolan (85) and was created with ©BioRender - biorender.com.

previous studies have shown that targeting vaccine Ag to defined populations of DCs can improve immunity and vaccine efficacy (91, 92), efforts are ongoing to better understand the precise interactions between diverse Ad types and DC subpopulations *in vivo*, as well as how we can engineer Ad vectors which are targeted to specific receptors on the surface of DCs (93, 94).

Receptors on the surface of dendritic cells (DCs) can permit entry of Ads independently of the classical CAR receptor, which is largely absent on DCs (95). Receptors proposed to be involved in Ad viral entry into human or murine DCs include Dendritic Cell-Specific Intercellular adhesion molecule-3-Grabbing Non-integrin (DC-SIGN) (95), CD46 (61, 96, 97), or CD80/CD86 (98). A vector based on chimpanzee Ad vector 1, ChAdV-1, was shown to efficiently transduce CD46-expressing murine DCs *in vitro* (97). Recombinant Ad5 vectors pseudotyped with the fiber knob from Ad3 (99) or porcine adenovirus type 4 (100), can increase entry into human DCs, via CD80/CD86 and surface glycans, respectively. Similarly, pseudotyping rAd5 with the fibers from species B, HAdV-B16 or species D, HAdV-D37 displayed increased entry into murine DCs compared with unmodified rAd5 (101). Interestingly, in the latter study, increased entry into DCs was not associated with improved cellular immunity following subcutaneous immunization. In support of this, species B Ad vectors, including Ad35, were long considered to hold great potential as potently immunogenic vaccine vectors due to their increased ability to target both myeloid and plasmacytoid human DCs via CD46. However, these vectors were subsequently shown to be some of the least potent Ad vaccines *in vivo* (5, 8). These observations and findings are important in highlighting that multiple parameters, such as post-entry intracellular trafficking kinetics or differential activation of innate immune signaling pathways, not just viral tropism, likely play key roles in the induction of robust immunogenicity.

Innate Immune Responses to Ad Vectors

The ability of diverse rAd vaccines to elicit robust cellular immune responses and confer protective immunity in animal models makes them an attractive vector platform for vaccine development (**Table 2**). In addition to this, their safety in clinical applications, compatibility with clinical-grade manufacturing and scale-up (102, 103) and their suitability for long-term storage (104), or thermo-stabilization (105–107) and stockpiling for cold-chain free storage, has solidified their appeal as vaccines for major infectious diseases (108). It is this clear translational potential which has emphasized the importance of improving our understanding of the mechanisms which underlie differences in the immunological potency of diverse Ad types. Ad vectors are capable of triggering multiple innate immune sensors at several steps in the viral entry pathway (109, 110), in a process which does not require viral replication or gene expression (111). Viral penton RGD:cellular integrin-mediated internalization and subsequent escape from the endosome is considered to be a crucial step in activating many innate immune responses to Ad vaccines (112). It is considered that preferential stimulation (or avoidance) of defined innate immune signaling pathways could impact on the downstream immunogenicity of distinct Ad vectors. With regard to assessing the differential stimulation of innate immune signaling pathways, this is complicated by the fact that many vectors have not been compared side-by-side, and published data proposing roles for these pathways in the immunological potency of different Ad vectors are often contradictory. However, a number of pathways which have been implicated in innate immune sensing of Ad vectors and the caveats associated, are described below.

TLRs

Recombinant Ad vectors contain PAMPs which can be sensed by cell-surface or endosomal pattern recognition receptors (PRRs) such as the Toll-like receptors (TLRs). TLRs implicated in the sensing of Ad vectors include TLR2 (113), TLR4 (114), and endosomally located TLR9 (61, 113), which can trigger the down-stream activation and transcription of anti-viral genes including NF-κB, mitogen-activated protein kinases (MAPK) and interferon-regulatory factors (IRFs). The intracellular adaptor protein MyD88 has been reported to play a major role in the induction of Ag-specific cellular immune responses following TLR-mediated sensing of Ad vaccines (109, 113). Importantly, the ability to engage multiple MyD88-dependent signaling pathways simultaneously, is believed to contribute to the robust immunogenicity associated with Ad vaccines. However, their immunological potency is also attributed to the fact that innate immune activation by recombinant Ad vaccines can occur not only via TLR-dependent mechanisms, but also through numerous TLR-independent pathways (86, 109, 110, 113, 114).

cGAS/STING

The viral DNA itself can play a crucial role in triggering innate immune responses. In recent years it has been demonstrated that following rupture of the endosomal membrane, Ad viral DNA can also be sensed by the cytosolic DNA sensor cGAS (115, 116). The engagement of cGAS triggers a signaling cascade involving the adaptor STING (117) and activation of the kinase TBK1, which initiate the induction of IRF3-responsive genes (115), such as Type I interferons (IFNs). It has been shown that the absence of cGAS or STING results in reduced activation of early innate immunity (i.e., IFN-β, cytokines, chemokines) but does not impact adaptive anti-vector immune responses in mice. However, the latter studies were performed in the context of *i.v.* delivery and anti-vector, not transgene-specific immunity (116), and as such, the relative importance of DNA sensor pathways in the immunogenicity of Ads as vaccine vectors is less clear. It has recently has been suggested that Ag expression is a more crucial predictor of Ag-specific memory T cells (33), as abrogation of STING and Type I IFN responses during Ad vaccination in mice merely altered the early kinetics of $CD8^+$ T cells, but did not impair the magnitude of T cell memory responses (33). In the latter study, it was shown that STING could act as a dominant innate PRR sensor for many Ad vectors. Interestingly, abrogation of STING accelerated the kinetics of Ag-specific T cell responses following vaccination with ChAdV-63, a chimpanzee Ad vector, but was dispensable for the early induction of $CD8^+$ T cell responses for Ad5 and rare species HAdV-D28-based vaccines (33). This supports the idea that a complex interplay between multiple PRR-mediated signaling pathways exists, and that different Ad vectors are differentially impacted by these pathways. Our understanding of this is confounded by differences in receptor usage, *in vivo* tropism, engagement of PRRs in diverse hematopoietic and non-hematopoietic cells, and by differences in putative PAMPs on diverse Ad particles.

The NLRP3 inflammasome

In addition to inducing the expression of anti-viral genes, infection with Ad vectors also triggers pro-inflammatory responses through cytosolic DNA-sensing mechanisms which are independent of TLR9 and IRFs (111). In macrophages, recognition of Ad viral DNA has been shown to be mediated by the innate cytosolic molecular complex, or inflammasome, in a process involving NLRP3 and (ASC), which is independent of viral gene expression or replication (117). The multi-protein inflammasome complex mediates caspase-1 activity, resulting in the processing of pro-interleukin-1β into its active and secreted form. IL-1β subsequently induces signaling cascades of pro-inflammatory cytokines and chemokines through the IL-1RI both *in vitro* and *in vivo* in response to Ad infection. However, alternative and contradictory mechanisms of immune activation in macrophages by Ads have also been identified which are independent of the NLRP3 inflammasome and its components. Di Paolo et al. showed that direct interactions between the RGD motif within the penton base of the Ad virion and the β3 subunit of integrins on the surface of macrophages were responsible for activating IL-1α. The authors also proposed that IL-1α, not IL-1β, was the predominant activator of innate immune responses to Ad5 *in vivo* (77).

One very important caveat which complicates our ability to systematically investigate how innate immune responses contribute to downstream adaptive immunity to Ad vaccines, is that many studies are performed *in vitro*, using defined

non-immune epithelial/endothelial cells or cultured immune cells including macrophages or dendritic cells (110, 115, 118). These cell type-specific findings often contradict subsequent *in vivo* studies using transgenic mice in which these "critical" mediators of innate immunity are knocked-out (77, 116). For example, despite numerous reports describing an important role for TLR9 *in vitro*, comparisons of wildtype and TLR9$^{-/-}$ mice have demonstrated that the impact of TLR9 in innate immune sensing of Ad particles *in vivo* is minimal (77), at least for *i.v.* administration of Ad5. Similarly, although cGAS or STING were shown to be pivotal in *early* immune sensing of Ad *in vivo*, studies using cGAS$^{-/-}$ or STING$^{-/-}$ mice showed that these molecular effectors have little impact on subsequent adaptive immunity and antibody production (116). These discrepancies are obviously further complicated by the known capacity of Ad vectors to engage multiple innate signaling pathways simultaneously, rendering individual pathways at least partially redundant *in vivo* (110). In addition to this, differences in the route of Ad vector delivery (i.e., *i.m*, *i.v.,* or intranasal) and access to different cell types, the multiplicity of infection (MOI) or injected dose, the timing or method of analysis reported in published work and the use of non-human or rare species Ad vectors with differential receptor usage, also limits our ability to fully dissect out the key contributing pathways (118, 119). Collectively, these factors highlight the many challenges facing the field and explain why we currently lack consensus on precisely which innate signaling pathways could contribute to protective immunity following vaccination with diverse Ad vectors.

Stimulation of type I IFNs

It has been proposed that *minimal* induction of Type I IFNs (44, 102, 120), in conjunction with sustained transgene expression (33), are hallmarks of potently immunogenic Ad vaccine vectors *in vivo*. Excessive stimulation of Type I IFN pathways at early time-points following immunization has been shown to lead to decreased transgene expression and subsequently reduced Ag-specific antibody (Ab) responses, following immunization with a chimpanzee Ad vector, ChAdV-68 (120). The authors demonstrated that these effects could be reversed by immunizing mice which have a defective type I IFN receptor IFNAR$^{-/-}$, resulting in an increased Ab response, thereby confirming that Type I IFN stimulation can have a detrimental impact on humoral immunity directed toward the Ad-encoded transgene Ag (120). In support of these findings, Quinn et al. also showed that abrogation of Type I IFN and STING could increase transgene expression from rAd vaccines, and that the development of protective cellular immunity correlated with this increased transgene expression (33). Following immunization with rare species and non-human Ad vectors, the authors used a systems biology-based, gene expression analysis approach at several time-points to confirm the differential modulation of IFN responsive genes. They determined that Type I and Type II IFNs were upregulated at 8 h post-immunization, which was followed by the induction of ISGs by 24 h. Interestingly, the most protective rAds identified in their study (i.e., Ad5 and chimpanzee Ad, ChAdV-3) exhibited the weakest transcriptional activation of these pathways. However, only the impact of innate gene activation on CD8^{+} T cell responses, but not transgene-specific Abs, was investigated (33). Nonetheless, collectively, these studies support the concept of robust, persistent Ag expression combined with low innate gene stimulation in contributing to the potency of rAd vaccines (33, 102). This is also supported by the knowledge that relative to rare species human and non-human Ad vectors (33, 120), immunization with the potently immunogenic Ad5 vector is well-established to result in robust, persistent Ag expression (33, 36, 41, 121, 122), while triggering minimal Type I IFN responses *in vivo*. Future studies which aim to comprehensively characterize the contribution of early innate immune activation and correlate this with the downstream immunological potency and efficacy of lead Ad vaccine platforms will be required.

Magnitude and Persistence of Antigen Expression

Non-replicating Ad5-based vectors are well-established for their ability to confer robust transgene expression following immunization (36). Furthermore, low level transgene expression can persist long-term (41, 122), with transcriptionally active Ad vector genomes being maintained in muscle at the injection site, or within draining lymph nodes (36, 122), depending on the route of administration. As previously outlined, it has been proposed that it is this magnitude and persistence of transgene Ag expression which is crucial for the induction of robust and protective T cell responses following Ad vaccination (33). As described above, Quinn et al. demonstrated that strong activation of innate immune gene expression profiles in the draining lymph nodes (dLNs) correlated with limiting Ad-mediated transgene expression for many rare or non-human Ad types (33). The Ad vectors with the highest levels of transgene Ad expression in dLNs, Ad5, and chimpanzee Ad vector ChAdV-3, also had the most attenuated IFN induction. The latter vectors were both potently immunogenic following immunization in mice. In agreement with this, similar comparative immunogenicity studies in mice have shown that transgene expression levels within muscle and dLNs are lower following immunization with a chimpanzee Ad vector, ChAdOx1, when compared with Ad5, and that this translates to superior immunogenicity observed with Ad5 (123).

To directly address the question of how persistence of Ag contributes to the induction of the robust immunogenicity of Ad vaccines, Finn et al. constructed an Ad vaccine with a doxycycline-regulated transgene expression cassette (121). By switching off transgene expression at early vs. late time-points post-immunization, the authors confirmed the importance of presence of Ag in expanding and maintaining memory T cell responses up to D30, but showed that the maintenance of memory responses at later time-points (D60) is independent of transgene expression.

As discussed above, it is apparent that a combination of multiple parameters influences the extent of transgene expression. These factors include the receptor usage and cellular tropism of each Ad vector, the presence and accessibility of specific cell types at the site of injection, in addition to differences in the induction of early innate immunity by diverse Ad

vectors. Collectively, these parameters shape subsequent adaptive immune responses.

Route of Administration

The successful transduction of cells at the site of vaccine administration, and subsequent engagement of defined and desirable PRRs which result in robust transgene expression, depend on the cell type and the specific Ad vector being studied. With this in mind, much of the evidence to date has focused on characterizing the induction of innate immune responses *in vitro* in APCs such as DCs or macrophages, which play important roles in initiating anti-viral immune responses. It is considered that inflammation induced at the injection site, can lead to an influx of APCs (monocytes or DCs) which carry Ag to the dLNs (124). Immature DCs residing at the site of vaccination respond to innate immune signals (i.e., stimulation of TLR pathways) by undergoing maturation, upregulating co-stimulatory molecules and migrating to dLNs where they present Ag to naïve T cells (124). However, non-professional APCs expressing MHC I (125, 126), such as tissue-specific epithelial or endothelial cells, could also contribute to the immune sensing of Ad vectors at the site of injection (39). Therefore, it is clear that the route of vaccine administration (45, 127, 128), the abundance and accessibility of cell types at those locations, as well as the surface expression of suitable entry receptors, will profoundly affect the immunological potency and protective efficacy of a chosen Ad vector.

As a result of the long history of experimental use of Ad vectors as oncolytic agents aimed at treating disseminated metastases, a significant amount of information exists in the literature regarding interactions between Ad vectors, immune cells (28, 77, 129), parenchymal cells (18, 63, 113, 130–134), and stromal cells (130) following *i.v.* delivery of Ad vectors (18, 112, 135). However, *i.v.* vaccination would be impractical for widespread population use and so immunization by *i.m.* or *i.n.* administration is preferable, particularly for vaccination against respiratory pathogens. Unfortunately, less is known about the precise interactions which occur at the site of injection or within dLNs *in vivo* following *i.m.* or *i.n.* immunization with Ads in animal models, and these questions are even more difficult to address in humans, without the use of invasive procedures (such as fine needle aspirates of lymph nodes) (136).

Intramuscular delivery

The cell types present when vaccine is administered *i.m.* include myocytes, skeletal muscle cells, fibroblasts and endothelial cells, with APCs such as DCs or macrophages representing a minority when compared with the abundance of murine skeletal muscle cells (87). Early studies by Mercier et al. demonstrated that transduction of different cell types can modulate the outcome and phenotype of the humoral immune response following Ad vaccination. The authors transduced DCs (professional APCs), myoblasts (progenitor cells which give rise to muscle cells) and endothelial cells *ex vivo* with Ad5 expressing a model antigen β-galactosidase (β-gal) (87), and vaccinated mice *i.m.* with the Ad-transduced cells. The authors found that all transduced cell types elicited humoral immune responses to the β-gal transgene to a similar extent (albeit with differences in their temporal kinetics), but that the IgG isotype subclass profile differed. Injection of transduced DCs or endothelial cells resulted in production of Ag-specific Abs which were exclusively IgG_{2a}, whereas vaccination with Ad-transduced myoblasts elicited a more balanced Ab response with equivalent IgG_1:IgG_{2a}. Interestingly, only mice immunized with Ad-transduced DCs elicited robust $CD8^+$ T cell responses, as did vaccination with control virus Ad-β-gal, suggesting that Ad interactions with different cell types *in vivo* could influence divergent arms of the adaptive immune response.

Bassett et al. also demonstrated that Ag presentation by non-lymphoid cells, in cooperation with hematopoietic APCs, contributes to the kinetics of primary $CD8^+$ T cell expansion, the maintenance of memory responses and to the functional phenotype of the cellular immune response following Ad vaccination (39). Through a series of investigations, the authors showed that although dLNs act as the site of immunological priming in response to Ad vaccination, primary expansion of the Ag-specific $CD8^+$ T cell response requires a source of sustained Ag expression outside of dLNs (39). They hypothesized that this cell type was of non-hematopoietic origin, due to their prior findings that a radioresistant population of cells was capable of priming $CD8^+$ T cell responses in mice leukopenic mice (137). Therefore, it is feasible that several modes of Ag presentation take place following *i.m.* immunization with Ad vectors, all of which contribute to different facets of the ensuing immune response. These interactions are summarized in **Figure 4**, showing that Ag presentation could take place not only within dLNs, but also at the site of injection, with or without the involvement of professional APCs.

It is important to note that the majority of detailed mechanistic studies into the immunogenicity of Ad vectors have been performed using Ad5-based vaccines and as such, similar information regarding the *in vivo* cellular tropism of rare species or non-human Ad vectors, is much more limited (123). It will therefore be crucial to outline the precise factors which confer a hierarchy of potency between Ad vectors in the future, as many Ad vectors are already under clinical investigation, or are advancing rapidly into clinical trials. This improved knowledge would allow us to engineer optimal platform vectors which combine multiple attributes associated with potent immunogenicity and long-lived protective efficacy.

Aerosolized or intranasal delivery

Mucosal *i.n.* or aerosolized (*a.e.*) delivery of Ad vectors is particularly attractive for the development of vaccines against respiratory pathogens (108, 139, 140). Ad vectors are capable of eliciting both humoral and cellular immune responses following *i.n.* (4, 140–142) and *a.e.* (143) vaccination in animal models, both in the bronchoalveolar lavage (BAL) and within the lung interstitium (15, 144). Many wildtype adenoviruses are common respiratory pathogens (i.e., HAdV-C5, HAdV-E4), highlighting their potential suitability for targeting vaccine Ag to mucosal surfaces within the respiratory tract. However, several chimpanzee Ad vectors, which are not associated with respiratory infections, have displayed superior immunogenicity to Ad5 when

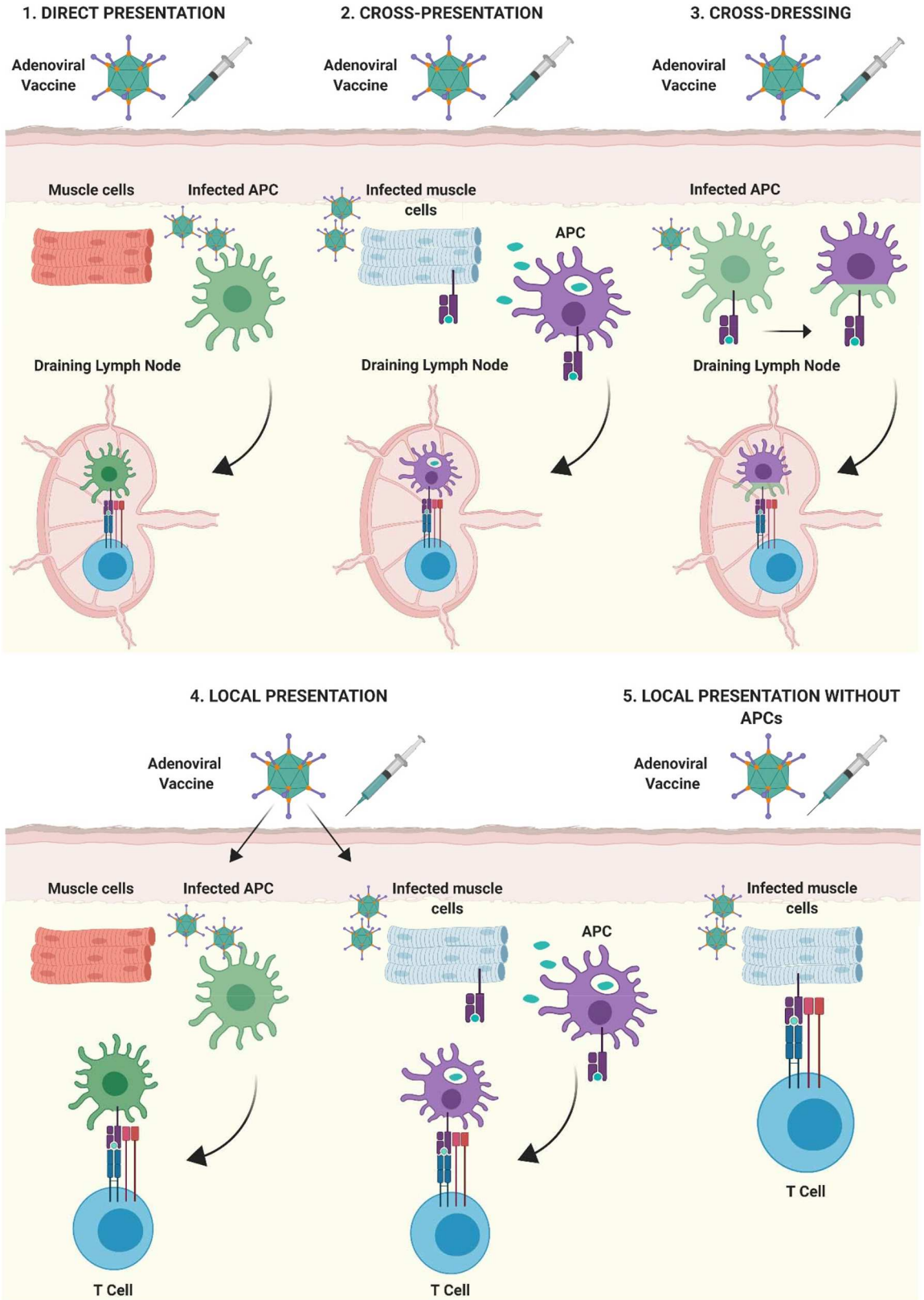

FIGURE 4 | Mechanisms of antigen presentation after intramuscular immunization with adenoviral vectored vaccines. **(1)** *Direct-presentation:* Adenoviral vaccine transduces APCs at the site of injection. APCs migrate to draining lymph nodes (dLNs) where they present processed vaccine antigen to T cells.

(Continued)

FIGURE 4 | (2) *Cross-presentation:* Vaccine antigen debris from Ad vaccine transduced cells is phagocytosed by professional APCs at the site of injection, transferred to dLNs by APCs and presented to lymphocytes. **(3)** *Cross-dressing:* Peptide:MHC complexes from Ad-transduced APCs may be transferred to naïve APCs by a process of membrane gnawing called trogocytosis. **(4)** APCs present at, or infiltrating into the site of injection, can present antigen directly to T lymphocytes. **(5)** Non-professional APCs such as parenchymal cells at the site of injection (muscle cells shown as an example) can present antigenic peptide on MHC I to infiltrating $CD8^+$ T lymphocytes, outside of secondary lymphoid organs. Figure is updated from Coughlan et al. (108) and Holst and Thomsen (138) and was created with ©BioRender - biorender.com.

administered by the *i.n.* route in mice, including a ChAdV-68-based vaccine against pulmonary tuberculosis (TB) (144) and a ChAdV-7 vaccine against *Pseudomonas aeruginosa* (145).

A major limitation in the application of rAd vaccines to mucosal respiratory surfaces may be the rapid scavenging and degradation of Ad vaccine vector particles by tissue resident alveolar macrophages in the lung, as it has previously been estimated that ∼70% of Ad vector genomes are lost within the first 24h following lung delivery in mice (intratracheal) (66). Furthermore, alveolar macrophages were found to be the predominant cell type responsible for initial inflammatory cytokine induction (68). However, depending on the balance of innate immune stimulation and the retention of a certain level of transgene expression within the respiratory tract, these interactions could be beneficial for the induction of subsequent adaptive immune responses.

Alveolar macrophages may play a role in trafficking to dLNs to facilitate Ag priming, or the inflammatory cytokines they release could signal the recruitment of lymphoid cells which could further potentiate immune responses to Ad-encoded transgene Ag. The many studies which have confirmed the induction of protective immunity following *i.n.* vaccination with Ad vectors support this possibility, but the precise mechanistic factors which underlie these effects and the specific cell types which contribute to vaccine efficacy are not extensively described. As differences in the phenotype and trafficking potential of $CD8^+$ T cells has been observed when comparing *i.m.* vs. *i.n.* vaccination of mice with Ad vectors, it will be important to identify the optimal Ad vaccine platform which elicits the correct correlates of protection for a specific disease target, before deciding on the ideal route of vaccine administration (128).

Structural Basis for Immune Activation by Ad Particles

The ability to engage and activate multiple, diverse innate immune signaling pathways simultaneously (excluding Type I IFN) can allow rAd vectors to act as an effective self-adjuvant, relative to other vaccination platforms (109, 110, 146). These attributes suggest that Ad virions themselves possess several PAMPs. In fact, it is considered that the native receptor determinants or entry factors of a particular Ad vector may, at least in part, regulate innate immune activation. In support of this, binding of the fiber knob domain to CAR is sufficient to activate p38MAPK, p44/42MAPK (ERK1/2), and NF-κB pathways (147), resulting in the transcription of pro-inflammatory cytokines both *in vitro* and *in vivo* (148). Similarly, Ad vectors which are capable of using CD46 as a receptor have been shown to display preferential activation of TLR9 to CAR-binding Ad vectors *in vitro* (61). However, CD46 distribution is limited to the expression in the testes in mice, rats and guinea pigs, in contrast to its widespread expression in humans (149). Therefore, this likely has little contribution to the immunological potency of CD46-using Ad vectors in murine models.

The fiber knob domain of Ad5-based vectors has been shown to contribute to the maturation of murine DCs, as recombinant knob protein, full-length fiber protein and penton capsomers (penton plus fiber), but not hexon or penton alone, were capable of exerting this effect (90). In support of this, Teigler et al. previously suggested that fiber-receptor interactions were important for triggering innate immune responses to rare species Ad vectors (26). Furthermore, studies using HAdV-B35 vectors pseudotyped with the fiber knob from Ad5 were shown to be more immunogenic in mice and NHP, suggesting that the fiber knob domain could contribute substantially to immunological potency (150). However, similar studies in which the entire fiber and penton RGD motif from rAd5 were swapped into chimpanzee Ad vector ChAdOx1, failed to increase the immunogenicity of ChAdOx1 relative to Ad5, suggesting that factors beyond fiber/penton capsomer interactions confer immune responses to ChAdOx1 (123).

More recently it has been shown that a member of the vitamin-K dependent protein family, growth arrest specific protein (Gas6), can bind differentially to the fiber of rAd vectors (151), interacting with a putative epitope which is outside of the fiber knob domain, such as the fiber shaft. Interestingly, Gas6 bound efficiently to the fiber of CAR-binding Ad5, without affecting its ability to enter cells, but significantly reduced the induction of type I IFNs, resulting in prolonged transgene expression. Conversely, Gas6 failed to bind to the fibers of non-Ad5 and non-CAR binding viruses, such as a species D Ad vectors HAdV-D28, which has been shown to display reduced immunogenicity in mice when compared with rAd5 (152). In support of this, HAdV-D28 has been shown to elicit robust IFN-α and had increased stimulation of IFN-responsive genes when compared with Ad5 (44). Importantly, immunization of $IFNR1^{-/-}$ mice with HAdV-D28 resulted in robust cellular immune responses, comparable to Ad5 (44). These data support the hypothesis by several other groups that Ad vectors which trigger robust type I IFN responses exhibit reduced transgene expression and impaired vaccine immunogenicity (33, 120). Therefore, one strategy to overcome stimulation of IFN-α could be to identify the precise amino acid binding epitopes for Gas6 and genetically engineer this region into the fiber of non-Gas6 binding Ad vectors in an effort to increase their immunogenicity (151).

In addition to interactions with CAR, interactions between the RGD motif within the penton base and cellular integrins can contribute to the induction of innate immune signaling pathways both *in vitro* (153) and *in vivo* (77). Following *i.v.* administration

of Ad5, interactions between the β3 subunit of cellular integrins and the RGD motif on MARCO$^+$ marginal zone macrophages in the spleen were required for triggering IL-1α-dependent innate immune signaling in mice (77). However, it is unclear how these interactions affect immune responses following immunization by other routes of administration. Finally, the Ad virion itself and its major capsid protein, the hexon, has been described as a potent adjuvant, capable of activating CD4$^+$ and CD8$^+$ cellular immune responses to a model immunogen mixture in mice (146). Although the precise mechanism underlying this effect has not been identified, subsequent studies have suggested that the HVR regions, particularly HVR1, are involved in enhancing interactions with scavenging macrophages (76, 78).

Novel Approaches to Increasing the Immunological Potency of Ad Vectors

One approach to identifying lead vaccine candidates is to perform head-to-head comparisons of immunogenicity in animal models to identify the most immunogenic vectors, followed by detailed and systematic experimental studies to try to identify the underlying mechanisms which contribute to immunological potency (i.e., transgene expression magnitude and duration, innate immune stimulation). However, in the interim, efforts are ongoing to try to maximize immune recognition of the Ad encoded Ag, in an effort to compensate for the reduced immunogenicity associated with certain Ad vectors which are otherwise an ideal platform (i.e., low seroprevalence, high titer growth, stability). Furthermore, this type of modification could permit dose-sparing, which would have cost saving effects, as well as minimizing any vector-induced reactogenicity, without compromising on immunogenicity. Such approaches include the use of molecular or genetic adjuvants, namely in the form of fusion proteins with the vaccine antigen of interest, which help to potentiate immunogenicity by enhancing Ag presentation or dissemination [reviewed in detail by Neukirch et al. (154)].

One such approach which has previously been described includes the generation of fusion-Ag cassettes which enhance MHC presentation. This can be achieved by fusing vaccine Ag to β-microglobulin for enhanced MHC I presentation (155), or to the invariant chain of MHC II (156–159). These approaches were capable of enhancing antigen-specific CD8$^+$ T cells responses in mice following immunization with an Ad vector encoding the Ii or β2-microglobulin fusion antigen. In a separate approach, we recently have shown that encoding vaccine Ag cassettes in which a model antigen, enhanced green fluorescent protein (EGFP), is fused to a protein domain known to tether proteins to the surface of extracellular vesicles (EVs), can dramatically improve the humoral immunogenicity of both Ad5 and chimpanzee Ad vector ChAdOx1 in mice following *i.m.* and *i.n* vaccination. EVs play important roles in regulating immune responses and are conveyors of cellular communication signals (15). As EVs are frequently implicated in host-pathogen interactions and have been shown to transfer antigenic material to APCs (81, 82), we reasoned that directed targeting of a vaccine Ag to their surface could potentiate immune responses. Although cellular immunity was largely unaffected, Ag-specific humoral immune responses were increased up to 400-fold when compared with unmodified EGFP (15). The choice of molecular or genetic adjuvant will depend on the predicted correlates of protection for a specific disease target: in certain cases, a robust humoral immune response will be more important than a cellular immune response. Further to this, some adjuvanting technologies will work for one Ag but not for another, and structural constraints may limit the ability to modify complex, multimeric Ags. This will require the optimization and selection of different components to be combined and assembled into customized Ad vectors which are tailored to specific pathogens.

Clinical Evaluation of Ad Vaccines for Infectious Disease; Challenges; and Advances

Challenges

A number of promising animal studies solidified the appeal of Ad5 as a platform vaccine vector for infectious diseases. In particular, a study by Sullivan et al. demonstrated that a single-shot, low dose (1×10^{10} vp) immunization with Ad5 expressing Ebola virus glycoprotein (GP) could provide 100% protection from challenge in NHPs (160). Similar studies using Ad5 based vectors expressing SIV gag demonstrated its superiority to plasmid DNA or modified vaccinia Ankara (MVA) in attenuating viremia following virus challenge (12). On the basis of these promising early results, a multicenter Phase II clinical trial called the Merck STEP study was initiated, in which a vaccine composed of a mixture of Ad5 vectors expressing HIV-1 *gag*, *pol,* and *nef* genes was administered to participants at high risk for HIV-1 acquisition (161, 162). Phase I safety and immunogenicity studies in healthy, HIV-seronegative adults showed that this vaccine could elicit antigen-specific IFN-γ ELISpot responses in both Ad5 seronegative and seropositive individuals (163). However, the Phase II study was terminated prematurely due to futility and failure to meet pre-defined endpoints: an interim analysis determined that the vaccine would not be efficacious in preventing HIV-1 infection, or in reducing viral-load setpoint in seroconverters, despite eliciting T cell responses in most participants (162, 163). Subsequent to this, a *post-hoc* analysis of the study suggested an association between vaccination with the Ad5 vaccine and increased acquisition of HIV-1 (161). On multivariate analyses, this increase was largely restricted to a defined sub-set of participants: uncircumcised men with high baseline antibody titers against Ad5. Several hypotheses were proposed to explain the increase in HIV-1 acquisition, including the formation of immune complexes (IC) between anti-Ad5 antibodies and DCs, which were shown to enhance HIV-1infection of T cells in DC-T cell co-cultures *in vitro* (164). An alternative hypothesis suggested that Ad5 immunization induced the expansion of Ad-specific memory CD4$^+$ T cells which upregulate CCR5 expression and/or homing markers for mucosal sites, thereby increasing the pool of HIV-1 susceptible cells at the site of infection (165). Although the latter hypothesis has been challenged (166), the precise mechanisms underlying the increased acquisition of HIV-1 in the Merck Step trial remain inconclusive (166). However, it is important to note that the effects were shown to wane over time (167). Nonetheless,

this outcome led to a dampening in enthusiasm for the broad application of Ad5-based vaccines for major infectious diseases, prompting the investigation of novel rare species human or non-human Ad viruses as alternative vaccine platforms.

Advances

Several rare species or non-human Ad vaccines are now leading the way in human clinical trials, namely species C vector HAdV-C6 and species D vector HAdV-26, as well as chimpanzee Ad vectors ChAdV-3, PanAdV-3, ChAdV-63, and ChAdOx1, which cluster phylogenetically with species C or E human Ads (see **Table 1**). Many of these vector candidates had previously been identified in animal studies as being potently immunogenic, and in some cases were comparable to the potency of Ad5 [(5, 168); **Table 2**]. In particular, HAdV-C6 and ChAdV-3 appear to possess attributes which make them an attractive platform vector (22%, 12% seroprevalence, respectively) (2, 5), and as a result, have been developed for clinical testing as vaccines against major global pathogens, hepatitis C virus (HCV) (2) and HIV-1 (169). Both HAdV-C6 and ChAdV-3 were shown to be safe and immunogenic in humans when used as a vaccine to elicit immunity against HCV, although HAdV-C6 appeared to be superior in its ability to cellular immune responses with increased magnitude and breadth at lower doses (i.e., 5×10^8 vp) (2). With regard to ChAdV-3, part of its appeal includes its ability to elicit long-lived cellular and humoral immune responses directed toward the encoded vaccine antigen. Immunization of NHPs with ChAdV-3 expressing HIV *gag* resulted in cellular immune responses which persisted for more than 5 years (5). A heterologous boost with PanAdV-3 at week 299 facilitated an expansion of gag-specific IFN-γ secreting T cells, in addition to boosting antibodies to HIV-1 gag. As such, there is broad interest in using these rare vectors in heterologous prime:boost vaccination regimens in an effort to confer long-lived protective immunity against challenging pathogens. In support of this, a Phase I clinical trial to test the HAdV-C6 and ChAdV-3 vectors expressing HCV antigens demonstrated that heterologous boost immunizations resulted in long-lived, polyfunctional effector, and central memory T cell responses which were sustained for up to 1 year in humans (2).

PanAdV-3 expressing Respiratory Syncytial Virus (RSV) fusion (F), nucleocapsid (N), and matrix (M2-1) antigens has also been tested in humans following *i.n.* and *i.m.* administration (37). Neutralizing antibodies to RSV F were increased following *i.m.,* but not *i.n.* prime immunization. Similar trends were observed for antigen-specific T cell responses to the vaccine inserts, although increases were minimal following PanAdV-3 *i.m.* prime only. This vaccine was also evaluated in older adults (60–75 years) who are at increased risk of severe RSV disease, with similar results (170). Immune responses elicited by PanAdV-3 were improved upon boosting with an MVA vector which also encoded the RSV transgene antigen. ChAdV-63, also identified as a clinically viable Ad vector with low seroprevalence which displayed protective efficacy in animal studies (**Table 2**), has been shown to be safe and immunogenic in children and adults (171–174). When ChAdV-63 has been used in a prime:boost vaccination regimen with MVA expressing malaria antigens, promising efficacy was observed in UK and Kenyan adults (175, 176), but has recently been associated with disappointing efficacy in field trials in young children in Burkina Faso, a highly endemic malaria transmission region (177). ChAdOx-1 is a species E chimpanzee Ad vector developed by the Jenner Institute at University of Oxford which has been tested clinically as a vaccine for influenza virus as a standalone vector or for use in prime:boost with MVA (1, 3), and for several other infectious disease targets such as Chikungunya Fever (NCT03590392), malaria (NCT03203421), and tuberculosis (NCT01829490). Numerous additional trials are currently ongoing or actively recruiting participants, including a recently initiated study to test a novel vaccine for COVID-19 (NCT04324606).

In addition to vectors derived from NHPs, promising advances have been the development of HAdV-D26 vectors. With a number of clinical trials registered on ClinicalTrials.gov, this platform has advanced into clinical studies as a vaccine against Ebola virus (178–180), RSV (181), HIV-1 (6, 182, 183), and has also very recently been announced as a candidate vectored vaccine against COVID-19. The first-in-human testing of HAdV-D26 expressing HIV-1 Env demonstrated that the vaccine was safe and well-tolerated and elicited Env-specific antibodies and antigen-specific ELISpot responses in all participants (182). Although HIV-1 specific neutralizing antibodies were not detected, the study reported multi-functional readouts for the non-neutralizing antibodies elicited, including effector functions such as antibody-dependent cell-mediated phagocytosis (ADCP), antibody-dependent cell-mediated virus inhibition (ADCVI) (183). This vaccine platform was subsequently improved upon by encoding polyvalent "mosaic" HIV-1 antigens, Env, Gag and Pol, representing computationally optimized sequences aimed at maximizing recognition of T cell epitopes (184). Evaluation of the HAdV-D26 platform in various prime:boost regimens is ongoing and preliminary data suggest that it is immunogenic, capable of eliciting Env-specific antibodies which exhibit ADCP and cellular immune responses out to week 50. Importantly, these assays were found to be correlates of protection in a parallel SHIV challenge model in rhesus monkeys (*Macaca mulatta*) (6). The HAdV-D26 mosaic HIV-1 vaccine is currently in Phase IIb efficacy studies in sub-saharan Africa (NCT03060629).

In Conclusion

Based on the literature, it appears that Ad vectors derived from species C, D, or E are most likely to be immunogenic vectors. Requirements for selecting specific vectors will vary depending on whether the required application is as a stand-alone vaccine or as part of a prime:boost regimen. For standalone vaccination regimens aimed at eliciting a rapid, protective response during an emerging pandemic, the magnitude of response to an identified correlate of protection following a single shot is crucial. Secondary considerations for an evolving pandemic scenario would be rapid immunogenicity at a low dose, and the capacity for lyophilization or stabilization, to facilitate dose-sparing, vaccine cost-effectiveness and pandemic preparedness. In this regard, of the Ad vectors evaluated to date, ChAdV-3 and HAdV-C6 appear promising. For protection against more complex

pathogens which require long-lived polyfunctional responses, or sustained humoral immunity with extensive breadth (i.e., universal influenza vaccine, HIV-1 or HCV), heterologous prime:boost vaccination regimens should be evaluated using diverse Ad vectors, or Ads in combination with MVA or protein based immunogens at different intervals. It is difficult to predict which Ad vectors should take precedence as the encoded antigen will need to be tailored to elicit the correct phenotype of immunity against a defined correlate of protection for each specific disease target. However, underpinning the evaluation of all Ad-based vaccines in pre-clinical animal studies, should be the inclusion of species C Ad5 vector controls to represent a benchmark of immunological potency. In addition, Ad vaccine candidates should be compared at several doses to evaluate the maintenance of vaccine potency upon dose de-escalation. The field should also make efforts to improve our understanding of the basic biology of many of these novel Ad vectors, as insights into the receptor usage, interactions of Ad vectors with different cell types following immunization and subsequent stimulation of differential innate signaling pathways will all impact on their downstream immunogenicity and ability to confer protective efficacy. Unfortunately, one major challenge in performing these types of head-to-head comparisons is the lack of widespread availability of many of these rare species or non-human Ad vectors to academic investigators, as many of these are being developed by large pharmaceutical companies.

SUMMARY

It is clear that a hierarchy exists in the immunological potency observed between rare species human and non-human Ad vectors in various animal species. As outlined above, Ad vector immunogenicity is most likely dependent on a complex combination of factors, rather than any particular factor in isolation. An ideal Ad vaccine platform will combine the following attributes; (i) low seroprevalence in humans, (ii) robust immunogenicity with potential for dose-sparing, and (iii) suitable manufacturing characteristics (i.e., growth to high titers, genome stability). Better understanding of the mechanisms which define effective vaccines, will enable us to design and customize improvements to existing Ad vaccine vectors, enhancing their potential for future clinical use.

AUTHOR CONTRIBUTIONS

LC: writing and editing—original and final draft.

FUNDING

LC was supported in part by funding from NIH/NIAID 1R21AI146529-01, CEIRS (HHSN272201400008C, Option 17C) and the 2018 *Pichichero Family Foundation Research Development Vaccines for Children Initiative Award in Pediatric Infectious Diseases* from the Pediatric Infectious Disease Society (PIDS).

ACKNOWLEDGMENTS

Thanks to Prof. Peter Palese, ISMMS, for helpful and constructive discussion of this review. Figures were created with ©BioRender - biorender.com.

REFERENCES

1. Antrobus RD, Coughlan L, Berthoud TK, Dicks MD, Hill AV, Lambe T, et al. Clinical assessment of a novel recombinant simian adenovirus ChAdOx1 as a vectored vaccine expressing conserved Influenza A antigens. *Mol Ther*. (2014). 22:668–74. doi: 10.1038/mt.2013.284
2. Barnes E, Folgori A, Capone S, Swadling L, Aston S, Kurioka A, et al. Novel adenovirus-based vaccines induce broad and sustained T cell responses to HCV in man. *Sci Transl Med*. (2012). 4:115ra111. doi: 10.1126/scitranslmed.3003155
3. Coughlan L, Sridhar S, Payne R, Edmans M, Milicic A, Venkatraman N, et al. Heterologous two-dose vaccination with simian adenovirus and poxvirus vectors elicits long-lasting cellular immunity to influenza virus A in healthy adults. *EBioMedicine*. (2018). 29:146–54. doi: 10.1016/j.ebiom.2018.02.011
4. Green CA, Scarselli E, Voysey M, Capone S, Vitelli A, Nicosia A, et al. Safety and immunogenicity of novel respiratory syncytial virus (RSV) vaccines based on the RSV viral proteins F, N and M2-1 encoded by simian adenovirus (PanAd3-RSV) and MVA (MVA-RSV); protocol for an open-label, dose-escalation, single-centre, phase. 1 clinical trial in healthy adults. *BMJ Open*. (2015) 5:e008748. doi: 10.1136/bmjopen-2015-008748
5. Colloca S, Barnes E, Folgori A, Ammendola V, Capone S, Cirillo A, et al. Vaccine vectors derived from a large collection of simian adenoviruses induce potent cellular immunity across multiple species. *Sci Transl Med*. (2012) 4:115ra112. doi: 10.1126/scitranslmed.3002925
6. Barouch DH, Tomaka FL, Wegmann F, Stieh DJ, Alter G, Robb ML, et al. Evaluation of a mosaic HIV-1 vaccine in a multicentre, randomised, double-blind, placebo-controlled, phase 1/2a clinical trial (APPROACH) and in rhesus monkeys (NHP 13-19). *Lancet*. (2018) 392:232–43. doi: 10.1016/S0140-6736(18)31364-3
7. Ewer K, Rampling T, Venkatraman N, Bowyer G, Wright D, Lambe T, et al. A monovalent chimpanzee adenovirus Ebola vaccine boosted with MVA. *New Engl J Med*. (2016) 374:1635–46. doi: 10.1056/NEJMoa1411627
8. Quinn KM, Da Costa A, Yamamoto A, Berry D, Lindsay RW, Darrah PA, et al. Comparative analysis of the magnitude, quality, phenotype, and protective capacity of simian immunodeficiency virus gag-specific CD8+ T cells following human-, simian-, and chimpanzee-derived recombinant adenoviral vector immunization. *J Immunol*. (2013) 190:2720–35. doi: 10.4049/jimmunol.1202861
9. Casimiro DR, Chen L, Fu TM, Evans RK, Caulfield MJ, Davies ME, et al. Comparative immunogenicity in rhesus monkeys of DNA plasmid, recombinant vaccinia virus, and replication-defective adenovirus vectors expressing a human immunodeficiency virus type 1 gag gene. *J Virol*. (2003) 77:6305–13. doi: 10.1128/jvi.77.11.6305-6313.2003
10. Tatsis N, Ertl HC. Adenoviruses as vaccine vectors. *Mol Ther*. (2004) 10:616–29. doi: 10.1016/j.ymthe.2004.07.013
11. Geisbert TW, Bailey M, Hensley L, Asiedu C, Geisbert J, Stanley D, et al. Recombinant adenovirus serotype 26 (Ad26) and Ad35 vaccine vectors bypass immunity to Ad5 and protect nonhuman primates against Ebolavirus challenge. *J Virol*. (2011) 85:4222–33. doi: 10.1128/JVI.02407-10
12. Shiver JW, Fu TM, Chen L, Casimiro DR, Davies ME, Evans RK, et al. Replication-incompetent adenoviral vaccine vector elicits effective anti-immunodeficiency-virus immunity. *Nature*. (2002) 415:331–5. doi: 10.1038/415331a

13. Robinson CM, Singh G, Lee JY, Dehghan S, Rajaiya J, Liu EB, et al. Molecular evolution of human adenoviruses. *Sci Rep*. (2013) 3:1812. doi: 10.1038/srep01812
14. Singh G, Robinson CM, Dehghan S, Schmidt T, Seto D, Jones MS, et al. Overreliance on the hexon gene, leading to misclassification of human adenoviruses. *J Virol*. (2012) 86:4693–5. doi: 10.1128/JVI.06969-11
15. Bliss CM, Parsons AJ, Nachbagauer R, Hamilton JR, Cappuccini F, Ulaszewska M, et al. Targeting antigen to the surface of EVs improves the *in vivo* immunogenicity of human and non-human adenoviral vaccines in mice. *Mol Ther Methods Clin Dev*. (2020) 16:108–25. doi: 10.1016/j.omtm.2019.12.003
16. Zhang W, Fu J, Liu J, Wang H, Schiwon M, Janz S, et al. An engineered virus library as a resource for the spectrum-wide exploration of virus and vector diversity. *Cell Rep*. (2017) 19:1698–709. doi: 10.1016/j.celrep.2017.05.008
17. Russell WC. Adenoviruses: update on structure and function. *J Gen Virol*. (2009) 90:1–20. doi: 10.1099/vir.0.003087-0
18. Coughlan L, Alba R, Parker AL, Bradshaw AC, McNeish IA, Nicklin SA, et al. Tropism-modification strategies for targeted gene delivery using adenoviral vectors. *Viruses*. (2010) 2:2290–355. doi: 10.3390/v2102290
19. Zhang W, Fu J, Ehrhardt A. Novel vector construction based on alternative adenovirus types via homologous recombination. *Hum Gene Ther Methods*. (2018) 29:124–34. doi: 10.1089/hgtb.2018.044
20. Duffy MR, Alonso-Padilla J, John L, Chandra N, Khan S, Ballmann MZ, et al. Generation and characterization of a novel candidate gene therapy and vaccination vector based on human species D adenovirus type 56. *J Gen Virol*. (2018) 99:135–47. doi: 10.1099/jgv.0.000978
21. Roy S, Gao G, Lu Y, Zhou X, Lock M, Calcedo R, et al. Characterization of a family of chimpanzee adenoviruses and development of molecular clones for gene transfer vectors. *Human Gene Ther*. (2004) 15:519–30. doi: 10.1089/10430340460745838
22. Kovesdi I, Hedley SJ. Adenoviral producer cells. *Viruses*. (2010) 2:1681–703. doi: 10.3390/v2081681
23. Gurwith M, Lock M, Taylor EM, Ishioka G, Alexander J, Mayall T, et al. Safety and immunogenicity of an oral, replicating adenovirus serotype 4 vector vaccine for H5N1 influenza: a randomised, double-blind, placebo-controlled, phase 1 study. *Lancet Infect Dis*. (2013) 13:238–50. doi: 10.1016/S1473-3099(12)70345-6
24. Liebowitz D, Gottlieb K, Kolhatkar NS, Garg SJ, Asher JM, Nazareno J, et al. Efficacy, immunogenicity, and safety of an oral influenza vaccine: a placebo-controlled and active-controlled phase 2 human challenge study. *Lancet Infect Dis*. (2020) 20:435–44. doi: 10.1016/S1473-3099(19)30584-5
25. Sebastian S, Lambe T. Clinical advances in viral-vectored influenza vaccines. *Vaccines*. (2018) 6:29. doi: 10.3390/vaccines6020029
26. Teigler JE, Iampietro MJ, Barouch DH. Vaccination with adenovirus serotypes 35, 26, and 48 elicits higher levels of innate cytokine responses than adenovirus serotype 5 in rhesus monkeys. *J Virol*. (2012) 86:9590–8. doi: 10.1128/JVI.00740-12
27. Dicks MD, Spencer AJ, Edwards NJ, Wadell G, Bojang K, Gilbert SC, et al. A novel chimpanzee adenovirus vector with low human seroprevalence: improved systems for vector derivation and comparative immunogenicity. *PLoS ONE*. (2012) 7:e40385. doi: 10.1371/journal.pone.0040385
28. Coughlan L, Bradshaw AC, Parker AL, Robinson H, White K, Custers J, et al. Ad5:Ad48 hexon hypervariable region substitutions lead to toxicity and increased inflammatory responses following intravenous delivery. *Mol Ther*. (2012). 20:2268–81. doi: 10.1038/mt.2012.162
29. Abbink P, Lemckert AA, Ewald BA, Lynch DM, Denholtz M, Smits S, et al. Comparative seroprevalence immunogenicity of six rare serotype recombinant adenovirus vaccine vectors from subgroups B and D. *J Virol*. (2007) 81:4654–663. doi: 10.1128/JVI.02696-06
30. Mennechet FJD, Paris O, Ouoba AR, Salazar Arenas S, Sirima SB, Takoudjou Dzomo GR, et al. A review of 65 years of human adenovirus seroprevalence. *Expert Rev Vaccines*. (2019) 18:597–613. doi: 10.1080/14760584.2019.1588113
31. Sayedahmed EE, Hassan AO, Kumari R, Cao W, Gangappa S, York I, et al. A bovine adenoviral vector-based H5N1 influenza -vaccine provides enhanced immunogenicity and protection at a significantly low dose. *Mol Ther Methods Clin Dev*. (2018) 10:210–22. doi: 10.1016/j.omtm.2018.07.007
32. Xiang ZQ, Yang Y, Wilson JM, Ertl HC. A replication-defective human adenovirus recombinant serves as a highly efficacious vaccine carrier. *Virology*. (1996) 219:220–7. doi: 10.1006/viro.1996.0239
33. Quinn KM, Zak DE, Costa A, Yamamoto A, Kastenmuller K, Hill BJ, et al. Antigen expression determines adenoviral vaccine potency independent of IFN and STING signaling. *J Clin Invest*. (2015) 125:1129–46. doi: 10.1172/JCI78280
34. Yang TC, Dayball K, Wan YH, Bramson J. Detailed analysis of the CD8+ T-cell response following adenovirus vaccination. *J Virol*. (2003) 77:13407–11. doi: 10.1128/jvi.77.24.13407-13411.2003
35. Sullivan NJ, Hensley L, Asiedu C, Geisbert TW, Stanley D, Johnson J, et al. CD8+ cellular immunity mediates rAd5 vaccine protection against Ebola virus infection of nonhuman primates. *Nat Med*. (2011) 17:1128–31. doi: 10.1038/nm.2447
36. Tatsis N, Fitzgerald JC, Reyes-Sandoval A, Harris-McCoy KC, Hensley SE, Zhou D, et al. Adenoviral vectors persist *in vivo* and maintain activated CD8+ T cells: implications for their use as vaccines. *Blood*. (2007) 110:1916–23. doi: 10.1182/blood-2007-02-062117
37. Green CA, Scarselli E, Sande CJ, Thompson AJ, de Lara CM, Taylor KS, et al. Chimpanzee adenovirus- and MVA-vectored respiratory syncytial virus vaccine is safe and immunogenic in adults. *Sci Transl Med*. (2015). *7*:300ra126. doi: 10.1126/scitranslmed.aac5745
38. Fejer G, Freudenberg M, Greber UF, Gyory I. Adenovirus-triggered innate signalling pathways. *Eur J Microbiol Immunol*. (2011) 1:279–88. doi: 10.1556/EuJMI.1.2011.4.3
39. Bassett JD, Yang TC, Bernard D, Millar JB, Swift SL, McGray AJ, et al. CD8+ T-cell expansion and maintenance after recombinant adenovirus immunization rely upon cooperation between hematopoietic and nonhematopoietic antigen-presenting cells. *Blood*. (2011) 117:1146–55. doi: 10.1182/blood-2010-03-272336
40. Jimenez-Chillaron JC, Newgard CB, Gomez-Foix AM. Increased glucose disposal induced by adenovirus-mediated transfer of glucokinase to skeletal muscle *in vivo*. *FASEB J*. (1999) 13:2153–60. doi: 10.1096/fasebj.13.15.2153
41. Juillard V, Villefroy P, Godfrin D, Pavirani A, Venet A, Guillet JG. Long-term humoral and cellular immunity induced by a single immunization with replication-defective adenovirus recombinant vector. *Eur J Immunol*. (1995) 25:3467–73. doi: 10.1002/eji.1830251239
42. Tan WG, Jin HT, West EE, Penaloza-MacMaster P, Wieland A, Zilliox MJ, et al. Comparative analysis of simian immunodeficiency virus gag-specific effector and memory CD8+ T cells induced by different adenovirus vectors. *J Virol*. (2013) 87:1359–72. doi: 10.1128/JVI.02055-12
43. Penaloza-MacMaster P, Provine NM, Ra J, Borducchi EN, McNally A, Simmons NL, et al. Alternative serotype adenovirus vaccine vectors elicit memory T cells with enhanced anamnestic capacity compared to Ad5 vectors. *J Virol*. (2013) 87:1373–84. doi: 10.1128/JVI.02058-12
44. Johnson MJ, Petrovas C, Yamamoto T, Lindsay RW, Lore K, Gall JG, et al. Type I IFN induced by adenovirus serotypes 28 and 35 has multiple effects on T cell immunogenicity. *J Immunol*. (2012) 188:6109–18. doi: 10.4049/jimmunol.1103717
45. Holst PJ, Orskov C, Thomsen AR, Christensen JP. Quality of the transgene-specific CD8+ T cell response induced by adenoviral vector immunization is critically influenced by virus dose and route of vaccination. *J Immunol*. (2010) 184:4431–9. doi: 10.4049/jimmunol.0900537
46. Lord R, Parsons M, Kirby I, Beavil A, Hunt J, Sutton B, et al. Analysis of the interaction between RGD-expressing adenovirus type 5 fiber knob domains and alphavbeta3 integrin reveals distinct binding profiles and intracellular trafficking. *J Gen Virol*. (2006) 87:2497–2505. doi: 10.1099/vir.0.81620-0
47. Wickham TJ, Mathias P, Cheresh DA, Nemerow GR. Integrins alpha v beta 3 and alpha v beta 5 promote adenovirus internalization but not virus attachment. *Cell*. (1993) 73:309–19. doi: 10.1016/0092-8674(93)90231-e
48. Suomalainen M, Luisoni S, Boucke K, Bianchi S, Engel DA, Greber UF. A direct and versatile assay measuring membrane penetration of adenovirus in single cells. *J Virol*. (2013) 87:12367–79. doi: 10.1128/JVI.01833-13
49. Burckhardt CJ, Suomalainen M, Schoenenberger P, Boucke K, Hemmi S, Greber UF. Drifting motions of the adenovirus receptor CAR and immobile integrins initiate virus uncoating and membrane lytic protein exposure. *Cell Host Microbe*. (2011) 10:105–17. doi: 10.1016/j.chom.2011.07.006

50. Greber UF, Willetts M, Webster P, Helenius A. Stepwise dismantling of adenovirus 2 during entry into cells. *Cell*. (1993) 75:477–86. doi: 10.1016/0092-8674(93)90382-z
51. Stewart PL, Fuller SD, Burnett RM. Difference imaging of adenovirus: bridging the resolution gap between X-ray crystallography and electron microscopy. *EMBO J*. (1993) 12:2589–99.
52. Wodrich H, Henaff D, Jammart B, Segura-Morales C, Seelmeir S, Coux O, et al. A capsid-encoded PPxY-motif facilitates adenovirus entry. *PLoS Pathog*. (2010) 6:e1000808. doi: 10.1371/journal.ppat.1000808
53. Maier O, Marvin SA, Wodrich H, Campbell EM, Wiethoff CM. Spatiotemporal dynamics of adenovirus membrane rupture and endosomal escape. *J Virol*. (2012) 86:10821–828. doi: 10.1128/JVI.01428-12
54. Wiethoff CM, Wodrich H, Gerace L, Nemerow GR. Adenovirus protein VI mediates membrane disruption following capsid disassembly. *J Virol*. (2005) 79:1992–2000. doi: 10.1128/JVI.79.4.1992-2000.2005
55. Gaggar A, Shayakhmetov DM, Liszewski MK, Atkinson JP, Lieber A. Localization of regions in CD46 that interact with adenovirus. *J Virol*. (2005) 79:7503–13. doi: 10.1128/JVI.79.12.7503-7513.2005
56. Sirena D, Lilienfeld B, Eisenhut M, Kalin S, Boucke K, Beerli RR, et al. The human membrane cofactor CD46 is a receptor for species B adenovirus serotype 3. *J Virol*. (2004) 78:4454–62. doi: 10.1128/jvi.78.9.4454-4462.2004
57. Gaggar A, Shayakhmetov DM, Lieber A. CD46 is a cellular receptor for group B adenoviruses. *Nat Med*. (2003) 9:1408–12. doi: 10.1038/nm952
58. Wang H, Li ZY, Liu Y, Persson J, Beyer I, Moller T, et al. Desmoglein 2 is a receptor for adenovirus serotypes 3, 7, 11 and 14. *Nat Med*. (2011) 17:96–104. doi: 10.1038/nm.2270
59. Baker AT, Mundy RM, Davies JA, Rizkallah PJ, Parker AL. Human adenovirus type 26 uses sialic acid-bearing glycans as a primary cell entry receptor. *Sci Adv*. (2019) 5:eaax3567. doi: 10.1126/sciadv.aax3567
60. Shayakhmetov DM, Li ZY, Ternovoi V, Gaggar A, Gharwan H, Lieber A. The interaction between the fiber knob domain and the cellular attachment receptor determines the intracellular trafficking route of adenoviruses. *J Virol*. (2003) 77:3712–23. doi: 10.1128/jvi.77.6.3712-3723.2003
61. Iacobelli-Martinez M, Nemerow GR. Preferential activation of Toll-like receptor nine by CD46-utilizing adenoviruses. *J Virol*. (2007) 81:1305–12. doi: 10.1128/JVI.01926-06
62. Maler MD, Nielsen PJ, Stichling N, Cohen I, Ruzsics Z, Wood C, et al. Key role of the scavenger receptor MARCO in mediating adenovirus infection and subsequent innate responses of macrophages. *mBio*. (2017) 8:e00670-17. doi: 10.1128/mBio.00670-17
63. Shayakhmetov DM, Li ZY, Ni S, Lieber A. Analysis of adenovirus sequestration in the liver, transduction of hepatic cells, and innate toxicity after injection of fiber-modified vectors. *J Virol*. (2004) 78:5368–81. doi: 10.1128/jvi.78.10.5368-5381.2004
64. Tao N, Gao GP, Parr M, Johnston J, Baradet T, Wilson JM, et al. Sequestration of adenoviral vector by Kupffer cells leads to a nonlinear dose response of transduction in liver. *Mol Ther*. (2001) 3:28–35. doi: 10.1006/mthe.2000.0227
65. Carey B, Staudt MK, Bonaminio D, van der Loo JC, Trapnell BC. PU.1 redirects adenovirus to lysosomes in alveolar macrophages, uncoupling internalization from infection. *J Immunol*. (2007) 178:2440–7. doi: 10.4049/jimmunol.178.4.2440
66. Worgall S, Leopold PL, Wolff G, Ferris B, Van Roijen N, Crystal RG. Role of alveolar macrophages in rapid elimination of adenovirus vectors administered to the epithelial surface of the respiratory tract. *Human Gene Ther*. (1997) 8:1675–84. doi: 10.1089/hum.1997.8.14-1675
67. Stichling N, Suomalainen M, Flatt JW, Schmid M, Pacesa M, Hemmi S, et al. Lung macrophage scavenger receptor SR-A6 (MARCO) is an adenovirus type-specific virus entry receptor. *PLoS pathog*. (2018) 14:e1006914. doi: 10.1371/journal.ppat.1006914
68. Zsengeller Z, Otake K, Hossain SA, Berclaz PY, Trapnell BC. Internalization of adenovirus by alveolar macrophages initiates early proinflammatory signaling during acute respiratory tract infection. *J Virol*. (2000) 74:9655–9667. doi: 10.1128/jvi.74.20.9655-9667.2000
69. Manickan E, Smith JS, Tian J, Eggerman TL, Lozier JN, Muller J, et al. Rapid Kupffer cell death after intravenous injection of adenovirus vectors. *Mol Ther*. (2006) 13:108–17. doi: 10.1016/j.ymthe.2005.08.007
70. Schiedner G, Bloch W, Hertel S, Johnston M, Molojavyi A, Dries V, et al. A hemodynamic response to intravenous adenovirus vector particles is caused by systemic kupffer cell-mediated activation of endothelial cells. *Human Gene Ther*. (2003) 14:1631–41. doi: 10.1089/104303403322542275
71. Xu Z, Tian J, Smith JS, Byrnes AP. Clearance of adenovirus by Kupffer cells is mediated by scavenger receptors, natural antibodies, and complement. *J Virol*. (2008) 82:11705–13. doi: 10.1128/JVI.01320-08
72. Cotter MJ, Zaiss AK, Muruve DA. Neutrophils interact with adenovirus vectors via Fc receptors and complement receptor 1. *J Virol*. (2005) 79:14622–31. doi: 10.1128/JVI.79.23.14622-14631.2005
73. Zaiss AK, Vilaysane A, Cotter MJ, Clark SA, Meijndert HC, Colarusso P, et al. Antiviral antibodies target adenovirus to phagolysosomes and amplify the innate immune response. *J Immunol*. (2009) 182:7058–68. doi: 10.4049/jimmunol.0804269
74. Haisma HJ, Boesjes M, Beerens AM, van der Strate BW, Curiel DT, Pluddemann A, et al. Scavenger receptor A: a new route for adenovirus 5. *Mol Pharm*. (2009) 6:366–74. doi: 10.1021/mp8000974
75. Canton J, Neculai D, Grinstein S. Scavenger receptors in homeostasis and immunity. *Nat Rev*. (2013) 13:621–34. doi: 10.1038/nri3515
76. Khare R, Reddy VS, Nemerow GR, Barry MA. Identification of adenovirus serotype 5 hexon regions that interact with scavenger receptors. *J Virol*. (2012) 86:2293–301. doi: 10.1128/JVI.05760-11
77. Di Paolo NC, Miao EA, Iwakura Y, Murali-Krishna K, Aderem A, Flavell RA, et al. Virus binding to a plasma membrane receptor triggers interleukin-1 alpha-mediated proinflammatory macrophage response *in vivo*. *Immunity*. (2009) 31:110–21. doi: 10.1016/j.immuni.2009.04.015
78. Alemany R, Suzuki K, Curiel DT. Blood clearance rates of adenovirus type 5 in mice. *J Gen Virol*. (2000) 81:2605–9. doi: 10.1099/0022-1317-81-11-2605
79. Furumoto K, Nagayama S, Ogawara K, Takakura Y, Hashida M, Higaki K, et al. Hepatic uptake of negatively charged particles in rats: possible involvement of serum proteins in recognition by scavenger receptor. *J Control Rel*. (2004) 97:133–41. doi: 10.1016/j.jconrel.2004.03.004
80. Dolan BP, Gibbs KD Jr., Ostrand-Rosenberg S. Dendritic cells cross-dressed with peptide MHC class I complexes prime CD8+ T cells. *J Immunol*. (2006) 177:6018–24. doi: 10.4049/jimmunol.177.9.6018
81. Thery C, Duban L, Segura E, Veron P, Lantz O, Amigorena S. Indirect activation of naive CD4+ T cells by dendritic cell-derived exosomes. *Nat Immunol*. (2002). *3*:1156–62. doi: 10.1038/ni854
82. Thery C, Ostrowski M, Segura E. Membrane vesicles as conveyors of immune responses. *Nat Rev*. (2009) 9:581–93. doi: 10.1038/nri2567
83. Denzer K, van Eijk M, Kleijmeer MJ, Jakobson E, de Groot C, Geuze HJ. Follicular dendritic cells carry MHC class II-expressing microvesicles at their surface. *J Immunol*. (2000) 165:1259–65. doi: 10.4049/jimmunol.165.3.1259
84. Segura E, Guerin C, Hogg N, Amigorena S, Thery C. CD8+ dendritic cells use LFA-1 to capture MHC-peptide complexes from exosomes *in vivo*. *J Immunol*. (2007) 179:1489–96. doi: 10.4049/jimmunol.179.3.1489
85. Yewdell JW, Dolan BP. Immunology: cross-dressers turn on T cells. *Nature*. (2011) 471:581–2. doi: 10.1038/471581a
86. Lindsay RW, Darrah PA, Quinn KM, Wille-Reece U, Mattei LM, Iwasaki A, et al. CD8+ T cell responses following replication-defective adenovirus serotype 5 immunization are dependent on CD11c+ dendritic cells but show redundancy in their requirement of TLR and nucleotide-binding oligomerization domain-like receptor signaling. *J Immunol*. (2010) 185:1513–21. doi: 10.4049/jimmunol.1000338
87. Mercier S, Gahery-Segard H, Monteil M, Lengagne R, Guillet JG, Eloit M, et al. Distinct roles of adenovirus vector-transduced dendritic cells, myoblasts, and endothelial cells in mediating an immune response against a transgene product. *J Virol*. (2002) 76:2899–911. doi: 10.1128/jvi.76.6.2899-2911.2002
88. Korst RJ, Mahtabifard A, Yamada R, Crystal RG. Effect of adenovirus gene transfer vectors on the immunologic functions of mouse dendritic cells. *Mol Ther*. (2002) 5:307–15. doi: 10.1006/mthe.2002.0538
89. Morelli AE, Larregina AT, Ganster RW, Zahorchak AF, Plowey JM, Takayama T, et al. Recombinant adenovirus induces maturation of dendritic cells via an NF-kappaB-dependent pathway. *J Virol*. (2000) 74:9617–28. doi: 10.1128/jvi.74.20.9617-9628.2000
90. Molinier-Frenkel V, Prevost-Blondel A, Hong SS, Lengagne R, Boudaly S, Magnusson MK, et al. The maturation of murine dendritic cells induced by

human adenovirus is mediated by the fiber knob domain. *J Biol Chem*. (2003) 278:37175–82. doi: 10.1074/jbc.M303496200
91. Bonifaz L, Bonnyay D, Mahnke K, Rivera M, Nussenzweig MC, Steinman RM. Efficient targeting of protein antigen to the dendritic cell receptor DEC-205 in the steady state leads to antigen presentation on major histocompatibility complex class I products and peripheral CD8+ T cell tolerance. *J Exp Med*. (2002) 196:1627–38. doi: 10.1084/jem.20021598
92. Johnson TS, Mahnke K, Storn V, Schonfeld K, Ring S, Nettelbeck DM, et al. Inhibition of melanoma growth by targeting of antigen to dendritic cells via an anti-DEC-205 single-chain fragment variable molecule. *Clin Cancer Res*. (2008) 14:8169–77. doi: 10.1158/1078-0432.CCR-08-1474
93. Pereboev AV, Nagle JM, Shakhmatov MA, Triozzi PL, Matthews QL, Kawakami Y, et al. Enhanced gene transfer to mouse dendritic cells using adenoviral vectors coated with a novel adapter molecule. *Mol Ther*. (2004) 9:712–20. doi: 10.1016/j.ymthe.2004.02.006
94. Korokhov N, de Gruijl TD, Aldrich WA, Triozzi PL, Banerjee PT, Gillies SD, et al. High efficiency transduction of dendritic cells by adenoviral vectors targeted to DC-SIGN. *Cancer Biol Ther*. (2005) 4:289–94. doi: 10.4161/cbt.4.3.1499
95. Adams WC, Bond E, Havenga MJ, Holterman L, Goudsmit J, Karlsson Hedestam GB, et al. Adenovirus serotype 5 infects human dendritic cells via a coxsackievirus-adenovirus receptor-independent receptor pathway mediated by lactoferrin DC-SIGN. *J Gen Virol*. (2009) 90:1600–10. doi: 10.1099/vir.0.008342-0
96. Lore K, Adams WC, Havenga MJ, Precopio ML, Holterman L, Goudsmit J, et al. Myeloid and plasmacytoid dendritic cells are susceptible to recombinant adenovirus vectors and stimulate polyfunctional memory T cell responses. *J Immunol*. (2007) 179:1721–9. doi: 10.4049/jimmunol.179.3.1721
97. Tatsis N, Blejer A, Lasaro MO, Hensley SE, Cun A, Tesema L, et al. A CD46-binding chimpanzee adenovirus vector as a vaccine carrier. *Mol Ther*. (2007) 15:608–17. doi: 10.1038/sj.mt.6300078
98. Short JJ, Pereboev AV, Kawakami Y, Vasu C, Holterman MJ, Curiel DT. Adenovirus serotype 3 utilizes CD80 (B7.1) and CD86 (B7.2) as cellular attachment receptors. *Virology*. (2004) 322:349–59. doi: 10.1016/j.virol.2004.02.016
99. Chondronasiou D, Eisden T, Stam AGM, Matthews QL, Icyuz M, Hooijberg E, et al. Improved induction of anti-melanoma t cells by adenovirus-5/3 fiber modification to target human DCs. *Vaccines*. (2018) 6:42. doi: 10.3390/vaccines6030042
100. Wilkinson-Ryan I, Kim J, Kim S, Ak F, Dodson L, Colonna M, et al. Incorporation of porcine adenovirus 4 fiber protein enhances infectivity of adenovirus vector on dendritic cells: implications for immune-mediated cancer therapy. *PLoS ONE*. (2015) 10:e0125851. doi: 10.1371/journal.pone.0125851
101. Hsu C, Boysen M, Gritton LD, Frosst PD, Nemerow GR, Von Seggern DJ. *In vitro* dendritic cell infection by pseudotyped adenoviral vectors does not correlate with their *in vivo* immunogenicity. *Virology*. (2005) 332:1–7. doi: 10.1016/j.virol.2004.11.014
102. Vitelli A, Folgori A, Scarselli E, Colloca S, Capone S, Nicosia A. Chimpanzee adenoviral vectors as vaccines - challenges to move the technology into the fast lane. *Expert Rev Vaccines*. (2017) 16:1241–52. doi: 10.1080/14760584.2017.1394842
103. Vemula SV, Mittal SK. Production of adenovirus vectors and their use as a delivery system for influenza vaccines. *Expert Opin Biol Ther*. (2010). 10:1469–1487. doi: 10.1517/14712598.2010.519332
104. Capelle MAH, Babich L, van Deventer-Troost JPE, Salerno D, Krijgsman K, Dirmeier U, et al. Stability and suitability for storage and distribution of Ad26.ZEBOV/MVA-BN(R)-Filo heterologous prime-boost Ebola vaccine. *Eur J Pharm Biopharm*. (2018) 129:215–21. doi: 10.1016/j.ejpb.2018.06.001
105. Afkhami S, LeClair DA, Haddadi S, Lai R, Toniolo SP, Ertl HC, et al. Spray dried human and chimpanzee adenoviral-vectored vaccines are thermally stable and immunogenic *in vivo*. *Vaccine*. (2017) 35:2916–24. doi: 10.1016/j.vaccine.2017.04.026
106. Alcock R, Cottingham MG, Rollier CS, Furze J, De Costa SD, Hanlon M, et al. Long-term thermostabilization of live poxviral and adenoviral vaccine vectors at supraphysiological temperatures in carbohydrate glass. *Sci Transl Med*. (2010) 2:19ra12. doi: 10.1126/scitranslmed.3000490
107. Wang C, Dulal P, Zhou X, Xiang Z, Goharriz H, Banyard A, et al. A simian-adenovirus-vectored rabies vaccine suitable for thermostabilisation and clinical development for low-cost single-dose pre-exposure prophylaxis. *PLoS Negl Trop Dis*. (2018) 12:e0006870. doi: 10.1371/journal.pntd.0006870
108. Coughlan L, Mullarkey C, Gilbert S. Adenoviral vectors as novel vaccines for influenza. *J Pharm Pharmacol*. (2015) 67:382–399. doi: 10.1111/jphp.12350
109. Rhee EG, Blattman JN, Kasturi SP, Kelley RP, Kaufman DR, Lynch DM, et al. Multiple innate immune pathways contribute to the immunogenicity of recombinant adenovirus vaccine vectors. *J Virol*. (2011) 85:315–23. doi: 10.1128/JVI.01597-10
110. Zhu J, Huang X, Yang Y. Innate immune response to adenoviral vectors is mediated by both Toll-like receptor-dependent and -independent pathways. *J Virol*. (2007) 81:3170–80. doi: 10.1128/JVI.02192-06
111. Muruve DA, Petrilli V, Zaiss AK, White LR, Clark SA, Ross PJ, et al. The inflammasome recognizes cytosolic microbial and host DNA and triggers an innate immune response. *Nature*. (2008) 452:103–7. doi: 10.1038/nature06664
112. Atasheva S, Shayakhmetov DM. Adenovirus sensing by the immune system. *Curr Opin Virol*. (2016) 21:109–13. doi: 10.1016/j.coviro.2016.08.017
113. Appledorn DM, Patial S, McBride A, Godbehere S, Van Rooijen N, Parameswaran N, et al. Adenovirus vector-induced innate inflammatory mediators, MAPK signaling, as well as adaptive immune responses are dependent upon both TLR2 and TLR9 *in vivo*. *J Immunol*. (2008) 181:2134–44. doi: 10.4049/jimmunol.181.3.2134
114. Appledorn DM, Patial S, Godbehere S, Parameswaran N, Amalfitano A. TRIF, and TRIF-interacting TLRs differentially modulate several adenovirus vector-induced immune responses. *J Innate Immun*. (2009) 1:376–88. doi: 10.1159/000207194
115. Lam E, Stein S, Falck-Pedersen E. Adenovirus detection by the cGAS/STING/TBK1 DNA sensing cascade. *J Virol*. (2014) 88:974–81. doi: 10.1128/JVI.02702-13
116. Anghelina D, Lam E, Falck-Pedersen E. Diminished innate antiviral response to adenovirus vectors in cGAS/STING-deficient mice minimally impacts adaptive immunity. *J Virol*. (2016) 90:5915–27. doi: 10.1128/JVI.00500-16
117. Burdette DL, Monroe KM, Sotelo-Troha K, Iwig JS, Eckert B, Hyodo M, et al. STING is a direct innate immune sensor of cyclic di-GMP. *Nature*. (2011) 478:515–8. doi: 10.1038/nature10429
118. Hartman ZC, Appledorn DM, Amalfitano A. Adenovirus vector induced innate immune responses: impact upon efficacy and toxicity in gene therapy and vaccine applications. *Virus Res*. (2008) 132:1–4. doi: 10.1016/j.virusres.2007.10.005
119. Hendrickx R, Stichling N, Koelen J, Kuryk L, Lipiec A, Greber UF. Innate immunity to adenovirus. *Human Gene Ther*. (2014) 25:265–84. doi: 10.1089/hum.2014.001
120. Hensley SE, Cun AS, Giles-Davis W, Li Y, Xiang Z, Lasaro MO, et al. Type I interferon inhibits antibody responses induced by a chimpanzee adenovirus vector. *Mol Ther*. (2007) 15:393–403. doi: 10.1038/sj.mt.6300024
121. Finn JD, Bassett J, Millar JB, Grinshtein N, Yang TC, Parsons R, et al. Persistence of transgene expression influences CD8+ T-cell expansion and maintenance following immunization with recombinant adenovirus. *J Virol*. (2009) 83:12027–36. doi: 10.1128/JVI.00593-09
122. Yang TC, Millar J, Groves T, Grinshtein N, Parsons R, Takenaka S, et al. The CD8+ T cell population elicited by recombinant adenovirus displays a novel partially exhausted phenotype associated with prolonged antigen presentation that nonetheless provides long-term immunity. *J Immunol*. (2006) 176:200–10. doi: 10.4049/jimmunol.176.1.200
123. Dicks MD, Spencer AJ, Coughlan L, Bauza K, Gilbert SC, Hill AV, et al. Differential immunogenicity between HAdV-5 and chimpanzee adenovirus vector ChAdOx1 is independent of fiber and penton RGD loop sequences in mice. *Sci Rep*. (2015) 5:16756. doi: 10.1038/srep16756
124. Pulendran B, Ahmed R. Translating innate immunity into immunological memory: implications for vaccine development. *Cell*. (2006) 124:849–63. doi: 10.1016/j.cell.2006.02.019
125. Thomas S, Kolumam GA, Murali-Krishna K. Antigen presentation by nonhemopoietic cells amplifies clonal expansion of effector CD8 T cells in a pathogen-specific manner. *J Immunol*. (2007) 178:5802–11. doi: 10.4049/jimmunol.178.9.5802

126. Dzierszinski F, Pepper M, Stumhofer JS, LaRosa DF, Wilson EH, Turka LA, et al. Presentation of *Toxoplasma gondii* antigens via the endogenous major histocompatibility complex class I pathway in nonprofessional and professional antigen-presenting cells. *Infect Immun*. (2007) 75:5200–9. doi: 10.1128/IAI.00954-07
127. Lambe T, Carey JB, Li Y, Spencer AJ, van Laarhoven A, Mullarkey CE, et al. Immunity against heterosubtypic influenza virus induced by adenovirus and MVA expressing nucleoprotein and matrix protein-1. *Sci Rep*. (2013) 3:1443. doi: 10.1038/srep01443
128. Kaufman DR, Bivas-Benita M, Simmons NL, Miller D, Barouch DH. Route of adenovirus-based HIV-1 vaccine delivery impacts the phenotype and trafficking of vaccine-elicited CD8+ T lymphocytes. *J Virol*. (2010) 84:5986–5996. doi: 10.1128/JVI.02563-09
129. Coughlan L, Vallath S, Gros A, Gimenez-Alejandre M, Van Rooijen N, Thomas GJ, et al. Combined fiber modifications both to target alpha(v)beta(6) and detarget the coxsackievirus-adenovirus receptor improve virus toxicity profiles *in vivo* but fail to improve antitumoral efficacy relative to adenovirus serotype 5. *Human Gene Ther*. (2012) 23:960–79. doi: 10.1089/hum.2011.218
130. Alba R, Bradshaw AC, Coughlan L, Denby L, McDonald RA, Waddington SN, et al. Biodistribution and retargeting of FX-binding ablated adenovirus serotype 5. *Vectors Blood*. (2010) 116:2656–64. doi: 10.1182/blood-2009-12-260026
131. Shayakhmetov DM, Gaggar A, Ni S, Li ZY, Lieber A. Adenovirus binding to blood factors results in liver cell infection and hepatotoxicity. *J Virol*. (2005) 79:7478–91. doi: 10.1128/JVI.79.12.7478-7491.2005
132. Waddington SN, McVey JH, Bhella D, Parker AL, Barker K, Atoda H, et al. Adenovirus serotype 5 hexon mediates liver gene transfer. *Cell*. (2008) 132:397–409. doi: 10.1016/j.cell.2008.01.016
133. Bradshaw AC, Coughlan L, Miller AM, Alba R, van Rooijen N, Nicklin SA, et al. Biodistribution and inflammatory profiles of novel penton and hexon double-mutant serotype 5 adenoviruses. *J Control Rel*. (2012) 164:394–402. doi: 10.1016/j.jconrel.2012.05.025
134. Bradshaw AC, Parker AL, Duffy MR, Coughlan L, van Rooijen N, Kahari VM, et al. Requirements for receptor engagement during infection by adenovirus complexed with blood coagulation factor X. *PLoS Pathog*. (2010) 6:e1001142. doi: 10.1371/journal.ppat.1001142
135. Atasheva S, Yao J, Shayakhmetov DM. Innate immunity to adenovirus: lessons from mice. *FEBS Lett*. (2019) 593:3461–83. doi: 10.1002/1873-3468.13696
136. Havenar-Daughton C, Newton IG, Zare SY, Reiss SM, Schwan B, Suh MJ, et al.. Normal human lymph node T follicular helper cells and germinal center B cells accessed via fine needle aspirations. *J Immunol Methods*. (2020) 479:112746. doi: 10.1016/j.jim.2020.112746
137. Grinshtein N, Yang TC, Parsons R, Millar J, Denisova G, Dissanayake D, et al. Recombinant adenovirus vaccines can successfully elicit CD8+ T cell immunity under conditions of extreme leukopenia. *Mol Ther*. (2006) 13:270–9. doi: 10.1016/j.ymthe.2005.09.018
138. Holst P, Thomsen A. Harnessing the potential of adenovirus vectored vaccines. In: *Viral Gene Therapy*. (2011). Available online at: https://www.intechopen.com/books/viral-gene-therapy/harnessing-the-potential-of-adenovirus-vectored-vaccines/
139. Coughlan L, Palese P. Overcoming barriers in the path to a universal influenza virus vaccine. *Cell Host Microbe*. (2018). 24:18–24. doi: 10.1016/j.chom.2018.06.016
140. Kim MH, Kim HJ, Chang J. Superior immune responses induced by intranasal immunization with recombinant adenovirus-based vaccine expressing full-length Spike Protein of Middle East respiratory syndrome coronavirus. *PLoS ONE*. (2019) 14:e0220196. doi: 10.1371/journal.pone.0220196
141. Jia W, Channappanavar R, Zhang C, Li M, Zhou H, Zhang S, et al. Single intranasal immunization with chimpanzee adenovirus-based vaccine induces sustained and protective immunity against MERS-CoV infection. *Emerg. Microbes Infect*. (2019) 8:760–72. doi: 10.1080/22221751.2019.1620083
142. Matchett WE, Anguiano-Zarate SS, Barry MA. Comparison of systemic and mucosal immunization with replicating Single cycle Adenoviruses. *Glob Vaccines Immunol*. (2018) 3:128. doi: 10.15761/GVI.1000128
143. Bolton DL, Song K, Tomaras GD, Rao S, Roederer M. Unique cellular and humoral immunogenicity profiles generated by aerosol, intranasal, or parenteral vaccination in rhesus macaques. *Vaccine*. (2017) 35:639–46. doi: 10.1016/j.vaccine.2016.12.008
144. Jeyanathan M, Thanthrige-Don N, Afkhami S, Lai R, Damjanovic D, Zganiacz A, et al. Novel chimpanzee adenovirus-vectored respiratory mucosal tuberculosis vaccine: overcoming local anti-human adenovirus immunity for potent TB protection. *Mucosal Immunol*. (2015) 8:1373–87. doi: 10.1038/mi.2015.29
145. Krause A, Whu WZ, Xu Y, Joh J, Crystal RG, Worgall S. Protective anti-Pseudomonas aeruginosa humoral and cellular mucosal immunity by AdC7-mediated expression of the *P. aeruginosa* protein OprF. *Vaccine*. (2011) 29:2131–9. doi: 10.1016/j.vaccine.2010.12.087
146. Molinier-Frenkel V, Lengagne R, Gaden F, Hong SS, Choppin J, Gahery-Segard H, et al. Adenovirus hexon protein is a potent adjuvant for activation of a cellular immune response. *J Virol*. (2002) 76:127–35. doi: 10.1128/jvi.76.1.127-135.2002
147. Tamanini A, Nicolis E, Bonizzato A, Bezzerri V, Melotti P, Assael BM, et al. Interaction of adenovirus type 5 fiber with the coxsackievirus and adenovirus receptor activates inflammatory response in human respiratory cells. *J Virol*. (2006) 80:11241–54. doi: 10.1128/JVI.00721-06
148. Schoggins JW, Nociari M, Philpott N, Falck-Pedersen E. Influence of fiber detargeting on adenovirus-mediated innate and adaptive immune activation. *J Virol*. (2005) 79:11627–37. doi: 10.1128/JVI.79.18.11627-11637.2005
149. Miwa T, Nonaka M, Okada N, Wakana S, Shiroishi T, Okada H. Molecular cloning of rat and mouse membrane cofactor protein (MCP, CD46): preferential expression in testis and close linkage between the mouse Mcp and Cr2 genes on distal chromosome 1. *Immunogenetics*. (1998) 48:363–71. doi: 10.1007/s002510050447
150. Nanda A, Lynch DM, Goudsmit J, Lemckert AA, Ewald BA, Sumida SM, et al. Immunogenicity of recombinant fiber-chimeric adenovirus serotype 35 vector-based vaccines in mice and rhesus monkeys. *J Virol*. (2005) 79:14161–8. doi: 10.1128/JVI.79.22.14161-14168.2005
151. Nidetz NF, Gallagher TM, Wiethoff CM. Inhibition of type I interferon responses by adenovirus serotype-dependent Gas6 binding. *Virology*. (2018) 515:150–7. doi: 10.1016/j.virol.2017.12.016
152. Kahl CA, Bonnell J, Hiriyanna S, Fultz M, Nyberg-Hoffman C, Chen P, et al. Potent immune responses and *in vitro* pro-inflammatory cytokine suppression by a novel adenovirus vaccine vector based on rare human serotype 28. *Vaccine*. (2010) 28:5691–702. doi: 10.1016/j.vaccine.2010.06.050
153. Tibbles LA, Spurrell JC, Bowen GP, Liu Q, Lam M, Zaiss AK, et al. Activation of p38 and ERK signaling during adenovirus vector cell entry lead to expression of the C-X-C chemokine IP-10. *J Virol*. (2002) 76:1559–68. doi: 10.1128/jvi.76.4.1559-1568.2002
154. Neukirch L, Fougeroux C, Andersson AC, Holst PJ. The potential of adenoviral vaccine vectors with altered antigen presentation capabilities. *Expert Rev Vaccines*. (2020) 19:25–41. doi: 10.1080/14760584.2020.1711054
155. Holst PJ, Bartholdy C, Stryhn A, Thomsen AR, Christensen JP. Rapid and sustained CD4(+) T-cell-independent immunity from adenovirus-encoded vaccine antigens. *J Gen Virol*. (2007) 88:1708–16. doi: 10.1099/vir.0.82727-0
156. Mikkelsen M, Holst PJ, Bukh J, Thomsen AR, Christensen JP. Enhanced and sustained CD8+ T cell responses with an adenoviral vector-based hepatitis C virus vaccine encoding NS3 linked to the MHC class II chaperone protein invariant chain. *J Immunol*. (2011) 186:2355–64. doi: 10.4049/jimmunol.1001877
157. Spencer AJ, Cottingham MG, Jenks JA, Longley RJ, Capone S, Colloca S, et al. Enhanced vaccine-induced CD8+ T cell responses to malaria antigen ME-TRAP by fusion to MHC class ii invariant chain. *PLoS ONE*. (2014) 9:e100538. doi: 10.1371/journal.pone.0100538
158. Jensen S, Steffensen MA, Jensen BA, Schluter D, Christensen JP, Thomsen AR. Adenovirus-based vaccine against listeria monocytogenes: extending the concept of invariant chain linkage. *J Immunol*. (2013) 191:4152–64. doi: 10.4049/jimmunol.1301290
159. Halbroth BR, Sebastian S, Poyntz HC, Bregu M, Cottingham MG, Hill AVS, et al. Development of a molecular adjuvant to enhance antigen-specific CD8(+) T cell responses. *Sci Rep*. (2018) 8:15020. doi: 10.1038/s41598-018-33375-1

160. Sullivan NJ, Geisbert TW, Geisbert JB, Shedlock DJ, Xu L, Lamoreaux L, et al. Immune protection of nonhuman primates against Ebola virus with single low-dose adenovirus vectors encoding modified GPs. *PLoS Med*. (2006) 3:e177. doi: 10.1371/journal.pmed.0030177
161. Buchbinder SP, Mehrotra DV, Duerr A, Fitzgerald DW, Mogg R, Li D, et al. Efficacy assessment of a cell-mediated immunity HIV-1 vaccine (the Step Study): a double-blind, randomised, placebo-controlled, test-of-concept trial. *Lancet*. (2008) 372:1881–93. doi: 10.1016/S0140-6736(08)61591-3
162. McElrath MJ, De Rosa SC, Moodie Z, Dubey S, Kierstead L, Janes H, et al. HIV-1 vaccine-induced immunity in the test-of-concept Step Study: a case-cohort analysis. *Lancet*. (2008) 372:1894–905. doi: 10.1016/S0140-6736(08)61592-5
163. Priddy FH, Brown D, Kublin J, Monahan K, Wright DP, Lalezari J, et al. Safety and immunogenicity of a replication-incompetent adenovirus type 5 HIV-1 clade B gag/pol/nef vaccine in healthy adults. *Clin Infect Dis*. (2008) 46:1769–81. doi: 10.1086/587993
164. Perreau M, Pantaleo G, Kremer EJ. Activation of a dendritic cell-T cell axis by Ad5 immune complexes creates an improved environment for replication of HIV in T cells. *J Exp Med*. (2008) 205:2717–25. doi: 10.1084/jem.20081786
165. Benlahrech A, Harris J, Meiser A, Papagatsias T, Hornig J, Hayes P, et al. Adenovirus vector vaccination induces expansion of memory CD4 T cells with a mucosal homing phenotype that are readily susceptible to HIV-1. *Proc Natl Acad Sci USA*. (2009) 106:19940–5. doi: 10.1073/pnas.0907898106
166. O'Brien KL, Liu J, King SL, Sun YH, Schmitz JE, Lifton MA, et al. Adenovirus-specific immunity after immunization with an Ad5 HIV-1 vaccine candidate in humans. *Nat Med*. (2009) 15:873–5. doi: 10.1038/nm.1991
167. Duerr A, Huang Y, Buchbinder S, Coombs RW, Sanchez J, del Rio C, et al. Extended follow-up confirms early vaccine-enhanced risk of HIV acquisition and demonstrates waning effect over time among participants in a randomized trial of recombinant adenovirus HIV vaccine (Step Study). *J Infect Dis*. (2012) 206:258–66. doi: 10.1093/infdis/jis342
168. Capone S, Meola A, Ercole BB, Vitelli A, Pezzanera M, Ruggeri L, et al. A novel adenovirus type 6 (Ad6)-based hepatitis C virus vector that overcomes preexisting anti-ad5 immunity and induces potent and broad cellular immune responses in rhesus macaques. *J Virol*. (2006) 80:1688–99. doi: 10.1128/JVI.80.4.1688-1699.2006
169. Harro C, Sun X, Stek JE, Leavitt RY, Mehrotra DV, Wang F, et al. Safety and immunogenicity of the Merck adenovirus serotype 5 (MRKAd5) and MRKAd6 human immunodeficiency virus type 1 trigene vaccines alone and in combination in healthy adults. *Clin Vaccine Immunol*. (2009) 16:1285–92. doi: 10.1128/CVI.00144-09
170. Green CA, Sande CJ, Scarselli E, Capone S, Vitelli A, Nicosia A, et al. Novel genetically-modified chimpanzee adenovirus and MVA-vectored respiratory syncytial virus vaccine safely boosts humoral and cellular immunity in healthy older adults. *J Infect*. (2019) 78:382–92. doi: 10.1016/j.jinf.2019.02.003
171. Mensah VA, Roetynck S, Kanteh EK, Bowyer G, Ndaw A, Oko F, et al. Safety and immunogenicity of malaria vectored vaccines given with routine expanded program on immunization vaccines in Gambian infants and neonates: a randomized controlled trial. *Front Immunol*. (2017). 8:1551. doi: 10.3389/fimmu.2017.01551
172. Bliss CM, Drammeh A, Bowyer G, Sanou GS, Jagne YJ, Ouedraogo O, et al. Viral Vector malaria vaccines induce high-level T cell and antibody responses in West African children and infants. *Mol Ther*. (2017). 25:547–59. doi: 10.1016/j.ymthe.2016.11.003
173. Bliss CM, Bowyer G, Anagnostou NA, Havelock T, Snudden CM, Davies H, et al. Assessment of novel vaccination regimens using viral vectored liver stage malaria vaccines encoding ME-TRAP. *Sci Rep*. (2018) 8:3390. doi: 10.1038/s41598-018-21630-4
174. Afolabi MO, Tiono AB, Adetifa UJ, Yaro JB, Drammeh A, Nebie I, et al. Safety and Immunogenicity of ChAd63 and MVA ME-TRAP in West African children and infants. *Mol Ther*. (2016). 24:1470–1477. doi: 10.1038/mt.2016.83
175. Hodgson SH, Ewer KJ, Bliss CM, Edwards NJ, Rampling T, Anagnostou NA, et al. Evaluation of the efficacy of ChAd63-MVA vectored vaccines expressing circumsporozoite protein and ME-TRAP against controlled human malaria infection in malaria-naive individuals. *J Infect Dis*. (2015) 211:1076–86. doi: 10.1093/infdis/jiu579
176. Ogwang C, Kimani D, Edwards NJ, Roberts R, Mwacharo J, Bowyer G, et al. Prime-boost vaccination with chimpanzee adenovirus and modified vaccinia Ankara encoding TRAP provides partial protection against plasmodium falciparum infection in Kenyan adults. *Sci Transl Med*. (2015) 7:286re285. doi: 10.1126/scitranslmed.aaa2373
177. Tiono AB, Nebie I, Anagnostou N, Coulibaly AS, Bowyer G, Lam E, et al. First field efficacy trial of the ChAd63 MVA ME-TRAP vectored malaria vaccine candidate in 5-17 months old infants and children. *PLoS ONE*. (2018) 13:e0208328. doi: 10.1371/journal.pone.0208328
178. Callendret B, Vellinga J, Wunderlich K, Rodriguez A, Steigerwald R, Dirmeier U, et al. A prophylactic multivalent vaccine against different filovirus species is immunogenic and provides protection from lethal infections with Ebolavirus and Marburgvirus species in non-human primates. *PLoS ONE*. (2018) 13:e0192312. doi: 10.1371/journal.pone.0192312
179. Anywaine Z, Whitworth H, Kaleebu P, Praygod G, Shukarev G, Manno D, et al. Safety and Immunogenicity of a 2-dose heterologous vaccination regimen with Ad26.ZEBOV and MVA-BN-Filo Ebola vaccines: 12-month data from a phase 1 randomized clinical trial in Uganda and Tanzania. *J Infect Dis*. (2019) 220:46–56. doi: 10.1093/infdis/jiz070
180. Milligan ID, Gibani MM, Sewell R, Clutterbuck EA, Campbell D, Plested E, et al. Safety and immunogenicity of novel adenovirus type 26- and modified vaccinia Ankara-vectored Ebola vaccines: a randomized clinical trial. *JAMA*. (2016) 315:1610–23. doi: 10.1001/jama.2016.4218
181. Salisch NC, Izquierdo Gil A, Czapska-Casey DN, Vorthoren L, Serroyen J, Tolboom J, et al. Adenovectors encoding RSV-F protein induce durable and mucosal immunity in macaques after two intramuscular administrations. *NPJ Vaccines*. (2019) 4:54. doi: 10.1038/s41541-019-0150-4
182. Baden LR, Walsh SR, Seaman MS, Tucker RP, Krause KH, Patel A, et al. First-in-human evaluation of the safety and immunogenicity of a recombinant adenovirus serotype 26 HIV-1 Env vaccine (IPCAVD 001). *J Infect Dis*. (2013) 207:240–47. doi: 10.1093/infdis/jis670
183. Barouch DH, Liu J, Peter L, Abbink P, Iampietro MJ, Cheung A, et al. Characterization of humoral and cellular immune responses elicited by a recombinant adenovirus serotype 26 HIV-1 Env vaccine in healthy adults (IPCAVD 001). *J Infect Dis*. (2013) 207:248–56. doi: 10.1093/infdis/jis671
184. Barouch DH, O'Brien KL, Simmons NL, King SL, Abbink P, Maxfield LF, et al. Mosaic HIV-1 vaccines expand the breadth and depth of cellular immune responses in rhesus monkeys. *Nat Med*. (2010) 16:319–23. doi: 10.1038/nm.2089

Conflict of Interest: The author declares that the research was conducted in the absence of any commercial or financial relationships that could be construed as a potential conflict of interest.

frontiers in Immunology

ORIGINAL RESEARCH
published: 19 June 2020
doi: 10.3389/fimmu.2020.01254

Toll-Like Receptor Ligand Based Adjuvant, PorB, Increases Antigen Deposition on Germinal Center Follicular Dendritic Cells While Enhancing the Follicular Dendritic Cells Network

Christina Lisk[1], *Rachel Yuen*[2], *Jeff Kuniholm*[2], *Danielle Antos*[3], *Michael L. Reiser*[4] *and Lee M. Wetzler*[1,2]*

[1] Section of Infectious Diseases, Department of Medicine, Boston Medical Center, Boston, MA, United States, [2] Department of Microbiology, Boston University School of Medicine, Boston, MA, United States, [3] Department of Microbiology and Immunology, University of Pittsburgh School of Medicine, Pittsburgh, PA, United States, [4] DRK-Blutspendedienst, BaWü-Hessen gGmbH, Frankfurt, Germany

OPEN ACCESS

Edited by:
Michael Schotsaert, Icahn School of Medicine at Mount Sinai, United States

Reviewed by:
Srinivasa Reddy Bonam, École supérieure de biotechnologie Strasbourg (ESBS), France
Xuguang Li, Health Canada, Canada

***Correspondence:**
Lee M. Wetzler
lwetzler@bu.edu

Specialty section:
This article was submitted to Vaccines and Molecular Therapeutics, a section of the journal Frontiers in Immunology

Received: 06 March 2020
Accepted: 18 May 2020
Published: 19 June 2020

Citation:
Lisk C, Yuen R, Kuniholm J, Antos D, Reiser ML and Wetzler LM (2020) Toll-Like Receptor Ligand Based Adjuvant, PorB, Increases Antigen Deposition on Germinal Center Follicular Dendritic Cells While Enhancing the Follicular Dendritic Cells Network. Front. Immunol. 11:1254. doi: 10.3389/fimmu.2020.01254

Vaccines are arguably one of the greatest advancements in modern medicine. Subunit vaccines comprise the majority of current preparations and consist of two main components—antigen and adjuvant. The antigen is a small molecule against which the vaccine induces an immune response to provide protection via the immunostimulatory ability of the adjuvant. Our laboratory has investigated the adjuvant properties of Toll-like receptor (TLR) ligand-based adjuvants, especially the outer membrane protein from *Neisseria mengingitidis*, PorB. In this current study we used PorB, along with CpG, an intracellular TLR9 agonist, and a non-TLR adjuvant, aluminum salts (Alum), to further investigate cellular mechanisms of adjuvanticity, focusing on the fate of intact antigen in the germinal center and association with follicular dendritic cells (FDCs). FDCs are located in the B cell light zone of the germinal center and are imperative for affinity maturation. They are stromal cells that retain whole intact antigen allowing recognition by the B cell receptor of the germinal center B cells. Our studies demonstrate that TLR ligands, but not Alum, increase the FDC network, while PorB and Alum increased colocalization of FDC and the model soluble antigen, ovalbumin (OVA). As PorB is the only adjuvant tested that induces both a higher number of FDCs and increased deposition of antigen on FDCs, it has the greatest ability to increase FDC-antigen interaction, essential for induction of B cell affinity maturation. These studies demonstrate a further mechanism and potential superiority of PorB as an adjuvant and its influence on antibody production.

Keywords: adjuvants, TLR-ligand based adjuvants, PorB, neisseria, TLR2, follicular dendritic cells, dendritic cells, antigen deposition

INTRODUCTION

Vaccines are one of the most significant advancements in modern medicine (1–5). Utilizing vaccines, smallpox has been eradicated and measles infection rate dropped by 80% from 2000 to 2017 (6). Yet there are still infectious diseases where the empirical methods have failed to produce a successful vaccine (7–10). In order to produce more effective vaccines, researchers have developed subunit vaccines, which consist of two main components—antigen and adjuvant (11–14). The antigen is a small molecule against which a protective response can be induced, but only with the addition of the adjuvant, which provides immunostimulation to induce this response (15–17). Antigen alone is usually unable to sufficiently provide protection therefore the addition of adjuvants has become critical. Adjuvants were described by Charles Janeway as the immunologist "dirty little secret" which defined pathogen associated molecular patterns (PAMPs) from microbial origins (18). PAMPS are recognized as "non-self" molecules by pattern recognition receptors (PRRs) on innate immune cells (19). There are multiple families of PRRs including membrane-bound receptors and cytoplasmic receptors. One subclass of PRRs are Toll-like receptors (TLRs). TLRs can be extracellularly located or within endosomes (20–22). TLR engagement activates downstream intracellular signaling cascades and induce cellular activation, activation marker expression and cytokine and chemokine production (19, 23–32). These characteristics account for the fact that many TLR-ligands are effective vaccine adjuvants (21, 33–38). Investigators can select certain TLR-ligand based adjuvants to examine specific cellular pathways within the immune system and draw conclusions based on protection and adaptive immune responses (36, 39–43).

Our laboratory has investigated the adjuvant properties of the major outer membrane protein from *Neisseria mengingitidis*, PorB. PorB is a TLR2/1 ligand, and is able to significantly increase co-stimulatory ligand expression and cytokine production in antigen presenting cells (APC) (44). In addition, PorB can increase antigen loaded APC trafficking to the lymph node (45), induce germinal center formation (46), and enhance antigen specific antibody production, $CD4^+$ T cell activation (47), and cross presentation allowing for $CD8^+$ T cell activation (45). We have mainly used subcutaneous immunizations for these studies; however, the effect of adjuvants of the microenvironment of the draining lymph nodes from these injections has not be extensively investigated. In the current studies, utilizing fluorochrome labeled antigen, we investigated the fate of intact antigen in the draining lymph nodes 24 h post-immunization in mice and whether adjuvants influence this process. In addition to PorB, we have also examined the effect of CpG, a TLR-9 agonist used as an intracellular TLR-ligand based adjuvant, and a non-TLR adjuvant, aluminum salts (Alum). Both of these adjuvants have been shown to increase cytokine expression in innate immune cells (48), and increase antigen specific antibodies (49). To date, the exact cellular interaction from immune cells to illicit a protective response after vaccination including adjuvants have not been fully described.

Multiple cellular interactions are needed to induce a protective antibody response. One critical initial step is antigen reaching the lymph node, either by trafficking as processed antigen in dendritic cells (DCs) or as free intact antigen from the lymphatic vessels. DCs are the primary APC during vaccine induced immune responses, taking up antigen at the immunization site, processing such antigen while trafficking to the secondary lymphoid organs (SLO) (50). The antigen containing DCs are needed to stimulate T follicular helper cells (Tfh), which can then further enhance antigen specific B cell activation during the germinal center response (51). Free intact antigen exits lymphatic drainage via subcapsular marginal zone macrophages and are eventually deposited on follicular dendritic cells (FDCs), likely by a non-cognate B, though this is unclear (52). FDCs are stromal cells within the lymph nodes and spleen which are located in the B cell light zone of the germinal center and are vital for induction of B cell somatic hypermutation and antibody (Ab) affinity maturation. They could also be involved with B cell differentiation into memory B cells or long-lived plasma cells (53). FDCs recycle antigen and antigen-antibody complex (known as immune complexes, IC) to the cell surface via actin-requiring processes (54) without proteolytically processing the antigen. Once the B cell receptor is engaged with the native antigen on the FDC, cytokines and chemokines are secreted for induction of B cell survival, allowing for: (1) exiting of the germinal center completely if high affinity interactions with intact antigen occur, (2) re-entering the B cell dark zone of the germinal center if moderate affinity to intact antigen occurs, for further activation by antigen specific Tfhs along with induction of somatic hypermutation, or (3) apoptosis if they have low affinity for their antigen (55). To date, very few studies have investigated how adjuvants influence this process, especially in regards to antigen association with FDCs (56, 57).

The studies presented here were designed to determine the effect of adjuvants on the initial steps involved in induction of B cell activation in the germinal center, which would subsequently lead to induction of high affinity antibodies. We examined the effect of adjuvants on the level of intact antigen present in the lymph node, deposition of this antigen on FDCs and the overall quality of the FDC network. These studies highlight the manner by which adjuvants, especially PorB, may influence desired vaccine antigen interaction with cells in the germinal center to influence antibody production essential for vaccine efficacy. We have published multiple papers describing PorB's adjuvant characteristic which resulted in higher antigen specific antibody levels as well as more diverse antigen specific subtypes than other adjuvants tested (44, 46) which substantiates our approach taken in these studies.

METHODS

Animals

Four to eight-week-old female and male C57Bl/6J (referred to as "wild type," stock #000664) mice were obtained from Jackson Laboratories (Bar Harbor, ME). All mice were maintained within the Laboratory Animals Science Center (LASC) at Boston University School of Medicine. The Boston University

Institutional Animal Care and Use Committee (IACUC) approved all research conducted using animal models (protocol number 201800024). All experiments involving the mice were performed in accordance within the relevant guidelines and regulations as defined by our IACUC.

Murine Immunizations

Groups of mice received one of the following immunization preparations: ovalbumin (OVA) fluorescently labeled with Alexa 594 (OVA-A594) alone (Life technologies), OVA-A594 + PorB, OVA-A594 + CpG (Invitrogen, Cat#ODN1826), or OVA-A594 + Alum (Aluminum hydroxide, Sigma, Cat#A8222). OVA was used at 10 μg per mouse, PorB and CpG at 10 μg per mouse and Alum at 200 μg per mouse based on previous publications (44, 46). An initial kinetic study using OVA-A594 given alone or with PorB, as above, was performed to determine the optimal time point for lymph node isolation to examine effects of adjuvants on antigen deposition on FDCs (**Supplemental Figure 1A**). All mice were injected subcutaneously near the base of the tail. Draining lymph nodes were isolated after euthanasia 24, 48, or 72 h after immunization (69). The nodes were embedded in optimal cutting temperature (OCT) medium (Richard Allan Scientific, Kalamazoo, MI, USA) in molds and used for immunohistochemistry.

Immunohistochemistry

Draining iliac and inguinal lymph nodes were isolated 24 h after immunization (46) and put into molds containing OCT medium and frozen on dry ice. Tissues were sectioned on a Microm HM 550 (Microm International GmBH, Germany). Eight micrometer sections were obtained and placed on Colorfrost Plus slides and stored at −80°C until staining. Sections were air dried for 15 min at room temperature, fixed in acetone at −20°C for 10 min, and air dried for 10 min. Sections were re-hydrated in TBS buffer with 0.05% Tween-20 (TBS-T) then blocked for 1 h at room temperature with TBS-T with 5% BSA. Sections were rinsed with PBS and then stained with conjugated (CD11c, Biolegend, Cat#117309) and primary (FDC-M1, BD Biosciences, Cat#551320) antibodies overnight at 4°C followed by three rinses with PBS. Secondary antibody (anti-rat 488, Biolegend, Cat#405418) was added to the slides for 1 h at room temperature followed by three washed in PBS. Antibody concentration for the primary was 1:100. Conjugated and secondary was used at 1:200 dilution. Stained sections were mounted in Fluoroshield mounting medium with DAPI (Abcam), dried overnight, and sealed with clear nail polish. A Leica SP5 confocal microscope (Leica AG) was used to examine the sections using the Leica LAS AF software using the 10x (HC PL FLUORTAR 10.0X0.3 Dry) and 63x oil immersion objectives. All images were captured with 4 lines average at 200 Hz. The images were arranged and analyzed using FIJI/ImageJ (NIH).

Image Analysis

After images were obtained from the Lecia SP5 and imported into FIJI/ImageJ (NIH). The background was subtracted for each image separately using a rolling ball radius of 20.0 pixels. Mean fluorescence intensity (MFI) was determined using the ImageJ and the measurement tool. Colocalization between DCs or FDCs and OVA was determined using the JaCoP plugin in ImageJ calculating the Pearson Colocalization Coefficient (**Supplemental Figures 1B,C**). To determine the MFI of OVA associated with DCs and FDCs, Mander's correlation coefficient was determined from the JaCoP plugin as a percentage of OVA (58) (**Supplemental Figure 2**) and then multiplied by the total MFI of OVA within the lymph node.

Flow Cytometry of Follicular Dendritic Cells and Dendritic Cells

Single cell suspensions were created from inguinal lymph nodes 24 h post injection. Briefly, lymph nodes were placed in cold PBS and were manually minced on a petri dish with a scalpel. The samples were transferred to a 24-well plate (Fisher Scientific, Cat #08-772-1H), incubated with DMEM containing 2% FBS (ThermoFisher, Cat#26140079), 33.3 mg/ml collagenase type IV (ThermoFisher, Cat#17104019), and 2,500 U/mL DNase I (ThermoFisher, Cat#18047019). Samples were incubated for 1 h at 37°C. After which, the samples were strained through 70 μm filter. Cells were incubated with a live/dead stain (Biolegend, Cat#423105) for 30 min, in the dark at 4°C. Cells were then washed with 5x FACS Buffer (PBS, 0.5%BSA, and 2% EDTA) and spun down. Cells were then incubated with CD16/CD32 Fc block (eBioscience, 48-0032-82) for 10 min in the dark at room temperature. Cells were then plated in a 96 V-well bottom plate (Corning, CLS3896-48EA) and stained. All dilutions were 1:200. Antibodies included: CD19-BUV395 (BD Horizon, 563557), CD3—eFlour (Invitrogen, 48-0032-82), CD11c—APC (BD Pharmigen, 550261). Cells were the analyzed on an LSRII. The gating strategy is shown in **Supplemental Figures 3A,B**. Animals were vaccinated with OVA lacking the Alexa594 fluorochrome as negative controls as shown in **Supplemental Figure 3C**. Single cell suspensions for FDCs were performed similarly. The samples were strained through 70 μm filter, although not pushed through to ensure the integrity of the FDCs remained intact. Samples were then stained for live/dead, Fc block, and conjugated antibodies. All antibody dilutions were 1:200 unless otherwise noted. CD21/CD35—BV421, CD45—APC, CD19—BUV395 (1:400), ICAM-1—FITC. Gating strategy is shown in **Supplemental Figure 4A**. A fluorescence minus one (FMO) was stained for all colors within the panel excluding CD21/CD35 shown in **Supplemental Figure 4B**. All samples were analyzed on an LSRII, a machine available within the Boston University flow core, on a low flow setting.

Statistics

Statistics were calculated in GraphPad Prism (version 8.0). Pearson Correlation Coefficients were analyzed as described above. ANOVA with Sidak's multiple comparisons test was used for all other analysis. ns, not significant, $^{*}p < 0.05$, $^{**}p < 0.01$, $^{***}p < 0.001$, $^{****}p < 0.0001$

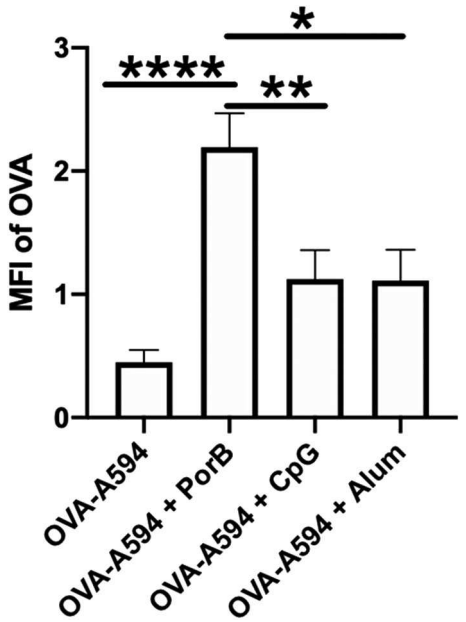

FIGURE 1 | PorB increases antigen presence in draining lymph node. Mean fluorescent intensity (MFI) of antigen (OVA) in draining lymph nodes 24 h post vaccination of either OVA-A594, OVA-A594 + PorB, OVA-A594 + CpG, or OVA-A594 + Alum. MFI of OVA was quantified by the ImageJ measurement tool after the subtraction of the background. Representative of three experiments. $n = 5–7$, $^{*}p < 0.05$, $^{**}p < 0.01$, $^{****}p < 0.001$.

RESULTS

Mean Fluorescence Intensity of OVA Increased With PorB Injections

At first, we needed to confirm that adjuvants could influence the presence of intact antigen in the SLO. This outcome is essential because antigen presence within the lymph node is a primary factor contributing to the establishment of an adaptive immune response. The groups we analyzed consisted of mice immunized with OVA labeled with Alexa594 (OVA-A594), OVA-A594 + PorB, OVA-A594 + CpG, and OVA-A594 + Alum. To determine whether adjuvants influenced antigen presence within the lymph nodes of the animals in this study, the average MFI of OVA in the draining lymph nodes was calculated from immunohistochemistry (IHC) images (**Figure 1**). Interestingly, only PorB appeared to increase the amount of labeled OVA within the lymph nodes. This increase was significant over other adjuvants used in these studies.

Follicular Dendritic Cell Networks Are Increased by TLR-Ligand Based Adjuvants

To determine if the adjuvants directly affected the quality of the FDC networks, we performed immunofluorescent staining on draining lymph nodes from immunized mice using primary antibody FDC-M1, which is the common marker for FDCs, and an Alexa 488 secondary antibody. This study included mice immunized with four different preparation as previously described: OVA-A594, OVA-A594 + PorB, OVA-A594 + CpG, and OVA-A594 + Alum. Samples were analyzed by ImageJ to calculate the MFI values for FDC-M1. **Figure 2A** displays representative images of FDC-M1 labeling in draining lymph nodes 24 h post immunization as a heat map, where white indicates the highest signal to pixel ratio and blue shows the lowest signal to pixel ratio. Lymph node FDC-M1 labeling was low in mice immunized with OVA alone or Alum + OVA. However, it was greatly increased when TLR-ligand based adjuvants (PorB and CpG) were used as shown in both **Figures 2A,B**.

To confirm these results, flow cytometry was utilized to quantify FDC numbers in the draining lymph nodes. The gating strategy is shown in **Supplemental Figure 4A**. FDCs were defined as $CD19^{-}CD45^{-}Cr1/Cr2^{+}ICAM\text{-}1^{+}$. Fluorescence minus one (FMO) was used to ensure the cells isolated were $Cr1/Cr2^{+}$ (**Supplemental Figure 4B**). As shown in **Figures 2C,D**, the flow cytometry data matched the IHC data both in frequency and cell counts of FDC. Animals vaccinated with PorB or CpG with OVA-A594 demonstrated a significant increase in FDC numbers in the draining lymph nodes as compared to the use of Alum + OVA-A594 or OVA-A594 alone. To further confirm that the increase in FDCs were not just due to measuring an increase in expression of activation markers intercellular adhesion molecule 1 (ICAM1) or complement receptors 1 and 2 (CR1/2), mean fluorescent intensity was calculated via FlowJo. As shown in **Figure 2** *Immunology* E and F, no significant differences were measured for ICAM1 or CR1/2. These results, in addition to the IHC measurements, led us to concluded that TLR-ligand based adjuvants, PorB and CpG, significantly increased FDC numbers within the germinal centers of draining lymph node 24 h post subcutaneous injection.

Antigen Deposition on Follicular Dendritic Cells Is Increased With PorB and Alum

As antigen deposition on FDCs is important and more biologically relevant than FDC numbers, the ability of adjuvants to influence antigen deposition onto FDCs was examined. Draining lymph nodes from immunized mice described above were examined by immunofluorescence microscopy to determine colocalization of labeled OVA with FDCs. As displayed in **Figure 3A,** non-adjuvanted OVA-A594 was minimally present in the lymph node 24 h post-immunization. When adjuvants were included, OVA-A594 was detectable within the lymph node, regardless of the adjuvant administered. Lymph nodes from mice given OVA-A594 + PorB had the most OVA present. Lymph nodes from mice given OVA-A594 + PorB or OVA-A594 + Alum had multiple areas of colocalization of OVA with FDC (shown by yellow arrows). There appeared to be less colocalization when CpG was used. JaCoP was used to quantify colocalization between OVA and FDC signal in each tissue section, as previously performed in our lab (45). The Pearson Correlation coefficient from JaCoP confirmed significant increases of colocalization in the lymph nodes from mice given OVA-A594 + PorB and OVA-A594 + Alum as compared to lymph nodes from mice given OVA-A594 alone (**Figure 3B**).

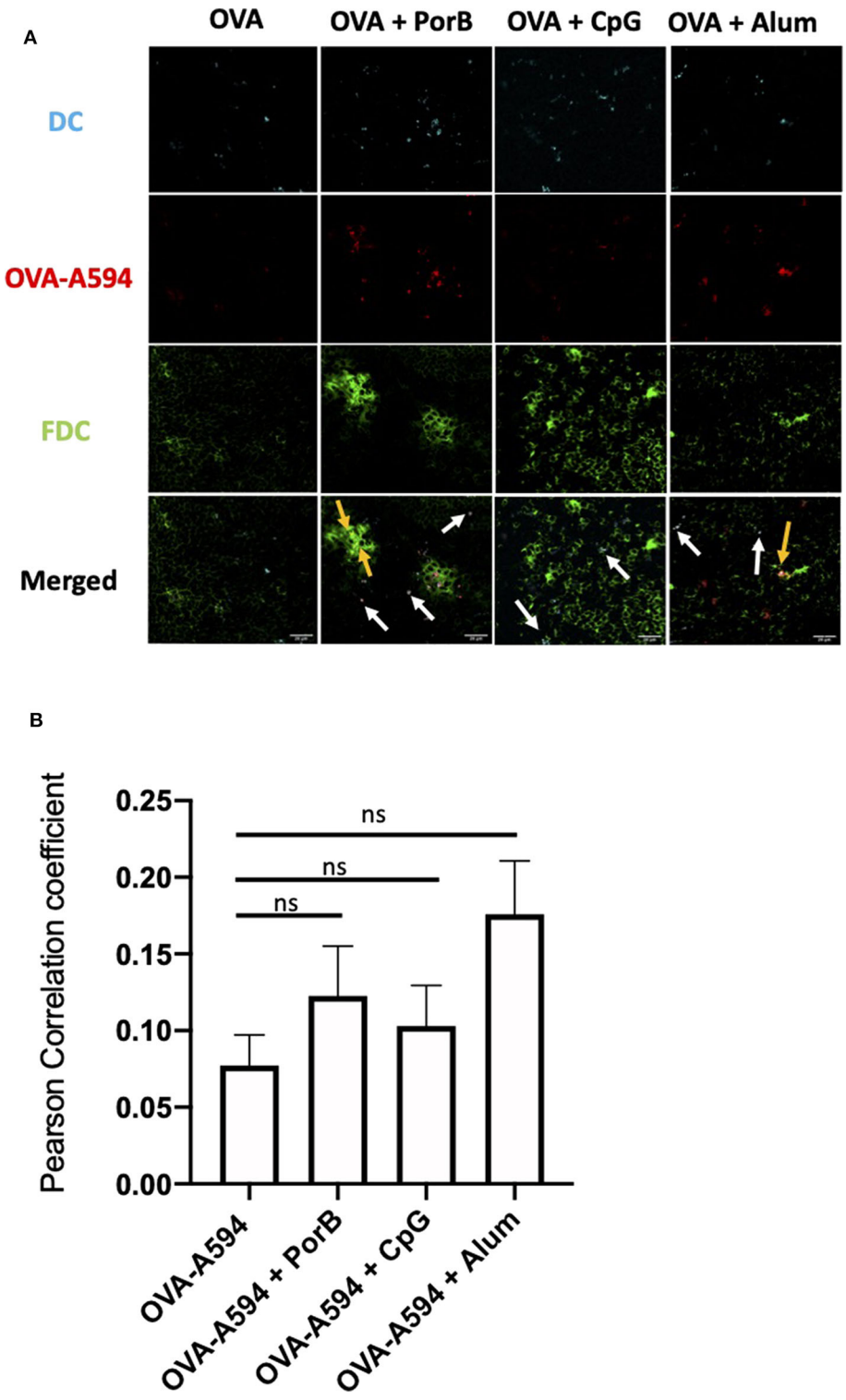

FIGURE 2 | Evaluation of the effect of Adjuvants on FDC Networks. **(A)** Representative images for FDC expression in draining lymph nodes 24 h post subcutaneous injections of either OVA-A594, OVA-A594 + PorB, OVA-A594 + CpG, or OVA-A594 + Alum. FDC expression is shown as a heat map where white indicates the highest signal to pixel ratio and blue sows the lowest signal to pixel ratio. Scale bar is 100 μM. One of 3 representative experiments is shown. **(B)** Mean fluorescence intensity (MFI) quantification from ImageJ of FDC networks in draining lymph nodes 24 h post injection of either OVA-A594, OVA-A594 + PorB, OVA-A594 + CpG, or

(Continued)

FIGURE 2 | OVA-A594 + Alum. Multiple FDC networks were measured within individual lymph nodes. $n = 9$/group. $^{*}p < 0.05$, $^{***}p < 0.001$ **(C)** Frequency of FDC in draining lymph nodes 24 h post subcutaneous injections with OVA-A594 ± adjuvants. Gating strategy is shown in **Supplemental Figure 4**. **(D)** Cell counts of FDC in draining lymph nodes 24 h post subcutaneous injections with OVA-A594 ± adjuvants. **(E)** MFI of intercellular adhesion molecule 1 (ICAM-1) from FDC gate in draining lymph nodes 24 h post subcutaneous injections with OVA-A594 ± adjuvants. **(F)** MFI of complement receptors 1 and 2 (CR1/2) from FDC gate in draining lymph nodes 24 h post subcutaneous injections with OVA-A594 ± adjuvants. $n = 9$ per group $^{*}p < 0.05$, $^{**}p < 0.01$; ns, not significant.

FDC Colocalization Is Independent of Antigen Loaded Dendritic Cells

To ensure the OVA correlation with FDCs was not due to concomitant presence antigen loaded DCs, we first examined draining lymph nodes by IHC for DCs (as labeled by anti-CD11c fluorochrome labeled Ab) along with the FDCs staining to determine if the two colocalized. **Figure 4A** demonstrates that a majority of the OVA colocalized with either DCs or FDCs in all treatment groups. The white arrows emphasize areas of colocalization between DCs and OVA, whereas the yellow arrow illustrates FDCs colocalization with OVA. JaCoP was used to determine whether OVA colocalization with FDCs vs. DCs were uniquely and separate. As shown in **Figure 4B**, the Pearson Correlation coefficient was not significant for any of the adjuvants tested for induction of direct association between DCs and FDCs. These data emphasize that the OVA deposition on FDCs is increased with adjuvants when compared to OVA alone and, in general, is independent of $CD11c^{+}$ DCs trafficking OVA within the lymph node.

PorB Significantly Increases OVA Association With FDCs and DCs as Compared to CpG or Alum

We next determined how the increase of antigen within the SLO was distributed between antigen loaded DCs, antigen deposition onto FDC, or unassociated with either of these cell types. Mander's correlation coefficients (JaCop within ImageJ) were used to determine the percentage of OVA that was associated with either DCs, FDCs, or neither. This correlation coefficient allows for spilt channels of correlation to be determined (58). The percentages of OVA correlated with either DCs or FDCs were then multiplied by the MFI of OVA (**Figure 1**) to determine the MFI of OVA associated with DCs, FDCs, or neither. All adjuvants had a significant increase in MFI of OVA associated with DCs, but PorB's increase was significantly greater than the other adjuvants tested (**Figure 5A**), which is consistent with our previous data (45). OVA association with FDCs was also significantly increased when PorB was used, as compared to the other adjuvants (**Figure 5B**). Lastly, levels of "unassociated OVA," which we defined as the remaining percentage of OVA that was not associated with either DCs or FDCs (Unassociated OVA = 1-[Mander's coefficient for OVA/DC + Mander's coefficient for OVA/FDC]) was determined. **Figure 5C** shows that OVA-A594 + PorB had the only significant decrease in unassociated OVA. Interestingly, OVA-A594 + CpG had a significant increase in unassociated OVA. These data emphasize that the PorB, as an adjuvant, induced a significant increase in antigen associated with both DCs and FDCs when compared to other adjuvants.

Dendritic Cells Numbers in Draining Lymph Node Were Increased With the Use of Adjuvants

DCs are a critical APC for the adaptive immune responses. To determine if adjuvants influence the number of DCs present in within draining lymph nodes after immunization, single cell suspensions of these lymph nodes were obtained 24 h post injection with OVA-A594, OVA-A594 + PorB, OVA-A594 + CpG, or OVA-A594 + Alum. We have previously examined this parameter for PorB (45) but have never compared this to other adjuvants, the gating strategy is shown in **Supplemental Figure 3A**. Our analysis showed a significant increase in cell count with PorB adjuvanted vaccines as well as a significant increase in DCs within the draining lymph node (**Figures 6A,B**). Interestingly, and supporting our previous work, PorB vaccinations showed a significant increase in antigen loaded DCs 24 h post subcutaneous injections (**Figure 6C**).

,

DISCUSSION

In order to understand the influence of different adjuvants on multiple immune response related pathways within the lymph node, we utilized the following vaccine adjuvants: PorB, a TLR1/2 ligand-based adjuvant, well-studied in our lab (59), along with CpG, a TLR9 agonist that has been previously used as an adjuvant, and Alum, a TLR-independent adjuvant. PorB, CpG and Alum have all been shown to increase antigen-specific antibody responses by our group and (46, 60–65). OVA-A594 was used as our model antigen based on previous studies in our laboratory as, on its own, does not induce innate immune activation or adaptive immune responses. Moreover, previous studies utilized tools and reagents unique for OVA, including defined T cell epitopes, MHC tetramers and TCR transgenic mice that recognize these epitopes (45, 46). Initially, we demonstrated that PorB was able to significantly increase the presence of OVA within the draining lymph nodes 24 h post subcutaneous immunization as compared to CpG or Alum (**Figure 1**). The specificity of the adaptive immune response is dependent on the presence of intact antigen on FDCs in the lymph node and processed antigen trafficked by DCs to the lymph node (54).

FDCs are critical for antibody production by providing intact antigen to B cell receptors (BCR) (55, 66). Depending on the affinity of the BCR, the B cell will either leave the germinal center, return to the dark zone for further somatic hypermutation, or become apoptotic based on cytokine expression from the FDCs (55). Here-in we investigated how adjuvants may affect these cells, especially in regards to antigen deposition. We demonstrated that TLR-ligand based adjuvants, PorB and CpG,

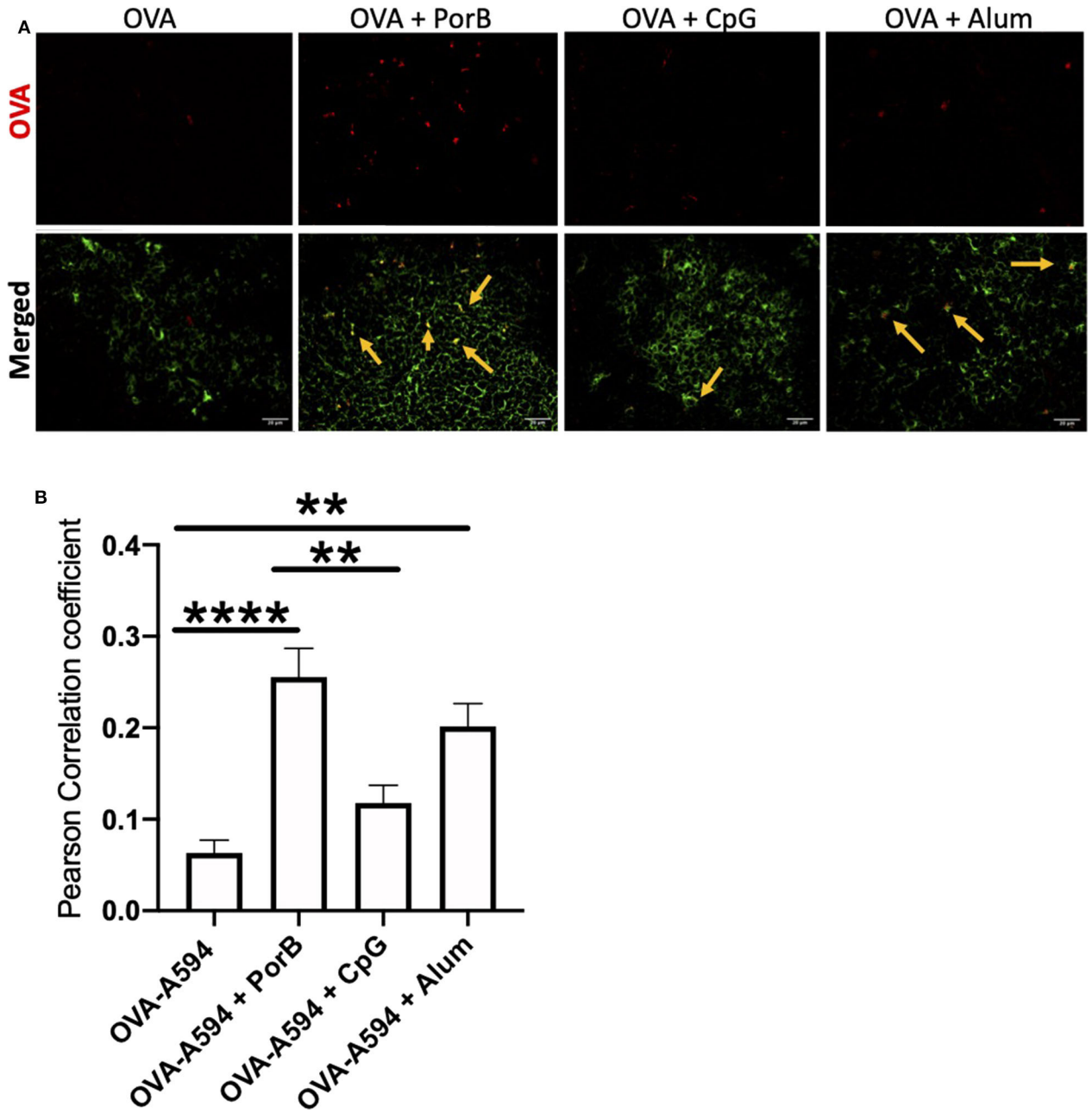

FIGURE 3 | Adjuvants effect colocalization of antigen onto FDCs. **(A)** Representative IHC images from draining lymph nodes from B6 control mice 24 h post subcutaneous injections. FDCs are shown in green. OVA-594, used as a non-immunogenic antigen, is shown in red. Areas of colocalization are shown with yellow arrows. Scale bar represents 20 μM. One out of 3 representative experiments is shown. Images were taken at 63x objective using a Leica SP5 microscope. **(B)** Quantification of Colocalization of fluorescently labeled OVA-A594 with FDCs within draining lymph nodes 24 h post subcutaneous injections. Colocalization was assessed using Pearson Correlation coefficients calculated with JaCoP plugin in ImageJ after background subtraction. $n = 9–12$, $^{**}p < 0.01$, $^{****}p < 0.001$.

both significantly increased the FDC network 24 h after a subcutaneous immunization by both confocal microscopic and flow cytometric analyses without significant increases in overall MFI of either ICAM-1 or CR1/2 within the FDC gating strategy (**Figure 2**). FDCs are stromal cells within the lymph node (67, 68); the increase is likely due to an overall increase in cellularity induced by the adjuvants (45). An increase in FDCs would allow for more surface area onto which more intact antigen can be deposited during the initiation of the adaptive immune response. This could lead to greater interaction with B cells and increased B cell receptor specificity by allowing for more B cells to come in contact with the deposited antigen, and increasing the kinetics of developing high affinity BCRs and antibodies. Interestingly, the use of PorB or Alum as adjuvants with OVA, significantly increased antigen deposition on the FDCs, as opposed to the use of CpG (**Figure 3**). However, Alum did not increase the

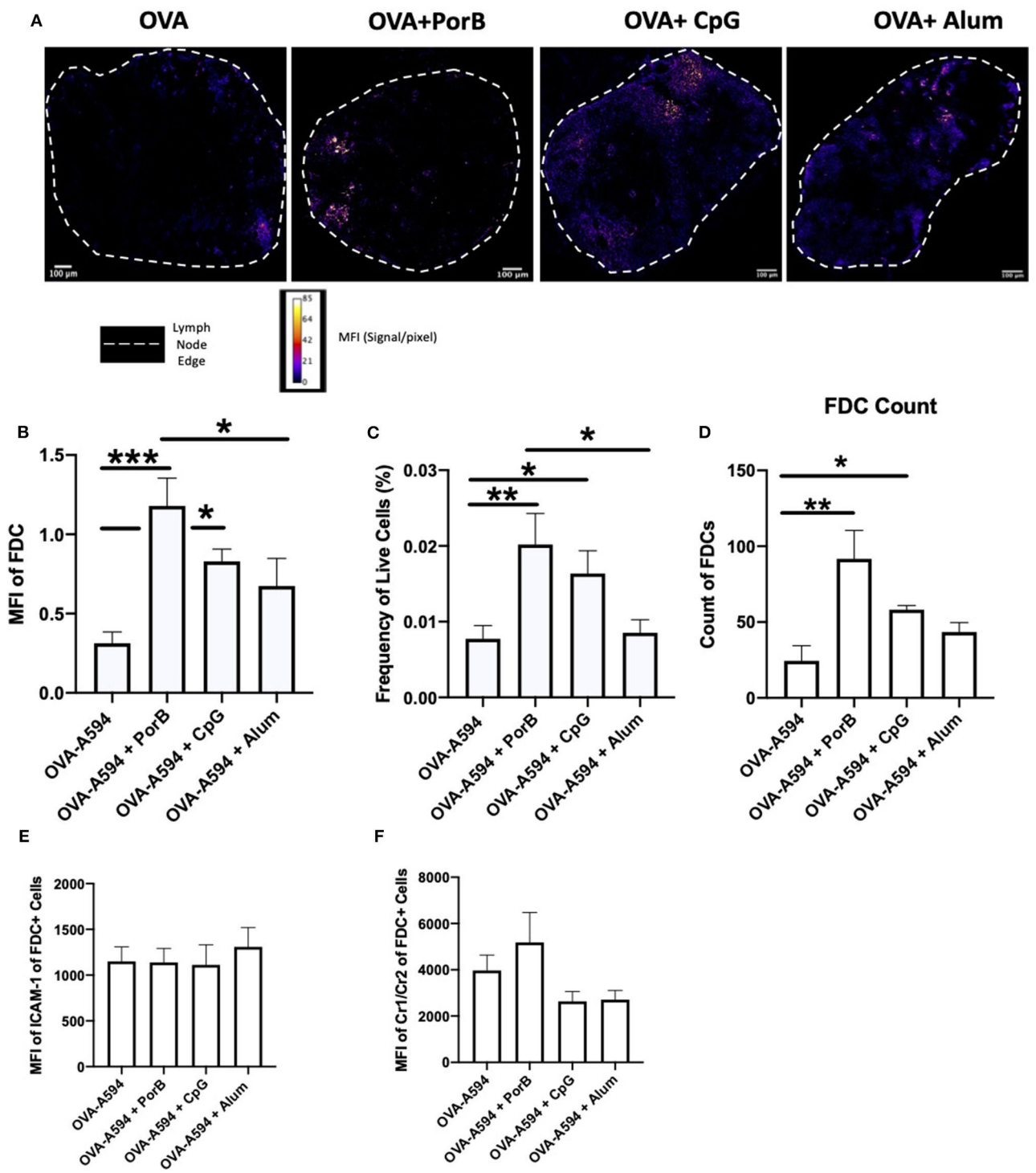

FIGURE 4 | FDC antigen deposition is independent of antigen loaded DCs. Representative IHC images of draining lymph nodes from mice 24 h post subcutaneous injections are shown in **(A)** where FDC is shown in green, OVA-594, used as a non-immunogenic antigen, is shown in red and dendritic cells (DCs, CD11c) are shown in cyan. Areas of colocalization between DC and OVA are shown with white arrows. Areas of colocalization between FDC and OVA are shown with yellow arrows.

(Continued)

FIGURE 4 | Images were taken at 63x objective using a Leica SP5 microscope. One out of 2 representative experiments is shown. **(B)** Pearson's correlation coefficient between FDC and DC (CD11c) in draining lymph nodes 24 h post subcutaneous injections. Colocalization was assessed using Pearson Correlation coefficients calculated with JaCoP plugin in ImageJ after subtracting the background and using an unsharp mask filter. $n = 7$/group. **(C)** Frequency of live FDCs from the draining lymph node 24 h after injections quantified by flow cytometry. **(D)** FDC count from the draining lymph node 24 h after injections quantified by flow cytometry. **(E)** MFI of ICAM-1 within the FDC+ gating strategy from the draining lymph node 24 h after injections. **(F)** MFI of Cr1/Cr2 within the FDC+ gating strategy from the draining lymph node 24 h after injections. $^{*}p < 0.05$, $^{**}p < 0.01$, $^{***}p < 0.0001$.

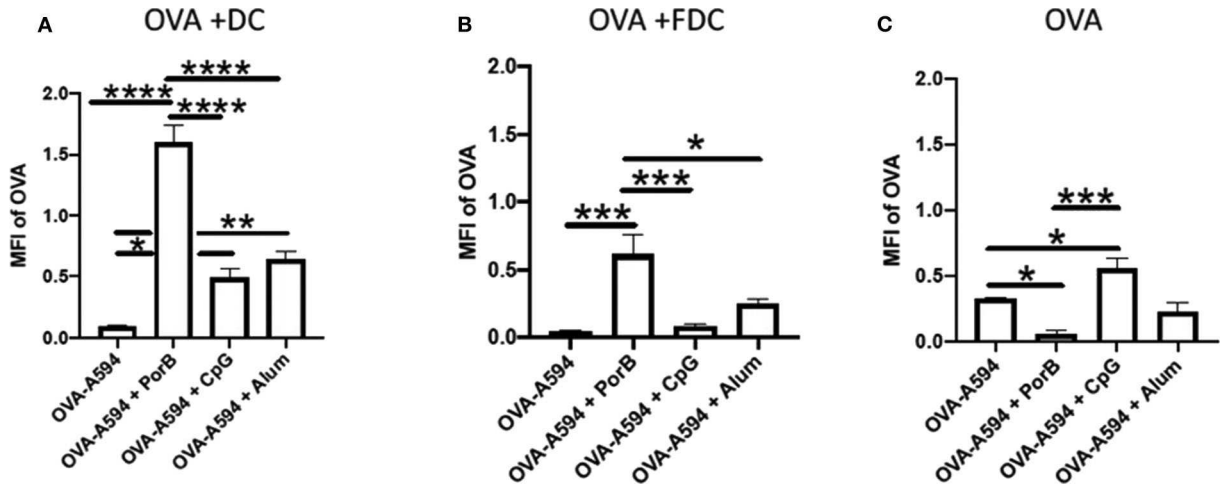

FIGURE 5 | OVA-A594 distribution between DC, FDC, and unassociated OVA within draining lymph node 24 h post subcutaneous injection. MFI of OVA associated with DC **(A)**, FDC **(B)**, or unassociated OVA **(C)** was assessed using the JaCoP plugin within ImageJ and determining the Mander's correlation coefficient after subtracting the background. The correlation coefficient is the percentage of DCs or FDCs associated with OVA. This percentage was then multiplied by the total MFI of OVA within the lymph node (**Figure 1**) to determine MFI of OVA associated with either DCs or FDCs. These data were assessed in draining lymph nodes 24 h post injection of either OVA-A594, OVA-A594 + PorB, OVA-A594 + CpG, or OVA-A594 + Alum. $n = 5$–7 $^{*}p < 0.05$, $^{**}p < 0.01$, $^{***}p < 0.001$, $^{****}p < 0.0001$.

number of FDCs overall; PorB was the only adjuvant studied that both increased FDC number and intact antigen deposition. Other studies have focused on passive immune complex (IC) injections to show deposition onto FDCs (52). While these passive studies are important, antigen still needs to be deposited on the FDCs to allow for BCR interactions allowing for B cell somatic hypermutation and enhanced Ab affinity. Our studies uniquely focused on primary exposures to antigen and the deposition onto FDCs.

The effect of PorB and the other adjuvants on DC trafficking to the lymph nodes and antigen association with DCs was also analyzed. DCs are a critical APCs for the adaptive immune response (50). Usage of PorB or Alum as an adjuvant increased the numbers DCs within the draining lymph nodes (**Figure 6B**). More importantly, however, only PorB demonstrated significant increases of antigen loaded DCs in these same draining lymph nodes (**Figure 6C**) (45). The effect of PorB and other adjuvants on DC antigen uptake and trafficking to the lymph nodes is a crucial step for antigen specificity during the adaptive immune response as DCs are the primary cell to present antigen to T cells in the SLO and subsequent activation of antigen specific B cells (50).

The effect of adjuvants on OVA distribution in the lymphoid follicle and germinal center demonstrates, for the first time, the ability of PorB to more efficiently direct intact antigen toward cellular pathways directly involved in antibody production as compared to other adjuvants tested. **Figure 5** demonstrates that immunizations including PorB as an adjuvant resulted in the majority of labeled OVA MFI in the lymphoid follicle and germinal center to be associated with either FDCs or DCs (CD11c). As stated, both of these cell types are imperative for effective antibody production due to FDCs interactions with B cells and DC interactions with Tfh cells. Interestingly, PorB was also the only adjuvant to show a significant decrease in OVA MFI that was not associated with either cell type. This emphasizes that PorB has a more targeted effect toward the adaptive immune responses than other adjuvants investigated here.

Overall, these studies emphasize the role adjuvants have on specific cellular mechanisms involved in vaccine induced antibody production. For the first time, follicular dendritic cells were demonstrated to be increased in numbers by both extracellular TLR1/2 agonist, PorB, and intracellular TLR9 agonist, CpG. Of these two, only PorB also increased antigen deposition onto the FDCs. The timepoint for these analyzes were chosen to investigate early innate responses that are involved in the initiation of adaptive immune responses. Yuen and Kuniholm have recently highlighted how PorB has major influences on the immune system as part of its highly effective adjuvant effect such as increasing costimulatory molecule expression on and cytokine production in dendritic cell, s as well as increasing production antigen-specific IgG antibodies including IgG1, IgG2b, and IgG3 subtypes (59). In the studies described above, we have further shown that PorB is able to increase draining lymph node antigen levels, FDC numbers, and increase antigen deposition on these FDCs. This is certainly related to its significant ability to enhance antigen specific antibody production (44). Moreover,

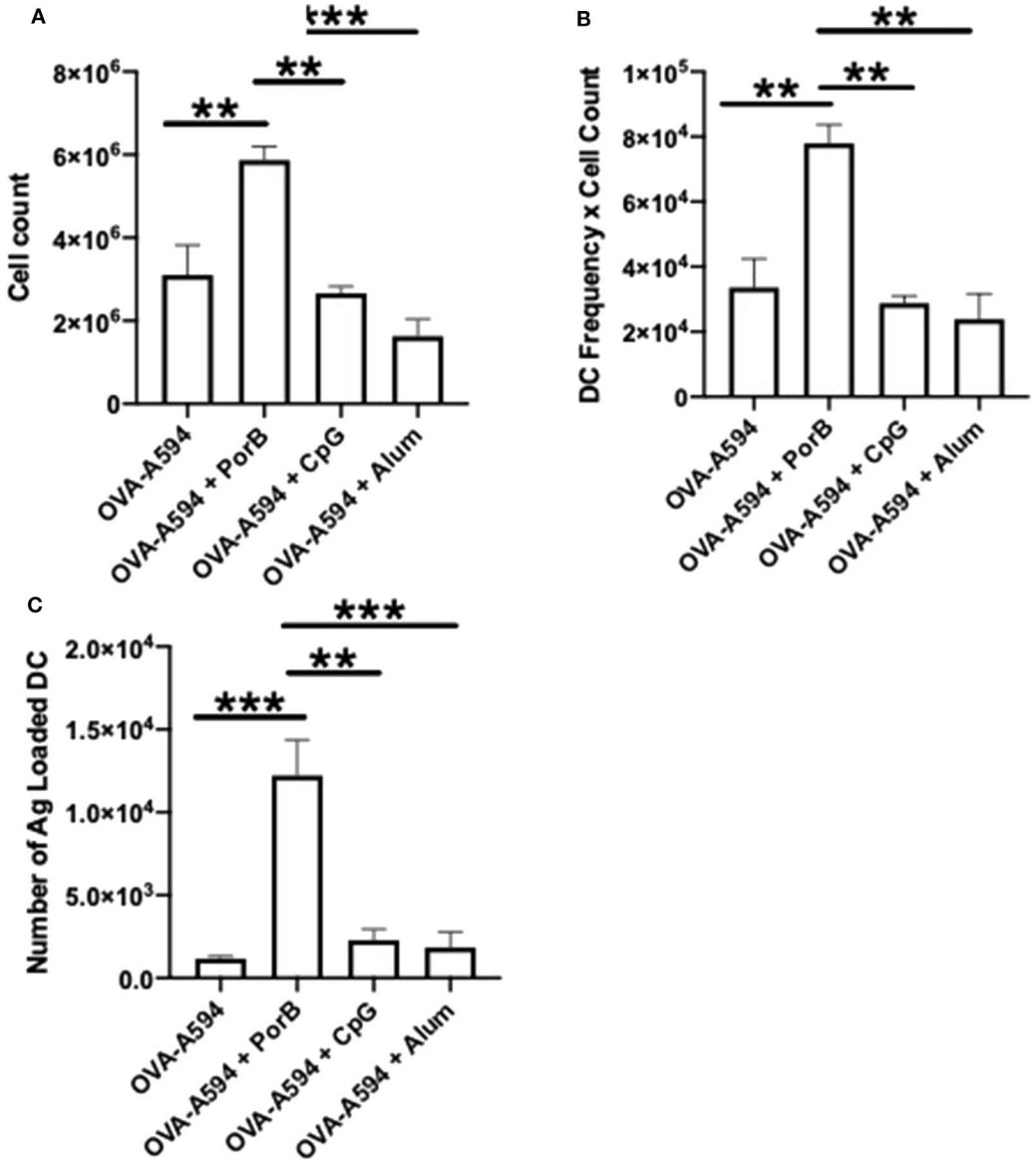

FIGURE 6 | PorB increases cell count, DCs, and antigen loaded DCs. **(A)** Single cell suspensions were used to calculate cell counts within the draining lymph node 24 h post injection of either OVA-A594, OVA-A594 + PorB, OVA-A594 + CpG, or OVA-A594 + Alum. **(B)** DCs from draining lymph nodes of animals 24 h post injection from either OVA-A594, OVA-A594 + PorB, OVA-A594 + CpG, or OVA-A594 + Alum. Gating strategy is shown in **Supplemental Figure 3A**. Statistics were calculated by ordinary one-way ANOVA with Sidak's multiple comparisons test. $^{*}p < 0.05$, $^{**}p < 0.01$ **(C)** Antigen loaded DCs from draining lymph nodes of animals 24 h post injection from either OVA-A594, OVA-A594 + PorB, OVA-A594 + CpG, or OVA-A594 + Alum. Gating strategy is shown in **Supplemental Figures 3B,C**. Statistics were calculated by ordinary one-way ANOVA with Sidak's multiple comparisons test. $n = 3$, data represents one of 3 experiments. $^{*}p < 0.05$, $^{**}p < 0.01$, $^{***}p < 0.0001$.

consistent with previous data (45), PorB increases trafficking of antigen loaded DCs to the lymph node, separate from the intact antigen deposition on the FDCs. This will allow for both increased B cell affinity maturation and increased antigen specific T cell induction and activation. Together, these data emphasize the pivotal role of adjuvants in immune processes leading to antibody production, along with evidence that PorB has characteristics that may make it a superior adjuvant as compared to others.

DATA AVAILABILITY STATEMENT

All datasets generated for this study are included in the article/**Supplementary Material**.

ETHICS STATEMENT

The animal study was reviewed and approved by Boston University IACUC.

AUTHOR CONTRIBUTIONS

The work was performed by CL, with help and advice form RY, JK, and MR and technical help from DA. All the work was planned with LW and CL. LW wrote and edited the manuscript. All authors contributed to the article and approved the submitted version.

FUNDING

These studies were funded by NIH Grant AI0404944 (LW), CL was funded by the Boston University Training Program in Inflammatory Disorders T32AI138933.

ACKNOWLEDGMENTS

We would like to thank Paola Massari and Xiuping Liu for help in purifying Neisserial PorB for the experiments conducted in this manuscript. We greatly appreciate the usage and technical assistance from the Boston University School of Medicine flow and imaging core.

SUPPLEMENTARY MATERIAL

The Supplementary Material for this article can be found online at: https://www.frontiersin.org/articles/10.3389/fimmu.2020.01254/full#supplementary-material

REFERENCES

1. Gould K. Vaccine safety: evidence-based research must prevail. *Dimens Crit Care Nurs.* (2017) 36:145–7. doi: 10.1097/DCC.0000000000000250
2. Orenstein WA, Ahmed R. Simply put: vaccination saves lives. *Proc Natl Acad Sci USA*. (2017)114:4031–3. doi: 10.1073/pnas.1704507114
3. Hinman AR, Orenstein WA, Schuchat A. Vaccine-preventable diseases, immunizations, and the epidemic intelligence service. *Am J Epidemiol.* (2011) 174:S16–22. doi: 10.1093/aje/kwr306
4. Plotkin SA. Vaccines, vaccination, and vaccinology. *J Infect Dis.* (2003) 187:1349–59. doi: 10.1086/374419
5. Andre FE, Booy R, Bock HL, Clemens L, Datta SK, John TJ, et al. Vaccination greatly reduces disease, disability, death and inequity worldwide. *Bull World Health Organ.* (2008) 86:140–6. doi: 10.2471/blt.07.040089
6. Immunization. (2019). Available online at: https://data.unicef.org/topic/child-health/immunization/
7. Kaufmann SH, Fensterle J, Hess J. The need for a novel generation of vaccines. *Immunobiology*. (1999) 201:272–82. doi: 10.1016/S0171–2985(99)80067–9
8. Taylor K, Nguyen A, Stephenne J. The need for new vaccines. *Vaccine.* (2009) 27(Suppl 6):G3–8. doi: 10.1016/j.vaccine.2009.10.014
9. Rappuoli R, Pizza M, Del Giudice G, de Gregorio E. Vaccines new opportunities for a new society. *Proc Natl Acad Sci USA*. (2014) 111:12288–93. doi: 10.1073/pnas.1402981111
10. Gutierrez AH, Spero DM, Gay C, Zimic M, de Groot AS. New vaccines needed for pathogens infecting animals and humans: one health. *Hum Vacc Immunother.* (2012) 8:971–8. doi: 10.4161/hv.20202
11. Moyle PM, Toth I. Self–adjuvanting lipopeptide vaccines. *Curr Med Chem.* (2008) 15:506–16. doi: 10.2174/092986708783503249
12. Demento SL, Siefert AL, Bandyopadhyay A, Sharp FA, Fahmy TM. Pathogen–associated molecular patterns on biomaterials: a paradigm for engineering new vaccines. *Trends Biotechnol.* (2011) 29:294–306. doi: 10.1016/j.tibtech.2011.02.004
13. Moyle PM, Toth I. Modern subunit vaccines: development, components, and research opportunities. *Chem Med Chem.* (2013) 8:360–76. doi: 10.1002/cmdc.201200487
14. Rueckert C, Guzmán CA. Vaccines: from empirical development to rational design. *PLoS Pathog.* (2012) 8:e1003001. doi: 10.1371/journal.ppat.1003001
15. Moyer TJ, Zmolek AC, Irvine DJ. Beyond antigens and adjuvants: formulating future vaccines. *J Clin Invest.* (2016) 126:799–808. doi: 10.1172/JCI81083
16. Reed SG, Orr MT, Fox CB. Key roles of adjuvants in modern vaccines. *Nat Med.* (2013) 19:1597–608. doi: 10.1038/nm.3409
17. Di Pasquale A, Preiss S, Tavares Da Silva F, Garçon N. Vaccine adjuvants: from 1920 to 2015 and beyond. *Vaccines.* (2015) 3:320–43. doi: 10.3390/vaccines3020320
18. Janeway CA Jr. Approaching the asymptote? Evolution and revolution in immunology. *Cold Spring Harb Symp Quant Biol.* (1989) 54(Pt 1):1–13.
19. Janeway CA Jr, Medzhitov R. Innate immune recognition. *Annu Rev Immunol.* (2002) 20:197–216. doi: 10.1146/annurev.immunol.20.083001.084359
20. Akira S, Uematsu S, Takeuchi O. Pathogen recognition, and innate immunity. *Cell.* (2006) 124:783–801. doi: 10.1016/j.cell.2006.02.015
21. Iwasaki A, Medzhitov R. Toll–like receptor control of the adaptive immune responses. *Nat Immunol.* (2004) 5:987–95. doi: 10.1038/ni1112
22. Averett DR, Fletcher SP, Li W, Webber SE, Appleman JR. The pharmacology of endosomal TLR agonists in viral disease. *Biochem Soc Trans.* (2007) 35:1468–72. doi: 10.1042/BST0351468
23. Chaturvedi A, Pierce SK. How location governs toll–like receptor signaling. *Traffic.* (2009) 10:621–8. doi: 10.1111/j.1600–0854.2009.00899.x
24. Kawai T, Akira S. The role of pattern–recognition receptors in innate immunity: update on Toll–like receptors. *Nat Immunol.* (2010) 11:373–84. doi: 10.1038/ni.1863
25. Kawasaki T, Kawai T. Toll–like receptor signaling pathways. *Front Immunol.* (2014) 5:461. doi: 10.3389/fimmu.2014.00461
26. Napolitani G, Rinaldi A, Bertoni F, Sallusto F, Lanzavecchia A. Selected Toll–like receptor agonist combinations synergistically trigger a T helper type 1–polarizing program in dendritic cells. *Nat Immunol.* (2005) 6:769–76. doi: 10.1038/ni1223
27. Zhu Q, Egelston C, Vivekanandhan A, Uematsu S, Akira S, Klinman DM, et al. Toll-like receptor ligands synergize through distinct dendritic cell pathways to induce T cell responses: implications for vaccines. *Proc Natl Acad Sci USA*. (2008) 105:16260–5. doi: 10.1073/pnas.0805325105
28. Tross D, Petrenko L, Klaschik S, Zhu Q, Klinman DM. Global changes in gene expression and synergistic interactions induced by TLR9 and TLR3. *Mol Immunol.* (2009) 46:2557–64. doi: 10.1016/j.molimm.2009.05.011
29. Liu Q, Ding JL. The molecular mechanisms of TLR–signaling cooperation in cytokine regulation. *Immunol Cell Biol.* (2016) 94:538–42. doi: 10.1038/icb.2016.18
30. Medzhitov R. Recognition of microorganisms and activation of the immune response. *Nature.* (2007) 449:819–26. doi: 10.1038/nature06246
31. Beutler BA. TLRs and innate immunity. *Blood*. (2009) 113:1399–407. doi: 10.1182/blood-2008-07-019307
32. Gibson SJ, Lindh JM, Riter TR, Gleason MR, Rogers LM, Fuller AE, et al. Plasmacytoid dendritic cells produce cytokines and mature in response to the TLR7 agonists, imiquimod and resiquimod. *Cell Immunol.* (2002) 218:74–86. doi: 10.1016/s0008–8749(02)00517–8
33. Steere AC, Sikand VK, Meurice F, Parenti DL, Fikrig E, Schoen RL, et al. Vaccination against Lyme disease with recombinant Borrelia burgdorferi outer–surface lipoprotein a with adjuvant. Lyme Disease Vaccine Study Group. *N Engl J Med.* (1998) 339:209–15. doi: 10.1056/NEJM199807233390401
34. Beran J, De Clercq N, Dieussaert I, van Hoecke C. Reactogenicity and immunogenicity of a Lyme disease vaccine in children 2-5 years old. *Clin Infect Dis.* (2000) 31:1504–7. doi: 10.1086/317479
35. Durier C, Launay O, Meiffrédy V, Saïdi Y, Salmon D, Lévy Y, et al. Clinical safety of HIV lipopeptides used as vaccines in healthy volunteers and HIV-infected adults. *AIDS.* (2006) 20:1039–49. doi: 10.1097/01.aids.0000222077.68243.22

36. Pulko V, Liu X, Krco CJ, Harris KJ, Frigola X, Kwon ED, et al. TLR3-stimulated dendritic cells up-regulate B7-H1 expression and influence the magnitude of CD8 T cell responses to tumor vaccination. *J Immunol.* (2009) 183:3634–41. doi: 10.4049/jimmunol.0900974
37. Tomai MA, Solem LE, Johnson AG, Ribi E. The adjuvant properties of a nontoxic monophosphoryl lipid A in hyporesponsive and aging mice. *J Biol Response Mod.* (1987) 6:99–107.
38. Johnson AG, Tomai M, Solem L, Beck L, Ribi E. Characterization of a nontoxic monophosphoryl lipid A. *Rev Infect Dis.* (1987) 9(Suppl. 5):S512–6. doi: 10.1093/clinids/9.supplement_5.s512
39. Rharbaoui F, Drabner B, Borsutzky S, Winckler U, Morr M, Ensoli B, et al. The mycoplasma-derived lipopeptide MALP-2 is a potent mucosal adjuvant. *Eur J Immunol.* (2002) 32:2857–65. doi: 10.1002/1521–4141(2002010)32:10<2857::AID–IMMU2857>3.0.CO2–R
40. Deres K, Schild H, Wiesmuller KH, Jung G, Rammensee HG. *In vivo* priming of virus–specific cytotoxic T lymphocytes with synthetic lipopeptide vaccine. *Nature.* (1989) 342:561–4. doi: 10.1038/342561a0
41. Moore A, McCarthy L, Mills KH. The adjuvant combination monophosphoryl lipid A and QS21 switches T cell responses induced with a soluble recombinant HIV protein from Th2 to Th1. *Vaccine.* (1999) 17:2517–27. doi: 10.1016/s0264–410x(99)00062–6
42. Huleatt JW, Jacobs AR, Tang J, Desai P, Kopp EB, Huang Y, et al. Vaccination with recombinant fusion proteins incorporating Toll–like receptor ligands induces rapid cellular and humoral immunity. *Vaccine.* (2007) 25:763–75. doi: 10.1016/j.vaccine.2006.08.013
43. Caron G, Duluc D, Frémaux I, Jeannin P, David C, Gascan H, et al. Direct stimulation of human T cells via TLR5 and TLR7/8: flagellin and R-848 up-regulate proliferation and IFN-gamma production by memory CD4+ T cells. *J Immunol.* (2005) 175:1551–7. doi: 10.4049/jimmunol.175.3.1551
44. Platt A, Macleod H, Massari P, Liu X, Wetzler L. *In vivo*, and *in vitro* characterization of the immune stimulating activity of the neisserial Porin PorB. *PLoS ONE.* (2013) 8:e82171. doi: 10.1371/journal.pone.0082171
45. Reiser ML, Mosaheb MM, Lisk C, Platt A, Wetzler LM. The TLR2 binding neisserial Porin PorB enhances antigen presenting cell trafficking and cross–presentation. *Sci Rep.* (2017) 7:736. doi: 10.1038/s41598–017–00555–4
46. Mosaheb MM, Reiser ML, Wetzler LM. Toll–like receptor ligand–based vaccine adjuvants require intact MyD88 signaling in antigen–presenting cells for germinal center formation and antibody production. *Front Immunol.* (2017) 8:225. doi: 10.3389/fimmu.2017.00225
47. Mosaheb M, Wetzler LM. Meningococcal PorB induces a robust and diverse antigen specific T cell response as a vaccine adjuvant. *Vaccine.* (2018) 36:7689–99. doi: 10.1016/j.vaccine.2018.10.074
48. Kumagai Y, Takeuchi O, Akira S. TLR9 as a key receptor for the recognition of DNA. *Adv Drug Deliv Rev.* (2008) 60:795–804. doi: 10.1016/j.addr.2007.12.004
49. Gupta RK. Aluminum compounds as vaccine adjuvants. *Adv Drug Deliv Rev.* (1998) 32:155–72.
50. Alvarez D, Vollmann EH, von Andrian UH. Mechanisms and consequences of dendritic cell migration. *Immunity.* (2008) 29:325–42. doi: 10.1016/j.immuni.2008.08.006
51. Förster R, Braun A, Worbs T. Lymph node homing of T cells and dendritic cells via afferent lymphatics. *Trends Immunol.* (2012) 33:271–80. doi: 10.1016/j.it.2012.02.007
52. Phan TG, Green JA, Gray EE, Xu Y, Cyster JG. Immune complex relay by subcapsular sinus macrophages and noncognate B cells drives antibody affinity maturation. *Nat Immunol.* (2009) 10:786–93. doi: 10.1038/ni.1745
53. Allen CD, Cyster JG. Follicular dendritic cell networks of primary follicles and germinal centers: phenotype and function. *Sem Immunol.* (2008) 20:14–25. doi: 10.1016/j.smim.2007.12.001
54. Nossal GJ, Ada GL, Austin CM, Pye J. Antigens in immunity. 8. Localization of 125–I–labelled antigens in the secondary response. *Immunology.* (1965) 9:349–57.
55. Kranich J, Krautler NJ. How follicular dendritic cells shape the B–cell antigenome. *Front Immunol.* (2016) 7:225. doi: 10.3389/fimmu.2016.00225
56. Cantisani R, Pezzicoli A, Cioncada R, Malzone C, de Gregorio E, D'Oro U, et al. Vaccine adjuvant MF59 promotes retention of unprocessed antigen in lymph node macrophage compartments and follicular dendritic cells. *J Immunol.* (2015) 194:1717–25. doi: 10.4049/jimmunol.1400623
57. Cantisani R, Piccioli D. Vaccine adjuvants confer an advantage to the kinetics of activation of follicular dendritic cells that are sensitive to peripheral tissue's injury. *Scand J Immunol.* (2015) 82:144–6. doi: 10.1111/sji.12313
58. Bolte S, Cordelieres FP. A guided tour into subcellular colocalization analysis in light microscopy. *J Microsc.* (2006) 224:213–2. doi: 10.1111/j.1365–2818.2006.01706.x
59. Yuen R, Kuniholm J, Lisk C. Wetzler LM. Neisserial PorB immune enhancing activity and use as a vaccine adjuvant. *Hum Vacc Immunother.* (2019) 15:2778–81. doi: 10.1080/21645515.2019.1609852
60. Klinman DM, Xie H, Little SF, Currie D, Ivins BE. CpG oligonucleotides improve the protective immune response induced by the anthrax vaccination of rhesus macaques. *Vaccine.* (2004) 22:2881–6. doi: 10.1016/j.vaccine.2003.12.020
61. Klinman DM, Klaschik S, Sato T, Tross D. CpG oligonucleotides as adjuvants for vaccines targeting infectious diseases. *Adv Drug Deliv Rev.* (2009) 61:248–55. doi: 10.1016/j.addr.2008.12.012
62. Tross D, Klinman DM. Effect of CpG oligonucleotides on vaccine–induced B cell memory. *J Immunol.* (2008) 181:5785–90. doi: 10.4049/jimmunol.181.8.5785
63. Gavin AL, Hoebe K, Duong B, Ota T, Martin C, Beutler B, et al. Adjuvant–enhanced antibody responses in the absence of toll–like receptor signaling. *Science.* (2006) 314:1936–8. doi: 10.1126/science.1135299
64. Nemazee D, Gavin A, Hoebe K, Beutler B. Immunology: toll–like receptors and antibody responses. *Nature.* (2006) 441:E4. doi: 10.1038/nature04875
65. Palm NW, Medzhitov R. Immunostimulatory activity of haptenated proteins. *Proc Natl Acad Sci USA.* (2009) 106:4782–7. doi: 10.1073/pnas.0809403105
66. Bajénoff M, Germain RN. B–cell follicle development remodels the conduit system and allows soluble antigen delivery to follicular dendritic cells. *Blood.* (2009) 14:4989–97. doi: 10.1182/blood−2009–06–229567
67. El Shikh MEM, Pitzalis C. Follicular dendritic cells in health and disease. *Front Immunol.* (2012) 3:292. doi: 10.3389/fimmu.2012.00292
68. Usui K, Honda SI, Yoshizawa Y, Nakahashi-Oda C, Tahara-Hanaoka S, Shibuya K, et al. Isolation and characterization of naïve follicular dendritic cells. *Mol Immunol.* (2012) 50:172–6. doi: 10.1016/j.molimm.2011.11.010
69. Harrell MI, Iritani BM, Ruddell A. Lymph node mapping in the mouse. *J Immunol Methods.* (2008) 332:170–4. doi: 10.1016/j.jim.2007.11.012

Conflict of Interest: The authors declare that the research was conducted in the absence of any commercial or financial relationships that could be construed as a potential conflict of interest.

frontiers in Immunology

ORIGINAL RESEARCH
published: 16 July 2020
doi: 10.3389/fimmu.2020.01458

Efficient Induction of Cytotoxic T Cells by Viral Vector Vaccination Requires STING-Dependent DC Functions

Cornelia Barnowski[1†], Gregor Ciupka[1†], Ronny Tao[1], Lei Jin[2], Dirk H. Busch[3], Sha Tao[1] and Ingo Drexler[1]*

[1] *Institute for Virology, Düsseldorf University Hospital, Heinrich-Heine-University, Düsseldorf, Germany,* [2] *Division of Pulmonary, Critical Care and Sleep Medicine, Department of Medicine, University of Florida, Gainesville, FL, United States,* [3] *Institute of Microbiology, Immunology and Hygiene, Technical University Munich, Munich, Germany*

OPEN ACCESS

Edited by:
Matthias Tenbusch, University Hospital Erlangen, Germany

Reviewed by:
Guus Rimmelzwaan, University of Veterinary Medicine Hannover, Germany
Brian J. Ferguson, University of Cambridge, United Kingdom

***Correspondence:**
Ingo Drexler
ingo.drexler@med.uni-duesseldorf.de

[†] *These authors have contributed equally to this work*

Specialty section:
This article was submitted to Vaccines and Molecular Therapeutics, a section of the journal Frontiers in Immunology

Received: *29 January 2020*
Accepted: *04 June 2020*
Published: *16 July 2020*

Citation:
Barnowski C, Ciupka G, Tao R, Jin L, Busch DH, Tao S and Drexler I (2020) Efficient Induction of Cytotoxic T Cells by Viral Vector Vaccination Requires STING-Dependent DC Functions. Front. Immunol. 11:1458. doi: 10.3389/fimmu.2020.01458

Modified Vaccinia virus Ankara (MVA) is an attenuated strain of vaccinia virus and currently under investigation as a promising vaccine vector against infectious diseases and cancer. MVA acquired mutations in host range and immunomodulatory genes, rendering the virus deficient for replication in most mammalian cells. MVA has a high safety profile and induces robust immune responses. However, the role of innate immune triggers for the induction of cytotoxic T cell responses after vaccination is incompletely understood. Stimulator of interferon genes (STING) is an adaptor protein which integrates signaling downstream of several DNA sensors and therefore mediates the induction of type I interferons and other cytokines or chemokines in response to various dsDNA viruses. Since the type I interferon response was entirely STING-dependent during MVA infection, we studied the effect of STING on primary and secondary cytotoxic T cell responses and memory T cell formation after MVA vaccination in STING KO mice. Moreover, we analyzed the impact of STING on the maturation of bone marrow-derived dendritic cells (BMDCs) and their functionality as antigen presenting cells for cytotoxic T cells during MVA infection *in vitro*. Our results show that STING has an impact on the antigen processing and presentation capacity of conventionel DCs and played a crucial role for DC maturation and type I interferon production. Importantly, STING was required for the induction of efficient cytotoxic T cell responses *in vivo*, since we observed significantly decreased short-lived effector and effector memory T cell responses after priming in STING KO mice. These findings indicate that STING probably integrates innate immune signaling downstream of different DNA sensors in DCs and shapes the cytotoxic T cell response via the DC maturation phenotype which strongly depends on type I interferons in this infection model. Understanding the detailed functions of innate immune triggers during MVA infection will contribute to the optimized design of MVA-based vaccines.

Keywords: viral vector vaccine, dendritic cells, STING, modified vaccinia virus Ankara MVA, cytotoxic T cells, type I interferon

INTRODUCTION

Vaccinia virus (VACV) is a member of the genus *Orthopoxvirus* and belongs to the family *Poxviridae*. It has a complex structure with a long double-stranded DNA (dsDNA). In contrast to other DNA viruses the replication takes place in the cytoplasm within special organelles called viral factories (1–4). Modified vaccinia virus Ankara (MVA) was derived from the chorioallantois vaccinia virus Ankara (CVA) by serial passaging in chicken embryo fibroblasts (CEFs) (5, 6) causing large deletions and numerous mutations in the viral genome affecting virulence and various immune evasion factors (e.g., factors interacting with host receptors for interferon-γ, interferon-α/β, and CC-chemokines) (7–10). Consequently, the virus is unable to produce infectious particles in most mammalian cells including humans (11, 12). The expression of viral genes is programmed to occur in three consecutive stages: early (118 ORFs), intermediate (53 ORFs), and late (38 ORFs) gene expression (13, 14). Despite the abortive infection, MVA allows for early through late gene expression (15). Due to its high safety profile MVA is currently tested as a recombinant vaccine candidate for various infectious diseases and cancer (16–18).

The innate immune system acts as the first line of defense against invading pathogens involving various cell types such as macrophages, dendritic cells (DCs), neutrophilic granulocytes, natural killer cells, and congenital lymphatic cells (19–21). Viruses activate innate immune system components e.g., by interaction of viral pathogen-associated molecular patterns (PAMPs) with cellular pattern recognition receptors (PRRs) (22). The detection of viral PAMPs via PRRs such as TLRs (toll-like receptors) or CDSs (cytosolic DNA sensors) activates intracellular signaling cascades which amongst others lead to the secretion of type I interferons (e.g., IFN-α, -β), proinflammatory cytokines and chemokines and induce an increased expression of costimulatory molecules such as CD40, CD80, and CD86 e.g., on DCs (23). Particularly for DNA viruses, stimulator of interferon genes (STING) plays a crucial role in this respect. STING is activated after recognition of foreign DNA from bacteria and viruses as well as own cellular DNA that has been released by cell stress or dysfunction (24, 25). The cyclic GMP-AMP synthase (cGAS) is an unusual innate immune sensor as it functions simultaneously as a receptor and as a biosynthetic enzyme (26, 27). The binding of dsDNA to the zinc finger domain of cGAS rearranges the active side of cGAS and enables the synthesis of the secondary messenger cyclic GMP-AMP (cGAMP) (26, 28–31). 2'3'-cGAMP activates the IFN-I signal cascade via the ER-resident homodimer receptor STING. The ability of a single cGAS enzyme to produce multiple cGAMP molecules provides a mechanism that can generate a rapidly amplifying immune response by small amounts of cytosolic DNA (32–34). A conformational change allows the recruitment of TANK-binding kinase 1 (TBK1) which phosphorylates the C-terminal domain of STING and thus leads to further recruitment of the transcription factor IRF3 (35, 36). TBK1 phosphorylates IRF3, IRF3 dimers are formed, and translocated into the nucleus. In the nucleus, IRF3 mediates the transcription of IFN-β and other coregulated genes. It has been recently shown that the expression of type I interferons in MVA-infected bone marrow-derived dendritic cells (BMDC) was completely dependent on STING (37). It should also be noted that STING can activate other signal transduction pathways involving NF-κB-, MAP kinases or STAT6 (38–40) indicating the importance of STING for the induction of potent innate immune responses.

During an infection, naïve cytotoxic $CD8^+$ T cells (CTL) are initially activated (primed) by antigen-presenting cells (APCs) in secondary lymphatic organs such as lymph node and spleen (41). The first major cell population in contact with the pathogen in secondary lymphoid organs are $CD169^+$ macrophages lining the subcapsular sinus area. Although macrophages may present antigens very effectively, $CD8^+$ T effector cells are primarily induced by professional APCs such as dendritic cells. It has been recently demonstrated, that optimal CTL responses induced by MVA vaccines require antigen presentation by infected DC as well as cross-presentation of antigen by non-infected bystander DC with both pathways being executed by distinct DC subsets (42, 43). The accurate killing of infected target cells is mediated by the release of cytotoxic granules (e.g., Granzymes and Perforin) from lysosomal compartments (44, 45). During degranulation, the lysosomal membrane proteins are transiently translocated to the cell surface of the $CD8^+$ T-effector cell which thereby become identifiable by the expression of lysosome-associated membrane proteins (LAMP-1 and LAMP-2) (46, 47). The understanding of the molecular interactions between innate and adaptive immunity, particularly with regard to the induction of efficient cytotoxic immune responses, is an important requirement for the development and optimization of MVA-based vaccines.

In the present study, we investigated the role of STING for the induction of an efficient cytotoxic T cell response after viral vector vaccination using recombinant MVA. We demonstrate that STING is crucial for the induction of efficient $CD8^+$ T cell responses *in vivo*. Interestingly, mainly the immunodominant CTL response was reduced and only short-lived effector and effector memory T cells were impaired, while long-term memory was unaffected. The proinflammatory cytokine and chemokine response was broadly impaired in infected mice lacking STING. Our *in vitro* findings suggest that the impaired $CD8^+$ T cell response in these mice was at least partly due to the abrogated type I interferon response in DCs which resulted in inefficient DC maturation and impaired antigen-processing and presentation capacity.

MATERIALS AND METHODS

Mice and Vaccination

Homozygous $MPYS^{-/-}$ mice (STING KO) and $MPYS^{+/+}$ wildtype littermates (STING WT) were originally obtained from B. Opitz, Charité, Berlin, and have been described elsewhere (48). C57BL/6 mice were purchased from Janvier. Transgenic mice were derived from in-house breeding "Zentrale Einrichtung für Tierforschung und wissenschaftliche Tierschutzaufgaben (ZETT)" under specific pathogen-free conditions following institutional guidelines. Animal experiments have been conducted according to the German Animal Welfare Act (Tierschutzgesetz) and have been approved by the regional

authorities (North Rhine-Westphalia State Environment Agency -LUA NRW, Germany). Female mice between 8 and 12 weeks old were used.

Viruses

Recombinant modified vaccinia virus Ankara (MVA) expressed OVA under the control of the early/late promoter P7.5 or PH5 (49). MVA-P7.5-NP-SIINFEKL-eGFP expressed the influenza A virus nucleoprotein fused to the class I (Kb)-restricted SIINFEKL-peptide epitope of OVA fused to eGFP (50) and MVA-PK1L-OVA expressing OVA under the control of the early promoter PK1L (49). All viruses were purified by two consecutive ultracentrifugation steps through a 36% (wt/vol) sucrose cushion and titrated by using standard methods (51).

Vaccination

Mice were vaccinated at 8-10 weeks of age by intraperitoneal (i. p.) or intramuscular (i. m.) application of 10^7 infectious units (IU) MVA-p7.5-OVA in 200 or 100 µl of vaccination buffer (20 mM Tris-HCl, 280 mM NaCl, pH 7.4), respectively. For the i. m. immunization mice were injected with 50 µl virus per leg. Vaccinated mice were either sacrificed on day 7 post-infection (p. i.) or boosted i. p. on day 28 post prime with 10^7 IU MVA-p7.5-OVA and sacrificed 5 days after the second vaccination. Spleens were harvested and induced $CD8^+$ T cell responses analyzed as described below.

Ex vivo T Cell Analysis

Spleens of vaccinated animals were collected and processed into a single-cell suspension by mechanical disruption using a 70 µm cell strainer and a plunger. Erythrocytes were lysed by incubation in lysis buffer (BD Pharm Lyse™) for 1 min at room temperature. Cells were passed through a 70 µm cell strainer and counted using a Neubauer cell counting chamber. Thereafter, 4×10^6 splenocytes were plated at 100 µl per well of a 96-well plate and further incubated with 2 µg/ml of MVA-specific or control peptides and 1 µg/ml brefeldin A (Merck) for 5 h. Peptides were $A19_{47-56}$ (VSLDYINTM), $B8_{20-27}$ (TSYKFESV), $K3_{6-15}$ (YSLPNAGDVI), $A3_{270-277}$ (KSYNYMLL), or $D13_{118-126}$ (NCINNTIAL) derived from MVA and $OVA_{257-264}$ (SIINFEKL) peptide derived from ovalbumin. K3 and D13-derived peptides are H2-D^b-restricted, all other peptides are H2-K^b- restricted. All peptides were purchased from Biosynthan (Germany). Beta-galactosidase (β-Gal) peptide was used as negative control as a non-cognate ligand. As an additional control, T cells were stimulated in a non-antigen-specific manner using anti-mouse CD3e antibody (clone 500A2, BD Pharmingen 553238) at 1,25 µg/ml. For the determination of CD107a expression, splenocytes were additionally incubated in the presence of anti-CD107a antibody (eBioscience).

Generation of BMDCs

Femur and tibiae from 12 to 16 weeks old mice were flushed with M2 medium and erythrocytes were lysed by incubation with 5 ml of diluted BD Pharm Lyse buffer™ for 1 min at room temperature. 5×10^6 bone marrow cells were plated in 10 ml M2 medium (containing 10% heat inactivated FCS, 50 µM 2-mercaptoethanol) and 10% GM-CSF (conditioned medium obtained as supernatant from B16 cells expressing GM-CSF; originally kindly provided by Georg Häcker, Freiburg, Germany) in 10 cm Petri-dishes. On day 3 and 6 cultures were replaced with 10 ml of fresh M2 medium containing 10% GM-CSF, respectively. BMDCs cultures were used for experiments on day 7.

BMDC Infection

Semiadherent BMDCs were scraped, counted using a Neubauer cell counting chamber and 4×10^6 BMDCs were spun down at 319 xg. After centrifugation, cell pellets were resuspended in 200 µl M2 medium (RPMI 1640 containing 10% heat inactivated FCS, 50 µM 2-mercaptoethanol) and BMDCs were infected at a multiplicity of infection (MOI) of 5 and incubated for 12 h at 37°C and 5% CO_2. In the first hour of infection BMDCs were softly shaken every 10 min to keep them in suspension. Thereafter, cells were seeded in a 6 cm Petri-dish and incubated at 37°C and 5% CO_2 for the remaining infection time.

Cross-Presentation Assay

Murine Cloudman S91 melanoma cells (ATCC CCL-53.1; MHC I haplotype H-2^d) were used as MHC I-mismatched feeder cells. Feeder cells were trypsinized, counted using a Neubauer cell counting chamber and 2×10^6 feeder cells were spun down at 319 xg. After centrifugation, cell pellets were resuspended in 200 µl of M2 medium (RPMI 1640 containing 10% heat inactivated FCS, 50 µM 2-mercaptoethanol). Cells were infected at MOI 1 and incubated for 16 h at 37°C and 5% CO_2. In the first hour of infection, feeder cells were softly shaken every 10 min to keep them in suspension and in the second hour of infection, every 20 min. Thereafter, cells were seeded in a 6-well plate and incubated at 37°C and 5% CO_2 for the remaining infection time. Infected feeder cells and mock controls were treated with 0.3 µg/ml psoralen for 15 min prior to irradiation with UVA (PUVA) for 15 min at room temperature. 2×10^6 feeder cells were washed and cocultured with 2×10^6 BMDCs in a 6 cm Petri-dish at 37°C and 5% CO_2. Cross-presenting BMDCs were analyzed at 12 h post co-cultivation for their ability to reactivate antigen-specific $CD8^+$ T cell lines, described below, or at 20 h post co-cultivation for their SIINFEKL/K^b-loading ability and maturation phenotype.

$CD8^+$ T Cell Activation Assay

Peptide-specific $CD8^+$ T cell lines were used as read-out for the antigen presentation capacity of infected or non-infected cross-presenting BMDCs. 2×10^5 $CD8^+$ were co-cultured with 4 x 10^5 BMDCs for 4 h in the presence of 1 µg/ml brefeldin A (Merck) at 37°C and 5% CO_2. T cell activation of $CD8^+$ T cells was determined by cytokine production analyzed by intracellular cytokine staining (ICS) as described below. For detection of SIINFEKL/K^b complexes at the cell surface, anti-SIINFEKL/K^b APC antibody (eBioscience 25-D1.16) was used after CD16/32-Fc-blockade (2.4G2, BD) and viability dye (Invitrogen). FACS analysis was performed on BD FACS CantoII and FlowJo 6.4.2 software.

Generation and Maintenance of CD8$^+$ T Cell Lines

LPS blasts were produced by incubating 1×10^6 splenocytes/ml derived from naïve C57BL/6 mice with 25 µg/ml LPS (Sigma-Aldrich) and 7 µg/ml dextran-SO_4 (Sigma-Aldrich) for 4 days at 37°C and 5% CO_2. After irradiation of LPS-blasts with 30 Gy, cells were washed with RPMI 1640 medium and incubated in 1 ml RPMI 1640 medium containing 5 µg/ml β-microglobulin and 1 ng/ml of the appropriate peptide for 30 min at 37°C and 5% CO_2. Peptides were $A19_{47-56}$ (VSLDYINTM), $B8_{20-27}$ (TSYKFESV), $K3_{6-15}$ (YSLPNAGDVI), $A3_{270-277}$ (KSYNYMLL), or $D13_{118-126}$ (NCINNTIAL) derived from MVA and $OVA_{257-264}$ (SIINFEKL) peptide derived from ovalbumin. K3 and D13-derived peptides are H2-D^b-restricted, all other peptides are H2-K^b- restricted. All peptides were purchased from Biosynthan (Germany). Cells were washed with medium prior to co-cultivation of 3×10^6 peptide-loaded LPS-blasts with 7×10^6 splenocytes from MVA-PK1L-OVA vaccinated C57BL/6 mice for 8 days at 37°C and 5% CO_2.

CD8$^+$ T cells were maintained by weekly restimulation using peptide loaded EL.4 cells (ATCC TIB-39), naïve splenocytes and M2 medium containing 5% TCGF [conditioned medium containing supernatant from rat splenocytes stimulated with 5 µg/ml Concanavalin A, produced as described (52)]. EL.4 cells and splenocytes were irradiated with 100 Gy or 30 Gy, respectively prior to peptide-loading and/or incubation with CD8$^+$ T cells.

Antibodies and Flow Cytometry

Cells were washed with PBS (Life Technologies, Darmstadt, Germany) and dead cells were excluded by viability dye staining (eBioscience™ Fixable Viability Dye eFluor™ 506) for 20 min on ice. Prior to the surface staining of CD8$^+$ T cells or BMDCs, cells were washed twice with staining buffer (1% BSA, 0,02% NaN_3 in PBS). To analyze activated CD8$^+$ T cells, cells were stained for CD8 using anti-CD8-PB (eBioscience) for 30 min on ice. Thereafter, intracellular staining was performed, as described below. Alternatively, BMDCs were analyzed for their SIINFEKL/K^b-loading ability using anti-CD11c-PE, -I-A/I-E-PB, -Kb-PE/Cy7, and -SIINFEKL/H2-K^b-PE/Cy7 (all from eBioscience) or for their maturation phenotype using anti-CD11c-APC/Cy7, -CD86-APC, I-A/I-E-PE antibodies (all BD Pharmingen), or anti-CD40-PB antibody (Biolegend). Antibodies were added after blocking of Fc-receptors using CD16/32 antibodies (Fc-Block™, BD Biosciences). After incubation on ice for 30 min, cells were washed and fixed with 1% paraformaldehyde and stored at 8°C until flow cytometry was performed using BD FACS Canto II (BD Biosciences, Heidelberg, Germany).

Intracellular Staining (ICS)

Cells were washed twice and permeabilized for 15 min on ice using BD Cytofix/Cytoperm™ solution. After an additional washing step, cells were incubated with anti-IFNγ and/or anti-MIP1-α (both Bioscience) for 30 min in the dark on ice. Finally, cells were washed and fixed with 1% paraformaldehyde. Flow cytometry was performed using BD FACS Canto II (BD Biosciences, Heidelberg, Germany).

Phenotypical Analysis of Memory T Cell Subsets *ex vivo*

STING KO mice and wild-type littermates were immunized as described above. Spleens were removed 7 days after primary immunization. Isolated splenocytes were directly used for staining with B8- or OVA-reactive tetramers. Briefly, splenocytes were washed with PBS and dead cells excluded by viability dye staining (eBioscience™ Fixable Viability Dye eFluor™ 506). Thereafter, cells were washed twice with staining buffer (1% BSA, 0.02% NaN_3 in PBS) and Fc-receptors blocked using CD16/32 antibodies (Fc-Block™, BD Biosciences). After washing, cells were incubated with B8- and OVA-reactive tetramers for 15 min and incubated in the dark on ice. Anti-CD8-PB, -CD127-APC, and -CD62L-PE/Cy7 (all eBioscience) antibodies were added to the tetramer-stained cells and incubated for additional 20 min in the dark on ice. Samples were analyzed by flow cytometry using BD FACS Canto II (BD Biosciences, Heidelberg, Germany).

Cytokine/Chemokine Response in Supernatants

Supernatants of MVA- or mock-infected BMDCs were harvested 12 h post-infection and supernatants of cross-presenting BMDCs were collected after overnight co-cultivation (12-15 h). Detection of IFN-α (LumiKine™ mIFN-α) and -β (LumiKine™ Xpress mIFN-β) was performed according to the manufacturer's protocol. LEGENDPlex™ assays (Mouse Proinflammatory Chemokine Panel and Mouse Anti-Virus Response Panel Mix and Match Subpanel; Biolegend) were performed to monitor cytokine/chemokine expression. Briefly, spleens were collected and carefully homogenized in 500 µl ice-cold PBS plus protease inhibitor cocktail (Roche). The supernatants were collected after centrifugation and stored at −80°C till usage. A volume of 25 µl supernatant was used following the manufacturer's protocol.

For the analysis of cytokines and chemokines produced by MVA- or mock-infected feeder cells, supernatants were harvested at 12 h p. i. and analyzed according to the manufacturer's protocol. Samples were analyzed by flow cytometry on a FACS CantoII (BD Bioscience). Data were analyed using LEGENDPlex software (Biolegend).

Generation of STING KO Feeder Cells

STING KO feeder cells were generated using CRISPR/Cas9 KO (TMEM173 CRISPR/Cas9 KO plasmid sc-428364) and HDR (TMEM173 HDR plasmid sc-428364-HDR) plasmids from Santa Cruz. Cells were seeded the day before in a 6-well plate and transfected at 80% confluency with both CRISPR/Cas9 plasmids using FuGENE HD Transfection Reagent according to the manufacturer's protocol. After 2 days cells were selected for 5 days with media containing 0.5 µg/ml puromycin (Sigma) which was renewed after 2 days of puromycin treatment. The phenotype of gene-edited cells was verified by western blot analysis, as described below.

Phagocytosis Activity and Endosomal Function

4×10^6 STING KO or WT BMDCs were transferred to a 6-well each and incubated with 10 μL of OVA-AF594 or OVA-DQTM (10 ng/mL) for 2 h at 37°C and 4°C. DQ-Ovalbumin is a self-quenching conjugate which shows a bright green fluorescence during proteolytic degradation. Cells were washed and stained with a vitality dye (eBioscience™ Fixable Viability Dye eFluor™ 660) as well as anti-CD11c-PE/Cy7 (eBioscience) and analyzed by flow cytometry using BD FACS Canto II (BD Biosciences, Heidelberg, Germany).

Western Blot Analysis

The expression of STING protein was analyzed in order to verify gene-editing of TEMEM173 by CRISPR/Cas9. Cell lysates were prepared from STING KO and control feeder cells and a SDS-PAGE and blotting on nitrocellulose membranes performed, as described elsewhere (53). Membranes were blocked using 5% BSA in Tris-buffered saline containing 0.1% Tween 20 (Merck) for 1 h at room temperature. Rabbit anti-STING (cell signaling) and mouse anti-β-actin (Sigma) were diluted according to the manufacturer's protocol and incubated over night with the membrane. Incubation of peroxidase-conjugated goat anti-rabbit or anti-mouse IgG (Jackson) for 1 h at room temperature allowed the detection by chemoluminescence using Super Signal West Dura Chemoluminescent Substrate (Thermo Scientific).

Statistical Analysis

All statistical analyses were performed using Graphpad Prism software version 7. Statistical comparisons of two groups were conducted using the unpaired, two-tailed Student's *t*-test. The results were depicted as mean ± standard deviation (SD) either pooled or representative from an indicated number of independent experiments. Statistical significance (P) is represented as: $^{*}P \leq 0.05$; $^{**}P \leq 0.01$; $^{***}P \leq 0.001$; $^{****}P \leq 0.0001$.

RESULTS

STING Is Crucial for the Induction of Efficient CD8$^+$ T Cell Responses After Infection With MVA

STING plays an important immunoregulatory role after recognition of cytosolic foreign DNA which is delivered by many DNA viruses including MVA. Next to innate immune activation, there may be STING-dependent effects on adaptive immunity such as CTL responses. In order to investigate a possible role of STING in MVA vaccination, we immunized STING KO and STING WT mice, which were genotypically confirmed by PCR (**Supplementary Figure 1A**), intraperitoneally (i.p.) or intramuscularly (i. m.) with 10^7 IU ovalbumin (OVA)-expressing MVA (MVA-P7.5-OVA). On day 7, spleens were harvested, splenocytes shortly restimulated with peptides and subsequently used for intracellular cytokine staining and analyzed by flow cytometry (**Figure 1A**). CD8$^+$ T-cells were examined for IFNγ, MIP-1α, and CD107a expression, respectively (**Figures 1B–D**). In addition, antigen-specific CD8$^+$ T cells were determined for the recombinant antigen OVA and for vaccinia virus for the immunodominant viral antigen B8 by specific multimers and further discriminated into memory cell subpopulations (**Figure 2A**). Interestingly, the specific CD8$^+$ T cell response against the immunodominant antigen B8 was significantly reduced in STING KO mice for all markers examined, while responses against subdominant viral epitopes (A3, K3, A19) as well as against OVA were comparable, yet with a slight tendency for a decrease in STING KO mice (**Figures 1B–D**). Moreover, we show that the dependency on STING as well as immunodominance of B8 was independent of the immunization route since primary B8-specific CD8$^+$ T cell responses in STING KO mice were significantly decreased for all markers tested with the exception of MIP-1α after i.m. vaccination (**Supplementary Figure 2**). Interestingly, we additionally found decreased T cell frequencies for subdominant OVA and A3 epitopes with the ability for IL2 (OVA) or CD107a (OVA and A3) expression which we had not seen before after i.p. administration. In addition to the functional analysis, antigen-specific memory cell subpopulations were phenotypically analyzed during the acute phase. Differentiation between central and effector memory cells as well as effector T cells was carried out by monitoring the activation and maturation markers CD62L (L-selectin) and CD127 (α subunit of the Interleukin-7 receptor) within the multimer-positive (antigen-specific) CD8$^+$ T cell population (**Figure 2A**). The overall frequency (**Figure 2B**) as well as absolute numbers (**Figure 2C**) of B8-specific CD8$^+$ T cells in STING KO mice, as determined by B8-specific tetramer reactivity, were significantly reduced compared to STING WT mice. Interestingly, predominantly short-lived effector T cells were reduced in frequency (**Figure 2D**) and absolute numbers (**Figure 2E**). Furthermore, B8-specific effector memory CD8$^+$ T cells were significantly reduced in absolute numbers (**Figure 2E**). In contrast, frequencies and distribution of memory subpopulations were comparable for OVA tetramer-reactive CTL in STING KO or WT mice.

Moreover, STING KO mice and WT-littermates were vaccinated i. p. with 10^7 IU MVA-P7.5-OVA on day 0 (prime) followed by a secondary immunization at day 28 (boost). Five days after the boost antigen-specific CD8$^+$ T cells were analyzed *ex vivo* by flow cytometry for their functionality (**Figure 3A**). As expected, since we failed to see an influence of STING for developing long-term memory, STING was neglectable for efficient secondary expansion as indicated by comparable functionality of CD8$^+$ T cell responses after MVA prime/boost vaccination in KO or WT mice (**Figures 3B–D**).

Effector T Cell Activation by STING KO BMDCs Is Not Impaired *in vitro*

It has been shown recently that both direct as well as cross-presentation of antigen is important for the induction of optimal CD8$^+$ T cell responses during MVA vaccination (42). To elucidate the underlying mechanisms of the impaired CD8$^+$ T cell response we had observed in STING KO mice during infection with recombinant MVA, we first

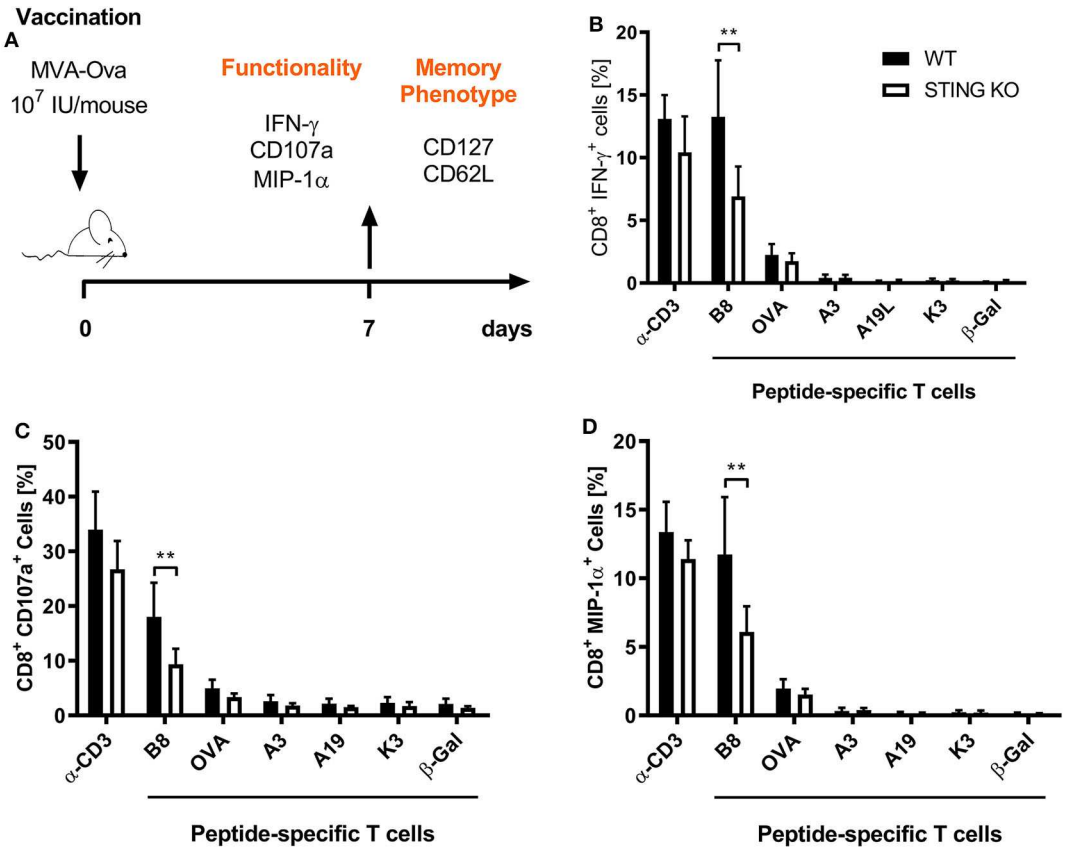

FIGURE 1 | STING has a strong impact on shaping the immunodominance of MVA-specific primary immune responses particularly acting on the immunodominant B8 antigen. **(A)** STING KO mice (STING KO) and WT-littermates (WT) were vaccinated on day 0 i. p. with 10^7 IU MVA-P7.5-OVA. Seven days after priming antigen-specific $CD8^+$ T cells were analyzed *ex vivo* by flow cytometry for their functionality by expression of **(B)** IFN-γ, **(C)** CD107a, and **(D)** MIP-1α. Anti-CD3 antibody (α-CD3) and β-galactosidase (β-Gal) peptides were used for stimulation as positive and negative controls, respectively. Data are represented as mean ± SD of $n = 8$ mice per group pooled from three independent experiments. Statistical significance (*P*); $^{**}P \leq 0.01$.

analyzed the ability of STING KO and WT bone-marrow-derived dendritic cells (BMDCs) to reactivate $CD8^+$ T cells *in vitro* in the setting of antigen cross- as well as direct presentation (**Supplementary Figures 1B, 3**). The purity of BMDC cultures and the expression of maturation markers prior to experimental use was comparable for STING KO or WT (**Supplementary Figures 4A,B**). By using $CD8^+$ T cell lines, specific for the viral antigens B8, K3, A3, and A19 or the recombinant antigen OVA, we observed a comparable T cell activation by infected STING KO and WT BMDCs (direct presentation) (**Figure 4A**). In order to investigate the antigen presentation capability of cross-presenting BMDCs, we used MVA-infected MHC I-mismatched feeder cells unable to directly present antigen to CTL lines. BMDC derived from WT (**Supplementary Figure 4C**) and KO mice (**Supplementary Figure 4D**) showed comparable marker expression profiles in the cross-presentation setting when co-cultivated with mock infected feeder cells. Only cocultivation with infected feeder cells changed the BMDC phenotype. Washing and PUVA treatment of infected feeder cells prevented false-positive results caused by directly antigen presenting BMDCs accidentally infected with input virus. After co-culturing STING KO or WT BMDCs with MVA-infected feeder cells, we did not observe any impact of STING deficiency in cross-presenting BMDCs on T cell activation for all epitope-specificities tested (**Figure 4B**). Considering the possibility that the phenotype of feeder cells may have an impact on their ability to be cross-presented e.g., by licensing DCs for cross-presentation, we generated STING KO feeder cells (**Supplementary Figure 5**) and tested these cells as an antigenic source for BMDCs for cross-presentation. Interestingly, all $CD8^+$ T cell-specificities showed comparable IFN-γ production after incubation with WT BMDC co-cultured with either STING KO or WT feeder cells (**Figure 4C**). Since our T cell lines represent pre-activated effector cells known to become already activated by a low epitope density on the cell surface of antigen-presenting cells, it was likely that there may be differences in the antigen presentation ability of STING-deficient BMDCs which were not obvious in the cytokine production assay (ICS) such as the expression rate or density of peptide/MHC I-complexes at the cell surface.

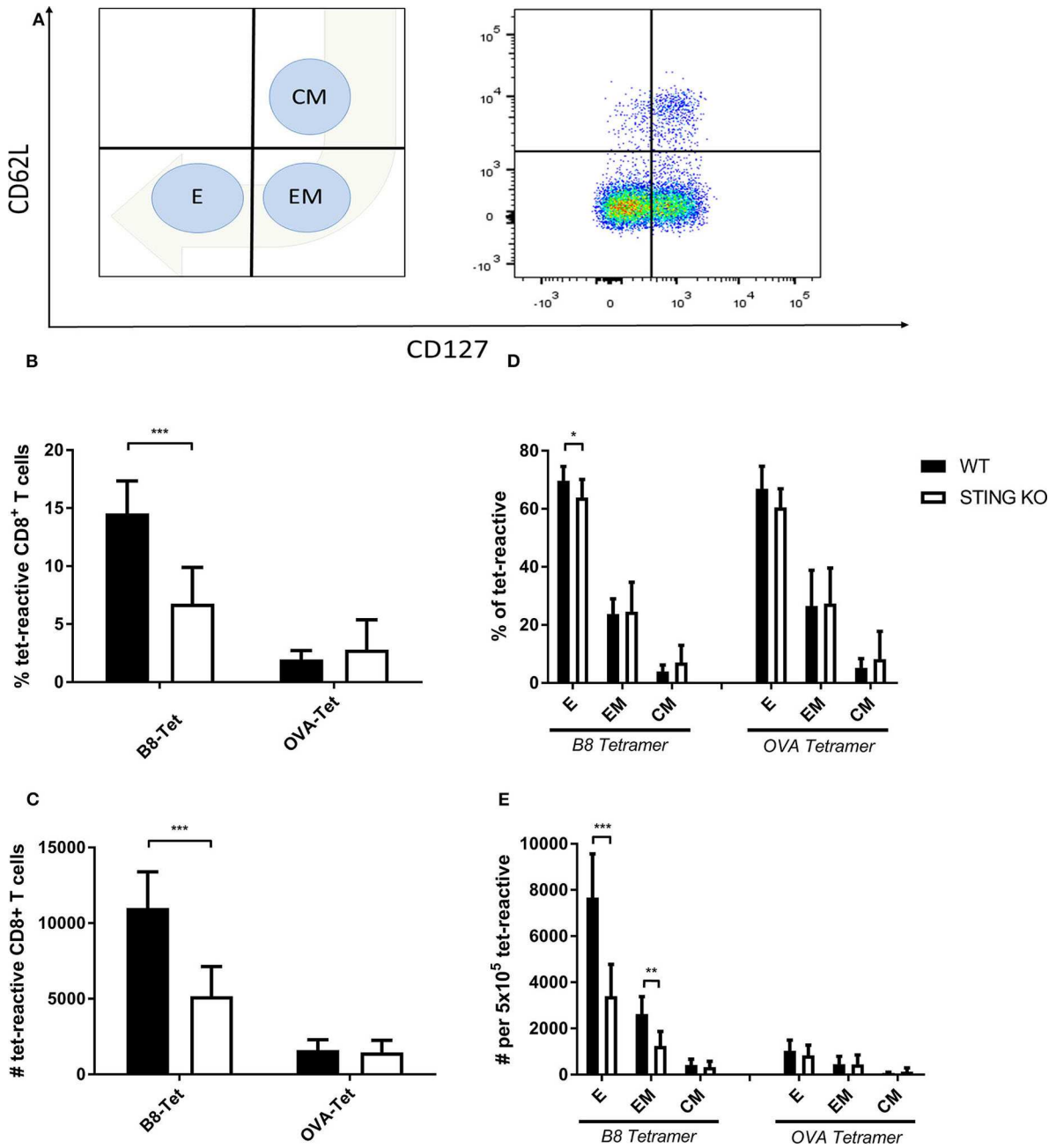

FIGURE 2 | Maturation and differentiation of B8-specific immunodominant CD8$^+$ T cells is STING-dependent. STING KO mice (STING KO) and WT-littermates (WT) were vaccinated on day 0 i. p. with 107 IU MVA-P7.5-OVA. Seven days after the prime antigen-specific CD8$^+$ T cells were analyzed *ex vivo* by flow cytometry for their memory phenotype by expression of CD62L and CD127. **(A)** Presentation of the gating strategy and division into the individual memory subtypes. Analysis of the **(B)** relative frequency (%) and **(C)** absolute numbers of B8- or OVA-specific CD8$^+$ T cell responses determined by tetramer staining (tet-reactive). In addition, the respective memory T cell subpopulations [effector T cells (E), effector memory T cells (EM) and central memory T cells (CM)] within the tetramer-reactive fraction are shown in **(D)** frequencies and **(E)** absolute numbers. B8 tetramer: $n = 13$; OVA tetramer: $n = 11$. Data are represented as mean ± SD of $n = 13$ (for B8 tetramer) or $n = 11$ (for OVA tetramer) mice per group pooled from three independent experiments for B. Statistical significance (P); $^*P \leq 0.05$; $^{**}P \leq 0.01$; $^{***}P \leq 0.001$.

STING Deficiency Results in a Reduced Antigen Processing and Presentation Capacity

Next to CD8$^+$ T cell activation as a more indirect effect of antigen-presentation by BMDCs, we examined antigen processing and presentation by monitoring the surface expression of SIINFEKL peptide/K^b complexes of BMDCs after infection with recombinant MVA expressing OVA. Infected STING KO BMDCs showed a significantly reduced frequency of SIINFEKL/K^b positive cells (**Figure 5A**) as well as a decreased

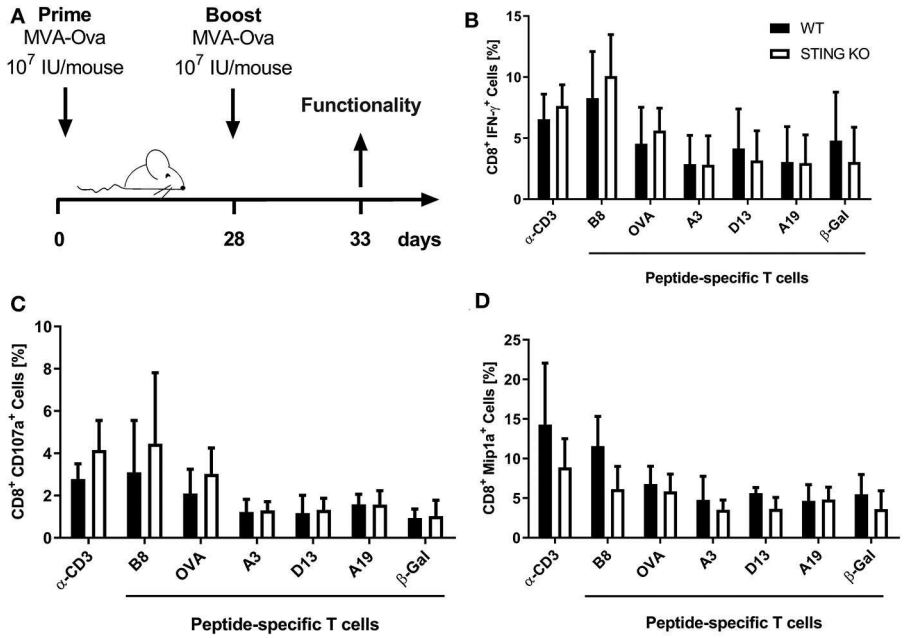

FIGURE 3 | STING is not relevant for developing long term memory and efficient secondary expansion of $CD8^+$ T cell responses in prime/boost vaccination. **(A)** STING KO mice (STING KO) and WT-littermates (WT) were vaccinated i. p. with 10^7 IU MVA-P7.5-OVA on day 0 (prime) and 28 (boost). Five days after the boost antigen-specific $CD8^+$ T cells were analyzed *ex vivo* by flow cytometry for their functionality by expression of **(B)** IFN-γ, **(C)** CD107a, and **(D)** MIP-1α. Anti-CD3 antibody (α-CD3) and β-galactosidase (β-Gal) peptides were used for stimulation as positive and negative controls, respectively. Data are represented as mean ± SD of $n = 9$ mice per group pooled from three independent experiments.

density of SIINFEKL/K^b complexes as compared to STING WT BMDCs (**Figure 5B**). To study whether antigen processing and presentation is altered in cross-presenting STING deficient BMDCs, we performed an assay with a setting similar to the cross-presentation assay described above using either MVA-infected STING KO or WT feeder cells which were co-cultured either with non-infected STING KO or WT BMDCs, but without adding CTL. Interestingly, we observed significant differences in the ability to produce SIINFEKL/K^b complexes for both settings with STING deficiency on either presenter BMDC or feeder cell side (**Figures 5C,D**). The lack of STING in BMDCs only resulted in significant decrease of SIINFEKL/K^b expressing cells (**Figure 5C**) as well as significant reduction of the amount of SIINFEKL/K^b complexes on individual STING KO BMDCs compared to WT BMDCs (**Figure 5D**). Unexpectedly, co-incubation of infected STING KO feeder cells resulted in a highly significant increase in SIINFEKL/K^b expressing BMDCs which was higher in STING WT compared to KO cells (**Figure 5C**). Of note, increased MFIs for SIINFEKL/K^b were mainly depending on STING in BMDCs (**Figure 5D**) indicating that the presence or absence of STING in feeder cells had only a limited impact on the amount of SIINFEKL/K^b complexes at the cell surface of BMDCs. Nevertheless, there was a significant reduction, when BMDCs were STING-deficient (**Figure 5D**). Taken together, these data indicate that STING has a strong impact on the efficiency of antigen processing and presentation in directly infected as well as cross-presenting BMDCs. In addition, the absence of STING in infected feeder cells, serving as a source for antigen, had no impact on the efficiency of antigen presentation, but significantly enhanced the number of BMDCs which were able to cross-present antigen. This may be an indication that STING is highly relevant for licensing feeder cells to activate DCs for cross-presentation, while STING in cross-presenting DCs supports their efficiency in SIINFEKL/K^b loading and/or presentation.

To exclude that the observed differences in SIINFEKL/Kb surface expression in STING KO and WT BMDCs were not due to differential phagocytosis activity or endosomal function, we analyzed the ability of STING-deficient and WT BMDCs to endocytose and process fluorophore-conjugated OVA. Using OVA labeled with either the fluorophore AF488 or DQ, we observed comparable numbers of OVA-$AF488^+$ $CD11c^+$ (**Figure 6A**) or DQ-OVA^+ $CD11c^+$ cells (**Figure 6B**) for STING KO and control BMDC cell cultures at 37°C. In addition, STING KO and WT BMDCs endocytosed comparable amounts of OVA-$AF488^+$ (**Figure 6C**) as well as DQ-OVA (**Figure 6D**, **Supplementary Figure 6**), indicating a similar phagocytic and endosomal activity.

STING Supports Efficient DC Maturation

Considering the connection between type I interferon and maturation of DCs which has been shown by previous research (54–57), we assessed whether STING is involved in the maturation process of DCs during infection with recombinant MVA by analyzing the BMDC maturation phenotype in the direct infection as well as the cross-presentation setting. Using

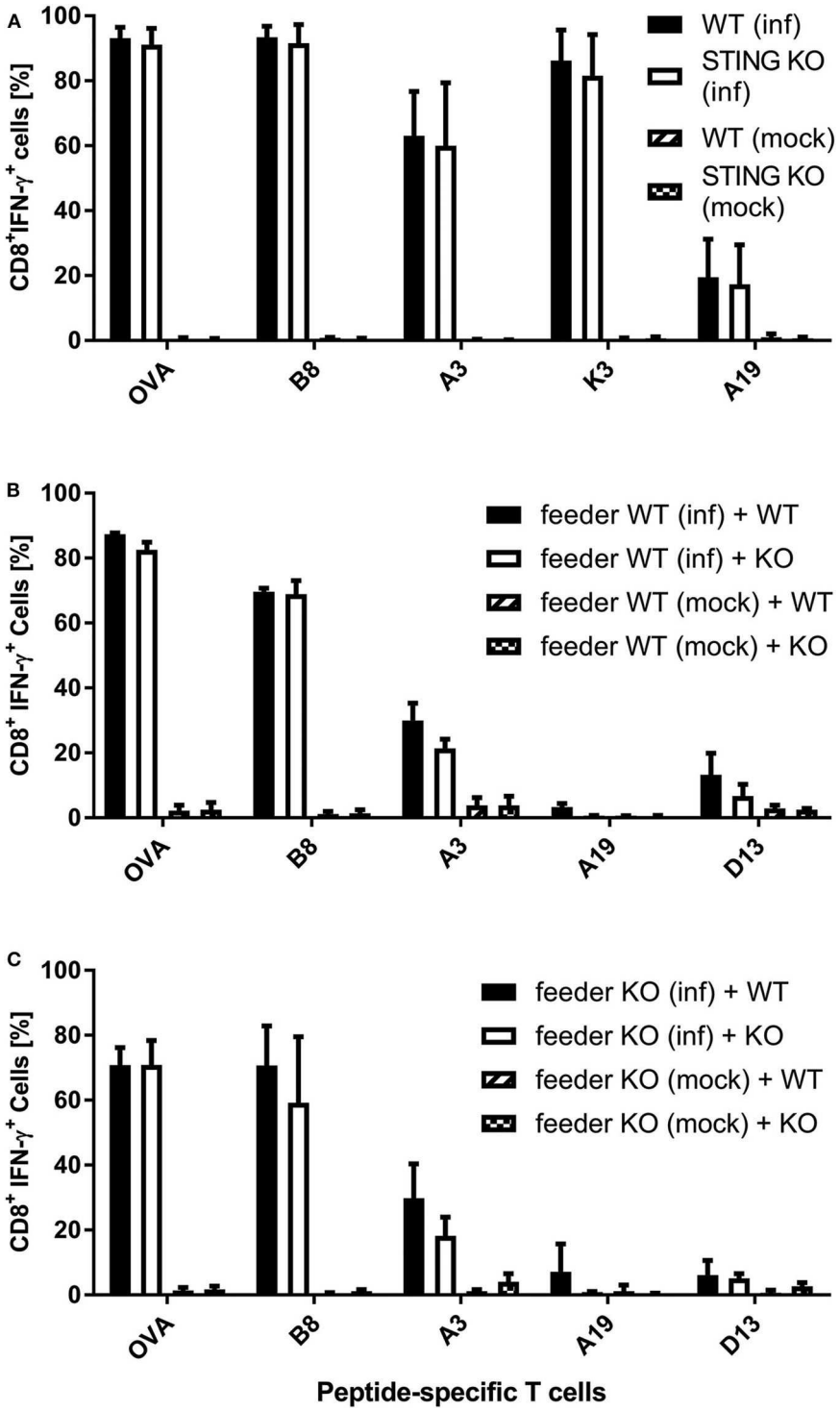

FIGURE 4 | Re-activation of antigen-specific $CD8^+$ T cells by infected or cross-presenting STING KO BMDC is not impaired. **(A)** BMDCs from STING KO mice (STING KO) or wildtype-littermates (WT) were infected with MVA-PK1L-OVA at MOI 1 (inf) or mock infected (mock) for 12 h. **(B)** MHC I-mismatched wildtype feeder cells (feeder WT) expressing STING were infected with MVA-PK1L-OVA at MOI 1 (inf) or mock infected (mock) for 12 h, treated with PUVA, washed and co-cultured with BMDCs derived from either STING KO mice (KO) or WT littermates (WT). **(C)** MHC I-mismatched STING KO (feeder KO) were infected with MVA-PK1L-OVA at MOI 1 (inf) or mock infected (mock), treated with PUVA, washed and co-cultured with BMDCs generated from either STING KO (KO) or wildtype mice expressing STING (WT). **(A)** BMDCs were analyzed 12 h post-infection or **(B,C)** 12 h post co-cultivation for their ability to activate $CD8^+$ T cell lines to produce IFN-γ as determined by ICS followed by FACS analysis. $CD8^+$ T cell activation was determined as frequency of IFN-γ expressing T cells specific for the indicated peptides derived from OVA or MVA antigens (B8, A3, K3, A19, D13). Data are represented as mean ± SD of **(A)** $n = 3$ or **(B,C)** $n = 2$ BMDC preparations from individual mice per group pooled from **(A)** three or **(B,C)** two independent experiments.

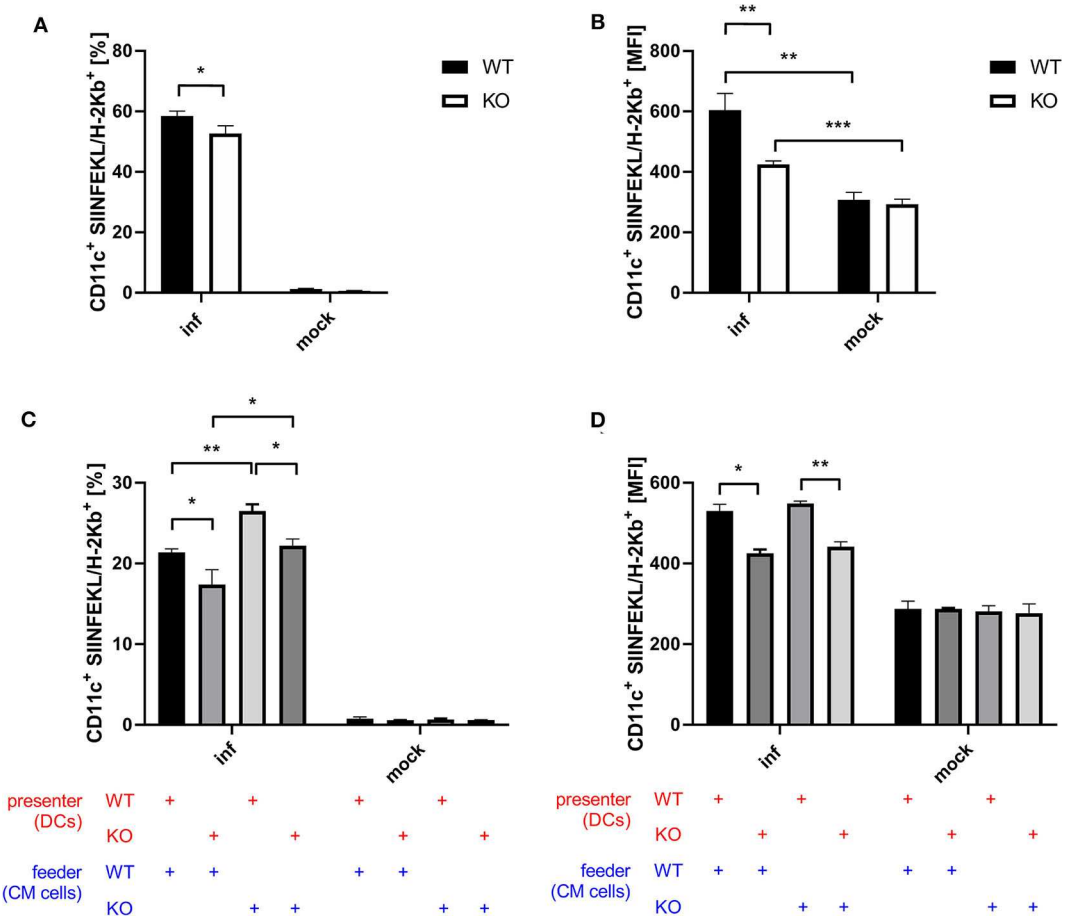

FIGURE 5 | STING in BMDC is crucial for efficient antigen processing and presentation while STING in feeder cells increases the size of the DC pool available for cross-presentation. **(A,B)** GM-CSF-BMDCs generated from STING KO mice (KO) or WT-littermates (WT) were infected with MVA-PK1L-OVA at MOI 1 (inf) or mock infected (mock). At 12 h post-infection SIINFEKL/K^b surface expression was determined. **(C,D)** The SIINFEKL/K^b loading ability of cross-presenting BMDCs was analyzed after co-culturing MVA-infected STING KO (feeder KO) or WT Cloudman (CM) feeder cells (feeder WT) with either STING KO (presenter KO) or WT BMDCs (presenter WT) for 20 h. Data are representative for one of two independent experiments and are presented as **(A,C)** frequencies (%) or **(B,D)** mean fluorescent intensities (MFI) and represent the mean ± SD of $n = 3$ BMDC preparations from individual mice per group. Statistical significance (P); $^*P \leq 0.05$; $^{**}P \leq 0.01$; $^{***}P \leq 0.001$.

recombinant MVA expressing SIINFEKL linked to eGFP for the infection of STING KO and WT BMDCs, we were able to distinguish infected (GFP-positive) from uninfected bystander BMDCs (GFP-negative). Interestingly, we observed that STING deficiency resulted in significantly reduced CD86 and MHC II expression in infected BMDCs and a significant decrease in the amount of MHC II (MFI) in MHC II high expressing BMDCs in the bystander population (**Figure 7A**). These results indicate that signaling via STING is not only relevant for maturation of directly infected BMDCs, but is also important for the maturation of bystander BMDCs. Furthermore, we tested if the presence or absence of STING in feeder cells or cross-presenting BMDCs has an effect on the maturation of BMDCs by co-culturing either MVA-infected STING KO or WT feeder cells with non-infected STING KO or WT BMDCs in a cross-presentation assay-like setting but without CTL (**Figures 7B,C**). CD40-expressing mature BMDCs were significantly diminished when infected STING-deficient feeder cells were used for co-cultivation, while there was no effect on CD86 or MHC II expression, if STING was absent in feeder cells (**Figure 7B**). STING deficiency in BMDC did not affect CD40 expression (**Figure 7B**), nor CD40 expression levels (MFI) of all groups (**Figure 7C**). In contrast, when STING was absent in BMDCs, we did not only observe a massive drop in CD86 and MHC II high expressing cells (**Figure 7B**), but also found a significantly reduced amount of these markers (MFI) on STING KO BMDCs (**Figure 7C**). Our data suggest that STING supports efficient maturation of directly infected BMDCs as well as bystander and cross-presenting BMDCs during infection with recombinant MVA.

STING Is Crucial for the Induction of Type I Interferon *in vitro* and *in vivo*

Dai et al. (37) demonstrated that the type I interferon response in BMDCs after infection with MVA is completely STING-dependent. Consistent with these results, we observed a

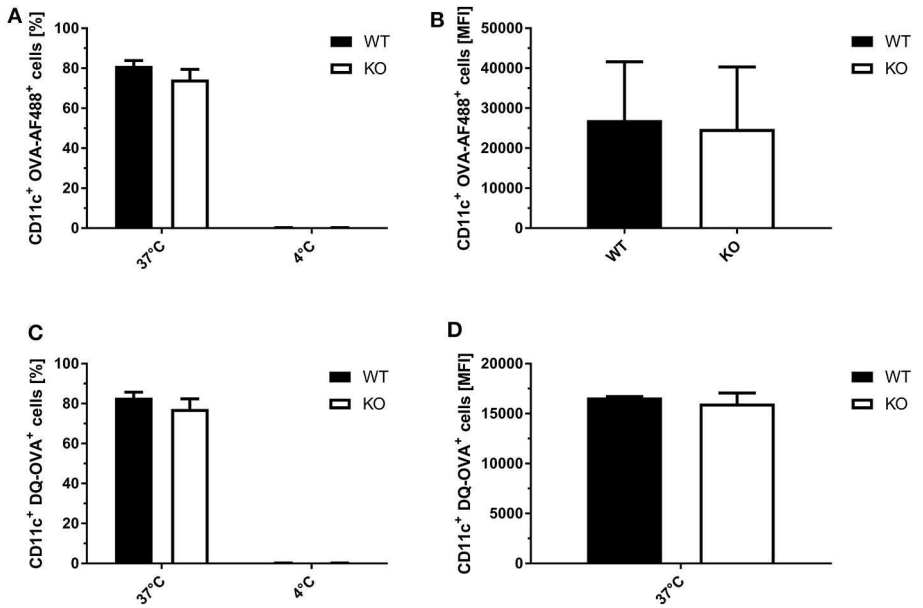

FIGURE 6 | STING KO and WT BMDCs showed comparable phagocytosis activity and endosomal function. **(A)** GM-CSF-BMDCs were generated from STING KO (KO) mice or wildtype littermates (WT). The phagocytic activity was analyzed using **(A,C)** OVA-AF488 or **(B,D)** DQ-OVA at 4 and 37°C. In addition, DQ-OVA **(B,D)** allowed to measure proteolytic activity resulting in increased fluorescence. Data are presented as **(A,B)** frequencies (%) or **(C,D)** mean fluorescent intensities (MFI) and represent the mean ± SD of $n = 3$ BMDC preparations from individual mice per group pooled from three independent experiments.

completely abrogated interferon-α (IFN-α) and -β (IFN-β) response determined *in vitro* in supernatants from infected STING-deficient BMDCs (**Figure 8A**). Similarly, cross-presenting BMDCs had no IFN-α and -β response when they were deficient for STING (**Figure 8B**). However, the presence or absence of STING in feeder cells had no impact on the induced type I interferon response in cross-presenting BMDCs (**Figure 8B**). Importantly, the observed type I interferon response arose from BMDCs only, because feeder cells were unable to produce type I interferons with or without MVA infection (**Supplementary Figure 7**). In line with the above findings, we observed the complete loss of IFN-β production when using spleen supernatants from vaccinated STING KO mice (**Figure 9A**). Furthermore, we saw a significantly reduced cytokine (**Figure 9A**) as well as chemokine response in STING-deficient mice (**Figure 9B**) affecting proinflammatory cytokines such as IL-1α, IL-6, MCP-1 (CCL2), IL-27 as well as IFN-γ (**Figure 9A**) and chemokines involved in T cell recruitment such as RANTES, MIP-1α/β, and MDC (**Figure 9B**).

DISCUSSION

The induction of a potent long-lasting antigen-specific $CD8^+$ T cell response is a fundamental aim of prophylactic and therapeutic vaccination strategies against many intracellular pathogens such as viruses. To achieve this goal, it is essential to understand the mechanisms and factors which determine the quality and quantity of vaccine-induced $CD8^+$ T cell immunity. Dai et al. (37) recently demonstrated that the production of type I interferon after infection of BMDCs with MVA *in vitro* was strictly STING-dependent. We were interested whether STING is also involved in the generation of an efficient type I interferon response *in vivo* and relevant for $CD8^+$ T cell immunity after viral vector vaccination using recombinant MVA. We showed in this study that an intact STING signaling pathway was crucial for the priming and development of a fully functional vaccinia virus-specific $CD8^+$ T cell response particularly in the acute phase (**Figures 1**, **2**). The absence of STING in vaccinated mice led to an overall reduced $CD8^+$ T cell response, but particularly affected the immunodominant B8-specific CTL response which is directed against an early gene product (**Figure 1**, **Supplementary Figure 2**). The entire genome replication of vaccinia virus and subsequent viral intermediate and late gene expression and translation takes place in organelles called viral factories (3, 58, 59). As a consequence late viral antigens such as A19 or D13 induce low $CD8^+$ T cell responses, not only because of a delayed expression kinetic in infected cells, but also due to the detention of late antigens in viral factories (**Figure 4A**) (50). Likewise, late antigens showed a reduced availability for cross-presentation by antigen presenting cells during infection (**Figures 4B,C**) (50, 60, 61). On the other hand, our *in vivo* data correlate with the results obtained from the phenotypical analysis of BMDC maturation (**Figure 7**). Since cross-priming plays a decisive role for the quality and quantity of the $CD8^+$ T cell response generated by MVA vaccination (42, 43), an intact and effective bystander BMDC maturation is likely essential. In fact, recent research demonstrated that the initial activation of $CD4^+$ and $CD8^+$ T cells is accomplished through both directly infected DCs

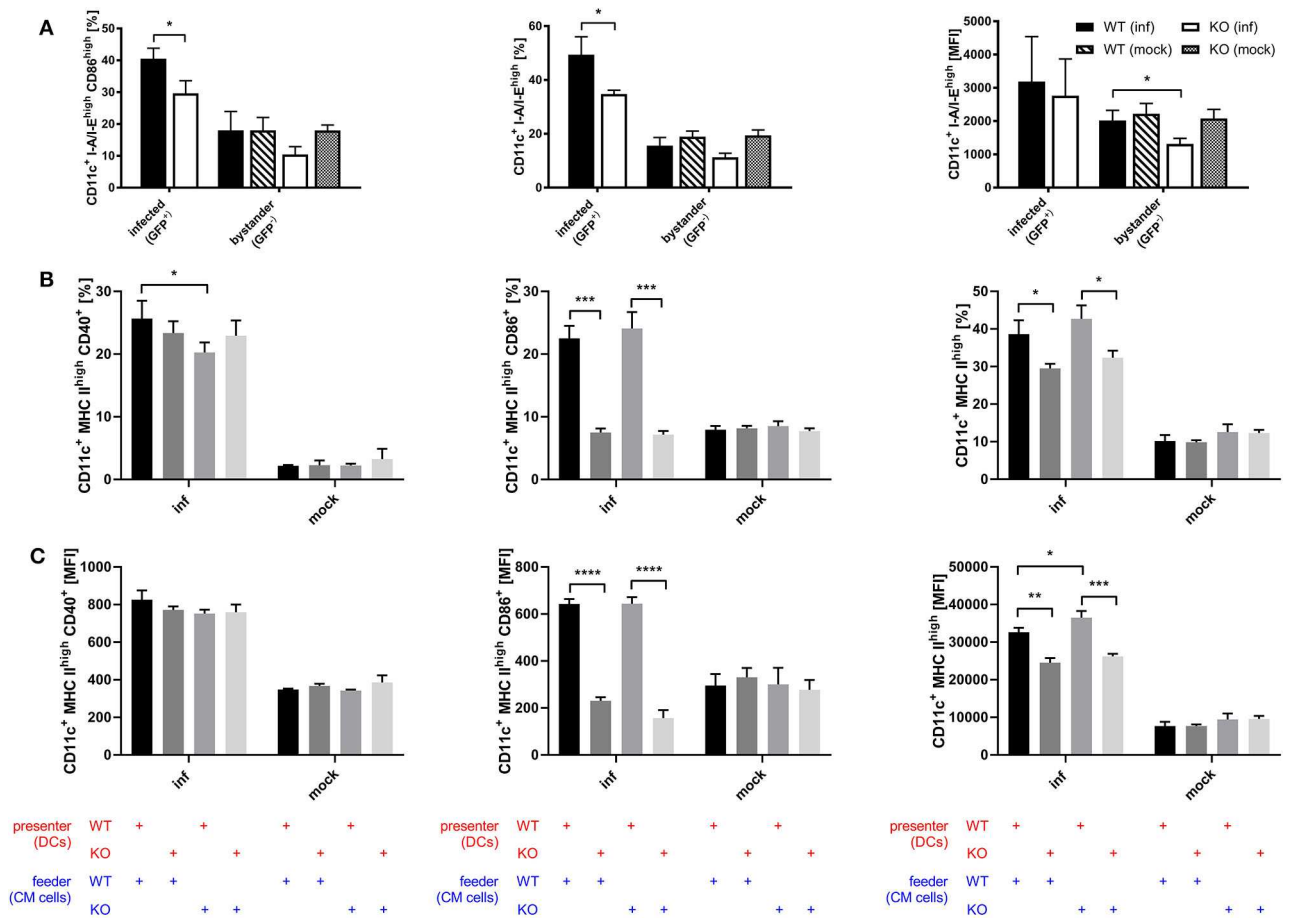

FIGURE 7 | STING strongly supports DC maturation. **(A)** GM-CSF-BMDCs were generated from STING KO mice (KO) and WT-littermates (WT), directly infected with MVA-P7.5-NP-SIINFEKL-eGFP at MOI 5 and analyzed 12 h post-infection for the expression of CD86 and MHC II. Here, infected BMDC were determined by GFP expression (GFP+), whereas accompanying non-infected bystander DC showed no GFP expression (GFP-). **(B,C)** The maturation of cross-presenting BMDCs was analyzed after co-culturing of MVA-PK1L-OVA-infected STING KO (feeder KO) or WT feeder cells (feeder WT) at MOI 1 with either STING KO (presenter KO) or WT BMDCs (presenter WT) for 20 h. Data are depicted as **(B)** frequencies (%) or **(C)** mean fluorescent intensities (MFI) for the expression of CD40, CD86, and MHC II and are presented as mean ± SD of $n = 3$ BMDC preparations from individual mice per group **(A)** pooled from three independent experiments or **(B,C)** representative for one of two independent experiments, each with $n = 3$ BMDC preparations from individual mice per group. Statistical significance (*P*); $^{*}P \leq 0.05$; $^{**}P \leq 0.01$; $^{***}P \leq 0.001$; $^{****}P \leq 0.0001$.

and non-infected bystander DCs (42, 62). In this context, non-infected XCR1$^+$ (CD8α$^+$) DCs were critical and responsible for the initial activation of naive CD8$^+$ T cells by cross-priming at later time points of infection and were supported by previously primed CD4$^+$ T cells (42, 62). Notably, a study by Brewitz et al. (63) indicates that also pDCs play a key role for a potent CD8$^+$ T cell response during viral infection. In particular, pDC depletion induced in Clec4c$^+$/DTR mice significantly impaired the host immune response to MVA infection. Animals without pDCs showed significantly reduced B8-specific IFN-γ-producing CD8$^+$ T cells which were mainly attributed to a lack of maturation of non-infected bystander (cross-presenting) XCR1$^+$ DC population due to a reduction of pDC-derived IFN-α. Interestingly, this was a strictly local effect as the total amount of IFN-α in the lymph nodes remained unaltered (63). Furthermore, we demonstrate for i.p. and i.m administration that the reduced function of CD8$^+$ T cells affected cytokine and chemokine production (**Figure 1**, **Supplementary Figure 2**). IFN-γ, CD107α and dependent on the route also MIP-1α were significantly reduced in immunodominant B8-specific CD8$^+$ T cells derived from STING KO compared to WT mice suggesting a broader functional impairment. The establishment of immunodominance depends on various factors (e.g., naïve T cell precursor frequency, T cell avidity, antigen processing efficacy, epitope binding affinity, etc.) which most likely differ for each ligand. As recently shown (64), there may be variations between vaccinia virus vaccine delivery platforms such as replication-competent vs. -deficient viruses, different insertion loci for target gene expression or the presence/absence of viral thymidine kinase by which immunodominance can be shaped to a certain degree, but it will not be reversed even in the absence of the immunodominant B8 epitope (49). In contrast

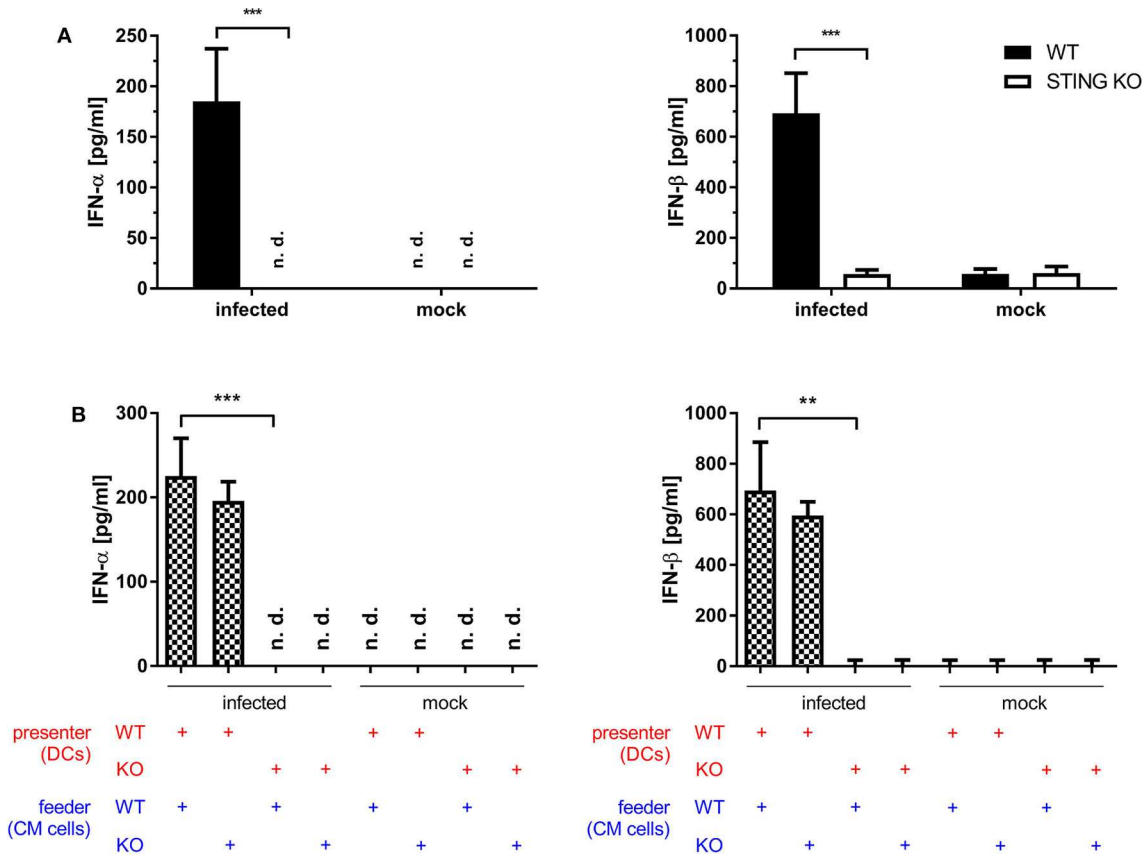

FIGURE 8 | STING is crucial for the induction of type I interferon *in vitro*. **(A)** GM-CSF-BMDCs generated from STING KO mice or WT-littermates were either directly infected with MVA-PK1L-OVA at MOI 1 or mock infected or **(B)** left uninfected, but co-cultivated with feeder cells which were infected with MVA-PK1L-OVA at MOI 1 for 12 h or left uninfected (mock). Supernatants were collected at **(A)** 12 h post-infection or **(B)** 12 h post co-cultivation and **(A,B)** concentrations of IFN-α and -β were determined by ELISA. In the co-culture setting, supernatants from co-cultures with either infected STING KO (feeder KO) or wildtype feeder cells (feeder WT) with either uninfected STING KO (presenter KO) or WT BMDCs (presenter WT) were taken at 12 h post co-culturing and tested. Data represent the mean ± SD of **(A)** $n = 4$ and **(B)** $n = 3$ BMDC preparations from individual mice per group pooled from three independent experiments. Statistical significance (P); $^{**}P \leq 0.01$; $^{***}P \leq 0.001$; n. d. = not detected.

to the systemic i.p. route, peripheral i.m. application resulted in additional decrease of T cells specific for some subdominant epitopes such as OVA and A3 in STING KO mice. A possible explanation may be the lower amount of CD86 on STING KO BMDCs making costimulation a limiting factor in these mice. This hypothesis is supported by Lin et al. (65) demonstrating that immunodominance was sharpened by peripheral i.d. or s.c. application of replication-competent vaccinia virus strain WR, but immunodomination of B8 could be reduced using recombinant WR expressing CD80 and CD86 for priming.

A potent activation of $CD8^+$ T cells leading to clonal expansion and effector function requires three signals: (I) TCR/antigen/MHC-I complex formation, (II) co-stimulatory receptor/ligand binding and (III) cytokine signals. STING-deficiency in infected as well as in cross-presenting BMDCs resulted in a decreased ability and efficiency in SIINFEKL/K^b-loading (**Figures 5A,B**), indicating defects in antigen processing and presentation. Importantly, we demonstrated that phagocytosis and endocytic uptake and degradative processing was not impaired in BMDCs when STING was absent (**Figure 6**, **Supplementary Figure 5**). However, STING-deficiency in these APC could not impair activation of antigen-specific $CD8^+$ T cell lines *in vitro* (**Figure 4**). Since effector $CD8^+$ T cells including our T cell lines need rather low epitope densities on the cell surface of antigen-presenting cells to become reactivated (66, 67), even significant differences in the amount of peptide/MHC I-complexes presented by STING KO and control BMDCs will result in comparable reactivation of primed or memory T cells. In contrast, priming of naïve T cells will be much more sensitive to reduced amounts of peptide/MHC I complexes and/or co-stimulatory molecules (68) which is in line with the reduced primary T cell response seen *in vivo* after vaccination (**Figures 1**, **2**). Similarly to infected BMDCs, the SIINFEKL/K^b-loading ability and efficacy of cross-presenting BMDCs was only impaired when STING was absent in the BMDC (**Figures 5C,D**). In addition, we showed that the STING phenotype of feeder cells had no impact on the epitope density of cross-presenting BMDCs (**Figure 5D**). Surprisingly, we noticed that STING

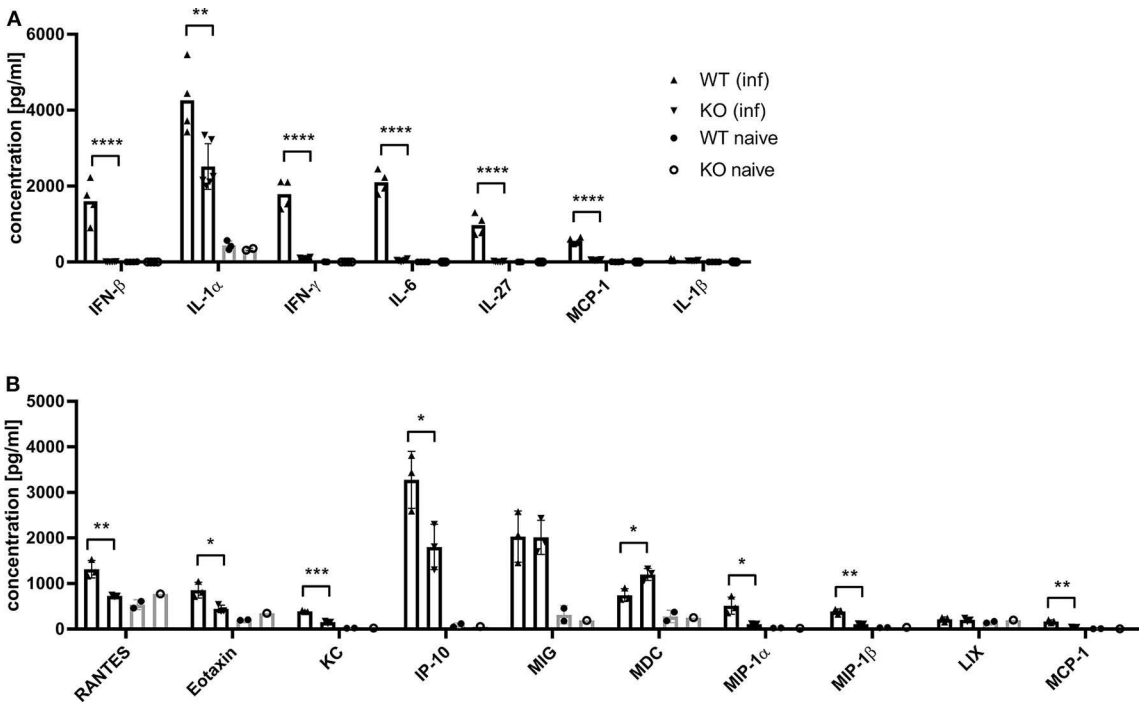

FIGURE 9 | MVA-vaccinated STING KO mice show a decreased cytokine and chemokine response. C57BL/6 mice (WT) and STING KO (KO) were i. p. infected with 1×10^8 IU MVA-PH5-OVA. After 6 h of infection, spleens were harvested, cell suspensions prepared and **(A)** cytokines or **(B)** chemokines were determined in spleen supernatants by cytoplex assay. Data from infected groups (WT inf, KO inf) are represented as mean ± SD of $n = 4$-6 (cytokines) and $n = 3$ (chemokines) mice per group pooled from two independent experiments. Naïve STING KO (KO naïve) and wildtype (WT naïve) mice were used as control and data are depicted as mean ± SD of $n = 2$-3 (cytokines) and $n = 2$ (chemokines) mice per group. Statistical significance (P); $^*P \leq 0.05$; $^{**}P \leq 0.01$; $^{***}P \leq 0.001$; $^{****}P \leq 0.0001$.

deficiency in feeder cells appeared to be highly beneficial for the activation of cross-presenting BMDCs promoting a dramatic increase of SIINFEKL/K^{b+} BMDCs (**Figure 5C**), suggesting that either alternative sensing pathways for MVA in STING KO feeder cells may be active (69) or STING in feeder cells may alter the ability of BMDCs to execute cross-presentation.

Optimal activation of T cell responses not only depends on the peptide/MHC complex density, but also on the correct DC phenotype namely mature or immature (63, 70). Maturation involves the expression of co-stimulatory molecules as well as the upregulation of MHC molecules, particularly MHC class II. Both are crucial for the generation of efficient T cell responses. CD86 which binds CD28 and CTLA-4 (71, 72) as well as CD40 interacting with CD40L (73) are important ligands for co-stimulation. We observed a dramatically reduced maturation in STING-deficient BMDCs with regard to the expression of CD86 and MHC II in directly as well as bystander and cross-presenting BMDCs, respectively (**Figure 7**). Interestingly, CD40 expression was not dependent on STING in BMDCs, but was significantly reduced when infected STING-deficient feeder cells were used in the cross-presentation setting indicating that exogenous STING-dependent signals other than type I IFN which was absent in feeder cells contributed to DC maturation.

Previous research has shown that many melanoma cells and cell lines have variable defects in interferon signaling pathways (74–76), which was also observed in the melanoma cell line that we used as feeder cells for this study (77, 78). Moreover, compared to infected BMDCs, we observed in MVA-infected S91 feeder cells a severely limited cytokine/chemokine response with a complete lack of type I and II interferons (**Supplementary Figure 7**). We anticipate that the most important factor related to STING deficiency in this model is likely the missing third signal from cytokines such as type I and type II interferons. In T cells, type I interferon triggers many important signaling cascades that are responsible for survival, proliferation and differentiation of effector cells (71, 79). An intact type I interferon response is essential for effective cross-priming *in vitro* and *in vivo* (80–82), and especially STING has been shown to be crucial for the expression of type I interferon (38, 39). In line with the findings of Dai et al. (37), we observed that production of type I interferon was completely STING-dependent in directly (**Figure 8A**) as well as cross-presenting BMDCs (**Figure 8B**). Ma et al. (83) showed that IFNAR1 knockout macrophages permit a lower induction of IFN-α4 and IFN-β compared to wildtype macrophages. They concluded that an intact IFNAR feedback loop was mandatory for optimal production of cGAMP-dependent type I interferons (83). It is also well-known that type I interferon suppresses the expression of various cytokines, including IL-12, and promotes the simultaneous expression of IFN-α and -β through a positive

feedback loop (84, 85). In this respect, Frenz et al. (86) were able to demonstrate that MVA infection in IFNAR knockout mice triggers the induction of IL-12 but fails to induce a type I interferon response. We therefore conclude that type I interferon and possibly other cytokines induced by MVA in a STING-dependent manner may act simultaneously on $CD8^+$ T cells as well as on dendritic cells to promote optimal T cell responses after a single vaccination *in vivo*.

In addition, STING was particularly important for the expansion/proliferation of immunodominant B8-specific $CD8^+$ T cells (**Figures 1B–D**, **2B,C**). Importantly, short-lived effector as well as effector memory T cells were significantly reduced in STING KO mice (**Figures 2D,E**). Berard et al. (87) and Mattei et al. (88) described that type I interferon together with IL-15 promote the homeostatic proliferation and maintenance of $CD8^+$ T memory cells *in vivo*. Similarly, IFN-α promotes the development of human $CD8^+$ T cells into memory cells (89). These findings correlate with our data indicating an impaired development of short-lived T cell memory with significant decrease of effector memory (EM) T cells (**Figure 2E**). This underlines the importance of STING-mediated type I interferon production during MVA infection for the quality of the acute response including effector and effector memory T cells. Interestingly, STING deficiency did not affect the long-term memory response mediated by central memory (CM) T cells (**Figures 2D,E**). The establishment of comparable long-term memory was corroborated by comparable T cell expansion seen after boost vaccinations at day 28 after priming in STING KO and WT mice (**Figure 3**), which indicates that STING is not required for efficient reactivation of memory T cells after secondary vaccination. It may be speculated that this also implies full protective capacity of vaccine-induced memory CTL against pathogen encounter.

Thus, STING signaling seems crucial for the innate and adaptive immune defense as demonstrated by the deficit production of a large array of cytokines and chemokines affecting the quality and quantity of relevant APC as well as anti-viral $CD8^+$ T cells. STING plays a decisive role for the primary induction and development of $CD8^+$ T cell responses in the acute phase during MVA infection *in vivo* which may allow for more rapid control and elimination of relevant pathogens in the vaccination setting. However, STING seems to be dispensable for the development of long-term CTL memory.

DATA AVAILABILITY STATEMENT

All datasets generated for this study are included in the article/**Supplementary Material**.

ETHICS STATEMENT

The animal study was reviewed and approved by North Rhine-Westphalia State Agency for Nature, Environment and Consumer Protection (LANUV), Germany.

AUTHOR'S NOTE

Parts of the study have been presented at the 17th International Congress of Immunology, Beijing, China, and an abstract is available as a conference paper at https://onlinelibrary.wiley.com/doi/abs/10.1002/eji.201970400.

AUTHOR CONTRIBUTIONS

CB, GC, and ST conducted experiments and analyzed the data. RT generated recMVA. DB provided multimers. LJ provided STING KO mice and WT littermates. ID designed the study and interpreted the data. ID, CB, and GC wrote the manuscript. All authors contributed to the article and approved the submitted version.

FUNDING

This work was supported by research funding from Deutsche Forschungsgemeinschaft (DFG) grant GK1949/1 to ID and the MOI III Graduate School.

ACKNOWLEDGMENTS

We thank Stefanie Weidtkamp-Peters (CAi-Center for Advanced Imaging, HHU, Düsseldorf) for support at the imaging facility. We are grateful to Maria Patra for generating MVA-Pe/l-Np-SIIN-eGFP and JW Yewdell (NIH, USA) for originally providing us with Np-SIIN-eGFP plasmid.

SUPPLEMENTARY MATERIAL

The Supplementary Material for this article can be found online at: https://www.frontiersin.org/articles/10.3389/fimmu.2020.01458/full#supplementary-material

REFERENCES

1. Cairns J. The initiation of vaccinia infection. *Virology*. (1960) 11:603–23. doi: 10.1016/0042-6822(60)90103-3
2. Dahl R, Kates JR. Intracellular structures containing vaccinia DNA: isolation and characterization. *Virology*. (1970) 42:453–62. doi: 10.1016/0042-6822(70)90288-6
3. Katsafanas G, Moss CB. Colocalization of transcription and translation within cytoplasmic poxvirus factories coordinates viral expression and subjugates host functions. *Cell Host Microbe*. (2007) 2:221–8. doi: 10.1016/j.chom.2007.08.005
4. Schramm B, de Haan C, Young A, Doglio J, Schleich L, Locker S, et al. Vaccinia-virus-induced cellular contractility facilitates the subcellular localization of the viral replication sites. *Traffic*. (2006) 7:1352–67. doi: 10.1111/j.1600-0854.2006.00470.x
5. Mayr A, Stickl H, Muller HK, Danner K, Singer H. [The smallpox vaccination strain MVA: marker, genetic structure, experience gained with the parenteral vaccination and behavior in organisms with a debilitated defence mechanism (author's transl)]. *Zentralbl Bakteriol B*. (1978) 167:375–90.
6. Mayr A, Munz E. [Changes in the vaccinia virus through continuing passages in chick embryo fibroblast cultures]. *Zentralbl Bakteriol Orig*. (1964) 195:24–35.
7. Meyer H, Sutter G, Mayr A. Mapping of deletions in the genome of the highly attenuated vaccinia virus MVA and their influence on virulence. *J Gen Virol*. (1991) 72(Pt 5):1031–8. doi: 10.1099/0022-1317-72-5-1031

8. Antoine G, Scheiflinger F, Dorner F, Falkner FG. The complete genomic sequence of the modified vaccinia Ankara strain: comparison with other orthopoxviruses. *Virology*. (1998) 244:365–96. doi: 10.1006/viro.1998.9123
9. Drexler I, Staib C, Kastenmuller W, Stevanovic S, Schmidt B, Lemonnier F, et al. Identification of vaccinia virus epitope-specific HLA-A*0201-restricted T cells and comparative analysis of smallpox vaccines. *Proc Natl Acad Sci USA*. (2003) 100:217–22. doi: 10.1073/pnas.262668999
10. Meisinger-Henschel C, Spath M, Lukassen S, Wolferstatter M, Kachelriess H, Baur K, et al. Introduction of the six major genomic deletions of modified vaccinia virus Ankara (MVA) into the parental vaccinia virus is not sufficient to reproduce an MVA-like phenotype in cell culture and in mice. *J Virol*. (2010) 84:9907–19. doi: 10.1128/JVI.00756-10
11. Carroll M, Moss WB. Host range and cytopathogenicity of the highly attenuated MVA strain of vaccinia virus: propagation and generation of recombinant viruses in a nonhuman mammalian cell line. *Virology*. (1997) 238:198–211. doi: 10.1006/viro.1997.8845
12. Drexler I, Heller K, Wahren B, Erfle V, Sutter G. Highly attenuated modified vaccinia virus Ankara replicates in baby hamster kidney cells, a potential host for virus propagation, but not in various human transformed and primary cells. *J Gen Virol*. (1998) 79(Pt 2):347–52. doi: 10.1099/0022-1317-79-2-347
13. Baldick CJ, Moss B Jr. Characterization and temporal regulation of mRNAs encoded by vaccinia virus intermediate-stage genes. *J Virol*. (1993) 67:3515–27. doi: 10.1128/JVI.67.6.3515-3527.1993
14. Yang Z, Maruri-Avidal L, Sisler J, Stuart C, Moss AB. Cascade regulation of vaccinia virus gene expression is modulated by multistage promoters. *Virology*. (2013) 447:213–20. doi: 10.1016/j.virol.2013.09.007
15. Sutter G, Moss B. Nonreplicating vaccinia vector efficiently expresses recombinant genes. *Proc Natl Acad Sci USA*. (1992) 89:10847–51. doi: 10.1073/pnas.89.22.10847
16. De Vries RD, Altenburg AF, Nieuwkoop NJ, De Bruin E, Van Trierum SE, Pronk MR, et al. Induction of cross-clade antibody and T-cell responses by a modified vaccinia virus ankara-based influenza A(H5N1) vaccine in a randomized phase 1/2a clinical trial. *J Infect Dis*. (2018) 218:614–23. doi: 10.1093/infdis/jiy214
17. Guo ZS, Lu B, Guo Z, Giehl E, Feist M, Dai E, et al. Vaccinia virus-mediated cancer immunotherapy: cancer vaccines and oncolytics. *J Immunother Cancer*. (2019) 7:6. doi: 10.1186/s40425-018-0495-7
18. Samreen B, Tao S, Tischer K, Adler H, Drexler I. ORF6 and ORF61 Expressing MVA vaccines impair early but not late latency in murine gammaherpesvirus MHV-68 infection. *Front Immunol*. (2019) 10:2984. doi: 10.3389/fimmu.2019.02984
19. Akira S, Uematsu S, Takeuchi O. Pathogen recognition and innate immunity. *Cell*. (2006) 124:783–801. doi: 10.1016/j.cell.2006.02.015
20. Beutler B, Eidenschenk C, Crozat K, Imler J, Takeuchi L, Akira O, et al. Genetic analysis of resistance to viral infection. *Nat Rev Immunol*. (2007) 7:753–66. doi: 10.1038/nri2174
21. Medzhitov R. Recognition of microorganisms and activation of the immune response. *Nature*. (2007) 449:819–26. doi: 10.1038/nature06246
22. Iwasaki A, Medzhitov R. Regulation of adaptive immunity by the innate immune system. *Science*. (2010) 327:291–5. doi: 10.1126/science.1183021
23. Takeuchi O, Akira S. Pattern recognition receptors and inflammation. *Cell*. (2010) 140:805–20. doi: 10.1016/j.cell.2010.01.022
24. Goubau D, Deddouche S, Reis e Sousa C. Cytosolic sensing of viruses. *Immunity*. (2013) 38:855–69. doi: 10.1016/j.immuni.2013.05.007
25. O'Neill LA. Immunology. Sensing the dark side of DNA. *Science*. (2013) 339:763–4. doi: 10.1126/science.1234724
26. Kranzusch PJ, Lee AS, Berger JM, Doudna JA. Structure of human cGAS reveals a conserved family of second-messenger enzymes in innate immunity. *Cell Rep*. (2013) 3:1362–8. doi: 10.1016/j.celrep.2013.05.008
27. Sun L, Wu J, Du F, Chen X, Chen ZJ. Cyclic GMP-AMP synthase is a cytosolic DNA sensor that activates the type I interferon pathway. *Science*. (2013) 339:786–91. doi: 10.1126/science.1232458
28. Civril F, Deimling T, de Oliveira Mann CC, Ablasser A, Moldt M, Witte G, et al. Structural mechanism of cytosolic DNA sensing by cGAS. *Nature*. (2013) 498:332–7. doi: 10.1038/nature12305
29. Gao P, Ascano M, Wu Y, Barchet W, Gaffney B, Patel L, et al. Cyclic [G(2',5')pA(3',5')p] is the metazoan second messenger produced by DNA-activated cyclic GMP-AMP synthase. *Cell*. (2013) 153:1094–107. doi: 10.1016/j.cell.2013.04.046
30. Li X, Shu C, Yi G, Chaton C, Shelton T, Li C, et al. Cyclic GMP-AMP synthase is activated by double-stranded DNA-induced oligomerization. *Immunity*. (2013) 39:1019–31. doi: 10.1016/j.immuni.2013.10.019
31. Zhang X, Wu J, Du F, Xu H, Sun L, Chen Z, et al. The cytosolic DNA sensor cGAS forms an oligomeric complex with DNA and undergoes switch-like conformational changes in the activation loop. *Cell Rep*. (2014) 6:421–30. doi: 10.1016/j.celrep.2014.01.003
32. Ishikawa H, Barber GN. STING is an endoplasmic reticulum adaptor that facilitates innate immune signalling. *Nature*. (2008) 455:674–8. doi: 10.1038/nature07317
33. Ablasser A, Goldeck M, Cavlar T, Deimling T, Witte G, Rohl I, et al. cGAS produces a 2'-5'-linked cyclic dinucleotide second messenger that activates STING. *Nature*. (2013) 498:380–4. doi: 10.1038/nature12306
34. Zhang X, Shi H, Wu J, Zhang X, Sun L, Chen C, et al. Cyclic GMP-AMP containing mixed phosphodiester linkages is an endogenous high-affinity ligand for STING. *Mol Cell*. (2013) 51:226–35. doi: 10.1016/j.molcel.2013.05.022
35. Liu S, Cai X, Wu J, Cong Q, Chen X, Li T, et al. Phosphorylation of innate immune adaptor proteins MAVS, STING, and TRIF induces IRF3 activation. *Science*. (2015) 347:aaa2630. doi: 10.1126/science.aaa2630
36. Chen Q, Sun L, Chen ZJ. Regulation and function of the cGAS-STING pathway of cytosolic DNA sensing. *Nat Immunol*. (2016) 17:1142–9. doi: 10.1038/ni.3558
37. Dai P, Wang W, Cao H, Avogadri F, Dai L, Drexler I, et al. Modified vaccinia virus Ankara triggers type I IFN production in murine conventional dendritic cells via a cGAS/STING-mediated cytosolic DNA-sensing pathway. *PLoS Pathog*. (2014) 10:e1003989. doi: 10.1371/journal.ppat.1003989
38. McWhirter SM, Barbalat R, Monroe KM, Fontana MF, Hyodo M, Joncker NT, et al. A host type I interferon response is induced by cytosolic sensing of the bacterial second messenger cyclic-di-GMP. *J Exp Med*. (2009) 206:1899–911. doi: 10.1084/jem.20082874
39. Chen H, Sun H, You F, Sun W, Zhou X, Chen L, et al. Activation of STAT6 by STING is critical for antiviral innate immunity. *Cell*. (2011) 147:436–46. doi: 10.1016/j.cell.2011.09.022
40. Abe T, Barber GN. Cytosolic-DNA-mediated, STING-dependent proinflammatory gene induction necessitates canonical NF-kappaB activation through TBK1. *J Virol*. (2014) 88:5328–41. doi: 10.1128/JVI.00037-14
41. Bajénoff M, Egen JG, Koo LY, Laugier JP, Brau F, Glaichenhaus N, et al. Stromal cell networks regulate lymphocyte entry, migration, and territoriality in lymph nodes. *Immunity*. (2006) 25:989–1001. doi: 10.1016/j.immuni.2006.10.011
42. Eickhoff S, Brewitz A, Gerner MY, Klauschen F, Komander K, Hemmi H, et al. Robust anti-viral immunity requires multiple distinct t cell-dendritic cell interactions. *Cell*. (2015) 162:1322–37. doi: 10.1016/j.cell.2015.08.004
43. Gasteiger G, Kastenmuller W, Ljapoci R, Sutter G, Drexler I. Cross-priming of cytotoxic T cells dictates antigen requisites for modified vaccinia virus Ankara vector vaccines. *J Virol*. (2007) 81:11925–36. doi: 10.1128/JVI.00903-07
44. Kagi D, Ledermann B, Burki K, Seiler P, Odermatt B, Olsen K, et al. Cytotoxicity mediated by T cells and natural killer cells is greatly impaired in perforin-deficient mice. *Nature*. (1994) 369:31–7. doi: 10.1038/369031a0
45. Wolint P, Betts MR, Koup RA, Oxenius A. Oxenius: Immediate cytotoxicity but not degranulation distinguishes effector and memory subsets of CD8+ T cells. *J Exp Med*. (2004) 199:925–36. doi: 10.1084/jem.20031799
46. Liu D, Bryceson Y, Meckel T, Vasiliver-Shamis T, Dustin G, Long M, et al. Integrin-dependent organization and bidirectional vesicular traffic at cytotoxic immune synapses. *Immunity*. (2009) 31:99–109. doi: 10.1016/j.immuni.2009.05.009
47. Krzewski K, Gil-Krzewska A, Nguyen V, Peruzzi G, Coligan JE. LAMP1/CD107a is required for efficient perforin delivery to lytic granules and NK-cell cytotoxicity. *Blood*. (2013) 121:4672–83. doi: 10.1182/blood-2012-08-453738
48. Jin L, Hill KK, Filak H, Mogan J, Knowles H, Zhang B, et al. MPYS is required for IFN response factor 3 activation and type I IFN production in the response of cultured phagocytes to bacterial second messengers cyclic-di-AMP and cyclic-di-GMP. *J Immunol*. (2011) 187:2595–601. doi: 10.4049/jimmunol.1100088

49. Kastenmuller W, Gasteiger G, Gronau J, Baier H, Ljapoci R, Drexler R, et al. Cross-competition of CD8(+) T cells shapes the immunodominance hierarchy during boost vaccination. *J Exp Med.* (2007) 204:2187–98. doi: 10.1084/jem.20070489
50. Tao S, Tao R, Busch DH, Widera M, Schaal H, Drexler I. Sequestration of late antigens within viral factories impairs MVA vector-induced protective memory CTL responses. *Front Immunol.* (2019) 10:2850. doi: 10.3389/fimmu.2019.02850
51. Drexler I, Staib C, Sutter G. Modified vaccinia virus Ankara as antigen delivery system: how can we best use its potential? *Curr Opin Biotechnol.* (2004) 15:506–12. doi: 10.1016/j.copbio.2004.09.001
52. Beeton C, Chandy KG. Preparing T cell growth factor from rat splenocytes. *J Vis Exp.* (2007). doi: 10.3791/402
53. Thiele F, Tao S, Zhang Y, Muschaweckh A, Zollmann T, Protzer U, et al. Modified vaccinia virus Ankara-infected dendritic cells present CD4+ T-cell epitopes by endogenous major histocompatibility complex class II presentation pathways. *J Virol.* (2015) 89:2698–709. doi: 10.1128/JVI.03244-14
54. Vatner RE, Janssen EM. STING, DCs and the link between innate and adaptive tumor immunity. *Mol Immunol.* (2019) 110:13–23. doi: 10.1016/j.molimm.2017.12.001
55. Laursen MF, Christensen E, Degn LL, Jønsson K, Jakobsen MR, Agger R, et al. CD11c-targeted delivery of DNA to dendritic cells leads to cGAS- and STING-dependent Maturation. *J Immunother.* (2018) 41:9–18. doi: 10.1097/CJI.0000000000000195
56. Dai P, Wang W, Yang N, Serna-Tamayo C, Ricca J, Deng M, et al. Intratumoral delivery of inactivated modified vaccinia virus Ankara (iMVA) induces systemic antitumor immunity via STING and Batf3-dependent dendritic cells. *Sci Immunol.* (2017) 2:eaal1713. doi: 10.1126/sciimmunol.aal1713
57. Rudd BD, Luker GD, Luker KE, Peebles RS, Lukacs NW. Type I interferon regulates respiratory virus infected dendritic cell maturation and cytokine production. *Viral Immunol.* (2007) 20:531–40. doi: 10.1089/vim.2007.0057
58. Lin YC, Evans DH. Vaccinia virus particles mix inefficiently, and in a way that would restrict viral recombination, in coinfected cells. *J Virol.* (2010) 84:2432–43. doi: 10.1128/JVI.01998-09
59. Tolonen N, Doglio L, Schleich S, Krijnse Locker J. Vaccinia virus DNA replication occurs in endoplasmic reticulum-enclosed cytoplasmic mini-nuclei. *Mol Biol Cell.* (2001) 12:2031–46. doi: 10.1091/mbc.12.7.2031
60. Tewalt EF, Grant JM, Granger EL, Palmer DC, Heuss ND, Gregerson DS, et al. Viral sequestration of antigen subverts cross presentation to CD8(+) T cells. *PLoS Pathog.* (2009) 5:e1000457. doi: 10.1371/journal.ppat.1000457
61. Niu TK, Princiotta MF, Sei JJ, Norbury CC. Analysis of MHC class i processing pathways that generate a response to vaccinia virus late proteins. *Immunohorizons.* (2019) 3:559–72. doi: 10.4049/immunohorizons.1900074
62. Hor JL, Whitney PG, Zaid A, Brooks AG, Heath WR, Mueller SN. Spatiotemporally distinct interactions with dendritic cell subsets facilitates CD4+ and CD8+ T cell activation to localized viral infection. *Immunity.* (2015) 43:554–65. doi: 10.1016/j.immuni.2015.08.018
63. Brewitz A, Eickhoff S, Dahling S, Quast T, Bedoui S, Kroczek R, et al. CD8(+) T cells orchestrate pDC-XCR1(+) dendritic cell spatial and functional cooperativity to optimize priming. *Immunity.* (2017) 46:205–19. doi: 10.1016/j.immuni.2017.01.003
64. Wong YC, Croft S, Smith SA, Lin LC, Cukalac T, La Gruta NL, et al. Modified vaccinia virus ankara can induce optimal CD8(+) T cell responses to directly primed antigens depending on vaccine design. *J Virol.* (2019) 93:e01154–19. doi: 10.1128/JVI.01154-19
65. Lin LC, Flesch IE, Tscharke DC. Immunodomination during peripheral vaccinia virus infection. *PLoS Pathog.* (2013) 9:e1003329. doi: 10.1371/journal.ppat.1003329
66. González PA, Carreño LJ, Coombs D, Mora JE, Palmieri E, Goldstein B, et al. T cell receptor binding kinetics required for T cell activation depend on the density of cognate ligand on the antigen-presenting cell. *Proc Natl Acad Sci USA.* (2005) 102:4824–9. doi: 10.1073/pnas.0500922102
67. Krogsgaard M, Davis MM. How T cells 'see' antigen. *Nat Immunol.* (2005) 6:239–45. doi: 10.1038/ni1173
68. Pennock ND, White JT, Cross EW, Cheney EE, Tamburini BA, Kedl RM. T cell responses: naive to memory and everything in between. *Adv Physiol Educ.* (2013) 37:273–83. doi: 10.1152/advan.00066.2013
69. Delaloye J, Roger T, Steiner-Tardivel Q, Le Roy G, Knaup Reymond D, Calandra M, et al. Innate immune sensing of modified vaccinia virus Ankara (MVA) is mediated by TLR2-TLR6, MDA-5 and the NALP3 inflammasome. *PLoS Pathog.* (2009) 5:e1000480. doi: 10.1371/journal.ppat.1000480
70. Pascutti MF, Rodríguez AM, Falivene J, Giavedoni L, Drexler I, Gherardi MM. Interplay between modified vaccinia virus ankara and dendritic cells: phenotypic and functional maturation of bystander dendritic cells. *J Virol.* (2011) 85:5532–45. doi: 10.1128/JVI.02267-10
71. Crouse J, Kalinke U, Oxenius A. Regulation of antiviral T cell responses by type I interferons. *Nat Rev Immunol.* (2015) 15:231–42. doi: 10.1038/nri3806
72. Thiel M, Wolfs MJ, Bauer S, Wenning AS, Burckhart T, Schwarz EC, et al. Efficiency of T-cell costimulation by CD80 and CD86 cross-linking correlates with calcium entry. *Immunology.* (2010) 129:28–40. doi: 10.1111/j.1365-2567.2009.03155.x
73. Elgueta R, Benson MJ, De Vries VC, Wasiuk A, Guo Y, Noelle RJ. Molecular mechanism and function of CD40/CD40L engagement in the immune system. *Immunol Rev.* (2009) 229:152–72. doi: 10.1111/j.1600-065X.2009.00782.x
74. Alavi S, Stewart AJ, Kefford RF, Lim SY, Shklovskaya E, Rizos H. Interferon signaling is frequently downregulated in melanoma. *Front Immunol.* (2018) 9:1414. doi: 10.3389/fimmu.2018.01414
75. Respa A, Bukur J, Ferrone S, Pawelec G, Zhao Y, Wang E, et al. Association of IFN-gamma signal transduction defects with impaired HLA class I antigen processing in melanoma cell lines. *Clin Cancer Res.* (2011) 17:2668–78. doi: 10.1158/1078-0432.CCR-10-2114
76. Rodriguez T, Mendez R, Del Campo A, Jimenez P, Aptsiauri N, Garrido F. Distinct mechanisms of loss of IFN-gamma mediated HLA class I inducibility in two melanoma cell lines. *BMC Cancer.* (2007) 7:34. doi: 10.1186/1471-2407-7-34
77. Kameyama K, Tanaka S, Ishida Y, Hearing VJ. Interferons modulate the expression of hormone receptors on the surface of murine melanoma cells. *J Clin Invest.* (1989) 83:213–21. doi: 10.1172/JCI113861
78. Peter I, Mezzacasa A, LeDonne P, Dummer R, Hemmi S. Comparative analysis of immunocritical melanoma markers in the mouse melanoma cell lines B16, K1735 and S91-M3. *Melanoma Res.* (2001) 11:21–30. doi: 10.1097/00008390-200102000-00003
79. Welsh RM, Bahl K, Marshall HD, Urban SL. Type 1 interferons and antiviral CD8 T-cell responses. *PLoS Pathog.* (2012) 8:e1002352. doi: 10.1371/journal.ppat.1002352
80. Lorenzi S, Mattei F, Sistigu A, Bracci L, Spadaro F, Sanchez M, et al. Type I IFNs control antigen retention and survival of CD8alpha(+) dendritic cells after uptake of tumor apoptotic cells leading to cross-priming. *J Immunol.* (2011) 186:5142–50. doi: 10.4049/jimmunol.1004163
81. Schiavoni G, Mattei F, Gabriele L. Type I interferons as stimulators of DC-mediated cross-priming: impact on anti-tumor response. *Front Immunol.* (2013) 4:483. doi: 10.3389/fimmu.2013.00483
82. Spadaro F, Lapenta C, Donati S, Abalsamo L, Barnaba V, Belardelli F, et al. IFN-α enhances cross-presentation in human dendritic cells by modulating antigen survival, endocytic routing, and processing. *Blood.* (2012) 119:1407–17. doi: 10.1182/blood-2011-06-363564
83. Ma F, Li B, Yu Y, Iyer SS, Sun M, Cheng G. Positive feedback regulation of type I interferon by the interferon-stimulated gene STING. *EMBO Rep.* (2015) 16:202–12. doi: 10.15252/embr.201439366
84. Cousens LP, Peterson R, Hsu S, Dorner A, Altman JD, Ahmed R, et al. Two roads diverged: interferon alpha/beta- and interleukin 12-mediated pathways in promoting T cell interferon gamma responses during viral infection. *J Exp Med.* (1999) 189:1315–28. doi: 10.1084/jem.189.8.1315
85. Dalod M, Salazar-Mather TP, Malmgaard L, Lewis C, Asselin-Paturel C, Brière F, et al. Interferon α/β and interleukin 12 responses to viral infections: pathways regulating dendritic cell cytokine expression *in vivo*. *J Exp Med.* (2002) 195:517–28. doi: 10.1084/jem.20011672
86. Frenz T, Waibler Z, Hofmann J, Hamdorf M, Lantermann M, Reizis B, et al. Concomitant type I IFN receptor-triggering of T cells and of DC is required to promote maximal modified vaccinia virus Ankara-induced T-cell expansion. *Eur J Immunol.* (2010) 40:2769–77. doi: 10.1002/eji.201040453

87. Berard M, Brandt K, Bulfone-Paus S, Tough DF. IL-15 promotes the survival of naive and memory phenotype CD8+ T cells. *J Immunol.* (2003) 170:5018–26. doi: 10.4049/jimmunol.171.4.2170-a
88. Mattei F, Schiavoni G, Belardelli F, Tough DF. IL-15 is expressed by dendritic cells in response to type I IFN, double-stranded RNA, or lipopolysaccharide and promotes dendritic cell activation. *J Immunol.* (2001) 167:1179–87. doi: 10.4049/jimmunol.167.3.1179
89. Ramos HJ, Davis AM, Cole AG, Schatzle JD, Forman J, Farrar JD. Reciprocal responsiveness to interleukin-12 and interferon-alpha specifies human CD8+ effector versus central memory T-cell fates. *Blood.* (2009) 113:5516–25. doi: 10.1182/blood-2008-11-188458

Conflict of Interest: The authors declare that the research was conducted in the absence of any commercial or financial relationships that could be construed as a potential conflict of interest.

frontiers in Immunology

ORIGINAL RESEARCH
published: 24 September 2020
doi: 10.3389/fimmu.2020.575818

The Human-Specific STING Agonist G10 Activates Type I Interferon and the NLRP3 Inflammasome in Porcine Cells

Sheng-Li Ming†, Lei Zeng†, Yu-Kun Guo†, Shuang Zhang, Guo-Li Li, Ying-Xian Ma, Yun-Yun Zhai, Wen-Ru Chang, Le Yang, Jiang Wang, Guo-Yu Yang* and Bei-Bei Chu**

College of Veterinary Medicine, Henan Agricultural University, Zhengzhou, China

OPEN ACCESS

Edited by:
Michael Schotsaert, Icahn School of Medicine at Mount Sinai, United States

Reviewed by:
Guangxun Meng, Institut Pasteur of Shanghai (CAS), China
Kailang Wu, Wuhan University, China
Jianguo Wu, Wuhan University, China

***Correspondence:**
Guo-Yu Yang
haubiochem@163.com
Bei-Bei Chu
chubeibei_hau@hotmail.com
Jiang Wang
wangjiang_hau@hotmail.com

† These authors have contributed equally to this work

Specialty section:
This article was submitted to Molecular Innate Immunity, a section of the journal Frontiers in Immunology

Received: *24 June 2020*
Accepted: *28 August 2020*
Published: *24 September 2020*

Citation:
Ming S-L, Zeng L, Guo Y-K, Zhang S, Li G-L, Ma Y-X, Zhai Y-Y, Chang W-R, Yang L, Wang J, Yang G-Y and Chu B-B (2020) The Human-Specific STING Agonist G10 Activates Type I Interferon and the NLRP3 Inflammasome in Porcine Cells. Front. Immunol. 11:575818. doi: 10.3389/fimmu.2020.575818

Pigs have anatomical and physiological characteristics comparable to those in humans and, therefore, are a favorable model for immune function research. Interferons (IFNs) and inflammasomes have essential roles in the innate immune system. Here, we report that G10, a human-specific agonist of stimulator of interferon genes (STING), activates both type I IFN and the canonical NLRP3 inflammasome in a STING-dependent manner in porcine cells. Without a priming signal, G10 alone transcriptionally stimulated Sp1-dependent *p65* expression, thus triggering activation of the nuclear factor-κB (NF-κB) signaling pathway and thereby priming inflammasome activation. G10 was also found to induce potassium efflux- and NLRP3/ASC/Caspase-1-dependent secretion of IL-1β and IL-18. Pharmacological and genetic inhibition of NLRP3 inflammasomes increased G10-induced type I IFN expression, thereby preventing virus infection, suggesting negative regulation of the NLRP3 inflammasome in the IFN response in the context of STING-mediated innate immune activation. Overall, our findings reveal a new mechanism through which G10 activates the NLRP3 inflammasome in porcine cells and provide new insights into STING-mediated innate immunity in pigs compared with humans.

Keywords: STING agonist, NLRP3 inflammasome, interferon, negative regulation, innate immunity

INTRODUCTION

The innate immune system detects pathogen-associated molecular patterns (PAMPs) or danger-associated molecular patterns (DAMPs) *via* germline-encoded pattern recognition receptors (PRRs) (1). Subsequently, innate immune responses are activated, and inflammatory cytokines, such as interferons (IFNs), proinflammatory cytokines, and chemokines, are generated. DAMPs and PAMPs comprise self- and foreign-derived double-stranded DNA in the cytosol (2). Stimulator of interferon genes (STING) is an ER-resident adaptor protein that is critical in mediating the signaling triggered by cytosolic nucleic acids (3, 4). After activation by an agonist, STING undergoes a conformational change resulting in the recruitment of TANK binding kinase (TBK1) to STING (5, 6). TBK1 subsequently phosphorylates IFN-regulated factor 3 (IRF3) and nuclear factor-κB (NF-κB), which translocate into the nucleus and stimulate expression of type I IFN and proinflammatory cytokines (7). Given the importance of the STING-mediated pathway in the activation of innate immunity and host protection from pathogens, harnessing the innate immunity activated by STING agonists is a promising strategy for antiviral and antitumor therapeutics (8, 9). G10 is

a synthetic small molecule that indirectly activates human STING and triggers IRF3-dependent IFNs expression but not NF-κB activation, thereby protecting against infection with emerging alphaviruses (10).

Inflammasomes are intracellular supramolecular complexes that assemble in response to the detection of microbial infection or stress-associated stimuli in innate immunity. The assembly of inflammasomes is a well-regulated process initiated by the recognition of DAMPs and PAMPs by PRRs (11). The nucleotide-binding domain, leucine-rich-repeat-containing proteins (NLRs), including NLRP1, NLRP3, NLRP6, NLRP7, and NLRP9, are notable inflammasome-forming PRRs (12–17). The NLRP3 inflammasome, the best-characterized inflammasome, contains NLRP3, the adaptor protein apoptosis-associated speck-like protein containing a caspase-recruitment domain (ASC) and the proinflammatory protein Caspase-1 (18). Activation of the NLRP3 inflammasome requires a priming signal and an activating signal. The priming process often involves TLRs, which activate NF-κB, thus resulting in the expression and activation of NLRP3, pro–IL-1β, and pro–IL-18 (19). Canonical activation is characterized by the oligomerization of NLRP3, ASC, and pro–Caspase-1, thus leading to the maturation of the proinflammatory cytokines IL-1β and IL-18, and the induction of pyroptotic cell death (20). The NLRP3 inflammasome is activated after exposure to a broad range of signals, including potassium efflux, calcium mobilization, mitochondrial damage, and reactive oxygen species (ROS) (21–24).

Activation of innate immunity by DAMPs and PAMPs usually leads to type I IFN expression and inflammasome activation. Because IL-1β, IL-18, and type I IFN are key players in both infectious and autoimmune diseases, reciprocal regulation between IFNs and inflammasome is essential for immune homeostasis. Type I IFN has been reported to induce Caspase-11 expression, thereby activating non-canonical inflammasome (25), whereas other studies have suggested that type I IFN inhibits inflammasome activation (26). IFN-inducible PYRIN domain (PYD)-only protein 3 interferes with the interaction between absent in melanoma 2 (AIM2) and ASC, thus inhibiting the AIM2 inflammasome (27). Another IFN-inducible protein, cholesterol 25-hydroxylase, converts cholesterol into 25-hydroxycholesterol, thus inhibiting pro–L-1β transcription and inflammasome activation (28). In contrast, type I IFN is antagonized by inflammasomes (29, 30). Caspase-1 cleaves cyclic GMP-AMP synthase (cGAS), thus inhibiting cGAS-STING-mediated type I IFN production (31).

Pigs are a validated model for use in biomedical research fields, such as xenotransplantation and immune disorders (32, 33). However, the interplay between type I IFN and inflammasomes has not been well documented in pigs to date. Here, we report that G10 triggers the activation of a STING-dependent type I IFN response and the NLRP3 inflammasome in porcine cells. G10 provides priming and activating signals, both of which are required for NLRP3 inflammasome activation. Furthermore, the NLRP3 inflammasome negatively regulates the type I IFN response in porcine cells after G10 treatment. Our results reveal a new mechanism through which G10 activates the NLRP3 inflammasome in porcine cells.

MATERIALS AND METHODS

Antibodies and Reagents

The antibodies anti-P65 (#8242), anti-p-P65 (#3033), and anti-Lamin B1 (#13435) were from Cell Signaling Technology; anti-Flag M2 (F1804) was from Sigma; anti-Sp1 (10500-1-AP), anti-ASC (21962-1-AP), and anti-β-actin (20536-1-AP) were from Proteintech; anti-IL-1β was from R&D Systems (AF-401-NA); anti-Caspase-1 was from Santa Cruz Biotechnology (sc-398715).

G10 (HY-19711), LPS (HY-D1056), ATP (HY-B2176), nigericin (HY-127019), MCC950 (HY-12815), and VX765 (HY-13205) were from MedChemExpress; and CL097 (tlrl-c97) was from InvivoGen.

Cells and Viruses

PK-15 (CCL-33, ATCC), 3D4/21 (CRL-2843, ATCC), HEK293 (CRL-1573, ATCC), HEK293T (CRL-11268, ATCC), and Vero (CL-81, ATCC) were cultured in DMEM (10566-016, GIBCO) supplemented with 10% FBS (10099141C, GIBCO), 100 units/ml penicillin, and 100 μg/ml streptomycin sulfate (B540732, Sangon). THP-1 (TIB-202, ATCC) were cultured in RPMI 1640 (21870-076, GIBCO) supplemented with 10% FBS, 100 units/ml penicillin, and 100 μg/ml streptomycin sulfate. All cells were grown in monolayers at 37°C under 5% CO_2. PRV-QXX was used as previously described (34).

THP-1 Macrophage Differentiation

THP-1 cells were differentiated overnight with DMEM/10% FBS supplemented with 100 ng/ml phorbol-12-myristate 13-acetate (P1585, Sigma). After being washed three times with PBS, the cells were re-plated in DMEM/10% FBS and allowed to recover for 2 days.

Cell Stimulation

For NLRP3 inflammasome activation, cells were primed by incubation with LPS (1 μg/ml) at 37°C for 3 h. Then, NLRP3 inflammasomes were activated by incubation of cells with nigericin (2.5 μM, denoted LPS + Nig) or ATP (5 mM, denoted LPS + ATP) for the indicated times.

Plasmids

The plasmids pcDNA3-N-Flag-NLRP3 (#75127) and pLEX-MCS-ASC-GFP (#73957) were from Addgene. The human STING-Flag plasmid was a gift from Chun-Fu Zheng (Fujian Medical University, China).

To clone individual small guide RNAs (sgRNAs), 24-bp oligonucleotides containing the sgRNA sequences were synthesized (Sangon). These sequences included a 4-bp overhang in the forward (CACC) and complementary reverse (AAAC) oligonucleotides to enable cloning into the *Bsm*BI site of the lentiCRISPR v2 (#52961, Addgene). The sgRNA sequences were as follows: *p65*-sgRNA1: 5′-GCGCTCAGCCGGCAGTATCC-3′; *p65*-sgRNA2: 5′-GCTCTCGCCCGGGATACTGC-3′; *Nlrp3*-sgRNA: 5′-GTGCAAGCTGGCTCGTTACC-3′; *Asc*-sgRNA: 5′-GAAGCTCGTCAACTACTACC-3′; and *Caspase-1*-sgRNA:

5′-GAACGCTACAGTTATGGATA-3′. The sgRNA sequences for *Sting*, *Tbk1*, *Irf3*, and *Ifnar1*were used as previously described (34).

For luciferase reporter assays, the porcine *p65* promoter 1800 bp upstream of the transcription initiation site (+1), as well as Sp1 binding site mutants, were synthesized (Genscript) and cloned into pGL3-Basic (E1751, Promega) through the *Kpn*I and *Hind*III sites to generate *p65*-Luc plasmids. Sp1 binding site 1 (−698) of 5′-CCGGCAGTGA-3′ was mutated to 5′-ACAAAAAAAC-3′ (*p65*-Luc mut1). Sp1 binding site 2 (−1300) of 5′-GAGGCACGGA-3′ was mutated to 5′-ACAAACAAAC-3′ (*p65*-Luc mut2). Sp1 binding site 3 (−482) of 5′-CCGGCAGTGA-3′ was mutated to 5′-AAAAACAGAC-3′ (*p65*-Luc mut3).

RT-qPCR

Total RNA was extracted from cells with TRIzol Reagent (9108, TaKaRa) and reverse-transcribed to cDNA with a PrimeScript RT reagent Kit (RR047A, TaKaRa) according to the manufacturer's instructions. RT-qPCR was performed in triplicate with SYBR Premix Ex Taq (RR820A, TaKaRa) according to the manufacturer's instructions. The results were normalized to the level of β-actin expression. Amounts were quantified with the $2^{-\Delta\Delta Ct}$ method. Primer sequences are as follows: porcine IFN-β-Fw: 5′-AGTTGCCTGGGACTCCTCAA-3′, porcine IFN-β-Rv: 5′-CCTCAGGGACCTCAAAGTTCAT-3′; porcine IL-1β-Fw: 5′-GCCCTGTACCCCAACTGGTA-3′, porcine IL-1β-Rv: 5′-CCAGGAAGACGGGCTTTTG-3′; porcine IL-18-Fw: 5′-AGGGACATCAAGCCGTGTTT-3′, porcine IL-18-Rv: 5′-CGGTCTGAGGTGCATTATCTGA-3′; porcine P65-Fw: 5′-GCATCCACAGCTTCCAGAAC-3′, porcine P65-Rv: 5′-GC ACAGCATTCAGGTCGTAG-3′; porcine ISG15-Fw: 5′-AAGG TGAAGATGCTGGGAGG-3′, porcine ISG15-Rv: 5′-CAGGATG CTCAGTGGGTCTC-3′; porcine NLRP1-Fw: 5′-TGAGTGAGG AGCAGTATGA-3′, porcine NLRP1-Rv: 5′-CAGAGCAGGTGT TCAGAC-3′; porcine NLRP3-Fw: 5′-AGAGGAGGAGGAGG AAGA-3′, porcine NLRP3-Rv: 5′-CACCAATCGCTGAGAATAT G-3′; porcine β-actin-Fw: 5′-CTGAACCCCAAAGCCAACCGT-3′, porcine β-actin-Rv: 5′-TTCTCCTTGATGTCCCGCACG-3′.

Immunoblotting Analysis

Cells were washed once in PBS and lysed with cell lysis buffer (50 mM Tris–HCl, pH 8.0, 150 mM NaCl, 1% Triton X-100, 1% sodium deoxycholate, 0.1% SDS, and 2 mM $MgCl_2$) supplemented with protease and phosphatase inhibitor cocktails (HY-K0010 and HY-K0022, MedChemExpress). Lysates were then centrifuged at 13,000 rpm for 15 min, and the insoluble fraction was removed. Protein concentrations were measured with a BCA Protein Assay Kit (BCA01, DINGGUO Biotechnology). Equal amounts of protein were loaded onto each lane and separated by SDS-PAGE, transferred to nitrocellulose membranes (ISEQ00010, Millipore), and incubated in 5% nonfat milk (A600669, Sangon) for 1 h at room temperature. The membranes were incubated with primary antibody at 4°C overnight and then incubated with horseradish-peroxidase-conjugated secondary antibody (709-035-149 or 715-035-150, Jackson ImmunoResearch Laboratories) for 1 h. Immunoblotting results were visualized with Luminata Crescendo Western HRP Substrate (WBLUR0500, Millipore) on a GE AI600 imaging system.

Nuclear and Cytoplasmic Extraction

Nuclear and cytoplasmic extraction was performed with NE-PER Nuclear and Cytoplasmic Extraction Reagents (78833, Thermo Fisher Scientific) according to the manufacturer's instructions. The extracted fractions were subjected to immunoblotting analysis.

ASC Speck Oligomerization Assay

Cells were lysed in homogenization buffer (20 mM HEPES-KOH, pH 7.5, 10 mM KCl, 1.5 mM $MgCl_2$, 1 mM EDTA, 1 mM EGTA, and 320 mM sucrose) supplemented with protease inhibitor cocktail via passage through a 21-gage needle 30 times. The lysates were subjected to centrifugation at 1500 rpm for 10 min. The supernatants were diluted with 1 volume of CHAPS buffer (20 mM HEPES-KOH, pH 7.5, 5 mM $MgCl_2$, 0.5 mM EGTA, and 0.1% CHAPS) supplemented with protease inhibitor cocktail and were centrifuged at 5000 rpm for 10 min. The pellets were washed three times with ice-cold PBS and then re-suspended in 30 μl of CHAPS buffer supplemented with 2 mM DSS crosslinker (21655, Thermo Fisher Scientific). After incubation at 37°C for 20 min, the reaction was quenched by the addition of Laemmli buffer, and the samples were subjected to SDS-PAGE.

Immunofluorescence Analysis

Cells were grown on coverslips (12-545-80, Thermo Fisher Scientific) in 12-well plates and fixed with PBS/4% paraformaldehyde at room temperature for 30 min. The cells were then permeabilized with PBS/0.1% Triton X-100 at room temperature for 3 min. After being washed twice with PBS, the cells were incubated with PBS/10% FBS supplemented with the primary antibody at room temperature for 1 h. After being washed three times with PBS, the cells were labeled with 10% FBS/PBS supplemented with fluorescent secondary antibody (#A-11034, Thermo Fisher Scientific) at room temperature for 1 h. Images were captured under a Zeiss LSM 800 confocal microscope and processed in ImageJ software for quantitative image analysis.

Dual Luciferase Reporter Assays

Cells cultured in 24-well plates were co-transfected with pCMV–Renilla (normalization plasmid) and *p65*–Luc (luciferase reporter plasmid) with Lipofectamine 3000 (L3000015, Invitrogen). At 24 h post transfection, luciferase reporter assays were performed with the Dual-Luciferase Reporter Assay System (E1910, Promega) according to the manufacturer's instructions. The luminescence signal was detected with a Fluoroskan Ascent FL Microplate Fluorometer (Thermo Fisher Scientific).

Chromatin Immunoprecipitation Assays

Cells grown in 10-cm dishes were cross-linked with DMEM containing 1% formaldehyde for 15 min, and then the crosslinking was stopped by the addition of 125 mM glycine for 5 min. After being washed twice with PBS, the cells were

incubated in lysis buffer (10 mM Tris–HCl, pH 7.5, 10 mM KCl, 5 mM $MgCl_2$, and 0.5% NP40) supplemented with protease inhibitor cocktail on ice for 10 min and centrifuged at 2000 rpm for 5 min. The cell pellets containing chromatin were suspended in SDS lysis buffer (50 mM Tris–HCl, pH 7.9, 10 mM EDTA, and 0.5% SDS) supplemented with protease inhibitor cocktail and sonicated into fragments with an average length of 1 kb. Chromatin immunoprecipitation (ChIP) assays were performed with IgG or antibody against Sp1. Primer specific for *p65* promoter was as follows: Fw: 5′-CCCCTCGGTGCCTTCT-3′ and Rv: 5′-CGATGGGTGCACGCTA-3′.

Lentivirus Production

HEK293T cells were seeded at 4×10^6 cells per 10-cm dish in DMEM/10% FBS. Cells were cultured for 24 h and transfected with 2 μg/dish lentiviral construct, 1.5 μg/dish psPAX2 (packaging plasmid, #12260, Addgene), and 0.5 μg/dish pMD2.G (envelope plasmid, #12259, Addgene) with Lipofectamine 3000 (Invitrogen). After 18 h, the medium was aspirated and replaced with 10 ml of DMEM/10% FBS. Lentivirus particles were harvested at 48 and 72 h post transfection and stored at −80°C.

Generation of Gene Knockout Cell Lines via CRISPR/Cas9

Sting$^{-/-}$, *Tbk1*$^{-/-}$, *Irf3*$^{-/-}$, and *Ifnar1*$^{-/-}$ PK15 cells were used as previously described (34). *Sting*$^{-/-}$ and *Ifnar1*$^{-/-}$ 3D4/21 cells were generated through the same procedure as *Sting*$^{-/-}$ and *Ifnar1*$^{-/-}$ PK15 cells (34). *p65*$^{-/-}$, *Nlrp3*$^{-/-}$, *Asc*$^{-/-}$, and *Caspase-1*$^{-/-}$ PK15 cells and *p65*$^{-/-}$, *Nlrp3*$^{-/-}$ and *Asc*$^{-/-}$, *Caspase-1*$^{-/-}$ 3D4/21 cells were generated by infection of the cells with lentivirus particles containing SpCas9 and the sgRNAs of interest for 48 h and then selected with puromycin (4 μg/ml) for 7 days. Single clonal knockout cells were obtained by serial dilution and verified by Sanger sequencing.

RNA Interference

Cells were seeded in 60-mm dishes at a density of 4×10^5 cells per dish and were transfected with small interfering RNA (siRNA, GenePharma, Shanghai) at a final concentration of 0.12 nM. Transfections were performed with Lipofectamine RNAiMAX Reagent (13778500, Invitrogen) according to the manufacturer's instructions in Opti-MEM reduced serum medium (31985062, GIBCO). The medium was replaced with DMEM containing 10% FBS at 8 h post-transfection. The knockdown efficacy was assessed by immunoblotting analysis at 48 h post-transfection. The siRNA sequences were as follows: siControl: 5′-UUCUCCGAACGUGUCACGU-3′; siSp1–1: 5′-GCAACAUCAUUGCUGCUAU-3′; siSp1–2: 5′-GGGAAACGCUUCACACGUU-3′; and siSp1–3: 5′-CCAUUAAUAUCAGUGGCAA-3′.

ELISA

Concentrations of IFN-β and interleukins were measured in the cell supernatants with ELISA kits from R&D Systems (human IL-1β, PDLB50 and porcine IL-1β, PLB00B) and Advanced BioChemical (porcine IFN-β, ABCE-EL-P1819 and porcine IL-18, ABCE-EL-P007), according to the manufacturers' instructions.

Caspase-1 Activity Assays

Caspase-1 activity was assessed with a Caspase-Glo 1 Inflammasome Assay kit (G9951, Promega) with cell lysates treated as indicated, according to the manufacturer's instructions.

The Tissue Culture Infective Dose Assays

Vero cells were seeded in 96-well plates at a density of 1×10^4 cells per well. On the next day, the cells were inoculated with serially diluted viruses (10^{-1}–10^{-12}-fold) for 1 h at 37°C. The excess viral inoculum was removed by washing with PBS. Then, 200 μl of DMEM/2% FBS was added to each well, and the cells were further cultured for 3–5 days. The cells demonstrating the expected cytopathic effects were observed daily, and the tissue culture infective dose ($TCID_{50}$) value was calculated with the Reed–Muench method.

Plaque Assays

Vero cells were cultured just to confluency in six-well plates and inoculated with serially diluted viruses (10^{-1}–10^{-7}-fold) for 1 h at 37°C. The excess viral inoculum was removed by washing with PBS. Then, 4 ml of DMED/1% methylcellulose (M8070, Solarbio) was added to each well, and the cells were further cultured for 4–5 days. The cells were fixed with 4% paraformaldehyde for 15 min and stained with 1% crystal violet for 30 min before the plaques were counted.

Statistical Analysis

GraphPad Prism 7 software was used for data analysis. Data are shown as mean ± standard deviations from three independent experiments. Statistical significance between two groups was analyzed with two-tailed unpaired Student's *t*-test or one-way ANOVA.

RESULTS

G10 Activates the Type I IFN Response in Porcine Cells

G10 is a human-specific STING agonist that activates the IFN response (**Figure 1A**) (10). We aimed to determine whether G10 might activate porcine STING-mediated type I IFN activation. We found that G10 up-regulated the transcription of IFN-β mRNA in both porcine PK15 kidney epithelial cells and 3D4/21 alveolar macrophages, in a manner dependent on STING and its downstream effectors TBK1 and IRF3, but not on IFNAR1 (**Figures 1B,C**). Ablation of *Sting* abolished G10-stimulated IFN-β secretion in PK15 and 3D4/21 cells (**Figure 1D**). We further detected the expression of IFN-stimulated gene 15 (ISG15) under G10 treatment by using RT-qPCR analysis. As shown in **Figure 1E**, challenge of *Sting*$^{-/-}$, *Tbk1*$^{-/-}$, *Irf3*$^{-/-}$, and *Ifnar1*$^{-/-}$ PK15 cells with G10 had no effect on *ISG15* transcription. This finding was also confirmed in *Sting*$^{-/-}$ and

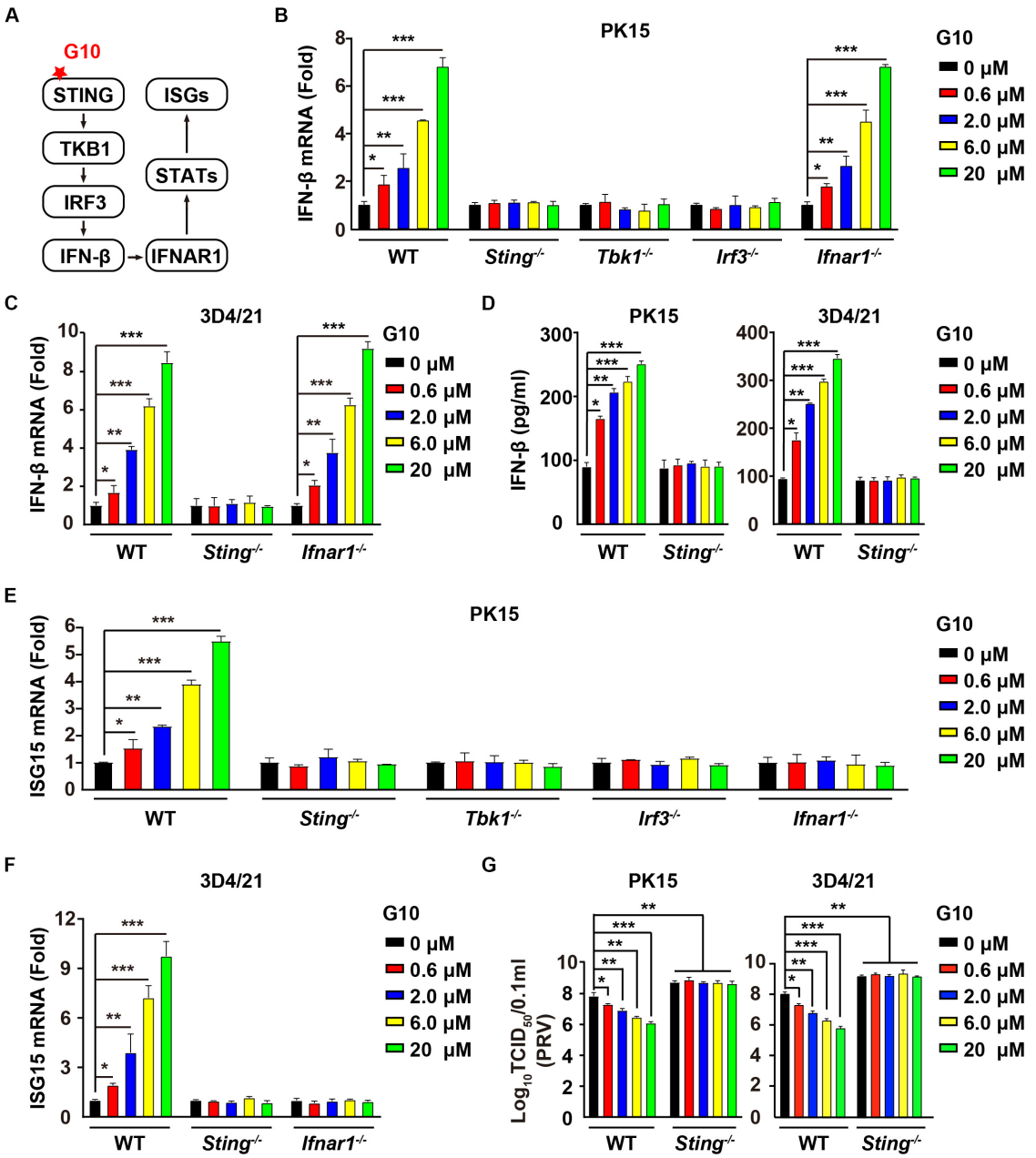

FIGURE 1 | G10 elicits a type I IFN response in porcine cells. **(A)** Schematic representation of the STING-mediated type I IFN response. **(B)** WT, *Sting*$^{-/-}$, *Tbk1*$^{-/-}$, *Irf3*$^{-/-}$, and *Ifnar1*$^{-/-}$ PK15 cells were seeded in 12-well plates at a density of 1 × 10^5 per well. On the next day, cells were treated with G10 at the indicated concentrations for 24 h. Total mRNA was then reverse-transcribed to cDNA and IFN-β mRNA was assessed by RT-qPCR analysis. The results were normalized to the level of β-actin expression. *$P < 0.05$, **$P < 0.01$, ***$P < 0.001$ determined by two-tailed Student's *t*-test. **(C)** WT, *Sting*$^{-/-}$, and *Ifnar1*$^{-/-}$ 3D4/21 cells were seeded in 12-well plates at a density of 1 × 10^5 per well. On the next day, cells were treated as in **B**. IFN-β mRNA was assessed by RT-qPCR analysis. The results were normalized to the level of β-actin expression. *$P < 0.05$, **$P < 0.01$, ***$P < 0.001$ determined by two-tailed Student's *t*-test. **(D)** WT and *Sting*$^{-/-}$ PK15 and 3D4/21 cells were seeded in 12-well plates at a density of 1 × 10^5 per well. On the next day, cells were treated as in **B**. The medium was then harvested and IFN-β secretion was quantified by ELISA. *$P < 0.05$, **$P < 0.01$, ***$P < 0.001$ determined by two-tailed Student's *t*-test. **(E)** WT, *Sting*$^{-/-}$, *Tbk1*$^{-/-}$, *Irf3*$^{-/-}$, and *Ifnar1*$^{-/-}$ PK15 cells were seeded in 12-well plates at a density of 1 × 10^5 per well. On the next day, cells were treated as in **B**. ISG15 mRNA was assessed by RT-qPCR analysis. The results were normalized to the level of β-actin expression. *$P < 0.05$, **$P < 0.01$, ***$P < 0.001$ determined by two-tailed Student's *t*-test. **(F)** WT, *Sting*$^{-/-}$, and *Ifnar1*$^{-/-}$ 3D4/21 cells were seeded in 12-well plates at a density of 1 × 10^5 per well. On the next day, cells were treated as in **B**. ISG15 mRNA was assessed by RT-qPCR analysis. The results were normalized to the level of β-actin expression. *$P < 0.05$, **$P < 0.01$, ***$P < 0.001$ determined by two-tailed Student's *t*-test. **(G)** WT and *Sting*$^{-/-}$ PK15 and 3D4/21 cells were seeded in 12-well plates at a density of 1 × 10^5 per well. On the next day, cells were infected with PRV-QXX (MOI = 1) and simultaneously treated with G10 as in **B**. Virus was harvested by three freeze–thaw cycles and PRV titer was assessed with $TCID_{50}$ assays. *$P < 0.05$, **$P < 0.01$, ***$P < 0.001$ determined by one-way ANOVA.

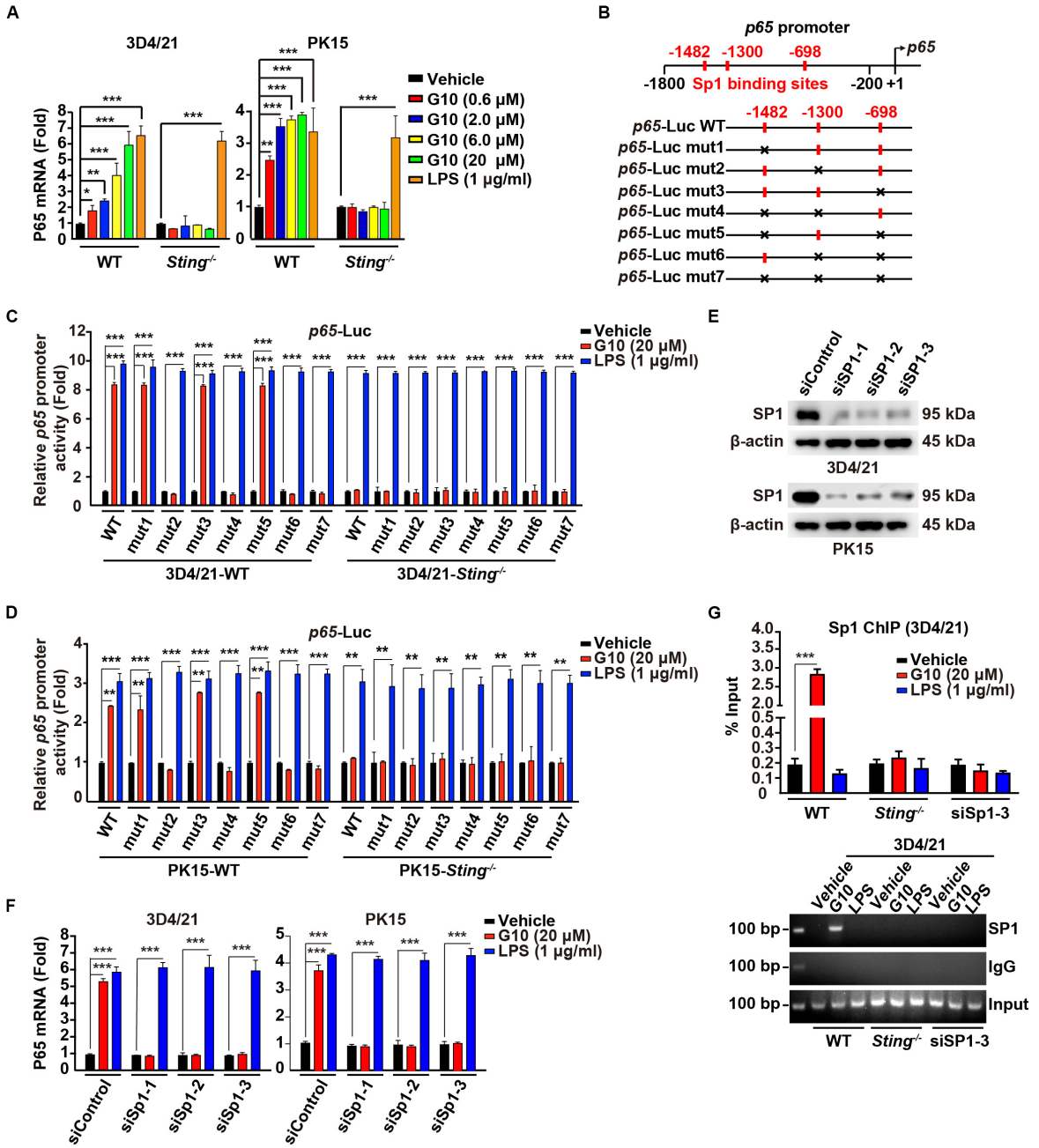

FIGURE 2 | G10 stimulates Sp1-dependent *p65* transcription in porcine cells. **(A)** WT and *Sting*$^{-/-}$ 3D4/21 and PK15 cells were seeded in 12-well plates at a density of 1 × 10^5 per well. On the next day, cells were treated with vehicle (DMSO), G10 (0.6–20 μM), and LPS (1 μg/ml) for 24 h. Total mRNA was then reverse-transcribed to cDNA and P65 mRNA was assessed by RT-qPCR analysis. The results were normalized to the level of β-actin expression. *$P < 0.05$, **$P < 0.01$, ***$P < 0.001$ determined by two-tailed Student's *t*-test. **(B)** Diagrams of the P65 promoter and the various mutants, with the Sp1 binding sites indicated. **(C)** WT and *Sting*$^{-/-}$ 3D4/21 cells were seeded in 12-well plates at a density of 1 × 10^5 per well. On the next day, cells were transfected with 0.1 μg/well *p65*–Luc variants and 0.02 μg/well pCMV-Renilla. At 24 h post transfection, cells were treated with vehicle (DMSO), G10 (20 μM), and LPS (1 μg/ml) for 6 h. *p65* promoter activity was assessed with dual luciferase reporter assays. ***$P < 0.001$ determined by two-tailed Student's *t*-test. **(D)** *p65* promoter activity was assessed with dual luciferase reporter assays in WT and *Sting*$^{-/-}$ PK15 cells the same as in C. **$P < 0.01$, ***$P < 0.001$ determined by two-tailed Student's *t*-test. **(E)** 3D4/21 and PK15 cells were seeded in 60-mm dishes at a density of 4 × 10^5 per dish. On the next day, cells were transfected with indicated siRNA for 48 h. Sp1 protein was assessed with immunoblotting analysis. β-actin served as loading control. **(F)** 3D4/21 and PK15 cells were seeded in 12-well plates at a density of 1 × 10^5 per well. On the next day, cells were transfected with indicated siRNA for 48 h. Then cells were treated with vehicle (DMSO), G10 (20 μM), and LPS (1 μg/ml) for 24 h. Total mRNA was then reverse-transcribed to cDNA and P65 mRNA was assessed by RT-qPCR analysis. The results were normalized to the level of β-actin expression. ***$P < 0.001$ determined by two-tailed Student's *t*-test. **(G)** WT and *Sting*$^{-/-}$ 3D4/21 cells were seeded in 60-mm dishes at a density of 4 × 10^5 per dish. On the next day, 3D4/21 cells were transfected with siSp1-3 for 48 h. Then WT, *Sting*$^{-/-}$, and siSp1-3 transfected 3D4/21 cells were treated with vehicle (DMSO), G10 (20 μM), and LPS (1 μg/ml). Sp1 ChIP assays were performed at 24 h post treatment. ***$P < 0.001$ determined by two-tailed Student's *t*-test.

Ifnar1$^{-/-}$ 3D4/21 cells, thus suggesting that G10 activates type I IFN and IFN signaling in porcine cells (**Figure 1F**).

We next assessed the antiviral activity of G10 against pseudorabies virus (PRV), a member of the subfamily Alphaherpesvirinae in the family Herpesviridae, and the causative pathogen of Aujeszky's disease in pigs (35). G10 treatment inhibited PRV infection in porcine PK15 and 3D4/21 cells (**Figure 1G**). STING deficiency in PK15 and 3D4/21 cells abrogated the antiviral activity of G10 and enhanced PRV infection (**Figure 1G**). These findings demonstrate that G10 acts on STING, resulting in activation of type I IFN and antiviral activity in porcine cells.

G10 Activates P65 Gene Transcription in Porcine Cells

G10 activates human STING and triggers IRF3-dependent IFNs expression but not NF-κB activation. Unexpectedly, porcine 3D4/21 and PK15 cells showed significant P65 mRNA up-regulation in response to G10 in a dose-dependent manner (**Figure 2A**). Knockout of STING inhibited G10-, but not LPS-induced *p65* transcription in 3D4/21 and PK15 cells (**Figure 2A**). Replenishment of STING expression in *Sting*$^{-/-}$ 3D4/21 cells rescued G10-induced *p65* transcription (**Supplementary Figure S1A**).

We next sought to address how G10 transcriptionally activates porcine *p65* expression. We analyzed the promoter of the porcine *p65* gene and found three consensus binding sites for the transcriptional factor Sp1 (**Figure 2B**). Promoter mutation analysis with dual luciferase reporter assays indicated that the second Sp1 binding site (−1300) in the *p65* promoter was essential for G10-mediated induction of *p65* expression in a STING-dependent manner in 3D4/21 and PK15 cells (**Figures 2C,D**). However, LPS-stimulated *p65* transcription was not dependent on these three Sp1 binding sites or on STING (**Figures 2C,D**). In addition, knockdown of Sp1 with RNA interference affected the expression of P65 mRNA in 3D4/21 and PK15 cells under G10 treatment (**Figures 2E,F**). Knockdown of Sp1 did not prevent LPS-induced *p65* transcription, thus suggesting that G10 and LPS regulate *p65* transcription through different mechanisms in porcine cells (**Figure 2F**). Furthermore, ChIP assays showed that Sp1 was recruited to the promoter of *p65* after G10 treatment, in a manner dependent on either STING or Sp1 (**Figure 2G**). Collectively, these data suggest that G10 induces *p65* transcription through STING and Sp1 in porcine cells.

G10 Activates the Porcine NF-κB Signaling Pathway

On the basis of the above findings, we attempted to determine whether G10 might activate the porcine NF-κB signaling pathway. We first addressed whether G10 induced the translocation of P65 into the nucleus. G10 did not stimulate P65 translocation into the nucleus, as indicated by immunofluorescence in human THP-1 cells (**Supplementary Figure S1B**). However, treatment of wild-type (WT) 3D4/21 and PK15 cells with G10 significantly promoted STING-dependent nuclear localization of P65 (**Figure 3A**). However, the percentage of cells with nuclear localized P65 in WT and *Sting*$^{-/-}$ 3D4/21 and PK15 cells was unchanged by LPS treatment (**Figure 3A**). LPS, but not G10, induced P65 translocation into the nucleus in *Sting*$^{-/-}$ 3D4/21 cells, as indicated by immunoblotting of nuclear and cytoplasmic extracts (**Figure 3B**).

We next investigated the transcription of the NF-κB target genes *Il-1*β and *Il-18* (36). G10 treatment significantly induced the transcription of IL-1β and IL-18 mRNA in 3D4/21 and PK15 cells, in a manner dependent on STING (**Figures 3C,D**). Knockdown of Sp1 abrogated G10- but not LPS-induced transcription of IL-1β and IL-18 mRNA (**Figures 3E,F**). Furthermore, we ablated *p65* with CRISPR/Cas9 editing in 3D4/21 and PK15 cells (**Figure 3G** and **Supplementary Figure S1C**). The mRNA levels of IL-1β and IL-18 were not up-regulated by the treatment of G10 and LPS in *p65*$^{-/-}$ 3D4/21 and PK15 cells, thus suggesting that G10- and LPS-induced expression of IL-1β and IL-18 mRNA was dependent on P65 (**Figures 3H,I**). These data indicate that G10 activates the NF-κB signaling pathway in porcine cells.

G10 Induces IL-1β and IL-18 Secretion in Porcine Cells

We asked whether G10 might promote porcine IL-1β and IL-18 secretion. Stimulation of human THP-1 cells with G10 did not affect IL-1β secretion (**Supplementary Figure S1D**). As a positive control, incubation of LPS-primed THP-1 cells with nigericin (LPS + Nig) significantly induced IL-1β secretion (**Supplementary Figure S1D**). However, G10 treatment stimulated STING-dependent secretion of IL-1β and IL-18 in 3D4/21 and PK15 cells (**Figures 4A,B**). IL-1β and IL-18 secretion was unchanged in WT and *Sting*$^{-/-}$ 3D4/21 and PK15 cells treated with LPS + Nig (**Figures 4A,B**).

To further establish the role of G10 in IL-1β and IL-18 secretion in porcine cells, we assessed the secretion of these cytokines in cells with Sp1 or P65 expression interference. Knockdown of Sp1 by RNA interference decreased G10-induced IL-1β and IL-18 secretion in 3D4/21 and PK15 cells (**Figures 4C,D**). IL-1β and IL-18 secretion was constitutively up-regulated in response to LPS + Nig treatment, regardless of Sp1 deficiency (**Figures 4C,D**). In addition, P65-deficient 3D4/21 and PK15 cells, compared with WT cells, did not respond to G10 or to LPS + Nig in terms of induction of IL-1β and IL-18 secretion (**Figures 4E,F**). G10 promoted mature IL-1β secretion in 3D4/21 cells in a STING-dependent manner, as indicated by immunoblotting analysis of mature IL-1β (**Figure 4G**). Transfection of STING-Flag plasmid into *Sting*-deficient 3D4/21 cells resulted in G10-induced IL-1β and IL-18 secretion, to levels comparable to those in WT cells (**Figure 4H**). Together, these data demonstrate that STING-mediated NF-κB activation is essential for G10-induced IL-1β and IL-18 secretion in porcine cells.

G10-Induced ASC Oligomerization and Caspase-1 Activation Promote IL-1β and IL-18 Maturation in Porcine Cells

IL-1β and IL-18 maturation requires nucleation of the adaptor protein ASC, which controls Caspase-1 activation

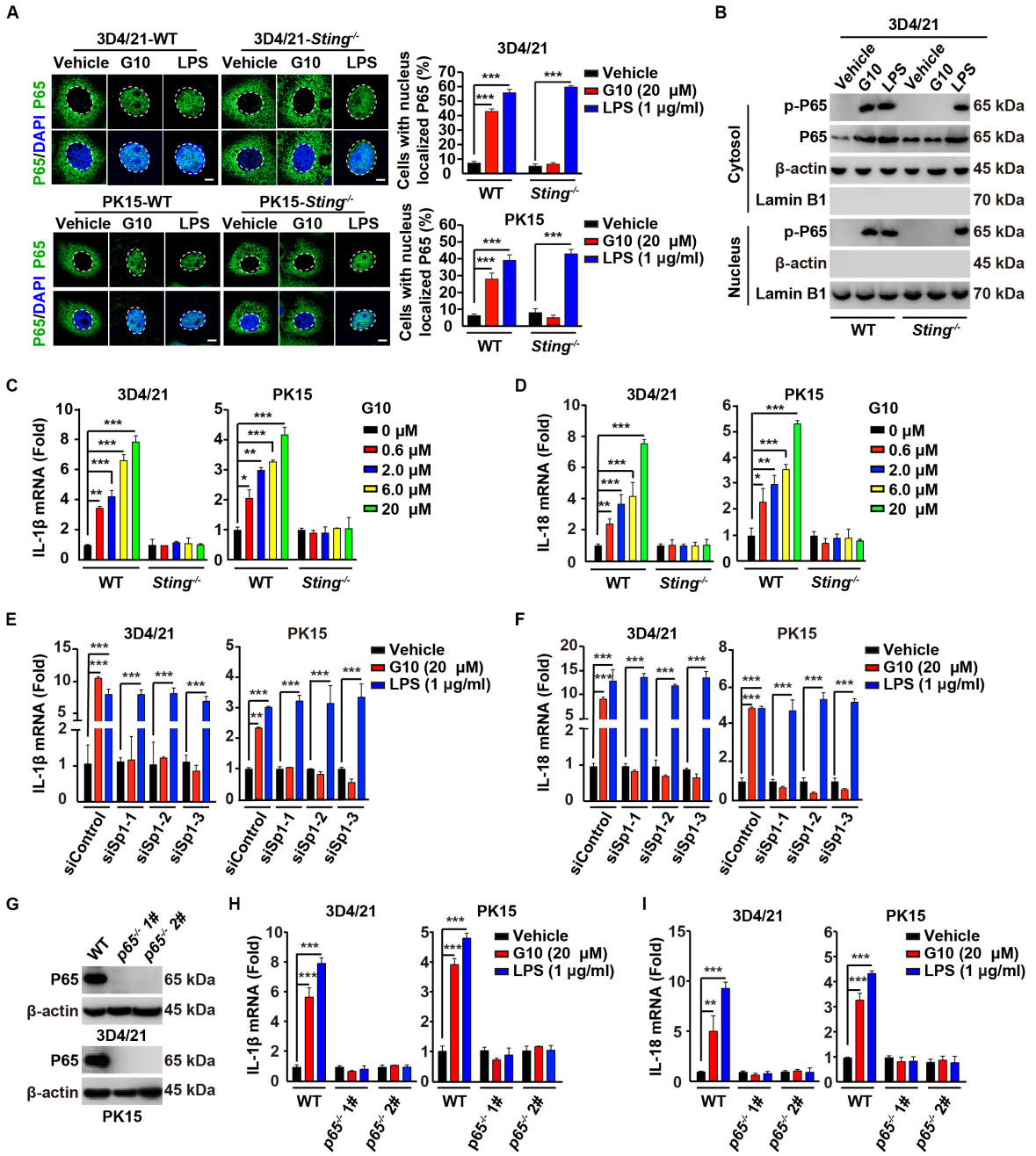

FIGURE 3 | G10 activates the NF-κB signaling pathway in porcine cells. **(A)** WT and *Sting*$^{-/-}$ 3D4/21 and PK15 cells were seeded in 12-well plates with coverslips at a density of 1 × 10^5 per well. On the next day, cells were treated with vehicle (DMSO), G10 (20 μM), and LPS (1 μg/ml) for 24 h. Translocation of P65 into the nucleus (DAPI) was assessed by immunofluorescence analysis with antibody against P65. Quantification of cells with nuclear localized P65 is shown on the right (n = 30 cells). Scale bar, 10 μm. ***P < 0.001 determined by two-tailed Student's t-test. **(B)** WT and *Sting*$^{-/-}$ 3D4/21 cells were seeded in 60-mm dishes at a density of 4 × 10^5 per dish. On the next day, cells were treated as in **A**. Phospho-P65 and P65 were assessed with immunoblotting analysis in the cytosol and nuclei fraction. β-actin (indicating cytosol) and Lamin B1 (indicating nuclei) served as loading controls. **(C,D)** WT and *Sting*$^{-/-}$ 3D4/21 and PK15 cells were seeded in 12-well plates at a density of 1 × 10^5 per well. On the next day, cells were treated with G10 at the indicated concentration for 24 h. Total mRNA was then reverse-transcribed to cDNA and IL-1β **(C)** and IL-18 **(D)** mRNAs were assessed by RT-qPCR analysis. The results were normalized to the level of β-actin expression. *P < 0.05, **P < 0.01, ***P < 0.001 determined by two-tailed Student's t-test. **(E,F)** 3D4/21 and PK15 cells were seeded in 12-well plates at a density of 1 × 10^5 per well. On the next day, cells were transfected with indicated siRNAs for 48 h. Then, cells were treated as in **A**. Total mRNA was then reverse-transcribed to cDNA and IL-1β **(E)** and IL-18 **(F)** mRNAs were assessed by RT-qPCR analysis. The results were normalized to the level of β-actin expression. **P < 0.01, ***P < 0.001 determined by two-tailed Student's t-test. **(G)** P65 protein was assessed with immunoblotting analysis in WT, *p65*$^{-/-}$ 1#, and *p65*$^{-/-}$ 2# 3D4/21 and PK15 cells. β-actin served as loading control. **(H,I)** WT, *p65*$^{-/-}$ 1#, and *p65*$^{-/-}$ 2# 3D4/21 and PK15 cells were seeded in 12-well plates at a density of 1 × 10^5 per well. On the next day, cells were treated as in **A**. Total mRNA was then reverse-transcribed to cDNA and IL-1β **(H)** and IL-18 **(I)** mRNAs were assessed by RT-qPCR analysis. The results were normalized to the level of β-actin expression. **P < 0.01, ***P < 0.001 determined by two-tailed Student's t-test.

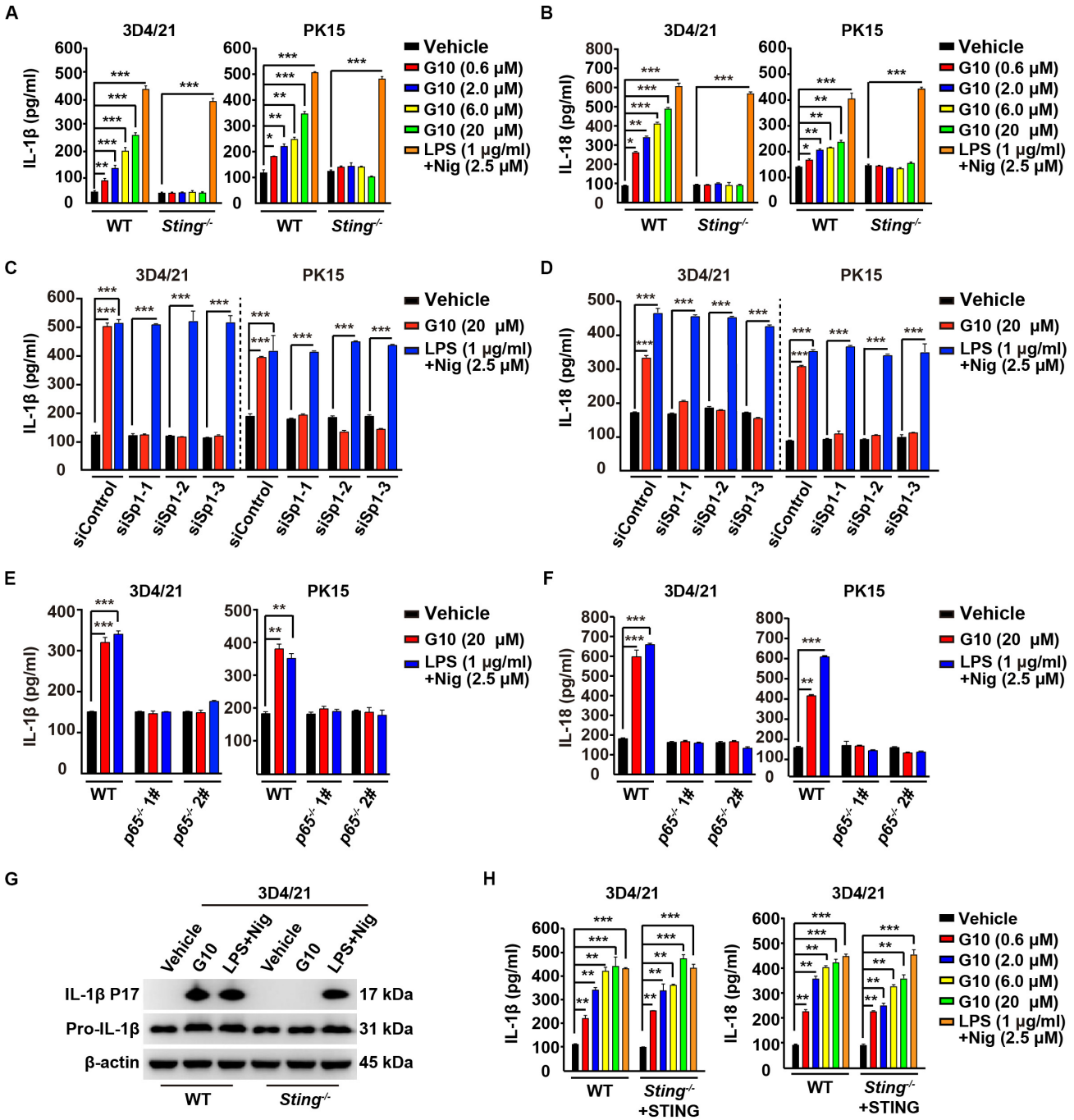

FIGURE 4 | G10 promotes IL-1β and IL-18 secretion in porcine cells. **(A,B)** WT and *Sting*$^{-/-}$ 3D4/21 and PK15 cells were seeded in 12-well plates at a density of 1×10^5 per well. On the next day, cells were treated with vehicle (DMSO), G10, and LPS + Nig at indicated concentrations for 24 h. The medium was then harvested and IL-1β **(A)** and IL-18 **(B)** secretion was quantified by ELISA. *$P < 0.05$, **$P < 0.01$, ***$P < 0.001$ determined by two-tailed Student's *t*-test. **(C,D)** 3D4/21 and PK15 cells were seeded in 12-well plates at a density of 1×10^5 per well. On the next day, cells were transfected with indicated siRNA for 48 h. Then, cells were treated with vehicle (DMSO), G10, and LPS + Nig at indicated concentrations for 24 h. The medium was then harvested and IL-1β **(C)** and IL-18 **(D)** secretion was quantified by ELISA. ***$P < 0.001$ determined by two-tailed Student's *t*-test. **(E,F)** WT, *p65*$^{-/-}$ 1#, and *p65*$^{-/-}$ 2# 3D4/21 and PK15 cells were seeded in 12-well plates at a density of 1×10^5 per well. On the next day, cells were treated as in **C**. The medium was then harvested and IL-1β **(E)** and IL-18 **(F)** secretion was quantified by ELISA. **$P < 0.01$, ***$P < 0.001$ determined by two-tailed Student's *t*-test. **(G)** WT and *Sting*$^{-/-}$ 3D4/21 cells were seeded in 60-mm dishes at a density of 4×10^5 per dish. On the next day, cells were treated as in **C**. The medium was harvested to analyze mature IL-1β (P17) secretion, and the cells were harvested to analyze pro-IL-1β by immunoblotting analysis. **(H)** WT and *Sting*$^{-/-}$ 3D4/21 cells were seeded in 12-well plates at a density of 1×10^5 per well. On the next day, *Sting*$^{-/-}$ 3D4/21 cells were transfected with plasmid for expression of STING-Flag plasmid (4 μg) for 24 h. Then, cells were treated as in **A**. The medium was then harvested and IL-1β and IL-18 secretion was quantified by ELISA. **$P < 0.01$, ***$P < 0.001$ determined by two-tailed Student's *t*-test.

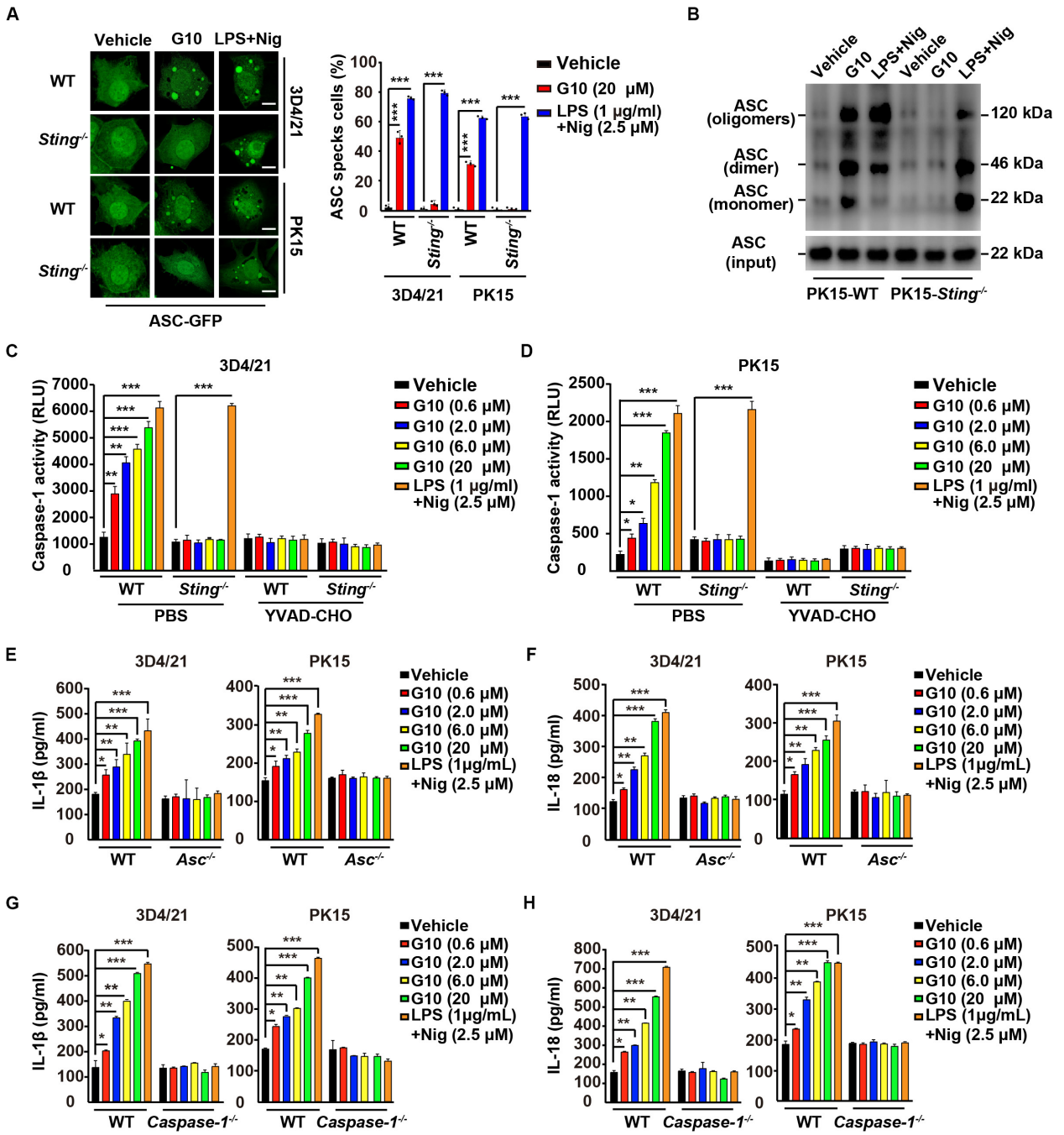

FIGURE 5 | G10 induces ASC oligomerization and Caspase-1 activation in porcine cells. **(A)** WT and *Sting*$^{-/-}$ 3D4/21 and PK15 cells were seeded in 12-well plates with coverslips at a density of 1 × 10^5 per well. On the next day, cells were transfected with plasmid for expression of ASC-GFP (2 μg) for 24 h. Then, cells were treated with vehicle (DMSO), G10, and LPS + Nig at the indicated concentrations for 24 h. ASC oligomerization was assessed by fluorescence microscopy. Quantification of cells with ASC specks is shown on the right (n = 30 cells). Scale bar, 10 μm. ***P < 0.001 determined by two-tailed Student's t-test. **(B)** WT and *Sting*$^{-/-}$ PK15 cells were seeded in 60-mm dishes at a density of 4 × 10^5 per dish. On the next day, cells were treated as in A. ASC oligomerization was assessed by immunoblotting analysis. **(C,D)** WT and *Sting*$^{-/-}$ 3D4/21 and PK15 cells were seeded in 12-well plates at a density of 1 × 10^5 per well. On the next day, cells were treated with vehicle (DMSO), G10, and LPS + Nig at the indicated concentrations in the absence (PBS) or presence of Caspase-1 inhibitor YVAD-CHO (5 μM) for 24 h. Caspase-1 activity was assessed with a Caspase-Glo 1 Inflammasome Assay kit. *P < 0.05, **P < 0.01, ***P < 0.001 determined by two-tailed Student's t-test. **(E,F)** WT and *Asc*$^{-/-}$ 3D4/21 and PK15 cells were seeded in 12-well plates at a density of 1 × 10^5 per well. On the next day, cells were treated with vehicle (DMSO), G10 and LPS + Nig at the indicated concentrations for 24 h. The medium was then harvested and IL-1β **(E)** and IL-18 **(F)** secretion were quantified by ELISA. *P < 0.05, **P < 0.01, ***P < 0.001 determined by two-tailed Student's t-test. **(G,H)** WT and *Caspase-1*$^{-/-}$ 3D4/21 and PK15 cells were seeded in 12-well plates at a density of 1 × 10^5 per well. On the next day, cells were treated as in **E**. The medium was then harvested and IL-1β **(G)** and IL-18 **(H)** secretion were quantified by ELISA. *P < 0.05, **P < 0.01, ***P < 0.001 determined by two-tailed Student's t-test.

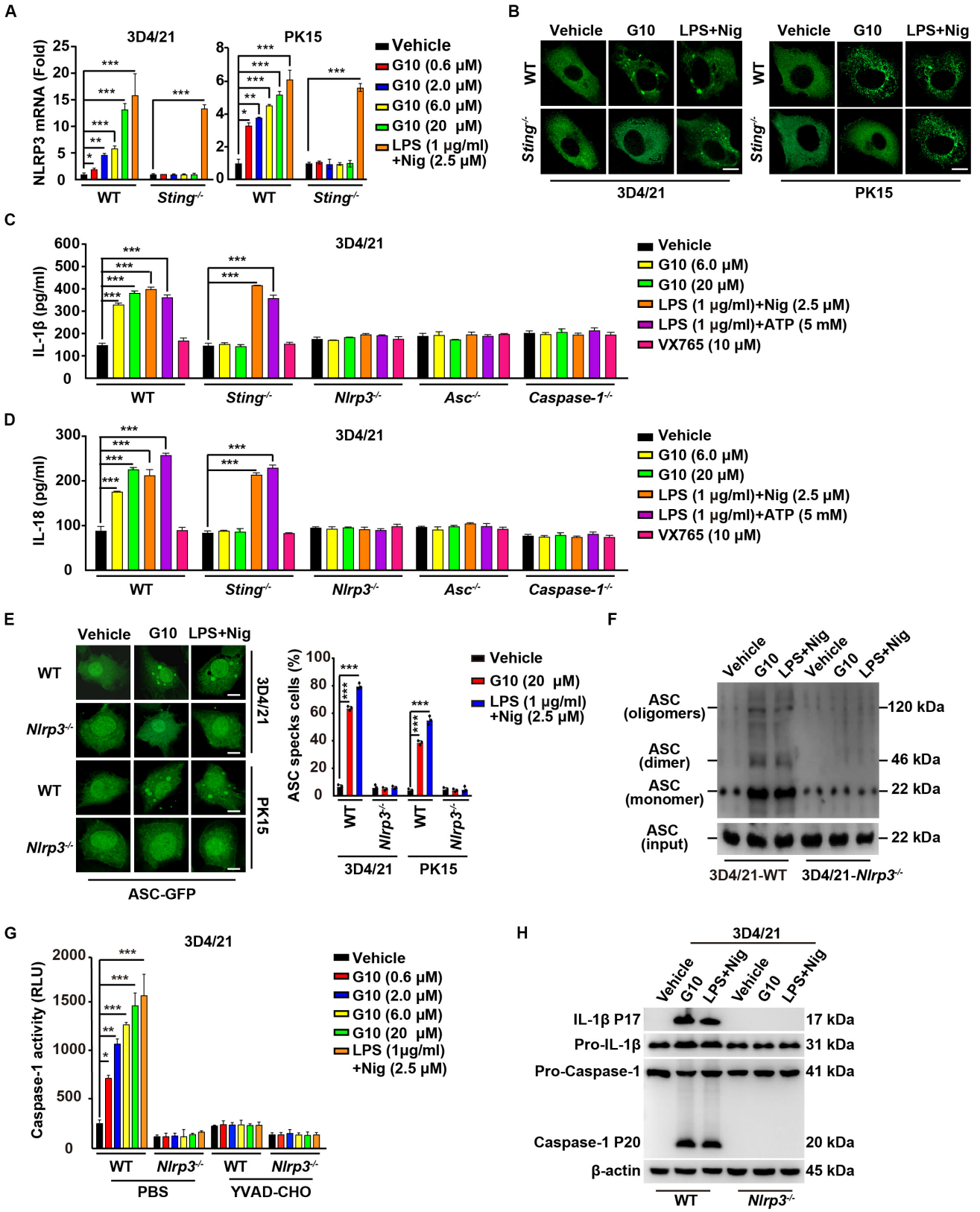

FIGURE 6 | Continued

FIGURE 6 | G10 activates the NLRP3 inflammasome in porcine cells. **(A)** WT and *Sting*$^{-/-}$ 3D4/21 and PK15 cells were seeded in 12-well plates at a density of 1 × 10^5 per well. On the next day, cells were treated with vehicle (DMSO), G10, and LPS + Nig at the indicated concentrations for 24 h. Total mRNA was then reverse-transcribed to cDNA and NLRP3 mRNA was assessed by RT-qPCR analysis. The results were normalized to the level of β-actin expression. *$P < 0.05$, **$P < 0.01$, ***$P < 0.001$ determined by two-tailed Student's *t*-test. **(B)** WT and *Sting*$^{-/-}$ 3D4/21 and PK15 cells were seeded in 12-well plates with coverslips at a density of 1 × 10^5 per well. On the next day, cells were transfected with plasmid for expression of NLRP3-Flag (2 μg) for 24 h. Then, cells were treated with vehicle (DMSO), G10 (20 μM), and LPS + Nig (1 μg/ml + 2.5 μM) for 24 h. NLRP3 activation was assessed by immunofluorescence analysis with antibody against Flag. Scale bar, 10 μm. **(C,D)** WT, *Sting*$^{-/-}$, *Nlrp3*$^{-/-}$, *Asc*$^{-/-}$, and *Caspase-1*$^{-/-}$ 3D4/21 cells were seeded in 12-well plates at a density of 1 × 10^5 per well. On the next day, cells were treated with vehicle (DMSO), G10, LPS + Nig, LPS + ATP, and VX765 at the indicated concentrations for 24 h. The medium was then harvested and IL-1β **(C)** and IL-18 **(D)** secretion were quantified by ELISA. ***$P < 0.001$ determined by two-tailed Student's *t*-test. **(E)** WT and *Nlrp3*$^{-/-}$ 3D4/21 and PK15 cells were seeded in 12-well plates with coverslips at a density of 1 × 10^5 per well. On the next day, cells were transfected with plasmid for expression of ASC-GFP (2 μg) for 24 h. Then, cells were treated as in **B**. ASC oligomerization was assessed by fluorescence microscopy. Quantification of cells with ASC specks is shown on the right ($n = 30$ cells). Scale bar, 10 μm. ***$P < 0.001$ determined by two-tailed Student's *t*-test. **(F)** WT and *Nlrp3*$^{-/-}$ 3D4/21 cells were seeded in 60-mm dishes at a density of 4 × 10^5 per dish. On the next day, cells were treated as in **B**. ASC oligomerization was assessed by immunoblotting analysis. **(G)** WT and *Nlrp3*$^{-/-}$ 3D4/21 cells were seeded in 12-well plates at a density of 1 × 10^5 per well. On the next day, cells were treated with vehicle (DMSO), G10, and LPS + Nig at the indicated concentrations in the absence (PBS) or presence of Caspase-1 inhibitor YVAD-CHO (5 μM) for 24 h. Caspase-1 activity was assessed with a Caspase-Glo 1 Inflammasome Assay kit. *$P < 0.05$, **$P < 0.01$, ***$P < 0.001$ determined by two-tailed Student's *t*-test. **(H)** WT and *Nlrp3*$^{-/-}$ 3D4/21 cells were seeded in 60-mm dishes at a density of 4 × 10^5 per dish. On the next day, cells were treated as in **B**. The medium was harvested to analyze mature IL-1β (P17) secretion, and the cells were harvested to analyze pro-IL-1β, pro-Caspase-1, and cleaved Caspase-1 (P20) by immunoblotting analysis.

and subsequent cleavage of pro–IL-1β and pro–IL-18 (37). We observed that G10 treatment induced bright fluorescent ASC specks in WT but not *Sting*$^{-/-}$ 3D4/21 and PK15 cells, whereas induction of ASC specks by LPS + Nig treatment was independent of STING (**Figure 5A**). Moreover, STING was responsible for G10-mediated induction of ASC oligomerization in PK15 cells, as indicated by immunoblotting analysis (**Figure 5B**).

Next, we investigated whether Caspase-1 might be activated by G10 treatment. As shown in **Figures 5C,D**, G10 dramatically increased Caspase-1 activity in 3D4/21 and in PK15 cells through STING. An inhibitor of Caspase-1, YVAD-CHO, blocked G10- and LPS + Nig-induced Caspase-1 activation (**Figures 5C,D**). Additionally, we examined the roles of ASC and Caspase-1 in G10-induced IL-1β and IL-18 secretion in *Asc*$^{-/-}$ and *Caspase-1*$^{-/-}$ 3D4/21 and PK15 cells generated by CRISPR/Cas9 editing (**Supplementary Figures S1E,F**). Knockout of ASC and Caspase-1 in 3D4/21 and PK15 cells abolished IL-1β and IL-18 secretion when cells were treated with G10 or LPS + Nig (**Figures 5E–H**). These data suggest that the STING/ASC/Caspase-1 axis is essential for G10-induced IL-1β and IL-18 secretion in porcine cells.

G10 Activates the NLRP3 Inflammasome in Porcine Cells

Because our data suggested that G10 is a bona fide inflammasome activator, we sought to investigate which PRRs might be involved in G10-mediated activation of inflammasomes. We first analyzed the mRNA expression of inflammasome effectors under G10 treatment. As indicated by RT-qPCR analysis, G10 did not induce NLRP1 transcription in 3D4/21 and PK15 cells (**Supplementary Figures S2A,B**). However, NLRP3 mRNA was significantly up-regulated by G10 treatment in WT but not in *Sting*$^{-/-}$ 3D4/21 and PK15 cells (**Figure 6A**). Because NLRP3 inflammasome activation leads to NLRP3 aggregation (38), we detected NLRP3 aggregation by immunofluorescence. We observed that multiple puncta of NLRP3 appeared after G10 treatment in WT but not STING-deficient 3D4/21 and PK15 cells (**Figure 6B**). We stimulated 3D4/21 cells with G10 to observe whether STING co-localized to NLRP3. No obvious co-localization was observed when cells were treated with DMSO (**Supplementary Figure S2C**). G10 treatment induced multiple puncta of STING formation, some of which co-localized with NLRP3 (**Supplementary Figure S2C**). These results demonstrated that G10 activates porcine NLRP3.

We then established the roles of NLRP3 in IL-1β and IL-18 secretion, ASC oligomerization, and Caspase-1 activation in response to G10 treatment. After G10 treatment, knockout of STING, NLRP3, ASC, and Caspase-1 in 3D4/21 and PK15 cells suppressed IL-1β and IL-18 secretion (**Supplementary Figure S2D** and **Figures 6C,D**). Treatment of WT and *Sting*$^{-/-}$ 3D4/21 and PK15 cells with LPS + Nig or LPS + ATP [another canonical NLRP3 activator (24)] stimulated IL-1β and IL-18 secretion (**Figures 6C,D**). An inhibitor of Caspase-1, VX756 (39), prevented WT, *Sting*$^{-/-}$, *Nlrp3*$^{-/-}$, and *Asc*$^{-/-}$ 3D4/21 and PK15 cells from secreting IL-1β and IL-18 in response to G10, LPS + Nig, or LPS + ATP (**Figures 6C,D**). ASC oligomerization disappeared in G10- and LPS + Nig-treated *Nlrp3*$^{-/-}$ cells, as indicated by fluorescence analysis of ASC specks (**Figure 6E**) or by immunoblotting analysis of ASC oligomerization (**Figure 6F**). Caspase-1 was not activated in *Nlrp3*$^{-/-}$ 3D4/21 cells treated with G10 or LPS + Nig (**Figure 6G**). The cleavage of pro-IL-1β and pro-Caspase-1 induced by G10 and LPS + Nig did not occur, owing to the NLRP3 ablation in 3D4/21 cells (**Figure 6H**). Together, these data indicate that G10 promotes canonical NLRP3 inflammasome activation in porcine cells.

G10 Induces Potassium Efflux, Thus Activating the NLRP3 Inflammasome in Porcine Cells

Several mechanisms have been proposed to be critical for NLRP3 inflammasome activation, such as potassium efflux, calcium mobilization, mitochondrial damage, and ROS (21–24). We sought to address the mechanism through which G10 activates the NLRP3 inflammasome. Because potassium efflux has been proposed to play a central role in NLRP3 inflammasome activation (40), we tested whether K^+ replenishment might rescue the effects on IL-1β and IL-18

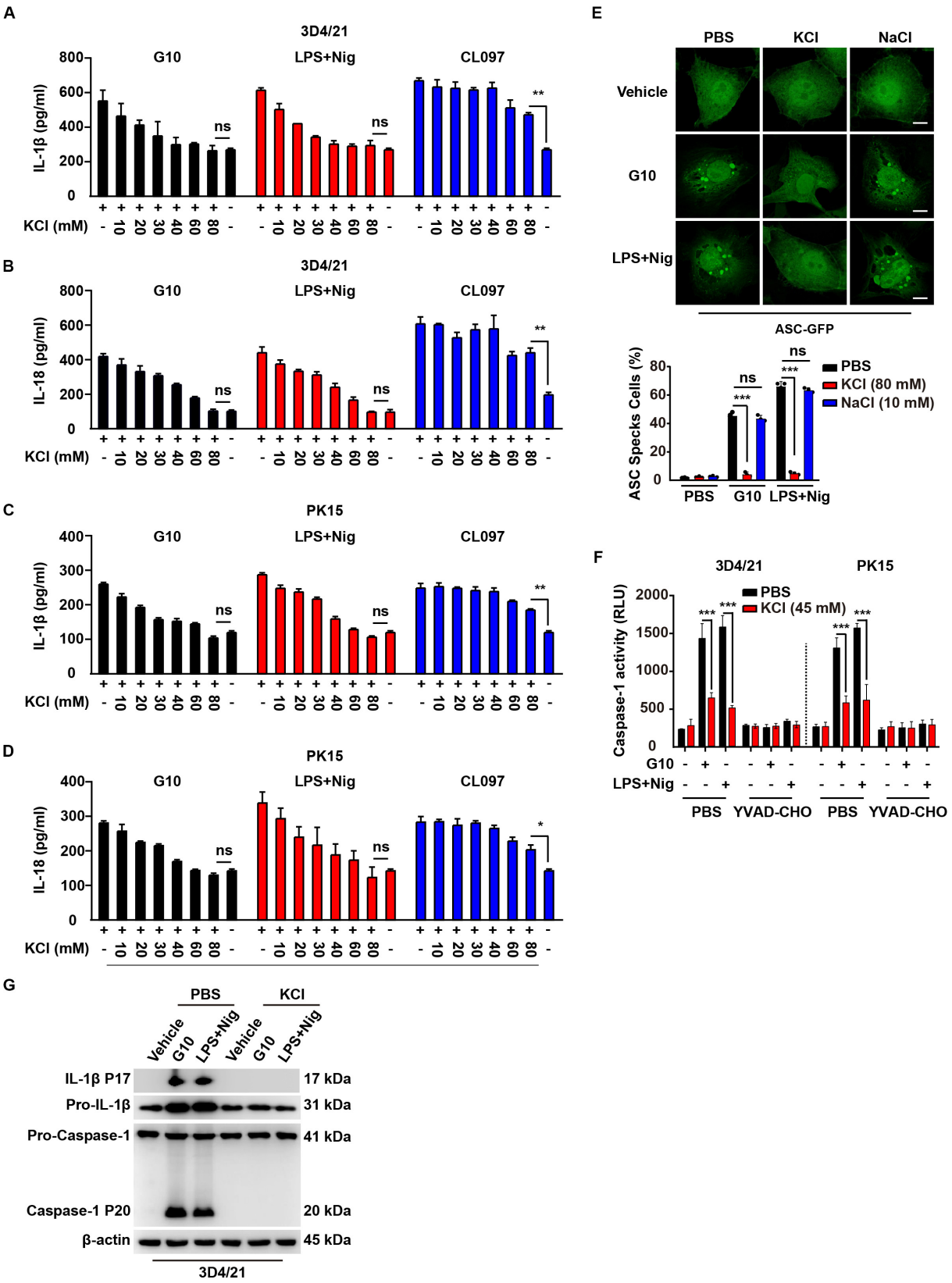

FIGURE 7 | Continued

FIGURE 7 | G10-mediated activation of the NLRP3 inflammasome requires potassium flux in porcine cells. **(A–D)** 3D4/21 **(A,B)** and PK15 **(C,D)** cells were seeded in 12-well plates at a density of 1×10^5 per well. On the next day, cells were treated with G10 (20 μm), LPS + Nig (1 μg/ml + 2.5 μM), and CL097 (70 μM) in the absence or presence of KCl (10–80 mM) for 24 h. The medium was then harvested and IL-1β **(A,C)** and IL-18 **(B,D)** secretion were quantified by ELISA. $^*P < 0.05$, $^{**}P < 0.01$ determined by two-tailed Student's *t*-test. ns, no significance. **(E)** 3D4/21 cells were seeded in 12-well plates with coverslips at a density of 1×10^5 per well. On the next day, cells were transfected with plasmid for expression of ASC-GFP (2 μg) for 24 h. Then, cells were treated with vehicle (DMSO), G10 (20 μm), and LPS + Nig (1 μg/ml + 2.5 μM) in the absence (PBS) or presence of KCl (80 mM) and NaCl (10 mM) for 24 h. ASC oligomerization was assessed by fluorescence microscopy. Quantification of cells with ASC specks is shown at the bottom ($n = 30$ cells). Scale bar, 10 μm. $^{***}P < 0.001$ determined by two-tailed Student's *t*-test. ns, no significance. **(F)** 3D4/21 and PK15 cells were seeded in 12-well plates at a density of 1×10^5 per well. On the next day, cells were treated with G10 (20 μm) and LPS + Nig (1 μg/ml + 2.5 μM) as indicated in the absence (PBS) or presence of KCl (45 mM) and Caspase-1 inhibitor YVAD-CHO (5 μM) for 24 h. Caspase-1 activity was assessed with a Caspase-Glo 1 Inflammasome Assay kit. $^{***}P < 0.001$ determined by two-tailed Student's *t*-test. **(G)** 3D4/21 cells were seeded in 60-mm dishes at a density of 4×10^5 per dish. On the next day, cells were treated with vehicle (DMSO), G10 (20 μm), and LPS + Nig (1 μg/ml + 2.5 μM) in the absence (PBS) or presence of KCl (80 mM) for 24 h. The medium was harvested to analyze mature IL-1β (P17) secretion, and the cells were harvested to analyze pro-IL-1β, pro-Caspase-1 and cleaved Caspase-1 (P20) by immunoblotting analysis.

secretion induced by G10. ELISA of IL-1β and IL-18 indicated that supplementation with K^+ gradually down-regulated G10-induced secretion of IL-1β and IL-18 from 3D4/21 and PK15 cells to basal levels (**Figures 7A–D**). Nigericin is an ionophore that induces potassium efflux, thus promoting NLRP3 inflammasome activation (40), and K^+ replenishment also down-regulated LPS + Nig-induced IL-1β and IL-18 secretion to the levels observed in untreated cells (**Figures 7A–D**). NLRP3 inflammasome activation by CL097 is K^+ efflux-independent (41). Extracellular K^+ did not completely abrogate CL097-stimulated IL-1β and IL-18 secretion, as expected (**Figures 7A–D**).

G10 and LPS + Nig induced formation of ASC specks in 3D4/21 cells, and this effect was reversed by K^+ replenishment but not Na^+ replenishment (**Figure 7E**). Extracellular K^+ inhibited Caspase-1 activation in 3D4/21 and PK15 cells under G10 or LPS + Nig treatment (**Figure 7F**). K^+ replenishment inhibited G10- and LPS + Nig-induced cleavage of pro-IL-1β and pro-Caspase-1 in 3D4/21 cells (**Figure 7G**). Together, these results suggest that G10 activates the NLRP3 inflammasome through K^+ efflux in porcine cells.

Inhibition of the NLRP3 Inflammasome Enhances G10-Induced Type I IFN in Porcine Cells

Type I IFN and inflammasomes are reciprocally regulated, in a process essential for immune homeostasis (42). Therefore, we defined the role of the NLRP3 inflammasome in the regulation of type I IFN in response to G10 in porcine cells. Ablation of *p65* further increased G10-, but not LPS-induced IFN-β and ISG15 mRNA transcription, as well as IFN-β secretion in 3D4/21 and PK15 cells (**Supplementary Figures S3A,B** and **Figure 8A**). Inhibition of the NLRP3 inflammasome by MCC950, or of Caspase-1 by VX765, prevented G10-mediated induction of IL-1β and IL18 secretion and enhanced IFN-β secretion in 3D4/21 and PK15 cells (**Supplementary Figures S3C,D** and **Figures 8B,C**). In addition, G10-induced *Nlrp3*$^{-/-}$, *Asc*$^{-/-}$, *Caspase-1*$^{-/-}$, and *p65*$^{-/-}$ 3D4/21 and PK15 cells generated more IFN-β than WT and *Ifnar1*$^{-/-}$ cells (**Figures 8D,E**). These data demonstrate that inhibition of the NLRP3 inflammasome enhances G10-induced type I IFN expression in porcine cells.

We then asked whether G10 might effectively prevent PRV infection through inhibition of the NLRP3 inflammasome in porcine cells. Viral titer assays indicated that G10 combined with MCC950 or VX765 had greater antiviral activity against PRV than G10 alone in 3D4/21 and PK15 cells, but not in *Ifnar1*$^{-/-}$ 3D4/21 cells (**Figures 8F,G** and **Supplementary Figures S3E,F**). Knockout of *Sting* or *Ifnar1* promoted PRV proliferation, whereas knockout of *Nlrp3*, *Asc*, *Caspase-1*, and *p65* inhibited PRV proliferation (**Figures 8H,I**). Compared with WT 3D4/21 and PK15 cells, *Nlrp3*$^{-/-}$, *Asc*$^{-/-}$, *Caspase-1*$^{-/-}$, and *p65*$^{-/-}$ cells treated with G10 showed significantly repressed PRV proliferation (**Figures 8H,I**). Collectively, these data indicate that G10-induced NLRP3 inflammasome activation negatively regulates type I IFN in porcine cells.

DISCUSSION

In this study, we demonstrated that G10 activates the porcine type I IFN response, in line with previous observations in human cells. Intriguingly, we further demonstrate that G10 primes the NLRP3 inflammasome through up-regulation of NLRP3, pro–IL-1β, and pro–IL-18 through STING, in contrast to the process in human cells. Furthermore, G10 induces potassium efflux and the oligomerization of NLRP3 and ASC, thus resulting in the formation of active Caspase-1, which in turn induces the secretion of mature IL-1β and IL-18. Treatment of NLRP3 inflammasome-deficient cells with G10 enhanced type I IFN expression and effectively inhibited viral infection. Our data indicate that type I IFN is negatively regulated by the NLRP3 inflammasome in porcine cells (**Figure 9**).

Nuclear factor-κB, a central mediator of immune and stress responses, is activated by multiple intra- and extracellular stimuli (43, 44). Our work shows that G10 can activate the NF-κB pathway in porcine cells, but this activation does not occur in human cells. We found that G10 induces porcine *p65* transcription through STING and Sp1. A previous study has indicated that the human *p65* promoter lacks both TATA and CCAAT consensus sequences and contains three consensus binding sites for Sp1 (45). Human cytomegalovirus (HCMV) infection increases Sp1 expression and activates transcription of *p65* through its promoter Sp1-binding sites (46, 47). Because cGAS and STING are key sensors of HCMV in primary human monocyte-derived DCs and macrophages (48, 49), our data may explain the mechanism through which HCMV infection activates *p65* transcription. We also show that LPS-induced

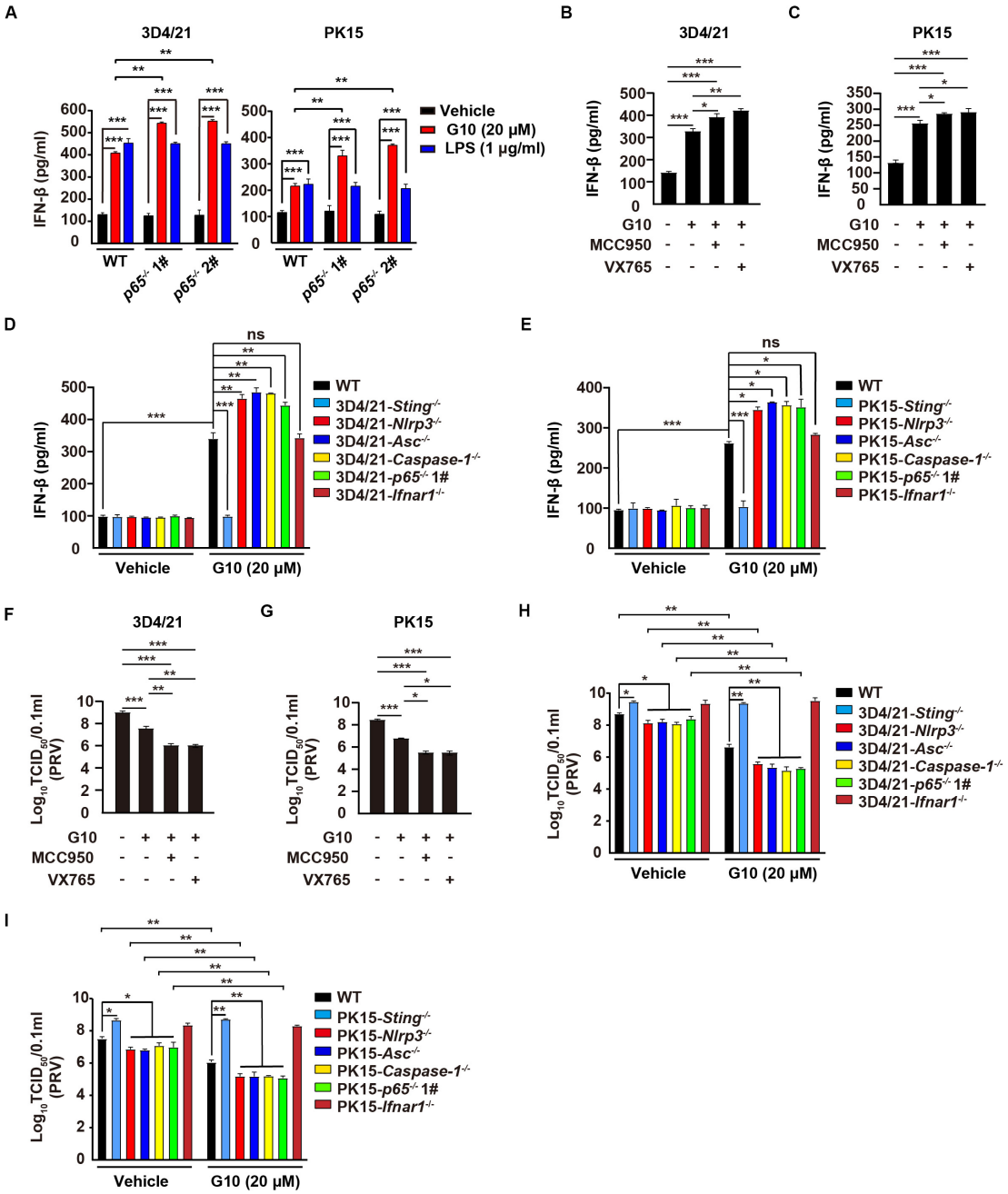

FIGURE 8 | Inhibition of the NLRP3 inflammasome augments G10-induced type I IFN and antiviral activity in porcine cells. **(A)** WT, $p65^{-/-}$ 1#, and $p65^{-/-}$ 2# 3D4/21 and PK15 cells were seeded in 12-well plates at a density of 1×10^5 per well. On the next day, cells were treated with vehicle (DMSO), G10 (20 μM), and LPS (1 μg/ml) for 24 h. The medium was then harvested and IFN-β secretion was quantified by ELISA. $^{**}P < 0.01$, $^{***}P < 0.001$ determined by one-way ANOVA. **(B,C)** 3D4/21 **(B)** and PK15 **(C)** cells were seeded in 12-well plates at a density of 1×10^5 per well. On the next day, cells were treated with G10 (20 μM), MCC950 (10 μM), and VX765 (10 μM) as indicated for 24 h. The medium was then harvested and IFN-β secretion was quantified by ELISA. $^{*}P < 0.05$, $^{**}P < 0.01$, $^{***}P < 0.001$ determined by one-way ANOVA. **(D,E)** WT, *Sting*$^{-/-}$, *Nlrp3*$^{-/-}$, *Asc*$^{-/-}$, *Caspase-1*$^{-/-}$, *p65*$^{-/-}$ 1#, and *Ifnar1*$^{-/-}$ 3D4/21 **(D)** and WT, *Sting*$^{-/-}$, *Nlrp3*$^{-/-}$, *Asc*$^{-/-}$, *Caspase-1*$^{-/-}$, *p65*$^{-/-}$ 1#, and *Ifnar1*$^{-/-}$ PK15 **(E)** cells were seeded in 12-well plates at a density of 1×10^5 per well. On the next day, cells were treated with vehicle (DMSO) or G10 (20 μM) for 24 h. The medium was then harvested and IFN-β secretion was quantified by ELISA. $^{*}P < 0.05$, $^{**}P < 0.01$, $^{***}P < 0.001$ determined by one-way ANOVA. ns, no significance. **(F,G)** 3D4/21 **(F)** and PK15 **(G)** cells were seeded in 12-well plates at a density of 1×10^5 per well. On the next day, cells were infected with PRV-QXX (MOI = 1) and simultaneously treated as in **B**. Virus was harvested by three freeze–thaw cycles and PRV titer was assessed with $TCID_{50}$ assays. $^{*}P < 0.05$, $^{**}P < 0.01$, $^{***}P < 0.001$ determined by one-way ANOVA. **(H,I)** WT, *Sting*$^{-/-}$, *Nlrp3*$^{-/-}$, *Asc*$^{-/-}$, *Caspase-1*$^{-/-}$, *p65*$^{-/-}$ 1#, and *Ifnar1*$^{-/-}$ 3D4/21 **(H)** and WT, *Sting*$^{-/-}$, *Nlrp3*$^{-/-}$, *Asc*$^{-/-}$, *Caspase-1*$^{-/-}$, *p65*$^{-/-}$ 1#, and *Ifnar1*$^{-/-}$ PK15 **(I)** cells were seeded in 12-well plates at a density of 1×10^5 per well. On the next day, cells were treated as in **D**. Virus was harvested by three freeze–thaw cycles and PRV titer was assessed with $TCID_{50}$ assays. $^{*}P < 0.05$, $^{**}P < 0.01$ determined by one-way ANOVA.

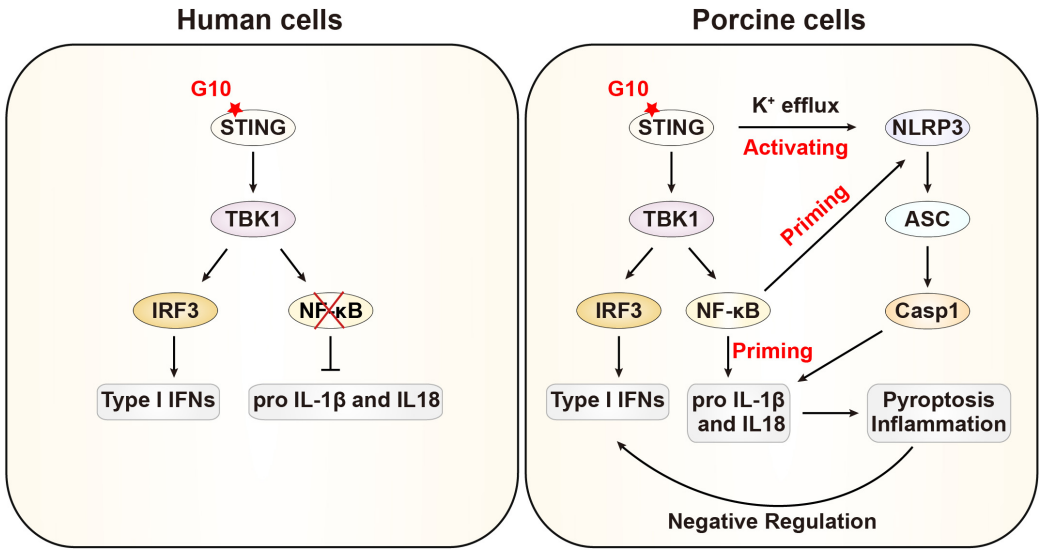

FIGURE 9 | Schematic model showing G10 activation of the NLRP3 inflammasome in porcine cells. In human cells, G10 activates only type I IFN. In porcine cells, G10 also activates the NF-κB signaling pathway, which is a priming signal for NLRP3 inflammasome activation. G10 induces potassium efflux and triggers NLRP3 inflammasome activation, which negatively regulates type I IFN.

p65 transcription is independent of STING and Sp1 in porcine cells. LPS activates NF-κB through Toll-like receptor 4-mediated signaling and causes Sp1 protein degradation by an LPS-inducible Sp1-degrading enzyme (50). Therefore, these findings combined with our current findings suggest that NF-κB is regulated by diverse stimuli through distinct mechanisms in different species.

Several studies have suggested that STING is involved in inflammasome activation. The cyclic dinucleotides 3′5′-diadenylate and 3′5′-diguanylate are bacterial second messengers that activate STING-mediated innate immune responses (51). They stimulate robust secretion of IL-1β through NLRP3 inflammasome signaling that is independent of STING (52). The intrinsic STING agonist cGAMP is catalyzed by cGAS from GTP and ATP (53), and it induces inflammasome activation through a STING, AIM2, NLRP3, ASC, and Caspase-1 dependent process in human and mouse cells (54). Cyclic dinucleotides from prokaryotes and eukaryotes are involved in different pathways of STING-mediated activation of inflammasomes. Nevertheless, our data demonstrate that STING is essential for G10-mediated activation of the canonical NLRP3 inflammasome in porcine cells. We did not determine whether AIM2 is involved in G10-induced NLRP3 inflammasome activation, because AIM2 is not present in pigs (55). Importantly, given that STING is a promising target for cancer immunotherapy, our results suggest that the roles of STING agonist-induced type I IFN in inflammasome activation should be assessed in clinical trials.

The sustained robust inflammation may lead to collateral damage due to the overproduction of inflammatory cytokines (56). Aside from the antimicrobial functions of IFNs, aberrant IFN production is associated with a variety of autoimmune disorders (57). We demonstrated that the NLRP3 inflammasome negatively regulates type I IFN, which may be essential for immune homeostasis in pigs. Multiple reports have demonstrated that the NLRP3 inflammasome can induce and regulate the development of adaptive immunity (58). Both IL-1β and IL-1β are involved in T cell activation and memory cell formation (59–62). Additionally, IL-1β and IL-18 have adjuvant capacity. Moreover, IL-1β enhances humoral immunity (63), and IL-18 augments IgE antibody production (64). Therefore, these beneficial aspects on the NLRP3 inflammasome may support the use of G10 as an effective vaccine adjuvant in the pig industry.

CONCLUSION

Stimulator of interferon genes is an ER-resident transmembrane protein that integrates cytosolic dsDNA-triggered activation of innate immune responses. G10 is a synthetic agonist of human STING that stimulates only STING-dependent IFN expression. However, we found that G10 acts on STING and activates both type I IFN and the canonic NLRP3 inflammasome. G10 activates the NLRP3 inflammasome in porcine cells through simultaneous priming and activation. Our data indicate that the G10-activated NLRP3 inflammasome negatively regulates type I IFN, a process that may be essential for immune homeostasis in pigs.

DATA AVAILABILITY STATEMENT

All datasets presented in this study are included in the article/**Supplementary Material**.

AUTHOR CONTRIBUTIONS

S-LM, LZ, Y-KG, G-YY, JW, and B-BC: project conception and design. S-LM, LZ, Y-KG, SZ, GL-L, Y-XM, YY-Z, W-RC, and

LY: data collection. S-LM, LZ, Y-KG, SZ, and G-LL: data analysis and interpretation. S-LM, G-YY, JW, and B-BC: original manuscript drafting. JW and B-BC: manuscript review, editing, and final approval. All authors contributed to the article and approved the submitted version.

FUNDING

This work was supported by grants from the Ten Thousand Talents Program for Young Talents (W03070106), Outstanding Talents of Henan Agricultural University (30600773), and Ministry of Agriculture and Rural Affairs of China (2016ZX08006001-006).

SUPPLEMENTARY MATERIALS

The Supplementary Material for this article can be found online at: https://www.frontiersin.org/articles/10.3389/fimmu.2020.575818/full#supplementary-material

FIGURE S1 | G10 activates porcine NF-κB signaling pathway. **(A)** WT and *Sting*$^{-/-}$ 3D4/21 cells were seeded in 12-well plates at a density of 1 × 10^5 per well. On the next day, *Sting*$^{-/-}$ 3D4/21 cells were transfected with plasmid for expression of STING-Flag (4 μg) for 24 h. Then cells were treated with vehicle (DMSO), G10 and LPS + Nig at the indicated concentrations for 24 h. Total mRNA was then reverse-transcribed to cDNA and P65 mRNA was assessed by RT-qPCR analysis. The results were normalized to the level of β-actin expression. $^*P < 0.05$, $^{**}P < 0.01$, $^{***}P < 0.001$ determined by two-tailed Student's *t*-test. **(B)** THP-1 cells were seeded and differentiated in 12-well plates with coverslips at a density of 2 × 10^5 per well. On the next day, cells were treated with DMSO, G10 (20 μM) and LPS (1 μg/ml) for 24 h. Translocation of P65 into the nucleus (DAPI) was assessed by immunofluorescence analysis with antibody against P65. Quantification of cells with nuclear localized P65 is shown on the right (n = 30 cells). Scale bar, 10 μm. $^{***}P < 0.001$ determined by two-tailed Student's *t*-test. ns, no significance. **(C)** Schematic representation of the porcine *p65* genomic structure and DNA sequencing results for the indicated knockout cells. Protospacer sequence is shown in red. The PAM sequence is framed by black boxes. **(D)** THP-1 cells were seeded and differentiated in 12-well plates with coverslips at a density of 2 × 10^5 per well. On the next day, cells were treated as in **A**. The medium was then harvested and IL-1β secretion was quantified by ELISA. $^{***}P < 0.001$ determined by two-tailed Student's *t*-test. **(E,F)** Schematic representations of the porcine *Asc* **(E)** and *Caspase-1* **(F)** genomic structure and DNA sequencing results for the indicated knockout cells. Protospacer sequences are shown in red. The PAM sequences are framed by black boxes.

FIGURE S2 | G10 activates porcine NLRP3 inflammasome. **(A,B)** WT, *Sting*$^{-/-}$ 3D4/21 **(A)** and WT, *Sting*$^{-/-}$ PK15 **(B)** cells were seeded in 12-well plates at a density of 1 × 10^5 per well. On the next day, cells were treated with vehicle (DMSO), G10 and LPS + Nig at the indicated concentrations for 24 h. Total mRNA was then reverse-transcribed to cDNA and NLRP1 mRNA was assessed by RT-qPCR analysis. The results were normalized to the level of β-actin expression. **(C)** 3D4/21 cells were seeded in 12-well plates with coverslips at a density of 1 × 10^5 per well. On the next day, cells were transfected with plasmid for expression of NLRP3-Flag (2 μg) for 24 h. Then cells were treated with DMSO and G10 (20 μM) for 24 h. Co-localization of STING and NLRP3 was assessed by immunofluorescence analysis with antibodies against STING and Flag. Scale bar, 10 μm. **(D)** Schematic representations of the porcine *Nlrp3* genomic structure and DNA sequencing results of *Nlrp3*$^{-/-}$ 3D4/21 and PK15 cells. The protospacer sequence is shown in red. The PAM sequence is framed by a black box.

FIGURE S3 | Inhibition of inflammasome activation enhances G10-induce type I IFN response. **(A,B)** WT, *p65*$^{-/-}$ 1#, *p65*$^{-/-}$ 2# 3D4/21, and PK15 cells were seeded in 12-well plates at a density of 1 × 10^5 per well. On the next day, cells were treated with vehicle (DMSO), G10 (20 μM) and LPS (1 μg/ml) for 24 h. Total mRNA was then reverse-transcribed to cDNA and IFN-β **(A)** and ISG15 **(B)** mRNA was assessed by RT-qPCR analysis. The results were normalized to the level of β-actin expression. $^{**}P < 0.01$, $^{***}P < 0.001$ determined by two-tailed Student's *t*-test. **(C)** 3D4/21 cells were seeded in 12-well plates at a density of 1 × 10^5 per well. On the next day, cells were untreated or treated with G10 (20 μM), MCC950 (10 μM), and VX765 (10 μM) as indicated for 24 h. The medium was then harvested and IL-1β and IL-18 secretion was quantified by ELISA. $^{***}P < 0.001$ determined by two-tailed Student's *t*-test. ns, no significance. **(D)** PK15 cells were seeded in 12-well plates at a density of 1 × 10^5 per well. On the next day, cells were treated as in **C**. The medium was then harvested and IL-1β and IL-18 secretion was quantified by ELISA. $^{**}P < 0.01$ determined by two-tailed Student's *t*-test. ns, no significance. **(E)** WT and *Ifnar1*$^{-/-}$ 3D4/21 cells were seeded in 12-well plates at a density of 1 × 10^5 per well. On the next day, cells were treated as in **C**. Virus was harvested by three freeze-thaw cycles and PRV titer was assessed with $TCID_{50}$ assays. $^{**}P < 0.01$, $^{***}P < 0.001$ determined by one-way ANOVA. **(F)** PRV titer was assessed with plaque assays from **E**. $^*P < 0.05$, $^{**}P < 0.01$, $^{***}P < 0.001$ determined by one-way ANOVA.

REFERENCES

1. Takeuchi O, Akira S. Pattern recognition receptors and inflammation. *Cell*. (2010) 140:805–20. doi: 10.1016/j.cell.2010.01.022
2. Paludan SR, Bowie AG. Immune sensing of DNA. *Immunity*. (2013) 38:870–80. doi: 10.1016/j.immuni.2013.05.004
3. Ishikawa H, Barber GN. STING is an endoplasmic reticulum adaptor that facilitates innate immune signalling. *Nature*. (2008) 455:674–8. doi: 10.1038/nature07317
4. Ishikawa H, Ma Z, Barber GN. STING regulates intracellular DNA-mediated, type I interferon-dependent innate immunity. *Nature*. (2009) 461:788–92. doi: 10.1038/nature08476
5. Wu J, Sun L, Chen X, Du F, Shi H, Chen C, et al. Cyclic GMP-AMP is an endogenous second messenger in innate immune signaling by cytosolic DNA. *Science*. (2013) 339:826–30. doi: 10.1126/science.1229963
6. Ablasser A, Goldeck M, Cavlar T, Deimling T, Witte G, Rohl I, et al. cGAS produces a 2′-5′-linked cyclic dinucleotide second messenger that activates STING. *Nature*. (2013) 498:380–4. doi: 10.1038/nature12306
7. Tanaka Y, Chen ZJ. STING specifies IRF3 phosphorylation by TBK1 in the cytosolic DNA signaling pathway. *Sci Signal*. (2012) 5:ra20. doi: 10.1126/scisignal.2002521
8. Ma Z, Ni G, Damania B. Innate sensing of DNA virus genomes. *Annu Rev Virol*. (2018) 5:341–62. doi: 10.1146/annurev-virology-092917-043244
9. Su T, Zhang Y, Valerie K, Wang XY, Lin S, Zhu G. STING activation in cancer immunotherapy. *Theranostics*. (2019) 9:7759–71. doi: 10.7150/thno.37574
10. Sali TM, Pryke KM, Abraham J, Liu A, Archer I, Broeckel R, et al. Characterization of a novel human-specific STING agonist that elicits antiviral activity against emerging alphaviruses. *PLoS Pathog*. (2015) 11:e1005324. doi: 10.1371/journal.ppat.1005324
11. de Zoete MR, Palm NW, Zhu S, Flavell RA. Inflammasomes. *Cold Spring Harb Perspect Biol*. (2014) 6:a016287. doi: 10.1101/cshperspect.a016287
12. Martinon F, Burns K, Tschopp J. The inflammasome: a molecular platform triggering activation of inflammatory caspases and processing of proIL-beta. *Mol Cell*. (2002) 10:417–26. doi: 10.1016/s1097-2765(02)00599-3
13. Agostini L, Martinon F, Burns K, McDermott MF, Hawkins PN, Tschopp J. NALP3 forms an IL-1beta-processing inflammasome with increased activity in Muckle-Wells autoinflammatory disorder. *Immunity*. (2004) 20:319–25. doi: 10.1016/s1074-7613(04)00046-9
14. Elinav E, Strowig T, Kau AL, Henao-Mejia J, Thaiss CA, Booth CJ, et al. NLRP6 inflammasome regulates colonic microbial ecology and risk for colitis. *Cell*. (2011) 145:745–57. doi: 10.1016/j.cell.2011.04.022
15. Khare S, Dorfleutner A, Bryan NB, Yun C, Radian AD, de Almeida L, et al. An NLRP7-containing inflammasome mediates recognition of microbial

lipopeptides in human macrophages. *Immunity*. (2012) 36:464–76. doi: 10.1016/j.immuni.2012.02.001
16. Zhu S, Ding S, Wang P, Wei Z, Pan W, Palm NW, et al. Nlrp9b inflammasome restricts rotavirus infection in intestinal epithelial cells. *Nature*. (2017) 546:667–70. doi: 10.1038/nature22967
17. Franchi L, Amer A, Body-Malapel M, Kanneganti TD, Ozoren N, Jagirdar R, et al. Cytosolic flagellin requires Ipaf for activation of caspase-1 and interleukin 1beta in *salmonella*-infected macrophages. *Nat Immunol*. (2006) 7:576–82. doi: 10.1038/ni1346
18. Zhou R, Yazdi AS, Menu P, Tschopp J. A role for mitochondria in NLRP3 inflammasome activation. *Nature*. (2011) 469:221–5. doi: 10.1038/nature09663
19. Bauernfeind FG, Horvath G, Stutz A, Alnemri ES, MacDonald K, Speert D, et al. Cutting edge: NF-kappaB activating pattern recognition and cytokine receptors license NLRP3 inflammasome activation by regulating NLRP3 expression. *J Immunol*. (2009) 183:787–91. doi: 10.4049/jimmunol.0901363
20. Sharma D, Kanneganti TD. The cell biology of inflammasomes: mechanisms of inflammasome activation and regulation. *J Cell Biol*. (2016) 213:617–29. doi: 10.1083/jcb.201602089
21. Petrilli V, Papin S, Dostert C, Mayor A, Martinon F, Tschopp J. Activation of the NALP3 inflammasome is triggered by low intracellular potassium concentration. *Cell Death Differ*. (2007) 14:1583–9. doi: 10.1038/sj.cdd.4402195
22. Murakami T, Ockinger J, Yu J, Byles V, McColl A, Hofer AM, et al. Critical role for calcium mobilization in activation of the NLRP3 inflammasome. *Proc Natl Acad Sci USA*. (2012) 109:11282–7. doi: 10.1073/pnas.1117765109
23. Liu Q, Zhang D, Hu D, Zhou X, Zhou Y. The role of mitochondria in NLRP3 inflammasome activation. *Mol Immunol*. (2018) 103:115–24. doi: 10.1016/j.molimm.2018.09.010
24. Cruz CM, Rinna A, Forman HJ, Ventura AL, Persechini PM, Ojcius DM. ATP activates a reactive oxygen species-dependent oxidative stress response and secretion of proinflammatory cytokines in macrophages. *J Biol Chem*. (2007) 282:2871–9. doi: 10.1074/jbc.M608083200
25. Rathinam VA, Vanaja SK, Waggoner L, Sokolovska A, Becker C, Stuart LM, et al. TRIF licenses caspase-11-dependent NLRP3 inflammasome activation by gram-negative bacteria. *Cell*. (2012) 150:606–19. doi: 10.1016/j.cell.2012.07.007
26. Guarda G, Braun M, Staehli F, Tardivel A, Mattmann C, Forster I, et al. Type I interferon inhibits interleukin-1 production and inflammasome activation. *Immunity*. (2011) 34:213–23. doi: 10.1016/j.immuni.2011.02.006
27. Khare S, Ratsimandresey RA, de Almeida L, Cuda CM, Rellick SL, Misharin AV, et al. The PYRIN domain-only protein POP3 inhibits ALR inflammasomes and regulates responses to infection with DNA viruses. *Nat Immunol*. (2014) 15:343–53. doi: 10.1038/ni.2829
28. Reboldi A, Dang EV, McDonald JG, Liang G, Russell DW, Cyster JG. Inflammation. 25-Hydroxycholesterol suppresses interleukin-1-driven inflammation downstream of type I interferon. *Science*. (2014) 345:679–84. doi: 10.1126/science.1254790
29. Banerjee I, Behl B, Mendonca M, Shrivastava G, Russo AJ, Menoret A, et al. Gasdermin D restrains type I interferon response to cytosolic DNA by disrupting ionic homeostasis. *Immunity*. (2018) 49:413–26.e5. doi: 10.1016/j.immuni.2018.07.006
30. Liu BC, Sarhan J, Panda A, Muendlein HI, Ilyukha V, Coers J, et al. Constitutive interferon maintains GBP expression required for release of bacterial components upstream of pyroptosis and anti-DNA responses. *Cell Rep*. (2018) 24:155–68.e5. doi: 10.1016/j.celrep.2018.06.012
31. Wang Y, Ning X, Gao P, Wu S, Sha M, Lv M, et al. Inflammasome activation triggers caspase-1-mediated cleavage of cGAS to regulate responses to DNA virus infection. *Immunity*. (2017) 46:393–404. doi: 10.1016/j.immuni.2017.02.011
32. Vadori M, Cozzi E. The immunological barriers to xenotransplantation. *Tissue Antigens*. (2015) 86:239–53. doi: 10.1111/tan.12669
33. Mair KH, Sedlak C, Kaser T, Pasternak A, Levast B, Gerner W, et al. The porcine innate immune system: an update. *Dev Comp Immunol*. (2014) 45:321–43. doi: 10.1016/j.dci.2014.03.022
34. Wang J, Wang CF, Ming SL, Li GL, Zeng L, Wang MD, et al. Porcine IFITM1 is a host restriction factor that inhibits pseudorabies virus infection. *Int J Biol Macromol*. (2019) 151:1181–93. doi: 10.1016/j.ijbiomac.2019.10.162
35. Mettenleiter TC. Aujeszky's disease (pseudorabies) virus: the virus and molecular pathogenesis–state of the art, June 1999. *Vet Res*. (2000) 31:99–115. doi: 10.1051/vetres:2000110
36. Hayden MS, Ghosh S. NF-kappaB in immunobiology. *Cell Res*. (2011) 21:223–44. doi: 10.1038/cr.2011.13
37. Man SM, Kanneganti TD. Regulation of inflammasome activation. *Immunol Rev*. (2015) 265:6–21. doi: 10.1111/imr.12296
38. Chen J, Chen ZJ. PtdIns4P on dispersed trans-Golgi network mediates NLRP3 inflammasome activation. *Nature*. (2018) 564:71–6. doi: 10.1038/s41586-018-0761-3
39. Wannamaker W, Davies R, Namchuk M, Pollard J, Ford P, Ku G, et al. (S)-1-((S)-2-{[1-(4-amino-3-chloro-phenyl)-methanoyl]-amino}-3,3-dimethyl-butanoyl)-pyrrolidine-2-carboxylic acid ((2R,3S)-2-ethoxy-5-oxo-tetrahydro-furan-3-yl)-amide (VX-765), an orally available selective interleukin (IL)-converting enzyme/caspase-1 inhibitor, exhibits potent anti-inflammatory activities by inhibiting the release of IL-1beta and IL-18. *J Pharmacol Exp Ther*. (2007) 321:509–16. doi: 10.1124/jpet.106.111344
40. Munoz-Planillo R, Kuffa P, Martinez-Colon G, Smith BL, Rajendiran TM, Nunez G. K(+) efflux is the common trigger of NLRP3 inflammasome activation by bacterial toxins and particulate matter. *Immunity*. (2013) 38:1142–53. doi: 10.1016/j.immuni.2013.05.016
41. Gross CJ, Mishra R, Schneider KS, Medard G, Wettmarshausen J, Dittlein DC, et al. K(+) efflux-independent NLRP3 inflammasome activation by small molecules targeting mitochondria. *Immunity*. (2016) 45:761–73. doi: 10.1016/j.immuni.2016.08.010
42. Labzin LI, Lauterbach MA, Latz E. Interferons and inflammasomes: cooperation and counterregulation in disease. *J Allergy Clin Immunol*. (2016) 138:37–46. doi: 10.1016/j.jaci.2016.05.010
43. Li Q, Verma IM. NF-kappaB regulation in the immune system. *Nat Rev Immunol*. (2002) 2:725–34. doi: 10.1038/nri910
44. Pahl HL. Activators and target genes of Rel/NF-kappaB transcription factors. *Oncogene*. (1999) 18:6853–66. doi: 10.1038/sj.onc.1203239
45. Ueberla K, Lu Y, Chung E, Haseltine WA. The NF-kappa B p65 promoter. *J Acquir Immune Defic Syndr*. (1993) 6:227–30.
46. Yurochko AD, Kowalik TF, Huong SM, Huang ES. Human cytomegalovirus upregulates NF-kappa B activity by transactivating the NF-kappa B p105/p50 and p65 promoters. *J Virol*. (1995) 69:5391–400.
47. Yurochko AD, Mayo MW, Poma EE, Baldwin AS Jr., Huang ES. Induction of the transcription factor Sp1 during human cytomegalovirus infection mediates upregulation of the p65 and p105/p50 NF-kappaB promoters. *J Virol*. (1997) 71:4638–48.
48. Paijo J, Doring M, Spanier J, Grabski E, Nooruzzaman M, Schmidt T, et al. cGAS senses human cytomegalovirus and induces type I interferon responses in human monocyte-derived cells. *PLoS Pathog*. (2016) 12:e1005546. doi: 10.1371/journal.ppat.1005546
49. Lio CW, McDonald B, Takahashi M, Dhanwani R, Sharma N, Huang J, et al. cGAS-STING signaling regulates initial innate control of Cytomegalovirus infection. *J Virol*. (2016) 90:7789–97. doi: 10.1128/JVI.01040-16
50. Ye X, Liu SF. Lipopolysaccharide causes Sp1 protein degradation by inducing a unique trypsin-like serine protease in rat lungs. *Biochim Biophys Acta*. (2007) 1773:243–53. doi: 10.1016/j.bbamcr.2006.09.013
51. Abdul-Sater AA, Grajkowski A, Erdjument-Bromage H, Plumlee C, Levi A, Schreiber MT, et al. The overlapping host responses to bacterial cyclic dinucleotides. *Microbes Infect*. (2012) 14:188–97. doi: 10.1016/j.micinf.2011.09.002
52. Abdul-Sater AA, Tattoli I, Jin L, Grajkowski A, Levi A, Koller BH, et al. Cyclic-di-GMP and cyclic-di-AMP activate the NLRP3 inflammasome. *EMBO Rep*. (2013) 14:900–6. doi: 10.1038/embor.2013.132
53. Sun L, Wu J, Du F, Chen X, Chen ZJ. Cyclic GMP-AMP synthase is a cytosolic DNA sensor that activates the type I interferon pathway. *Science*. (2013) 339:786–91. doi: 10.1126/science.1232458
54. Swanson KV, Junkins RD, Kurkjian CJ, Holley-Guthrie E, Pendse AA, Morabiti R. El, et al. A noncanonical function of cGAMP in inflammasome priming and activation. *J Exp Med*. (2017) 214:3611–26. doi: 10.1084/jem.20171749
55. Dawson HD, Smith AD, Chen C, Urban JF Jr. An in-depth comparison of the porcine, murine and human inflammasomes; lessons from the porcine genome

and transcriptome. *Vet Microbiol*. (2017) 202:2–15. doi: 10.1016/j.vetmic.2016.05.013
56. Chen GY, Nunez G. Sterile inflammation: sensing and reacting to damage. *Nat Rev Immunol*. (2010) 10:826–37. doi: 10.1038/nri2873
57. Ivashkiv LB, Donlin LT. Regulation of type I interferon responses. *Nat Rev Immunol*. (2014) 14:36–49. doi: 10.1038/nri3581
58. Chen M, Wang H, Chen W, Meng G. Regulation of adaptive immunity by the NLRP3 inflammasome. *Int Immunopharmacol*. (2011) 11:549–54. doi: 10.1016/j.intimp.2010.11.025
59. Ghiringhelli F, Apetoh L, Tesniere A, Aymeric L, Ma Y, Ortiz C, et al. Activation of the NLRP3 inflammasome in dendritic cells induces IL-1beta-dependent adaptive immunity against tumors. *Nat Med*. (2009) 15:1170–8. doi: 10.1038/nm.2028
60. Sutton C, Brereton C, Keogh B, Mills KH, Lavelle EC. A crucial role for interleukin (IL)-1 in the induction of IL-17-producing T cells that mediate autoimmune encephalomyelitis. *J Exp Med*. (2006) 203:1685–91. doi: 10.1084/jem.20060285
61. Gris D, Ye Z, Iocca HA, Wen H, Craven RR, Gris P, et al. NLRP3 plays a critical role in the development of experimental autoimmune encephalomyelitis by mediating Th1 and Th17 responses. *J Immunol*. (2010) 185:974–81. doi: 10.4049/jimmunol.0904145
62. Nakanishi K, Yoshimoto T, Tsutsui H, Okamura H. Interleukin-18 is a unique cytokine that stimulates both Th1 and Th2 responses depending on its cytokine milieu. *Cytokine Growth Factor Rev*. (2001) 12:53–72. doi: 10.1016/s1359-6101(00)00015-0
63. Curtsinger JM, Schmidt CS, Mondino A, Lins DC, Kedl RM, Jenkins MK, et al. Inflammatory cytokines provide a third signal for activation of naive CD4+ and CD8+ T cells. *J Immunol*. (1999) 162:3256–62.
64. Yoshimoto T, Mizutani H, Tsutsui H, Noben-Trauth N, Yamanaka K, Tanaka M, et al. IL-18 induction of IgE: dependence on CD4+ T cells, IL-4 and STAT6. *Nat Immunol*. (2000) 1:132–7. doi: 10.1038/77811

Conflict of Interest: The authors declare that the research was conducted in the absence of any commercial or financial relationships that could be construed as a potential conflict of interest.

frontiers in Immunology

REVIEW
published: 20 October 2020
doi: 10.3389/fimmu.2020.02172

Modulation of Immune Responses to Influenza A Virus Vaccines by Natural Killer T Cells

John P. Driver[1], *Darling Melany de Carvalho Madrid*[1], *Weihong Gu*[1], *Bianca L. Artiaga*[2] *and Jürgen A. Richt*[2]*

[1] Department of Animal Sciences, University of Florida, Gainesville, FL, United States, [2] Diagnostic Medicine/Pathobiology, College of Veterinary Medicine, Kansas State University, Manhattan, KS, United States

Influenza A viruses (IAVs) circulate widely among different mammalian and avian hosts and sometimes give rise to zoonotic infections. Vaccination is a mainstay of IAV prevention and control. However, the efficacy of IAV vaccines is often suboptimal because of insufficient cross-protection among different IAV genotypes and subtypes as well as the inability to keep up with the rapid molecular evolution of IAV strains. Much attention is focused on improving IAV vaccine efficiency using adjuvants, which are substances that can modulate and enhance immune responses to co-administered antigens. The current review is focused on a non-traditional approach of adjuvanting IAV vaccines by therapeutically targeting the immunomodulatory functions of a rare population of innate-like T lymphocytes called invariant natural killer T (iNKT) cells. These cells bridge the innate and adaptive immune systems and are capable of stimulating a wide array of immune cells that enhance vaccine-mediated immune responses. Here we discuss the factors that influence the adjuvant effects of iNKT cells for influenza vaccines as well as the obstacles that must be overcome before this novel adjuvant approach can be considered for human or veterinary use.

Keywords: natural killer T (NKT) cells, influenza A virus, vaccines, immune modulation, adjuvant

OPEN ACCESS

Edited by:
Jordi Ochando, Icahn School of Medicine at Mount Sinai, United States

Reviewed by:
Mark L. Lang, University of Oklahoma Health Sciences Center, United States
Estanislao Nistal-Villan, San Pablo CEU University, Spain

***Correspondence:**
Jürgen A. Richt
jricht@ksu.edu

Specialty section:
This article was submitted to Vaccines and Molecular Therapeutics, a section of the journal Frontiers in Immunology

Received: *30 May 2020*
Accepted: *10 August 2020*
Published: *20 October 2020*

Citation:
Driver JP, de Carvalho Madrid DM, Gu W, Artiaga BL and Richt JA (2020) Modulation of Immune Responses to Influenza A Virus Vaccines by Natural Killer T Cells. Front. Immunol. 11:2172. doi: 10.3389/fimmu.2020.02172

INTRODUCTION

Influenza A viruses (IAVs) are a genetically diverse group of segmented RNA viruses capable of infecting birds and mammals, including swine, bats, and humans (1–3). IAV infections result in a highly contagious acute respiratory disease that is capable of causing substantial morbidity but usually low mortality (4, 5). IAVs are a significant burden to human and animal health and have the potential to occasionally cause pandemics. Vaccination is a cornerstone of IAV mitigation. However, the high genetic/antigenic diversity of IAVs, which is a result of (i) the rapid IAV mutation rates ("genetic drift") and (ii) the reassortment ability between genetically different IAV strains ("genetic shift"), inherently limits vaccine effectiveness (6). The genetic evolution of IAVs by genetic drift and shift associated with the heterogeneous and complex immune response to influenza vaccines requires annual updates of human IAV vaccines and often results in vaccine failure (2, 7). For example, the 2018–2019 influenza vaccines for humans were reported to have an estimated vaccine effectiveness of 29% (8), based on the relative difference in influenza risk between vaccinated and unvaccinated participants (9). This low effectiveness was due to the circulation of an influenza H3N2 virus which was antigenically drifted from the H3N2 virus isolate included in the vaccine (8). The use of adjuvants that increase the scope, scale, and quality of innate and adaptive

immune responses can improve the effectiveness of IAV vaccines significantly (10). Most adjuvants fall into two categories. The first is delivery systems that enhance antigen release, stability, and uptake (11). The second uses immune stimulatory molecules, such as Toll-like receptor ligands, that induce the release of cytokines and chemokines from innate immune cells, which drives antigen-presenting cell (APC) maturation and licensing and, therefore, improves immunogenicity of the respective antigens (12).

Although conventional adjuvants can stimulate cellular and humoral immune responses and reduce the antigen dose required in the vaccine, they seldom improve long-term immunity and cross-reactivity against heterologous (i.e., belong to the same subtype but are genetically different IAV isolates) and heterosubtypic (i.e., belong to different IAV subtypes) IAV strains, which is greatly needed (13). This has led researchers to explore using non-traditional adjuvants to improve vaccine efficacy, including the powerful immunoregulatory effects of innate T lymphocyte populations, such as γδT cells, and CD1- and MR-1-resticted T cells. Unlike the major histocompatibility complex (MHC)-restricted T cells, these cells possess a restricted repertoire of T cell receptors (TCR), perform rapid effector responses, and recognize a limited selection of non-peptide molecules, including small metabolites and lipids (14). Currently, the innate T cell population with the most potential to enhance vaccines is natural killer T (NKT) cells, which recognize lipid and glycolipid ligands presented by the MHC class I-like molecule CD1d (14). These cells have phenotypic characteristics of both T cells and NK cells and express a semi-invariant TCR (14). Upon activation, NKT cells rapidly release large quantities of multiple cytokines and chemokines capable of boosting adaptive immune responses. Importantly, a subset of NKT cells known as type I or invariant NKT (iNKT) cells that express an invariant αβ TCR, can be globally and specifically activated using derivatives of the prototypic antigen known as (2S,3S,4R)-1-*O*-(α-D-galactopyranosyl)-N-hexacosanoyl-2-amino-1,3,4-octadecanetriol, also called α-galactosylceramide (α-GalCer), which was first isolated from a marine sponge (*Agelas mauritianus*) (15, 16). Activation with α-GalCer induces iNKT cells to generate a potent immune response to a wide range of co-delivered antigens.

Since the discovery of α-GalCer, numerous studies have explored how iNKT cell responses can adjuvant vaccines against different infectious diseases [reviewed in (17–20)]. However, most of these studies have used the mouse model of IAV infection, largely because it is well-established and easy to work with. These studies have almost invariably reported that iNKT cells are capable of substantially enhancing the quality and the scale of IAV vaccine responses (21–33). In this review, we summarize the current knowledge about therapeutically harnessing iNKT cell activities to improve IAV vaccines in mice and other animal models. We also address important factors that influence the adjuvant effects of therapeutically activated iNKT cells, which must be considered to safely and effectively exploit the adjuvant potential of iNKT cells for human or livestock vaccines.

NKT CELL CHARACTERISTICS

Although the name "natural killer T cell" first appeared in the literature in 1995 (34), these cells were first described in 1987 as a subset of T cells with moderate levels of αβ TCRs and NK1.1, a marker characteristic of natural killer cells (35–38). Over the subsequent decade, it was established that NKT cells express a highly restricted TCR repertoire (39), produce developmentally regulated Th1 and Th2 cytokines (40), bind CD1d as their antigen presenting molecule (41), and recognize glycolipid/lipid ligands (15, 42). It was further discovered that NKT cells can be divided into two functionally distinct classes: type I and type II NKT cells (43). Type I NKT or iNKT cells express a highly restricted TCR repertoire which recognizes CD1d-bound α-GalCer (44, 45). Type II NKT cells, also known as diverse NKT cells, express a less restricted TCR repertoire and recognize different glycolipids than iNKT cells, such as sulfatides (46). This review will discuss iNKT cells as it is this subset which can be therapeutically targeted using glycolipid antigens.

iNKT cells recognize both endogenous and exogenous ligands (42). Their recognition of endogenous ligands enables iNKT cells to interact with inflamed or injured tissues which overexpress lipid molecules (47). Most exogenous iNKT cell antigens are glycolipid and phospholipid components of bacterial cell walls, such as mycobacterial phosphatidylinositolmannosides and monoglycosylceramides from gram-negative bacteria (42, 48). iNKT cells also respond to antigens from protozoan parasites, including phospholipids from *Leishmania* and glycophosphatidylinositol from *Plasmodium* and *Trypanosoma* (49, 50). iNKT cells in most species react to α-GalCer and its synthetic analog KRN7000 (51–53). These molecules have been widely used to study iNKT cell function since they strongly activate these cells. α-GalCer stimulated mouse iNKT cells produce a wide variety of cytokines, including IFN-γ, IL-2, IL-3, IL-4, IL-5, IL-9, IL-10, IL-13, IL-17, IL-21, IL-22, and tumor necrosis factor (TNF)-α and -β (54–57). Stimulated mouse iNKT cells also secrete chemokines, including RANTES (regulated on activation, normal T cell expressed and secreted), monocyte chemoattractant protein (MCP)-1, eotaxins, and macrophage inflammatory protein (MIP)-1α and MIP-1β (58–61). Many of these cytokines modulate cellular and humoral immune responses against foreign antigens, which is why α-GalCer activated iNKT cells can enhance the scale and the scope of vaccine responses against a wide variety of pathogens.

iNKT CELL-CD1d SYSTEM IN MAMMALS

The defining feature of iNKT cells is the expression of a TCR with an invariant Vα chain rearrangement and limited Vβ chain usage. Mouse iNKT cells express a single α chain (Vα14-Jα18) that is paired with a limited number of Vβ chains (Vβ2, Vβ7, or Vβ8.2) (39, 62, 63). Rats use a homologous Vα14-Jα18 rearrangement paired with Vβ8.2 chains but have four Vα14 genes with differential tissue expression (64). The human invariant receptor is composed of a Vα24-Jα18 rearrangement paired with Vβ11 (39, 65, 66), while the porcine iNKT TCR is composed of a Vα10-Jα18 chain paired with a Vβ25-chain, both of which are

highly homologous to the human Vα24-Jα18 and Vβ11 TCR chains (67). A consequence of the remarkably conserved nature of the TCR-CD1d system is that CD1d tetramers often cross-react among different animal species. For instance, human CD1d tetramers cross-react with mouse iNKT cells and *vice versa* (45), and both mouse and human CD1d tetramers cross-react with pig iNKT cells (68). Interestingly, rat iNKT cells are only partially identified by mouse CD1d tetramers and require the use of rat CD1d molecules in glycolipid-loaded tetramers (69). Overall, the CD1d-mediated recognition of α-GalCer by iNKT cells is highly conserved through mammalian evolution (70). This has the advantage that many aspects of glycolipid therapy research in preclinical mouse models can be directly translated to target animal species, including humans.

Not all mammals harbor CD1d genes in their genomes, and some that do, do not express functional transcripts and/or CD1d proteins that are capable of interacting with iNKT cells. Humans (71), primates (72, 73), mice (15), rats (64), cotton rats (74), pigs (75, 76), and dogs (77) have been reported to possess functional iNKT cell-CD1d systems and iNKT cells that react to α-GalCer. Ruminants were thought to harbor two copies of *CD1d* that are pseudogenes (*CD1d1* and *CD1d2*) due to a mutated start codon and a first intron that cannot be translated into functional proteins (78, 79). However, it was later discovered that the bovine *CD1d1* gene has an alternative start codon that produces CD1d proteins capable of being expressed on the cell surface (80). Interestingly, the antigen binding site in bovine CD1d1 is smaller than in human and mouse CD1d proteins, which prohibits α-GalCer from binding. Instead, bovine CD1d1 appears to present glycolipids with shorter alkyl chains than α-GalCer (80, 81). The sequences of the equine iNKT invariant α-chain TCR and CD1d have conserved residues that align with their human and mouse counterparts. Nevertheless, equine iNKT cells have yet to be isolated and horses do not respond to synthetic glycolipids that activate iNKT cells in other species (82).

MECHANISMS OF iNKT CELL ACTIVATION

iNKT cells can be directly activated by TCR signaling after engaging CD1d-bound glycolipid antigens, or indirectly via cytokines from pathogen recognition receptor-stimulated APCs. Indirect activation sometimes involves weak TCR signals from low-affinity microbial or self-lipid antigens but can also occur in the absence of TCR stimulation (83–88). Directly activated mouse iNKT cells secrete a mixture of Th1 and Th2 cytokines, which differs from iNKT cells indirectly activated through pro-inflammatory cytokines that mainly produce Th1-type cytokines (89, 90). The variety and the quantity of cytokines produced by directly activated iNKT cells depend on the strength of the interactions between the iNKT TCR and the lipid-CD1d complex (43, 83, 91, 92). However, additional factors, including different iNKT cell subsets, the half-life of TCR-ligand binding, ligand density, and the uptake and presentation of iNKT cell-activating glycolipids by APCs, may play a role in determining their cytokine bias (93–97). α-GalCer strongly activates iNKT cells, which induces the rapid upregulation of T cell activation markers and the secretion of several cytokines, especially IFN-γ, IL-2, and IL-4 within hours after stimulation. α-GalCer activated iNKT cells also proliferate and may expand up to 10-fold in some organs by 4 days post-treatment, after which they contract to baseline levels (98, 99). Unlike conventional T cells, iNKT cells do not possess memory functions. In fact, secondary α-GalCer administration actually results in a significantly weaker iNKT cell response compared to primary stimulation with this antigen, characterized by reduced proliferation and cytokine secretion (100, 101). This hyporesponsive state lasts for at least 1 month after initial activation (101–103). The same hyporesponsive state has been reported in mice challenged with bacterial pathogens (104–106), toxins (107), and TLR agonists (104). The response of iNKT cells to α-GalCer have been studied most extensively in mice. However, *in vivo* studies in humans, chimpanzees, macaques, swine, and cotton rats have found that α-GalCer can stimulate iNKT cell activities in a wide variety of mammals.

iNKT cells indirectly activated by APCs participate in immune responses against numerous microorganisms that lack cognate lipid antigens. Various pathogen-associated molecular patterns (PAMPs) and some danger-associated molecular patterns (DAMPs) have been shown to induce iNKT cell-activating cytokines (108–112), such as type I interferons, IL-12, IL-18, and IL-33 (88, 90, 113–115). Interleukin-12 signaling appears to be particularly important as iNKT cells express high baseline levels of the IL-12 receptor (116). Many bacterial and viral infections stimulate sufficient IL-12 to activate iNKT cells with low-affinity endogenous ligands or without TCR signaling (88, 89, 113, 117, 118). Indirect iNKT cell activation may also be induced by IFN-α and IFN-β from TLR-7- and TLR-9-activated APCs (113) or by a combination of IL-12 and IL-18, which are produced by TLR-4- and TLR-9-stimulated APCs (88, 90, 114). iNKT cells can also be activated *via* their NK receptors that provide both activation and regulation signals in response to stress-induced ligands (119–121). Indirectly activated iNKT cells develop distinct effector functions compared to directly activated iNKT cells. One important difference is that a large fraction of cytokine-activated iNKT cells acquire the ability to express perforin that may allow them to carry out cytolytic functions *in vivo* (54). Furthermore, indirectly activated iNKT cells secrete large quantities of IFN-γ without IL-4, whereas directly activated iNKT cells often produce both cytokines simultaneously (122). The weak TCR signaling that occurs during indirect iNKT cell activation promotes IFN-γ production by inducing histone H4 acetylation near the IFN-γ locus. This enables iNKT cells to produce IFN-γ upon subsequent exposure to IL-12 and IL-18 without concurrent TCR stimulation (114). Unlike during direct activation, iNKT cells remain motile during stimulation with cytokines, which may enable them to disseminate IFN-γ as they migrate, amplifying their impact on immune responses (114). It is likely that IAV vaccines trigger several indirect activation-mediated iNKT cell effector functions and that some of these responses will support (or perhaps counteract) the direct activation effects of co-delivered glycolipid antigens. In this scenario, achieving optimal IAV vaccine immunity will require studies to

evaluate combining different dosages of iNKT cell agonists and IAV vaccines.

HELPER FUNCTIONS OF iNKT CELLS

iNKT cells are capable of generating immune responses that in many ways mirror conventional $CD4^+$ T cell help (**Figure 1**). Activated iNKT cells induce APCs to mature when they engage antigen-bound CD1d on their surface (123). These iNKT cell-conditioned APCs, in turn, produce cytokines and T cell costimulatory molecules that further prime iNKT cells, causing them to upregulate CD40L, and secrete IFN-γ and granulocyte-macrophage colony-stimulating factor. This induces surrounding APCs to mature and activate additional iNKT cells (113, 123, 124). iNKT cell-licensed APCs prime conventional $CD4^+$ T cells against co-delivered peptide antigens, which results in enhanced cytotoxic $CD8^+$ T cell responses and induces $CD4^+$ T cells to become follicular helper T (T_{FH}) cells. iNKT cell-conditioned APCs also acquire the ability to cross-present peptide antigens to $CD8^+$ T cells (125–127). The mechanisms through which iNKT cells enhance humoral immune responses have been extensively reviewed (128–132). One mode involves iNKT cells directly interacting with B cells presenting glycolipid ligands on CD1d, which is referred to as cognate B cell help. Initially, iNKT cells recognize glycolipid antigens on dendritic cells (DCs) and differentiate into iNKT follicular helper ($iNKT_{FH}$) cells that adopt a phenotype similar to T_{FH} cells (133, 134). These $iNKT_{FH}$ cells then activate B cells specific for protein antigens through a process that requires CD1d expression by B cells, B7-1/B7-2, and CD40 ligation by the iNKT cells and the secretion of IFN-γ and IL-21. Cognate B cell help stimulates plasmablast expansion, germinal center formation, antibody class switching, and moderate affinity maturation (135, 136). iNKT cells can also provide non-cognate B cell help which occurs when iNKT cells indirectly activate B cells by inducing T_{FH} cells specific for protein antigens displayed by B cells (137). This mode of activation is thought to drive enhanced antibody production when α-GalCer is co-administered with immunizing antigens; protein and α-GalCer are internalized by DCs that simultaneously present peptide fragments of the protein antigen on MHC class II to naïve CD4+ T cells and α-GalCer on CD1d to iNKT cells. The T_{FH} cells that result provide CD1d-independent antigen-specific help for the proliferation of B cells in germinal centers, antibody class switching, affinity maturation, and the generation of plasma cells and memory B cells. In addition, activated iNKT cells trans-activate NK cells to produce large quantities of IFN-γ that stimulate B cells to secrete IgG (138). Non-cognate B cell help is probably important after virus exposure when iNKT cells may shape B cell responses by producing an early wave of IL-4 that seeds germinal centers and activates antigen-experienced B cells (139).

The benefit of eliciting T helper responses via iNKT cells compared to $CD4^+$ T cells is that iNKT cells constitute a much greater fraction of total T cells than any antigen-specific $CD4^+$ T cell clone (140, 141). Furthermore, iNKT cells can be globally and specifically activated using α-GalCer analogs due to the highly non-polymorphic CD1d molecule (67, 78, 142). Conversely, conventional $CD4^+$ T cells are restricted by the high level of inter-individual MHC class II polymorphism, which limits the efficacy of peptide-based vaccines in outbred populations. Co-administering iNKT cell ligands with vaccines that induce a wide array of conventional T helper cell responses has the potential to induce wide-ranging cellular and humoral immune responses capable of greatly improving the durability and the cross-protection of vaccines, including against IAVs.

ROLE OF iNKT CELLS IN IMMUNITY TO IAV INFECTIONS

Mice lacking iNKT cells are more susceptible to IAV infections than iNKT cell-intact mice (143–146), indicating that these cells contribute to IAV immunity. iNKT cell activation is likely through the indirect pathway as IAVs contain no known iNKT cell ligands. Nevertheless, stimulation may be enhanced by interactions with CD1d-bound endogenous glycolipids which often increase after viral infection (147). iNKT cells migrate to the lungs during the early stages of IAV infections, alongside the recruitment of neutrophils and the rapid induction of pro- and anti-inflammatory cytokines that prime immune cells, including iNKT cells (146, 148). Mouse studies have reported that airway-resident iNKT cells prevent virus replication and limit lung damage through a combination of (i) reducing the suppressive capacity of myeloid-derived suppressor cells that inhibit influenza-specific immune responses (143), (ii) activating lung-resident NK cells (145), and (iii) directly lysing IAV-infected monocytes (144). In addition, iNKT cells stimulated by IL-1β and IL-23 produce large amounts of IL-22 that protects the lung epithelium from influenza-mediated damage (149). iNKT cells have also been investigated for their role in shaping pre-existing immunity against re-infections with the same or heterologous influenza viruses. Benton et al. showed that CD1d knockout mice previously infected with A/Puerto Rico/8/34 (H1N1) or A/Philippines/2/82/X-79 (H3N2) and re-infected after 4 weeks with the correspondent homologous or heterologous H1N1 or H3N2 viruses were just as susceptible to re-infection as wildtype mice (150). These findings suggest that iNKT cell responses might be superfluous for generating immune memory or cross-protection after a natural IAV infection. This contrasts with other studies showing that therapeutically activated iNKT cells improve pre-existing immunity from IAV vaccination and suggests that immunity generated by iNKT cells might differ depending on whether they are activated indirectly during an IAV infection or *via* glycolipid antigens.

STUDIES USING iNKT CELL AGONISTS WITH IAV VACCINES

At least 17 publications have reported the effects of iNKT cell agonists for adjuvanting IAV vaccines (**Table 1**). Most of these studies have used mice because they are relatively inexpensive and compatible with a wide variety of vaccine formats. However, swine and non-human primates [pigtail

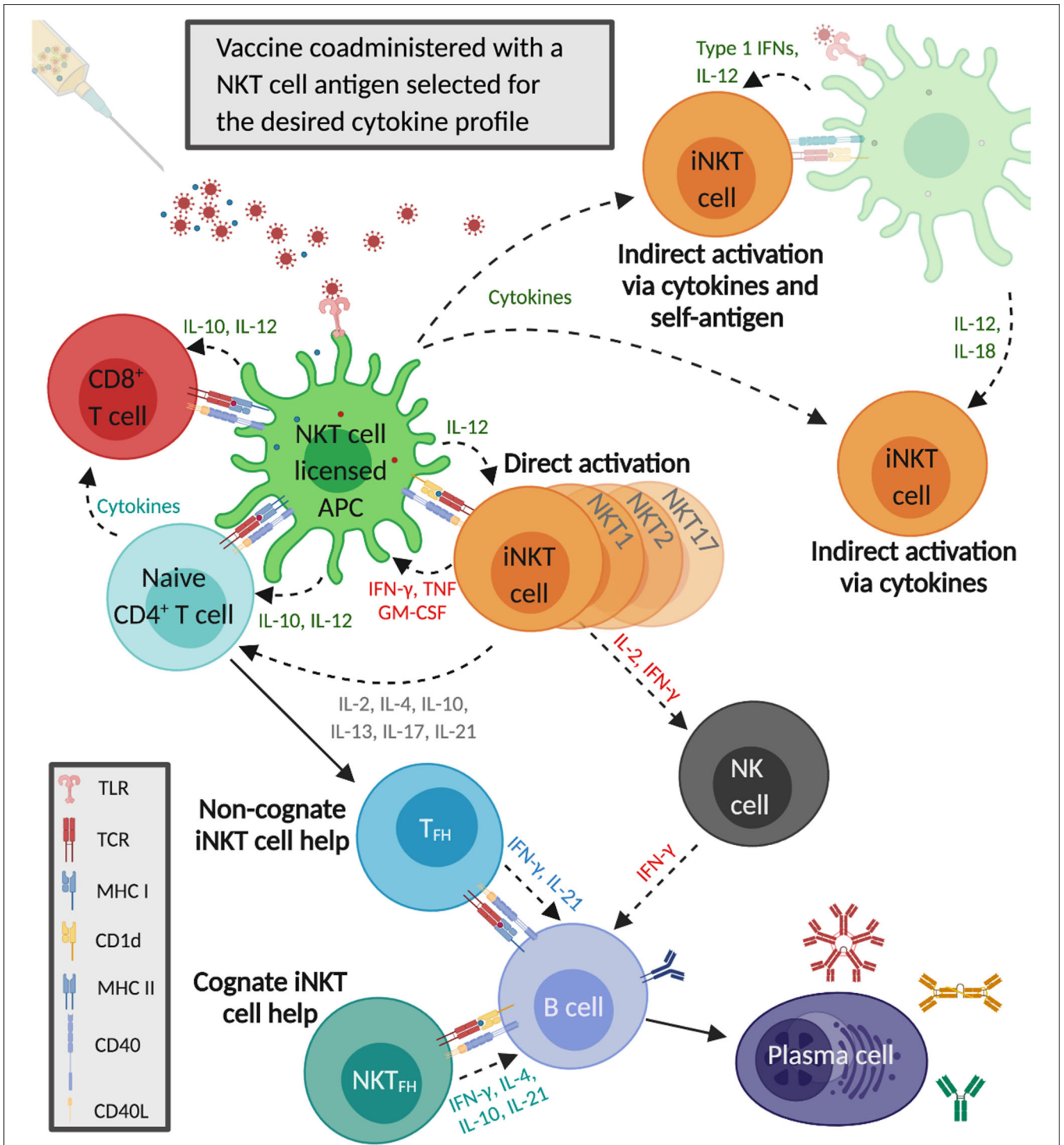

FIGURE 1 | Invariant natural killer T cells activate and regulate innate and adaptive immune responses that enhance influenza A virus (IAV) vaccine immunity. The co-administered IAV vaccine antigens and the selected α-GalCer analog are internalized by dendritic cells that simultaneously present the α-GalCer analog on CD1d to iNKT cells and IAV epitopes on major histocompatibility complex (MHC) II to $CD4^+$ T cells. Cytokines secreted by iNKT cells increase MHC class II and CD40 presentation to naïve $CD4^+$ T cells, which generates follicular T helper cells (T_{FH}) that provide non-cognate help to B cells. iNKT cells also undergo indirect activation in response to proinflammatory cytokines released by IAV-stimulated antigen-presenting cells (APCs), with or without engagement of the iNKT TCR by CD1d-presented self-antigens. iNKT cell-licensed dendritic cells (DCs) generate vaccine-specific $CD8^+$ T cells which become further activated by cytokines secreted by α-GalCer and IAV-stimulated APCs as well as iNKT cells and $CD4^+$ T cells. The iNKT cells recognizing α-GalCer on DCs differentiate into iNKT follicular helper ($iNKT_{FH}$) cells that provide cognate help to B cells specific for vaccine antigens. iNKT cells also boost humoral immunity by trans-activating natural killer cells that can stimulate B cells to secrete immunoglobulin G.

macaques (*Macaca nemestrina*)] have also been tested. To our knowledge, Ko et al. were the first group to explore adjuvanting IAV vaccines with iNKT cell agonists (26). They reported that BALB/c mice intranasally co-administered with three doses (1 week apart) of α-GalCer and HA antigen derived from the mouse-adapted A/PR/8/34 (PR8, H1N1) IAV were much better protected from a lethal dose of the homologous virus than mice immunized with vaccine alone. α-GalCer induced greater levels of mucosal and systemic IgA and IgG antibodies. The same group later demonstrated that a single intranasal vaccination with inactivated PR8 and α-GalCer was sufficient to induce long-lasting PR8-specific IgG and IgA that protected mice from PR8 infection 3 months after the vaccination (22).

iNKT cell agonists have also been assessed for their ability to improve vaccine-mediated cross-protection against heterologous and heterosubtypic virus infections. Kamijuku et al. administered α-GalCer to BALB/c mice in combination with HA-based vaccines derived from a variety of IAV strains. Strong protection was induced against heterologous IAV strains within the same HA vaccine subtype and partial protection was generated against the heterosubtypic strains (23). A follow-up study demonstrated that an inactivated whole-virion vaccine of H5N1 IAV generated robust cross-protection against a heterologous H5N1 IAV strain when administered intranasally with, but not without, α-GalCer. The cross-protective effects of iNKT cell activation were found to be mediated by mucosal IgA production and effector responses that require IL-4, but not IFN-γ (23).

Other strategies that have been tested include a study where the α-GalCer derivative α-C-galactosylceramide (α-C-GalCer) enhanced the immune response elicited by a live attenuated A/PR/8/34 virus expressing only the first 73 amino acids in the NS1 gene; NS1 is needed to inhibit critical innate host immune factors (27). BALB/c mice were co-administered the live attenuated virus (LAV) vaccine with different doses of α-C-GalCer ranging from 0 to 4 μg/mouse. Interestingly, only mice that received low doses of α-C-GalCer survived, while mice treated with the 4 μg dose or the LAV vaccine alone were not protected. This finding suggests that activating iNKT cells too strongly may be detrimental for LAV vaccine applications since their limited replication capacity might be abolished by iNKT cell-mediated innate immune responses before they have had an opportunity to induce vaccine-specific immunity. α-GalCer has also been used to adjuvant the normally poorly immunogenic IAV M2 ectodomain (M2e); BALB/c mice co-immunized with M2e and α-GalCer were fully protected against a highly pathogenic H5N1 avian IAV infection and exhibited significantly reduced morbidity and lung viral titers compared to mice that were immunized without α-GalCer (25). The enhanced protection was associated with augmented IgG1 and IgG2 antibody levels and greater IFN-γ and IL-4 upregulation after infection. Another study tested the efficacy of α-GalCer-peptide conjugated vaccines composed of synthetic long peptides (SLP) containing an immunogenic peptide covalently attached to α-GalCer by a cleavable linker (28). This ensures that the vaccine peptide and α-GalCer are delivered to the same APC and enables iNKT cells to license the same APCs involved in stimulating conventional $CD4^+$ and $CD8^+$ T cell responses against the vaccine antigen. C57BL/6 mice were vaccinated with α-GalCer conjugated SLPs composed of an immunogenic peptide of chicken ovalbumin and challenged 6 weeks later with a recombinant ovalbumin expressing IAV. The SLP vaccine provided much greater protection than previous infection with the backbone virus. However, it remains to be determined whether this approach provides protection against non-OVA-expressing IAVs. Another strategy used an "adjuvant vector cell" (aAVC) system comprised of $CD1d^+$ HA mRNA-transfected cell lines (NIH3T3 for mice and HEK293 cells for humans) loaded with α-GalCer. C57BL6/J mice immunized with aAVC-HA were protected from a lethal dose of PR8 2 weeks later. The efficacy of this approach seemed to depend on the formation of germinal centers and T_{FH} cells and was more effective than a co-administration of free antigen and α-GalCer (29).

Many articles reporting the adjuvant activities of iNKT cells for IAV vaccines have used the intranasal delivery route of administering α-GalCer because of the importance of this site for pulmonary immunity. α-GalCer administered by this route remains localized to the nasal-associated lymphoid tissues and cervical lymph nodes where it becomes concentrated in the intracellular vesicles of DCs. These DCs co-localize with iNKT cells that accumulate in these tissues through a process that requires the chemokine receptor CXCR6 and its ligand CXCL16 (23). α-GalCer can also induce effective immunity when delivered to tissues beyond the site of infection. For instance, Galli et al. showed that mice immunized *via* the intramuscular route with α-GalCer admixed with HA/NA subunits from human influenza viruses generated antibody titers that were 1–2 logs higher than mice immunized with protein alone and greatly enhanced survival after a lethal IAV infection (30).

iNKT cell responses have also shown promise for generating cross-reactive $CD8^+$ T cells against serologically distinct IAV subtypes, which is a major shortcoming of current IAV vaccines. Guillonneau et al. examined cytotoxic $CD8^+$ T cell responses in C57BL/6 mice subcutaneously immunized with an inactivated PR8 vaccine, with and without α-GalCer, that were infected with a heterosubtypic H3N2 IAV 6 weeks later (24). iNKT cell activation enhanced the survival of long-lived memory cytotoxic $CD8^+$ T cells capable of clearing virus from the lungs while paradoxically diminishing acute phase cytotoxic T cell responses through iNKT cell-dependent production of indoleamine 2,3-dioxygenase, an immune suppressive enzyme (24). The induction of long-lasting $CD8^+$ T cells was associated with the upregulation of *Bcl-2*, which is a pro-survival gene. The adjuvant effects of iNKT cells have also shown potential to improve DNA-based vaccines, which stimulate only modest immunity in humans. Two studies have demonstrated that vaccinating mice with α-GalCer derivatives and DNA vaccines encoding an HA consensus sequence of an H5N1 IAV or the IAV M2 protein induces M2-specific cellular and humoral immune responses and protection from virus challenge (21, 31).

Although mouse models have demonstrated that iNKT cell activities can greatly enhance IAV vaccines, it remains unclear whether the same approach would be successful in humans as mice are not natural IAV hosts and mouse and human iNKT cells differ considerably in frequency, subsets, and tissue

TABLE 1 | Summary of studies on modulating immune responses to influenza A virus (IAV) using invariant natural killer T (iNKT) cell agonists.

Animal model	Vaccination		Vaccine format	iNKT cell agonist (dose per animal)	Mode of action	References
	Route	Strain/subunit				
Mouse (BALB/c)	i.n.	H1N1 PR8	Immunization with PR8 HA antigen with α-GalCer three times at 1-week intervals. Infection with 20 LD_{50} PR8 2 weeks after final immunization.	α-GalCer (0.125, 0.5, 2 μg)	α-GalCer induced mucosal secretory IgA as well as systemic IgG antibody responses against virus-derived antigen and reduced clinical signs.	(26)
Mouse (BALB/c)	i.n.	H1N1 PR8	Immunization with inactivated PR8 with α-GalCer. Infection with 20 LD_{50} PR8 2 weeks and 3 months after immunization.	α-GalCer (0.5 μg)	α-GalCer induced both mucosal and systemic antibody responses, provided protective immunity against challenge with live PR8 and induced cytotoxic $CD8^+$ T cells.	(22)
Mouse (BALB/c)	i.n./i.m.	H1N1 PR8 H1N1A/Yamagata H3N2A/Guizhou B/Ibaraki	Immunization with PR8, A/Yamagata, A/Guizhou, or B/Ibaraki HA vaccine with α-GalCer twice at 4 weeks apart. Infection with 40 LD_{50} PR8 2 weeks after the second immunization.	α-GalCer (2 μg)	i.n., not i.m., vaccination (PR8 and A/Yamagata) with α-GalCer boosted IgA and IgG and cross-protection against heterosubtypic virus infection.	(23)
Mouse (BALB/c)	i.n.	H1N1 PR8	Immunization with PR8 with α-GalCer twice at 4 weeks apart. Infection with 40 LD_{50} A/Yamagata, A/Guizhou, or B/Ibaraki 2 weeks after the second immunization.	α-GalCer (2 μg)	i.n. vaccination with α-GalCer protected against challenge with homologous (A/PR8) and heterologous (A/Yamagata) viruses.	(23)
Mouse (BALB/c)	i.n.	H5N1 NIBRG14	Immunization with NIBRG14 (H5N1) inactivated vaccine with α-GalCer twice, 4 weeks apart. Infection with 10^3 PFU of A/Vietnam (H5N1) or A/HK483 (H5N1) influenza virus 2 weeks after the second immunization.	α-GalCer (2 μg)	i.n. vaccination with α-GalCer increased nasal IgA and serum IgG and induced cross-protection against H5N1 influenza infection.	(23)
Mouse (BALB/c)	i.n.	H1N1 rNS1 1-73	Immunization with live attenuated rNS1 1-73 with different amounts of α-C-GalCer. Infection with 100 LD_{50} PR8 3 weeks after the immunization.	α-C-GalCer (0.11, 0.33, 1, 2, 3, 4 μg)	α-C-GalCer used between 0.1 and 1 μg per mouse reduced mortality and morbidity. The adjuvant also increased the amount of influenza virus-specific total IgG, IgG1, and IgG2a antibodies as well as IFN-γ secreting $CD8^+$ T cells.	(27)
Mouse (BALB/c)	i.n.	H1N1 PR8	Immunization with inactivated PR8 with α-GalCer or α-GalCer analogs. Infection with 5 LD_{50} PR8 4 weeks after the immunization or 100 LD_{50} PR8 5 weeks after immunization.	α-GalCer (0.5 μg); KBC-007 (0.5 μg); KBC-009 (0.5 μg)	Co-immunization with α-GalCer, KBC-007 and KBC-009 increased PR8-specific systemic IgG and mucosal IgA. α-GalCer and KBC-009 (but not KBC-007) increased antigen-specific lymphocyte proliferation, cytokine production, and cytotoxic $CD8^+$ T cell activity and induced complete protection from live virus infection.	(32)
Mouse (C57BL/6)	i.v.	H1N1 PR8-OVA257	Immunization with SLP-conjugated vaccine PR8-OVA257 with α-GalCer. Infection with 10^4 PFU HKx31-OVA257 6–8 weeks after the immunization.	α-GalCer (76 ng)	α-GalCer-peptide conjugates induced OVA-specific T cell responses and protected against IAV infection.	(28)
Mice (C57BL/6)	i.m.	HA/NA from H3N2 PNM07	Immunization with PNM07 protein and α-GalCer twice at 2 weeks apart.	α-GalCer (0.1 μg)	Immunization with H3N2 PNM07 plus α-GalCer increased titers of H3N2-specific antibodies.	(30)
Mouse (C57BL/6)	i.m.	HA/NA from H1N1 NC20	Immunization with NC20 protein with α-GalCer twice at 2 weeks apart. Infection with 100 LD_{50} H1N1 A/WS/33 2 weeks after the second immunization.	α-GalCer (0.1 μg)	α-GalCer increased the survival rate after challenge.	(30)
Mouse (C57BL/6)	i.m.	H3N2 PNM07	Immunization with H3N2 PNM07 protein with α-GalCer twice at 0 and 2 weeks, boosted with PNM07 at 30 weeks.	α-GalCer (0.1 μg)	Immunization with H3N2 PNM07 plus α-GalCer resulted in a higher antibody response and increased expansion of the antigen-specific memory B cells.	(30)
Mouse (C57BL/6)	s.c.	H1N1 PR8	Immunization with inactivated PR8 with α-GalCer. Infection with 10^4 PFU of live H3N2 HKx31 6 weeks after immunization.	α-GalCer (1 μg)	Vaccination with α-GalCer increased the survival of long-lived memory cytotoxic $CD8^+$ T cell populations capable of boosting protection against heterologous IAV challenge.	(24)

(Continued)

TABLE 1 | Continued

Animal model	Vaccination		Vaccine format	iNKT cell agonist (dose per animal)	Mode of action	References
	Route	Strain/subunit				
Mouse (BALB/c)	i.m.	pCHA5 for H5N1	Immunization with pCHA5 with C34 twice at 3 weeks apart. Infection with 200 LD_{50} NIBRG14 (a reassortant H5N1 virus) 2 weeks after the immunization.	C34 (2 μg)	C34 increased titers of HA-specific antibodies and T cells and improved survival after challenge.	(31)
Mouse (C57BL/6)	i.v.	H1N1 PR8	Immunization with PR8 HA mRNA-transfected CD1d-allogeneic cells loaded with α-GalCer (aAVC-HA). Infection with 10^3 PFU PR8 2 weeks after the immunization.	5×10^5 aAVC-HA precultured with α-GalCer (500 ng/mL)	Vaccination with aAVC-HA preserved body weight, increased survival after infection, and increased titers of HA-specific IgG.	(29)
Mouse (BALB/c)	i.p.	M2e peptide	Immunization with M2e peptide with α-GalCer twice at 3 weeks apart. Infection with 10^3 PFU H5N1 3 weeks after the final immunization.	α-GalCer (1 μg)	α-GalCer co-administered with M2e peptide reduced morbidity, mortality and up-regulated IFN-γ, IL-4 after challenge.	(25)
Mouse (BALB/c)	i.m.	DNA vaccine encoding M2	Immunization with DNA vaccine encoding M2 with α-GalCer three times at 2-week intervals. Infection with 1 LD_{90} PR8 2 weeks after the final immunization.	α-GalCer (1 μg)	α-GalCer increased M2-specific IgG; lymphocyte proliferation; IFN-γ and IL-12 and IL-4 production; and survival rate after virus challenge.	(21)
Mouse (BALB/c)	i.m.	H1N1 CA07, A/Hong Kong (H3N2), B/Phuket, and B/Texas	Immunization with split influenza HA vaccine with 7DW8-5 twice at 2-week intervals. Infection with 10 MLD_{50} H1N1 CA04 3 weeks after the final immunization.	7DW8-5 (1 μg or 10 μg)	7DW8-5 was sufficient to protect the mice from lethal infection but did not completely prevent virus replication.	(33)
Pig	i.n.	H1N1 OH07	Immunization with inactivated SwIV OH07 with α-GalCer once. Infection with homologous SwIV OH07 (10^6 $TCID_{50}$ per pig) 3 weeks after the immunization.	α-GalCer (50 or 250 μg)	α-GalCer increased IAV-specific mucosal IgA and upregulated the expression of BAFF.	(151)
Pig	i.n.	H1N1 OH07	Immunization with inactivated SwIV OH07 with α-GalCer once. Infection with homologous SwIV OH07 (10^6 $TCID_{50}$ per pig) 3 weeks after the immunization.	α-GalCer (50 or 250 μg)	α-GalCer (250 μg) administration reduced pulmonary viral load and increased SwIV-specific IgA secretion both in the lungs and the airways.	(152)
Pig	i.m.	H1N1 CA04	Immunization with inactivated H1N1 CA04 with α-GalCer twice at 16-day intervals. Infection with 10^6 $TCID_{50}$ CA04 16 days after the immunization.	α-GalCer (100 μg/kg)	Vaccination with α-GalCer enhanced both systemic and mucosal influenza-specific antibodies and inhibited viral replication in the upper and the lower respiratory tracts.	(153)
Pigtail macaques	i.v.	Live-attenuated IAV encoding three distinct SIV epitopes (flu-SIV)	A single dose of α-GalCer pulsed onto whole blood for 2 h and re-infused with flu-SIV; additional vaccinations without α-GalCer on days 28, 56, and 119.	α-GalCer (5 μg)	α-GalCer reduced vaccine-specific $CD8^+$T cells and had no effect on the frequency of iNKT cells or IAV-specific antibodies; reduced influenza-specific $CD8^+$ T cells.	(72)

PR8, H1N1 strain A/Puerto Rico/8/34; NC20, H1N1 strain A/New Caledonia/20/99; A/WS/33, H1N1 strain A/Wilson-Smith/1933; PNM07, H3N2 strain A/Panama/2007/99; A/Yamagata, H1N1 strain A/Yamagata/120/86; A/Guizhou, H3N2 strain A/Guizhou/54/89; B/Ibaraki, B/Ibaraki/2/85; rNS1 1-73, a PR8 mutant virus expressing only the first 73 amino acids in the NS1 gene; NIBRG-14, reassortant virus derived from PR8 and A/Vietnam/1194/2004 (H5N1) virus (in which the polybasic HA cleavage site has been excised); M2e, ectodomain of M2 protein; CA07, A/California/07/2009 (H1N1) virus; A/Hong Kong, A/Hong Kong/4801/2014 (H3N2) virus; B/ Phuket, B/Phuket/3073/2013 (Yamagata lineage) virus; B/Texas, B/Texas/2/2013 (Victoria lineage) virus; OH07, a zoonotic SwIV H1N1 (Sw/OH/24366/07); CA04, H1N1pdm09 strain A/California/04/2009; α-C-GalCer, alpha-C galactosylceramide; α-GalCer, alpha-galactosylceramide; 7DW8-5, 4-fluorophenylundecanoyl-alpha-galactosylceramide; aAVC-HA, HA-expressing artificial adjuvant vector cells; i.m., intramuscular; i.n., intranasal; i.p., intraperitoneal; s.c., subcutaneous; i.v., intravenous; WB, whole blood.

distribution. Therapeutically activating iNKT cells failed to improve anti-IAV cellular and humoral immune responses when attempted in pigtail macaques, which are considered a good translational model for human IAV infections (72). Nevertheless, we previously reported that α-GalCer substantially increased the efficacy of a killed pandemic 2009 H1N1 IAV vaccine in pigs that were challenged with the homologous virus. Protection was associated with higher levels of vaccine-specific antibodies and T cells and reduced viral replication in the upper and lower respiratory tract compared to pigs that received the vaccine alone (153). Similar results were obtained in studies by Dwivedi et al. and Renu et al., who showed that intranasal co-administration of α-GalCer with UV-inactivated H1N1 vaccines increased mucosal IgA levels, upregulated lung expression of the B cell activation factor BAFF, and substantially reduced virus loads in pigs (151, 152). Collectively, these results are encouraging as swine and human iNKT cells share several key characteristics, and like humans, pigs are natural hosts of IAVs. Furthermore, there may also be potential to use iNKT cell antigens for vaccines against swine influenza and other pig pathogens.

FACTORS THAT INFLUENCE THE ADJUVANT POTENTIAL OF iNKT CELLS

Studies in mice have established that the effects of iNKT cell activation are influenced by a variety of interacting parameters, which should be considered when attempting to use these agents to adjuvant vaccines. Some of the main factors are discussed below.

iNKT Cell Subsets

The iNKT cell compartment consists of multiple subsets that play distinct roles during pathogen-host interactions and which produce different effector functions after glycolipid stimulation. Subset development occurs through a linear differentiation process characterized by sequential changes in surface markers and transcription factors. Human iNKT cells develop into $CD4^-$ or $CD4^+$ subsets that secrete Th1 or a mixture of Th1 and Th2 cytokines upon activation, respectively (54, 154). However, these differences in cytokine production are less apparent for mouse iNKT cells (85). Another difference is that the $CD4^+$ subset of iNKT cells predominates in mice (155), while human iNKT cells are mostly $CD4^-$ (54, 156, 157). Like humans, iNKT cells in pigs are mainly $CD4^-$ (52, 68, 75, 153), and both humans and pigs contain a subset of $CD8^+$ iNKT cells which is absent in mice (54, 68, 75, 156, 157).

Mouse iNKT cell subsets can be classified according to their development lineages that are acquired during thymic selection (**Table 2**). These are composed of the three major functionally distinct subsets, NKT1, NKT2, and NKT17, which express the master transcription factors T-bet, GATA-3, and RORγt that also, respectively, engender the fate of Th1, Th2, and Th17 T helper cell subsets as well as ILC1, ILC2, and ILC3 innate lymphoid cells (95, 158–161, 163–165). Each iNKT subset expresses different levels of the transcription factor PLZF, which is critical for the development and the innate functions of iNKT cells (168–170). Additional iNKT cell subsets that differentiate extrathymically have been identified, including NKT_{FH} and NKT10 cells. NKT_{FH} cells are characterized by the expression of Bcl-6 and the secretion of IL-21 and are located in the germinal centers of lymphoid organs. NKT_{FH} cells provide help to B cells during the formation of germinal centers and drive the affinity maturation of antibodies toward lipid antigens (134, 135). NKT10 cells are equivalent to type-1 regulatory T cells (T_{REGS}) and produce IL-10 and IL-2. This subset induces the differentiation of anti-inflammatory macrophages and provides help to T_{REGS}. Instead of expressing PLZF like other NKT cells, NKT10 express E4BP4, a transcription factor associated with IL-10 production (166).

Individual iNKT cell subsets differentially accumulate in lymphoid and non-lymphoid tissues (171). In mice, most liver iNKT cells are NKT1 cells, while NKT2 cells predominate in the lung, spleen, and mesenteric lymph nodes (56, 162, 171). NKT17 cells are most plentiful in the lymph nodes, lung, and skin (56, 162, 171), while NKT10 cells preferentially accumulate in adipose tissue (167, 171) and NKT_{FH} cells localize in germinal centers, especially in the spleen (134, 135). The effector functions of each subset are distinct and range from NKT1 cells that stimulate proinflammatory responses capable of suppressing cancer and infectious agents (83, 172) to tolerogenic NKT2 and NKT10 cells that inhibit autoimmune diseases (173–175). Such diversity in function needs to be considered when targeting the adjuvant activities of iNKT cell agonists because, depending on the route of vaccinations, some subsets may have more influence on shaping anti-IAV immune responses than others, which could considerably affect the quality and the durability of protection. Another consideration is the extensive variability in iNKT cell subset ratios among inbred mouse strains and genetically outbred humans and animals, which can result in extensive variability in outcomes. Indeed different ratios of NKT1/NKT2 subsets are thought to underlie the dimorphic responses that α-GalCer treatment elicits in C57BL/6 and BALB/c mice for a host of different diseases (95). Currently, a unifying model linking iNKT cell transcription factors and functions is lacking for humans (and other species). Nevertheless, iNKT cells are probably comprised of functionally distinct subsets in all species that expresses these cells. Accordingly, the variability in iNKT cell subsets should be considered a potential source of variation in people or animals administered glycolipids to stimulate iNKT cell adjuvant activities.

iNKT Cell Agonists

Since α-GalCer is the first iNKT cell ligand to be discovered and strongly activates iNKT cells, this agent and its synthetic derivative KRN7000 have been widely used to study the therapeutic potential of iNKT cells, including their adjuvant activities (18, 19, 176). α-GalCer is a glycosylceramide molecule, composed of an α-anomeric sugar linked to a 26-carbon-long fatty acid chain and an 18-carbon-long sphingosine base (15). While this glycolipid induces a mixed Th1/Th2 cytokine response, various structural analogs of α-GalCer that skew iNKT cell cytokine production toward a Th1 or Th2 response have been developed. These modifications include altering the length, saturation level, and branching of the alkyl and sphingosine chains, while other derivatives contain modifications at the glycosyl head (96, 97, 173, 177–181).

In general, α-GalCer analogs with truncated fatty acid chains or the addition of double bonds in the acyl chain, such as OCH ((2S,3S,4R)-1-*O*-(α-D-galactopyranosyl)-N-tetracosanoyl-2-amino-1,3,4-non-anetriol) and C20:2, skew iNKT cells toward producing Th2 cytokines (173, 177). In contrast, iNKT cells can be preferentially activated to produce Th1-like cytokines by (i) α-GalCer derivatives that contain a CH2 group in place of the glycosidic oxygen (180), (ii) α-C-GalCer analogs that contain an oxygen residue in the galactose sugar ring (182), and (iii) 7DW8-5 and C34 analogs that, respectively, possess methylene and aromatic residues inserted into their fatty acid chains (183, 184). Most studies on the adjuvant activities of iNKT cells use α-GalCer, which generates potent cellular and humoral immunity due to the mixed Th1/Th2 cytokines elicited. However, several Th1-inducing reagents, including 7DW8-5 and C-glycoside, substantially enhance vaccine responses against malaria, HIV, and IAV vaccines in mice (33, 180, 183). Some studies have reported that these agents are superior to α-GalCer for boosting vaccine-mediated immune responses due to a greater ability to

TABLE 2 | Key characteristics of the main invariant natural killer T (iNKT) cell subsets.

iNKT cell subset	Transcription factor	Signature cytokines	Tissue distribution	References
NKT1	T-bet, PLZF^{low}	IL-4, IFN-γ	Liver, spleen, lung, small intestine	(56, 95, 158–162)
NKT2	GATA3, PLZF^{hi}	IL-4, IL-5, IL-13	Lung, spleen, mesenteric lymph nodes	(56, 159–163)
NKT17	RORγt, PLZF^{int}	IL-17, IL-22	Lymph nodes, lung, skin	(56, 159–162, 164, 165)
NKT_{FH}	Bcl-6	IL-21	Germinal centers of lymphoid organs	(134, 135)
NKT10	E4BP4, PLZF^{-}	IL-10, IL-2	Adipose tissue	(166, 167)

trans-activate other immune cells, especially NK cells, to produce IFN-γ (92, 183).

The burgeoning list of synthetic iNKT cell ligands provides new opportunities to tune iNKT cell responses for a desired vaccine-supporting immune outcome. For IAV vaccines, the most promising iNKT cell-stimulating antigens are those which polarize mouse iNKT cells to produce Th1 cytokines or a mixture of Th1 and Th2 cytokines, which are naturally important for antiviral immune responses. Nevertheless, many of these reagents do not polarize human iNKT cells to the same degree as mouse iNKT cells due partially to the structural differences in mouse and human CD1d molecules that affect TCR/CD1d/antigen interactions (91, 92, 178). This is an important consideration for translating preclinical animal vaccine studies to humans.

Vaccine Format

Studies with different disease models have shown that α-GalCer treatment can have diverse immune effects depending on the timing, route, and dose of α-GalCer administration. Understanding how these parameters affect the adjuvant activities of therapeutically activated iNKT cells is critical for optimizing iNKT cell-adjuvanted IAV vaccines. The timing of α-GalCer treatment is a concern for prime-boost vaccination strategies that administer more than one α-GalCer dose. This is because the strong activation from a primary vaccination may render iNKT cells hypo-responsive to an additional stimulation. Most studies on the adjuvant activities of iNKT cell agonists for IAV vaccines employ multiple vaccine applications (**Table 1**) even though iNKT cells are reported to remain anergic to restimulation within 3 months after the initial stimulation. These reports seldom assess whether increases in immune responses are from the effects of iNKT cells stimulation or from the vaccine antigen alone. However, it has been shown that the intramuscular delivery of α-GalCer avoids iNKT cell anergy in both mice and pigs (21, 30, 52, 153), suggesting that the risk of iNKT cell hypo-responsiveness may be low if prime-boost vaccination strategies were employed with IAV vaccines using the i.m. route.

Studies that have employed inactivated IAV vaccines, viral peptides, and DNA vaccines have used a variety of immunization routes, although intramuscular injection is the most common. In contrast, iNKT-adjuvanted live attenuated IAV vaccines have mostly been delivered intranasally to induce protective immunity at the site of infection. In general, the systemic routes of vaccine and α-GalCer co-administration globally activate iNKT cells in a way that greatly enhances neutralizing antibodies (21, 23, 30). However, this route is not as effective as intranasal administration at inducing secretory IgA antibodies necessary for cross-protection against heterologous virus strains (23). Studies that have compared the efficacy of different vaccination sites include the report by Galli et al. which showed that the intraperitoneal, subcutaneous, intramuscular, and intravenous immunization routes were equally effective and better than intranasal administration at inducing vaccine-specific antibodies (30). Another study showed that BALB/c mice intranasally vaccinated with α-GalCer in combination with HA antigen derived either from A/PR8 (H1N1) or A/Yamagata (H1N1) were protected from subsequent infection with A/PR8 (H1N1) live virus and that the A/Yamagata HA antigen vaccine induced anti-PR8 HA IgA and IgG antibodies. In contrast, the same vaccines administered by the intramuscular route failed to induce IgA antibodies and did not provide cross-protective immunity (23). The same study compared the effect of intraperitoneally and intranasally delivered α-GalCer on an intranasally delivered A/PR8 (H1N1) vaccine. Despite strongly activating splenic and hepatic iNKT cells, intraperitoneally delivered α-GalCer did not induce anti-PR8 IgA and IgG antibodies as a response to the A/PR8 HA antigen vaccine administered intranasally, indicating that iNKT cell ligands must be co-administered with viral antigens to enhance an intranasally delivered vaccine (23).

The adjuvant effects of glycolipid-stimulated iNKT cells enhance immune responses to a wide variety of vaccine formats. Such versatility stems from the powerful immunoregulatory properties of iNKT cells, which affect almost every branch of the immune system and which are generally more diverse than the immunomodulatory effects induced by traditional adjuvants. A drawback of this potency is that iNKT cell responses can reduce the efficacy of live attenuated virus vaccines by inducing antiviral host responses that eliminate the weakened vaccine virus before it has had a chance to induce adaptive immunity. Consequently, it will be necessary to carefully titrate each glycolipid ligand to find a dose that increases, rather than decreases, immunity against live attenuated virus vaccines. Dosage is less important for non-attenuated vaccines, although high doses of glycolipid ligands may render iNKT cells anergic to secondary activation.

POTENTIAL PITFALLS

Several obstacles must be overcome before the immunomodulatory activities of iNKT cells can be used for human or livestock vaccines. Of paramount concern is the safety of this strategy as the potent cytokine responses generated by therapeutically activated iNKT cells can sometimes

result in immunopathological inflammation and/or disease exacerbation (185–187). This includes reports that α-GalCer administration can induce acute airway hyper-reactivity in mice (188), non-human primates (189), and pigs (76). In addition, the co-administration of α-GalCer and the model antigen ovalbumin resulted in allergic airway inflammation in mice (190). These results should serve as a note of caution that combining α-GalCer with intranasally administered IAV vaccines could cause potentially life-threatening airway inflammation. Another concern is that α-GalCer-stimulated iNKT cells may increase the risk of vaccine-associated enhanced respiratory disease. This phenomenon occurs when inactivated IAV vaccines include a virus strain of the same hemagglutinin subtype as a subsequent challenge virus, but with substantial antigenic shift (191). This occasionally generates IgG antibodies that cross-react with the heterologous virus proteins but lack the ability to neutralize the heterologous virus effectively. These antibodies might instead bind epitopes in the HA stem region (HA2) of the heterologous virus, which facilitates infection of host cells by enhancing virus fusion activity (191). As iNKT cell activation boosts the size and the complexity of humoral responses, it is possible that they will also increase non-neutralizing antibody responses against heterologous viruses. Another concern is the potential that immunity from iNKT cell-adjuvanted vaccines will be inconsistent and unpredictable due to the high interindividual variability in iNKT cell frequency and function in genetically outbred species, including humans (192, 193). Indeed some studies have reported that only patients with high iNKT cell frequencies were likely to benefit from iNKT cell-based treatments (194, 195). It is currently difficult to predict whether an individual's iNKT cells will produce an immunogenic or tolerogenic response to stimulation, and the danger exists that iNKT cell activation might actually reduce the efficacy of IAV vaccines. This is further complicated by the phenomenon that iNKT cells undergo substantial age-related alterations in concentration and effector functions that are likely to impact their response to glycolipid antigens (196–200). Finally, it is important to consider that most studies in this field were conducted using mouse models which, although they have provided extensive knowledge about the fundamental role of iNKT cells during IAV infections, do not closely mirror humans for iNKT cell physiology. Furthermore, mice are not natural hosts of IAV infections and usually develop much more severe disease than humans when infected with mouse-adapted IAV strains (201). Thus, another obstacle is the need for more studies in valid preclinical animal models to translate iNKT cell-adjuvanted vaccination to the clinic.

CONCLUDING REMARKS

Durable and broadly protective IAV vaccines are greatly needed to counteract the growing threats of morbidity, mortality, and economic losses from seasonal and pandemic IAV infections. Current vaccine formulations do not provide long-lasting and cross-protective immunity, partly because they do not induce sufficient T cell help from virus-specific T cells. iNKT cells may help to overcome this limitation because they can be uniformly and specifically activated by therapeutic glycolipid antigens to supply a universal form of T cell help capable of expanding virus-specific antibodies and $CD8^+$ T cells. Nevertheless, significant hurdles remain before the adjuvant activities of iNKT cells can be utilized in humans and livestock for vaccines against IAV and other pathogens. Future research should focus on testing this approach using preclinical animal models with high human translational potential, such as swine and non-human primates. Such studies will help determine the translatability of iNKT cell-adjuvanted vaccines for other respiratory diseases which have shown promise in mouse models (202).

AUTHOR CONTRIBUTIONS

JD and JR contributed to the conceptualization, writing, review, and editing. DC, WG, and BA contributed to the writing. All authors contributed to the article and approved the submitted version.

FUNDING

This work was supported by U.S. Department of Agriculture Grant 2016-09448 (to JD), National Institutes of Health Grant HD092286 (to JD and JR), the NIAID-funded Center of Excellence for Influenza Research and Surveillance (CEIRS, #HHSN272201400006C; JR), and the U.S. Department of Homeland Security under Grant Award Number DHS-2010-ST-061-AG0001 (JR) for the Center of Excellence for Emerging and Zoonotic Animal Disease (CEEZAD).

REFERENCES

1. Taubenberger JK, Kash JC. Influenza virus evolution, host adaptation, pandemic formation. *Cell Host Microbe.* (2010) 7:440–51. doi: 10.1016/j.chom.2010.05.009
2. Medina RA, García-Sastre A. Influenza A viruses: new research developments. *Nat Rev Microbiol.* (2011) 9:590–603. doi: 10.1038/nrmicro2613
3. Wu Y, Tefsen B, Shi Y, Gao GF. Bat-derived influenza-like viruses H17N10 and H18N11. *Trends Microbiol.* (2014) 22:183–91. doi: 10.1016/j.tim.2014.01.010
4. Kasowski EJ, Garten RJ, Bridges CB. Influenza pandemic epidemiologic and virologic diversity: reminding ourselves of the possibilities. *Clin Infect Dis.* (2011) 52(Suppl. 1):S44–9. doi: 10.1093/cid/ciq010
5. GBD 2017 Influenza Collaborators. Mortality, morbidity, and hospitalisations due to influenza lower respiratory tract infections, 2017: an analysis for the Global burden of disease study 2017. *Lancet Respir Med.* (2019) 7:69–89. doi: 10.1016/S2213-2600(18)30496-X
6. Bouvier NM, Palese P. The biology of influenza viruses. *Vaccine.* (2008) 26(Suppl.4):D49–53. doi: 10.1016/j.vaccine.2008.07.039
7. Kidd M. Influenza viruses: update on epidemiology, clinical features, treatment and vaccination. *Curr Opin Pulm Med.* (2014) 20:242–6. doi: 10.1097/MCP.0000000000000049

8. Flannery B, Kondor RJG, Chung JR, Gaglani M, Reis M, Zimmerman RK, et al. Spread of antigenically drifted Influenza A(H3N2) viruses and vaccine effectiveness in the United States during the 2018-2019 season. *J Infect Dis.* (2020) 221:8–15. doi: 10.1093/infdis/jiz543
9. Jackson ML, Nelson JC. The test-negative design for estimating influenza vaccine effectiveness. *Vaccine.* (2013) 31:2165–8. doi: 10.1016/j.vaccine.2013.02.053
10. Reed SG, Orr MT, Fox CB. Key roles of adjuvants in modern vaccines. *Nat Med.* (2013) 19:1597–608. doi: 10.1038/nm.3409
11. Henriksen-Lacey M, Christensen D, Bramwell VW, Lindenstrøm T, Agger EM, Andersen P, et al. Liposomal cationic charge and antigen adsorption are important properties for the efficient deposition of antigen at the injection site and ability of the vaccine to induce a CMI response. *J Control Release.* (2010) 145:102–8. doi: 10.1016/j.jconrel.2010.03.027
12. Maisonneuve C, Bertholet S, Philpott DJ, de Gregorio E. Unleashing the potential of NOD- and toll-like agonists as vaccine adjuvants. *Proc Natl Acad Sci USA.* (2014) 111:12294–9. doi: 10.1073/pnas.1400478111
13. Van Reeth K, Van Gucht S, Pensaert M. Investigations of the efficacy of European H1N1- and H3N2-based swine influenza vaccines against the novel H1N2 subtype. *Vet Rec.* (2003) 153:9–13. doi: 10.1136/vr.153.1.9
14. Godfrey DI, Uldrich AP, McCluskey J, Rossjohn J, Moody DB. The burgeoning family of unconventional T cells. *Nat Immunol.* (2015) 16:1114–23. doi: 10.1038/ni.3298
15. Kawano T, Cui J, Koezuka Y, Toura I, Kaneko Y, Motoki K, et al. CD1d-restricted and TCR-mediated activation of valpha14 NKT cells by glycosylceramides. *Science.* (1997) 278:1626–9. doi: 10.1126/science.278.5343.1626
16. Natori T, Koezuka Y, Higa T. Agelasphins, novel alpha-galactosylceramides from the marine sponge agelas-mauritianus. *Tetrahedron Lett.* (1993) 34:5591–2. doi: 10.1016/S0040-4039(00)73889-5
17. Carreño LJ, Kharkwal SS, Porcelli SA. Optimizing NKT cell ligands as vaccine adjuvants. *Immunotherapy.* (2014) 6:309–20. doi: 10.2217/imt.13.175
18. Speir M, Hermans IF, Weinkove R. Engaging natural killer T cells as 'universal helpers' for vaccination. *Drugs.* (2017) 77:1–15. doi: 10.1007/s40265-016-0675-z
19. Silk JD, Hermans IF, Gileadi U, Chong TW, Shepherd D, Salio M, et al. Utilizing the adjuvant properties of CD1d-dependent NK T cells in T cell-mediated immunotherapy. *J Clin Invest.* (2004) 114:1800–11. doi: 10.1172/JCI200422046
20. Cerundolo V, Silk JD, Masri SH, Salio M. Harnessing invariant NKT cells in vaccination strategies. *Nat Rev Immunol.* (2009) 9:28–38. doi: 10.1038/nri2451
21. Fotouhi F, Shaffifar M, Farahmand B, Shirian S, Saeidi M, Tabarraei A, et al. Adjuvant use of the NKT cell agonist alpha-galactosylceramide leads to enhancement of M2-based DNA vaccine immunogenicity and protective immunity against influenza A virus. *Arch Virol.* (2017) 162:1251–60. doi: 10.1007/s00705-017-3230-7
22. Youn HJ, Ko SY, Lee KA, Ko HJ, Lee YS, Fujihashi K, et al. A single intranasal immunization with inactivated influenza virus and alpha-galactosylceramide induces long-term protective immunity without redirecting antigen to the central nervous system. *Vaccine.* (2007) 25:5189–98. doi: 10.1016/j.vaccine.2007.04.081
23. Kamijuku H, Nagata Y, Jiang X, Ichinohe T, Tashiro T, Mori K, et al. Mechanism of NKT cell activation by intranasal coadministration of alpha-galactosylceramide, which can induce cross-protection against influenza viruses. *Mucosal Immunol.* (2008) 1:208–18. doi: 10.1038/mi.2008.2
24. Guillonneau C, Mintern JD, Hubert FX, Hurt AC, Besra GS, Porcelli S, et al. Combined NKT cell activation and influenza virus vaccination boosts memory CTL generation and protective immunity. *Proc Natl Acad Sci USA.* (2009) 106:3330–5. doi: 10.1073/pnas.0813309106
25. Li K, Luo J, Wang C, He H. α-Galactosylceramide potently augments M2e-induced protective immunity against highly pathogenic H5N1 avian influenza virus infection in mice. *Vaccine.* (2011) 29:7711–7. doi: 10.1016/j.vaccine.2011.07.136
26. Ko SY, Ko HJ, Chang WS, Park SH, Kweon MN, Kang CY. alpha-Galactosylceramide can act as a nasal vaccine adjuvant inducing protective immune responses against viral infection and tumor. *J Immunol.* (2005) 175:3309–17. doi: 10.4049/jimmunol.175.5.3309
27. Kopecky-Bromberg SA, Fraser KA, Pica N, Carnero E, Moran TM, Franck RW, et al. Alpha-C-galactosylceramide as an adjuvant for a live attenuated influenza virus vaccine. *Vaccine.* (2009) 27:3766–74. doi: 10.1016/j.vaccine.2009.03.090
28. Anderson RJ, Li J, Kedzierski L, Compton BJ, Hayman CM, Osmond TL, et al. Augmenting influenza-specific T cell memory generation with a natural killer T cell-dependent glycolipid-peptide vaccine. *ACS Chem Biol.* (2017) 12:2898–905. doi: 10.1021/acschembio.7b00845
29. Yamasaki S, Shimizu K, Kometani K, Sakurai M, Kawamura M, Fujii SI. *In vivo* dendritic cell targeting cellular vaccine induces CD4. *Sci Rep.* (2016) 6:35173. doi: 10.1038/srep35173
30. Galli G, Pittoni P, Tonti E, Malzone C, Uematsu Y, Tortoli M, et al. Invariant NKT cells sustain specific B cell responses and memory. *Proc Natl Acad Sci USA.* (2007) 104:3984–9. doi: 10.1073/pnas.0700191104
31. Hung JT, Tsai YC, Lin WD, Jan JT, Lin KH, Huang JR, et al. Potent adjuvant effects of novel NKT stimulatory glycolipids on hemagglutinin based DNA vaccine for H5N1 influenza virus. *Antiviral Res.* (2014) 107:110–8. doi: 10.1016/j.antiviral.2014.04.007
32. Lee YS, Lee KA, Lee JY, Kang MH, Song YC, Baek DJ, et al. An α-GalCer analogue with branched acyl chain enhances protective immune responses in a nasal influenza vaccine. *Vaccine.* (2011) 29:417–25. doi: 10.1016/j.vaccine.2010.11.005
33. Feng H, Nakajima N, Wu L, Yamashita M, Lopes TJS, Tsuji M, et al. A glycolipid adjuvant, 7DW8-5, enhances the protective immune response to the current split influenza vaccine in mice. *Front Microbiol.* (2019) 10:2157. doi: 10.3389/fmicb.2019.02157
34. Makino Y, Kanno R, Ito T, Higashino K, Taniguchi M. Predominant expression of invariant V alpha 14+ TCR alpha chain in NK1.1+ T cell populations. *Int Immunol.* (1995) 7:1157–61. doi: 10.1093/intimm/7.7.1157
35. Budd RC, Miescher GC, Howe RC, Lees RK, Bron C, MacDonald HR. Developmentally regulated expression of T cell receptor beta chain variable domains in immature thymocytes. *J Exp Med.* (1987) 166:577–82. doi: 10.1084/jem.166.2.577
36. Fowlkes BJ, Kruisbeek AM, Ton-That H, Weston MA, Coligan JE, Schwartz RH, et al. A novel population of T-cell receptor alpha beta-bearing thymocytes which predominantly expresses a single V beta gene family. *Nature.* (1987) 329:251–4. doi: 10.1038/329251a0
37. Ceredig R, Lynch F, Newman P. Phenotypic properties, interleukin 2 production, and developmental origin of a "mature" subpopulation of Lyt-2- L3T4- mouse thymocytes. *Proc Natl Acad Sci USA.* (1987) 84:8578–82. doi: 10.1073/pnas.84.23.8578
38. Sykes M. Unusual T cell populations in adult murine bone marrow. Prevalence of CD3+CD4-CD8- and alpha beta TCR+NK1.1+ cells. *J Immunol.* (1990) 145:3209–15.
39. Lantz O, Bendelac A. An invariant T cell receptor alpha chain is used by a unique subset of major histocompatibility complex class I-specific CD4+ and CD4-8- T cells in mice and humans. *J Exp Med.* (1994) 180:1097–6. doi: 10.1084/jem.180.3.1097
40. Moodycliffe AM, Maiti S, Ullrich SE. Splenic NK1.1-negative, TCR alpha beta intermediate CD4+ T cells exist in naive NK1.1 allelic positive and negative mice, with the capacity to rapidly secrete large amounts of IL-4 and IFN-gamma upon primary TCR stimulation. *J Immunol.* (1999) 162:5156–63.
41. Bendelac A, Lantz O, Quimby ME, Yewdell JW, Bennink JR, Brutkiewicz RR. CD1 recognition by mouse NK1+ T lymphocytes. *Science.* (1995) 268:863–5. doi: 10.1126/science.7538697
42. Mattner J, Debord KL, Ismail N, Goff RD, Cantu C, Zhou D, et al. Exogenous and endogenous glycolipid antigens activate NKT cells during microbial infections. *Nature.* (2005) 434:525–9. doi: 10.1038/nature03408
43. Rossjohn J, Pellicci DG, Patel O, Gapin L, Godfrey DI. Recognition of CD1d-restricted antigens by natural killer T cells. *Nat Rev Immunol.* (2012) 12:845–57. doi: 10.1038/nri3328
44. Benlagha K, Weiss A, Beavis A, Teyton L, Bendelac A. *In vivo* identification of glycolipid antigen-specific T cells using fluorescent CD1d tetramers. *J Exp Med.* (2000) 191:1895–903. doi: 10.1084/jem.191.11.1895
45. Matsuda JL, Naidenko OV, Gapin L, Nakayama T, Taniguchi M, Wang CR, et al. Tracking the response of natural killer T cells to a

glycolipid antigen using CD1d tetramers. *J Exp Med.* (2000) 192:741–54. doi: 10.1084/jem.192.5.741
46. Rhost S, Lofbom L, Rynmark BM, Pei B, Mansson JE, Teneberg S, et al. Identification of novel glycolipid ligands activating a sulfatide-reactive, CD1d-restricted, type II natural killer T lymphocyte. *Eur J Immunol.* (2012) 42:2851–60. doi: 10.1002/eji.201142350
47. Mempel M, Ronet C, Suarez F, Gilleron M, Puzo G, Van Kaer L, et al. Natural killer T cells restricted by the monomorphic MHC class 1b CD1d1 molecules behave like inflammatory cells. *J Immunol.* (2002) 168:365–71. doi: 10.4049/jimmunol.168.1.365
48. Fischer K, Scotet E, Niemeyer M, Koebernick H, Zerrahn J, Maillet S, et al. Mycobacterial phosphatidylinositol mannoside is a natural antigen for CD1d-restricted T cells. *Proc Natl Acad Sci USA.* (2004) 101:10685–90. doi: 10.1073/pnas.0403787101
49. Amprey JL, Im JS, Turco SJ, Murray HW, Illarionov PA, Besra GS, et al. A subset of liver NKT cells is activated during *Leishmania donovani* infection by CD1d-bound lipophosphoglycan. *J Exp Med.* (2004) 200:895–904. doi: 10.1084/jem.20040704
50. Schofield L, McConville MJ, Hansen D, Campbell AS, Fraser-Reid B, Grusby MJ, et al. CD1d-restricted immunoglobulin G formation to GPI-anchored antigens mediated by NKT cells. *Science.* (1999) 283:225–9. doi: 10.1126/science.283.5399.225
51. Liu Y, Goff RD, Zhou D, Mattner J, Sullivan BA, Khurana A, et al. A modified alpha-galactosyl ceramide for staining and stimulating natural killer T cells. *J Immunol Methods.* (2006) 312:34–9. doi: 10.1016/j.jim.2006.02.009
52. Artiaga BL, Whitener RL, Staples CR, Driver JP. Adjuvant effects of therapeutic glycolipids administered to a cohort of NKT cell-diverse pigs. *Vet Immunol Immunopathol.* (2014) 162:1–13. doi: 10.1016/j.vetimm.2014.09.006
53. Kobayashi E, Motoki K, Uchida T, Fukushima H, Koezuka Y. KRN7000, a novel immunomodulator, and its antitumor activities. *Oncol Res.* (1995) 7:529–34.
54. Gumperz JE, Miyake S, Yamamura T, Brenner MB. Functionally distinct subsets of CD1d-restricted natural killer T cells revealed by CD1d tetramer staining. *J Exp Med.* (2002) 195:625–36. doi: 10.1084/jem.20011786
55. Coquet JM, Chakravarti S, Kyparissoudis K, McNab FW, Pitt LA, McKenzie BS, et al. Diverse cytokine production by NKT cell subsets and identification of an IL-17-producing CD4-NK1.1- NKT cell population. *Proc Natl Acad Sci USA.* (2008) 105:11287–92. doi: 10.1073/pnas.0801631105
56. Lee YJ, Wang H, Starrett GJ, Phuong V, Jameson SC, Hogquist KA. Tissue-specific distribution of iNKT cells impacts their cytokine response. *Immunity.* (2015) 43:566–78. doi: 10.1016/j.immuni.2015.06.025
57. Goto M, Murakawa M, Kadoshima-Yamaoka K, Tanaka Y, Nagahira K, Fukuda Y, et al. Murine NKT cells produce Th17 cytokine interleukin-22. *Cell Immunol.* (2009) 254:81–4. doi: 10.1016/j.cellimm.2008.10.002
58. Chang YJ, Huang JR, Tsai YC, Hung JT, Wu D, Fujio M, et al. Potent immune-modulating and anticancer effects of NKT cell stimulatory glycolipids. *Proc Natl Acad Sci USA.* (2007) 104:10299–304. doi: 10.1073/pnas.0703824104
59. Kim JH, Chung DH. CD1d-restricted IFN-γ-secreting NKT cells promote immune complex-induced acute lung injury by regulating macrophage-inflammatory protein-1α production and activation of macrophages and dendritic cells. *J Immunol.* (2011) 186:1432–41. doi: 10.4049/jimmunol.1003140
60. Bilenki L, Yang J, Fan Y, Wang S, Yang X. Natural killer T cells contribute to airway eosinophilic inflammation induced by ragweed through enhanced IL-4 and eotaxin production. *Eur J Immunol.* (2004) 34:345–54. doi: 10.1002/eji.200324303
61. Faunce DE, Stein-Streilein J. NKT cell-derived RANTES recruits APCs and CD8+ T cells to the spleen during the generation of regulatory T cells in tolerance. *J Immunol.* (2002) 169:31–8. doi: 10.4049/jimmunol.169.1.31
62. Ohteki T, MacDonald HR. Stringent V beta requirement for the development of NK1.1+ T cell receptor-alpha/beta+ cells in mouse liver. *J Exp Med.* (1996) 183:1277–82. doi: 10.1084/jem.183.3.1277
63. Arase H, Arase N, Ogasawara K, Good RA, Onoé K. An NK1.1+ CD4+8- single-positive thymocyte subpopulation that expresses a highly skewed T-cell antigen receptor V beta family. *Proc Natl Acad Sci USA.* (1992) 89:6506–10. doi: 10.1073/pnas.89.14.6506
64. Matsuura A, Kinebuchi M, Chen HZ, Katabami S, Shimizu T, Hashimoto Y, et al. NKT cells in the rat: organ-specific distribution of NKT cells expressing distinct V alpha 14 chains. *J Immunol.* (2000) 164:3140–8. doi: 10.4049/jimmunol.164.6.3140
65. Exley M, Garcia J, Balk SP, Porcelli S. Requirements for CD1d recognition by human invariant Valpha24+ CD4-CD8- T cells. *J Exp Med.* (1997) 186:109–20. doi: 10.1084/jem.186.1.109
66. Dellabona P, Padovan E, Casorati G, Brockhaus M, Lanzavecchia A. An invariant V alpha 24-J alpha Q/V beta 11 T cell receptor is expressed in all individuals by clonally expanded CD4-8- T cells. *J Exp Med.* (1994) 180:1171–6. doi: 10.1084/jem.180.3.1171
67. Yang G, Artiaga BL, Lomelino CL, Jayaprakash AD, Sachidanandam R, Mckenna R, et al. Next generation sequencing of the pig αβ TCR repertoire identifies the porcine invariant NKT cell receptor. *J Immunol.* (2019) 202:1981–91. doi: 10.4049/jimmunol.1801171
68. Yang G, Artiaga BL, Lewis ST, Driver JP. Characterizing porcine invariant natural killer T cells: a comparative study with NK cells and T cells. *Dev Comp Immunol.* (2017) 76:343–51. doi: 10.1016/j.dci.2017.07.006
69. Pyz E, Naidenko O, Miyake S, Yamamura T, Berberich I, Cardell S, et al. The complementarity determining region 2 of BV8S2 (V beta 8.2) contributes to antigen recognition by rat invariant NKT cell TCR. *J Immunol.* (2006) 176:7447–55. doi: 10.4049/jimmunol.176.12.7447
70. Brossay L, Chioda M, Burdin N, Koezuka Y, Casorati G, Dellabona P, et al. CD1d-mediated recognition of an alpha-galactosylceramide by natural killer T cells is highly conserved through mammalian evolution. *J Exp Med.* (1998) 188:1521–8. doi: 10.1084/jem.188.8.1521
71. Spada FM, Koezuka Y, Porcelli SA. CD1d-restricted recognition of synthetic glycolipid antigens by human natural killer T cells. *J Exp Med.* (1998) 188:1529–34. doi: 10.1084/jem.188.8.1529
72. Fernandez CS, Jegaskanda S, Godfrey DI, Kent SJ. *In-vivo* stimulation of macaque natural killer T cells with α-galactosylceramide. *Clin Exp Immunol.* (2013) 173:480–92. doi: 10.1111/cei.12132
73. Motsinger A, Azimzadeh A, Stanic AK, Johnson RP, Van Kaer L, Joyce S, et al. Identification and simian immunodeficiency virus infection of CD1d-restricted macaque natural killer T cells. *J Virol.* (2003) 77:8153–8. doi: 10.1128/JVI.77.14.8153-8158.2003
74. Fichtner AS, Paletta D, Starick L, Schumann RF, Niewiesk S, Herrmann T. Function and expression of CD1d and invariant natural killer T-cell receptor in the cotton rat (*Sigmodon hispidus*). *Immunology.* (2015) 146:618–29. doi: 10.1111/imm.12532
75. Thierry A, Robin A, Giraud S, Minouflet S, Barra A, Bridoux F, et al. Identification of invariant natural killer T cells in porcine peripheral blood. *Vet Immunol Immunopathol.* (2012) 149:272–9. doi: 10.1016/j.vetimm.2012.06.023
76. Renukaradhya GJ, Manickam C, Khatri M, Rauf A, Li X, Tsuji M, et al. Functional invariant NKT cells in pig lungs regulate the airway hyperreactivity: a potential animal model. *J Clin Immunol.* (2011) 31:228–39. doi: 10.1007/s10875-010-9476-4
77. Yasuda N, Masuda K, Tsukui T, Teng A, Ishii Y. Identification of canine natural CD3-positive T cells expressing an invariant T-cell receptor alpha chain. *Vet Immunol Immunopathol.* (2009) 132:224–31. doi: 10.1016/j.vetimm.2009.08.002
78. Looringh van Beeck FA, Reinink P, Hermsen R, Zajonc DM, Laven MJ, Fun A, Troskie M, et al. Functional CD1d and/or NKT cell invariant chain transcript in horse, pig, African elephant and guinea pig, but not in ruminants. *Mol Immunol.* (2009) 46:1424–31. doi: 10.1016/j.molimm.2008.12.009
79. Van Rhijn I, Koets AP, Im JS, Piebes D, Reddington F, Besra GS, Porcelli SA, et al. The bovine CD1 family contains group 1 CD1 proteins, but no functional CD1d. *J Immunol.* (2006) 176:4888–93. doi: 10.4049/jimmunol.176.8.4888
80. Nguyen TK, Koets AP, Vordermeier M, Jervis PJ, Cox LR, Graham SP, et al. The bovine CD1D gene has an unusual gene structure and is expressed but cannot present alpha-galactosylceramide with a C26 fatty acid. *Int Immunol.* (2013) 25:91–8. doi: 10.1093/intimm/dxs092

81. Wang J, Guillaume J, Pauwels N, Van Calenbergh S, Van Rhijn I, Zajonc DM. Crystal structures of bovine CD1d reveal altered alphaGalCer presentation and a restricted A' pocket unable to bind long-chain glycolipids. *PLoS ONE.* (2012) 7:e47989. doi: 10.1371/journal.pone.0047989
82. Dossa RG, Alperin DC, Garzon D, Mealey RH, Brown WC, Jervis PJ, et al. In contrast to other species, alpha-Galactosylceramide (alpha-GalCer) is not an immunostimulatory NKT cell agonist in horses. *Dev Comp Immunol.* (2015) 49:49–58. doi: 10.1016/j.dci.2014.11.005
83. Brennan PJ, Brigl M, Brenner MB. Invariant natural killer T cells: an innate activation scheme linked to diverse effector functions. *Nat Rev Immunol.* (2013) 13:101–17. doi: 10.1038/nri3369
84. Brennan PJ, Tatituri RV, Brigl M, Kim EY, Tuli A, Sanderson JP, et al. Invariant natural killer T cells recognize lipid self antigen induced by microbial danger signals. *Nat Immunol.* (2011) 12:1202–11. doi: 10.1038/ni.2143
85. Van Kaer L, Parekh VV, Wu L. Invariant natural killer T cells: bridging innate and adaptive immunity. *Cell Tissue Res.* (2011) 343:43–55. doi: 10.1007/s00441-010-1023-3
86. Matsuda JL, Mallevaey T, Scott-Browne J, Gapin L. CD1d-restricted iNKT cells, the 'Swiss-Army knife' of the immune system. *Curr Opin Immunol.* (2008) 20:358–68. doi: 10.1016/j.coi.2008.03.018
87. Tupin E, Kinjo Y, Kronenberg M. The unique role of natural killer T cells in the response to microorganisms. *Nat Rev Microbiol.* (2007) 5:405–17. doi: 10.1038/nrmicro1657
88. Tyznik AJ, Tupin E, Nagarajan NA, Her MJ, Benedict CA, Kronenberg M. Cutting edge: the mechanism of invariant NKT cell responses to viral danger signals. *J Immunol.* (2008) 181:4452–6. doi: 10.4049/jimmunol.181.7.4452
89. Brigl M, Bry L, Kent SC, Gumperz JE, Brenner MB. Mechanism of CD1d-restricted natural killer T cell activation during microbial infection. *Nat Immunol.* (2003) 4:1230–7. doi: 10.1038/ni1002
90. Nagarajan NA, Kronenberg M. Invariant NKT cells amplify the innate immune response to lipopolysaccharide. *J Immunol.* (2007) 178:2706–13. doi: 10.4049/jimmunol.178.5.2706
91. Birkholz A, Nemčovič M, Yu ED, Girardi E, Wang J, Khurana A, et al. Lipid and carbohydrate modifications of α-galactosylceramide differently influence mouse and human type I natural killer T cell activation. *J Biol Chem.* (2015) 290:17206–17. doi: 10.1074/jbc.M115.654814
92. Sullivan BA, Nagarajan NA, Wingender G, Wang J, Scott I, Tsuji M, et al. Mechanisms for glycolipid antigen-driven cytokine polarization by Valpha14i NKT cells. *J Immunol.* (2010) 184:141–53. doi: 10.4049/jimmunol.0902880
93. Carreño LJ, Riquelme EM, González PA, Espagnolle N, Riedel CA, Valitutti S, et al. T-cell antagonism by short half-life pMHC ligands can be mediated by an efficient trapping of T-cell polarization toward the APC. *Proc Natl Acad Sci USA.* (2010) 107:210–5. doi: 10.1073/pnas.0911258107
94. González PA, Carreño LJ, Coombs D, Mora JE, Palmieri E, Goldstein B, et al. T cell receptor binding kinetics required for T cell activation depend on the density of cognate ligand on the antigen-presenting cell. *Proc Natl Acad Sci USA.* (2005) 102:4824–9. doi: 10.1073/pnas.0500922102
95. Lee YJ, Holzapfel KL, Zhu J, Jameson SC, Hogquist KA. Steady-state production of IL-4 modulates immunity in mouse strains and is determined by lineage diversity of iNKT cells. *Nat Immunol.* (2013) 14:1146–54. doi: 10.1038/ni.2731
96. Yu KO, Im JS, Molano A, Dutronc Y, Illarionov PA, Forestier C, et al. Modulation of CD1d-restricted NKT cell responses by using N-acyl variants of alpha-galactosylceramides. *Proc Natl Acad Sci USA.* (2005) 102:3383–8. doi: 10.1073/pnas.0407488102
97. Im JS, Arora P, Bricard G, Molano A, Venkataswamy MM, Baine I, et al. Kinetics and cellular site of glycolipid loading control the outcome of natural killer T cell activation. *Immunity.* (2009) 30:888–98. doi: 10.1016/j.immuni.2009.03.022
98. Wilson MT, Johansson C, Olivares-Villagómez D, Singh AK, Stanic AK, Wang CR, et al. The response of natural killer T cells to glycolipid antigens is characterized by surface receptor down-modulation and expansion. *Proc Natl Acad Sci USA.* (2003) 100:10913–8. doi: 10.1073/pnas.1833166100
99. Crowe NY, Uldrich AP, Kyparissoudis K, Hammond KJ, Hayakawa Y, Sidobre S, et al. Glycolipid antigen drives rapid expansion and sustained cytokine production by NKT cells. *J Immunol.* (2003) 171:4020–7. doi: 10.4049/jimmunol.171.8.4020
100. Fujii S, Shimizu K, Kronenberg M, Steinman RM. Prolonged IFN-gamma-producing NKT response induced with alpha-galactosylceramide-loaded DCs. *Nat Immunol.* (2002) 3:867–74. doi: 10.1038/ni827
101. Parekh VV, Wilson MT, Olivares-Villagómez D, Singh AK, Wu L, Wang CR, et al. Glycolipid antigen induces long-term natural killer T cell anergy in mice. *J Clin Invest.* (2005) 115:2572–83. doi: 10.1172/JCI24762
102. Uldrich AP, Crowe NY, Kyparissoudis K, Pellicci DG, Zhan Y, Lew AM, et al. NKT cell stimulation with glycolipid antigen *in vivo*: costimulation-dependent expansion, Bim-dependent contraction, and hyporesponsiveness to further antigenic challenge. *J Immunol.* (2005) 175:3092–101. doi: 10.4049/jimmunol.175.5.3092
103. Sullivan BA, Kronenberg M. Activation or anergy: NKT cells are stunned by alpha-galactosylceramide. *J Clin Invest.* (2005) 115:2328–9. doi: 10.1172/JCI26297
104. Kim S, Lalani S, Parekh VV, Vincent TL, Wu L, Van Kaer L. Impact of bacteria on the phenotype, functions, and therapeutic activities of invariant NKT cells in mice. *J Clin Invest.* (2008) 118:2301–15. doi: 10.1172/JCI33071
105. Chiba A, Dascher CC, Besra GS, Brenner MB. Rapid NKT cell responses are self-terminating during the course of microbial infection. *J Immunol.* (2008) 181:2292–302. doi: 10.4049/jimmunol.181.4.2292
106. Choi HJ, Xu H, Geng Y, Colmone A, Cho H, Wang CR. Bacterial infection alters the kinetics and function of iNKT cell responses. *J Leukoc Biol.* (2008) 84:1462–71. doi: 10.1189/jlb.0108038
107. Joshi SK, Lang GA, Larabee JL, Devera TS, Aye LM, Shah HB, et al. Bacillus anthracis lethal toxin disrupts TCR signaling in CD1d-restricted NKT cells leading to functional anergy. *PLoS Pathog.* (2009) 5:e1000588. doi: 10.1371/journal.ppat.1000588
108. Raftery MJ, Winau F, Giese T, Kaufmann SH, Schaible UE, Schönrich G. Viral danger signals control CD1d de novo synthesis and NKT cell activation. *Eur J Immunol.* (2008) 38:668–79. doi: 10.1002/eji.200737233
109. Montoya CJ, Jie HB, Al-Harthi L, Mulder C, Patiño PJ, Rugeles MT, et al. Activation of plasmacytoid dendritic cells with TLR9 agonists initiates invariant NKT cell-mediated cross-talk with myeloid dendritic cells. *J Immunol.* (2006) 177:1028–39. doi: 10.4049/jimmunol.177.2.1028
110. Karmakar S, Bhaumik SK, Paul J, De T. TLR4 and NKT cell synergy in immunotherapy against visceral leishmaniasis. *PLoS Pathog.* (2012) 8:e1002646. doi: 10.1371/journal.ppat.1002646
111. Chen T, Guo J, Han C, Yang M, Cao X. Heat shock protein 70, released from heat-stressed tumor cells, initiates antitumor immunity by inducing tumor cell chemokine production and activating dendritic cells via TLR4 pathway. *J Immunol.* (2009) 182:1449–59. doi: 10.4049/jimmunol.182.3.1449
112. Sharma AK, LaPar DJ, Stone ML, Zhao Y, Kron IL, Laubach VE. Receptor for advanced glycation end products (RAGE) on iNKT cells mediates lung ischemia-reperfusion injury. *Am J Transplant.* (2013) 13:2255–67. doi: 10.1111/ajt.12368
113. Paget C, Mallevaey T, Speak AO, Torres D, Fontaine J, Sheehan KC, et al. Activation of invariant NKT cells by toll-like receptor 9-stimulated dendritic cells requires type I interferon and charged glycosphingolipids. *Immunity.* (2007) 27:597–609. doi: 10.1016/j.immuni.2007.08.017
114. Wang X, Bishop KA, Hegde S, Rodenkirch LA, Pike JW, Gumperz JE. Human invariant natural killer T cells acquire transient innate responsiveness via histone H4 acetylation induced by weak TCR stimulation. *J Exp Med.* (2012) 209:987–1000. doi: 10.1084/jem.20111024
115. Ferhat MH, Robin A, Barbier L, Thierry A, Gombert JM, Barbarin A, et al. The impact of invariant NKT cells in sterile inflammation: the possible contribution of the alarmin/cytokine IL-33. *Front Immunol.* (2018) 9:2308. doi: 10.3389/fimmu.2018.02308
116. Kitamura H, Iwakabe K, Yahata T, Nishimura S, Ohta A, Ohmi Y, et al. The natural killer T (NKT) cell ligand alpha-galactosylceramide demonstrates its immunopotentiating effect by inducing interleukin (IL)-12 production by dendritic cells and IL-12 receptor expression on NKT cells. *J Exp Med.* (1999) 189:1121–8. doi: 10.1084/jem.189.7.1121
117. Brigl M, Tatituri RV, Watts GF, Bhowruth V, Leadbetter EA, Barton N, et al. Innate and cytokine-driven signals, rather than microbial antigens, dominate

in natural killer T cell activation during microbial infection. *J Exp Med.* (2011) 208:1163–77. doi: 10.1084/jem.20102555
118. Wesley JD, Tessmer MS, Chaukos D, Brossay L. NK cell-like behavior of Valpha14i NK T cells during MCMV infection. *PLoS Pathog.* (2008) 4:e1000106. doi: 10.1371/journal.ppat.1000106
119. Bendelac A, Savage PB, Teyton L. The biology of NKT cells. *Annu Rev Immunol.* (2007) 25:297–336. doi: 10.1146/annurev.immunol.25.022106.141711
120. Bendelac. Mouse NK1+ T cells. *Curr Opin Immunol.* (1995) 7:367–74. doi: 10.1016/0952-7915(95)80112-X
121. Kuylenstierna C, Björkström NK, Andersson SK, Sahlström P, Bosnjak L, Paquin-Proulx D, et al. NKG2D performs two functions in invariant NKT cells: direct TCR-independent activation of NK-like cytolysis and co-stimulation of activation by CD1d. *Eur J Immunol.* (2011) 41:1913–23. doi: 10.1002/eji.200940278
122. Brigl M, Brenner MB. How invariant natural killer T cells respond to infection by recognizing microbial or endogenous lipid antigens. *Semin Immunol.* (2010) 22:79–86. doi: 10.1016/j.smim.2009.10.006
123. Salio M, Speak AO, Shepherd D, Polzella P, Illarionov PA, Veerapen N, et al. Modulation of human natural killer T cell ligands on TLR-mediated antigen-presenting cell activation. *Proc Natl Acad Sci USA.* (2007) 104:20490–5. doi: 10.1073/pnas.0710145104
124. Yang OO, Racke FK, Nguyen PT, Gausling R, Severino ME, Horton HF, et al. CD1d on myeloid dendritic cells stimulates cytokine secretion from and cytolytic activity of V alpha 24J alpha Q T cells: a feedback mechanism for immune regulation. *J Immunol.* (2000) 165:3756–62. doi: 10.4049/jimmunol.165.7.3756
125. Yoo JK, Braciale TJ. IL-21 promotes late activator APC-mediated T follicular helper cell differentiation in experimental pulmonary virus infection. *PLoS ONE.* (2014) 9:e105872. doi: 10.1371/journal.pone.0105872
126. Taraban VY, Martin S, Attfield KE, Glennie MJ, Elliott T, Elewaut D, et al. Invariant NKT cells promote CD8+ cytotoxic T cell responses by inducing CD70 expression on dendritic cells. *J Immunol.* (2008) 180:4615–20. doi: 10.4049/jimmunol.180.7.4615
127. Hermans IF, Silk JD, Gileadi U, Salio M, Mathew B, Ritter G, et al. NKT cells enhance CD4+ and CD8+ T cell responses to soluble antigen in vivo through direct interaction with dendritic cells. *J Immunol.* (2003) 171:5140–7. doi: 10.4049/jimmunol.171.10.5140
128. Fujii SI, Yamasaki S, Sato Y, Shimizu K. Vaccine designs utilizing invariant NKT-licensed antigen-presenting cells provide NKT or T cell help for B cell responses. *Front Immunol.* (2018) 9:1267. doi: 10.3389/fimmu.2018.01267
129. Lang ML. How do natural killer T cells help B cells? *Expert Rev Vaccines.* (2009) 8:1109–21. doi: 10.1586/erv.09.56
130. Doherty DG, Melo AM, Moreno-Olivera A, Solomos AC. Activation and regulation of B cell responses by invariant natural killer T cells. *Front Immunol.* (2018) 9:1360. doi: 10.3389/fimmu.2018.01360
131. Vomhof-DeKrey EE, Yates J, Leadbetter EA. Invariant NKT cells provide innate and adaptive help for B cells. *Curr Opin Immunol.* (2014) 28:12–7. doi: 10.1016/j.coi.2014.01.007
132. Dellabona P, Abrignani S, Casorati G. iNKT-cell help to B cells: a cooperative job between innate and adaptive immune responses. *Eur J Immunol.* (2014) 44:2230–7. doi: 10.1002/eji.201344399
133. Barral P, Eckl-Dorna J, Harwood NE, de Santo C, Salio M, Illarionov P, et al. B cell receptor-mediated uptake of CD1d-restricted antigen augments antibody responses by recruiting invariant NKT cell help *in vivo*. *Proc Natl Acad Sci USA.* (2008) 105:8345–50. doi: 10.1073/pnas.0802968105
134. Chang PP, Barral P, Fitch J, Pratama A, Ma CS, Kallies A, et al. Identification of Bcl-6-dependent follicular helper NKT cells that provide cognate help for B cell responses. *Nat Immunol.* (2012) 13:35–43. doi: 10.1038/ni.2166
135. King IL, Fortier A, Tighe M, Dibble J, Watts GF, Veerapen N, et al. Invariant natural killer T cells direct B cell responses to cognate lipid antigen in an IL-21-dependent manner. *Nat Immunol.* (2012) 13:44–50. doi: 10.1038/ni.2172
136. Leadbetter EA, Brigl M, Illarionov P, Cohen N, Luteran MC, Pillai S, et al. NK T cells provide lipid antigen-specific cognate help for B cells. *Proc Natl Acad Sci USA.* (2008) 105:8339–44. doi: 10.1073/pnas.0801375105
137. Tonti E, Galli G, Malzone C, Abrignani S, Casorati G, Dellabona P. NKT-cell help to B lymphocytes can occur independently of cognate interaction. *Blood.* (2009) 113:370–6. doi: 10.1182/blood-2008-06-166249
138. Gray JD, Horwitz DA. Activated human NK cells can stimulate resting B cells to secrete immunoglobulin. *J Immunol.* (1995) 154:5656–64.
139. Gaya M, Barral P, Burbage M, Aggarwal S, Montaner B, Warren Navia A, et al. Initiation of antiviral B cell immunity relies on innate signals from spatially positioned NKT cells. *Cell.* (2017) 172:517–33.e20. doi: 10.1016/j.cell.2017.11.036
140. Berzins SP, Cochrane AD, Pellicci DG, Smyth MJ, Godfrey DI. Limited correlation between human thymus and blood NKT cell content revealed by an ontogeny study of paired tissue samples. *Eur J Immunol.* (2005) 35:1399–407. doi: 10.1002/eji.200425958
141. Long HM, Chagoury OL, Leese AM, Ryan GB, James E, Morton LT, et al. MHC II tetramers visualize human CD4+ T cell responses to Epstein-Barr virus infection and demonstrate atypical kinetics of the nuclear antigen EBNA1 response. *J Exp Med.* (2013) 210:933–49. doi: 10.1084/jem.20121437
142. Yu KKQ, Wilburn DB, Hackney JA, Darrah PA, Foulds KE, James CA, et al. Conservation of molecular and cellular phenotypes of invariant NKT cells between humans and non-human primates. *Immunogenetics.* (2019) 71:465–78. doi: 10.1007/s00251-019-01118-9
143. De Santo C, Salio M, Masri SH, Lee LY, Dong T, Speak AO, et al. Invariant NKT cells reduce the immunosuppressive activity of influenza A virus-induced myeloid-derived suppressor cells in mice and humans. *J Clin Invest.* (2008) 118:4036–48. doi: 10.1172/JCI36264
144. Kok WL, Denney L, Benam K, Cole S, Clelland C, McMichael AJ, et al. Pivotal advance: invariant NKT cells reduce accumulation of inflammatory monocytes in the lungs and decrease immune-pathology during severe influenza A virus infection. *J Leukoc Biol.* (2012) 91:357–68. doi: 10.1189/jlb.0411184
145. Ishikawa H, Tanaka K, Kutsukake E, Fukui T, Sasaki H, Hata A, et al. IFN-γ production downstream of NKT cell activation in mice infected with influenza virus enhances the cytolytic activities of both NK cells and viral antigen-specific CD8+ T cells. *Virology.* (2010) 407:325–32. doi: 10.1016/j.virol.2010.08.030
146. Paget C, Ivanov S, Fontaine J, Blanc F, Pichavant M, Renneson J, et al. Potential role of invariant NKT cells in the control of pulmonary inflammation and CD8+ T cell response during acute influenza A virus H3N2 pneumonia. *J Immunol.* (2011) 186:5590–602. doi: 10.4049/jimmunol.1002348
147. Kulkarni RR, Haeryfar SM, Sharif S. The invariant NKT cell subset in anti-viral defenses: a dark horse in anti-influenza immunity? *J Leukoc Biol.* (2010) 88:635–43. doi: 10.1189/jlb.0410191
148. Ho LP, Denney L, Luhn K, Teoh D, Clelland C, McMichael AJ. Activation of invariant NKT cells enhances the innate immune response and improves the disease course in influenza A virus infection. *Eur J Immunol.* (2008) 38:1913–22. doi: 10.1002/eji.200738017
149. Paget C, Ivanov S, Fontaine J, Renneson J, Blanc F, Pichavant M, et al. Interleukin-22 is produced by invariant natural killer T lymphocytes during influenza A virus infection: potential role in protection against lung epithelial damages. *J Biol Chem.* (2012) 287:8816–29. doi: 10.1074/jbc.M111.304758
150. Benton KA, Misplon JA, Lo CY, Brutkiewicz RR, Prasad SA, Epstein SL. Heterosubtypic immunity to influenza A virus in mice lacking IgA, all Ig, NKT cells, or gamma delta T cells. *J Immunol.* (2001) 166:7437–45. doi: 10.4049/jimmunol.166.12.7437
151. Renu S, Dhakal S, Kim E, Goodman J, Lakshmanappa YS, Wannemuehler MJ, et al. Intranasal delivery of influenza antigen by nanoparticles, but not NKT-cell adjuvant differentially induces the expression of B-cell activation factors in mice and swine. *Cell Immunol.* (2018) 329:27–30. doi: 10.1016/j.cellimm.2018.04.005
152. Dwivedi V, Manickam C, Dhakal S, Binjawadagi B, Ouyang K, Hiremath J, et al. Adjuvant effects of invariant NKT cell ligand potentiates the innate and adaptive immunity to an inactivated H1N1 swine influenza virus vaccine in pigs. *Vet Microbiol.* (2016) 186:157–63. doi: 10.1016/j.vetmic.2016.02.028
153. Artiaga BL, Yang G, Hackmann TJ, Liu Q, Richt JA, Salek-Ardakani S, et al. α-Galactosylceramide protects swine against influenza infection when administered as a vaccine adjuvant. *Sci Rep.* (2016) 6:23593. doi: 10.1038/srep23593
154. Lee PT, Benlagha K, Teyton L, Bendelac A. Distinct functional lineages of human V(alpha)24 natural killer T cells. *J Exp Med.* (2002) 195:637–41. doi: 10.1084/jem.20011908

155. Chen YG, Tsaih SW, Serreze DV. Genetic control of murine invariant natural killer T-cell development dynamically differs dependent on the examined tissue type. *Genes Immun.* (2012) 13:164–74. doi: 10.1038/gene.2011.68
156. Gadola SD, Dulphy N, Salio M, Cerundolo V. Valpha24-JalphaQ-independent V, CD1d-restricted recognition of alpha-galactosylceramide by human CD4(+) and CD8alphabeta(+) T lymphocytes. *J Immunol.* (2002) 168:5514–20. doi: 10.4049/jimmunol.168.11.5514
157. Takahashi T, Chiba S, Nieda M, Azuma T, Ishihara S, Shibata Y, et al. Cutting edge: analysis of human V alpha 24+CD8+ NK T cells activated by alpha-galactosylceramide-pulsed monocyte-derived dendritic cells. *J Immunol.* (2002) 168:3140–4. doi: 10.4049/jimmunol.168.7.3140
158. Townsend MJ, Weinmann AS, Matsuda JL, Salomon R, Farnham PJ, Biron CA, et al. T-bet regulates the terminal maturation and homeostasis of NK and Valpha14i NKT cells. *Immunity.* (2004) 20:477–94. doi: 10.1016/S1074-7613(04)00076-7
159. Engel I, Seumois G, Chavez L, Samaniego-Castruita D, White B, Chawla A, et al. Innate-like functions of natural killer T cell subsets result from highly divergent gene programs. *Nat Immunol.* (2016) 17:728–39. doi: 10.1038/ni.3437
160. Georgiev H, Ravens I, Benarafa C, Förster R, Bernhardt G. Distinct gene expression patterns correlate with developmental and functional traits of iNKT subsets. *Nat Commun.* (2016) 7:13116. doi: 10.1038/ncomms13116
161. Lee YJ, Starrett GJ, Lee ST, Yang R, Henzler CM, Jameson SC, et al. Lineage-specific effector signatures of invariant NKT cells are shared amongst γδ T, innate lymphoid, Th cells. *J Immunol.* (2016) 197:1460–70. doi: 10.4049/jimmunol.1600643
162. Constantinides MG, Bendelac A. Transcriptional regulation of the NKT cell lineage. *Curr Opin Immunol.* (2013) 25:161–7. doi: 10.1016/j.coi.2013.01.003
163. Kim PJ, Pai SY, Brigl M, Besra GS, Gumperz J, Ho IC. GATA-3 regulates the development and function of invariant NKT cells. *J Immunol.* (2006) 177:6650–9. doi: 10.4049/jimmunol.177.10.6650
164. Doisne JM, Becourt C, Amniai L, Duarte N, Le Luduec JB, Eberl G, et al. Skin and peripheral lymph node invariant NKT cells are mainly retinoic acid receptor-related orphan receptor (gamma)t+ and respond preferentially under inflammatory conditions. *J Immunol.* (2009) 183:2142–9. doi: 10.4049/jimmunol.0901059
165. Jaiswal AK, Sadasivam M, Hamad ARA. Syndecan-1-coating of interleukin-17-producing natural killer T cells provides a specific method for their visualization and analysis. *World J Diabetes.* (2017) 8:130–4. doi: 10.4239/wjd.v8.i4.130
166. Lynch L, Michelet X, Zhang S, Brennan PJ, Moseman A, Lester C, et al. Regulatory iNKT cells lack expression of the transcription factor PLZF and control the homeostasis of T(reg) cells and macrophages in adipose tissue. *Nat Immunol.* (2015) 16:85–95. doi: 10.1038/ni.3047
167. Wingender G, Sag D, Kronenberg M. NKT10 cells: a novel iNKT cell subset. *Oncotarget.* (2015) 6:26552–3. doi: 10.18632/oncotarget.5270
168. Savage AK, Constantinides MG, Han J, Picard D, Martin E, Li B, et al. The transcription factor PLZF directs the effector program of the NKT cell lineage. *Immunity.* (2008) 29:391–403. doi: 10.1016/j.immuni.2008.07.011
169. Kovalovsky D, Uche OU, Eladad S, Hobbs RM, Yi W, Alonzo E, et al. The BTB-zinc finger transcriptional regulator PLZF controls the development of invariant natural killer T cell effector functions. *Nat Immunol.* (2008) 9:1055–64. doi: 10.1038/ni.1641
170. Kovalovsky D, Alonzo ES, Uche OU, Eidson M, Nichols KE, Sant'Angelo DB. PLZF induces the spontaneous acquisition of memory/effector functions in T cells independently of NKT cell-related signals. *J Immunol.* (2010) 184:6746–55. doi: 10.4049/jimmunol.1000776
171. Crosby CM, Kronenberg M. Tissue-specific functions of invariant natural killer T cells. *Nat Rev Immunol.* (2018) 18:559–74. doi: 10.1038/s41577-018-0034-2
172. Wolf BJ, Choi JE, Exley MA. Novel approaches to exploiting invariant NKT cells in cancer immunotherapy. *Front Immunol.* (2018) 9:384. doi: 10.3389/fimmu.2018.00384
173. Miyamoto K, Miyake S, Yamamura T. A synthetic glycolipid prevents autoimmune encephalomyelitis by inducing TH2 bias of natural killer T cells. *Nature.* (2001) 413:531–4. doi: 10.1038/35097097
174. Baev DV, Caielli S, Ronchi F, Coccia M, Facciotti F, Nichols KE, et al. Impaired SLAM-SLAM homotypic interaction between invariant NKT cells and dendritic cells affects differentiation of IL-4/IL-10-secreting NKT2 cells in nonobese diabetic mice. *J Immunol.* (2008) 181:869–77. doi: 10.4049/jimmunol.181.2.869
175. Sag D, Krause P, Hedrick CC, Kronenberg M, Wingender G. IL-10-producing NKT10 cells are a distinct regulatory invariant NKT cell subset. *J Clin Invest.* (2014) 124:3725–40. doi: 10.1172/JCI72308
176. Yu KO, Porcelli SA. The diverse functions of CD1d-restricted NKT cells and their potential for immunotherapy. *Immunol Lett.* (2005) 100:42–55. doi: 10.1016/j.imlet.2005.06.010
177. Oki S, Chiba A, Yamamura T, Miyake S. The clinical implication and molecular mechanism of preferential IL-4 production by modified glycolipid-stimulated NKT cells. *J Clin Invest.* (2004) 113:1631–40. doi: 10.1172/JCI200420862
178. Oki S, Tomi C, Yamamura T, Miyake S. Preferential T(h)2 polarization by OCH is supported by incompetent NKT cell induction of CD40L and following production of inflammatory cytokines by bystander cells *in vivo*. *Int Immunol.* (2005) 17:1619–29. doi: 10.1093/intimm/dxh342
179. McCarthy C, Shepherd D, Fleire S, Stronge VS, Koch M, Illarionov PA, et al. The length of lipids bound to human CD1d molecules modulates the affinity of NKT cell TCR and the threshold of NKT cell activation. *J Exp Med.* (2007) 204:1131–44. doi: 10.1084/jem.20062342
180. Schmieg J, Yang G, Franck RW, Tsuji M. Superior protection against malaria and melanoma metastases by a C-glycoside analogue of the natural killer T cell ligand alpha-Galactosylceramide. *J Exp Med.* (2003) 198:1631–41. doi: 10.1084/jem.20031192
181. Wun KS, Cameron G, Patel O, Pang SS, Pellicci DG, Sullivan LC, et al. A molecular basis for the exquisite CD1d-restricted antigen specificity and functional responses of natural killer T cells. *Immunity.* (2011) 34:327–39. doi: 10.1016/j.immuni.2011.02.001
182. Tashiro T, Sekine-Kondo E, Shigeura T, Nakagawa R, Inoue S, Omori-Miyake M, et al. Induction of Th1-biased cytokine production by alpha-carba-GalCer, a neoglycolipid ligand for NKT cells. *Int Immunol.* (2010) 22:319–28. doi: 10.1093/intimm/dxq012
183. Li X, Fujio M, Imamura M, Wu D, Vasan S, Wong CH, et al. Design of a potent CD1d-binding NKT cell ligand as a vaccine adjuvant. *Proc Natl Acad Sci USA.* (2010) 107:13010–5. doi: 10.1073/pnas.1006662107
184. Lin KH, Liang JJ, Huang WI, Lin-Chu SY, Su CY, Lee YL, et al. *In vivo* protection provided by a synthetic new alpha-galactosyl ceramide analog against bacterial and viral infections in murine models. *Antimicrob Agents Chemother.* (2010) 54:4129–36. doi: 10.1128/AAC.00368-10
185. Osman Y, Kawamura T, Naito T, Takeda K, Van Kaer L, Okumura K, et al. Activation of hepatic NKT cells and subsequent liver injury following administration of alpha-galactosylceramide. *Eur J Immunol.* (2000) 30:1919–28. doi: 10.1002/1521-4141(200007)30:7<1919::AID-IMMU1919>3.0.CO;2-3
186. Kim HY, Kim S, Chung DH. FcgammaRIII engagement provides activating signals to NKT cells in antibody-induced joint inflammation. *J Clin Invest.* (2006) 116:2484–92. doi: 10.1172/JCI27219
187. Miellot-Gafsou A, Biton J, Bourgeois E, Herbelin A, Boissier MC, Bessis N. Early activation of invariant natural killer T cells in a rheumatoid arthritis model and application to disease treatment. *Immunology.* (2010) 130:296–306. doi: 10.1111/j.1365-2567.2009.03235.x
188. Meyer EH, Goya S, Akbari O, Berry GJ, Savage PB, Kronenberg M, et al. Glycolipid activation of invariant T cell receptor+ NK T cells is sufficient to induce airway hyperreactivity independent of conventional CD4+ T cells. *Proc Natl Acad Sci USA.* (2006) 103:2782–7. doi: 10.1073/pnas.0510282103
189. Matangkasombut P, Pichavant M, Yasumi T, Hendricks C, Savage PB, Dekruyff RH, et al. Direct activation of natural killer T cells induces airway hyperreactivity in nonhuman primates. *J Allergy Clin Immunol.* (2008) 121:1287–9. doi: 10.1016/j.jaci.2008.02.006
190. Kim JO, Kim DH, Chang WS, Hong C, Park SH, Kim S, et al. Asthma is induced by intranasal coadministration of allergen and natural killer T-cell ligand in a mouse model. *J Allergy Clin Immunol.* (2004) 114:1332–8. doi: 10.1016/j.jaci.2004.09.004
191. Khurana S, Loving CL, Manischewitz J, King LR, Gauger PC, Henningson J, et al. Vaccine-induced anti-HA2 antibodies promote virus fusion

and enhance influenza virus respiratory disease. *Sci Transl Med.* (2013) 5:200ra114. doi: 10.1126/scitranslmed.3006366
192. Rymarchyk SL, Lowenstein H, Mayette J, Foster SR, Damby DE, Howe IW, et al. Widespread natural variation in murine natural killer T-cell number and function. *Immunology.* (2008) 125:331–43. doi: 10.1111/j.1365-2567.2008.02846.x
193. Bernin H, Fehling H, Marggraff C, Tannich E, Lotter H. The cytokine profile of human NKT cells and PBMCs is dependent on donor sex and stimulus. *Med Microbiol Immunol.* (2016) 205:321–32. doi: 10.1007/s00430-016-0449-y
194. Metelitsa LS, Wu HW, Wang H, Yang Y, Warsi Z, Asgharzadeh S, et al. Natural killer T cells infiltrate neuroblastomas expressing the chemokine CCL2. *J Exp Med.* (2004) 199:1213–21. doi: 10.1084/jem.20031462
195. Schneiders FL, de Bruin RC, van den Eertwegh AJ, Scheper RJ, Leemans CR, Brakenhoff RH, et al. Circulating invariant natural killer T-cell numbers predict outcome in head and neck squamous cell carcinoma: updated analysis with 10-year follow-up. *J Clin Oncol.* (2012) 30:567–70. doi: 10.1200/JCO.2011.38.8819
196. DelaRosa O, Tarazona R, Casado JG, Alonso C, Ostos B, Peña J, et al. Valpha24+ NKT cells are decreased in elderly humans. *Exp Gerontol.* (2002) 37:213–7. doi: 10.1016/S0531-5565(01)00186-3
197. Tsukahara A, Seki S, Iiai T, Moroda T, Watanabe H, Suzuki S, et al. Mouse liver T cells: their change with aging and in comparison with peripheral T cells. *Hepatology.* (1997) 26:301–9. doi: 10.1002/hep.510260208
198. Faunce DE, Palmer JL, Paskowicz KK, Witte PL, Kovacs EJ. CD1d-restricted NKT cells contribute to the age-associated decline of T cell immunity. *J Immunol.* (2005) 175:3102–9. doi: 10.4049/jimmunol.175.5.3102
199. Mocchegiani E, Giacconi R, Cipriano C, Gasparini N, Bernardini G, Malavolta M, et al. The variations during the circadian cycle of liver CD1d-unrestricted NK1.1+TCR gamma/delta+ cells lead to successful ageing. Role of metallothionein/IL-6/gp130/PARP-1 interplay in very old mice. *Exp Gerontol.* (2004) 39:775–88. doi: 10.1016/j.exger.2004.01.014
200. Mocchegiani E, Giacconi R, Muti E, Rogo C, Bracci M, Muzzioli M, et al. Zinc, immune plasticity, aging, and successful aging: role of metallothionein. *Ann NY Acad Sci.* (2004) 1019:127–34. doi: 10.1196/annals.1297.023
201. Starbæk SMR, Brogaard L, Dawson HD, Smith AD, Heegaard PMH, Larsen LE, et al. Animal models for Influenza A virus infection incorporating the involvement of innate host defenses: enhanced translational value of the porcine model. *ILAR J.* (2018) 59:323–37. doi: 10.1093/ilar/ily009
202. Bai L, Deng S, Reboulet R, Mathew R, Teyton L, Savage PB, et al. Natural killer T (NKT)-B-cell interactions promote prolonged antibody responses and long-term memory to pneumococcal capsular polysaccharides. *Proc Natl Acad Sci USA.* (2013) 110:16097–102. doi: 10.1073/pnas.1303218110

Conflict of Interest: The authors declare that the research was conducted in the absence of any commercial or financial relationships that could be construed as a potential conflict of interest.

frontiers in Immunology

ORIGINAL RESEARCH
published: 30 November 2020
doi: 10.3389/fimmu.2020.579872

Innate Immune Responses to Chimpanzee Adenovirus Vector 155 Vaccination in Mice and Monkeys

Catherine Collignon[1‡], Vanesa Bol[1‡], Aurélie Chalon[1], Naveen Surendran[2†], Sandra Morel[1], Robert A. van den Berg[2], Stefania Capone[3], Viviane Bechtold[1§] and Stéphane T. Temmerman[1§]*

[1] Preclinical R&D, GSK, Rixensart, Belgium, [2] Discovery Performance Unit, GSK, Rockville, MD, United States, [3] Preclinical R&D, ReiThera Srl, Rome, Italy

OPEN ACCESS

Edited by:
Michael Schotsaert, Icahn School of Medicine at Mount Sinai, United States

Reviewed by:
Salvador Iborra, Universidad Complutense de Madrid, Spain
Francisco Sobrino Castello, Severo Ochoa Molecular Biology Center (CSIC-UAM), Spain

***Correspondence:**
Stéphane T. Temmerman
stephane.t.temmerman@gsk.com

†Present address:
Naveen Surendran, Bacterial Vaccines & Technologies, Pfizer Vaccines R&D, Pearl River, NY, United States

‡These authors share first authorship

§These authors share last authorship

Specialty section:
This article was submitted to Vaccines and Molecular Therapeutics, a section of the journal Frontiers in Immunology

Received: 03 July 2020
Accepted: 02 November 2020
Published: 30 November 2020

Citation:
Collignon C, Bol V, Chalon A, Surendran N, Morel S, van den Berg RA, Capone S, Bechtold V and Temmerman ST (2020) Innate Immune Responses to Chimpanzee Adenovirus Vector 155 Vaccination in Mice and Monkeys. Front. Immunol. 11:579872. doi: 10.3389/fimmu.2020.579872

Replication-deficient chimpanzee adenovirus (ChAd) vectors represent an attractive vaccine platform and are thus employed as vaccine candidates against several infectious diseases. Since inducing effective immunity depends on the interplay between innate and adaptive immunity, a deeper understanding of innate immune responses elicited by intramuscularly injected ChAd vectors in tissues can advance the platform's development. Using different candidate vaccines based on the Group C ChAd type 155 (ChAd155) vector, we characterized early immune responses in injected muscles and draining lymph nodes (dLNs) from mice, and complemented these analyses by evaluating cytokine responses and gene expression patterns in peripheral blood from ChAd155-injected macaques. In mice, vector DNA levels gradually decreased post-immunization, but local transgene mRNA expression exhibited two transient peaks [at 6 h and Day (D)5], which were most obvious in dLNs. This dynamic pattern was mirrored by the innate responses in tissues, which developed as early as 1–3 h (cytokines/chemokines) or D1 (immune cells) post-vaccination. They were characterized by a CCL2- and CXCL9/10-dominated chemokine profile, peaking at 6 h (with CXCL10/CCL2 signals also detectable in serum) and D7, and clear immune-cell infiltration peaks at D1/D2 and D6/D7. Experiments with a green fluorescent protein-expressing ChAd155 vector revealed infiltrating hematopoietic cell subsets at the injection site. Cell infiltrates comprised mostly monocytes in muscles, and NK cells, T cells, dendritic cells, monocytes, and B cells in dLNs. Similar bimodal dynamics were observed in whole-blood gene signatures in macaques: most of the 17 enriched immune/innate signaling pathways were significantly upregulated at D1 and D7 and downregulated at D3, and clustering analysis revealed stronger similarities between D1 and D7 signatures versus the D3 signature. Serum cytokine responses (CXCL10, IL1Ra, and low-level IFN-α) in macaques were predominantly observed at D1. Altogether, the early immune responses exhibited bimodal kinetics with transient peaks at D1/D2 and D6/D7, mostly with an IFN-associated signature, and these features were remarkably consistent across most analyzed parameters in murine tissues and macaque blood. These compelling

observations reveal a novel aspect of the dynamics of innate immunity induced by ChAd155-vectored vaccines, and contribute to ongoing research to better understand how adenovectors can promote vaccine-induced immunity.

Keywords: innate immunity, chimpanzee adenovirus, adenovirus vector, vaccine, mice, monkeys

INTRODUCTION

Replication-incompetent adenovirus (Ad) vectors, such as those based on the well-studied human Ad serotype 5 (Ad5), are employed as vaccine delivery vehicles due to their high manufacturing efficiency, versatility, and capacity to accommodate large transgenes (1). They also enable efficient transduction of dividing and non-dividing cells without chromosomal integration (2). Owing to their lower seroprevalence and thus decreased vector neutralization in humans as compared to human Ad5, chimpanzee Ad (ChAd) vectors represent an attractive vaccine platform (3–5). ChAd-vectored candidate vaccines against infectious diseases such as malaria, Ebola, and RSV have shown favorable immunogenicity and tolerability in humans (6–11). These vaccines drive robust intracellular antigen expression, thus promoting a $CD8^+$ T-cell-biased response, but were also shown to induce antigen-specific $CD4^+$ T-cell responses and antibodies. The latter responses can be enhanced by modifying the transgene-coding sequence to favor extracellular protein release. These properties have guided the selection of this platform for several vaccine candidates with a ChAd serotype 155 [ChAd155 (12, 13)] backbone. These vaccines include the pediatric RSV vaccine ChAd155-RSV (7) currently in Phase II development (NCT02927873), as well as the rabies vaccine ChAd155-RG and the therapeutic hepatitis B vaccine ChAd155-hIi-HBV, both in Phase I development (NCT04019444 and NCT03866187, respectively).

The development of persisting transgene-specific immunity requires activation of the innate arm of the immune system, for which the Ad vector's hexon protein may act as an intrinsic adjuvant (14). Upon intramuscular (i.m.) vaccination, the interplay between diverse innate signals——such as pattern-recognition receptor activation, immune-cell recruitment to the injection site, and cytokine production——shapes adaptive responses to the transgene (15). Innate immune recognition of the vector is thus necessary to trigger its self-adjuvanticity, but some murine and *in vitro* studies suggest that certain innate cues can also dampen Ad infection efficiency and antigen expression, either directly by killing infected cells, or indirectly *via* cytokine production (16–18). This balance between immune suppression and stimulation appears to be defined by levels of vector-induced effector cells (NK cells, neutrophils, monocytes/macrophages), and expression of interferon (IFN) signaling–related genes in the draining lymph node (dLN) (15–19). In addition, the innate response quality/magnitude is shaped by the vaccine delivery route, Ad serotype, and host, as well as by the anatomical site of the response (17–20). The latter influence is exemplified by the difference between blood and dLN expression levels of certain cell-associated transcripts seen after subcutaneous administration of Ad vectors in mice (17). Understanding how Ad vectors interact with the innate immune system is thus essential for optimal vaccine development. Several aspects of innate immunity to Ad vectors, administered *via* various delivery routes, have been unraveled in the context of vaccination, gene therapy, or infection (15–17, 21–24). However, for i.m. injection, the preferred route for human vaccines, there is a need for a more comprehensive understanding of the early events occurring not only in the dLN or serum, but also at the first point of entry, the muscle.

Here, we characterize the innate immune response to intramuscularly delivered ChAd155 vectors combined with different antigens [i.e., ChAd155-RSV, ChAd155-RG, or the green-fluorescent-protein (GFP)–expressing vector ChAd155-GFP] in two animal models. We first studied tissue-specific vector DNA levels, transgene expression, cytokines/chemokines expression, and immune-cell infiltration in the injected muscle and dLNs from C57BL/6 mice, and then explored cytokine/chemokine and gene expression in peripheral blood from the translationally more relevant non-human primate (NHP) model. We observed a remarkable concordance between the two models, with a bias toward IFN-associated responses, and, intriguingly, a bimodal dynamic pattern. By characterizing, for the first time, the early immune mechanisms induced by ChAd155-vectored vaccines, this study will contribute to our understanding of the adaptive immunity data that are currently emerging from the clinical trials evaluating these vaccines. Additionally, our data will help explain the immunogenicity profiles of adenoviral vaccines at large, and advance the vaccine platform.

MATERIALS AND METHODS

ChAd155-Vectored Vaccines

The ChAd155-RSV and ChAd155-RG candidate vaccines are based on the replication-defective (E1/E4-deleted) ChAd155 vector (7, 25). Vector construction and production have been described (12, 13, 25), and a GFP-expressing ChAd155 vector (ChAd155-GFP) was developed using similar procedures. In each of the investigated vaccines, the transcription of the transgene is driven by the human cytomegalovirus (hCMV) promoter, and the bovine growth hormone poly-adenylation signal sequence is downstream of the transgene stop codon. ChAd155-RSV encodes a secreted form of hRSV fusion (F) protein deleted of the transmembrane and cytoplasmic regions (F0ΔTM), and a fusion of nucleocapsid (N) and anti-termination (M2-1) proteins (7). ChAd155-RG encodes rabies virus glycoprotein (25).

Animals and Immunizations

The studies in mice and NHP were conducted at the AAALAC-accredited facilities of GSK (Rixensart, Belgium) and Aptuit (Verona, Italy), respectively. Animal husbandry and experiments were ethically reviewed and carried out in accordance with the European Directive 2010/63/EU and the GlaxoSmithKline Biologicals S.A. Policy on the Care, Welfare and Treatment of animals. The study in NHP was conducted in accordance with the Italian legislation, under approval of the facility's Committee on Animal Research and Ethics, and under authorization issued by the Italian Ministry of Health (Italian Ministry of Health Authorization n. 984/2015-PR; Aptuit Internal code no. 50000).

Female 6- to 8-week-old C57BL/6 mice (Harlan Horst) were randomly allocated across the study groups (n = 5/time point/group/experiment). They were immunized by i.m. injection (*gastrocnemius* muscle) with ChAd155-RSV, ChAd155-GFP, or placebo control (each at 10 µl/muscle) at Day (D)0. Injections were administered either unilaterally as one full dose in the left muscle [**Figure 1** (mRNA), **Figure 2**], or bilaterally as two half doses [**Figure 1** (DNA), **Figures 3** and **4**). ChAd155-RSV vector doses per animal were 5.0×10^8 vp in **Figure 1** and 1.0×10^8 vp in **Figures 2** and **3**. To ensure adequate flow cytometric analyses, and based on published data (17), a higher dose of ChAd155-RSV or ChAd155-GFP (i.e., 5.0×10^9 vp) was used in **Figure 4**. The controls were phosphate-buffered saline (PBS) in **Figure 3**, and A195 buffer (26) in all other experiments. In determinations of immune response kinetics (**Figures 2** and **3**), an additional control group of untreated mice was used to characterize baseline (D0) responses. The number of repeats performed for each experiment in mice is indicated in the individual analysis descriptions (see below) and figure legends. Blood samples, injected muscles and iliac dLNs were collected at different time points as indicated in the figures. The animals had free access to water and a maintenance diet. Nesting material was included in the cages, and social housing was applied.

Six 3-year-old cynomolgus macaques (*Macaca fascicularis*) weighing 3.17–4.05 kg were obtained from LCL-Cynologics IBL House; Port Louis, Mauritius. They received 300 µl ChAd155-RG (5×10^{10} vp; within the range of doses intended to be used in humans) administered as a single injection in the deltoid muscle at D0, as described (25). In that study, blood samples for assessment of humoral responses were taken at prevaccination and from weeks 2 to 48 post first vaccination, and virus-neutralizing antibody titers in sera were measured as described (25). Blood samples for whole-blood gene expression and serum cytokine analyses were collected five days before immunization ("Pre"), and at D1, D3, and D7 post-immunization. For ethical reasons, these experiments were performed only once. The animals were housed in communicating steel cages (maintained at 21°C –23°C; RH 45%–65%; lighting between 06:00 and 18:00 h with 30 min dawn-sunset light system), with access to environmental enrichment devices. No clinical signs were noted either before or after immunization (25).

Anti-RSV F Antibody Response in Mice

Anti-RSV F immunoglobulin (Ig)G concentrations in sera from mice immunized with ChAd155-RSV (10^8 vp/animal) at D0 were measured using an ELISA developed in-house with a cutoff of 50 ELISA units (EU)/ml. Blood samples were collected daily

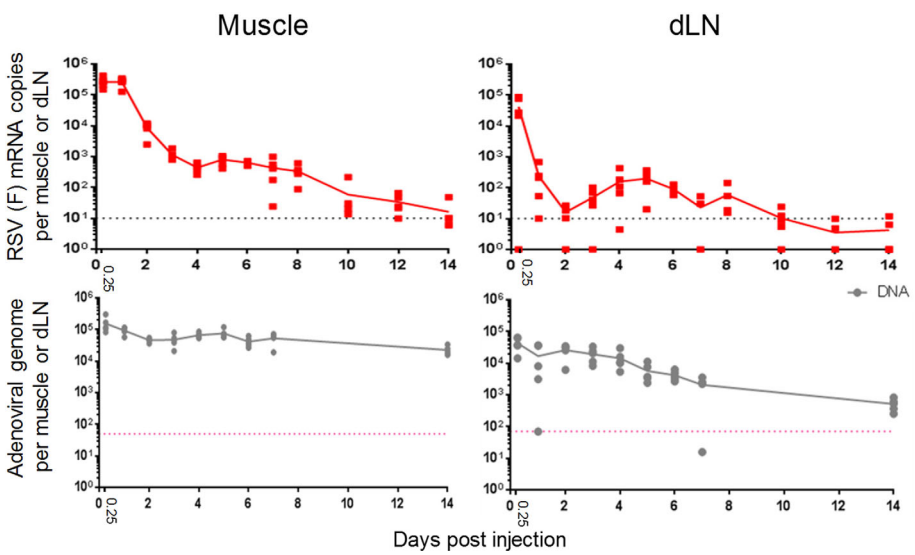

FIGURE 1 | Different kinetics of transgene mRNA expression *versus* viral vector DNA levels in mice. Expression levels of RSV fusion (F) mRNA and ChAd155 viral DNA levels (top and bottom panels, respectively) detected in murine muscles (left) and draining lymph nodes (dLN; right) are shown. Mice (N = 5/time point) were injected intramuscularly with ChAd155-RSV (5×10^8 vp) or buffer (control) at Day 0. Injections were performed either unilaterally as one full dose for mRNA quantification, or bilaterally as two half doses for DNA quantification. Depending on the time point, graphs represent data from two or three (mRNA) or one or two (DNA) independent experiments. Solid lines represent mean expression levels; symbols represent means or single values per animal. Dotted lines represent the lower limits of quantitation.

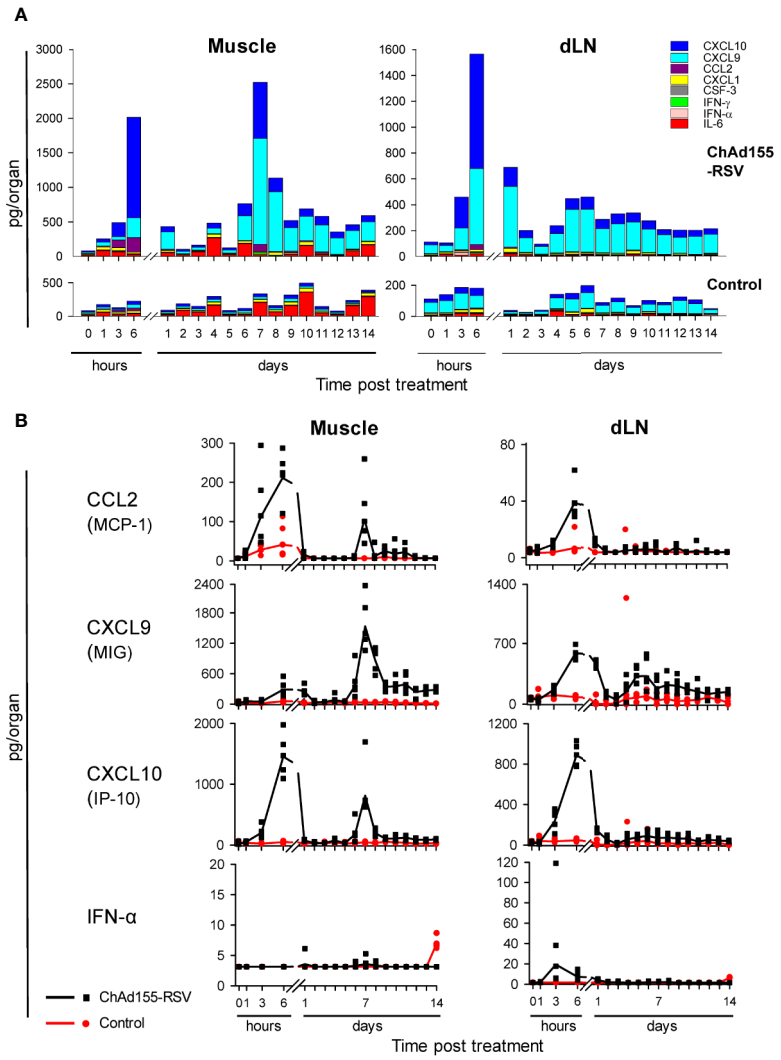

FIGURE 2 | Local cytokine responses in mice are dominated by CXCL10 and CXCL9. Cytokine responses in homogenates of the injected muscles and draining lymph nodes (dLN) collected from mice treated with ChAd155-RSV (10^8 vp) or buffer ("Control") are shown (n = 5/group/time point). Injections (10 µl) were performed unilaterally in the left gastrocnemius muscle at Day 0. Tissues were collected before immunization (0 h), and after immunization at 1, 3, and 6 h, and then daily from 24 h (Day 1) through Day 14. Graphs represent data from a single experiment. Cytokine levels (expressed in pg/organ) were detected in homogenate supernatants of the indicated tissues collected from the injected side of each animal. Geometric mean concentrations are presented as cumulative bars **(A)** or lines **(B)**. Each symbol in **(B)** represents one animal.

up to D14 (n = 5/time point), and then, in a separate experiment, at D14, D21, D34, D56, and D77 (n = 10/time point).

Monitoring of RSV Transgene Expression in Mice

Total RNA was isolated by homogenizing murine muscle and dLN tissues in Tripure (Sigma) used in quantities adapted according to the tissue's volume, and extracted with phenol/chloroform, then treated using the RNeasy Mini kit (Qiagen). The RNeasy column was treated with DNase I (Qiagen). RNA yields were quantified using a NanoDrop 2000c spectrophotometer. The total RNA profile was analyzed using the RNA6000 Nano kit with the 2100 Bioanalyzer for muscle tissue, and the High Sensitivity RNA Screen Tape kit in Tape Station 4200 (Agilent) for dLNs. RSV transcripts were quantified by qPCR using TaqMan Gene Expression Master Mix Plus on a ViiA7 sequence detection system (Applied Biosystems). The primers and probe encoding the F0ΔTM sequence in ChAd155-RSV were: 5′-cgagcccat catcaacttct-3′ forward primer; 5′-caggctctggttgatcttctc-3′ reverse primer; and 5′-6FAM-cgagttcgacgccagcatca-BHQ1-3′ probe. For each sample, 200 ng (muscle) or 50 ng (dLN) RNA were reverse transcribed in 20 µl with SuperScript III (Invitrogen), and volumes of 2 µl (muscle) or 4 µl (dLN) were analyzed. Expression was measured against a dilution curve of ChAd155-RSV (5×10^7–5 copies). Amplifications were performed in duplicate. Taqman Gene Expression assay was used to detect *Tfrc* expression

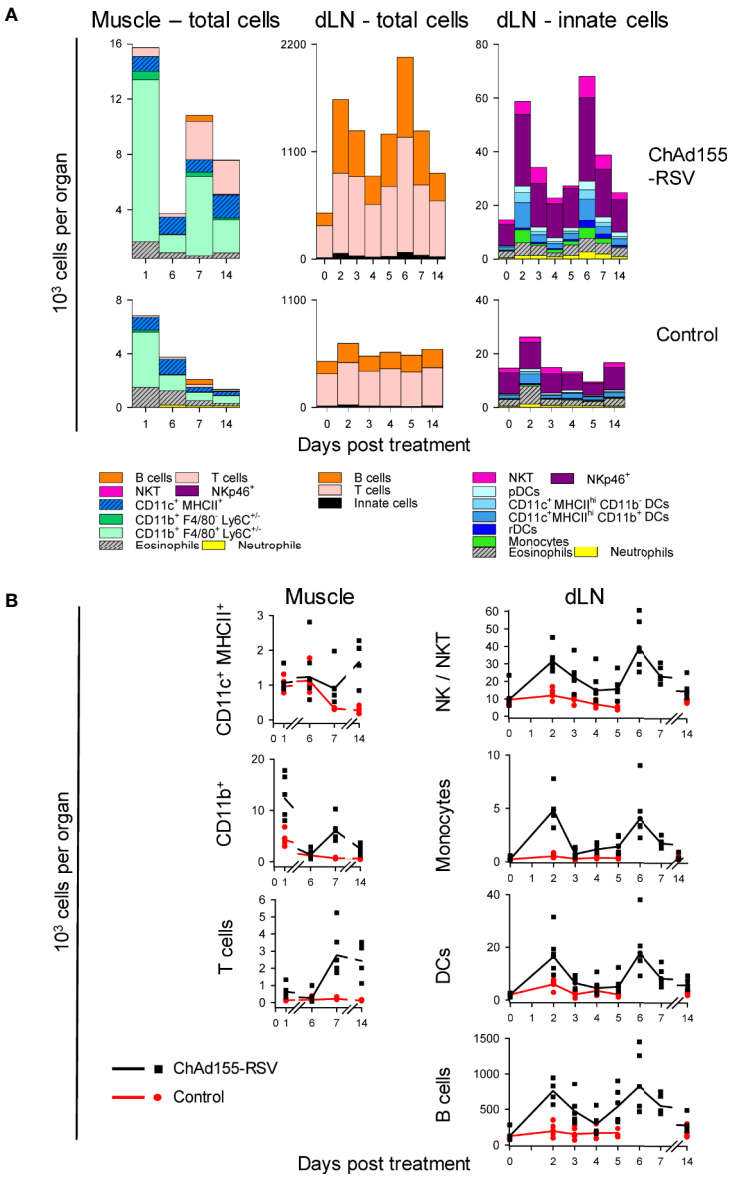

FIGURE 3 | Kinetics of immune cell infiltration in mice. The composition of immune cell infiltrates in muscles and draining lymph nodes (dLNs) collected from mice (n = 5/group/time point) immunized with ChAd155 RSV (10^8 vp) or phosphate-buffered saline ("Control") are shown. Injections were performed bilaterally as two half doses (10 µl each) in both gastrocnemius muscles at Day 0. Injected muscles were collected after immunization (Days 1, 6, 7, and 14); dLNs were collected both before (0 h) and after immunization (Days 2–7 and 14; note the discontinuity in time points on x-axes). All cells recovered from muscles and 10^6 cells of the total recovered dLN cells were stained and analyzed by flow cytometry; values represent both the cell count per tissue and the number of total events detected by FACS (i.e., $CD45^+$ living muscle cells and total living dLN cells). Geometric means of number of cells per tissue are presented as cumulative bars **(A)** or lines **(B)**. Each symbol in **(B)** represents one animal. Graphs represent data from single experiments performed for each tissue.

(Mm00441941_m1; Applied Biosystems). Depending on the time point, experiments were performed in triplicate (6 h, D2, D6) or duplicate (other time points).

Monitoring of Viral DNA in Mice

For adenoviral genome DNA quantification, tissues were lysed (3 h, 56°C) in 40 µl Proteinase K (Qiagen), using 160 µl ATL buffer per whole dLN or per 20-mg muscle tissue, then 200 µl of the homogenized lysates were incubated (10 min, 70°C) with 200 µl AL buffer (all Qiagen). Mice genomic DNA and adenoviral DNA were co-extracted with the QIAamp DNA Mini purification kit (Qiagen) according to the manufacturer's instructions, and quantified using a NanoDrop 2000c spectrophotometer (Thermo Fisher Scientific). DNA quantification by qPCR was performed on 10 µl per sample (corresponding to 10% of the total volume of available DNA) using TaqMan Gene Expression Master Mix on a ViiA7 sequence detection system (Applied Biosystems), against a

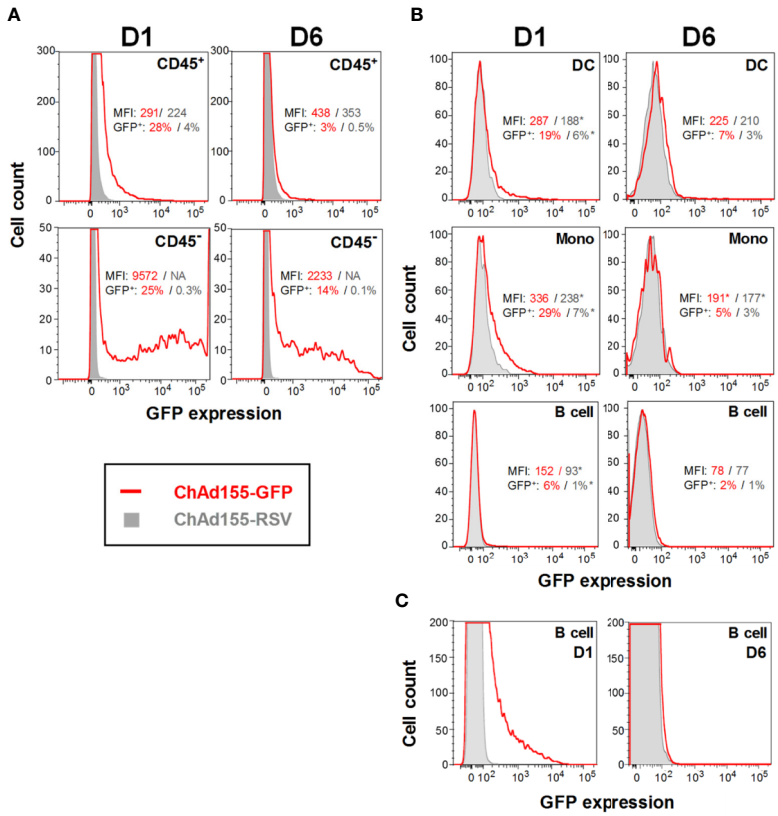

FIGURE 4 | Antigen expression and distribution in local cell populations after vaccination. Histograms representing green fluorescent protein (GFP)-expressing cells detected in either hematopoietic ($CD45^+$) or non-hematopoietic ($CD45^-$) cell subsets in muscle cell suspensions **(A)**, or in immune-cell subsets in draining lymph node (dLN) cell suspensions **(B)** are shown. Given the loss of detail with the scaling of **(B)** which was needed to accommodate the different population sizes, a detail-zoom of the dLN B cells is presented in **(C)**. Mice were immunized with ChAd155-GFP or the control vaccine ChAd155-RSV (both at 5×10^9 vp; typically n = 5/time point). Injections were performed in both gastrocnemius muscles at 2.5×10^9 vp/muscle. Tissues were collected at 1 or 6 days post-immunization (D1, D6). Experiments were performed once (muscle) or in duplicate (dLN). Graphs represent data generated for a single representative animal. Geometric means of the mean fluorescence intensity ("MFI") values and of the frequencies of GFP-expressing ("GFP^+") cells measured in the ChAd155-GFP group (red font) and ChAd155-RSV group (grey font) are indicated in each graph; asterisks denote values that were calculated from only 1 or 2 samples (as MFI was not measured for samples with <50 positive events). DC, dendritic cells; including plasmacytoid DCs, resident DCs and migratory $CD11b^{+/-}$ DCs. Mono, monocytes. B cell, $CD19^+$ cell populations.

ChAd155-RSV dilution curve (10^8–10 copies). Primers and probe (IDT) were directed at the hCMV promoter sequence in ChAd155-RSV [hCMV1 primers left (cagtacatcaatgggcgtggatag) and right (attttggaaagtcccgttgattttg); hCMV1 probe (6FAM-cggggatttccaagtctccacc-BHQ1)]. Taqman Copy Number Reference assay (Applied Biosystems, ThermoFisher Scientific cat. #4458366) was used to detect the housekeeping gene (HKG) transferrin receptor (*Tfrc*). Depending on the time point, experiments were performed in duplicate (6 h, D2, D6) or only once (other time points).

Cytokine Levels in Mice and Monkeys

Cytokine levels were measured in murine and monkey sera, and in murine tissues. Tissue samples dissected from muscles and dLN were individually homogenized, and cytokine levels were measured in tissue-homogenate supernatants as described previously (27, 28). Due to the high number of time points analyzed, the experiments in mice were performed only once. Analyzed cytokines included IFN-γ, IFN-α, IL-6, CXCL1, CSF-3, CCL2, CXCL9, and CXCL10 in mice, and 30 cytokines (IFN-γ, IFN-α, CXCL-10, CXCL11, CXCL9, IL-1β, IL1Ra, IL-7, IL-8, IL-6, IL-18, CCL2, CCL4, CCL3, CXCL12, CCL11, CXCL13, CSF-3, CSF-1, IL-15, IL-10, IL-12p70, sCD40L, IL-4, IL-5, IL-13, IL-17A, IL-2, IL-23, and TNF-α) in monkeys. ELISA kits were used to measure levels of IFN-γ (R&D Systems; in mice), IFN-α (PBL Assay Science; in mice/NHP), or CXCL10 (R&D systems human kit; in NHP). All other cytokines were measured by multiplex assays, using Luminex xMAP (Millipore) for murine samples (including sera, and muscle- and dLN-tissue homogenates), and ProcartaPlex (Invitrogen) for monkey sera. For calculation of geometric mean concentrations (GMCs) or medians, concentrations below the assay's lower limit of quantitation (LLOQ) were assigned a value of either half the manufacturer's LLOQ (for the NHP multiplex assay and IFN-α ELISA), or equal to the manufacturer's limit of detection (LOD; for the NHP CXCL10 ELISA, and the mouse multiplex assay and IFN-α ELISA). In NHP, statistically significant differences between

post- and pre-vaccination levels were calculated using an analysis of variance (ANOVA) model with repeated measures including the time point as fixed effect. The model was fitted on $\log_{10}$-transformed cytokine concentrations. A compound symmetry covariance structure was selected, and homogeneity of variances was assumed. The level of significance was set at $P < 0.05$.

Murine Muscle and dLN Cell Phenotyping Using Flow Cytometry

From each mouse, both injected muscles were homogenized in GentleMACS in a solution of DMEM containing 1% FCS, 100 µg/ml Dnase I (Roche) and 0.1 U/ml Liberase TM (Roche) at 37° C. After 1 h, the enzymatic reaction was stopped by addition of a cold solution of DMEM containing 1% FCS and 10 mM EDTA. After centrifugation and filtration, cells recovered were subjected to a Percoll density gradient. All cells subsequently recovered were transferred into 96 V-bottom wells and washed in FACS buffer (PBS containing 2 mM EDTA and 2% FCS). Both dLNs were treated individually by mechanical dissociation in 2 ml RPMI medium + 2% FCS. After addition of Dnase I and Liberase (at 150 µg/ml and 0.13 U/ml, respectively; Roche), and incubation (30 min; room temperature; under agitation), digestion was stopped by addition of 10 mM EDTA and incubation on ice. The dLN cells were filtered (100 µM nylon cell strainer, BD Biosciences), washed and resuspended in PBS containing 2 mM EDTA and 2% FCS before counting. All cells recovered from the muscle, and 10^6 dLN cells, were treated with CD16/32 (clone 2.4G2; BD Pharmingen) and CD16.2 (clone 9e9; Biolegend) antibodies (10 min, 4°C) to block the Fc receptor, and stained (30 min, 4°C) with the anti-mouse antibodies described below.

For kinetics characterization (**Figure 3**), cells extracted from muscles were stained with anti-CD90.2-FITC, anti-CD45-PE, anti-SiglecF-PECF594, anti-CD43-BV510, anti-Ly6C-BV605, and anti-Ly6G-BV711 from BD Pharmingen; anti-F4/80-APC from Miltenyi Biotec; anti-CD335-PE/Dazzle 594, anti-CD19-BV421, and anti-CD11b-BV785 from Biolegend; anti-CD11c-PE-Cy7 and anti-MHCII-Alexa Fluor 700 from eBiosciences; and Live/Dead Near-IR from Invitrogen. The dLNs were stained with anti-NK1.1-PE, anti-CD43-BV500, anti-Ly6C-BV605, and anti-Ly6G-BV711 from BD Pharmingen; anti-SiglecH-APC, anti-CD19-BV421, and anti-CD11b-BV785 from Biolegend; anti-TCRb-PercpCy5.5, anti-CD11c-PE-Cy7, and anti-MHCII-Alexa Fluor 700 from eBiosciences; and Live/Dead Near-IR from Invitrogen. Due to the high number of time points analyzed, these experiments were performed only once.

In experiments using ChAd155-GFP (**Figure 4**), cells recovered from muscles were stained with anti-CD45-APC and Live/Dead Near-IR from Invitrogen, and dLN cells were stained with the same dLN antibody panel as described above. These experiments were performed once (muscle) or in duplicate (dLN).

Fluorescent events were acquired using an LSR2 flow cytometer (BD Biosciences), and analyzed using FlowJo software v9 (Tree Star); see **Figure S1** for the gating strategies applied for each tissue. For statistical analyses in the experiments with ChAd155-GFP, the following subsets were pooled: neutrophils and eosinophils ("granulocytes"), plasmacytoid DCs, resident DCs and migratory $CD11b^{+/-}$ DCs ("DCs"), and $TCR\beta^+$ $NK1.1^+$ cells and $NK1.1^+$ cells ("total NK cells").

Whole Blood Gene Expression in NHP Using Nanostring

Total RNA was isolated from whole blood from NHP that was collected in PAXgene Blood RNA tubes (PreAnalytiX), using the RNeasy RNA purification kit and the BioRobot MDx system (both Qiagen, Valencia, CA, USA) according to the manufacturer's guidelines. RNA concentrations were measured by ND-1000 spectrophotometer (NanoDrop Technologies). RNA integrity numbers (RINs) were determined using the Agilent 2100 Bioanalyzer and Agilent RNA 6000 Nano kit (Agilent Technologies). RNA with RIN >7 was included in the analysis. Total RNA samples were analyzed using a pre-designed gene expression code-set targeting 730 immune-related NHP genes (nCounter NHP Immunology Panel, NanoString Technologies). Probeset-target RNA hybridization reactions, using 50 ng total RNA/reaction, were performed according to the manufacturer's protocol. Purified probeset-target RNA complexes from each reaction were processed and immobilized on nCounter cartridges using the nCounter Flex Prep Station, and transcripts were quantified on the nCounter Digital Analyzer GEN 2 (all NanoString Technologies). Raw data was analyzed using Nanostring nSolver 4.0 software and the Advanced Analysis Module 2.0 plugin, as described [(29, 30) and **Supplementary Methods**]. For pathway scoring, scores were calculated as the first principal component of the normalized expression (raw counts) of the genes included in a dedicated pathway. For this analysis, at least one co-variate was chosen against which the scores were plotted (i.e., the time points), thus reflecting any factor(s) emerging as the main driver(s) of variability in the gene expression of that particular gene set.

For the gene-set analysis, pathways enriched by the DEGs were determined by the directed significance for a covariate, as determined by the cumulative evidence of DEGs in a pathway, and calculated as the square root of the mean squared t-statistics of the genes. The presence of over- or under-expressed genes in a pathway was determined by the directed global significance, taking the direction of the t-statistics sign into account (31).

Whole Blood Gene Expression in NHP Using qPCR

To validate Nanostring data, expression of 84 immune-related genes was assessed by qPCR. RNA quality and quantity were assessed as described above. Reverse transcription was performed using the RT^2 First Strand Kit (Qiagen; 400 ng RNA/reaction). Transcription levels of 89 immune-related genes and the HKGs GAPDH, LOC709186 and RPL13A were measured by qPCR using the RT^2 Profiler Rhesus Macaque Innate & Adaptive Immune Responses arrays (Qiagen) and a ViiA7 real-time cycler. Each qPCR reaction was qualified and validated in a specific range of threshold cycle (Ct) values. For values higher than the LOQ (Ct = 32), the value was replaced by

"LOQ + 1". Geometric means of the Ct of the three HKG and means of the Ct for each duplicated target gene were calculated, with the following normalization for each target gene: ΔCt = geomean Ct_{HKG} − mean $Ct_{target\ gene}$. The impact of vaccination on the mRNA levels was expressed in ΔΔCt values, representing the relative quantification of the ΔCt values at D1, D3, or D7 over the ΔCt at pre-vaccination (D-5), by calculating ΔΔCt = ΔCt post − ΔCt pre. Fold changes (FCs) were calculated as $2^{\Delta\Delta Ct}$. Genes with FC > |2.0| were considered differentially expressed. Genes with discrepancies between the *Macaca mullata*-specific primes and *Macaca fascularis* sequences were excluded from the analyses.

RESULTS

Transgene Expression and Viral Vector DNA Levels Follow Different Kinetics in Murine Tissues

Immunogenicity of a single i.m. immunization with ChAd155-RSV (10^8 vp/animal) in C57BL/6 mice was confirmed by assessing RSV F-specific antibody responses in sera. Data from two separate experiments revealed detectable responses from D8, in 40% of the animals (**Figure S2**). All animals exhibited a response by D10. Geometric mean concentrations increased up to D12 and then plateaued through D77, with responses persisting in all mice.

We then initiated our main analysis by evaluating the local events following i.m. ChAd155 vaccination. The kinetics of RSV F mRNA expression and viral vector DNA persistence were characterized in tissues from ChAd155-RSV-treated mice, using mock-treated mice as control group. For both parameters, levels in muscles and dLNs were measured at 6 h and D1 post-immunization, then daily or every other day up to D14 (mRNA), or daily up to D7 and at D14 (DNA; **Figure 1**).

In the muscle, RSV F mRNA levels were maintained at levels exceeding 10^5 copies between 6 and 24 h, but then decreased by 1-log by D2, and by 2-log by D4. Levels remained relatively constant through D8, to gradually decrease to near-undetectable levels by D14. By contrast, viral DNA levels were relatively stable, though with an overall 1-log decrease, up to D14.

Unlike the early (≤ 24 h) gene expression in the muscle, mRNA expression in the dLN showed already from 6 h a rapid and pronounced (4-log) decrease, to reach negligible levels at D1-D2. This was followed by a 1-log increase until D5, and gradual contraction to non-quantifiable levels from D10 onward. As in the muscle, DNA levels only gradually decreased (by 2-log) and remained detectable up to at least D14.

The kinetics of DNA levels may be consistent with the ≥7-week persistence of ChAd155 DNA levels in muscles and dLNs of ChAd155-RG injected rats (25), and suggest that the decline in transgene expression seen here in both tissues within the first few days post-immunization was not caused by limiting levels of viral particles, but rather by regulation at the level of mRNA. We next characterized local immune responses to ChAd155 vectors.

Early Cytokine Responses to ChAd155 Are Dominated by IFN-Related Chemokines and Follow Bimodal Kinetics

To elucidate the vector's ability to promote early cytokine production following i.m. vaccination, we compared the cytokine/chemokine responses in injected muscles and dLNs from ChAd155-RSV-immunized mice with those in mock (buffer)-treated mice, up to two weeks after a single injection at D0.

At the muscle injection site, cytokine responses were initiated as early as 1 h post-treatment, and reflected at 6 h a CCL2-, CXCL9-, and CXCL10-dominated peak (**Figures 2A, B**, *left*). After contracting to baseline at D1 or D2, this response was followed by a second peak of these cytokines at D7, this time dominated by CXCL9 and coinciding with a low IFN-γ peak (**Figure S3A**, *left*). This bimodal kinetic pattern could also be discerned, though less obvious, in the dLN (**Figures 2A, B** and **Figure S3A**; *right*). In this tissue, a minor IFN-α signal at 3 h was followed at 6 h by a low IFN-γ response and higher CCL2, CXCL9, and CXCL10 responses, all of which had contracted by D2 or D3. For CXCL9, this first response was followed by a second (lower) increase around D5–D7, which was still detectable at D14. The minor IFN-α response observed in both tissues from control mice at D14 was considered an anomaly. The late time point, and the fact that it was neither detected in vaccinated mice at D14, nor at any of the preceding time points in the control mice, suggest that it was unlikely to be related to the placebo injection.

In serum, the vaccine elicited at 6 h only CCL2 and CXCL10 responses (**Figure S3B**). Neither the tissues nor the serum exhibited substantial vaccine-induced responses of the neutrophil-associated chemokines CXCL1 and CSF-3, or of the pro-inflammatory cytokine IL-6, at any of the time points measured.

Given the roles of the detected chemokines in recruitment of immune cells such as lymphocytes (IFN-inducible chemokines CXCL9 and CXCL10), monocytes (CXCL10 and CCL2), and DCs (CCL2) (32–34), we next investigated immune-cell infiltration in the same tissues.

Immune Cell Infiltration Coincides With Chemokine Responses

To characterize the dynamics of local cell recruitment, we analyzed the composition of immune-cell infiltrates in muscles and dLNs from ChAd155-RSV-treated and mock-treated mice up to D14, using flow cytometry (see **Figure S1** for tissue-specific gating strategies).

In the muscle, recruited cells consisted predominantly of ($CD11b^+$ $F4/80^+$ $Ly6C^{+/-}$) monocytes or monocyte-derived macrophages (**Figure 3A**, *left*). Recruitment of these cells occurred in two separate peaks, at D1 and D7 (cell counts at D1/D6/D7: $12/1/6 \times 10^3$ cells/muscle), coinciding with the two CCL2 peaks in this tissue (see **Figure 2**). This suggested that locally produced CCL2 induced recruitment of mainly patrolling ($CD11b^+$ $F4/80^+$ $Ly6C^-$) monocytes to the muscle injection site. In addition, increased numbers of $CD11c^+$ $MHCII^+$ DCs (D14) and T cells (D7, D14) were detected in ChAd155-injected muscles, while

NK (NKT/NKp46$^+$) cells were not detected in either group at any of the four time points tested.

In the dLN, total cell numbers had tripled from baseline levels at D2, then contracted at D4, and more than doubled again at D6 (D2/D4/D6 cell counts: ~1,600/900/2,100 × 10^3 per dLN; **Figure 3A**, *middle*). Both peaks were characterized by a strong lymphocyte component, as T and B cells constituted 97% of all dLN cells, with the second peak possibly representing the initiation of the adaptive response. Deeper analysis of the dLN innate-cell compartment demonstrated that NK cells constituted approximately half of the recruited innate cells at D2 (**Figure 3A**, *right*), suggesting a link with the CXCL9/10 responses (see **Figure 2**). Slightly lower responses of DCs and monocytes were also observed. Neutrophil recruitment was negligible, consistent with the absence of CXCL1 or CSF-3 responses.

Thus, the two temporally distinct peaks in chemokine production were reflected in the cell recruitment patterns, with a 1-day delay in the dLN possibly reflecting the time-span the chemokine signal required to promote such spatial recruitment. The response was dominated by CD11b$^+$ cells in the muscle and NK, T, B cells and DCs in the dLN. This prompted us to determine the relative contributions of these cells to antigen expression.

ChAd155 Infects Mostly B Cells and Monocytes in the dLN

To complement chemokine-production and cell-migration patterns, we next determined the cellular tropism of a GFP-encoding ChAd155 vector at the response peaks (D1, D6) in tissues, by identifying the cell subsets preferentially targeted by the vector. ChAd155-RSV was used as control, to track potential interference due to cell auto-fluorescence (a common limitation of *in vivo* GFP detection).

Upon CD45 staining of muscle cells, both the non-hematopoietic (CD45$^-$) and hematopoietic (CD45$^+$) subsets expressed GFP (**Figure 4A**), suggesting that muscle-resident non-immune cells, likely myocytes, as well as infiltrating blood cells are targets of ChAd155. Though the gated cells did not represent the full cell population in the muscle due to experimental procedures (see Materials and Methods), mean fluorescence intensity (MFI) was higher in the non-hematopoietic subset [D1 geometric means: 9572 (CD45$^-$) vs. 291 (CD45$^+$)]. Coinciding with the kinetics of the main infiltrating subset in the muscle (CD11b$^+$ F4/80$^+$ Ly6C$^{+/-}$ cells; **Figure 3**), GFP$^+$ CD45$^+$ cell frequencies declined sharply from D1 to D6, while fluorescence signals remained relatively stable [D1/D6 geometric means: 28%/3%; 291/438 (MFI)]. A more moderate decline in GFP$^+$ cell frequencies was seen in CD45$^-$ cells (D1/D6 geometric means: 25%/14%).

In the dLN, cells with potential APC functionalities including DCs and monocytes (**Figure 4B**), as well as B cells (**Figures 4B, C**) also exhibited GFP expression at both time points, aligned with the kinetics of immune cell infiltration (**Figure 3**). In addition, the D6 signals in B cells (**Figures 4B, C**) could be aligned with the initiation of the antibody response detected from D8 in serum (**Figure S2**). For other cell types, levels detected in the ChAd155-GFP group were ambiguous (granulocytes), or relatively low and/or similar to controls (NK and T cells; data not shown). While our analyses did not allow discrimination between signals emanating from transduced cells or from phagocytosed infected cells, the late time points and detected intensities suggested that the former process was responsible for the bulk of these signals.

IFN Pathway Activation and Gene Expression Kinetics in NHP Blood Are Consistent With Chemokine Signatures in Murine Tissues

Previous studies illustrated discrepancies in Ad vector-induced innate cytokine profiles between NHP and mice, potentially related to differences in receptor binding, i.e., to CD46, which is lacking in mice, vs. to coxsackievirus and Ad receptor (CAR) (20). We therefore aimed to bridge the local analyses in mice with systemic (serum) responses in NHP. Cytokine levels and immune-related gene expression were evaluated at pre-vaccination (D-5) and D1, D3, and D7 post-vaccination, in serum from macaques previously injected with ChAd155-RG at D0. The humoral and cell-mediated adaptive immunogenicity of a single dose of this vaccine was previously demonstrated in the same animals, by characterizing the rabies virus-neutralizing antibody responses and rabies-specific IFN-γ–expressing T-cell responses in peripheral blood (25).

Of the panel of 30 immune-related cytokines, growth factors or activation markers, only nine cytokines were detected, and only five were modulated by vaccination (**Figure 5**). As compared to pre-vaccination baseline, we detected slightly increased IFN-α levels at D1, and stronger increases of both CXCL10, at D1 and D7, and of the anti-inflammatory marker IL1Ra, at D1. Statistical analysis by ANOVA revealed that these increases were borderline significant for IFN-α and significant for CXCL10 and IL1Ra (see figure legend for details). We also detected significantly decreased levels of the neutrophil chemoattractant IL-8 at D7, and a statistically non-significant trend toward decreased CCL2 levels at D3 and D7. Thus, while the CXCL10 and IFN responses corresponded with murine data, the absence of CCL2 increases did not, though comparisons may be obfuscated by the fewer time points investigated in the NHP model. Baseline CXCL12, CCL11, CCL4, and IL-7 levels were unchanged after vaccination (data not shown).

We then evaluated the dynamic regulation and signatures of whole-blood transcriptomic responses by differential gene expression analyses (P-value < 0.05), performed with NanoString technology on a 730-gene panel. Consistent with the response kinetics in murine tissues, numbers of differentially expressed genes (DEG) revealed a bimodal kinetic pattern, with higher numbers of upregulated [$\log_2$ fold-change (FC) >1] DEGs at D1 and D7 as compared to D3 (upregulated/total DEGs D1, D3, and D7: 61/318, 3/149, and 36/285, respectively; **Table S1**).

Gene-set enrichment analyses revealed 17 enriched pathways associated with innate and adaptive immunity (see **Table S2** for genes annotated into each pathway). Pathway scores obtained using principal component analysis followed a similar dynamic

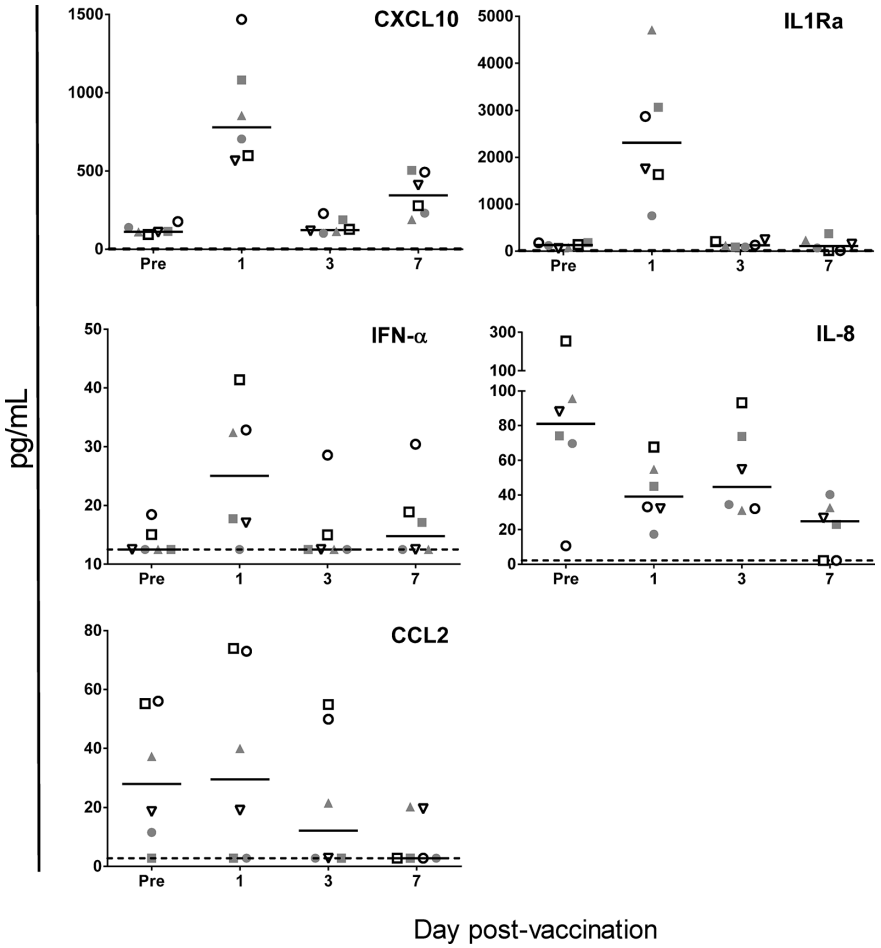

FIGURE 5 | ChAd155-vectored rabies vaccine elicits few serum cytokine responses in macaques. Cytokine levels were measured at pre-vaccination ("Pre", Day-5) and 1, 3, and 7 days post- vaccination in serum collected from six macaques injected intramuscularly with ChAd155-RG rabies vaccine (5×10^{10} vp) at Day 0. Graphs shown [CXCL10, IFN-α (both ELISA), IL1Ra, IL-8, and CCL2 (multiplex assay)] represent the only five analytes found to be modulated by vaccination, out of the panel of 30 immune-related cytokines, growth factors or activation markers tested. Each symbol represents the same animal across the graphs. Solid lines represent medians; dashed lines represent limits of detection applied for statistical calculations. An ANOVA model of the $\log_{10}$-transformed geometric mean concentrations revealed significant changes as compared to prevaccination for CXCL10 at Days 1 and 7, IL-1RA at Day 1 (all $P < 0.001$) and IL-8 at Day 7 ($P < 0.01$), as well as a borderline significant change ($P = 0.05$) for IFN-α at Day 1.

pattern, with scores for most modulated pathways increasing from baseline to D1, then decreasing to levels at or below baseline at D3, followed by a second increase at D7 (**Figure 6A**). Consequently, gene-set and clustering analyses based on $\log_2$ fold-changes over baseline (P-value < 0.05) revealed a greater similarity between the D1 and D7 expression profiles as compared to the D3 profile (**Figure 6B**). The highest enrichment scores were observed for the IFN signaling-related pathway, both at D1 and D7. Interestingly, most genes associated with the NF-kB pathway (regulating apoptosis, inflammatory responses and cell growth) and the adaptive immunity pathway were upregulated at all three time points, indicating these processes were less impacted by the mechanisms underlying the downregulation of the other pathways. Five pathways followed different kinetics as they were not upregulated at either D1 (complement system- or extracellular matrix organization-associated pathways) and/or D7 (pathways associated with MAPK signaling, Fc receptor signaling, cellular stress, or extracellular matrix organization), but they were all downregulated at D3.

Subsequent qPCR validation performed for 84 genes identified 12 genes that were differentially expressed ($\log_2$ FC >1) on at least one time point post-vaccination (**Table S3**). Trends and kinetics of expression levels (typically D1 > D7 > D3) and the bias toward IFN-associated genes (9/12 of DEGs) were consistent with those seen for the broader (Nanostring) gene panel. Overall, the predominance of IFN-associated protein and gene signatures, and the bimodal kinetic pattern of these transcriptomic responses corroborated the patterns seen in murine local tissues.

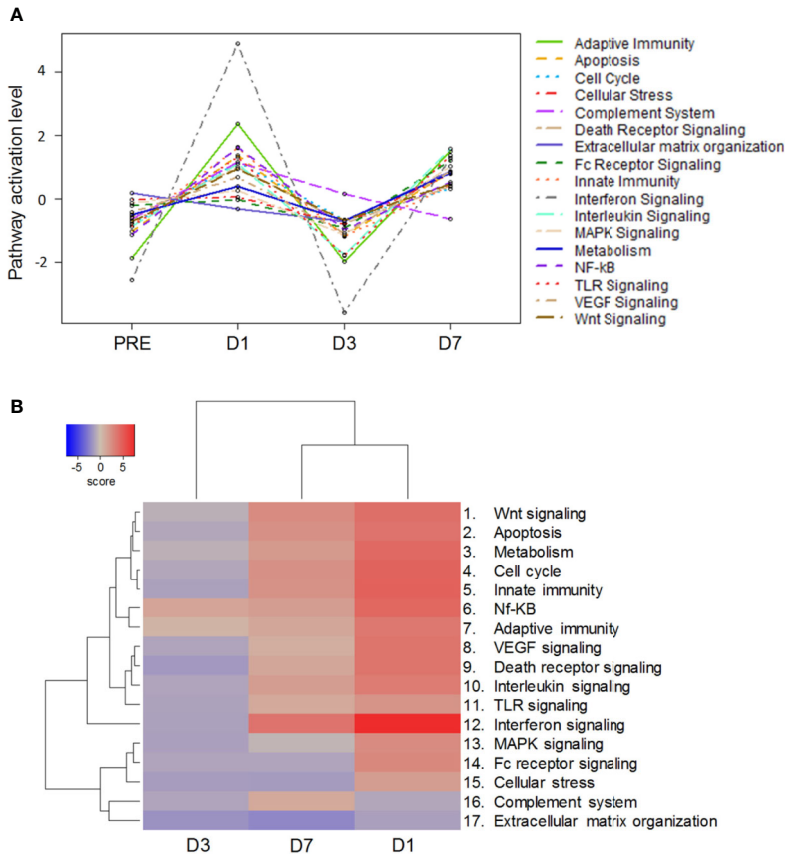

FIGURE 6 | Bimodal kinetic pattern of gene signatures in ChAd155-RG-immunized macaques. Whole blood was collected at pre-vaccination ("PRE") and 1, 3 and 7 days post vaccination (D1, D3, D7) from six macaques injected intramuscularly with ChAd155-RG rabies vaccine (5×10^{10} vp) at Day 0. Modulation of gene expression across timepoints was analyzed through pathway scoring **(A)** and gene set analysis **(B)**, with both methods leading to analysis of pathway modulation at the different timepoints. Significantly enriched immune-related pathways are listed at the right side of each panel (see **Table S2** for gene lists per pathway). **(A)** For pathway scoring, principal component (PC) analysis was performed for each sample using a linear combination (weighted average) of its gene expression values, weighing specific genes to capture the greatest possible variability in the data. The first PC reflects any factor(s) emerging as main driver(s) of variability in gene expression of that particular gene set. **(B)** Gene expression values were expressed as $\log_2$ fold-changes over baseline (P-value < 0.05). Differential expression and pathway enrichment analyses were performed by direct global significance analyses using NanoString nSolver 4.0 with Advanced Analysis 2.0 plugin (730-gene panel).

DISCUSSION

Innate immunity is required to orchestrate the sequence of immunological events resulting in the desired transgene-specific adaptive response (15). A deeper understanding of the kinetics and nature of innate immunity in tissues elicited after i.m. vaccination is thus essential for future improvement of adenoviral vaccine design. We have characterized for the first time the innate mechanisms underlying the adaptive immunogenicity of vaccines based on the clinically relevant ChAd155 vector. Using ChAd155 vectors expressing different antigens, we characterized the early immune responses in injected muscles and dLNs from mice, and compared these data with the protein and gene-expression patterns in blood from macaques. There was a remarkable concordance in innate immune patterns between both animal models, and three key observations were made. First, from 6 or 24 h post-immunization, ChAd155-vectored vaccines induced local tissue-specific innate cell population changes and cytokine production, which, along with local transgene expression and blood transcriptomic responses, mostly followed a bimodal temporal profile. Second, innate immune activation was in both animal models dominated by IFN-associated signatures. Last, the vector induced only low-level responses of either inflammatory cytokines in blood (both models) or tissues (mice), or inflammatory cell-infiltrates in tissues in mice.

Based on our dataset (see overview in **Figure 7A**), we propose the following hypothetical mechanism. In the injected muscle, the vaccine vector infected hematopoietic cells [generally present in very low quantities before injection (35–37)] and muscle cells, and both subsets probably contributed to transgene mRNA expression at 6 h. This led to production of danger signals, stimulating muscle-resident innate sentinels to engulf the vector and secrete cytokines (e.g., CXCL10, and CCL2) within a few hours. In turn, this promoted monocyte/macrophage chemotaxis to the muscle (D1)——likely aligned with the concurrent

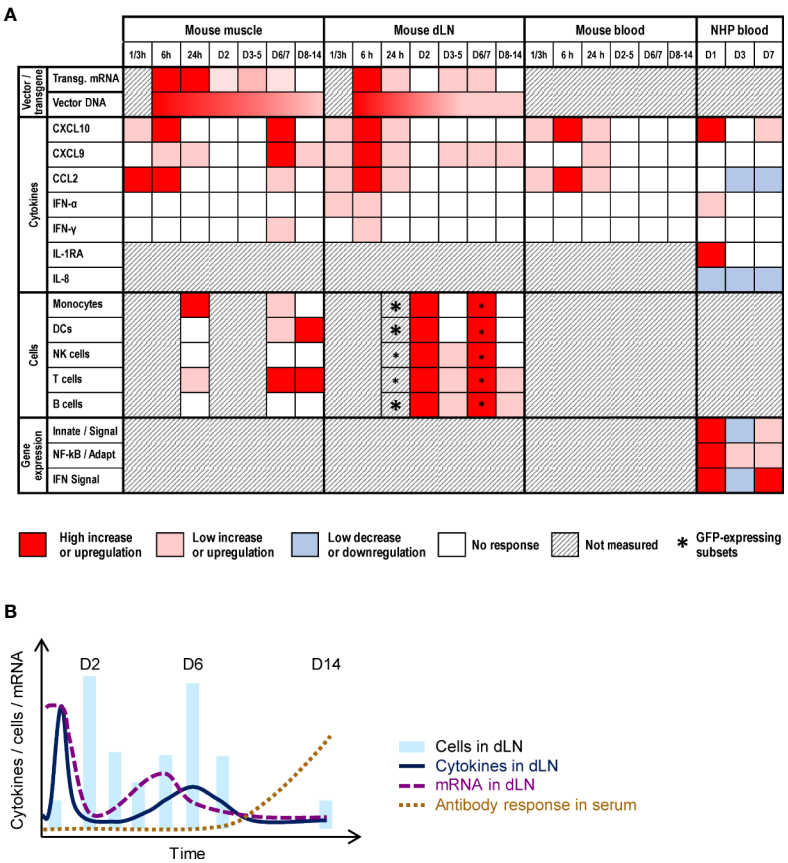

FIGURE 7 | Conceptual data integration. **(A)** Conceptual heat map representing the response levels in the injected muscle or draining lymph node (dLN) from mice, or in peripheral blood from mice or non-human primates (NHP) after intramuscular immunization with ChAd155-vectored vaccines. Blood responses were measured in serum (cytokines, in both animal models) or whole blood (gene expression). Colors represent the qualitative response intensity as compared to pre-vaccination levels, as indicated in the color key below the figure. Asterisk sizes correspond to relative response levels. Indicated gene expression refers to the following pathways in **Figure 6B**: "Innate/signal", innate immunity signaling pathways (nos. 1–5 and 8–11); "NF-KB/Adapt", NF-kB and adaptive immunity pathways (nos. 6 and 7); and "IFN signal", interferon signaling pathway (no. 12). **(B)** Diagram representing hypothetical model of transgene mRNA expression and immune response in the dLN elicited after immunization. Transgene mRNA expression peaks shortly after injection, but is rapidly dampened, likely by the first wave of cytokine/chemokine release and subsequent cell mobilization (D2). Upon contraction of this first innate response wave around D4–D5, a residual reservoir of ChAd155-infected cells instigates a reactivation of viral gene expression, and consequently also of innate immune responses (D6–D7). These responses are then followed by adaptive immunity, including the antigen-specific antibody response which was detectable in the serum from D8.

upregulation of innate/IFN transcriptomic pathways in (NHP) blood——resulting in further local cytokine secretion, removal of free antigen and cellular debris, and reduction of infected cells. Collectively this could instigate IFN-mediated downregulation of transgene transcription (D2–D4).

In the dLN, the transgene mRNA levels detected at 6 h suggested that antigen may have localized to this tissue in different capacities, such as in free-flowing viral particles or as cargo within phagocytotic cells. The kinetics of the immune response (i.e., cellular migration, cytokine responses) and viral mRNA expression suggest a temporal interplay between host and vector (**Figure 7B**). Indeed, apart from the effects as a result of the drainage described above, secretion of CXCL9/10, and, to a lesser extent, CCL2, IFN-γ, and IFN-α, may also be responsible for the D1/D2 cell influx (supposedly followed by antigen uptake in subcapsular sinuses). This concurred with a sharp decline in mRNA levels from 6 h to D2, which was likely due to regulation at the mRNA level considering the coinciding persistent DNA levels. Indeed, since the hCMV promoter used in ChAd155 vectors to drive transgene transcription (12, 13), is reportedly inhibited by IFN-γ (38), this steep drop in mRNA levels may be linked to the early cytokine signals. Additionally, as DC and monocyte levels subsequently decreased more quickly from the dLN relative to NK-cell levels, the reduced transcription may also be mediated *via* NK-cell action, possibly activated by IFN-α (16). These patterns in murine tissues were consistent with the downregulation of innate pathways in monkey blood at D3. Of note, considering that in ChAd-vectored vaccines, the noninfectious particles vastly outnumber infectious particles (39), lack of mRNA production following the uptake of noninfectious particles by APCs will have skewed the mRNA/DNA balance strongly to the side of DNA (**Figure 1**).

Remarkably, a second, lower-level immune activation in tissues was seen at D6/D7. This was possibly linked to residual expression of (likely biologically active) mRNA remaining in myocytes around D2/D3. This mRNA could subsequently have accumulated in the absence of concurrent robust innate and cytokine responses. The transient D6/D7 innate immune activation could be in keeping with a possible reversion of the putative IFN-γ–mediated inhibition of expression (38) after the first innate response peak had receded. The response in tissues was aligned with the second upregulation of innate/IFN-related pathways at D7 in (NHP) blood, and we hypothesize that this secondary response contained higher frequencies of antigen-specific T cells as compared to the D1 activation. Though T-cell CXCR3 expression was not analyzed, this sequence of immune events would fit a previously described model of CXCR3-dependent immunosurveillance and elimination of infected cells by CD8 T cells (40, 41). In this model, immune cells, such as monocytes or DCs, upregulate production of CXCL9 and CXCL10 upon encountering the vector, with particularly for the latter chemokine a possible contribution from infected non-immune cells such as muscle cells (42, 43). These chemokine signals activate the CXCR3 receptor present on effector and memory CD8 T cells, instigating CD8 T cell priming and differentiation, and tissue infiltration of these cells due to chemotaxis along the CXCL9/CXCL10 gradient. The subsequent antigen recognition, due to their interaction with either infected immune or muscle cells, or with cells which phagocytosed an infected cell or viral particle, triggers these T cells to produce IFN-γ. Of note, IFN-γ–expressing T cell responses to ChAd155-RG were previously detected in spleens from immunized mice, and in peripheral blood from the immunized macaques described here (25). Possibly aligned, the NF-kB-associated pathway, linking to both innate and adaptive regulation, and the adaptive immunity-related pathway both appeared to be more upregulated in blood at D7 vs. D3.

Interestingly, similar kinetics, with a second cytokine peak at D7, was seen in serum from NHP injected with a comparable dose of the (Group D) Ad48 vector, but not with Ad5, Ad26, or Ad35 vectors (20), suggesting that this pattern may be vector serotype-specific. Since Ad48, Ad26 and Ad35 utilize the CD46 receptor, while Ad5 and ChAd155 [which has high genome similarity with Ad5 (12)] supposedly use mainly CAR, these data suggest that the involved immune determinants are not limited to receptor usage. For Ad48, it has been proposed that this bimodal pattern was specific to its hexon hypervariable region, and that in addition to fiber-receptor interactions, other Ad capsid components could also induce innate immune responses (20). This hypothesis may warrant further investigation for ChAd155.

In both models, the vector elicited only low IFN-α and IFN-γ responses relative to baseline/control, as seen for Ad5 in monkeys (20), but also clear IFN-associated response patterns, comprising increased CXCL9/10 levels and IFN-related gene expression in blood and/or tissues. For another (subcutaneously delivered) C-serotype ChAd vector, IFN/STING signaling-related gene expression had a negative impact on the $CD8^+$ T-cell kinetics, which was mediated, amongst others, by suppressed antigen translation in DCs (17). We detected local transgene expression in both tissues, with DNA levels in muscle up to D14 possibly representing a reservoir that is necessary to mount adaptive immunity. In addition, in both animal models, the presented (**Figure S2**) or published (25) antibody or T-cell data suggest that at least for this vector, IFN-associated responses and robust antigen-specific adaptive immunity can co-exist. It should be noted however that the conclusion of an IFN/STING-mediated impact on adaptive immunity drawn in the former study (17), was mainly based on gene expression in murine blood and dLNs, without supporting characterization of local cytokines and immune cell infiltration. Comparison of our data with that study is also obfuscated by differences in the delivery method, which is known to affect vaccine responses (19), and in the number of analysis time points. Finally, the same study, as well as a study using intramuscularly injected vectors, also revealed vector group-dependent differences in IFN expression and transgene expression (17, 44), with a tendency toward higher levels of transgene expression for Group E vectors as compared to Group C vectors. Altogether, further mechanistic research is needed to investigate the interplay between innate and adaptive immunity for ChAd155-vectors and vectors from other groups, which could be guided by the current observations.

Finally, we note that i.m.-delivered ChAd155 vectors did not appear to elicit substantial inflammatory responses. This considering our data obtained for murine tissues—low-level neutrophil or eosinophil infiltration, negligible CXCL1, CSF-3, or IL-6 responses relative to controls——and for NHP blood, i.e., decreased IL-8 and increased IL1Ra levels relative to baseline. This may be of interest since blood cytokine profiles can be Ad serotype-specific, given the pro-inflammatory cytokine (IL-6, IL-1β, TNF-α) responses seen in NHP with (Group B/D) Ad35 or Ad48 vectors, but not with an Ad5 vector (20). Still, whether our data can be linked to either the absence of clinical symptoms in ChAd155-RG-injected NHP (25) or the low-grade reactogenicity of ChAd155-RSV in humans (7), remains to be elucidated.

We conclude that the observed response dynamics was consistent across most of the read-outs and seen in both animal models. Further investigation using the i.m. route, e.g., by confocal analysis of both the injected muscle and the dLN after ChAd-GFP injection, is still warranted. This may help to (i) link these early responses to the adaptive immunity induced by these ChAd-vectored vaccines, (ii) extend the current blood transcriptomic data to local gene expression in NHP, and (iii) determine to what extent our data can be translated to other serotypes, vector doses and host immune systems, which may be particularly relevant for recently developed adeno-vectored candidate vaccines against COVID-19 (45, 46). Another critical aspect with respect to the latter and other Ad-based vaccines is the boostability of the response. Indeed, in macaques, adaptive responses to the first dose of ChAd155-RG appeared to be boostable by a second dose administered 48 weeks later (25). Boostability was also observed for SARS-CoV-2 vaccines based on ChAdOx1, in mice and pigs (47) as well as in a Phase1/2 trial in humans (48). However, it was inconsistently observed across read-outs in human ChAd155-RSV vaccinees, possibly due to the presence of baseline anti-vector responses in some subjects (7). Collectively these studies

demonstrate that multiple determinants are at play, such as vector identity and dose, the time interval between doses, and the immune status of the host.

Nonetheless, we show for the first time that the local innate immunity to i.m. injected ChAd155 vector mostly followed a distinctly bimodal kinetic pattern with tissue-specific response characteristics, and a propensity toward IFN pathway-associated responses. These findings represent promising avenues for future research, which may facilitate design of novel ChAd-based vaccines, and could ultimately advance the adenoviral vaccine platform at large.

DATA AVAILABILITY STATEMENT

NanoString gene expression data has been made available through Supplementary data in manuscript. Additional data can be made available upon request to corresponding author.

ETHICS STATEMENT

The animal study was reviewed and approved by AAALAC-accredited facilities of GSK (Rixensart, Belgium) and Aptuit (Verona, Italy). Animal husbandry and experiments were ethically reviewed and carried out in accordance with the European Directive 2010/63/EU and the GlaxoSmithKline Biologicals S.A. Policy on the Care, Welfare and Treatment of animals. The study in NHP was conducted in accordance with the Italian legislation, under approval of the facility's Committee on Animal Research and Ethics, and under authorization issued by the Italian Ministry of Health (Italian Ministry of Health Authorization n. 984/2015-PR; Aptuit Internal code no. 50000).

AUTHOR CONTRIBUTIONS

CC and AC were involved in the conception and design of the studies and/or the development of study protocols. CC, AC, and VBo participated to the acquisition of data. CC, AC, and VBo analyzed and interpreted the results. All authors contributed to the article and approved the submitted version.

FUNDING

This work was sponsored by GlaxoSmithKline Biologicals SA, which was involved in all stages of the study conduct and analysis and took responsibility for all costs incurred in publishing.

ACKNOWLEDGMENTS

The authors would like to acknowledge Isabelle Carletti and Caroline Ego (both GSK) for their contribution to the statistical analysis of the data, and Cédric Vanderhaegen, Jennifer Dalcq, Benoît Bozzetti, Laurie Dumont, Ouafaâ Tahmaoui and Christel Verachtert (all GSK) for technical assistance. They also thank Ellen Oe and Robert Lin (both GSK) for scientific writing services in the manuscript's development, and publication management, respectively.

SUPPLEMENTARY MATERIAL

The Supplementary Material for this article can be found online at: https://www.frontiersin.org/articles/10.3389/fimmu.2020.579872/full#supplementary-material

REFERENCES

1. Ertl HC. Viral Vectors as Vaccine Carriers. *Curr Opin Virol* (2016) 21:1–8. doi: 10.1016/J.Coviro.2016.06.001
2. Feuerbach FJ, Crystal RG. Progress in Human Gene Therapy. *Kidney Int* (1996) 49(6):1791–4. doi: 10.1038/Ki.1996.269
3. Guo J, Mondal M, Zhou D. Development of Novel Vaccine Vectors: Chimpanzee Adenoviral Vectors. *Hum Vaccin Immunother* (2018) 14 (7):1679–85. doi: 10.1080/21645515.2017.1419108
4. Capone S, D'Alise AM, Ammendola V, Colloca S, Cortese R, Nicosia A, et al. Development of Chimpanzee Adenoviruses as Vaccine Vectors: Challenges and Successes Emerging From Clinical Trials. *Expert Rev Vaccines* (2013) 12 (4):379–93. doi: 10.1586/Erv.13.15
5. Vitelli A, Folgori A, Scarselli E, Colloca S, Capone S, Nicosia A. Chimpanzee Adenoviral Vectors as Vaccines - Challenges to Move the Technology Into the Fast Lane. *Expert Rev Vaccines* (2017) 16(12):1241–52. doi: 10.1080/14760584.2017.1394842
6. Colloca S, Barnes E, Folgori A, Ammendola V, Capone S, Cirillo A, et al. Vaccine Vectors Derived From a Large Collection of Simian Adenoviruses Induce Potent Cellular Immunity Across Multiple Species. *Sci Transl Med* (2012) 4(115):115ra2. doi: 10.1126/Scitranslmed.3002925
7. Cicconi P, Jones C, Sarkar E, Silva-Reyes L, Klenerman P, De Lara C, et al. First-in-Human Randomized Study to Assess the Safety and Immunogenicity of an Investigational Respiratory Syncytial Virus (RSV) Vaccine Based on Chimpanzee-Adenovirus-155 Viral Vector-Expressing RSV Fusion, Nucleocapsid, and Antitermination Viral Proteins in Healthy Adults. *Clin Infect Dis* (2020) 70(10):2073–81. doi: 10.1093/Cid/Ciz653
8. Green CA, Sande CJ, Scarselli E, Capone S, Vitelli A, Nicosia A, et al. Novel Genetically-Modified Chimpanzee Adenovirus and MVA-Vectored Respiratory Syncytial Virus Vaccine Safely Boosts Humoral and Cellular Immunity in Healthy Older Adults. *J Infect* (2019) 78(5):382–92. doi: 10.1016/J.Jinf.2019.02.003
9. Swadling L, Capone S, Antrobus RD, Brown A, Richardson R, Newell EW, et al. A Human Vaccine Strategy Based on Chimpanzee Adenoviral and MVA Vectors That Primes, Boosts, and Sustains Functional HCV-Specific T Cell Memory. *Sci Transl Med* (2014) 6(261):261ra153. doi: 10.1126/Scitranslmed.3009185
10. Tapia MD, Sow SO, Ndiaye BP, Mbaye KD, Thiongane A, Ndour CT, et al. Safety, Reactogenicity, and Immunogenicity of a Chimpanzee Adenovirus Vectored Ebola Vaccine in Adults in Africa: a Randomised, Observer-Blind, Placebo-Controlled, Phase 2 Trial. *Lancet Infect Dis* (2020) 20(6):707–18. doi: 10.1016/S1473-3099(20)30016-5
11. Tapia MD, Sow SO, Mbaye KD, Thiongane A, Ndiaye BP, Ndour CT, et al. Safety, Reactogenicity, and Immunogenicity of a Chimpanzee Adenovirus Vectored Ebola Vaccine in Children in Africa: a Randomised, Observer-Blind, Placebo-Controlled, Phase 2 Trial. *Lancet Infect Dis* (2020) 20(6):719–30. doi: 10.1016/S1473-3099(20)30019-0
12. Colloca S. *Inventor. Novel Adenovirus. International Patent Publication Number WO2017017049A1*. (2017).
13. Glaxosmithkline Biologicals. *Chad155-RSV Part 1 (Council Decision 2002/813/EC) Summary Notification Information Format for the Release of Genetically Modified Organisms Other Than Higher Plants in Accordance*

With Article 11 of Directive 2001/18/EC. Eudract Number: 2018-000431-27 (2018). (Accessed 07-06-2020).
14. Molinier-Frenkel V, Lengagne R, Gaden F, Hong SS, Choppin J, Gahery-Ségard H, et al. Adenovirus Hexon Protein Is a Potent Adjuvant for Activation of a Cellular Immune Response. *J Virol* (2002) 76(1):127–35. doi: 10.1128/Jvi.76.1.127-135.2002
15. Rhee EG, Blattman JN, Kasturi SP, Kelley RP, Kaufman DR, Lynch DM, et al. Multiple Innate Immune Pathways Contribute to the Immunogenicity of Recombinant Adenovirus Vaccine Vectors. *J Virol* (2011) 85(1):315–23. doi: 10.1128/JVI.01597-10
16. Johnson MJ, Björkström NK, Petrovas C, Liang F, Gall JG, Loré K, et al. Type I Interferon-Dependent Activation of NK Cells by Rad28 or Rad35, But Not Rad5, Leads to Loss of Vector-Insert Expression. *Vaccine* (2014) 32(6):717–24. doi: 10.1016/J.Vaccine.2013.11.055
17. Quinn KM, Zak DE, Costa A, Yamamoto A, Kastenmuller K, Hill BJ, et al. Antigen Expression Determines Adenoviral Vaccine Potency Independent of IFN and STING Signaling. *J Clin Invest* (2015) 125(3):1129–46. doi: 10.1172/JCI78280
18. Hensley SE, Cun AS, Giles-Davis W, Li Y, Xiang Z, Lasaro MO, et al. Type I Interferon Inhibits Antibody Responses Induced by a Chimpanzee Adenovirus Vector. *Mol Ther* (2007) 15(2):393–403. doi: 10.1038/Sj.Mt.6300024
19. Roy S, Jaeson MI, Li Z, Mahboob S, Jackson RJ, Grubor-Bauk B, et al. Viral Vector and Route of Administration Determine the ILC and DC Profiles Responsible for Downstream Vaccine-Specific Immune Outcomes. *Vaccine* (2019) 37(10):1266–76. doi: 10.1016/J.Vaccine.2019.01.045
20. Teigler JE, Iampietro MJ, Barouch DH. Vaccination With Adenovirus Serotypes 35, 26, and 48 Elicits Higher Levels of Innate Cytokine Responses Than Adenovirus Serotype 5 in Rhesus Monkeys. *J Virol* (2012) 86(18):9590–8. doi: 10.1128/JVI.00740-12
21. Hendrickx R, Stichling N, Koelen J, Kuryk L, Lipiec A, Greber UF. Innate Immunity to Adenovirus. *Hum Gene Ther* (2014) 25(4):265–84. doi: 10.1089/Hum.2014.001
22. Chen RF, Lee CY. Adenoviruses Types, Cell Receptors and Local Innate Cytokines in Adenovirus Infection. *Int Rev Immunol* (2014) 33(1):45–53. doi: 10.3109/08830185.2013.823420
23. Lindsay RW, Darrah PA, Quinn KM, Wille-Reece U, Mattei LM, Iwasaki A, et al. $CD8^+$ T Cell Responses Following Replication-Defective Adenovirus Serotype 5 Immunization Are Dependent on $CD11c^+$ Dendritic Cells But Show Redundancy in Their Requirement of TLR and Nucleotide-Binding Oligomerization Domain-Like Receptor Signaling. *J Immunol* (2010) 185(3):1513–21. doi: 10.4049/Jimmunol.1000338
24. Quinn KM, Da Costa A, Yamamoto A, Berry D, Lindsay RW, Darrah PA, et al. Comparative Analysis of the Magnitude, Quality, Phenotype, and Protective Capacity of Simian Immunodeficiency Virus Gag-Specific $CD8^+$ T Cells Following Human-, Simian-, and Chimpanzee-Derived Recombinant Adenoviral Vector Immunization. *J Immunol* (2013) 190(6):2720–35. doi: 10.4049/Jimmunol.1202861
25. Napolitano F, Merone R, Abbate A, Ammendola V, Horncastle E, Lanzaro F, et al. A Next Generation Vaccine Against Human Rabies Based on a Single Dose of a Chimpanzee Adenovirus Vector Serotype C. *PLoS Negl Trop Dis* (2020) 14(7):E0008459. doi: 10.1371/Journal.Pntd.0008459
26. Evans RK, Nawrocki DK, Isopi LA, Williams DM, Casimiro DR, Chin S, et al. Development of Stable Liquid Formulations for Adenovirus-Based Vaccines. *J Pharm Sci* (2004) 93(10):2458–75. doi: 10.1002/Jps.20157
27. Didierlaurent AM, Morel S, Lockman L, Giannini SL, Bisteau M, Carlsen H, et al. AS04, an Aluminum Salt- and TLR4 Agonist-Based Adjuvant System, Induces a Transient Localized Innate Immune Response Leading to Enhanced Adaptive Immunity. *J Immunol* (2009) 183(10):6186–97. doi: 10.4049/Jimmunol.0901474
28. Didierlaurent AM, Collignon C, Bourguignon P, Wouters S, Fierens K, Fochesato M, et al. Enhancement of Adaptive Immunity by the Human Vaccine Adjuvant AS01 Depends on Activated Dendritic Cells. *J Immunol* (2014) 193(4):1920–30. doi: 10.4049/Jimmunol.1400948
29. Vandesompele J, De Preter K, Pattyn F, Poppe B, Van Roy N, De Paepe A, et al. Accurate Normalization of Real-Time Quantitative RT-PCR Data by Geometric Averaging of Multiple Internal Control Genes. *Genome Biol* (2002) 3(7):RESEARCH0034. doi: 10.1186/Gb-2002-3-7-Research0034
30. Wang H, Horbinski C, Wu H, Liu Y, Sheng S, Liu J, et al. Nanostringdiff: a Novel Statistical Method for Differential Expression Analysis Based on Nanostring Ncounter Data. *Nucleic Acids Res* (2016) 44(20):E151. doi: 10.1093/Nar/Gkw677
31. Tomfohr J, Lu J, Kepler TB. Pathway Level Analysis of Gene Expression Using Singular Value Decomposition. *BMC Bioinf* (2005) 6:225. doi: 10.1186/1471-2105-6-225
32. Welsh RM, Bahl K, Marshall HD, Urban SL. Type 1 Interferons and Antiviral CD8 T-Cell Responses. *PLoS Pathog* (2012) 8(1):E1002352. doi: 10.1371/Journal.Ppat.1002352
33. Groom JR. Regulators of T-Cell Fate: Integration of Cell Migration, Differentiation and Function. *Immunol Rev* (2019) 289(1):101–14. doi: 10.1111/Imr.12742
34. Hauser AE, Debes GF, Arce S, Cassese G, Hamann A, Radbruch A, et al. Chemotactic Responsiveness Toward Ligands for CXCR3 and CXCR4 Is Regulated on Plasma Blasts During the Time Course of a Memory Immune Response. *J Immunol* (2002) 169(3):1277–82. doi: 10.4049/jimmunol.169.3.1277
35. Langlet C, Tamoutounour S, Henri S, Luche H, Ardouin L, Gregoire C, et al. CD64 Expression Distinguishes Monocyte-Derived and Conventional Dendritic Cells and Reveals Their Distinct Role During Intramuscular Immunization. *J Immunol* (2012) 188(4):1751–60. doi: 10.4049/Jimmunol.1102744
36. Calabro S, Tortoli M, Baudner BC, Pacitto A, Cortese M, O'Hagan DT, et al. Vaccine Adjuvants Alum and MF59 Induce Rapid Recruitment of Neutrophils and Monocytes That Participate in Antigen Transport to Draining Lymph Nodes. *Vaccine* (2011) 29(9):1812–23. doi: 10.1016/J.Vaccine.2010.12.090
37. Liang F, Ploquin A, Hernández JD, Fausther-Bovendo H, Lindgren G, Stanley D, et al. Dissociation of Skeletal Muscle for Flow Cytometric Characterization of Immune Cells in Macaques. *J Immunol Methods* (2015) 425:69–78. doi: 10.1016/J.Jim.2015.06.011
38. Sung RS, Qin L, Bromberg JS. Tnfa and Ifng Induced by Innate Anti-Adenoviral Immune Responses Inhibit Adenovirus-Mediated Transgene Expression. *Mol Ther* (2001) 3(5 Pt 1):757–67. doi: 10.1006/Mthe.2001.0318
39. Tatsis N, Tesema L, Robinson ER, Giles-Davis W, Mccoy K, Gao GP, et al. Chimpanzee-Origin Adenovirus Vectors as Vaccine Carriers. *Gene Ther* (2006) 13(5):421–9. doi: 10.1038/Sj.Gt.3302675
40. Beura LK, Masopust D. Infected Cells Call Their Killers to the Scene of the Crime. *Immunity* (2015) 42(3):399–401. doi: 10.1016/J.Immuni.2015.03.001
41. Hickman HD, Reynoso GV, Ngudiankama BF, Cush SS, Gibbs J, Bennink JR, et al. CXCR3 Chemokine Receptor Enables Local $CD8^+$ T Cell Migration for the Destruction of Virus-Infected Cells. *Immunity* (2015) 42(3):524–37. doi: 10.1016/J.Immuni.2015.02.009
42. Afzali AM, Muntefering T, Wiendl H, Meuth SG, Ruck T. Skeletal Muscle Cells Actively Shape (Auto)Immune Responses. *Autoimmun Rev* (2018) 17(5):518–29. doi: 10.1016/J.Autrev.2017.12.005
43. Crescioli C, Sottili M, Bonini P, Cosmi L, Chiarugi P, Romagnani P, et al. Inflammatory Response in Human Skeletal Muscle Cells: CXCL10 as a Potential Therapeutic Target. *Eur J Cell Biol* (2012) 91(2):139–49. doi: 10.1016/J.Ejcb.2011.09.011
44. Dicks MD, Spencer AJ, Coughlan L, Bauza K, Gilbert SC, Hill AV, et al. Differential Immunogenicity Between Hadv-5 and Chimpanzee Adenovirus Vector Chadox1 Is Independent of Fiber and Penton RGD Loop Sequences in Mice. *Sci Rep* (2015) 21:16756. doi: 10.1038/Srep16756
45. Zhu FC, Li YH, Guan XH, Hou LH, Wang WJ, Li JX, et al. Safety, Tolerability, and Immunogenicity of a Recombinant Adenovirus Type-5 Vectored COVID-19 Vaccine: a Dose-Escalation, Open-Label, Non-Randomised, First-in-Human Trial. *Lancet* (2020) 395(10240):1845–54. doi: 10.1016/S0140-6736(20)31208-3
46. van Doremalen N, Lambe T, Spencer A, Belij-Rammerstorfer S, Purushotham JN, Port JR. ChAdOx1 nCoV-19 vaccine prevents SARS-CoV-2 pneumonia in rhesus macaques. *Nature* (2020) 586(7830):578–82. doi: 10.1038/s41586-020-2608-y
47. Graham SP, Mclean RK, Spencer AJ, Belij-Rammerstorfer S, Wright D, Ulaszewska M, et al. Evaluation of the Immunogenicity of Prime-Boost Vaccination With the Replication-Deficient Viral Vectored COVID-19

Vaccine Candidate Chadox1 Ncov-19. *NPJ Vaccines* (2020) 5:69. doi: 10.1038/S41541-020-00221-3

48. Folegatti PM, Ewer KJ, Aley PK, Angus B, Becker S, Belij-Rammerstorfer S, et al. Safety and Immunogenicity of the Chadox1 Ncov-19 Vaccine Against SARS-Cov-2: a Preliminary Report of a Phase 1/2, Single-Blind, Randomised Controlled Trial. *Lancet* (2020) 396(10249):467–78. doi: 10.1016/S0140-6736(20)31604-4

Conflict of Interest: CC, VBo, AC, NS, SM, RB, VBe, and ST are, or were at the time of the study, employees of the GSK group of companies. RB, SM, VBe, and ST report ownership of GSK shares and/or restricted shares. SC is an employee of Reithera Srl.

Advantages of publishing in Frontiers

OPEN ACCESS
Articles are free to read for greatest visibility and readership

FAST PUBLICATION
Around 90 days from submission to decision

HIGH QUALITY PEER-REVIEW
Rigorous, collaborative, and constructive peer-review

TRANSPARENT PEER-REVIEW
Editors and reviewers acknowledged by name on published articles

Frontiers
Avenue du Tribunal-Fédéral 34
1005 Lausanne | Switzerland

Visit us: www.frontiersin.org
Contact us: frontiersin.org/about/contact

REPRODUCIBILITY OF RESEARCH
Support open data and methods to enhance research reproducibility

DIGITAL PUBLISHING
Articles designed for optimal readership across devices

FOLLOW US
@frontiersin

IMPACT METRICS
Advanced article metrics track visibility across digital media

EXTENSIVE PROMOTION
Marketing and promotion of impactful research

LOOP RESEARCH NETWORK
Our network increases your article's readership